

16TH INTERNATIONAL PLANETARY PROBE WORKSHOP

Oxford University, UK 8–12 July 2019

& Short Course titled • Ice Giants: Exciting Targets for
Solar System Entry Probes Exploration • 6–7 July



IPPW-2019

Abstract deadline • 8 March 2019
Further information • www.ippw2019.uk

Abstract Book



Oral Session Abstracts

Monday, July 8 2019

Science Instrumentation, Experiments, and In-Situ Measurements - Conveners: Manuel Dominguez, Rafael Lugo,				
2:45 PM	Poster Introductions			
2:57 PM	The PanCam instrument for the Rosalind Franklin (ExoMars 2020) rover	Andrew Coates	UCL Mullard Space Science Laboratory	
3:09 PM	TheJet Propulsion Laboratory, California Institute of Technology Venus Aerosol Mass Spectrometer Concept	Kevin Baines	Jet Propulsion Laboratory, California Institute of Technology	
3:21 PM	Dragonfly: In Situ Exploration of Titan's Organic Chemistry and Habitability	Elizabeth Turtle	Johns Hopkins Applied Physics Laboratory	
3:58 PM	The Entry Descent and Landing Instrumentation Suite for the Mars 2020 Mission	Todd White	NASA Ames Research Center	
4:10 PM	Piezo-Electric Inlet System For Atmospheric Descent Probe	Jurij Simcic	Jet Propulsion Laboratory, California Institute of Technology	
4:22 PM	Exploring The Performance Of A Miniature 3D Wind Sensor Under Extreme Martian Winds Up To The Dust Devil Scale	Manuel Dominguez-Pumar	Technical University of Catalonia	
4:34 PM	Assessing The Habitability Of Icy Ocean Worlds	Samuel Kounaves	Tufts University	
4:46 PM	i-Drill: An Instrumented Drill for Lunar Polar Volatiles	Ryan Timoney	University of Glasgow	Student
4:58 PM	Laser Nephelometer For In-Situ Particle Detection In Planetary Atmospheres	Vandana Jha	NASA Ames Research Center	

The PanCam instrument for the Rosalind Franklin (ExoMars 2020) rover

A.J. Coates¹ for the ExoMars 2020 PanCam team(*), ¹Mullard Space Science Laboratory, University College London, Holmbury St Mary, Dorking, RH5 6NT, UK (a.coates@ucl.ac.uk)

Brief Presenter Biography: Professor Andrew Coates gained a BSc in Physics from UMIST and MSc and D.Phil. from Oxford University. He has been at UCL's Mullard Space Science Laboratory (MSSL) since 1982, with temporary guest positions in Germany, USA and the BBC World service. He is Deputy Director (solar system) at UCL-MSSL. Space mission involvements include the ExoMars 2020 rover where he leads the PanCam team, Cassini, where he leads the electron spectrometer team (part of the Cassini Plasma Spectrometer), Venus Express, Mars Express and Giotto.

Introduction: The scientific objectives of the ExoMars Rosalind Franklin rover [1] are designed to answer several key questions in the search for life on Mars. In particular, the unique subsurface drill will address some of these questions for the first time, such as the possible existence and stability of sub-surface organics. PanCam [2] will establish the surface geological and morphological context for the mission, working in collaboration with other context instruments. Here, we describe the PanCam scientific objectives in geology, atmospheric science and 3D vision. We discuss the design of PanCam, which includes a stereo pair of Wide Angle Cameras (WACs), each of which has an 11 position filter wheel, and a High Resolution Camera (HRC) for high resolution investigations of rock texture at a distance. The cameras and electronics are housed in an optical bench that provides the mechanical interface to the rover mast and a planetary protection barrier. The electronic interface is via the PanCam Interface Unit (PIU), and power conditioning is via a DC-DC converter. PanCam also includes a calibration target mounted on the rover deck for radiometric calibration, fiducial markers for geometric calibration and a rover inspection mirror.

* A.J. Coates,^{1,2} R. Jaumann,³ A.D. Griffiths,^{1,2} M. Carter,^{1,2} C.E. Leff,^{1,2} N. Schmitz,³ J.-L. Josset,⁴ G. Paar,⁵ M. Gunn,⁶ E. Hauber,³ C.R. Cousins,⁷ P. Grindrod,⁸ J.C. Bridges,⁹ M. Balme,¹⁰ S. Gupta,¹¹ I.A. Crawford,^{2,12} P. Irwin,¹³ R. Stabbin,^{1,2} D. Tirsch,³ J.L. Vago,¹⁴ M. Caballo-Perucha,⁵ G.R. Osinski,¹⁵ and the PanCam Team

¹Mullard Space Science Laboratory, University College London, Dorking, UK (a.coates@ucl.ac.uk)

²Centre for Planetary Science at UCL/Birkbeck, London, UK.

³Institute of Planetary Research, German Aerospace Centre (DLR), Berlin, Germany.

⁴Space Exploration Institute, Neuchâtel, Switzerland.

⁵Joanneum Research, Graz, Austria.

⁶Department of Physics, Aberystwyth University, Aberystwyth, UK.

⁷Department of Earth & Environmental Sciences, University of St Andrews, St Andrews, UK.

⁸Natural History Museum, London, UK

⁹Space Research Centre, University of Leicester, Leicester, UK.

¹⁰Department of Earth Sciences, Open University, Milton Keynes, UK.

¹¹Department of Earth Science and Engineering, Imperial College London, UK.

¹²Department of Earth and Planetary Sciences, Birkbeck, University of London, London, UK.

¹³Department of Physics, University of Oxford, Oxford, UK.

¹⁴European Space Agency, Noordwijk, the Netherlands.

¹⁵Centre for Planetary Science & Exploration, U. Western Ontario, London, Canada

References:

[1] Vago, J.L., F. Westall, A.J. Coates, et al., *Astrobiology*, 17(6-7), 471-510, doi:10.1089/ast.2016.1533, Jul 2017. [2] Coates, A.J., R. Jaumann, A.D. Griffiths, et al., *Astrobiology*, 17 (6-7), 511-541, DOI: 10.1089/ast.2016.1548, Jul 2017.

THE JPL VENUS AEROSOL MASS SPECTROMETER CONCEPT.

K. H. Baines¹, J. A. Cutts², D. Nikolić³, S. M. Madzunkov⁴, M. L. Delitsky⁵, S. S. Limaye⁶, and K. McGouldrick⁷,
¹Jet Propulsion Laboratory/Caltech (M/S 183-601, 4800 Oak Grove Dr., Pasadena, CA, kevin.baines@jpl.nasa.gov),
²Jet Propulsion Laboratory/Caltech (M/S 321-360, 4800 Oak Grove Dr., Pasadena, CA, 91109, james.a.cutts@jpl.nasa.gov),
³Jet Propulsion Laboratory/Caltech (M/S 306-392, 4800 Oak Grove Dr., Pasadena, CA, 91109, Dragan.Nikolic@jpl.nasa.gov),
⁴Jet Propulsion Laboratory/Caltech (M/S 306-392, 4800 Oak Grove Dr., Pasadena, CA, 91109, stojan.m.madzunkov@jpl.nasa.gov),
⁵California Specialty Engineering, Pasadena CA,
⁶Space Science and Engineering Center, University of Wisconsin-Madison, Madison, WI 53706,
⁷Laboratory for Atmospheric and Space Physics, University of Colorado, Boulder, 3665 Discovery Dr., Boulder, CO 80303

Brief Presenter Biography: Kevin Baines is a Principal Scientist at the Jet Propulsion Laboratory and a Senior Scientist at the Space Science and Engineering Center at the University of Wisconsin-Madison. He specializes in the composition, cloud structures and dynamics of planetary atmospheres, particularly of Venus and the jovian planets. He was the NASA-named Lead NASA Scientist on the Venus Express Mission, and a Co-Investigator on the Cassini and Galileo missions to Saturn and Jupiter where he explored the nature of major meteorological features via near-infrared spectral imaging. He has participated as PI or Project Scientist on eight Discovery and New Frontiers proposals to Venus, including three involving long-duration globe-circling balloon platforms.

Introduction: Via both photo- and thermo-chemistry, Venus experiences complex chemical cycles involving both vapors and aerosols. Sulfuric acid clouds and hazes in the ~40-70 km altitude range result from photochemical processes involving SO₂ and H₂O, which, upon descent below ~40 km altitude, decompose back into their parent constituents. While such sulfuric acid aerosols are considered to comprise the bulk of Venusian aerosols, a significant admixture of constituents is evident by the surprisingly strong UV absorption observed within this cloud environment. Besides contributing a substantial amount of cloud heating that may play a significant role in the planet's radiative balance and global circulation, the uv-absorbing material provides evidence of poorly-understood chemical processes within the clouds. Biotic processes may even be involved [1].

To understand the chemical processes occurring within the cloud environment - most notably within H₂SO₄ cloud particles - we are developing a lightweight, low-power in-situ instrument to measure the composition of Venusian aerosols. This device would be used on future aerial missions, including on long-duration (multi-week) balloon missions and on short-duration (several hour) probes, and could be used on such missions to explore the clouds and hazes of Titan and the outer planets. For Venus, current design requirements

include the ability to measure mass ranges from 2 to 300 AMU at <0.02 AMU resolution, to, for example, measure the component of iron chloride (FeCl₃ - 158 AMU; [2]) and potential biotic species embedded within sulfur acid aerosols. Another requirement, based on the expected saturated equilibrium concentration of HCl in H₂SO₄ aerosols near the 55-km-altitude level [3] is to measure HCl/H₂SO₄ with a mixing ratio of 2×10^{-9} to better than 10% in less than 300 secs. Solution chemistry of H₂SO₄ with HCl and with its sister hydrogen halides HF and HBr [4,5] may produce significant amounts of associated sulfonic acids (e.g., ClSO₃H, FSO₃H, BrSO₃H) and their daughter products (e.g., SOCl₂ and SO₂Cl₂, SOF₂, SO₂F₂; [3, 6, 7]). Other potential species to be measured resident on or dissolved within H₂SO₄ particles include elemental sulfur polymers comprised principally of S₈ together with small admixtures of the metastable allotropes S₄ and S₃ [8], and [9]). Elemental sulfur particles may also be measured as standalone particles, unattached to H₂SO₄.

The heart of the Venus Aerosol Mass Spectrometer instrument is the Quadrupole Ion-Trap Mass Spectrometer (QITMS, [10,11]) a version of which has flown on the International Space Station [12] where it has reliably monitored toxic CO against a large background of N₂. The preliminary concept involves an inlet aerodynamic lens [13,14] together with an adjustable piezo-electric aperture that allows only aerosols of a selectable size range within an overall range of 0.3 to 3.0 μm radius into the QITMS. Upon entering the QITMS, aerosols are vaporized by its hot electrode surfaces (~320° C). Measurements of the entire mass spectrum are made every 0.05 seconds, and can be co-added to achieve superior precisions. Species with concentrations of 100 ppm can be determined to 10% precision in under 1.5 seconds; 1 ppm in 15 seconds; and 1 ppb in < 3 minutes.

References:

- [1] Limaye S. S. et al. (2018) *Astrobiology*, 18, #10, 1-18.
- [2] Krasnopolsky V. A. (2017) *Icarus*, 286,134-137.
- [3] Delitsky M. L. and Baines K. H. (2018) 50th

AAS/DPS. Abstract 102.01.[4] Sill, G. T. (1975) *J. Atm. Sci*, 32, 1201 - 1204.[5] Krasnopolsky V. A. (2017) *Icarus*, 293, 114-118. [6] Baines K. H. and Delitsky M. L. (2013) 45th AAS/DPS. Abstract 118.10. [7] Delitsky M. L. and Baines K. H. (2015) 47th AAS/DPS. Abstract 217.02. [8] Toon O. B. et al. (1982) *Icarus*, 51, 358 - 373. [9] Hartley K. M. et al. (1989) *Icarus*, 77, 382 -390. [10] Madzunkov, S. M. and Nikolic, D. (2014) *J. Am. Soc. for Mass Spectro.*, 25, 1841 - 1852. [11] Avicé, G. et al. (2019) *J. Anal. At. Spectrom.*, 34, 104-117. [12] Darrach, M et al (2010) *Proc. 40th Internat. Conf. Environmental Systems* [13] Schreiner, J et al (1999) *Science*, 283, 968. [14] Cziczó, D. J. et al (2004) *JGR*, 109.

DRAGONFLY: IN SITU EXPLORATION OF TITAN'S ORGANIC CHEMISTRY AND HABITABILITY.

E. Turtle¹, M. Trainer², J. Barnes³, R. Lorenz¹, K. Hibbard¹, D. Adams¹, P. Bedini¹, W. Brinckerhoff², M. Burks⁴, M. Cable⁵, C. Ernst¹, C. Freissinet⁶, K. Hand⁵, A. Hayes⁷, S. Hörst⁸, J. Johnson¹, E. Karkoschka⁹, J. Langelaan¹⁰, D. Lawrence¹, A. Le Gall⁶, J. Lora¹¹, S. MacKenzie¹, C. McKay¹², R. Miller¹, S. Murchie¹, C. Neish¹³, C. Newman¹⁴, J. Nunez¹, J. Palacios¹⁰, M. Panning⁵, A. Parsons², P. Peplowski¹, L. Quick¹⁵, J. Radebaugh¹⁶, S. Rafkin¹⁷, M. Ravine¹⁸, S. Schmitz¹⁰, J. Soderblom¹⁹, K. Sotzen¹, A. Stickle¹, E. Stofan¹⁵, C. Szopa⁶, T. Tokano²⁰, C. Wilson²¹, R. Yingst¹³, K. Zacny²², ¹APL, Laurel, MD (Elizabeth.Turtle@jhuapl.edu), ²NASA GSFC, Greenbelt, MD, ³Univ. Idaho, Moscow, ID, ⁴LLNL, Livermore, CA, ⁵JPL, Pasadena, CA, ⁶LATMOS, Guyancourt, France, ⁷Cornell Univ., Ithaca, NY, ⁸Johns Hopkins Univ., Baltimore, MD, ⁹Univ. Arizona, Tucson, AZ, ¹⁰Penn. State Univ., University Park, PA, ¹¹Yale Univ., New Haven, CT, ¹²NASA ARC, Moffett Field, CA, ¹³PSI, Tucson, AZ, ¹⁴Aeolis Research, Pasadena, CA, ¹⁵Smithsonian Inst., Washington, DC, ¹⁶BYU, Provo, UT, ¹⁷SWRI, Boulder, CO, ¹⁸MSSS, San Diego, CA, ¹⁹MIT, Cambridge, MA, ²⁰Univ. Köln, Köln, Germany, ²¹Oxford Univ., Oxford, UK, ²²Honeybee Robotics, Pasadena, CA.

Brief Presenter Biography: Dr. Elizabeth Turtle is a planetary scientist at the Johns Hopkins Applied Physics Laboratory (APL) with expertise in exploration of the outer planets and the Moon, having participated in *Galileo*, *Cassini*, and *LRO*. She is the Principal Investigator (PI) for the Europa Imaging System (EIS) on *Europa Clipper* and PI of the *Dragonfly* mission concept being studied under NASA's New Frontiers Program.

Introduction: Titan's abundant complex carbon-rich chemistry, interior ocean, and past presence of liquid water on the surface make it an ideal destination to study prebiotic chemical processes and document the habitability of an extraterrestrial environment [e.g., 1-7]. The diversity of the surface materials and environments [8] drives a scientific need to sample a variety of locations, thus mobility is key for *in situ* measurements.

Exploration Strategy: Titan's dense atmosphere provides the means for long-range exploration by a vehicle with aerial mobility. The *Dragonfly* mission concept, under study in NASA's New Frontiers Program, is a rotorcraft lander that would achieve wide-ranging *in situ* investigation by flying to access different geologic settings 10s–100s of km apart, performing multidisciplinary science measurements at each landing site.

Given Titan's dense atmosphere (4x that at Earth's surface) and low gravity (1.35 m/s²), heavier-than-air mobility is highly efficient [9-11]. Modern control electronics and recent developments in autonomous flight enable a multi-rotor vehicle to convey a capable instrument suite to explore multiple locations [12]. For a given vehicle mass and rotor diameter, the hover power required on Titan is 38x less than on Earth [9,12]. Flights are performed using power from a battery recharged via an MMRTG. Adopting rotors as a substitute for the retrorockets used for landing on other planets, the ability to take off and land elsewhere follows with little incremental cost and tremendous science enhancement. The interior of the lander is maintained at constant benign temperatures using 'waste' heat from the MMRTG, so only modest adaptation is needed for Titan's environment.

Science Objectives: At each landing site, *Dragonfly* can answer key scientific questions regarding habitability and prebiotic chemistry and put these measurements in the context of Titan's meteorology and methane cycle, local geologic setting and material properties [13], and geophysical measurements of the subsurface [14].

Surface material is sampled by drills and ingested using pneumatic transfer at near-ambient Titan temperatures into a mass spectrometer [15,16]. Laser desorption (LDMS) and pyrolysis gas chromatography (GCMS) operating modes can identify the chemical components and processes at work to produce biologically relevant compounds. Bulk elemental composition beneath the lander is determined by a neutron-activated gamma-ray spectrometer [17]. Meteorology and remote sensing measurements characterize the atmosphere and surface [18-20]. Seismic sensing can detect subsurface activity and probe subsurface structure [21], and aerial and surface imaging will characterize geologic features and provide context for sampling.

References: [1] Raulin *et al.* (2010) in *Titan from Cassini-Huygens* Brown *et al.* Eds. [2] Thompson & Sagan (1992), *Sympos. on Titan, ESA SP-338*, 167-176. [3] Neish *et al.* (2010) *Astrobiol.* 10, 337-347. [4] Neish *et al.* (2018) *Astrobiol.* 18, 571-585. [5] <https://astrobiology.nasa.gov/research/life-detection/ladder/> [6] Hand *et al.* (2018) *LPSC 49*, #2430. [7] Chyba *et al.* (1999) *LPSC 30*, #1537. [8] Barnes *et al.* (2018) *LPSC 49*, #2721. [9] Lorenz (2000) *J. British Interplanet. Soc.* 53, 218-234. [10] Lorenz (2001) *J. Aircraft* 38, 208-214. [11] Barnes *et al.* (2012) *Exp. Astron.* 33, 55-127. [12] Langelaan *et al.* (2017) *Proc. Aerospace Conf. IEEE*. [13] MacKenzie *et al.* (2019) *LPSC 50*. [14] Lorenz *et al.* (2019) *LPSC 50*. [15] Trainer *et al.* (2018) *LPSC 49*, #2586. [16] Zacny *et al.* (2017) *LPSC 48*, #1366. [17] Lawrence *et al.* (2017) *LPSC 48*, #2234. [18] Stofan *et al.* (2013) *Proc. Aerospace Conf. IEEE*, DOI: 10.1109/AERO.2013.6497165. [19] Wilson & Lorenz (2017) *LPSC 48*, #1859. [20] Lorenz *et al.* (2012) *Int'l Workshop Instr. Planet. Missions, LPI Contrib.* 1683, p.1072. [21] Lorenz & Panning (2018) *Icarus* 303, 273-279.

THE ENTRY DESCENT AND LANDING INSTRUMENTATION SUITE FOR THE MARS 2020 MISSION

T. R. White¹, C. D. Karlgaard², M. Mahzari³, C. Tang⁴, M. Schoenenberger⁵, B. A. Cruden⁶

¹NASA Ames Research Center, Todd.R.White@nasa.gov, ²Analytical Mechanics Associates, Inc. at NASA Langley Research Center, Chris.Karlgaard-1@nasa.gov, ³NASA Ames Research Center, Milad.Mahzari@nasa.gov, ⁴NASA Ames Research Center, Chun.Y.Tang@nasa.gov, ⁵NASA Langley Research Center, Mark.Schoenenberger@nasa.gov, ⁶Analytical Mechanics Associates, Inc. at NASA Ames Research Center, Brett.A.Crudon@nasa.gov.

Brief Presenter Biography: Todd White is a member of the NASA Ames Entry Systems and Vehicle Development Branch and the MEDLI2 Principle Investigator. He has contributed to many space missions and proposals, including Shuttle, Orion, OSIRIS-REx, InSight, MSL, MEDLI, and the current Mars Sample Return Earth Entry Vehicle.

Introduction: Because entry descent and landing (EDL) missions are infrequent and involve complex physics, space agencies and spacecraft designers are increasingly instrumenting in-situ sensor suites on spacecrafts so the EDL modelling community and future mission designers can validate their models with flight data. Over the last decade, NASA [1],[2], ESA [3], and JAXA [4] have seen a resurgence in the gathering of in-situ entry aerothermal and aerodynamic data using accurate temperature and pressure sensing systems. The availability of high-quality flight data coupled with increasingly more powerful computer systems has enabled the EDL community to refine their aerothermal, aerodynamic, and thermal protection system models for various planetary missions.

Mars 2020 & MEDLI2: The Mars 2020 mission will launch in July, 2020 and will enter the Martian atmosphere on February 18th, 2021. Like the Mars Science Laboratory (MSL) mission before it, Mars 2020 includes an aeroshell instrumentation suite to accurately measure the atmospheric conditions and vehicle entry state during EDL. The Mars 2020 instrumentation suite is shown in Figure 1, and is called the Mars Entry Descent and Landing Instrumentation Suite 2, or MEDLI2 [5]. MEDLI2 is a combined effort of NASA Langley and Ames; the Jet Propulsion Laboratories; and Lockheed Martin, which is responsible for the sensors, support electronics, and integration of MEDLI2 onto the aeroshell and to the rover computer systems. Mars 2020 is a flagship-class mission, and the MEDLI2 suite includes an array of previously demonstrated instrument types flown on MSL as well as new instruments to better characterize entry phenomena at Mars. MEDLI2 will gather approximately 10 minutes of data from these sensors, starting prior to atmospheric entry and down through heatshield separation. This dataset will allow aerospace engineers to reconstruct the aerodynamic and aerothermal environment with great accuracy.

Scope of the Presentation: This presentation will discuss the current state of each of the main measurements systems for MEDLI2. The first system

is a network of pressure transducers, the Mars Entry Atmospheric Data System (MEADS). Improving upon MEDLI, separate MEDLI2 pressure transducers span the measurement range suitable for both hypersonic and supersonic flows. The MEADS will also measure pressure on the backshell of the vehicle to better characterize the contribution of backshell pressure on the overall forces and moments on the entry probe. The second system is the thermal instrumentation, or Mars Instrumented Sensor Plugs. This system includes a network of high-temperature thermocouples embedded in the thermal protection system across the heatshield and backshell. The MISP also includes two types of sensors for directly measuring incident heatflux on the backshell of the vehicle. In addition, a radiometer is instrumented on the backshell to measure radiative heating.

The presentation will also cover the current state of the MEDLI2 hardware, expected environments that will be measured, and data analysis techniques being developed to infer vehicle entry performance from both the MISP and MEADS sensor systems.

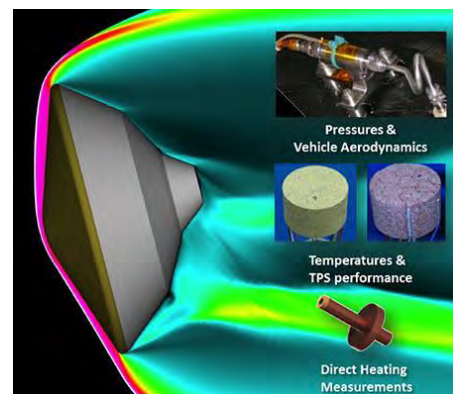


Figure 1 The MEDLI2 Sensor Suite

References:

- [1] M. Gazarik, A. Little, F. Cheatwood, M. Wright, J. Herath, E. Martinez, M. Munk, F. Novak, H. Wright, "Overview of the MEDLI Project" IEEE 2008.
- [2] K. Bibb, "Overview of Orion Aerodynamics: Database Development and Flight Test Comparisons" IPPW 2018.
- [3] A. Gülhan, et al. "Aerothermal Measurements from the ExoMars Schiaparelli Capsule Entry" Journal of Spacecraft and Rockets, 2018.

[4] T. Yamada, K. Yoshihara, K. Yamada, "Hayabusa-2 Reentry Capsule and its Verification Tests", IPPW11 (2014).

[5] H. Hwang, D. Bose, H. Wright, T. White, M. Schoenenberger, J. Santos, C. Karlgaard, C. Kuhl, T. Oishi, D. Trombetta, "Mars 2020 Entry, Descent, and Landing Instrumentation (MEDLI2)", AIAA 2016-3536.

PIEZO-ELECTRIC INLET SYSTEM FOR ATMOSPHERIC DESCENT PROBE

J. Simcic¹, J. C. Lee¹, S. Madzunkov¹, D. Nikolic¹, A. Belousov¹, ¹Jet Propulsion Laboratory, 4800 Oak Grove Dr., Pasadena, CA 91109, USA, jurij.simcic@jpl.nasa.gov

Brief Presenter Biography: Dr. Simcic is a research technologist at JPL, working on the design of quadrupole ion traps for miniature mass spectrometers (QITMS). He is a cognizant engineer for QITMS sensor for Spacecraft Atmosphere Monitor, which is expected to launch for ISS later in 2019. He is developing a miniature piezoelectric valve for atmospheric descent sampling and leading the JPL effort in designing a miniature sample chamber and gaseous discharge detector system for the Miniature Variable Pressure Scanning Electron Microscope.

Introduction: An inherent challenge with Spaceflight Mass Spectrometers is the introduction of the material being sampled (gas, solid, or liquid) into the instrument interior, which operates at vacuum. Especially, if being employed in an Atmospheric Descent Probe, Spaceflight Mass Spectrometers typically require a specially designed sample inlet system which ideally provides highly choked, nearly constant mass-flow intake, despite ambient pressure variations. In addition to being sufficiently low in conductance, an inlet leak for Spaceflight Mass Spectrometer must also be chemically inert, must not distort the gas composition being sampled by adsorbing or reacting with sampled gases differentially, and must have a reasonably fast response time (on the order of seconds or less). Finally, it must be simple, robust and operable over a wide temperature range. Past methods of producing such inlet systems have included pulled glass [1], crimped metal tubes [2,3], porous frits, micro-machined leaks [4-7] and pulsed piezoelectric valves [8,9]. So far none of these methods have produced an inlet system that would satisfy all the conditions mentioned above and be able to finely regulate sample mass-flow in a continuous fashion in wide pressure interval.

At JPL we have recently fabricated a miniature valve for atmospheric descent sampling using Micro-Electro-Mechanical Systems (MEMS) technology. The miniature valve consists of a custom-designed piezoelectric stack actuator bonded onto silicon valve components with the entire assembly contained within a metal housing. The valve seat configuration includes narrow-edge seating rings and tensile-stressed silicon tethers that enable the normally closed and leak-tight operation. A concentric series of narrow rings simulates a “knife-edge” seal by greatly reducing the valve contact area, thereby increasing the seating pressure and consequently reducing leak. The design of the device dates 12 years back when similar instrument was

developed at JPL for high pressure gas micro-propulsion applications [10]. The newly fabricated device is a fast reacting (less than a ms), and low power valve of variable conductance, capable of continuous regulation of mass-flow in very fine steps in the environment where external pressure can reach up to 100bar. It can operate in a static or pulsed mode, up to 1kHz. Leak testing of the miniature valve, conducted using a Helium leak detector, showed a leak rate of approximately 2×10^{-6} mbar l/s at 55 bar inlet pressure in its “normally closed” position. The miniature valve has been successfully coupled with JPL’s existing Quadrupole Ion Trap Mass Spectrometer (QITMS) [11], today’s smallest SMS, a compact, wireless instrument, with a mass of only 7.5 kg, capable of detecting a complete inventory of atmospheric chemical species at high speed (50 full-range mass spectra per second), with high sensitivity (up to 10^{14} counts/mbar/sec) and high resolution ($m/\Delta m = 20000$ at 40Da). The combination of the miniature piezo-electric valve and QITMS results in extremely powerful instrument, suitable for atmospheric descent probe missions. For example, a compact instrument based upon the QITMS design would have a sensitivity high enough to reach the precision on isotope ratios (*e.g.* better than 1% for $^{129,131}\text{Xe}/^{136}\text{Xe}/^{130}\text{Xe}$ ratios) [12] necessary for a scientific payload measuring noble gases collected in the Venus atmosphere.

References: [1] H. B. Niemann, D. N. Harpold, S. K. Atreya, (1992) *Space Sci. Rev.* 60, 111. [2] J. H. Hoffman, R. R. Hodges, K. D. Duerksen, (1979) *J. Vac. Sci. Technol.* 16, 692. [3] J. H. Hoffman, R. R. Hodges, Jr., M. B. McElroy, T. M. Donahue, and M. Kolpin (1979) *Science* 205, 49. [4] ROSES 2015: New Frontiers Homesteader, JPL, Madzunkov. [5] M. R. Darrach, S. Madzunkov, E. Neidholdt, J. Simcic (2016) IPM, Pasadena, CA. [6] B. G. Jamieson et al. (2007) *Rev. Sci. Inst.* 78, 065109. [7] NASA Tech Briefs (July 2016), Vol.40, No.7, p38. [8] K. V. Grechnev, V. G. Istomin, L. N. Ozerov, and V. G. Klimovitskii (1979) *Kosm. Issled.* 17,697. [9] V.G. Istomin, K.V. Grechnev and V.A. Kochnev (1979) *Pisma Astron. Zh.* 5, 211-216. [10] J. C. Lee, E.-H. Yang, S. M. Saeidi, and J. M. Khodadadi (2006) *Jour. of MEMS*, Vol. 15, No. 3, pg.686. [11] S. Madzunkov, & D. Nikolić (2014) *J. Am. Soc. Mass Spectrom.* 25: 1841. [12] G. Avice et al. (2019), *J. Anal. At. Spectrom.*, 34, 104.

Additional Information: The development of piezo-electric valve is being sponsored by NASA through NNN16ZDA001N-PICASSO.

EXPLORING THE PERFORMANCE OF A MINIATURE 3D WIND SENSOR UNDER EXTREME MARTIAN WINDS UP TO THE DUST DEVIL SCALE,

M. Dominguez-Pumar¹, L. Kowalski¹, V. Jimenez¹, I. Rodríguez², M. Soria²

¹MNT-Group, UPC-Campus Nord, Ed. C4, Jordi Girona 1-3, 08034 Barcelona, SPAIN.

²TUAREG-Group, UPC, Colom 11, Terrassa (Barcelona) 08222, Spain.
email: manuel.dominguez@upc.edu

Prof. M. Domínguez-Pumar: Associate Prof. at BarcelonaTech, Spain. He has participated in the REMS, TWINS and MEDA wind sensors for MSL, InSight and Mars2020. He also works in the design of nonlinear controls for sensors and in the optimization of their dynamics.

Introduction: The objective of this paper is to explore the performance of a miniature 3D spherical wind sensor for Mars atmosphere, [1-3], working under extreme wind speeds, up to the Dust Devil scale.

The experimental campaign has been made for winds in the range Reynolds 1000-2000, which for typical Mars conditions and the dimensions of the sensor, represent 65-130m/s wind velocities.

The experimental results further confirm high-fidelity numerical simulations of the fluid dynamics and heat transfer from a sphere for Reynolds 1000-10⁴ and Prandtl 0.7, recently published in [4], which indicate that it is possible to measure in this regime.

Sensor description: The sensor is composed of 4 equally shaped sectors, conforming a 10 mm diameter sphere, that are placed on two superimposed PCBs, which act as supporting structure and provide signal routing (see Figure 1). A customized silicon die which includes a Pt resistor is attached to each sector in order to sense temperature and provide heating power. Finally, two additional dice are placed on the supporting PCBs in order to control the temperature at the core of the sphere, on the PCBs. Maintaining the core at the same sector temperature, heat transfer between both elements is minimized.

The sensor is operated at the same constant temperature in the core and in all sectors. From the heating powers injected on the 4 resistors in the sectors and the air temperature, the thermal conductance of each sector is calculated. From these 4 signals 3D wind speed recovery can be made.

The performance of the sensor under typical Martian wind conditions (Reynolds below 200) has been previously explained [1]. The sensor presents a time response in the 1-2s range and its dynamics has been analyzed in [2-3].

Main result: The paper presents experimental results obtained under conditions representative of ex-

treme wind velocities in Mars atmosphere. Reynolds numbers in the range 1000-2000 have been attained by controlling pressure and wind speed in a wind tunnel inside a dry-air hypobaric chamber at room temperature. These Reynolds numbers represent wind speeds of 65m/s – 130m/s for typical Mars conditions (CO₂, 210K, 630Pa), and for the sensor diameter.



Fig. 1: Photograph of the 4-sector spherical sensor (10mm diameter).

Simulation results:

The results corroborate high-fidelity simulations in [4]. Direct numerical simulations (DNS) have been made for Re1000 and large-eddy simulations (LES) for Re10⁴. As an example, a snapshot of the temperature field in the wake of the sphere at Re1000 is shown in Figure 2. The scalar represented is the normalized temperature $\Phi = (T - T_{in}) / (T_{sph} - T_{in})$, where T_{sph} is the temperature on the surface of the sphere and T_{in} is the temperature of the fluid at the inlet.

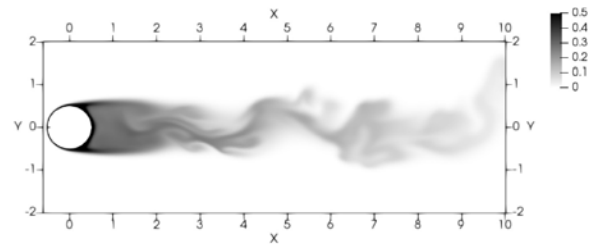


Fig. 2: Figure from [4] showing a snapshot of the temperature field in the wake of the sphere for Re1000 obtained from direct numerical simulations of the incompressible Navier-Stokes and energy equations.

Figure 3-left shows the local Nusselt number at Re1000 on the sphere. Figure 3-right shows a section of Figure 3-left corresponding to a triangular sector (a first approximation to the sectors of the sensor).

The objective is to analyze how the average Nu number on the triangular sector changes as a function of Yaw angle. This will provide information on the expected behavior at each sector of the sphere when the sensor is rotated. Figure 4 shows how the average Nu number of this sector changes as a function of the yaw angle of the incident wind, for Re1000. Figure 5 presents the equivalent result for Re10⁴.

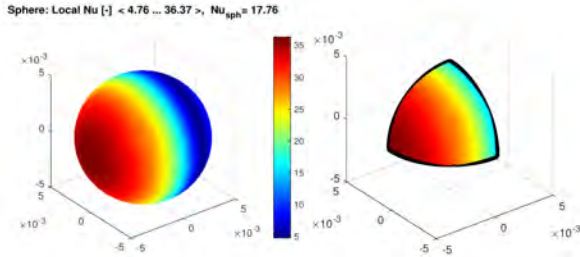


Fig. 3: (Left) Local Nusselt number on the sphere obtained from DNS simulations of Re1000. (Right) zoom corresponding to a triangular sector.

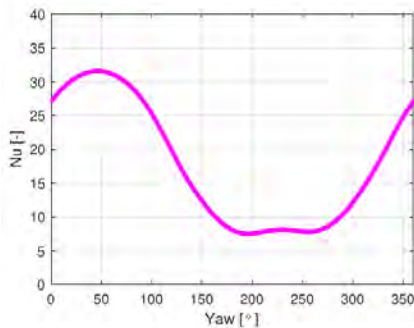


Fig. 4: Average Nu number for Re1000 on the triangle of Fig.3-right as a function of yaw angle.

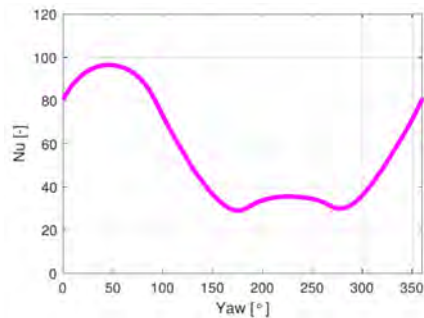


Fig. 5: Average Nu number for Re10⁴ on the triangle of Fig.3-right as a function of yaw angle.

Discussion: The simulations indicate that the average Nusselt of the sector as a function of the incident wind yaw angle presents a minimum region which widens for increasing Re numbers. This region presents a maximum between two minima. This represents a signature of the expected behavior of the sensor.

Experimental results: Figures 6 and 7 present the experimental curves obtained with the sensor in a wind tunnel inside a vacuum chamber at room temperature:

a) **Re1000:** Equivalent $U_{\text{Mars-flow}}$ of 65m/s (under typical Mars conditions). $U_{\text{dryair-flow}}$ in the chamber 6.5-7m/s, 250mbar, $T_{\text{air}}=22.9\text{C}$, $T_{\text{sph}}=35.6\text{C}$.

b) **Re2000:** Equivalent $U_{\text{Mars-flow}}$ 130m/s. $U_{\text{dryair-flow}}$ in the chamber 6.5-7m/s, 500mbar, $T_{\text{air}}=23.9\text{C}$, $T_{\text{sph}}=34.4\text{C}$.

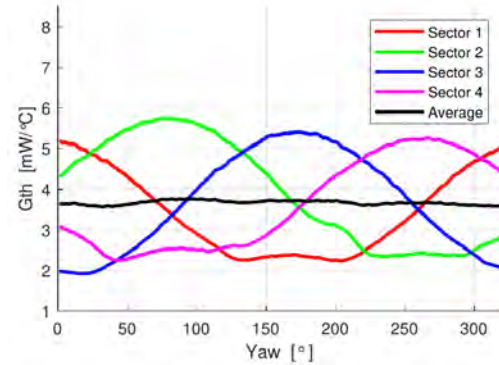


Fig. 6: Thermal conductances of each sector, and average value, as a function of Yaw angle for Re1000. Equivalent $U_{\text{Mars-flow}}$ velocity under typical Mars conditions of 65m/s.

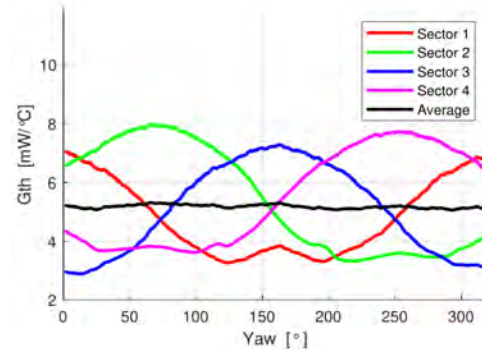


Fig. 7: Idem as Fig. 6 for Re2000 (equivalent $U_{\text{Mars-flow}}$ velocity under typical Mars conditions of 130m/s).

Conclusions: The thermal conductance of sectors follows the trend predicted by the simulations: for yaw angles leaving the sector in the wake of the sphere and for increasing Re numbers, the Gth presents widening minima and the maximum between them tends to increase.

These preliminary results indicate that 3D wind speed inference can be made in this extreme regime.

References:

[1] L. Kowalski, et al. (2016), *IEEE Sensors Journal*, 16, 1887-1897. [2] M. T. Atienza, et al. (2017) *Sens. and Act. A*, 267, 342-350. [3] M. Dominguez-Pumar et al. (2016), *IEEE Trans. Ind. Electr.*, 64 (1), (664-673). [4] I. Rodriguez, et al (2019), *Int. J. Heat and Fluid Flow*, 76, 141-153.

ASSESSING THE HABITABILITY OF ICY OCEAN WORLDS.

S. P. Kounaves¹, M. V. Clark¹, E. A. Jaramillo², N. Naz¹, A. C. Noell², R. C. Quinn³, and A. J. Ricco³

¹Tufts University (samuel.kounaves@tufts.edu), ²NASA Jet Propulsion Laboratory, California Institute of Technology, ³NASA Ames Research Center

Presenter Biography: Sam Kounaves is a professor at Tufts University and a visiting professor at Imperial College London. He was lead scientist for the Phoenix Mars lander wet chemistry laboratory (WCL). His research is aimed at unraveling fundamental questions in planetary science using modern *in-situ* analytical systems designed to analyze and study the biogeochemistry in these extreme remote environments.

Introduction: The Phoenix Lander descended onto the surface of Mars carrying four identical *Wet Chemistry Laboratory* (WCL) units (Figure 1). The goal of the Phoenix WCL was to analyze the aqueous geochemistry of the regolith in order to better understand the history of the water, biohabitability, available chemical energy sources, and the general geochemistry of the site. The WCL successfully performed all its tasks and provided the first direct wet chemical analysis of soil on another planet [1-3]. The power of wet chemical analysis to change how we view the martian surface chemistry clearly demonstrated that a fundamental understanding of the present habitability of any planetary body cannot be adequately made without direct knowledge of the aqueous chemistry of the regolith and its aqueous geochemistry.

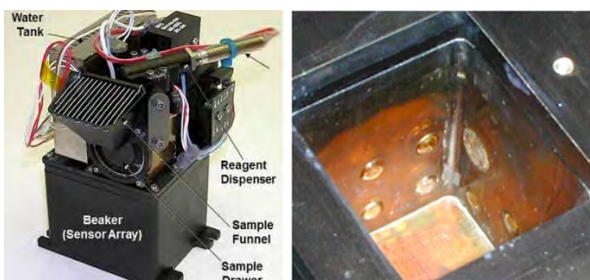


Figure 1. The flight-proven Phoenix Wet Chemistry Laboratory (WCL) and a view of its sensor array.

Determining the chemical composition and properties of the soluble species entrapped in the plume ejecta or surface coverage on icy worlds is fundamental science equivalent to the initial mineralogy studies that were accomplished on the surface materials of Mars. Although the icy moon oceans are likely 20-40 km below the surface, determining the chemistry of these subsurface environments can be accomplished by analyzing the materials that are brought to the surface. The plumes of Enceladus are especially tempting because they have been shown to erupt regularly, and that the silica particles found in the plume imply subsurface

hydrothermal activity [4]. On Europa this is made possible by what appears to be a highly active ice shell [5], and more recently observed potential plumes [6].

The Microfluidic-WCL: Just as the WCL determined both bulk and trace soluble cations and anions in the leached martian regolith, the *microfluidic-based WCL* (mWCL), shown in Figure 2, will determine similar species and properties of the material ejected in the plumes or on the surface of the icy moons. During the past two years, supported by NASA COLDTech and ICEE2 grants, we have designed, fabricated, and characterized this prototype device. Based on the Phoenix WCL, it has been redesigned to fit into a small-form factor, operate with milliliter or microliter volumes, and withstand the temperatures and radiation that would be encountered during a 5-10 year cruise to an icy world. Throughout the redesign a prime goal was to ensure that the mWCL would be able to use the flight-tested heritage WCL sensors.

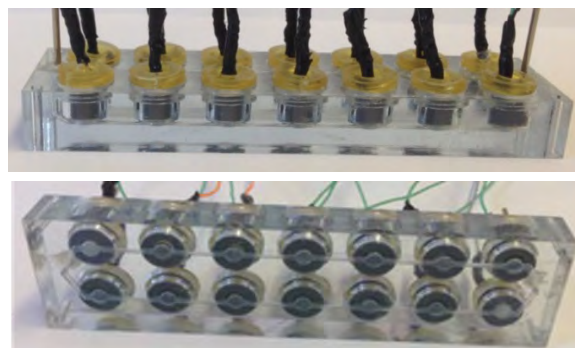


Figure 2. The microfluidic-WCL containing 14 ISE sensors interconnected by a sub-mm flow channel requiring only 100 μL of sample solution.

Results: The mWCL sensor array exhibited an order of magnitude improved LOD compared to the WCL, and responded faster and with improved sensitivity using a 100 μL volume. Interference tests using an Enceladus plume simulant showed the mWCL sensor array employing chemometric and AI algorithms can detect a variety of anions and cations in the presence of chloride levels expected in Enceladus' plume.

References:

- [1] Kounaves, S. P., et al. (2007) *JGR*, 115, E00E10.
- [2] Kounaves, S. P., et al. (2010) *GRL*, 37, L09201.
- [3] Quinn, R. C., et al. (2011) *GRL*, 38, L14202.
- [4] Hsu, H.W., et al. (2015) *Nature*, 519, 207-210.
- [5] Kattenhorn et al. (2014) *Nature Geosci*, 7, 762-767.
- [6] Roth, L., et al., (2014) *Science*, 343, 171-174.

i-Drill: An Instrumented Drill for Lunar Polar Volatiles

R. Timoney¹, K. Worrall¹, P. Harkness¹, S. Barber², S. Sheridan² and N. Murray³. ¹School of Engineer, University of Glasgow, Scotland, UK. G12 8QQ. r.timoney.1@research.gla.ac.uk. ²School of Physical Sciences, The Open University, Milton Keynes, UK. MK7 6AA. ³Dynamic Imaging Analytics, Milton Keynes, UK. MK16 6GD.

Brief Presenter Biography: Ryan is concluding his Ph.D. currently concluding his Ph.D. studies at the University of Glasgow having developed a number of planetary drilling technologies over the past four years. He has been fortunate enough to have spent time in Antarctica on two occasions during this period and has attended four previous IPPW.

Introduction: A recent European focus on the exploration of the Moon, may provide the scientific community with opportunities to further understand our nearest neighbour, both in its own right and as an indicator of the rich history of our Solar System. Numerous missions are planned, starting with in-situ robotic exploration but envisaged to later involve sample return and new human sorties to the lunar vicinity.

Many missions will target previously unsampled high-latitude and/or Permanently Shadowed Regions (PSRs), in a quest to provide ground truth for orbital measurements that suggest elevated concentrations of water and other volatiles associated with these low-temperature environments. Such species are of high intrinsic scientific value; moreover the use of these materials as a potential feedstock within the emerging field of in-situ resource utilisation (ISRU) additionally makes them of particular interest to future mission planners. To this end, the authors propose technologies capable of the extraction and analysis of these volatiles, as candidate payload elements on these upcoming missions.

‘i-Drill’ – an instrumented drill

i-Drill is an instrumented drill concept optimised to access the upper ~1 m of the lunar regolith. Thus i-Drill accesses both the surface layer that may exhibit signatures of transient surficial volatile enhancement and/or of contamination from the host spacecraft, and the deeper subsurface probed by remote sensing observations such as neutron detectors.

The concept shares many of its objectives with the Luna-27 PROSPECT package [1], with regolith being sampled by a drill and volatiles being released by heating for analysis in a mass spectrometer. However, whereas PROSPECT employs a complex, coring drill and an intermediate sample receiving and manipulation device to seal the cored sample and release volatiles by heating, i-Drill removes the need for precise robotic manipulation. This is accomplished by i-Drill employing a

hollow drill-string, such that volatiles bound to the regolith are released through the drilling process and diffuse up the string for analysis in a (PROSPECT-type) ion trap mass spectrometer supplied by The Open University (OU). Further advantages accrue because the drill can be operated for maximum penetration performance, and the resultant heat generated is beneficial in enabling efficient release and transfer of evolved volatiles. This is in contrast to a coring drill, which must be operated carefully in order to minimise the generation of heat at the bit that may introduce unwanted thermal alteration of the sample.

i-Drill also supports imaging of the sampled lunar regolith, enabling the volatiles profiles obtained to be interpreted in the wider geological context of the site. Imaging of the bottom of the borehole and of the cuttings is proposed and shall be achieved through the use of a dual camera suite of LUVMI heritage [2] and provided by Dynamic Imaging Analytics (DIA).

i-Drill was conceived at Glasgow, OU and DIA in response to a ESA RFI call on European payload contributions for future lunar missions. Harnessing knowledge gained through a rich heritage of technology development in their respective fields of subsurface sampling, in-situ analysis tools and space imaging, i-Drill provides a low resource solution for locating and extracting volatiles on future lightweight landed missions. Crucially, it occupies a ‘sweet-spot’ in the trade between payload mass/power requirements and its capability in terms of accessing ~1 m sub-surface and performing crucial volatiles investigations supported by contextual imagery. It is envisaged that this package of drill integrated with powerful and complementary mass spectrometer and imagers shall form a mass- and power-efficient payload applicable to various near-term small lunar landers.

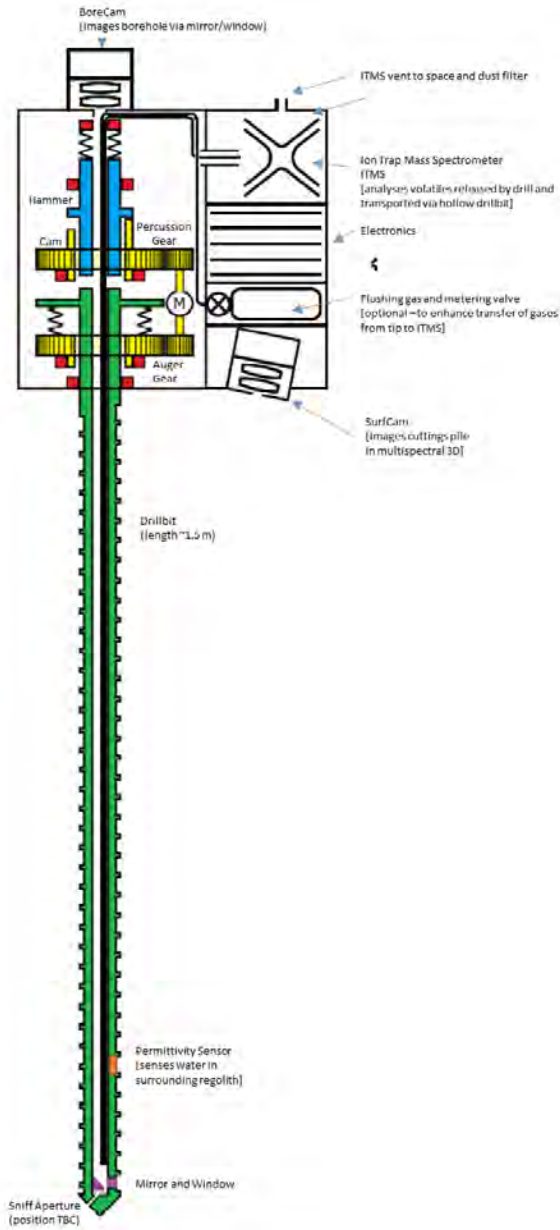


Figure 1: i-Drill Conceptual Schematic

References:

- [1] Trautner R. et al. (2018). IAC 2018. [2] Urbina D. et al. (2017) IAC 2017.

LASER NEPHELOMETER FOR IN-SITU PARTICLE DETECTION IN PLANETARY ATMOSPHERES

V. Jha¹, A. Colaprete¹, A. Cook^{1,2}, B. White¹, E. Bendek³, ¹NASA Ames Research Center, Moffett Field, CA, 94035, (vandana.jha@nasa.gov) ²Millennium Engineering & Integration, ³Bay Area Research Institute.

Brief Presenter Biography: Vandana Jha is a planetary atmospheres researcher in the space science division at NASA Ames Research Center. Her recent research focused on in-situ measurements of cloud condensation nuclei using a Forward Scattering Spectrometer Probe. She is currently part of the development team for a new nephelometer instrument for planetary atmosphere particle sensing.

Introduction: Proposed Venus and Saturn missions called out in the NASA Decadal Survey include atmospheric observations of clouds and aerosols. Remote sensing techniques to derive cloud properties, including density and particle size, are limited by the optical density of the respective atmospheres. A nephelometer is an instrument that makes in-situ measurements of the cloud particles it encounters as it descends, using a two-color backscattering process. A new nephelometer (derived from the Galileo version [1]) has been prototyped; the design benefits from lower volume and increased power efficiencies of near infrared diode lasers. This nephelometer measures the laser light scattered off of atmospheric particles. The reflected signal depends on particle density, size, and shape. Using two wavelengths allows discrimination over a range of particle sizes. Typical cloud particle sizes in the upper troposphere of Saturn and below are $>1.5 \mu\text{m}$ [2]. Number density estimates range from $\sim 10^6/\text{m}^3$ in tropospheric hazes to $\sim 10^9/\text{m}^3$ in a thick water condensation cloud. The addition of short wavelength filters on the detectors provides a measure of cloud particle single-scattering albedo and Rayleigh scattering. The estimated mass and power for this nephelometer are 1.7 kg and 1.5W, respectively. The system is suitable for a range of in-situ atmospheric missions, including descent probes and landers (NB: Galileo Nephelometer was 4.7kg, and averaged 11W).

Laser and Diode Description: The prototype consists of two diode lasers (785 and 1550 nm), two diode sensors, and control/readout electronics. To test the unit and calibrate sensitivity calculations, a dark air-flow chamber was designed and built. Air is mixed with calibrated particles and flowed through the chamber in the optical path of the sensor, enabling measurements of the sensor response to backscatter from each laser and particle size.

Initial data will test the possibility of operating the lasers in a growing-period pulse mode, allowing for Dynamic

Light Scattering approaches to determine the number of particles, and their size distribution.

Measurements: The active laser sensing works independent of lighting conditions at the probe descent location. Two pulsed diode lasers at 785 and 1550 nm, operating at frequencies up to 1.0 kHz, measure backscattered light to characterize cloud aerosol properties and number densities.

Pulsing the lasers minimizes the average power and, along with narrowband rejection filters over the laser detector, minimizes ambient background effects.

References: [1] Ragert B. et al. (1998) *JGR planet*, 103, 22891–22809. [2] Roman M. T. et al. (2013) *Icarus*, 225, 93-110.

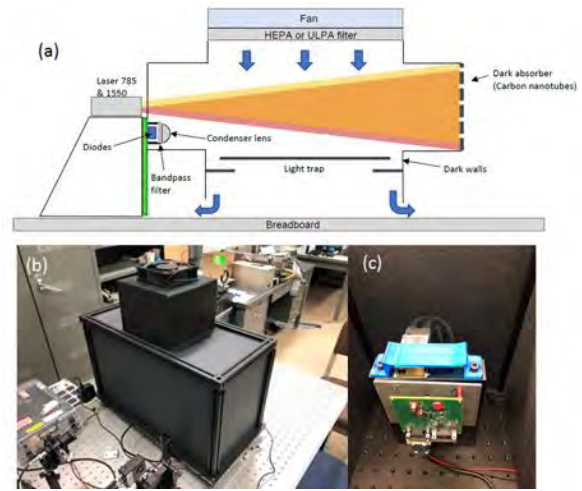


Figure 1a) Diagram of stand-off laser nephelometer instrument in test chamber (b) exterior of test chamber, and (c) laser nephelometer prototype in test chamber.

Tuesday, July 9 2019

Mars Exploration - Conveners: Ashley Korzun, David Mimoun, Michelle Munk, and Brooke Harper				
8:45 AM	InSight EDL Overview and As-Flown Performance	Rob Grover	Jet Propulsion Laboratory, California Institute of Technology	Invited
8:57 AM	Mars InSight Trajectory and Atmosphere Reconstruction	Chris Karlgaard	AMA, Inc. at NASA Langley Research Center	Invited
9:09 AM	InSight Approach Operations During Dust-Storm Season	Eugene Bonfiglio	Jet Propulsion Laboratory, California Institute of Technology	Invited
9:21 AM	Performance of the InSight Spacecraft During Entry, Descent, and Landing at Mars	Mark Johnson	Lockheed Martin Space	Invited
9:33 AM	EDL Comm featuring MarCO CubeSat Performance	Sanford Krasner	Jet Propulsion Laboratory, California Institute of Technology	Invited
9:45 AM	Simulation of InSight Plume Induced Surface Cratering and Validation Through Imagery Based 3D Topology Reconstruction	Peter Liever	CFD Research Corp.	Invited
9:57 AM	Comparison of the Reconstructed Entry, Descent, and Landing Phase of the InSight and Phoenix Mars Landers	Aline Zimmer	Jet Propulsion Laboratory, California Institute of Technology	Invited
10:30 AM	Reconstruction Of Schiaparelli And Comars Flight Data	Aaron Brandis	AMA Inc at NASA Ames Research Center	
10:42 AM	Mars 2020 Entry, Descent, and Landing Update	Allen Chen	Jet Propulsion Laboratory, California Institute of Technology	
10:54 AM	Mars 2020 EDL System Performance at Jezero Crater	David Way	NASA Langley Research Center	
11:06 AM	The Mars 2020 Lander Vision System: Architecture And V&V Results	James Montgomery	Jet Propulsion Laboratory, California Institute of Technology/Caltech	
11:18 AM	Exomars 2020 Entry, Descent And Landing System	Steve Lingard	Vorticity Ltd	
11:30 AM	Systems Analysis Of An Inflatable Entry Concept For Human Mars Mission	Jamshid Samareh	NASA Langley Research Center	
11:42 AM	Application of Direct Force Control to Human-Scale Mars Entry, Descent, and Landing.	Rafael Lugo	NASA Langley Research Center	
2:00 PM	Mars Sample Return - A reference campaign architecture for joint ESA-NASA studies and early mission concepts	Sanjay Vijendran	European Space Agency	
2:12 PM	Overview And Status Of The Mars Sample Return Study 2026 Opportunity	Martin Greco	Jet Propulsion Laboratory, California Institute of Technology	
2:24 PM	Mars Sample Return Edl Flight Performance Challenges And Mitigation Strategies	Mark Ivanov	Jet Propulsion Laboratory, California Institute of Technology	

INSIGHT EDL OVERVIEW AND AS-FLOWN PERFORMANCE.

M. R. Grover, M. A. Johnson, R. W. Maddock, E. P. Bonfiglio, S. R. Francis, E. A. Leylek, M. A. Lobbia, E. Sklyanskiy, C. H. Zumwalt, Jet Propulsion Laboratory, California Institute of Technology, Lockheed Martin Space, NASA Langley Research Center

Brief Presenter Biography: Rob Grover is the In-Sight Entry, Descent & Landing Team Lead at the Jet Propulsion Laboratory. Previous assignments include the EDL Phase Lead for NASA’s Constellation Program. Previous mission work includes Mars Odyssey, Mars Exploration Rovers, and the Mars Scout lander Phoenix. He has degrees from Oregon State University and the University of Washington.

Introduction: After a nearly seven month cruise to Mars, InSight successfully executed entry, descent and landing (EDL) on November 26, 2018. The EDL system owes its success to missions that came before, and from a robust and thorough engineering undertaking from the initiation of the InSight project in 2012. This presentation will provide a brief overview of the InSight EDL system, and a high level look at the as-flown performance of the system, with comparison to pre-landing predictions. In the process, the presentation will provide a preview of topics that will be covered in more detail in other InSight presentations and posters.

A First: Landing During Dust Storm Season:

The InSight EDL system is essentially a built-to-print version of the EDL system that successfully landed the Phoenix spacecraft in 2008. A significant difference in assessing system performance is the challenge InSight faced landing during dust storm season. This challenge led to a few design enhancements, an operations process designed to succeed across a range of possible arrival atmosphere conditions, and a significant increase in the range of environments in which the system needed to successfully perform, quadrupling the performance assessment space relative to the Phoenix system. On landing day, after years of assessing EDL system performance across a wide spectrum of predicted environments, the EDL Team was cautiously confident the EDL system would perform successfully.

Landing Day Performance:

The InSight Navigation Team and Spacecraft Team succeeded in delivering the spacecraft to entry interface with an entry flight path angle (EFPA) of -12.046° , well within the required corridor of $\pm 0.21^\circ$ centered on -12.0° [1]. With EDL event communications supported by the Mars Reconnaissance Orbiter (MRO), MarCO spacecraft and UHF ground stations, the EDL event was tracked by the InSight team in real-time, with a one-way

light delay. As the landing event unfolded, real-time telemetry allowed the team to see that the vehicle experienced a peak g-level somewhat higher than predicted. After landing, HiRISE imaging allowed the team to pinpoint the vehicle landing location, showing the landing site 13.8 km uptrack and somewhat crosstrack from the predicted landing point [1]. Consistent with the higher g, uptrack landing, the vehicle traversed the space from entry interface to touchdown in 5 minutes and 48 seconds, about 41 seconds faster than predicted [1]. The trajectory flown also resulted in parachute deployment at a lower altitude and lower Mach than predicted. Preliminary assessments attribute landing uptrack after flying a higher g, short timeline trajectory to a combination of factors including an atmosphere on landing day lower

Table 1. Preliminary predicted vs as-flown performance.

EDL Metric	Units	Req’t	Predict	Flight
Max Entry Load	g’s	< 13	7.61	8.25
Chute Deploy Mach	Mach	< 2.3	1.70	1.48
		> 1.1		
Chute Deploy Dynamic Pressure	Pa	< 750	520	550
		> 300		
Chute Deploy Total AoA	deg	< 9.7	1.39	2.78
Heatshield Sep. Attitude Rate	deg/s	< 100	50	20
Heatshield Sep. Mach	Mach	< 0.8	0.54	0.44
Leg Deploy Attitude Rate	deg/s	< 100	43	27
MRD Init Altitude	m	< 10051	6402	5369
		> 2497		
Lander Sep. Attitude Rate	deg/s	< 60	26	8.5
Touchdown Vert. Velocity	m/s	< 3.4	2.43	2.32
		> 1.4		
Touchdown Horiz. Velocity	m/s	< 1.4	0.22	0.33

in density at altitude than predicted, and an entry vehicle that appears to have trimmed at non-zero angle of attack through peak dynamic pressure resulting in a lift down trajectory. This placed some characteristics of EDL sys-

tem performance near the bounds of landing day predictions, but within the capability of the landing system. Table 1 shows a summary of a preliminary comparison of as-flown performance versus pre-landing predictions. Even with some EDL performance near predicted bounds, the system performed robustly resulting in a successful touchdown on Mars.

References:

[1] Abilleira, et al. “2018 Mars InSight Trajectory Reconstruction and Performance from Launch through Landing,” AAS 19-204, 29th AAS/AIAA Space Flight Mechanics Meeting.

© 2018 Jet Propulsion Laboratory, California Institute of Technology. Government sponsorship acknowledged.

MARS INSIGHT TRAJECTORY AND ATMOSPHERE RECONSTRUCTION.

C. D. Karlgaard¹, J. A. Tynis¹, A. M. Korzun², M. Schoenenberger², M. R. Grover³, and D. M. Kass³

¹Analytical Mechanics Associates, Inc., Hampton, VA, 23666, USA, ²NASA Langley Research Center, Hampton, VA, 23681, USA, ³Jet Propulsion Laboratory, California Institute of Technology, Pasadena, CA, 91109, USA.

Brief Presenter Biography: Chris Karlgaard received B.S. degrees in Mathematics and Aerospace Engineering from the University of Maryland, and M.S. and Ph.D. degrees from Virginia Tech. He has been employed by AMA Inc. since 2001, and his areas of expertise include flight mechanics, estimation, and trajectory reconstruction.

Introduction: The InSight probe successfully landed on the surface of Mars at Elysium Planitia on November 26th, 2018. The entry, descent, and landing (EDL) system made use of existing flight spare hardware from the Mars Phoenix that landed in 2008. Specifically the system consists of a 70 degree sphere cone aeroshell with 2.65 m diameter, an 11.769 m diameter disk-gap-band parachute, and a system of 12 220 N terminal descent engines. The onboard guidance, navigation, and control sensors include a Honeywell Miniature Inertial Measurement Unit providing 200 Hz acceleration and angular rate measurements, and a radar altimeter measuring height above the ground during terminal descent at a rate of 10 Hz.

This poster describes the reconstruction of the InSight EDL trajectory and atmosphere.

Trajectory Reconstruction: The InSight inertial trajectory was reconstructed using a n iterative extended Kalman filter/smoothen, configured to process orbit determination initial conditions, landing site coordinates, and on-board measurements of accelerations and angular rates from the inertial measurement unit and altitude above ground level from the radar altimeter. The process uses a forward and backward pass through the data as a fixed-interval smoothing problem to reconstruct the trajectory of the vehicle through inertial space [1].

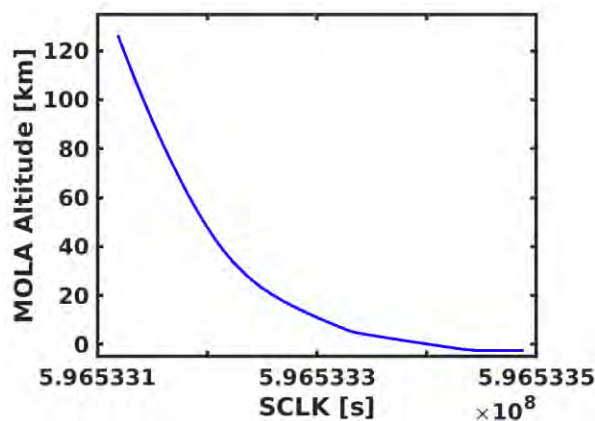


Figure 1 - Reconstructed Altitude

The reconstructed altitude time history is shown in Figure 1. The reconstruction was initialized at entry interface and terminated at landing.

Atmosphere Reconstruction: The as-flown atmosphere was reconstructed using the classical approach of solving for the density from the sensed accelerations and the nominal vehicle aerodynamic axial force coefficient. The process involves the solution to a system of nonlinear equations in which the angles of attack and sideslip are computed simultaneously with the density by using the ratios of the lateral to axial accelerations and ratios the corresponding force coefficients. Linear covariance analysis techniques are utilized to produce uncertainty estimates of the reconstructed quantities [2].

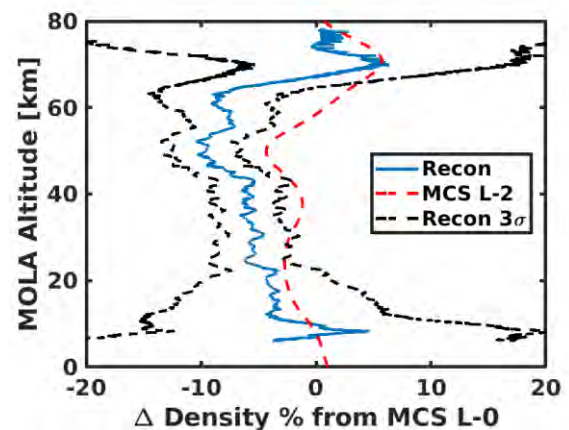


Figure 2 - Density Ratio Relative to Landing Day MCS

Preliminary results of the atmospheric reconstruction are shown in Figure 2, which shows the density ratio percent difference of the reconstruction relative to atmospheric profiles from the Mars Climate Sounder [3] (MCS) instrument on the day of landing, as well as the reconstruction uncertainties based on linear covariance analysis. Also shown for comparison is another profile from two days prior to landing.

References: [1] Karlgaard, C. D. et al (2013) *JSR*, 50, 641–661. [2] Kutty, P. (2014), M.S. Thesis, GA Tech. [3] McCleese, D. J. et al (2007), *JGR*, 112, E05S06.

INSIGHT APPROACH OPERATIONS DURING DUST-STORM SEASON

Eugene P. Bonfiglio, Devin Kipp, and Evgeniy Sklyanskiy, Jet Propulsion Laboratory¹, California Institute of Technology, 4800 Oak Grove Drive, Pasadena, CA 91109, ebonfiglio@jpl.nasa.gov; devin.kipp@gmail.com; evgeniy.sklyanskiy@jpl.nasa.gov

Brief Presenter Biography: Gene Bonfiglio received his Master's degree from Purdue University in 1999 studying orbital mechanics under Professor James Longuski. After graduating in the summer of 1999, Gene began working for the Jet Propulsion Laboratory as a member of the Outer Planets Solar Probe project and is currently a member of the EDL Guidance & Control Systems group in the Guidance & Control section at JPL. He has worked on many flight missions including the Spitzer Space Telescope, Phoenix Mars Lander, and Mars Curiosity Rover. Most recently he has worked as an EDL systems engineer for the InSight Mars Lander.

Abstract: The Interior Exploration Using Seismic Investigations, Geodesy, and Heat Transport (InSight) Mission launched on May 5th, 2018 and successfully executed entry, descent, and landing (EDL) on November 26, 2018, following a direct entry into the atmosphere from its interplanetary trajectory [1]. InSight was the first mission to land during Mars's dust storm season and was designed to successfully survive EDL during a global dust storm. Part of the design included ensuring the approach operations plan was robust to a large uncertainty in atmospheric dust levels on landing day.

The Navigation Plan for InSight used six trajectory correction maneuvers (TCMs) to target the desired entry state of Mars such that the targeted entry flight path angle (EFPA) results in the nominal trajectory landing at the desired latitude and longitude. The original navigation plan was to target an EFPA of exactly -12.0° .

In order for the TCMs to target the correct entry state, a simulation of the nominal EDL trajectory must be used in an iterative process with the maneuver targeting software. The EDL simulation uses an atmosphere model of the density, pressure, and temperature profiles as a function of altitude. Measurements of the atmosphere with a latency of less than 3-4 days from the Mars Reconnaissance Orbiter (MRO) were used to improve the accuracy of the atmosphere model in the EDL simulation [2]. During an Operational Readiness Test (ORT), the InSight team realized that updating the atmosphere model in the targeting software, while continuing to target an EFPA of exactly -12.0° , would change the nominal trajectory used in maneuver targeting. The designed TCM would compensate for that change in a way that had not been modeled previously, resulting in larger-than-expected maneuvers for the final TCM [3].

The relationship between the EDL team's operational plans for improving atmosphere knowledge and maneuver design is a very subtle and nuanced one and, as a result, the impact to TCM magnitude was not accounted for in the original estimate of propellant requirements. This dependency would be present for any unguided Mars lander planning to use low-latency atmosphere measurements to improve the atmosphere model in the EDL simulation. InSight is particularly sensitive to it because it landed at a time when the probability of dust storms is much higher, resulting in a larger variability in expected landing day atmosphere.

The team performed an investigation across multiple subsystems to understand the cause, mitigations, and impact to the system design of implementing the mitigations. The team ultimately determined that most of the maneuver impact which was unaccounted for could be eliminated by providing some tolerance to either the landing target or the nominal EFPA that is targeted with the final few maneuvers of the mission.

We will present the details of dependency between maneuver targeting and atmospheric updates as well as why the tolerance is required, consequences of ignoring the issue, and provide suggestions for how future Mars landing missions should accommodate this issue from the early design phase. The paper will discuss the as-flown EDL operations experience, the atmospheres that were actually measured by MRO near landing day and the impact the global dust storm of 2018 [4] could have had to the mission had it occurred closer to landing.

References:

- [1] Halsell, et al. "Orbiters, Navigation Performance of the 2018 InSight Mars Lander Mission," AAS 19-291, 29th AAS/AIAA Space Flight Mechanics Meeting
- [2] Tamppari, L. K., et al. (2010), Phoenix and MRO coordinated atmospheric measurements, J. Geophys. Res., 115, E00E17, [www.doi.org/10.1029/2009JE003415](https://doi.org/10.1029/2009JE003415)
- [3] Bonfiglio, et al. "Atmospheric impacts on EDL maneuver targeting for the InSight mission and unguided Mars landers," AAS 19-264, 29th AAS/AIAA Space Flight Mechanics Meeting
- [4] <https://mars.nasa.gov/weather/storm-watch-2018/>

Performance of the InSight Spacecraft During Entry, Descent, and Landing at Mars

M. A. Johnson¹, S. Francis¹, D. Eckart¹, C. Carson¹, B. White¹, B. Harper¹, ¹ Lockheed Martin Space, ² Jet Propulsion Laboratory

Brief Presenter Biography: Mark Johnson is a senior systems engineer and served as the InSight Entry, Descent, and Landing Mission Phase Lead at Lockheed Martin Space. Past roles have included Science Phase Lead for the MAVEN project, and Aerobraking Phase Lead for the MRO project. He has a B.S. in Engineering Mechanics and Astronautics from the University of Wisconsin – Madison, and a M.S. in Mechanical Engineering from The George Washington University.

Abstract: The Interior Exploration Using Seismic Investigations, Geodesy, and Heat Transport (InSight) mission to Mars made a successful entry, descent, and landing (EDL) onto the Martian surface on November 26, 2018. The spacecraft was designed to perform this task autonomously, with little interaction from the ground in the final few days before landing. The activities were driven by flight software and the EDL sequence, and was initiated 4 days prior to entry. The sequence was responsible for transitioning the spacecraft from its cruise configuration to one safe for hypersonic flight, to parachute flight, powered descent, and ultimately landed operations. Many of the transitions were determined by flight software (FSW) algorithms, tuned to trigger at the conditions deemed desirable by the EDL team.

Entry mass and propellant were tracked throughout cruise, with updates made available to the EDL team after every trajectory correction maneuver (TCM). Since later TCM's were expected to be small, a snapshot of the spacecraft mass after TCM-3 was used for tuning some of the EDL FSW. Uncertainties were maintained to cover the remaining variability in TCM performance and used in EDL simulations. Fuel usage in cruise was estimated to be 3.6 kg. Fuel usage in powered descent was calculated to be 40.4 kg based on telemetered thruster activity, resulting in a total of 44.0 kg, leaving 19.2 kg of usable propellant in the tanks at touchdown.

EDL simulations performed commensurate with each TCM opportunity generated updates to important GNC FSW parameters controlling the parachute deployment and radar activation. Although the trajectory timeline showed itself to be on the very short end, the triggers functioned correctly. Parachute deployment is estimated to have occurred at 527 Pa (target 525 Pa) and Mach 1.49. Radar activation occurred at approximately 5300 m AGL, subject to a minimum radar warmup duration, post-parachute deploy. This is safely inside the 2.4 – 10 km range constraint imposed on this event.

GNC performance was nominal, with no abnormal attitude behavior during the entry. As designed, no thrusters were fired during hypersonic flight. With a relatively low Mach at parachute deploy, angle-of-attack was seen to be growing, although the value at the mortar fire event was small. Peak attitude rates at parachute deploy, heatshield separation, and lander separation were low – well within design limits.

Lander separation occurred at 1235 m and 64.7 m/s. Terminal descent was typical, with max average duty cycle of 77% across the 12 descent engines. A backshell avoidance maneuver was executed to improve separation distance between the lander and backshell/parachute on the ground. Touchdown occurred at a vertical velocity of 2.4 m/s and a horizontal velocity of 0.3 m/s. Attitude was within 0.3 deg azimuth of desired. Landed tilt was determined to be 4.0 deg after post-landing gyrocompassing was performed.

Execution of deployments and separations were performed via pyrotechnic initiators. Examination of high rate IMU data indicated all events occurred on time. No recontact was observed during heatshield jettison or lander separation. The vehicle was observed to nearly bounce during the touchdown event – a brief period of zero-G motion was observed after first impact – however post-touchdown images do not suggest the lander footpads moved from their initial contact positions.

The spacecraft power performance was nominal, with a total depth of discharge of the batteries of approximately 15%. Minimum battery voltage was 32.45 V at touchdown.

Thermal behavior was also as predicted, with all temperatures remaining within expected ranges.

References: None

UHF Communications during InSight Entry, Descent and Landing featuring MarCO Performance.

Sanford Krasner¹, Kristoffer Bruvold, Andrew Klesh, Masatoshi Kobayashi, Jared Call, Ryan Lim, Kamal Oudrhiri, Norman Lay, Mark Wallace, David Morabito², Daniel Litton³

¹ Jet Propulsion Laboratory, California Institute of Technology, Pasadena, CA, skrasner@jpl.nasa.gov, ² Jet Propulsion Laboratory, California Institute of Technology, Pasadena, CA, ³ NASA Langley Research Center, Hampton, VA

Brief Presenter Biography: Sanford Krasner was the End-to-End Information Systems (EEIS) Engineer and the EDL Communications Lead for the InSight Mars Lander Project, and is now the EEIS Engineer for the NISAR project. He received a Bachelors (1975) and Masters degree (1976) in Aeronautics and Astronautics from the Massachusetts Institute of Technology (MIT). He has been at the Jet Propulsion Laboratory since 1979, specializing in End-to-End Information Systems Engineering for interplanetary missions.

Introduction: During Entry, Descent, and Landing (EDL), the InSight lander transmitted UHF (401 Mhz) telemetry and carrier “beacon” tones reporting the current state of the spacecraft. These data were displayed to operators in real-time. If the mission had failed, this data would have been used for failure analysis.

Five assets, two on Earth and three in the vicinity of Mars, received this EDL data and returned it to the operators at JPL and at Lockheed Martin Space in Littleton, CO: two CubeSats, named MarCO-A & -B, or Eva and Wall-E (from the movie Wall-E); the Mars Reconnaissance Orbiter (MRO); and Earth-bound radio telescopes at Green Bank, West Virginia and Effelsberg, Germany. All assets were able to observe the InSight signals from UHF turn-on prior to atmosphere entry through landing to UHF turn-off 5 minutes after landing.

MarCO: The MarCO CubeSats returned data to Earth in near-real-time, allowing ground operators to observe EDL in real-time (with a light-time delay of 8 minutes 7 seconds from Mars). They also relayed the first image from the InSight landing sight. These were the first CubeSats in deep space. They demonstrated cost effective access to deep space, and filled a critical gap in the plans for returning essential data from the InSight EDL.

The MarCOs have flown by Mars and gone silent. Contact may be re-established in late Summer 2019.

Radio Science: Radio science operators observing the data from the antennas at Green Bank, WV and Effelsberg were able to report the Doppler shift at chute deployment, and carrier “beacon” tones at touchdown.

Monte Carlo analysis: Monte Carlo simulations done to analyze landing safety were adapted to predict link margins for EDL data to each asset. These results

were used to optimize the MRO and MarCO trajectories for EDL data return. ^[1]

The Monte Carlo simulations were also used to design the MRO slew to track InSight, and planned acquisition of a HiRISE image of InSight descending on its parachute.

MRO HiRISE Parachute Image: Despite the unfavorable orbital geometry for imaging, an attempt was made to use MRO's HiRISE camera to capture an image of the parachute during descent. Unfortunately the resulting image was too over-saturated to be useful. Due to the steeper descent angle of the EDL trajectory than was predicted in the Monte Carlo analysis, the HiRISE image started 2 seconds after the parachute crossed the field of view.

Plasma Outage: All five assets were able to track EDL from UHF transmitter turn-on through landing to UHF turn-off. All assets experienced a degradation of signal around the time of peak aerodynamic heating, due to plasma formation around the spacecraft. An analysis of the received signal is being performed, along with aerothermal modelling, to characterize the plasma dynamics.

MRO Signal Degradation: The MRO Open-loop recording also showed a signal degradation prior to the plasma outage. The cause for this degradation is currently under investigation.

Summary: Overall, the InSight EDL communications design was shown to be robust. It brought EDL in real-time to the project mission operators, and to millions of people around the globe. The EDL communications experience demonstrated the usefulness of CubeSats in exploring interplanetary space, and provided a collection of data which would have been essential for failure analysis if necessary. It also provided an important contribution to the understanding of the Mars atmosphere, and to hypersonic entry.

References:

[1] MarkWallace, Daniel Litton, Tomas Martin-Mur, Sean Wagner, (2019) AAS/AIAA Flight Mechanics Meeting 19-291

Simulation of InSight Plume Induced Surface Cratering and Validation Through Imagery Based 3D Topology Reconstruction

M. Mehta¹, P. A. Liever², M. S. Manginelli¹, O. Thomas³, M. Gale² and D. Westra² ¹NASA Marshall Space Flight Center, Aerosciences Branch, Huntsville, AL (manish.mehta@nasa.gov), ²NASA Marshall Space Flight Center, Fluid Dynamics Branch, Huntsville, AL (peter.a.liever@nasa.gov), ³Cardinal Systems Inc., Flagler Beach, FL

Brief Presenter Biography: Dr. Manish Mehta is a subject matter expert in aerothermodynamics and rocket plume flow physics and has been working in this discipline for the last 15 years. Dr. Peter Liever is a Technical Fellow at CFD Research Corporation (CFDRC), with more than 30 years' experience in research, development and application of Computational Fluid Dynamics (CFD) modeling for launch vehicles, reentry vehicles, and planetary entry, descent and landing propulsion induced environments.

3D Imagery Topology Reconstruction: The quantification of the particulate erosion that occurs as a result of a rocket exhaust plume impinging on soil during extraterrestrial landings is critical for future robotic and human lander mission design. The aerodynamic environment that results from the reflected plumes results in dust lifting, site alteration and saltation, all of which create a potentially erosive and contaminant heavy environment for the lander vehicle and any surrounding structures [1]. The plume effects on the lander can result in high plume heating and aerodynamic destabilization [2]. In this work we seek to quantify plume soil interaction and its resultant soil erosion caused by the InSight Lander descent engines by performing three-dimensional digital terrain and elevation mapping of the InSight landing site. Aerial triangulation using Structures From Motion photogrammetric imaging techniques were used in developing a 3D model of the site-alteration. Images captured by the Instrument Deployment Camera (Figure 1) were used in this analysis. This data in conjunction with the high-rate telemetry data and preliminary soil properties can develop an average erosion rates which can be used as an important metric in comparing to computational models.

Computational Simulation: Computational simulations of the plume induced surface erosion and cratering are performed with the Gas-Granular Flow Solver (GGFS). GGFS solves the two-phase gas-particle interaction by modeling the surface regolith particles as an Eulerian fluid with detailed DEM-derived particle phase kinetics constitutive relations. GGFS is equipped to model the key processes involved in particle-particle and gas-particle interactions covering the range from tightly packed granular material (up to the packing limit) in the surface layer up to the dilute regime in the form of dust clouds. Models for mixtures of polydisperse, multi-material and irregularly-shaped non-spherical particles are implemented using DEM-derived

constitutive relations for inelastic collisions, kinetic interactions, inter-particle friction in densely packed particulates, interaction with gas-phase via drag forces and other required quantities. An integrated multi-physics computational simulation framework featuring the GGFS has been implemented by the MSFC Fluid Dynamics Branch for plume-surface interaction environment predictions for NASA program applications. The framework integrates the Loci/CHEM Computational Fluid Dynamics (CFD) simulation program, the Gas-Granular Flow Solver (GGFS), and the Debris Transport Analysis (DTA) toolkit to achieve end-to-end spacecraft landing plume-surface interaction effects predictions on vehicle dynamics, plume induced surface cratering, and regolith particle debris transport towards the vehicle and surrounding assets. Simulations of the InSight landing plume-surface interaction processes are performed with best available pre-landing surface material composition and will be update with post-landing information. Validation of the GGFS predictive capabilities is performed by comparison against post-landing imagery and the imagery-based 3D topology reconstruction.

References: [1] Mehta M. et al. (2011) *Icarus*, 211, pp. 172–194. [2] Mehta, M. et al. (2015) *AIAA Journal*, 51, pp. 2800-2818.



Figure 1. IDC Image of Site-Alteration

Comparison of the Reconstructed Entry, Descent, and Landing Phase of the InSight and Phoenix Mars Landers

A. K. Zimmer¹, E. D. Skulsky¹, and B. P. Harper¹, ¹Jet Propulsion Laboratory, California Institute of Technology, 4800 Oak Grove Drive, Pasadena, CA 91109.

Biography: Aline Zimmer is a systems engineer for Mars Entry, Descent, and Landing for InSight as well as Europa Deorbit, Descent, and Landing for the Europa Lander Concept. Since InSight’s successful landing in November 2018, Aline joined the Europa Clipper team as phase lead for the science tour phase. Aline received her M.Sc. in Aerospace Engineering from the Georgia Institute of Technology and her Ph.D. in Aerospace Engineering from the University of Stuttgart in Germany.

Abstract: The Interior Exploration Using Seismic Investigations, Geodesy, and Heat Transport (InSight) Mission successfully executed its Entry, Descent, and Landing (EDL) phase on November 26, 2018. The InSight spacecraft is based on the design of NASA’s Phoenix Mars Lander, with updates to accommodate InSight’s unique science payload and new mission requirements. The engineering for InSight’s EDL system in particular draws significantly on the technology of Phoenix and was designed under the guiding principle to stay within the predicted flight envelope for Phoenix. This presentation will shed some light on similarities and differences between the EDL designs of InSight and Phoenix and their respective predicts and reconstructed flight performance.

Some of the differences between the two spacecraft and EDL systems were due to differences in landing sites and expected atmospheric conditions at arrival: While Phoenix landed near Mars’ North Pole, InSight landed near the equator and at a higher elevation than Phoenix, leaving less atmosphere to use for deceleration. In addition, InSight was the first mission to land during Mars’ dust storm season. It was designed to be robust to a wide range of atmospheric dust levels and

survive landing even during a global dust storm. As a result, InSight’s heat shield was slightly thicker than the one used for the Phoenix mission to withstand being sandblasted by dust in the atmosphere during EDL. Furthermore, the suspension lines of InSight’s parachute were stronger to survive higher inflation loads resulting from InSight’s higher entry mass, higher expected speed at parachute deployment, as well as the possibly severe atmospheric conditions. These additional challenges compared to Phoenix also triggered changes to be made to InSight’s EDL timeline. An explicitly stated goal for InSight’s EDL timeline was to effectively decouple terminal descent from the earlier subphases of EDL, more so than was already the case for Phoenix.

As an example for differences in reconstructed performance, preliminary results for InSight seem to indicate that a major difference between the reconstructed performance of InSight and Phoenix is the total duration of EDL. The as-flown total duration of EDL for InSight appears to be distinctly on the short end of the predicted distribution; further analysis is required to fully understand the causes. Table 1 provides a comparison between predicted performance metrics as well as as-flown actuals, both for InSight and Phoenix [1,2]. The full reconstruction results will be available for this presentation.

References:

- [1] Grover, et al. “InSight EDL Overview and As-Flown Performance,” IPPW 2019.
- [2] Abilleira, et al. “Entry, Descent, and Landing Performance of the Mars Phoenix Lander,” Journal of Spacecraft and Rockets, Vol. 48, No. 5, September–October 2011.

Table 1. Predicted and as-flown performance metrics for InSight and Phoenix EDL. As-flown numbers for InSight are preliminary

ELD Metric	Units	Requirement	InSight		Phoenix		
			Predict (Mean)	Flight	Requirement	Predict (Mean)	Flight
Max Entry Load	Earth g	< 13	7.61	8.25	< 13	9.3	8.5
Chute Deploy Mach	Mach	< 2.3	1.7	1.48	< 2.13	1.64	1.7
		> 1.1			> 1.1		
Chute Deploy Dynamic Pressure	Pa	< 750	520	550	< 560	491	489
		> 300			> 300		
Chute Deploy Total AoA	deg	< 9.7	1.39	2.78	< 10.0	2.3	4.73
Heatshield Separation Attitude Rate	deg/s	< 100	50	20	< 100	15.5	16.5
Heatshield Separation Mach	Mach	< 0.8	0.54	0.44	< 0.8	0.51	N/A
Leg Deploy Attitude Rate	deg/s	< 100	43	27	< 100	12.6	5.8

Lander Separation Attitude Rate	deg/s	< 60	26	8.5	< 100	11.8	4.8
Touchdown Vertical Velocity	m/s	< 3.4	2.43	2.32	< 3.4	2.1	2.38
		>1.4			>1.0		
Touchdown Horizontal Velocity	m/s	< 1.4	0.22	0.33	< 1.4	0.5	0.06

RECONSTRUCTION OF SCHIAPARELLI AND COMARS FLIGHT DATA

A. Brandis¹, T. White², D. Saunders¹, J. Hill¹, and C. Johnston³, ¹AMA, Inc. at NASA Ames Research Center, Moffett Field, 94035, CA, USA: aaron.m.brandis@nasa.gov. ²NASA Ames Research Center, Moffett Field, 94035, CA, USA. ³NASA Langley Research Center, Hampton, 23666, VA, USA

Brief Presenter Biography: Aaron Brandis received his undergraduate Bachelor of Engineering (Mechanical and Space) in 2003 and his PhD from the University of Queensland and Ecole Central Paris, France in 2009. Dr Brandis is a senior research scientist employed by AMA, Inc. in the Aerothermodynamics branch at NASA Ames. He is currently the deputy PI for the Entry Systems Modeling project and PM/PI for NEQAIR, Co-PI for the Electric Arc Shock Tube, Aerothermal and ESI lead for Dragonfly.

Abstract: ESA recently flew an entry, descent, and landing demonstrator module called Schiaparelli that entered the atmosphere of Mars on the 19th of October, 2016. The instrumentation suite included heatshield and backshell pressure transducers and thermocouples (known as AMELIA) and backshell radiation and direct heatflux-sensing sensors (known as COMARS and ICOTOM). Due to the failed landing of Schiaparelli, only a subset of the flight data was transmitted before and after plasma black-out. The goal of this paper is to present comparisons of the flight data with calculations from NASA simulation tools, DPLR/NEQAIR and LAURA/HARA. DPLR and LAURA are used to calculate the flowfield around the vehicle and surface properties, such as pressure and convective heating. The flowfield data are passed to NEQAIR and HARA to calculate the radiative heat flux. Comparisons will be made to the COMARS total heat flux, radiative heat flux and pressure measurements. Results will also be shown against the reconstructed heat flux which was calculated from an inverse analysis of the AMELIA thermocouple data performed by Astrium. Preliminary calculations are presented in this abstract. The aerodynamics of the vehicle and certain as yet unexplained features of the inverse analysis and forebody data will be investigated.

Introduction: Researchers from the European Space Agency's ExoMars mission recently published flight data from the Schiaparelli descent module's entry into the Martian atmosphere [1,2]. The data obtained during Schiaparelli's descent are invaluable for further validating models used to design thermal protection systems for future Mars missions and can be used to complement the data MEDLI measured during the Mars Science Laboratory entry in 2012. In order to assess the performance of the heat shield, characterize the atmosphere and better understand the trajectory, the Atmospheric Mars Entry and Landing Investigations and Analysis (AMELIA) [3] package led out of the Università

degli Studi di Padova in Italy was integrated with Schiaparelli. Due to backshell environments having large uncertainties with high margins used during spacecraft design, up to 3x [4], DLR, the German Aerospace Center, developed the Combined Aerothermal and Radiation Sensor package, called COMARS+, to measure the total heat flux, pressure and radiative loads at different backshell positions on Schiaparelli [1]. COMARS+ consisted of three combined aerothermal sensors, one broadband radiometer sensor and an electronics box. The failed landing of Schiaparelli meant it was not possible to retrieve the complete data package. However, communications between the Schiaparelli module and the orbiter during entry allowed data to be transmitted at ten trajectory points.

Preliminary Results: Figure 1 shows the locations of the various COMARS sensors. More detail will be provided in the final paper; for the abstract, preliminary results are presented in Figure 2. Figure 2 shows a comparison of the total heat flux calculated by DPLR and NEQAIR with the COMARS 1 flight data and inverse analysis as performed by Pinaud et al. [3]. The preliminary unmarginined simulation results shown in Figure 2 generally over-predict the flight data and show trends similar to the inverse analysis. From these initial comparisons, it is clear that valuable flight data were gathered by both COMARS and AMELIA, even though some of the data were lost to radio black-out.

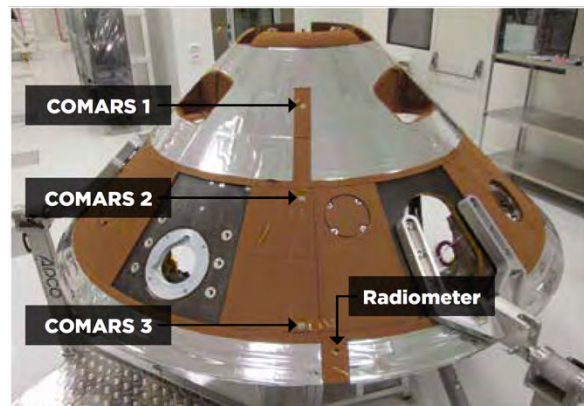


Figure 1. Location of COMARS sensors [1]

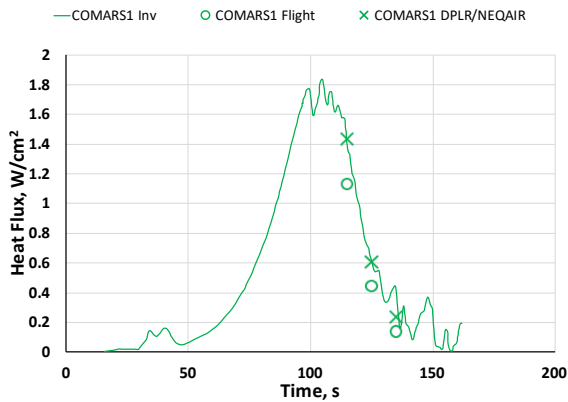


Figure 2. Preliminary comparison of simulations of total heat flux for COMARS 1 including the inverse analysis from [3].

References:

1. A. Gülhan. et al. “Aerothermal Measurements from the ExoMars Schiaparelli Capsule Entry,” Journal of Spacecraft and Rockets, 2018.
2. A. Gülhan, “Post Flight Analysis of the COMARS+ Data and Backcover Heating of the ExoMars Schiaparelli Capsule,” IPPW 2018.
3. G. Pinaud, “ExoMars 2016: A preliminary post-flight study of the entry module heat shield interactions with the Martian atmosphere,” IPPW 2018.
4. M. Wright et al., “Sizing and Margins Assessment of Mars Science Laboratory Aeroshell Thermal Protection System,” Journal of Spacecraft and Rockets, Vol. 51, 2014.

MARS 2020 ENTRY, DESCENT, AND LANDING UPDATE. Allen Chen, Paul Brugarolas, Richard Otero, Aaron Stehura, Erisa Stilley, Jet Propulsion Laboratory, California Institute of Technology (4800 Oak Grove Dr., Pasadena, CA, 91109, allen.chen@jpl.nasa.gov)

Brief Presenter Biography: Allen Chen is the Entry, Descent, and Landing (EDL) Phase Lead for the Mars 2020 project. Prior to that, he spent a really long time working on the Mars Science Laboratory EDL team. He holds S.B. and S.M. degrees in Aeronautics and Astronautics from the Massachusetts Institute of Technology and a M.B.A. from the University of California, Los Angeles.

Abstract: Building upon the success of Curiosity's landing and surface mission, the Mars 2020 project is a flagship-class science mission intended to address key questions about the potential for life on Mars and collect samples for possible return to Earth by a future mission [1]. Mars 2020 will also demonstrate technologies needed to enable future human expeditions to Mars. Utilizing the groundbreaking entry, descent, and landing (EDL) architecture pioneered by Mars Science Laboratory (MSL) [2], Mars 2020 will launch in July 2020 and land on Mars in February 2021.

The mission takes advantage of the favorable 2020 launch/arrival opportunity; this enables the delivery of a larger, heavier, and more capable rover to wider variety of potential landing sites. While Mars 2020 inherits much of its EDL architecture, software, and hardware from MSL, a number of changes have been made to correct deficiencies, improve performance, and increase the overall robustness of the system [3]. These include significant additions such as the addition of Range Trigger, the introduction of Terrain Relative Navigation (TRN), and the use of a strengthened supersonic parachute, tested via the Advanced Supersonic Parachute Inflation Research Experiment (ASPIRE) program.

Over the past year, the team has achieved a number of major accomplishments and dealt with unexpected challenges. The team performed a detailed safety assessment of four final landing site candidates. The safety assessment informed the ultimate selection of Jezero Crater as Mars 2020's landing site. The ASPIRE program successfully executed supersonic tests of Mars 2020's strengthened parachute at relevant conditions.

The unexpected failure of a MSL residual heatshield during static test has prompted the redesign, fabrication, and testing of a new heatshield. The EDL team also discovered an unexpected interaction between parachute hardware and the Descent Stage inertial measurement

unit (DIMU) during parachute deploy on MSL; measures have been taken on Mars 2020 to mitigate the risks identified. Despite these challenges, almost all major elements of the EDL system have been tested, delivered, and integrated into the spacecraft, including the TRN Lander Vision System (LVS) hardware and the landing radar. Additionally, the EDL flight software testing campaign is nearing completion, almost a year prior to launch, with the overall verification and validation program on track to be completed on schedule prior to launch.

This paper presents an update on the development and major milestones of the Mars 2020 EDL system, and a brief look at what remains ahead.

References:

- [1] Mustard, J., et al. (2013) "Report of the Mars 2020 Science Definition Team," Tech. rep., *Mars Exploration Program Analysis Group (MEPAG)*. [2] Steltzner, A. (2013) "*Mars Science Laboratory Entry, Descent, and Landing System Overview*," AAS 13-236. [3] A. Nellesen, et al., "*Mars 2020 Entry, Descent, and Landing System Overview*," (2019) *IEEE Aerospace Conference*.

Mars 2020 EDL System Performance at Jezero Crater.

David W. Way, NASA Langley Research Center

Brief Presenter Biography: David Way has served as an aerospace engineer at the NASA Langley Research Center in Hampton, VA, since 2001. He received his B.S in Aerospace Engineering from the United States Naval Academy and his M.S. and Ph.D. in Aerospace Engineering from the Georgia Institute of Technology. He is currently the lead engineer for Mars 2020's primary Entry, Descent, and Landing (EDL) System Performance Simulation.

Introduction: The Mars 2020 rover is NASA's next flagship mission, set to explore Mars in search of scientific evidence of past microbial life. Importantly, the rover will also, for the first time, have the ability to collect and cache rock and soil samples for retrieval and return to laboratories here on Earth.

A key step in the development of the Mars 2020 mission is the selection of a suitable landing site with the largest likelihood of meeting scientific goals. This decision is a complex and critical one that requires close interaction between the scientific and engineering communities. The chosen landing site must be both scientifically interesting --- providing the project with the greatest possible chance of gathering credible and defensible scientific evidence --- and also safe enough to attempt a landing in the first place. Thus, arguably one of the most important undertakings of the EDL (EDL) team, is to effectively enumerate, quantify, and communicate the landing risks to all of the stakeholders.

The culmination of this effort is the Landing Site Safety Assessment, which is a review commissioned by the project, presided over by the EDL SRB, and attended by management and science stakeholders, in which the EDL team communicates their assessment of the associated landing risks and the statistical probability of a successful landing at each of the final candidate landing sites. This assessment relies heavily on computer simulations of the EDL sequence.

Over the course of several Landing Site Workshops held over four years, approximately thirty candidate landing sites were evaluated for scientific interest and the potential to meet scientific objectives. These sites were ranked by the science community, with the highest ranked sites progressing to the next round. Through this process, three top candidates emerged: JEZ, NES, and CLH. These three sites, along with a fourth site located approximately half-way between JEZ and NES, were evaluated in detail by the EDL team for overall EDL performance and landing safety.

On November 19, 2018, NASA announced that Jezero Crater had been selected as the landing site for the Mars 2020 rover. This announcement marked the

end of a four-year process to choose where the rover will land on February 18, 2021, when it arrives at Mars.

In this paper, we will summarize the end-to-end EDL simulation results used in support of this assessment.

References:

- [1] A. Nelessen, C. Sackier, I. Clark, P. Brugarolas, G. Villar, A. Chen, A. Stehura, R. Otero, E. Stilley, D. Way, K. Edquist, S. Mohan, Cj Giovingo, and M. Lefland, "Mars 2020 Entry, Descent, and Landing System Overview," IEEE Aerospace Conference, Big Sky, MT, Mar 2019.

THE MARS 2020 LANDER VISION SYSTEM: ARCHITECTURE AND V&V RESULTS.

J. Montgomery,¹ A. Johnson¹, H. Ansari¹, C. Bergh¹, J. Chang¹, Y. Cheng¹, S. Mohan¹, S. Schroeder¹, A. Stehura¹, N. Trawny¹, N. Villaume¹, J. Zheng¹, ¹Jet Propulsion Laboratory, California Institute of Technology, 4800 Oak Grove Drive, Pasadena, CA 91109 (james.f.montgomery@jpl.nasa.gov).

Brief Presenter Biography: Dr. Jim Montgomery received his B.S. in Computer Science from the University of Michigan in 1986 and his Ph.D. in Computer Science/Autonomous Robotics from the University of Southern California in 1999. He joined JPL in 2000, working on a variety of autonomous robotic technology development tasks until 2006 when he joined the Mars Science Laboratory (MSL) team. He is currently the Mars 2020 Lander Vision System Systems Engineer, a role he has held since 2015.

Introduction: Human and robotic planetary lander missions require accurate surface relative position knowledge to land near science targets or next to pre-deployed assets. These accurate position estimates can be obtained in real-time by matching sensor data collected during descent to an on-board map. The Lander Vision System (LVS) being developed for the Mars 2020 mission generates landmark matches in descent imagery and combines these with inertial data to estimate vehicle position, velocity and attitude. The Mars 2020 Entry, Descent and Landing (EDL) system will use this position estimate to repurpose its heritage powered descent divert to avoid 100m scale hazards identified in the landing ellipse map prior to landing. This enables the selection of landing sites that have scientifically interesting terrain relief and were not selectable in the original implementation of MSL EDL [1] [2]. Mars scientists see great value in adding this capability to the Mars 2020 lander mission [3].

LVS technology development at JPL has been ongoing for more than a decade. A real-time flight-like prototype was flown in a helicopter field test conducted in February and March 2014 [4]. Position knowledge errors of less than 40m were demonstrated over a wide variety of terrains, illumination conditions, and attitude dynamics. The LVS prototype was reengineered into a smaller self-contained package and integrated with a terrestrial vertical take off and landing rocket to demonstrate a closed-loop Mars EDL scenario [5]. Follow-on work focused on LVS algorithm improvements and an analysis, using MSL flight data and other data sources, that demonstrated LVS could tolerate large changes in vertical motion [6]. The Mars 2020 flight design of the LVS occurred in parallel with this field testing and performance analysis and culminated in a preliminary design completed in November 2015. The LVS technology was baselined on the Mars 2020 mission in January 2016. Detailed hardware and software development, integration and test has been on-going since this time.

Architecture and V&V Results: This presentation describes the flight LVS architecture baselined for Mars 2020. It touches on all aspects of the architecture including the Vision Compute Element (VCE) processor, the LVS Camera (LCAM), the Map Relative Localization algorithms and firmware, the map used for landmark matching, and the flight software (VCEFSW). The verification and validation (V&V) relationships and flow from lower-level LVS components to the fully integrated LVS are described. The test venues, both simulation and hardware-in-the-loop (HWIL) testbeds are presented. The V&V activities performed on those venues, including those with an Engineering Model (EM) LVS on the HWIL testbed, are discussed and results presented.

References: [1] Golombek M., et al. (2018) Fourth Landing Site Workshop for the 2020 Mars Rover Mission, URL https://marsnext.jpl.nasa.gov/workshops/wkshp_2018_10.cfm. [2] “NASA Announces Landing Site for Mars 2020 Rover”, (2018) URL <https://mars.nasa.gov/news/8387/nasa-announces-landing-site-for-mars-2020-rover/>. [3] Mustard, J.F., et al., (2014) *Report of the Mars 2020 Science Definition Team* URL: http://mepag.jpl.nasa.gov/reports/MEP/Mars_2020_SDT_Report_Final.pdf. [4] Johnson, A. et al. (2015) “Real-Time Terrain Relative Navigation Test Results from a Relevant Environment for Mars Landing,” *AIAA Guidance, Navigation, and Control Conference*. [5] Trawny N. et al., (2016) “Flight testing of terrain-relative navigation and large-divert guidance on a VTVL rocket,” *AIAA Space Conference*. [6] Johnson A. (2016) “Design and Analysis of Map Relative Localization for Access to Hazardous Landing Sites on Mars,” *AIAA Guidance, Navigation, and Control Conference*.

EXOMARS 2020 ENTRY, DESCENT AND LANDING SYSTEM

Dr J.S. Lingard¹, J.C. Underwood² and S. Langlois³, ¹Technical Director, Vorticity Ltd, Monument Park, Chalgrove, OX44 7RW, United Kingdom, Steve.Lingard@vorticity-systems.com, ²Principal Engineer, Vorticity Ltd, John.Underwood@vorticity-systems.com, ³European Space Agency.

Brief Presenter Biography: John Underwood is the Principal Engineer at Vorticity Ltd. He has over 30 year's experience of delivering parachute systems for planetary landers including the NASA / ESA Huygens mission, Schiaparelli and ExoMars 2020. He regularly manages wind tunnel and free-flight tests of parachute systems.

Introduction: The ExoMars 2020 mission is the latest in a series of European missions designed to explore the environment of Mars and search for signs of exobiology.

The mission is a joint venture between the European Space Agency and Roscosmos. ESA provides the rover and elements of the EDLS while Roscosmos provides the surface platform, entry system and launcher.

The scientific payload includes a surface platform which is designed to characterize the surface environment at the landing site for a period of one Earth year and the first European Mars rover which carries a package of instruments which will characterize the physical and chemical composition of the surface and sub-surface to a depth of 1 m.

The 2000 kg entry module utilizes a conventional non-lifting entry system followed by a sequence of four parachutes and powered descent in order to land safely at the Oxia Planum landing site.

The parachute system has been designed to decelerate the entry module from Mach 2.1, the maximum for reliable parachute operation, to a suitable velocity for the Reaction Control System (RCS) to complete the landing sequence. The combination of high landing mass and low density atmosphere requires the parachute system to be optimised both in terms of performance and mass.

Mission Goals: The objective of the mission is to characterize a site which has a high potential for finding well-preserved organic material, particularly from the early history of the planet.

The rover carries a chemical analysis package and a drill which is able to collect samples from depths of up to two meters. It is expected to cover a distance of several kilometers during its mission.

The surface platform carries an instrument package to characterize the immediate surroundings of the landing point, the temperature and seismicity of the surface below and the properties of the atmosphere above.

Probe Configuration: The lander and surface platform are packaged together within a protective aeroshell. The 200 kg parachute system is mounted in the rear half of the aeroshell which remains attached to the rover until just before the start of the powered descent phase. The front shield is released once the probe has decelerated to subsonic velocity.

Parachute System: The parachute system consists of two main parachutes, each deployed by its own pilot chute. The first pilot chute, a 2.4 m Disk-Gap-Band (DGB), is deployed at Mach 2.1 using a pyrotechnic mortar (Figure 1 - 1) which ejects it through a breakout patch in the rear aeroshell. Two seconds after deployment, the lid of the parachute container is released

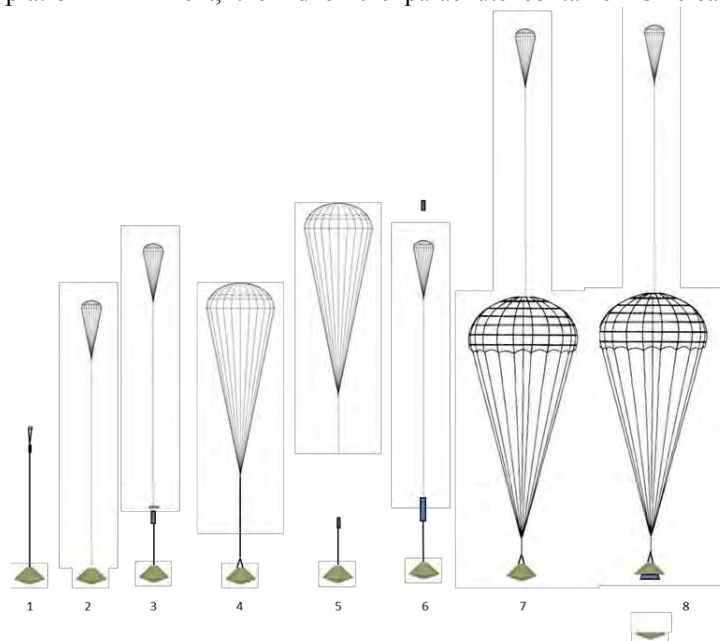


Figure 1: Parachute sequence

from the Entry and Descent Module (EDM) using three release nuts. The pilot chute pulls the lid away from the EDM (3), thus deploying the first main parachute, a 15 m DGB.

Over the next 20 seconds the EDM decelerates to less than Mach 0.7. At this point the first main parachute is released and the second pilot chute, a 4.8 m DGB, is deployed using a second mortar (5). The sec-

ond main parachute, a 35 m ring slot, is deployed immediately on inflation of the pilot chute (6). The main parachute is the largest ever deployed on a planetary mission.

Following inflation of the second main parachute, the front aeroshell is released (8), the landing legs deploy and the radar altimeter determines the optimal altitude for release of the rear aeroshell and activation of the RCS. The airspeed at the time of RCS activation is approximately 40 m/s.

System design: A parachute system with two main parachutes was chosen in order to allow optimization of each for its operation environment. The initial parachute flight takes place in the supersonic regime at a relatively high dynamic pressure of 1 kPa. The parachute system must also provide sufficient drag during terminal descent to achieve the desired terminal velocity prior to the start of powered descent. A single parachute solution would require a parachute which is large enough to achieve the terminal velocity whilst being robust enough to withstand inflation and flight at high dynamic pressure. A two parachute system allows a small, robust parachute to be used for the supersonic deceleration and a large, lower stressed parachute to achieve the terminal velocity.

A mortar-deployed pilot chute was chosen to deploy the first main parachute since direct mortar deployment would require a heavy mortar and would induce unacceptable reaction loads into the EDM.

A mortar-deployed pilot chute was also chosen to deploy the second parachute. The alternative of using the first main parachute to deploy the second directly was not feasible since it would result in too-high an extraction velocity which could damage the deploying parachute. A second advantage of using a pilot chute is that by leaving it attached to the deployed parachute it can control the rebound of the parachute during the initial inflation stage.

System qualification: The parachute system will be qualified using a sequence of tests starting with elementary tests of parachute materials and pyrotechnic gas generators and culminating with three drop tests of the parachute system.

The first drop test took place in March 2018. This was a low altitude test of the second main parachute. The objectives were to demonstrate the correct sequential deployment of the parachute when extracted by the pilot chute and the ability of the pilot chute to prevent rebound of the parachute during its initial inflation. The test used a 500 kg test vehicle which was lifted to an altitude of 1.2 km using a helicopter. On release from the helicopter the pilot chute was deployed by static line and was used to stabilize the probe as it accelerated to the deployment velocity. At this point the

pilot chute was released and deployed the test parachute. The parachute deployment and inflation were both nominal.

It was not possible to design a test on Earth which could reproduce the flight loads on both main parachutes within the same flight. Thus two high altitude tests are planned.

The second drop test is a high altitude full sequence drop test. This will be accomplished during May / June 2019, releasing from a high altitude balloon at an altitude of 28 km. This test will qualify the first main parachute at loads which are greater than the predicted flight loads and will demonstrate the full sequence using all mortars, parachutes and release mechanisms.

The final drop test, scheduled for August 2019 is a second high altitude test. In this case a heavier vehicle will be used with only the second main parachute and its pilot chute. This test will qualify the second parachute at flight-representative loads.



Figure 2: Low altitude drop test

SYSTEMS ANALYSIS OF AN INFLATABLE ENTRY CONCEPT FOR HUMAN MARS MISSION

J. A. Samareh, NASA Langley Research Center (jamshid.a.samareh@nasa.gov)

Introduction: Human Mars entry systems are complex with many critical design parameters and multiple criteria for concept assessment. The present work is built upon a previous Mars systems analysis effort for an entry, descent, and landing (EDL) concept [1]. The approach is based on a data-driven and physics-based parametric systems analysis and tradespace exploration for a human Mars entry system using hypersonic inflatable aerodynamic decelerator (HIAD) technology. The baseline system includes elements for Mars aerocapture (AC) and EDL segments of the mission. The use of a parametric mass model has enabled a systems analysis, vehicle sizing, and sensitivity analysis of the resulting design space. Results from these analyses will be presented and discussed at the workshop for the baseline entry system.

Concept of Operation (ConOps): The baseline ConOps starts at Mars arrival with a relative velocity of 6.2 km/s in a polar inclination. The entry system performs an AC maneuver into a Mars one-solar day (1-Sol) parking orbit, and then the AC HIAD is jettisoned. The rest of the vehicle may stay in orbit for up to one year. The EDL sequence starts with a deorbit burn at the apoapsis of the parking orbit. After hypersonic entry with the EDL HIAD, the entry system uses a supersonic retropropulsion maneuver to slow the vehicle for descent and landing. The vehicle is assumed to maintain a constant velocity of 2.5 m/s for 5 seconds prior to landing at 0 km relative to the Mars Orbiter Laser Altimeter (MOLA) ellipsoid.

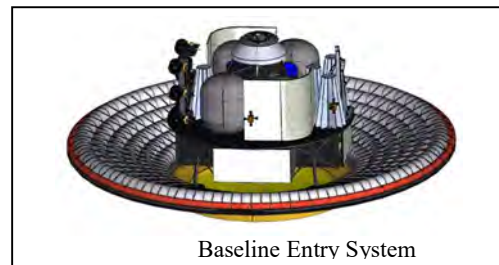
Systems Analysis and Design Space Evaluation: Systems analysis and evaluation of the design space provide a holistic view of systems and concepts. Systems analysis enables decision makers to gain an improved understanding of various entry concepts and their limitations based on quantitative simulation data. The traditional systems analysis process may take from several weeks to several years. The process has been significantly improved by automating and streamlining the analysis process, and these improvements have reduced the errors resulting from manual data transfer among discipline experts. This improved process has reduced time required for parametric studies, sensitivity analyses, and Monte Carlo analyses of the design space.

Entry System Models: The system includes a Mars Ascent Vehicle (MAV), Mars Descent Module (MDM), and two HIADs. The modeling approach follows parametric modeling presented in ref. [2].

The MDM includes a primary structure, tanks, engines, and radiators. The primary structure is represented as an aluminum-lithium (Al-Li) cruciform design

similar to the structural design of the Apollo Lunar Module. The cruciform planform layout results in four outer bays, with volume in the corners between outer bays to package landing gear. The central bay is reserved for packaging the MAV and the recessed MAV engines. Two of the outer bays package main propellant tanks, with one LOX and one CH₄ tank in each bay. The two remaining outer bays each package four rocket engine systems and associated support structure.

Each HIAD consists of an inflatable structure, flexible thermal protection system, gas, and gas generators. The HIAD design used in this study is a stacked-toroid concept with pairing loop straps and radial/chevron straps.



Baseline Entry System

Results: The baseline system was sized to land a 20-t payload on the Mars surface. It is assumed the vehicle arrives at 6.2 km/s relative velocity at 90° inclination and is captured to a 1-Sol parking orbit.

The baseline design includes many assumptions such as margins, arrival state, ConOps options, parking orbit, physical dimensions, and technology concepts. The impact of these parameters are characterized through systems-level sensitivity analyses. It is important to quantify systems-level sensitivities to capture the global impact—not at a component level—but at the systems level. The systems-level sensitivities expose major design drivers and importance of each assumption for a given design.

Evaluation of the design space examined a wide range of systems parameters and compared several possible design options. Studies were performed for the following input parameters: payload mass, AC/EDL ballistic coefficient, lander thrust to weight ratio (T/W) (surrogate for the maximum EDL g's), engine specific impulse (Isp), parking orbit, and inclination.

References:

[1] Samareh, J. A. and Komar, D. R., "Parametric Mass Modeling for Mars Entry, Descent and Landing System Analysis Study," AIAA-2011-1038.

[2] Samareh, A., A Multidisciplinary Tool for Systems Analysis of Planetary Entry, Descent, and Landing (SAPE), NASA-TM-2009-215950.

APPLICATION OF DIRECT FORCE CONTROL TO HUMAN-SCALE MARS ENTRY, DESCENT, AND LANDING.

R. A. Lugo¹, R. W. Powell², E. M. Queen¹, J. S. Green¹, A. M. Korzun¹, and A. D. Cianciolo¹, ¹ NASA Langley Research Center, Hampton, VA 23681, rafael.a.lugo@nasa.gov, ²Analytical Mechanics Associates, 21 Enterprise Pkwy., Suite 300, Hampton, VA 23666, richard.w.powell@nasa.gov.

Brief Presenter Biography: Rafael Lugo is an aerospace engineer at NASA Langley Research Center and is a member of the Atmospheric Flight and Entry Systems Branch. While at NASA, he has worked on materials testing for inflatable atmospheric decelerators, scale model aeroballistic testing for Orion and Mars Science Laboratory, and flight trajectory reconstruction for MSL. He currently supports simulation and design of robotic- and human-scale Lunar and Mars vehicle entry, descent, and landing trajectories.

Introduction: Historically, Mars entry guidance methods have utilized bank angle reversals to mitigate total range and crossrange targeting errors. While proven effective for landing robotic assets (<3.5 t), this approach does not provide sufficient landing accuracy and precision required for crewed and crew support landers (~40-50 t). Specifically, the finite number of bank reversals limits crossrange error mitigation performance, and the use of the bank angle magnitude for downrange error mitigation results in relatively large landing ellipses. Additionally, this approach couples the range errors because the time, number, and magnitude of bank reversals affect both crossrange and downrange errors.

Direct force control. Direct force control (DFC) enables the decoupling of these targeting parameters [1]. The simplest example is the use of a system that permits direct control of angle of attack and angle of sideslip. Consider a conventional airplane: elevators control angle of attack, and rudders control angle of sideslip. Similarly, an entry vehicle with the ability to directly control these wind angles would be able to manage landing range errors without requiring bank reversals, given an appropriate guidance scheme. By modulating angle of attack at intervals, the lift vector is adjusted such that the predicted downrange errors at landing are continuously minimized. Similarly, modulating angle of sideslip permits management of predicted crossrange errors. This example is illustrated in Figure 1, which shows a case in which the vehicle angle of attack is used to directly modulate downrange, and angle of sideslip is used to directly modulate crossrange. This approach is particularly effective when the entry vehicle lacks a significant roll moment due to sideslip ($C_{l\beta}$) term, which is generally the case with the entry capsules that have been used for all NASA Mars landing missions to date.

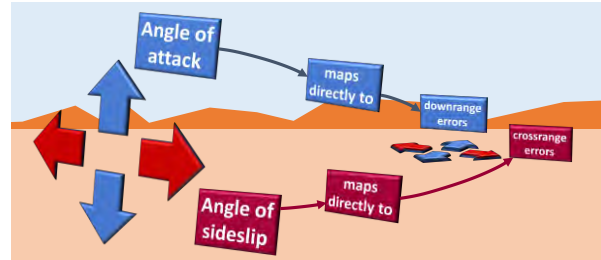


Figure 1. Illustration of direct force control using angle of attack and sideslip.

Guidance. A numerical predictor-corrector (NPC) guidance algorithm has been developed at NASA Langley Research Center (LaRC) as a flexible and robust method of spacecraft aerocapture and entry, descent, and landing (EDL) guidance [1, 4]. This NPC guidance will be used to demonstrate the application of DFC in a human-scale Mars EDL mission. An overview of the NPC guidance logic is shown in Figure 2.

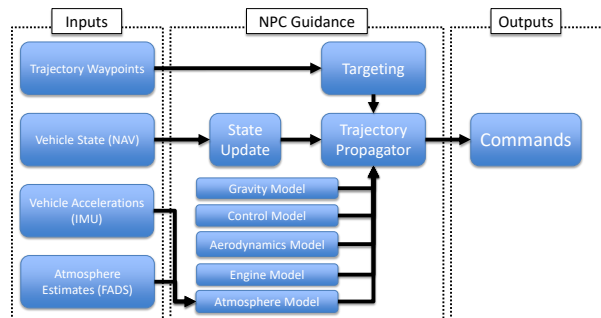


Figure 2. Outline of NPC Guidance.

Aerodynamics and supersonic retropropulsion. Control of the vehicle dynamics during hypersonic entry is provided by four deployable and actuated flaps, shown in Figure 3. The aerodynamic effects of the flaps are modeled and considered. In addition, recent efforts in predicting the effects of aerodynamic-propulsive interference on vehicle aerodynamics are considered in the present work. Supersonic retropropulsion (SRP) is an approach to powered flight used to reduce velocity during the descent and landing phases of EDL. If the engines are configured in such a way that they permit differential throttling or gimbaling, vehicle control authority during powered flight is enabled, and the NPC guidance can determine the time to start the engines, throttle setting, and thrust vector orientation.

Discussion: In the present work, a DFC guidance strategy using aerodynamic surface modulation and SRP is evaluated by simulating a human-scale Mars entry vehicle that utilizes a hypersonic inflatable aerodynamic decelerator (HIAD) with and the NPC guidance algorithm described previously. A rendered visualization of this vehicle during entry, with aerodynamic flaps deployed and exposed SRP engines, is shown in Figure 3. Effects of aerodynamics and engine transients during powered flight will also be presented, with emphasis on resultant landing accuracy and spacecraft performance effects.

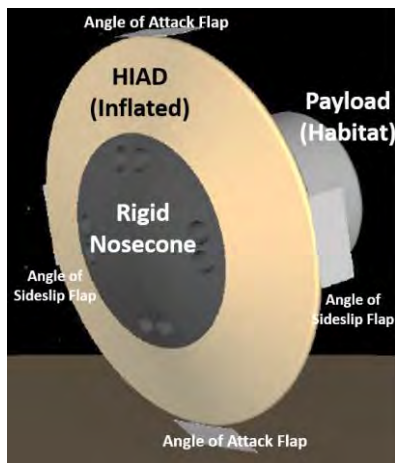


Figure 3. Representation of HIAD entry vehicle.

References:

- [1] Cianciolo, A. D., and Powell, R. W., "Entry, Descent, and Landing Guidance and Control Approaches to Satisfy Mars Human Mission Landing Criteria," AAS-17-254.
- [2] Cianciolo, A. D., and Polsgrove, T. T., "Human Mars Entry, Descent, and Landing Architecture Study Overview," AIAA SPACE 2016, 13-16 September 2016, Long Beach, CA, 10.2514/6.2016-5494.
- [3] Cianciolo, A., Striepe, S., Carson, J., Sostaric R., Woffinden, D., Karlgaard, C., Lugo, R., Powell, R., and Tynis, J., "Defining Navigation Requirements for Future Precision Lander Missions," SciTech 2019 AIAA Paper, submitted for publication, January 2019.
- [4] Fraysse, H., Powell, R., Rosseau, S., and Striepe, S., "CNES-NASA Studies of the Mars Sample Return Orbiter Aerocapture Phase," 51st International Astronautical Congress, 2-6 October, 2000, Rio De Janeiro, Brazil, IAF-00-A.6.05.

MARS SAMPLE RETURN ENGINEERING – A REFERENCE ARCHITECTURE FOR JOINT ESA-NASA STUDIES AND EARLY MISSION CONCEPTS

Sanjay Vijendran (1), Charles D. Edwards, Jr. (2), Brian K. Muirhead (2), Orson Sutherland (1), Jakob Huesing (1), Kelly Geelen (1), Ludovic Duvet (3), Friederike Beyer (1), Sarmad Aziz (1)

(1) European Space Agency-ESTEC, The Netherlands (sanjay.vijendran@esa.int) (2) Jet Propulsion Laboratory, California Institute of Technology, Pasadena, CA (3) European Space Agency-ECSAT, UK

Brief Presenter Biography: Presenter to be confirmed.

Introduction: The analysis in Earth laboratories of samples that could be returned from Mars is of extremely high interest to the international Mars exploration community. The NASA Mars 2020 sample-caching rover mission is the first component of a potential Mars Sample Return (MSR) campaign, so its existence constitutes a critical opportunity. On April 26, 2018, NASA and ESA signed a Statement of Intent¹ to work together to formulate, by the end of 2019, a joint plan for the retrieval missions that has a sufficient level of technical and programmatic maturity that will lead to an international agreement between the two agencies in time to be submitted for approval to their respective authorities at the end of 2019. This abstract describes the reference engineering architecture of the MSR campaign, which forms the basis on which ESA and NASA have been performing joint studies since early 2018. Some concepts for the retrieval flight elements will also be presented based on the recent and on-going studies.

The MSR reference architecture: The architecture is based on three major flight elements and one ground element as depicted in Figure 1.

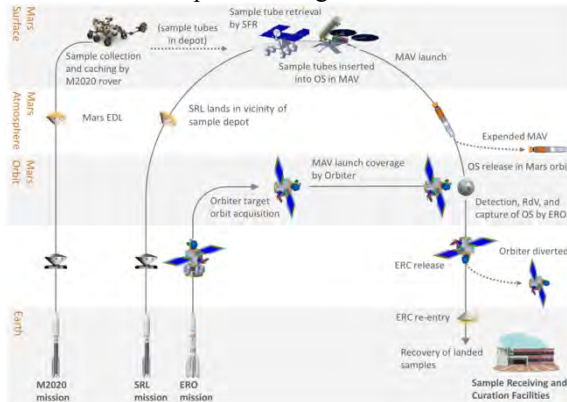


Figure 1: MSR reference architecture for joint ESA-NASA studies

The Mars 2020 sample caching rover mission, which would be the first element of this campaign, is already in full flight development and is planned for launch in 2020 with a nominal 1.25 Mars-year mission

to collect, analyze and cache samples for possible later retrieval.

The following two flights elements, not yet approved missions, are the main subjects of the joint studies.

The Sample Retrieval Lander (SRL) element is assumed to be led by NASA and would carry the Mars Ascent Vehicle (MAV), as well as an ESA-provided Sample Fetch Rover (SFR) and Sample Transfer Arm (STA).

The Earth Return Orbiter (ERO) element is assumed to be led by ESA and would carry a NASA-provided Capture and Containment System as well as an Earth Entry Vehicle.

For the purposes of the joint studies, launch dates as early as 2026 for both the SRL and ERO missions are being considered.

The fourth element of MSR, based on the ground, would constitute all post-landing handling, sample receiving and curation activities, collectively known as Mars Returned Sample handling (MRSB).

A key driver for the MSR campaign will be the backward planetary protection requirements as it falls under the COSPAR Category V “Restricted Earth Return” categorization.

The information provided about possible Mars sample return architectures is for planning and discussion purposes only. NASA and ESA have made no official decision to implement Mars Sample Return.

Acknowledgements:

A portion of the research described in this paper was carried out at the Jet Propulsion Laboratory, California Institute of Technology, under a contract with the National Aeronautics and Space Administration.

References:

[1] [https://mepag.jpl.nasa.gov/announcements/2018-04-26 NASA-ESA SOI \(Signed\).pdf](https://mepag.jpl.nasa.gov/announcements/2018-04-26%20NASA-ESA%20SOI%20(Signed).pdf)

OVERVIEW AND STATUS OF THE MARS SAMPLE RETURN STUDY 2026 OPPORTUNITY

M. E. Greco¹, ¹Jet Propulsion Laboratory, California Institute of Technology, 4800 Oak Grove Drive, Mail Stop 321-220, Pasadena, CA 91109, megreco@jpl.nasa.gov

Abstract: NASA has been studying how to retrieve a physical sample from the surface of Mars since the 1960s [1]. Recovering physical samples containing rock, soil and atmosphere would greatly increase the understanding of our nearest neighbor as well as how terrestrial planets evolve. As part of the Mars Exploration Program, NASA and the European Space Agency (ESA) are studying options for Mars Sample Return (MSR) mission concepts that could return the samples that the Mars 2020 rover mission will collect at Jezero crater starting in 2021. The Mars 2020 rover will collect core rock and soil samples and store some of them on the Martian surface encased in sample tubes [2]. The Mars 2020 mission will bring the goal of returning Martian samples one step closer to reality by performing the science, sample collection and caching, removing this requirement from future sample return vehicles. MSR would be one of the most important as well as complex efforts undertaken by the Mars Exploration Program under NASA and its partnership with ESA.

The current baseline MSR architecture requires the Earth launch of two independent spacecraft that must coordinate their operations at Mars. The two flight vehicles would be the ERO (Earth Return Orbiter) and the Mars Sample Return Vehicle (SRV) and are comprised of ten spacecraft elements. The ERO concept consists of the spacecraft bus capable of achieving Mars orbit and providing telecommunications relay support and the capability to capture the Mars sample and process it for Earth return via the CCRS (Capture, Containment and Return System) payload. The ERO would be capable of leaving the Martian orbit and execute the maneuvers needed for an Earth return. The EEV (Earth Entry Vehicle) would then execute the Earth entry to finally return the Mars samples to Earth. The SRV concept would be capable of making its trip from Earth and executing the EDL (Entry Descent and Landing) sequence onto the Martian surface. Once on the surface of Mars, the SRV would have the capability to seek out and gather the sample tubes that were collected by the Mars 2020 rover and prepare them to for launch on the MAV (Mars Ascent Vehicle). The SRV must not only be a capable EDL system but must also be capable of delivering samples to the OS and executing a MAV launch, requirements that sometimes are at odds with each other.

This presentation will provide an overview of the current sample return mission architecture and operational concepts. It will also discuss the technical challenges that must be overcome to ensure a successful mission. The SRV must be capable of safely landing

what is expected to be the largest mass ever landed on the surface of Mars [3]. A trade between SRV architectures will be presented including propulsive pallet and skycrane landing systems, as well as stationary and mobile MAV launching platforms. These architectures are evaluated for EDL capability, surface operations and the ability to serve as a capable MAV launch platform. Additionally, the presentation will touch on how technologies in the area of miniature electronics and mission timeline choices enable these SRV architectural options.

The scope and challenges of Mars Sample Return are something that NASA has not attempted since lunar samples were brought to Earth. The missions would rely heavily on the recent successful Mars missions, but new technological innovations are needed. These new engineering solutions are explored and evaluated based on the risk vs. reward to provide MSR the highest chance at success.

The information presented about potential MSR is pre-decisional and is provided for planning and discussion purposes only.

References:

- [1] P. D. Stabekis (2010) History Of Planning for a Mars Sample Return Mission, Presentation to the Planetary Protection Advisory Subcommittee
- [2] NASA (2019) <https://mars.nasa.gov/mars2020>
- [3] R. D. Braun, R. M. Manning (2006) Mars exploration entry, descent and landing challenges

MARS SAMPLE RETURN EDL FLIGHT PERFORMANCE CHALLENGES AND MITIGATION STRATEGIES. M. Ivanov¹, W. Strauss¹, ¹NASA Jet Propulsion Laboratory, California Institute of Technology (4800 Oak Grove Drive, Pasadena CA 91109).

Brief Presenter Biography: Mark Ivanov has worked in industry since 1986, leading flight dynamics, flight operations, and business development teams for General Dynamics, Lockheed Martin, EchoStar Communications, and from 2004, at NASA's Jet Propulsion Laboratory in Pasadena, California. At JPL, he has worked and lead several investigations into improving entry, descent, and landing (EDL) performance for robotic missions to Mars, including participation in Earth-based flight testing of parachutes intended for Mars applications. He is currently the EDL Flight Dynamics lead engineer for Mars Sample Return mission concept studies.

Abstract: NASA is studying potential Mars Sample Return (MSR) architectures to enable a unique investigative opportunity to study Martian soil and atmosphere samples here on Earth. The current notional MSR mission architecture is comprised of three interdependent operational elements: Sample Caching, Sample Retrieval, and Sample Return. The Mars 2020 rover mission will cache samples for possible return. M2020 could be followed by a separate Sample Retrieval Lander (SRL) mission launched as early as 2026, and a Earth Return Orbiter (ERO) mission, also launched around 2026. The SRL mission concept is currently a Pre-Phase A study but could transition to an official Phase A project in early 2020. The SRL mission element may consist of an EDL configuration hundreds of kilograms heavier than any other entry vehicle flown to Mars to date. Further, landing accuracy to within 100 meters of the intended target site may also be necessary (i.e. Pin-Point Landing)[1][2]. The engineering strategy is to design the SRL configuration utilizing elements similar to recent Mars missions (e.g. MSL, M2020, InSight) but add select augmentations necessary to overcome the performance challenges.

The current baseline SRL EDL configuration consists of a traditional entry aeroshell design with an internal descent and landing system that has yet to be determined as either a Skycrane (e.g. MSL, M2020) or a platform lander (e.g. InSight). For either option, the delivered mission specific hardware would include a Mars Ascent Vehicle (MAV) and a fetch rover, both of which would drive the overall mass of the system beyond the purely scientific payloads of past missions. The fetch rover would travel to one or more "depot" locations containing samples left by M2020 and transport them back to the SRL landing site for transfer to the MAV and eventual launch into Mars orbit. The

ERO vehicle would then rendezvous with the Orbiting Sample (OS) for capture and return to Earth.

The SRL EDL CONOPS would be similar to past missions in that the entry phase utilizes bank modulated guidance during entry, transition to a supersonic Disk Gap Band (DGB) parachute, and then separate a propulsive descent stage that softly lands the payload on the surface. Since the location of the depots would be known prior to entry, the propulsive stage may divert up to ~4km to a landing location close to one of the depots in order to ease the driving distance for the fetch rover. The magnitude of this divert may require upwards to ~200kg of additional propellant, further complicating entry performance[1].

Initial entry mass estimates for the configuration options under consideration are approaching ~4,000 kg (compared to M2020, which has an entry mass of ~3,450 kg). This additional mass increase results in an altitude loss at chute deploy that produces chute phase timing not sufficient to perform the operations necessary to prepare for descent stage separation. Therefore, one or more performance augmentations would be necessary to add timeline back into the chute phase.

EDL performance augmentation could include any of the following: higher Mach at chute deploy, reducing or eliminating operations during the chute phase (resulting in less required timeline), increasing entry L/D by flying at a higher angle of attack, using a ballute as a drag device prior to chute deploy, increasing the entry capsule diameter (thereby reducing the entry ballistic coefficient), and adding a trim tab to achieve the entry angle of attack without the need for heavy balance masses [3]. Each augmentation has a clear performance improvement benefit but also unique challenges when considering the detailed implementation. The presentation will focus on both defining the overall performance challenge as well as discussing some of the augmentations currently under consideration. The information presented about potential MSR is pre-decisional and is provided for planning and discussion purposes only.

References:

- [1] A. Wolf et al. (2012) *Improving The Landing Precision Of An MSL-Class Vehicle*, IEEE 978-1-4577-0557-1
- [2] B. Acikmese et al. (2012) *Flight Testing Of Trajectories Computed By GFOLD: Fuel Optimal Large Divert Guidance Algorithm For Planetary Landing*, AAS 13-386
- [3] M. Ivanov et al. (2011) *Entry, Descent and Landing Systems Analysis Study: Phase 2 Report on*

Mars Science Laboratory Improvement, NASA/TM-
2011-21698

Tuesday, July 9, 2019

Sample Return to Earth - Conveners: Scott Perino, Matthias Grott, Marcus Lobbia, Joern Helbert, and Sahadeo Ramjatan

2:48 PM	Robotic Mars Sample Return Earth Entry Vehicle Concept Development	Marcus Lobbia	Jet Propulsion Laboratory, California Institute of Technology	
3:00 PM	HEET Material Modeling and Earth Entry Vehicle Landing Analyses for Potential Mars Sample Return	Aaron Siddens	Jet Propulsion Laboratory, California Institute of Technology	
3:12 PM	Break the Chain and Containment Assurance Concepts for Mars Sample Return and Beyond	Morgan Hendry	Jet Propulsion Laboratory, California Institute of Technology	
3:24 PM	Conceptual Design Of Sample Return Capsule For CAESAR Mission	Kazuhiko Yamada	JAXA	Invited
3:36 PM	The DLR Sample Analysis Laboratory	Joern Helbert	DLR	
3:48 PM	Successes With Exo-Brake Development and Targeting for Future Sample Return Capability: TES-6,7,8 Flight Ex-eriments	Marcus Murbach	NASA Ames Research Center	

ROBOTIC MARS SAMPLE RETURN EARTH ENTRY VEHICLE CONCEPT DEVELOPMENT

S. V. Perino¹, J. M. Corliss², J. C. Vander Kam³, and M. A. Lobbia¹, ¹Jet Propulsion Laboratory, California Institute of Technology, ²NASA Langley Research Center, ³NASA Ames Research Center

Brief Presenter Biography: Marcus Lobbia is a Systems Engineer in the Entry Descent & Landing (EDL) Systems group at JPL, where he supports design and analysis of future planetary probe missions. Currently he is the EDL Systems Engineer for JPL's Mars Sample Return / Earth Entry Vehicle formulation team; he previously supported EDL operations for the Mars InSight lander and has worked on JPL proposals and concept studies. Marcus has a B.S. degree from the University of California, San Diego, and M.S. and Ph.D. degrees from the University of Tokyo.

Introduction: The most recent Planetary Science Decadal Survey indicated that the Mars Astrobiology Explorer-Cacher element of a potential robotic Mars Sample Return (MSR) architecture should be considered as the highest-priority large mission [1]. While MSR is still in the pre-formulation phase, NASA's upcoming Mars 2020 rover is being designed with a sample-caching system that could fulfil this role. Other elements of the notional architecture include MSR Orbiter and MSR Lander concepts. The last step of the overall MSR mission would be to bring the Mars samples back to Earth's surface via an Earth Entry Vehicle (EEV), where they would then be transferred to the Sample Receiving and Curation Facility.

Earth Entry Vehicle Design Considerations: Due to the expected stringent planetary protection concerns related to bringing Martian samples back to Earth, the EEV concept development has focused on high-reliability approaches to entry vehicle design. This includes a completely passive/ballistic system that could be targeted for landing at a site such as the Utah Test and Training Range. To increase reliability, no parachutes or active electronics/power are being considered in current concepts, which would result in the vehicle being designed for a high-speed landing on the order of 40 m/s.

Recent EEV concept studies have focused on a potential 2026 launch / 2029 or 2031 return architectures [2]. This results in relatively high entry velocities at Earth of approximately 12 to 13.5 km/s. The EEV must therefore be designed to withstand heat fluxes on the order of 1-2 kW/cm², depending on the entry flight path angle targeted. Several thermal protection system (TPS) options have been studied, and detailed concept designs (see Fig. 2) have been developed for concepts using Phenolic-Impregnated Carbon Ablator (PICA) and Heatshield for Extreme Entry Environment Technology (HEEET) TPS materials. Previous design cycles also

looked at the use of a "hot structure" concept using a Carbon-Carbon structure capable of operating at high temperatures [3].

This presentation will provide an overview of the current MSR/EEV concepts being matured, some of the trades being explored, and summarize the high-level differences in both design and performance. As an example, Fig. 2 shows a landing ellipse generated from Monte Carlo trajectory analyses conducted on an EEV concept using HEEET TPS material.

The information presented about potential MSR is pre-decisional and is provided for planning and discussion purposes only.

References: [1] Squyres, et al., "Visions and Voyages for Planetary Science in the Decade 2013-2022," National Academies Press (2011). [2] Perino, et al., "A New Era and a New Trade Space: Evaluating Earth Entry Vehicle Concepts for a Potential 2026 Mars Sample Return," 15th International Planetary Probe Workshop (2018). [3] Lobbia, et al., "Hot-Structure Earth Entry Vehicle Concept for Robotic Mars Sample Return," 15th International Planetary Probe Workshop (2018).

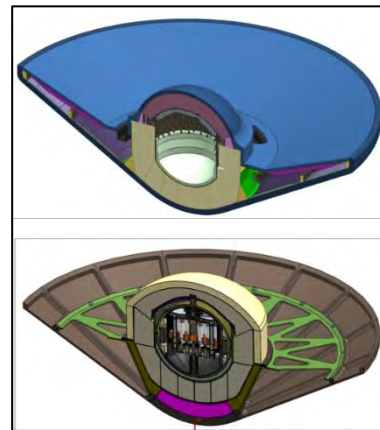


Fig. 1: Example of designs for EEV concepts using PICA TPS material (top) and Carbon-Carbon (bottom).

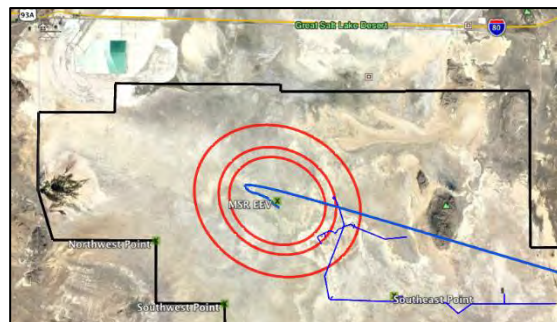


Fig. 2: Example of landing ellipse for an EEV concept using HEEET TPS material and a -25 deg. entry flight path angle.

HEEET Material Modeling and Earth Entry Vehicle Landing Analyses for Potential Mars Sample Return.

A. J. Siddens¹ and S. Kellas², ¹Jet Propulsion Laboratory, California Institute of Technology, aaron.j.siddens@jpl.nasa.gov. ²NASA Langley Research Center.

Brief Presenter Biography: Aaron Siddens is a Structures Engineer at the Jet Propulsion Laboratory. His work focuses on impact analysis and developing best practices for advanced numerical methods.

Introduction: NASA is studying a potential Mars Sample Return (MSR) campaign that would return samples from the surface of Mars to Earth in a multi-step series of mission concepts. A key part of the proposed campaign is the Earth Entry Vehicle (EEV), a passive vehicle that would enter the Earth's atmosphere and transport the sample container to the surface by impacting the ground at terminal velocity [1].

The EEV energy absorber component would be responsible for mitigating loads to the sample container during impact. It is composed of composite-wrapped foam cells that, when assembled and co-cured, form a foam-filled composite web structure [2]. Energy is dissipated by progressive folding and crushing of the webs and foam, with damage initiating at the nose of the EEV and progressing aft.

The notional impact location for an MSR EEV is the Utah Test and Training Range (UTTR). To attain a landing ellipse small enough to avoid most known hazards, such as roads and structures, a steep atmospheric entry flightpath angle may be required. The EEV entry conditions are such that traditional TPS materials, such as PICA, may be less suited for the aerothermal loading imposed by a steep entry.

For this and other reasons, the Heatshield for Extreme Entry Environment Technology (HEEET) is under consideration for the EEV. HEEET is a 3D woven dual-layer TPS material system [3]. The exterior recession layer (RL) is a high-density all-carbon fiber layer that mitigates recession during entry. The interior insulation layer (IL) is a lower density blended fiber layer that mitigates bond line temperatures and insulates the underlying structure from entry heating. While technically a 3D composite, the layer-to-layer interlocking fibers run predominantly in-plane and not in the through-thickness direction, making it a pseudo-3D or 2.5D composite material.

EEV Impact Landing and HEEET: With low-density TPS materials such as PICA, there is little contribution to the overall stiffness and energy absorption of the structure, and its influence is considered negligible during impact. In contrast, HEEET retains significant stiffness after processing.

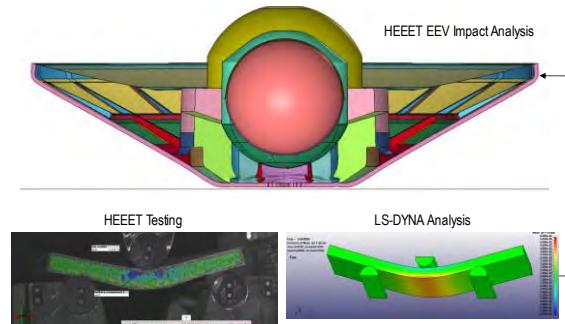


Fig. 1. HEEET material model development and HEEET EEV impact assessment

The dynamic response of HEEET and its influence on the existing EEV energy absorber performance during impact is unknown. The energy absorber is designed with the assumption that the TPS and forward shell readily deform during an off-nominal hard surface impact event, allowing the foam and composite webs to absorb energy by crumpling [2].

A concern with HEEET is that significant stiffness in the TPS could cause the energy absorber to be loaded in a way that was not intended, potentially degrading performance. In the extreme case, a very stiff TPS could prevent the intended front-end deformation altogether, requiring a different energy absorber approach.

To address this concern, testing was carried out to characterize the dynamic progressive damage response of HEEET. The primary goal of this testing was to provide data for material model development using LS-DYNA so that the influence of HEEET on the EEV during impact could be directly simulated. Separate RL and IL models were developed in order to accurately capture the influence of each on the EEV response.

HEEET Coupon Testing: 3-point bend tests were conducted on separate RL and IL coupons. Specimens with the beam length aligned with the (1) fill, and (2) $\pm 45^\circ$ bias orientation were made in order to characterize the anisotropic material response. While the warp direction should be interrogated as well, material for testing was limited, and it was determined that the fill and $\pm 45^\circ$ coupons were best for initial model development. Until more testing can be performed, the warp response is inferred from comparisons between warp and fill tensile testing.

Tests were conducted both at low rate (1.27 cm/s) on a load frame and at higher rates (7 and 17 m/s) on a drop tower in order to characterize strain-rate dependency in the material response. Load-displacement data

at the center loader and photogrammetry on one side of the coupon we obtained for use in model validation.

Testing revealed a complex material response. While HEEET is a 3D woven composite, the response of both the RL and IL was analogous to a 2D woven composite with inter-laminar connections that have a low damage threshold but a high failure threshold. The results suggested that an appropriate modeling approach might be one in which weakening of layer-to-layer coupling can be represented, but without completely decoupling the layers from one another.

HEEET Model Development: The coupon tests were simulated using LS-DYNA. A hybrid modeling approach was investigated in which the in-plane and inter-laminar failure responses are handled by separate models. This necessitated modeling the coupons using several layers of 8-noded hexagonal elements. The in-plane damage response is handled by these elements and their material formulation, while the inter-laminar damage response is primarily handled by the formulation of the connection between element layers.

For the in-plane response, candidate material models were identified that could capture different orthogonal behavior as well as capture the effect of fiber scissoring that occurs during loading in the $\pm 45^\circ$ bias orientation. For the inter-laminar response, cohesive formulations, strength-based approaches, and contact-based methods were investigated.

Once an approach was developed that gave sufficient accuracy, the HEEET RL and IL models were incorporated into simulations of EEV off-nominal impact, including hard surface impact. The TPS layer was modeled in the same manner as the coupons. Changes in sample container acceleration and loads at mount locations were key quantities of interest used to assess the effect of HEEET TPS on the EEV response.

A brief summary of the test results used for the HEEET model development, model validation efforts, and results of impact simulations of the EEV with a HEEET TPS will be presented.

References:

- [1] Mitcheltree, R., & Kellas, S. (1999) "A Passive Earth-Entry Capsule for Mars Sample Return."
- [2] Kellas, S. (2015) "Integrated Composite Stiffener Structure (ICoSS) Concept for Planetary Entry Vehicles."
- [3] Ellerby, D., et al. (2018) "Overview of Heatshield for Extreme Entry Environment Technology (HEEET) Project," *15th IPPW*.

Acknowledgment: The authors would like to acknowledge Dr. Justin Little at NASA Langley Research Center for performing the static and dynamic HEEET coupon testing and data collection.

A portion of the research described in this paper was carried out at the Jet Propulsion Laboratory, California Institute of Technology, under contract with the National Aeronautics and Space Administration. Pre-decisional information – for planning and discussion purposes only.

Break the Chain and Containment Assurance Concepts for Mars Sample Return and Beyond

M. L. Hendry¹, ¹Jet Propulsion Laboratory, California Institute of Technology, 4800 Oak Grove Drive, Pasadena, CA 91109

Brief Presenter Biography: Morgan Hendry joined JPL and the Mars Science Laboratory Chassis Team as a mechanical engineer in 2007 after completing his B.S and M.S. in Astronautics from the University of Southern California. In 2009, he transitioned to the role of project mass properties engineer for the Soil Moisture Active Passive mission. After a successful launch and spin-up of the SMAP instrument in 2015, Morgan began work as a mechanical systems engineer developing break the chain technology to support future Mars Sample Return missions. During the same period, he also worked to design and test new additively manufactured excavation and sampling technology for the exploration of Europa, Enceladus, and Titan.

Introduction: Sample return from solar system bodies has long been an important goal for many planetary science programs. While robotic exploration missions have yielded many groundbreaking discoveries, further progress requires the use of Earth-based tools, techniques, and equipment. Thus, there has been a push of late to bring back extraterrestrial material to Earth for study.

While the idea of sample return dates back to early lunar exploration and has been conducted on many bodies, Mars represents the first potential target that the scientific community believes could have realistically held the conditions for life at one point in its past. As such, backward planetary protection measures have been studied to ensure sample containment and protect Earth's biosphere. [1] This has included both biological research and technology development to create methods of both sterilizing and robustly containing material of interest. [2]

The latest Planetary Science Decadal Survey called Mars Sample Return one of the highest priorities for study. [3] Mars 2020 will collect samples for possible return by a future mission. Two concepts for subsequent missions are being studied, a Sample Return Lander and an Earth Return Orbiter. This talk will discuss the back planetary protection strategy for potential Mars Sample Return, both for "breaking the chain of contact" (Break the Chain, or BTC) with Mars and maintaining containment through our landing event (Containment Assurance).

Break the Chain: The first step in bringing samples back to Earth would require breaking the chain of contact with the body of origin. This would require a mission to leverage both active techniques and passive effects of the space environment to sequentially reduce

the probability of a viable microorganism entering Earth's biosphere.

A new wave of technology development has progressed over the past five years to rebuild and surpass capabilities that were in work for a proposed (and canceled) 2003/2005 MSR attempt. These included work in brazing, explosive welding, polymeric bagging, pyrotechnic paint, and plasma sterilization (amongst many others). [4] Some of these technologies have been traded, tested, and redesigned to fit within a subsystem called the Containment Module (CM) of a proposed MSR payload element called the Capture Containment and Return System (CCRS).

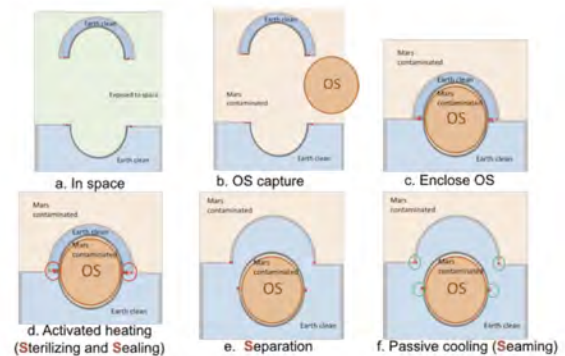


Figure 1: Schematic showing utilization of a double wall lid as part of a BTC concept

Recently, work has commenced on understanding particle transport and passive environmental inactivation of Mars material. This material control strategy would regulate the particle loading on both the surface and orbital elements to improve the performance of any containment and sterilization systems used. Things like exposure to UV energy and hard vacuum, orbital decay, solar pressure, and particle adhesion/emission are being considered as ways to reduce the number of particles of interest.

Containment Assurance: Once the chain of contact is broken, robust containment must be preserved through landing on Earth and transport to a sample handling facility. This includes the design of the containers themselves, the Earth Entry Vehicle, and its impact attenuation strategy.

The coupled EEV and Containment Assurance system would be designed to reduce the load environment on the sample containers. Current concepts feature crushable energy dissipating material surrounding the nested vessels. Motion limiting features are envisioned

between containers to ensure that all lids remain in compression and one container does not impact the lid of another. When latches are being used to retain lids, they are presently being designed to operate on a continuum (i.e. non-backlash).

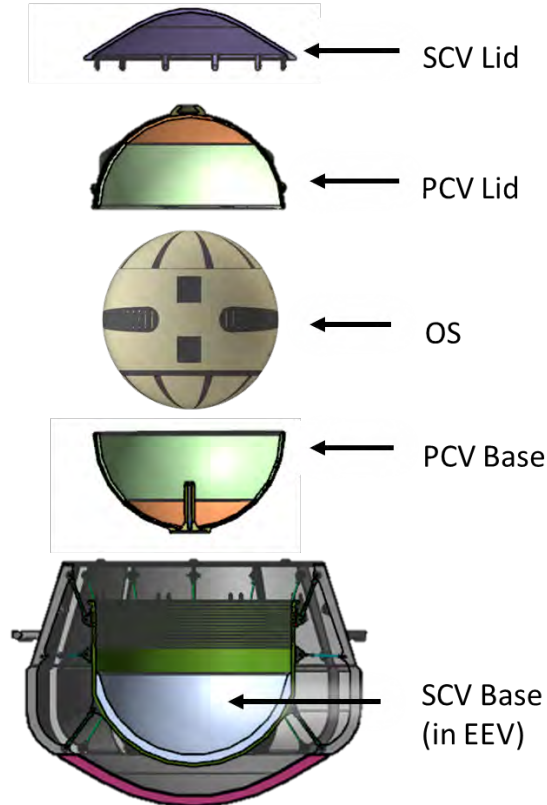


Figure 2: Redundant containment concept utilizing Primary and Secondary Containment (PCV and SCV) around the Orbiting Sample (OS)

Future Missions: While this work is being done to support concepts for Mars Sample Return, any sample return mission (Category V Restricted or otherwise) would benefit from the technology development, requirements definition, architecture, and V&V approach of this campaign. Additionally, some of the back planetary protection work may be applied for forward planetary protection problems to better sterilize and keep out-bound probes free of Earth contamination.

References: [1] “Mars Sample Return Issues and Recommendations”, National Academy Press, 1997. [2] NASA NID 8020.109A, March 30, 2017. [3] “Visions and Voyages for Planetary Science in the Decade 2013-2022”, The National Academies Press, 2011. [4] Gershman, R., et. al. Break-the-Chain Technology for Potential Mars Sample Return. IEEE Aerospace Conference. 2018.

Acknowledgment: A portion of the research described in this paper was carried out at the Jet Propulsion Laboratory, California Institute of Technology, under contract with the National Aeronautics and Space Administration. The decision to implement Mars Sample Return will not be finalized until NASA’s completion of the National Environmental Policy Act (NEPA) process. This document is being made available for information purposes only.

CONCEPTUAL DESIGN OF SAMPLE RETURN CAPSULE FOR CAESAR MISSION

Kazhiko Yamada¹ and CAESAR-SRC team, ¹Japan Aerospace Explartion Agency (3-1-1 Yoshinodai Chuo-ku Sagamihara Kanagawa Japan, yamada.kazuhiko@jaxa.jp)

Brief Presenter Biography: Dr. Kazuhiko Yamada is an associate professor at Department of Space Flight Systems, Institute of Space and Astronautical Science, Japan Aerospace Exploration Agency. He received his Ph.D. from the The University of Tokyo in Engineering in 2004. He works in JAXA/ISAS since 2004. His present focus is various re-entry technology, from conventional sample return capsule to innovative inflatable decelerator.

Introduction: A significance and its value of sample return missions to astral bodies in the deep space is recognized by HAYABUSA's successful sample return to asteroid ITOKAWA. The sample return mission became one of the keys in the planetary exploration. The sample return capsule is one of the important and indispensable key technologies to support the future sample return missions. Sample return missions in next generation require a large amount of sample, samples in deeper space and low temperature samples from the viewpoint of science. So, the evolution of the sample return capsule is necessary in order to realize these missions. JAXA and Japanese researchers and engineers continues the research and development of the sample return capsule evolved on the basis of HAYABUSA-SRC heritage[1]. Its sample return capsule technology in Japan can contribute not only Japanese domestic missions, but also international collaboration missions. For example, JAXA contribute the CAESAR (Comet Astrobiology Exploration Sample Return) [2] mission with its sample return capsule technology.



Fig. 1: Hayabusa's reentry and Hayabusa 2 sample return capsule

CAESAR mission : CAESAR (Comet Astrobiology Exploration Sample Return) is one of the finalist missions for next NASA's New Frontiers Program. CAESAR is the international collaboration mission which will return nonvolatile and volatile material from comet 67P/Churyumov-Gerasimenko. The Figure 2 is Artist's concept of CAESAR obtaining a sample from comet 67P. JAXA's researcher, engineers and Japanese scientists contributed to CAESAR for the concept study and the preparation of proposal documents. JAXA will play an important role in CAESAR mission. It is a development of the sample return capsule which is indispensable for sample return mission.



Fig. 2: Artist's concept of CAESAR obtaining a sample from comet 67P

Conceptual design of SRC : CAESAR requires to survive a severe aerodynamic and aerothermal environment during a direct reentry from interplanetary orbit for SRC. Its aerodynamic environment is same level as one of Hayabusa SRC. Additionally, CAESAR's SRC has to keep the comet's sample in low temperature and to carry a large payload system. The conceptual design of SRC was conducted to fulfill these mission and system requirements utilizing the heritage of Hayabusa's sample return capsule. The aerodynamic shape and heat shield material is same as Hayabusa SRC and the front heat shield can be jettisoned in descent phase, which is the same concept of Hayabusa SRC. However, the two stage parachute is adopted and the integration of inside devices including payload system is modified to meet the mission requirements to CAESAR SRC. Figure 3 shows conceptual design of CAESAR-SRC which is designed on the basis of heritage of HAYABUSA SRC.

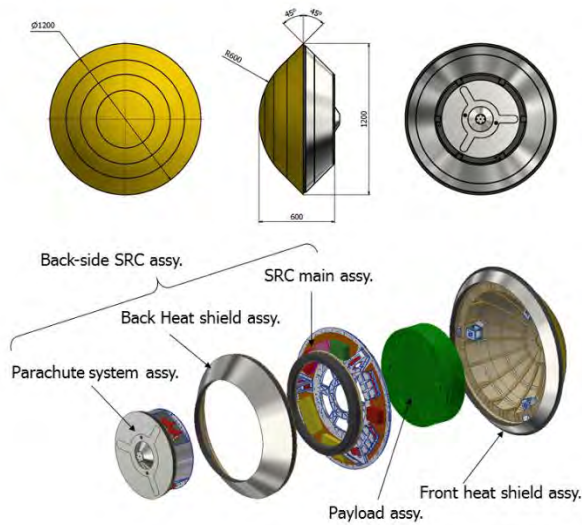


Fig. 3: Conceptual design of CAESAR SRC which is designed on the basis of heritage of HAYABUSA SRC.

Summary:

JAXA participates the CAESAR team and contributes the conceptual study of CAESAR mission. JAXA are developing advanced sample return capsule for next generation sample return mission for CAESAR mission. In this presentation, the conceptual design of CAESAR SRC and development status will be introduced.

References:

- [1] Yoshifumi Inatani and Nobuaki Ishii, "Design Overview of Asteroid Sample Return Capsule", The institute of Space and Astronautical Science Report SP No.17, March 2003. Page 1-15
- [2] S. W. Squyres, et, al. "The CAESAR New Frontiers Mission : 1. Overview", 49th Lunar and Planetary Science Conference 2018 (LPI Contrib. No. 2083, 1332.pdf) (2018)

Planetary Sample Analysis Laboratory (SAL) at DLR

J. Helbert¹, A. Maturilli¹ and the SAL team ¹Institute for Planetary Research, DLR, Germany, (joern.helbert@dlr.de)

Brief Presenter Biography: Jörn Helbert is a physicist by training and joined DLR in 1998. He is currently the head of the Planetary Spectroscopy Laboratories group. His scientific research focus on understand the surface composition of mainly airless bodies from remote sensing, in-situ and sample analysis. He has been involved in several planetary missions of ESA, NASA and JAXA and is one of the PIs of the MERTIS instrument on BepiColombo.

Introduction: Building on the available infrastructure and the long heritage in spectral studies of planetary (analog) materials DLR is creating a Sample Analysis Laboratory (SAL). The setup has started with the installation of a vis-IR-microscope at the Planetary Spectroscopy Laboratory in 2018.

Global reconnaissance of planetary surface can only be obtained by remote sensing methods. Optical spectroscopy from UV to far-infrared is playing a key role to determine surface mineralogy, texture, weathering processes, volatile abundances etc. It is a very versatile technique, which will continue to be of importance for many years to come. Providing ground truth by in-situ measurements and ultimately sample return can significantly enhanced the scientific return of the global remote sensing data. This motivates the planned extension of PSL with a SAL by support of the Astrobiology Laboratories.

SAL will focus on spectroscopy on the microscopic scale and geochemical and geo-microbiological analysis methods to study elemental composition and isotopic ratios in addition to mineralogy to derive information on the formation and evolution of planetary surfaces, search for traces of organic materials or even traces of extinct or extant life and inclusions of water.

Analysis of returned samples: SAL will add over the next 4 years capabilities for detailed mineralogical and geochemical characterization of material return by sample return missions in a clean room facility. The step-wise extension follows the successful development approach used for the Planetary Spectroscopy Laboratory (PSL) and Astrobiology Laboratories. The goal is to test and validate each extension step before planning the follow-up step.

A key driver for the design of the setup is the type of sample returned and the return method. The first step is focused on analyzing samples from asteroids missions like Hayabusa 2 mission, Osiris-REX and lunar sample return missions. SAL can later be extended to a full Sample Curation facility.

The DLR SAL will be operated as a community facility (much like PSL), supporting the larger German and European sample analysis community

Current facilities: PSL at DLR (<http://s.dlr.de/2siu>) is the only spectroscopic infrastructure in the world with the capability to measure emissivity of powder materials, in air or in vacuum, from low to very high temperatures [1-3], over an extended spectral range. Emissivity measurements are complimented by reflectance and transmittance measurements produced simultaneously with the same setup. It is the ground reference laboratory for the MERTIS thermal infrared spectral imager on the ESA BepiColombo mission [4, 5]. Members of the PSL group are team members of the MarsExpress, VenusExpress, MESSENGER and JAXA Hayabusa 2 missions [6]. For the latter mission PSL has performed ground calibration measurements. In addition PSL has been used extensively in support of the ESA Rosetta mission. The samples analyzed at PSL ranged from rocks, minerals, to meteorites and Apollo lunar soil samples.

In a climate-controlled environment PSL operates currently two Fourier Transform Infrared Spectrometer (FTIR) vacuum spectrometers, equipped with internal and external chambers, to measure emittance, transmittance and reflectance of powdered or solid samples in the wavelength range from 0.3 to beyond 100 micron. Recently a Hyperion 2000 microscope has been added in preparation of the SAL setup. For details on PSL see the accompanying presentation.

All laboratory facilities undergo regular evaluations as part of the DLR quality management process. The evaluations address laboratory protocols, documentation, safety, data archival and staff training.

PSL is a community facility as part of the “Distribute Planetary Simulation Facility” in European Union funded EuroPlanet Research Infrastructure (<http://www.europlanet-2020-ri.eu/>). Through this program (and its predecessor) over the last 7 years more than 60 external scientists have obtained time to use the PSL facilities. PSL has setup all necessary protocols to support visiting scientist, help with sample preparation, and archive the obtained data.

Sample Analysis Laboratory: The near-term goal of the first step is the preparation to receive samples from the Hayabusa 2 mission. The current PSL and Raman facilities are operating in climate-controlled rooms and follow well-established cleanliness standards. The SAL will be housed in two ISO 5 clean rooms. The cleanrooms are equipped with glove boxes to handle and prepare samples. All samples will be stored under

dry nitrogen and can be transported between the instruments in dry nitrogen filled containers.

To characterize and analysis the returned samples the existing analytical capabilities are currently been extended. PSL was just upgraded with a vis-IR-microscope to extend spectral analysis to the sub-mi-cron scale.

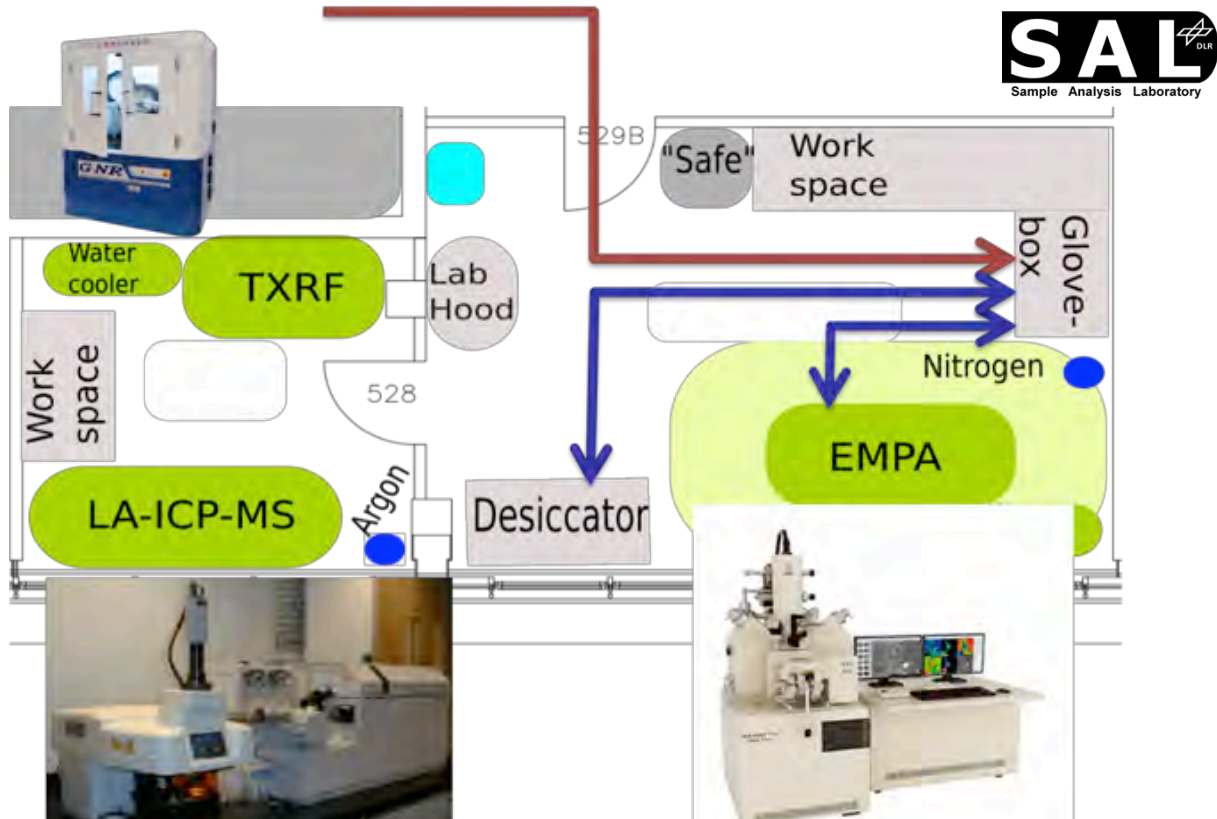
For the SAL this will be complemented by the following capabilities:

1. Electron Microprobe Analyse (EMPA) for elemental analysis
2. Laser ablated inductive coupled Plasma Mass Spectrometer for elemental and isotope analysis
3. Dual Source TXRF & Grazing Incidence ED-XRF for mineralogical and structural analysis
4. Supporting equipment incl. microtome to prepare thin sections, optical polarization microscope, etc.

Based on current planning the first parts of SAL will be operational and ready for certification by end of 2021. Analysis of first Hayabusa 2 samples can start by beginning to mid of 2022.

Outlook: DLR has started establishing a Sample Analysis Laboratory. Following the approach of a distributed European sample analysis and curation facility as discussed in the preliminary recommendations of EuroCares (<http://www.euro-cares.eu/>) the facility at DLR could be expanded to a curation facility. The timeline for this extension will be based on the planning of sample return missions. The details will depend on the nature of the returned samples. Through the BIOMEX project a collaboration has been established with the Robert-Koch Institute (RKI) (<http://www.rki.de>) for question of samples that might pose a bio-hazard. RKI is operating BSL 4 facilities, which might be used as part of the DLR curation facilities.

References: [1] Ferrari, S., et al., American Mineralogist, 2014. **99**(4): p. 786-792. [2] Maturilli, A. and J. Helbert, Journal of Applied Remote Sensing, 2014. **8**(1): p. 084985. [3] Helbert, J., et al., Earth and Planetary Science Letters, 2013. **371-372**: p. 252-257. [4] Hiesinger, H. and J. Helbert., Planetary and Space Science, 2010. **58**(1-2): p. 144-165. [5] Helbert, J., et al., *SPIE* 2008. **7082**: p. 70820L. [6] Okada, T., et al., Space Science Reviews, 2016.



Successes with Exo-Brake Development and Targeting for Future Sample Return Capability: TES-6,7,8 Flight Experiments

M. S. Murbach,¹ P. Papadopoulos,² A. Guarneros,¹ J. Wheless,¹ F. Tanner,¹ C. Priscal,¹ S. Smith,¹ A. Salas,¹ Z. Hughes,¹ R.D. Ntone Sike,¹ Sanny Omar,³ B. Soriano-Gama,¹ N. Williams,¹

¹NASA Ames Research Center, Moffett Field, CA 94035, ²San Jose State University, Aeronautical Engineering Department, One Washington Square, San Jose, CA, 95192, ³University of Florida, Gainesville, FL, 32611

Brief Presenter Biography: Marcus Murbach is the Principal Investigator and originator of the SOAREX (Sub-Orbital Aerodynamic Re-entry Experiments) and TechEdSat-n nano-satellite series. He is the lead inventor of the Exo-Brake as well as other related innovations. Working at the NASA Ames Research Center, he is also an Adjunct Professor at the local state university in the Aeronautics Department (San Jose State University), and works to have many student collaborators involved in flight experiments and research.

Abstract: The Exo-Brake is a deployable, non-propulsive means of de-orbiting small payloads from orbital platforms such as the International Space Station (ISS) [1,2]. Recent flight experiments involving the TechEdSat (TES) 6, 7, 8 will be presented in terms of both ‘targeted’ and ‘disposal’ de-orbit techniques. These build on the previous flight experiments in the TES-n flight series which had fixed surface areas and therefore a constant ballistic coefficient. The most recent three nano-sats, starting with TES-6, permitted either an abrupt step change or a gradual change in the projected front surface area caused by warping the support system.

The TES-6 was a 3U nano-satellite launched from the International Space Station (ISS) on November 20, 2017 and was designed with a variable ballistic coefficient graded in 10 steps. After the initial ballistic coefficient range determination, an uplink command could be sent to reset the Exo-Brake to the new position. The analysis team would then restart the orbit mechanic propagator (e.g., Satellite Tool Kit) at the new position, and determine if the de-orbit path would coincide with the target latitude/longitude at the Von Karman altitude (100km).

The TES-7 was a 2U nano-satellite awaiting integration into the experimental vehicle for launch in the Spring, 2019. The 500km circular orbit opportunity permitted the advancement of a high altitude ‘disposal’ Exo-Brake to be developed. The intent is to reduce the orbit lifetime from years to months, and to later permit a coarse targeting (scale of an ocean) suitable for earlier mission termination. By developing a compact version of the system with a straightforward interface, future nano-sats at the more problematic higher altitude can be provided options of disposal

without contributing more to the increasing problem of orbital debris. The design also features a system to release the Exo-Brake during the final orbit, abruptly changing the ballistic coefficient and permitting some targeting. To make this version of the Exo-Brake as compact as possible, non-rigid or flexible struts are used which are partially inflated with a gas.

The largest and most capable nano-sat in the series, TES-8 was jettisoned from the ISS on January 31, 2019 (TES-7 was out of sequence due to repeated delays in the launch vehicle). As a linear 6U in size, it permitted an array of communication experiments as well as the highest power capacity battery sub-system of any NASA nano-satellite in the same class. The Exo-Brake was also larger, permitting a wider range of ballistic coefficient. The telemetry system also affords multiple path for command/control from the use of the Iridium satellite network.

The analysis group uses an array of tools in order to develop the aerodynamic data base (e.g., DAC, CBAERO), trajectory simulation (e.g., STK, GMAT), and initial re-entry (TRAJ). In the future experiments, the orbit mechanic propagators will be placed on the on-board microprocessor for autonomous de-orbit and initial entry. High temperature versions of the Exo-Brake are being designed and tested in order to survive through maximum convective heating if necessary. This may help engender new techniques for sample return and hypersonic/entry experiments to be conducted in the future. [3]

References: [1] M.S. Murbach, K. Boronowsky, B. White, E. Fritzler (2010) AIAA 2010-2663. [2] E. Hill, M. Krihak, D. Reiss-Bubenheim (2008) NASA Internal Planning Document [3] M.S. Murbach, J. Drew, I. Cozmuta, A. Guarneros-Luna, A. Tanner, J. Wheless, A. Lavin (2016) IAC-16-B4.5.7x35738.



Figure 1. Exo-Brake experiment from the ISS.

Tuesday, July 9, 2019

Innovative Concepts for Exploration - Conveners: Robert Dillman, Dmitriy Shutin, Gilles Baillet, and Siddharth Krishnamoorthy

4:36 PM	Deployable Aeroshell Technology For Small-Class	Kazuhiko Yamada	JAXA	Invited
4:48 PM	Dragonfly: In situ Terrain Relative Navigation fo	Kenneth Hibbard	Johns Hopkins Applied Physics Laboratory	
5:00 PM	BioSats: Distributed Sensing of Venus' Atmosphe	Katharina Hildebrandt	European Space Agency	
5:12 PM	Swarm Navigation and Exploration for Planetary Surface Missions: Experimental Results	Emanuel Staudinger	German Aerospace Center (DLR)	
5:24 PM	Triple: Autonomous Subglacial Lake Exploration As A Stepping Stone Towards Icy Worlds Ocean Exploration	Christoph Waldmann	University of Bremen/MARUM	

DEPLOYABLE AEROSHELL TECHNOLOGY FOR SMALL-CLASS PLANETARY EXPLORATION MISSION.

Kazhiko Yamada¹, Kojiro Suzuki², Osamu Imamura³, Daisuke Akita⁴ and MAAC group, ¹ Japan Aerospace Exploration Agency (3-1-1 Yoshinodai Chuo-ku Sagami-hara Kanagawa Japan, yamada.kazuhiko@jaxa.jp), ²The University of Tokyo, ³Nihon University, ⁴Tokyo Institute of Technology.

Brief Presenter Biography: Dr. Kazuhiko Yamada is an associate professor at Department of Space Flight Systems, Institute of Space and Astronautical Science, Japan Aerospace Exploration Agency. He received his Ph.D. from the The University of Tokyo in Engineering in 2004. He works in JAXA/ISAS since 2004. His present focus is various re-entry technology, from conventional sample return capsule to innovative inflatable decelerator.

Introduction: The deployable and flexible aeroshell is promising as a future atmospheric-entry system for space transportations and planetary explorations. The atmospheric entry vehicle with a large and low-mass flexible aeroshell make its ballistic coefficient low and can reduce the aerodynamic heating during the atmospheric entry. Our group has been researched and developed on this technology to apply it to actual missions since 2000, focusing on a flare-type thin membrane aeroshell supported by a single inflatable ring. Two balloon drop tests were carried out in 2004 and 2009 and a re-entry demonstration from an altitude of 150km was carried out in 2012 using the S-310 sounding rocket^[1]. And a flight demonstration in low earth orbit (LEO) which is named EGG was carried out in 2017, utilizing an opportunity to deploy a nano-satellite from ISS.

SPUR mission: This deployable and flexible aeroshell is expected as one of the key technology to realize the full-blown planetary exploration by small-class spacecraft. Our group proposes the SPUR (Scattered nano Probes Unfolded Reconnaissance) mission, which utilize the deployment aeroshell. In SPUR mission, 100kg-class small-spacecraft is inserted in an orbit around a planet by aerocapture technology at first. After that, some several-kg-class nano-landers is ejected from orbiter. Each nano-lander enters into the atmosphere and is landed on difference location of planet surface. These nano-landers and the orbiter make the network for the distributed observation. Therefore, the main objective of SPUR mission is a demonstration of network observation on the planet for the future distributed planetary exploration using the small-class spacecraft. The figure 1 shows a conceptual image of network-type exploration in SPUR mission.

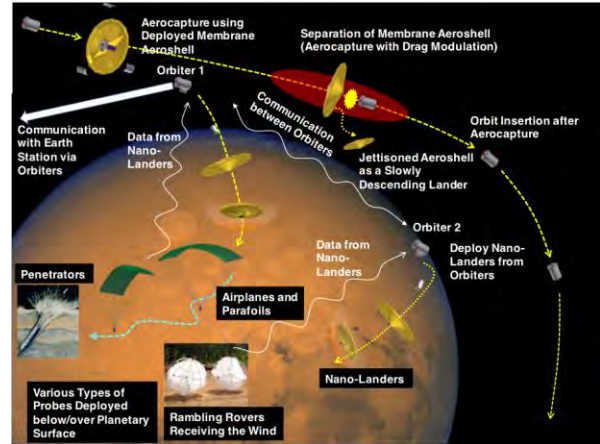


Fig. 1: Concept image of network-type exploration in 3D space around Mars

Application of deployable aeroshell: SPUR mission adopts the drag modulation aerocapture technology for the orbit insertion maneuver. The spacecraft with a low-mass and large-area deployable aeroshell jettisons its aeroshell at appropriate time during atmospheric entry in order to acquire the appropriate aerodynamic deceleration. The figure 2 is one of the mock-up of flare-type membrane aeroshell sustained by single inflatable ring, with a diameter of 3.5m. It is the largest aeroshell which our group has ever made. The results of atmospheric-entry trajectory simulation at Mars indicate the feasibility of drag modulation aerocapture for a 100kg-class small spacecraft and 3.5-meter-diameter of deployable aeroshell.



Fig. 2: The mock-up of inflatable aeroshell sustained by single inflatable ring with a diameter of 3.5m.

The deployable aeroshell has some advantage for the EDL system of nano-lander because of its simplicity in EDL phase and good packing efficiency. Our group is developing SMA(shape memory alloy)-type passive deployable aeroshell besides of gas injected inflatable type aeroshell. The SMA-type deployable aeroshell is more simple than inflatable aeroshell and it has a potential for application to a 1kg-class nano-lander. The figure 3 shows the demonstration of passive deployment of SMA-type aeroshell due to the aerodynamic heating in hypersonic wind tunnel.

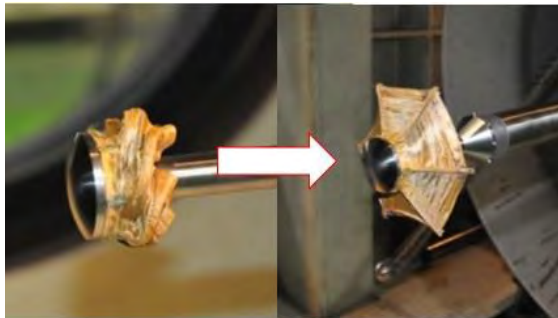


Fig. 3: Demonstration of passive deployment of SMA-type deployable aeroshell in the hypersonic wind tunnel test.

Summary:

The deployable aeroshell is one of the key technologies in order to realize the planetary exploration by a small-class spacecraft. The deployable aeroshell may realize both the orbit insertion of small spacecraft and nano-lander. In this presentation, the status and future plan of the research and development of its deployable aeroshell technology will be introduced.

References:

- [1] Yamada, K., et.al.: Suborbital Reentry Demonstration of Inflatable Flare-Type Thin-Membrane Aeroshell Using a Sounding Rocket, AIAA Journal of Spacecraft and Rockets, January, Vol. 52, No. 1(2015) : pp. 275-284
- [2] Yamada, K., et.al.: Re-entry Nano-Satellite with Gossamer Aeroshell and GPS/Iridium deployed from ISS, ISTS-paper, 2017-f-21, 2017

***Dragonfly*: In situ Terrain Relative Navigation for Titan Surface Exploration**

K. E. Hibbard,¹ D. S. Adams,¹ B. F. Villac,¹ C. A. Sawyer,¹ N. L. Mehta,¹ and A. A. Cocoros¹

¹Johns Hopkins Applied Physics Lab, 11100 Johns Hopkins Road, Laurel, MD 20723.

Presenter email: Kenneth.Hibbard@jhuapl.edu

Brief Presenter Biography: Kenneth Hibbard has worked at the Johns Hopkins Applied Physics Laboratory (APL) for 15 years, and at the Goddard Space Flight Center for 10 years prior, specializing in project systems engineering and the design, development, and implementation of robotic space missions. He has served on numerous flight missions including *ACE*, *SOHO*, *Swift*, *MESSENGER*, and *New Horizons* and has led the development of various NASA proposals and concepts, including the *Europa Clipper*, the *Venus Reconnaissance Observer (VRO)*, the *Io Volcano Observer (IVO)*, and the *Titan Mare Explorer (TiME)*. Mr. Hibbard is currently the Mission Systems Engineer for the proposed *Dragonfly* New Frontiers mission to Titan.

Introduction: *Dragonfly* is a proposed New Frontiers-class mission that will send a nuclear-powered rotorcraft lander to the surface of Titan to study the composition of a wide variety of surface sites and complete the first comprehensive *in situ* study of Titan's chemical diversity and complexity. This presentation will provide an overview of the approach to terrain-relative navigation (TRN) and safe landing site assessment, which was specifically adapted to the unique needs at Titan and thus enables flight of this "relocatable lander."

TRN is an element of *Dragonfly*'s "mobility" subsystem that is defined as all of the components supporting atmospheric flight on Titan. The mobility subsystem consists of sensors (flash lidar, radar, cameras, pressure altimeter, and IMU), actuators (motors and rotors), structure (booms and skids), electronics (processor and rotor drive electronics), and surface Guidance, Navigation, and Control (GNC) processing. All of the sensors have previous flight heritage, so the ongoing development is in the *Dragonfly*-specific software and TRN application. *Dragonfly*'s TRN is derived from decades of related work including legacy Digital Scene Matching Area Correlator (DSMAC) and Terrain Contour Matching (TERCOM) algorithms employed by APL on Tomahawk missiles, the Autonomous Landing and Hazard Avoidance Technology (ALHAT), which fed into previous lunar lander development activities, and our Autonomous Precision Landing Navigation (APL Nav) software.

Unlike navigation on Earth, the Moon, or Mars, flying at Titan does not have the benefit of existing high-resolution images, maps, or digital elevation models (DEMs). Therefore, *Dragonfly* employs image-to-image TRN [1], using images taken for the current and



previous flights only. The vehicle will scout out potential landing sites on previous flights and use that survey data to help navigate from one location to the next, using a flash lidar for landing site selection. By not requiring the generation of maps, or needing to correlate to existing data sets with an absolute surface reference, this implementation is highly streamlined through its use of only *in situ* relative positions, and also minimizes the amount of data that needs to be relayed back to Earth. Additionally, in order to generate position estimates at a rate required by *Dragonfly*, portions of TRN and landing site assessment algorithms are executed on a field-programmable gate array (FPGA) that excels in computer vision applications and reduces computational burden on the single board processor.

Building upon ALHAT algorithms [2] with the use of flash lidar data, *Dragonfly* can safely land, executing robust hazard detection. Lidar data collected during horizontal flight is used to generate an elevation map in realtime that is processed to identify potentially hazardous slopes and deviations (rocks, pits). The slope and deviation are calculated using well-established methods of numerical differentiation, and hazards identified using conservative threshold values. Safe landing zones are identified by calculating the distance to the nearest hazard, where potential safe sites are identified and ranked.

APL developed a correlation-based TRN algorithm that continuously estimates the relative lateral position change of the vehicle, which allows navigation even in the conservative case where limited optical features are available. *Dragonfly*'s TRN uses full-frame fast Fourier transform (FFT) correlation, with required warping, for optical navigation. Using a typical "leapfrog" flight scenario, images from a previous flight or on an earlier segment of the current flight, also referred to as "breadcrumbs," reduce errors in lateral drift and allow the

rotorcraft to localize to a previously recorded position. Otherwise, image-to-image navigation is used and a new breadcrumb is registered for future use. The algorithm's inputs are two images, along with their corresponding states and parameters.

The full presentation will provide additional details about the design of *Dragonfly*'s TRN and surface ConOps. Various graphics and animations to elucidate *Dragonfly*'s TRN execution and performance, and further demonstrate the concepts described here will also be presented.

References: [1] Witte et al. (2019), "No GPS? No Problem! Exploring the Dunes of Titan with *Dragonfly* Using Visual Odometry," AIAA SciTech 2019 Forum, [2] Johnson et al. (2008), "Analysis of On-Board Hazard Detection and Avoidance for Safe Lunar Landing," IEEE Aerospace Conference, pp. 1-9.

BioSats: Distributed Sensing of Venus' Atmosphere through Microprobes

K. Hildebrandt¹ and E. Ozturk², ¹European Space Research and Technology Center, Advanced Concepts Team (katharina.a.r.hildebrandt@gmail.com), ² European Space Research and Technology Center, Advanced Concepts Team (ekin4ozturk@gmail.com).

Brief Presenter Biography: Katharina Hildebrandt is currently a researcher in the Advanced Concepts Team at ESA in the area of Biomimetics for Space Technology. Prior to that she earned a Master's degree in Engineering for Flight and Space Flight from the University of Bremen (Germany). She earned her undergraduate degree from the University of Applied Sciences Bremen (Germany) and the New Jersey Institute of Technology (USA) in the area of Bio-inspired Engineering.

Introduction: The harsh Cytherean atmosphere is a hotbed of different phenomena from the super-rotation of the upper atmosphere [1] to the sulphuric acid clouds lurking in the 30 – 60 km range [2]. The dynamics of Venus' atmosphere have yet to be fully understood based on observations and numerical simulations due to an inability to obtain a global view of the atmosphere at different depths.

Current global observation methods for the Cytherean atmosphere use spectral imaging placed on various satellites orbiting Venus [3,4,5]. Though this gives a global overview of the atmosphere, it does not provide a direct way of computing a 3D map of the atmosphere at any given time.

Our solution to this is to use a distributed sensing approach whereby many microprobes are dispersed into the atmosphere of Venus and communicate measurements of temperature, pressure, electric and magnetic fields, and density.

In order to maximize the number of measurements, we propose using bio-inspired designs to increase the flight time of the probes. The design space was restricted to passively dispersed natural objects. This is a very broad selection, thus the available designs were screened based on the required aerodynamic properties.

Trajectories of the microprobes were computed utilizing a Newtonian motion model incorporating Cytherean atmospheric data based on observations by Venera [3], Venus Express [4] and Pioneer Venus [5]. Figure 1 shows the atmospheric profile of Venus as collated from these sources with some values interpolated based on the availability of data.

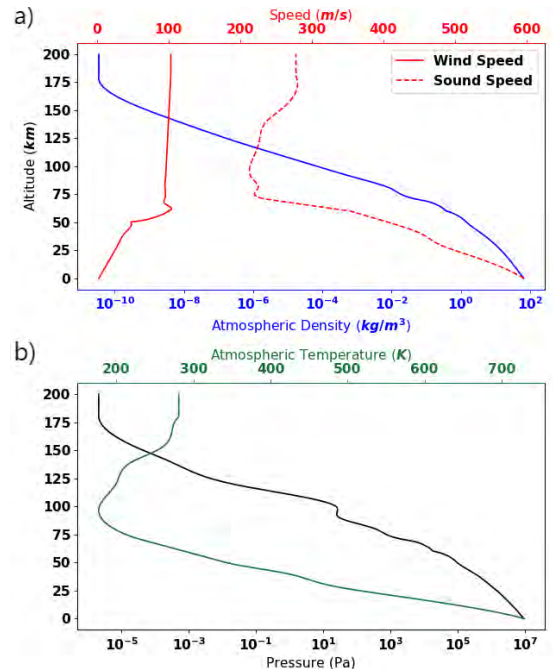


Figure 1 - Atmospheric Profile of Venus based on data from [3,4,5,6]. (a): The wind and sound speed, and the atmospheric density as a function of altitude. (b): The atmospheric temperature and pressure as a function of altitude.

These trajectories were used to obtain the relationship between the total flight time, and the drag and lift coefficients. Figure 2 shows an example descent profile for a microprobe dropped from an altitude of 100 km with a drag coefficient of 5 and a lift coefficient of 2.6. The area of the probe in the x, y and z directions were assumed to be 20 cm², 20 cm² and 144 cm² respectively.

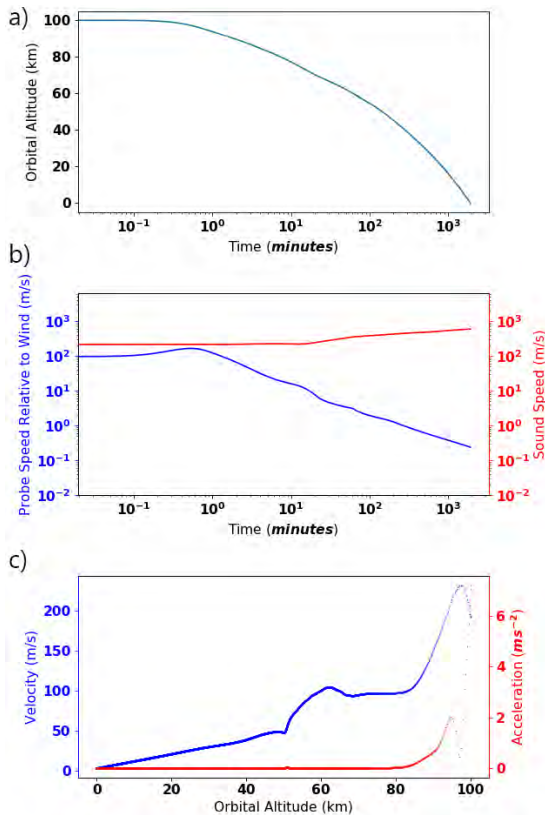


Figure 2 - Microprobe Atmospheric Descent Profile. (a): The orbital altitude as a function of time. (b): The probes relative velocity and the sound speed as a function of time. (c): The velocity and acceleration at each height.

From the descent profiles for various parameters, favourable lift and drag coefficients for enhanced flight times were determined. Consequently the *Alsomitra macrocarpa* gliding seed [6] and the *Acer spec.* rotating seed [7] were identified as good biomimetic design models with comparable aerodynamic properties. Figure 3 shows the pressure profile of a microprobe design inspired by the *Alsomitra macrocarpa* seed for a head-on wind of 10 m/s.

Naturally, the microprobe designs that were selected are scaled up in comparison to the actual seeds due to the payload requirements. The dimensions of possible payloads were based on the investigation of payloads for distributed sensing undertaken by Wells et al. [8] and Manchester and Peck [9].

CFD simulations were used to investigate the drag and lift coefficients of the microprobes subject to the expected relative velocity and the atmospheric density at various altitudes.

The next stage of this project is to optimize the designs for the maximised flight time given the data transmission, thermal and structural requirements. In order to determine the shape and structural design of the probe, an iterative CFD based optimization strategy is used.

This presentation will provide an overview of the project and the optimization methodology along with the resulting designs of the microprobes and potential improvements.

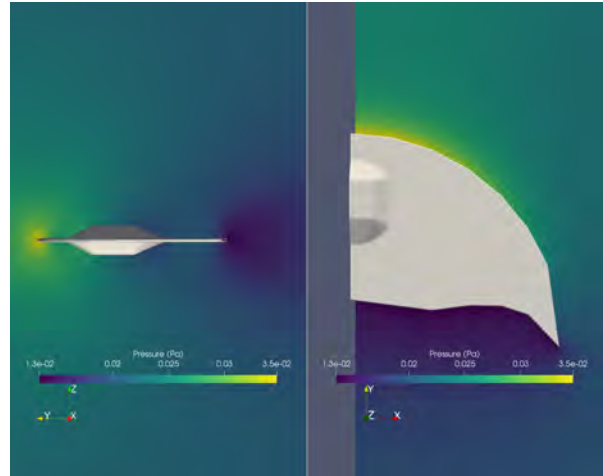


Figure 3 - Pressure Profile for *Alsomitra macrocarpa* based design of microprobe subject to a head-on wind speed of 10m/s at a pressure of 0.02 Pa and temperature of 200 K. The x-axis length of the probe, from the centerline to the wingtip, is 7cm.

References:

- [1] Read, P. L. and Lebonnois, S. (2018), Annual Review of Earth and Planetary Sciences, Vol. 46, 175-202
- [2] Limaye, S. S. et al. (2018), Astrobiology, Vol. 18, Nr. 9
- [3] Petropoulos, B. (1993), Earth, Moon, and Planets 63, 1 – 7
- [4] Gubenko, V. N. and Kirillovich, I. A. (2018) Cosmic Research, Vol. 56, Nr. 6, 471-479
- [5] Petropoulos, B. (1987), Earth, Moon and Planets 42, 29-40
- [6] Azuma, A. and Okuno, Y. (1987), Journal of theoretical Biology 129, 262-274
- [7] Lee, Y. J. (2012), Icarus 217, 599-609
- [8] Wells, N. J. et al. (2004), Proc. of 8th ESA Workshop on Advanced Space Technologies for Robotics and Automation ‘ASTRA 2004’, Noordwijk, The Netherlands
- [9] Manchester, Z. R. and Peck, M. A. (2011), AIAA Guidance, Navigation, and Control Conference, Portland, USA

SWARM NAVIGATION AND EXPLORATION FOR PLANETARY SURFACE MISSIONS: EXPERIMENTAL RESULTS

E. Staudinger, R. Pöhlmann, T. Wiedemann, S. Zhang, A. Dammann and D. Shutin, German Aerospace Center (DLR) e.V., Institute of Communications and Navigation (Emanuel.Staudinger@DLR.de)

Brief Presenter Biography: Emanuel Staudinger is leading the topic *Swarm Navigation* within the department Communication Systems of the Institute of Communications and Navigation of DLR. He obtained his PhD degree with distinction at the University of Bremen in 2015 and is working as scientific staff in DLR since 2010. He is actively working on experimental platforms for swarm navigation, its concepts and evaluations.

Introduction: Modern robotic platforms for in-situ space exploration are single-robots equipped with a number of specialized sensors providing scientists with unique information about a planet's surface. However, there is a number of exploration problems where larger spatial apertures of the exploration system are necessary, requiring a completely new perspective on in-situ space exploration and its required technologies. Large networks of robots, called swarm, pave the way: agents in a swarm span ad-hoc communication networks, localize themselves based on radio signals, share resources, process data and make inference over the network in a decentralized fashion. By cooperation, local information collected by agents becomes globally available.

In this work we present our recent results in development of swarm technologies for future in-situ space exploration missions: a wireless system jointly used for communication, localization and timing, and swarm navigation and exploration strategies to sample and reconstruct gas fields.

Swarm Navigation: We propose a concept for joint wireless communication, localization, and timing, enabling robot self-localization and time synchronization. The multi-user radio channel access is achieved with a decentralized time division multiple access (TDMA) scheme: no central coordinator is required. The design of the wireless system is based on orthogonal frequency division multiplex (OFDM) to combat multipath and enable high-rate communication among agents. The wireless signals used for communication are further exploited to estimate the distance among agents based on the round-trip time. Ad-hoc communication and precise ranging provide the basis for distributed localization of all agents in a Bayesian tracking framework realized as distributed particle filters. As a result, we obtain the formation of the swarm. In addition, we exploit so called multi-mode antennas for 3D bearing determination. As a result, once agents in a

swarm establish a network and are able to localize themselves, they can exploit this information to navigate and explore. Swarm navigation is understood as computationally data driven technique to optimize swarm movements: either for location-aware formation control to optimize self-localization, or to span a distributed phased array to determine the bearing of a low-frequency radio signal, e.g. to navigate back to the lander.

Swarm Exploration: We define swarm exploration as data driven and model based techniques to determine sample locations, where new measurements provide the highest information gain. To this end, robust communication, accurate localization, and synchronization are essential pre-requisites. In this work we focus on mapping the concentration of airborne trace substances in the exploration area with the goal to find emission sources. A-priori neither the number of sources, nor their strength, nor their location is known. These parameters should be estimated by the swarm cooperatively. Our exploration strategy exploits a physical model of gas diffusion based on a partial differential equations. This model based approach has three important properties: (i) It enables inference, as the gas sources are not directly measurable, however, inferable based on concentrations measurements, wind and the model. (ii) The a-priori information given by the physical model accelerates the exploration. (iii) We can quantify uncertainties in the exploration area based on the model leading to an information-driven exploration strategy.

The exploration strategy itself determines, where agents shall take the next measurements. Areas with high uncertainty offer the highest information gain, and thus are favoured candidates for the next concentration measurements. In addition to the exploration strategy a coordination scheme to avoid agent collisions must be used.

Experimental Results: We realized the main aspects of swarm navigation with software defined radios (SDRs) for communication and ranging, and with a JAVA based framework for localization. Six SDRs have been integrated into six rovers providing distance estimates to the particle filter, see Fig. 1. The particle filter estimates the location of each rover in real-time and provides a graphical output. A GNSS-RTK system is used as ground truth and visualized in parallel. Several localization experiments have been conducted

showing the gain of cooperation and resulting in localization errors in sub-meter value range.



Fig. 1: One of six rovers equipped with DLR's swarm navigation system. The rover is located in a large gravel pit as analog experimentation site.

The gas exploration strategy has been realized as hardware-in-the-loop (HIL) simulation within the robot operating system (ROS). In this HIL simulation we numerically simulate the wind conditions and the gas dispersion in the exploration area. The real six rovers drive autonomously in the exploration area based on their local communication and localization taking the simulated gas concentration into account. Besides, they consider the obstacle map and avoid inter-agent collisions.

Fig. 2 shows the simulated gas concentration field resulting from two emission sources. In the experiment based on our exploration strategy the rovers were guided towards the sources and were able to identify and localize the sources within a few minutes.



Fig. 2: Start of the gas exploration: two gas sources were simulated together with wind coming from the right. The gas concentration field is shown as overlay.

by the Federal Ministry for Economic Affairs and Energy on the basis of a decision by the German Bundestag, grant 50NA1520 administered by DLR Space Administration

Acknowledgements: This work was partially supported by the DLR project *Swarm Navigation & Exploration* and the project *VaMEx-CoSMiC* supported

TRIPLE: AUTONOMOUS SUBGLACIAL LAKE EXPLORATION AS A STEPPING STONE TOWARDS ICY WORLDS OCEAN EXPLORATION

Christoph Waldman¹, Dmitriy Shutin², Oliver Funke³,

¹MARUM-Center for Marine Environmental Sciences, University of Bremen, Leobener Str. 8, 28359 Bremen, Germany,

²German Aerospace Center (DLR), Institute for Communications and Navigation, 82234 Wessling, Germany,

³German Aerospace Center (DLR), Space Administration, 53227 Bonn, Germany,

Brief Presenter Biography: Christoph Waldmann graduated from the University of Kiel, Germany, in the field of physics in 1981 and received a Doctorate degree in 1985. He has been engaged in the field of ocean technology for over 30 years now specializing in the development of new sensing methods, instruments and mobile platforms. Since 1996 he has been working as a senior scientist at the University of Bremen, Germany.

Introduction: Search for life as we know it in our Solar system mainly implies search for presence liquid water. Among the many, so far discussed potential ocean worlds in our solar system, Europa and Enceladus are the most likely candidates to support life. Needless to say that human exploration of these worlds lies in a very far future. Robotic exploration, on the other hand, offers a possibility to answer the question whether life beyond Earth exists even in our lifetime. Nonetheless, at present such sophisticated robotic exploration systems are not yet available, since enabling key technologies still need to be developed or brought to a higher TRL. The TRIPLE initiative is set to fill this gap.

Three main system components: The acronym TRIPLE stands for *Technologies for Rapid Ice Penetration and subglacial Lake Exploration*, representing technology development for three required main components. Specifically, the so far engaged German teams are focusing on *i.)* a melting probe carrying a slim-shaped autonomous underwater vehicle, and the *ii.)* nanoAUV as a payload. This two-component system is foreseen for a series of terrestrial analog field tests with increasing technical challenges. In a final field test access and deployment of the nanoAUV into a subglacial lake is envisaged. The third component is the *iii.)* AstroBioLab for microbiologic sample analysis that will be operated at the ice surface.

Precursor projects: The TRIPLE initiative is part of the DLR Explorer Initiatives founded by DLR Space Administration, department of Navigation, in order to concentrate expertise from diverse running projects funded within Germany's national Space Program. The general purpose is to coordinate running activities (as for combined field tests), discussion and development of new approaches, early identification of

specific technical solutions and given synergies among these projects. In particular, the diverse EnEx (Enceladus Explorer) and EurEx (Europa Explorer) projects acted as precursors for the TRIPLE initiative:

In EnEx a fully maneuverable melting probe – the “EnEx-IceMole” – was developed. Equipped with corresponding technologies for positioning, navigation, and clean sampling, EnEx-IceMole was designed to autonomously melt its way into the ice surface of Enceladus at a depth of about 200 m and towards a water-filled crevasse that feeds a cryovolcano. The task of the probe is to take a liquid water sample from there for in-situ examination. In collaboration with the science team from the NSF funded MIDGE project (J. Mikucki, S. Tulaczyk) the probe was already successfully utilized in a terrestrial analog field test in Antarctica (November/December 2014) for retrieval of a clean water sample from a subglacial lake (Blood Falls experiment).

In the EurEx scenario likewise a melting probe was used, albeit it was acting as a shuttle carrying an Autonomous Underwater Vehicle (AUV) as a payload. In the project the ice penetrating shuttle “*Teredo*” and the AUV “*Leng*” were developed as first approach technology carriers and tested in laboratory and minor field tests. Although in these tests the system demonstrated the correctness of the followed approach, further miniaturization and increased TRL is required. This is the goal of TRIPLE.

Ambitious objectives: Within the TRIPLE initiative various parallel running projects are planned, funded and coordinated by DLR Space Administration. The final goal is demonstration of the technological capability of the TRIPLE system for a fully autonomous subglacial lake exploration. This shall be done in a terrestrial field test that resembles as much as possible the expected environmental conditions on Jupiter's moon Europa.

The technical challenges of designing a 2-stage device consisting of a melting probe equipped with a deployable AUV to search for biosignatures on Icy Moons are extremely demanding. It is actually unknown whether today's technology permits a successful exploration/landing mission on Europa or other planets. It is therefore of paramount importance to

embrace all necessary components and modules into a system engineering approach.

To this end, all subsystems developed within EnEx and EurEx projects need to be raised to the next technical readiness level in a coordinated manner. Indeed, diverse TRLs of individual subsystems would significantly slow down the mission design process and its management. Moreover, the interaction of those subsystems when assembled will stay unpredictable which constitutes a big risk for the mission as a whole.

Some of the major technical challenges can be identified already today. These are the establishment of a reliable communication link between the ground station and the 2-stage exploration platform, the safe autonomous operation of the nanoAUV in completely unknown environmental conditions, as well as a concept for miniaturization of the AUV while still preserving its required operational capabilities. All technological steps have to be guided by a systematic risk assessment process, which will create a better picture on where we stand today technologically.

TRIPLE road map: In November 2018 TRIPLE was started with a feasibility study (phase 0) with a duration of seven months. Within this study also different potential locations for the TRIPLE field tests (such as Antarctica or Canada) are considered and weighed against each other with respect to scientific and technological benefit on the one hand, and logistic restrictions/costs on the other hand. The next project steps are currently planned for fall 2019 with the design phase A/B1 with duration of about one year, followed by the development phase B2/C/D planned to start early in 2021. The final field test is envisaged for winter 2024/25. Results of the phase 0 study will be presented at IPPW 2019.

Wednesday, July 10 2019

Solar System Exploration I – Mercury, Venus, Giant Planets, and Titan - Conveners: Thibault Cavalie, Jacob Izraelevitz, Olivier Mousis, and David Atkinson				
8:30 AM	Poster Introductions			
8:42 AM	The Decade of Venus: Revitalizing Exploration of our Sister Planet	James Cutts	Jet Propulsion Laboratory, California Institute of Technology	
8:54 AM	Mercury Vapor Rankine Power Cycle For A Venus Surface Lander	Christopher Greer	The Pennsylvania State University	Student
9:06 AM	Long-Duration Venus Probes and Landers	Tibor Kremic	NASA Glenn Research Center	
9:18 AM	The Cupid's Arrow Mission Concept: Hypervelocity Sampling In The Upper Atmosphere Of Venus	Jason Rabinovitch	Jet Propulsion Laboratory, California Institute of Technology	
9:30 AM	Balloon-Borne Infrasond As A Remote Sensing Tool For Venus - Progress In 2018	James Cutts	Jet Propulsion Laboratory, California Institute of Technology	
9:42 AM	Altitude-Controlled Balloon Concepts for Venus and Titan: Energy, Mass, and Stability Tradeoffs	Jacob Izraelevitz	NASA Jet Propulsion Laboratory, California Institute of Technology	
10:18 AM	Advances In Mechanical Compression Altitude Control Balloon Technology For Venus And Titan	Maxim de Jong	Thin Red Line Aerospace	
10:30 AM	Sampling Titan'S Surface With Dragonfly	Ralph Lorenz	Johns Hopkins Applied Physics Laboratory	
10:42 AM	Study On ESA Contribution To NASA-Led Ice Giants Mission	Gonzalo Saavedra Criado	European Space Agency	
10:54 AM	The deep composition of Uranus and Neptune from mass spectrometry and thermochemical modeling	Thibault Cavalie	Laboratoire d'Astrophysique de Bordeaux	
11:06 AM	Key Atmospheric Signatures For Deciphering The Formation Conditions Of Uranus And Neptune In The Protosolar Nebula	Olivier Mousis	Laboratoire d'Astrophysique de Marseille	
11:18 AM	Ice Giant Aerocapture Using Low-L/D Aeroshells: Uncertainty Quantification and Risk Assessment	Athul Pradeepkumar Girija	Purdue University	Student
11:30 AM	Atmospheric Link Science And Communications With Planetary Entry Probes Via Direct-To-Earth And Relay Radio Link Methods.	Sami Asmar	Jet Propulsion Laboratory, California Institute of Technology	

THE DECADE OF VENUS: REVITALIZING EXPLORATION OF OUR SISTER PLANET. M. D. Dyar¹, N. Izenberg², J. Cutts³, G. Hunter⁴, J. G. O'Rourke⁵, and members of the VEXAG Steering committee. ¹Dept. of Astronomy, Mount Holyoke College, 50 College St., South Hadley, MA 01075, mdyar@mtholyoke.edu, ²Johns Hopkins Applied Physics Laboratory, ³Jet Propulsion Laboratory, California Institute of Technology, jcutts@jpl.nasa.gov, ⁴NASA Glenn Research Center, ⁵School of Earth and Space Exploration, Arizona State University.

Brief Presenter Biography: Darby Dyar, senior author, is Professor of Astronomy at Mount Holyoke College, Senior Scientist at the Planetary Science Institute, and the current chair of the Venus Exploration Analysis Group (VEXAG). Jim Cutts, presenter, is a Program Manager in the Solar System Exploration Directorate at JPL and is a member of VEXAG, where he leads the Venus Exploration Roadmap Focus Group.

Introduction: Venus and Earth are often described as twins. Their sizes, densities, and elemental building blocks are nearly identical and they stand out as being considerably more massive than other terrestrial planetary bodies. Yet the Venus that has been revealed through past exploration missions is hellishly hot, devoid of oceans, apparently lacking plate tectonics, and bathed in a thick, reactive atmosphere. A less Earth-like environment is hard to imagine. How, why and when did Earth's and Venus's evolutionary paths diverge?

Resolving these questions will require an exploration program involving many different types of exploration platform – orbiters, probes, landers and aerial platforms. A single platform and a single mission will not suffice. In the 1970s and 1980s, more than 30 missions went to Venus and established much of what we know today. Although orbital exploration has continued with recent and planned missions by ESA, JASA, Russia, and now ISRO, no further *in situ* missions have been conducted by NASA since 1985.

VEXAG's Decade of Venus: To address the challenge of revitalizing the exploration of Venus, VEXAG has conducted the first major update of its strategic documents since they were created in 2014. The Goals, Objectives and Investigations (GOI) document (1) spells out the science drivers for Venus Exploration. The Venus Roadmap (2) described the platforms needed to realize these objective and the mission that would deliver them. The Venus Technology Plan (3) describes the key technical capabilities needed to enable the missions and hence accomplish the science. Current versions of these guiding documents mentioned here can be accessed from the VEXAG Website [1].

Finally, the Venus Mission Goal revision recrafts the primary science objectives desirable for large mission to Venus. It recommends that the Venus priority for New Frontiers class "large missions" in the next Decadal Survey be renamed simply "Venus Explorer" in

recognition of the wide variety of modern mission types that can address important Venus science questions.

Many of the technical capabilities needed for restarting Venus exploration by NASA are ready today. The completion of the Heatshield for Extreme Entry Environment Technology (HEEET) technology program has enabled *in situ* missions at Venus, with entry probes that are already ready to go. A radar orbital mission that can image the surface of the planet with an order of magnitude higher resolution than Magellan accomplished 25 years ago is also technically mature. Other orbital science missions with either conventional spacecraft or SmallSats and CubeSats are being considered.

Technologies with the ability to extend *in situ* observations from hours to months or even years will also be ready for flight in the next decade. High temperature electronics technology developed under NASA's Long Lived In Situ System Explorer project now permits surface missions that can acquire new kinds of scientific data without physical or chemical protection despite surface temperatures up to 460°C. Aerial platforms, which conduct observations in the lower temperature "habitable zone" in Venus clouds can conduct revolutionary *in situ* studies of the atmosphere as well as advancing knowledge of the interior through infrasound seismology, magnetometry and gravity measurements

These developments mean that the long hiatus in Venus exploration by the United State should soon end. The Decade of Venus envisages a series of missions involving multiple platforms that advances Venus science on a broad front. In formulating the details of this plan, VEXAG has engaged the scientific and technological communities. This presentation to IPPW2019 is part of the effort to solicit input and develop a compelling case for returning to Venus. It focuses on *in situ* platforms and describes the linkages between the science, the missions and the key technologies enabling them.

Although the focus of this effort has been largely on U.S. missions, the plan recognizes the importance and relevance of international collaboration for this the most accessible of the planets. In particular, it will be vital to ensure the use of common standards for relay communications for *in situ* missions, as has been the case for Mars. Ways in which synergistic observations by spacecraft from different nations can advance the science must also be explored.

References: [1] <https://www.lpi.usra.edu/vexag/>

MERCURY VAPOR RANKINE POWER CYCLE FOR A VENUS SURFACE LANDER – POSTER & PRESENTATION. Christopher J. Greer¹, Anastasia A. Timofeeva¹, Michael V. Paul², and Alexander S. Rattner¹.
¹Department of Mechanical and Nuclear Engineering, The Pennsylvania State University, University Park, PA 16802. Email: czg5155@psu.edu, aat5318@psu.edu, alex.rattner@psu.edu.
²Applied Physics Laboratory, John Hopkins University, Laurel, MD 20723. Email: michael.paul@jhuapl.edu

Introduction: Reports for a Venus [1] surface mission concepts and the National Research Council’s Decadal Survey [2] have identified the scientific value for landing on the surface Venus. However, the extreme environment and low solar availability on the surface impose power and cooling challenges for future missions. The opacity of the Venusian atmosphere limits the use of solar photovoltaic generators for the desired power range of hundreds of Watts [3]. Because of this low solar availability, stored energy sources are necessary to power surface landers [4]. While electrochemical batteries represent a mature power system option, they significantly limit mission scope. The longest duration mission on the Venus surface was Venera 13, at just over two hours. This time constraint was due to reliance on battery power and limited cooling capacity.

Therefore, extended mission duration concepts have focused on Radioisotope Thermal Generators (RTG) power plants. Due to the RTG’s dependency on plutonium 238, a RTG powered mission effectively requires a New Frontiers (\$600M – \$1B) or Flagship-class (\$2B+) mission budget. Low cost, power, and mass radioisotope power systems have been proposed to meet this need, but have not yet been demonstrated [5]. Recently, a metal-fueled, combustion-based power plant has been proposed as a low-cost alternative for extended duration missions [4]. On many planetary bodies, the atmosphere could be used as in-situ oxidizer for reactive metal fuels (e.g., CO₂ on Venus), significantly reducing carried mass requirements. The main benefit of a metal combustion-based power plant is the more than three times greater system specific energy when compared with sodium-sulfur batteries for a Venus mission [4]. Detailed surveys of available power systems and the benefits for metal combustion-based power plants have been performed [4], [6], [7].

Present Investigation: For these combustion-based power plants to be a success, hot operating temperature power conversion systems will be required. An experimental study, funded by the NASA Hot Operating Temperature Technology (HOTTech) program, is under way to test the conversion of combustion heat to electrical power with a high-temperature turbine power cycle. This program is designed to increase the TRL levels of technology for the Venusian environment.

This study, named HOTLINE (Hot Operating Temperature Lithium combustion for IN-situ Energy and

power), will determine the feasibility of a mercury vapor Rankine cycle for powering a Venus surface lander and experimentally validate models for hardware design. This system will be powered by simulating a high-temperature combustion heat source and will operate at a simulated environment with temperatures approaching Venus surface conditions. The system is designed to provide hundreds of watts of electrical power to the spacecraft for hundreds of hours. The goal of this study is to increase the TRL level of the HOTLINE power generation cycle from TRL 2 up to TRL 4-5.

The LARC experimental facility (Figure 1) is currently under construction at Pennsylvania State University. The first iteration of this facility will be able to test the complete mercury working fluid Rankine cycle at temperatures up to 330°C. The experimental facility is shown in Figure 1 and the components for the Rankine cycle installed in the oven are shown in Figure 2. Figure 3 shows the full plumbing and instrumentation diagram for the facility.



Fig 1. LARC stand with control box

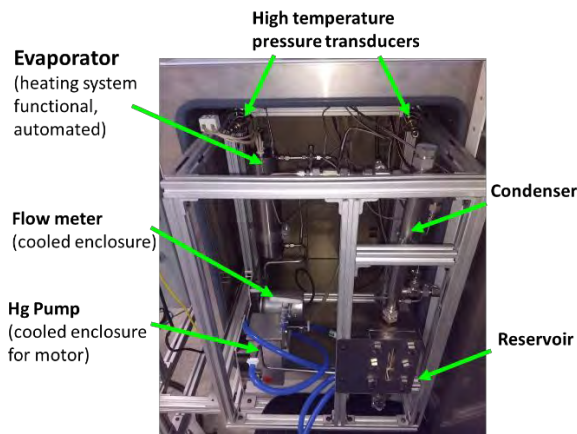


Fig 2. Rankine cycle components inside oven

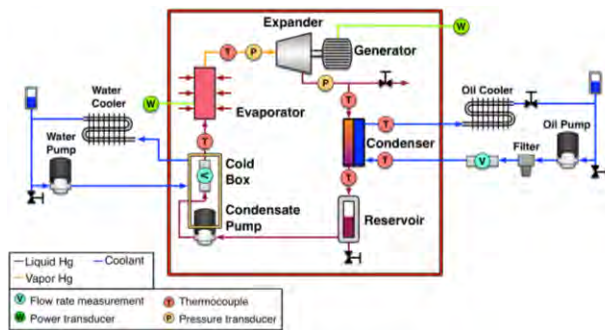


Fig 3. Rankine cycle diagram

A rotary vane expander is being designed for hot operating temperature conditions. Additionally collaborations with another HOTTEch study performed by Honeybee is underway to utilize their high temperature DC motor for Venus conditions.

Experimental data will be used to refine the system model and aid design of a future packaged prototype system. This combination of experimentation and modeling will enable the characterization of lithium combustion power and conversion technology for spacecraft applications.

Conclusions: The goal of the HOTLINE project is to experimentally demonstrate a complete power generation cycle with a mercury working fluid approaching Venus conditions. Current progress includes: analysis and selection of the working fluid (Mercury), experimental facility construction nearly complete and subsystems verified, rotary vane expander test stand construction complete, and performance measurements of the rotary vane expander in progress.

Experimental findings will be applied to validate and refine design models in support of future Venus power system technology maturation. With future technology maturation support, a rotary vane expander for a

mercury working fluid will be optimized for challenging hot operating temperature conditions, resulting in a complete, high-efficiency power generation system for extended duration Venus missions.

Acknowledgements: This work is supported through NASA's Planetary Science Division's HOTTECH funding.

References: [1] M. Bullock, J. L. Hall, D. A. Senske, J. A. Cutts, and R. Grammier, "Venus Flagship Study Report," National Aeronautics and Space Administration, Jet Propulsion Laboratory, Pasadena, California, 2009. [2] S. W. Squyers, "Vision and Voyages for Planetary Science in the Decade 2013-2022," Washington, DC, The National Academies Press, 2013. [3] G. a. Landis and E. Haag, "Analysis of solar cell efficiency for Venus atmosphere and surface missions," 11th International Energy Conversion Engineering Conference, vol. 2, no. V, Reston, Virginia: American Institute of Aeronautics and Astronautics, 2013. [4] T. F. Miller, M. V. Paul, and S. R. Oleson, "Combustion-based power source for Venus surface missions," *Acta Astronautica*, vol. 127, pp. 197–208, 2016. [5] J. F. Mondt, M. L. Underwood, and B. J. Nesmith, "Future Radioisotope Power Needs for Missions to the Solar System," in 32nd Intersociety Energy Conversion Engineering Conference, Honolulu, HI, USA, 1997, pp. 460–464. [6] T. Baker, T. F. Miller, M. Paul, and J. A. Peters, "The Use of Lithium Fuel with Planetary In Situ Oxidizers," in 10th Symposium on Space Resource Utilization, Grapevine, Texas, 2017, no. January, pp. 1–11. [7] Greer, C. J., Paul, M. V., & Rattner, A. S. (2018). Analysis of lithium-combustion power systems for extreme environment spacecraft. *Acta Astronautica*, 151(May), 68–79. <https://doi.org/10.1016/j.actaastro.2018.05.039>

Long-Duration Venus Probes and Landers

T. Kremic¹, M. S. Gilmore², G. W. Hunter¹, and C. M. Tolbert¹, ¹NASA Glenn Research Center (21000 Brookpark Rd., Cleveland, Ohio, 44135, USA or email at Tibor.Kremic@nasa.gov), ²Wesleyan University (45 Wyllys Ave, Middletown, Connecticut, 06459, USA, mgilmore@wesleyan.edu)

Brief Presenter Biography: Tibor Kremic is currently the Chief of the Space Science Project Office at NASA's Glenn Research Center. In this role he is responsible for the Centers' work in space science. Dr. Kremic has held various positions managing tasks, projects, and programs relating to technology development, science, and mission formulation. A prior program he managed was instrumental in developing entry system technologies that have applicability to probes and landers. One of his other current duties is serving as Principle Investigator for the Long-Lived In Situ Solar System Explorer, a project developing and long duration lander for Venus.

Introduction: Planetary probes have long been a tool used by scientists to gain early clues on environments and systems of new planetary targets. This not only fueled the scientific process but also helped prepare for future missions, such as landers, and helped ensure their success. Venus, Earth's sister planet, has been the target of more probes and landers than any other body in our solar system except for Earth and yet many fundamental questions are unanswered.

Challenge for Venus Surface Science: This lack of knowledge is a result of the challenging Venus environments [1]. Remote sensing of the surface and portions of the atmosphere is difficult at best [2] – [7] due to the thick layers of sulfuric acid clouds and the high pressure supercritical CO₂ atmosphere below those clouds. This has hampered the ability of orbiting missions to provide us insight into surface features and processes and thus hides potential clues on interior process from our view.

Surface probes and landers face an even more daunting challenge, which is the extreme temperature, pressure and unfriendly chemical composition of the near surface atmosphere. Over 10 assets have landed on the surface yet the longest surviving asset Venera-13 lasted only 127 minutes [1] before succumbing to the extreme temperature. While this and other landers provided valuable new data, the short life impacted ability to understand any temporal processes, for example meteorology, seismic active, and therefore very little is known about the interior and surface atmosphere interactions.

New Capability Offering Potential Solutions: Recent developments by NASA are offering hope of overcoming the technical challenges of surface operations and

life with the use of high temperature electronics and systems. Wide band gap, SiC based electronics have been demonstrated to function successfully for extended periods of time both at 500C, Venus surface temperatures as well as when temperature is combined with the reactive chemistry of the surface atmosphere and the high pressures (over 90 bar pressure at the surface). In addition to electronics a number of other subsystems are in development [8] including power in the form of high temperature batteries and power management devices, communications including antennas, transmitters and other components, materials [9], and structures and mechanisms. These are all activities under NASA's Long Lived In Situ Solar System Exploration (LLISSE) project. Other activities are also funded under NASA's HOTTech program.

Mission Applications and Concepts: One of the exciting opportunities these investments are making is in the form a complete, independent small long lived stations that can function on the surface of Venus for months. In fact under the LLISSE project tests of full scale engineering model hardware will occur and will demonstrate 2 months of operation in Venus conditions in NASA Glenn's GEER (Glenn Extreme Environment Rig) laboratory. Demonstration tests will occur in 2019, 2021 and finally a high fidelity engineering model test of full performance at Venus conditions by 2023.

These quickly evolving capabilities are changing the paradigm for Venus exploration, especially related to the surface and interior. Previous thinking was that long duration missions are decades out, which is no longer true. Evidence of the new opportunities is seen in the fact that just in the last year or so several funded studies have explored and developed mission concepts based around LLISSE and its capabilities. The joint Russia – US Venera-D study as assessed and baselined a 60 day long lived station (LLISSE) as part of the core mission that would entry and be mounted onto the much larger but short lived Venera-D lander [10] - [11]. One of the PSDS³ proposals selected for study was called SAEVe (Seismic and Atmospheric Exploration of Venus) [12] SAEVe built on the capabilities of LLISSE and other high temperature developments and generated a mission concept lasting 120 days. A third study, VBOSS [13] was one of two concepts funded by NASA to explore what compelling science a small mission (<\$200M) might be able to accomplish at Venus. This study also incorporated LLISSE capability, augmented with other

high temperature instruments and paired it with a small orbiter for synergistic science.

Conclusion: New technology and innovative operations approaches are opening up new opportunities to explore the deep Venus atmosphere and surface. This is changing the paradigm for Venus exploration in the next decade. Ongoing projects are quickly closing the gaps in preparation for a long-lived Venus lander. Demonstrations at Venus surface conditions are planned over the next couple of years culminating in high fidelity engineering model full scale test demonstrating performance and life. This paves the way for long duration Venus missions or mission elements in the mid 2020's and beyond.

References: [1] Linkin V. M. et al., (1986). *Sov. Astron. Lett.* 12, 40-42, 1986. [2] Garvin, J.B., et al., (1985). *JGR Solid Earth*, 90(B8), pp.6859-6871. [3] Ford, P.G. and Pettengill, G.H., (1992). *JGR Planets*, 97(E8), pp.13103-13114. [4] Campbell, B. and Campbell, D., (1992), *JGR Planets*, V97(E10), pp. 16293-16314. [5] Smrekar S, et al., *Science*, (2010). Vol. 328, Issue 5978, pp. 605-608. [6] Herrick, R. R. et al., (2012). *EOS*, 93, 125-126. [7] Mueller, N., et al., (2008). *JGR Planets*, 113(E5). [8] Neudeck, P. et al., *Physics Today*, (2017), <https://physicstoday.scitation.org/doi/10.1063/PT.3.3484>. [9] Costa, G., et. al., (2018). *Corrosion Science* 132, 260-271, 2018. [10] Venera-D JSDT. L. Zasova, et, al, (2017). *VEXAG 16th Meeting*, https://www.hou.usra.edu/meetings/vexag2018/pdf/vexag2018_program.htm. [11] Kremic, T., et al., (2017). *VEXAG 15th Meeting, Abstract #8*. [12] Kremic, T., et. al. LPS XLIX, Abstract #2744. [13] G. W. Hunter, V-BOSS: Venus Bridge Orbiter and Surface System Preliminary Report, Fifteenth Meeting of the Venus Exploration and Analysis Group (VEXAG), November 2017, https://www.lpi.usra.edu/vexag/meetings/archive/vexag_15/presentations/21-COMPASS-Venus-Bridge-Summary.pdf.

THE CUPID'S ARROW MISSION CONCEPT: HYPERVELOCITY SAMPLING IN THE UPPER ATMOSPHERE OF VENUS

Jason Rabinovitch¹, Arnaud Borner², Michael A. Gallis³, Christophe Sotin¹, and John Baker¹. ¹Jet Propulsion Laboratory, California Institute of Technology, 4800 Oak Grove Drive, Pasadena, CA, 91109, jason.rabinovitch@jpl.nasa.gov, ²STC at NASA Ames Research Center, MS 258-6 Moffett Field, CA, 94035, ³Sandia National Laboratories, P.O. Box 5800, Albuquerque, NM 87185.

Presenter Biography: Jason Rabinovitch is Mechanical Engineer in the Entry, Descent, and Landing & Formulation Group at the Jet Propulsion Laboratory, California Institute of Technology.

Introduction: Noble gases in planetary atmospheres are tracers of their geophysical evolution. They carry the fingerprints of processes driving atmospheric composition including original supply of volatiles from the solar nebula, delivery of volatiles by asteroids and comets, escape rate of planetary atmospheres, degassing of the interior, and its timing in the planet's history. However, a major observational missing link in our understanding of Venus' evolution is the elementary and isotopic pattern of noble gases and stable isotopes in its atmosphere, which remain poorly known [1]. The concentrations of heavy noble gases (Kr, Xe) and their isotopes are mostly unknown, and our knowledge of light noble gases (He, Ne, Ar) is incomplete and imprecise. NASA's community based forum, Venus Exploration Analysis Group (VEXAG), has placed a high priority on obtaining such measurements in its "Goals, Objectives, and Investigations" document (2014).

The Cupid's Arrow Mission Concept is small atmospheric probe that would sample Venus' atmosphere to measure the concentrations of noble gases and their isotopic ratios. Noble gases cannot be sensed remotely, and instead have to be measured in situ, below an altitude referred to as the homopause. Here atmospheric gases are well-mixed, and samples are representative of their naturally occurring concentrations. To date, planetary scientists have successfully made these challenging measurements at Earth, Mars, Jupiter and comet GC. An incomplete set of noble gases (Ar and Ne) were measured in Titan's atmosphere by the Huygens probe. The atmospheres of Saturn, Venus, and the Ice Giants, Uranus and Neptune, have not yet been explored in this fashion, leaving major gaps in our understanding.

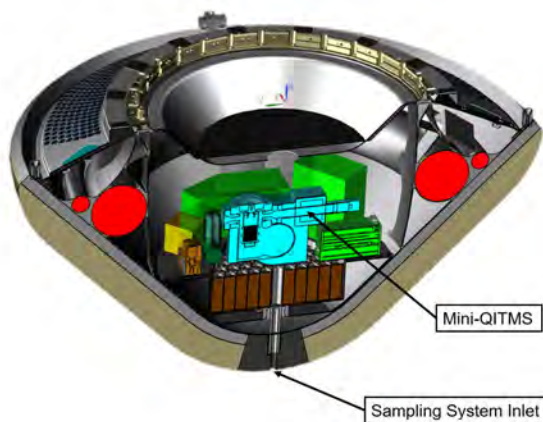


Figure 1: Possible spacecraft design for the Cupid's Arrow Mission Concept. A 45° sphere/cone aeroshell is shown, with the sampling system inlet located at the stagnation point of the vehicle.

Mission Concept: The Cupid's Arrow mission concept (Fig. 1) is a small atmospheric skimmer that would sample the Venus atmosphere below the homopause where the different atmospheric compounds are well mixed [2]. Four samples of Venus atmosphere would be acquired at periapsis, and then noble gas concentrations for each sample would be determined with a miniaturized Quadrupole Ion Trap Mass Spectrometer (QITMS) [3], [4]. A demonstration QITMS' ability to accurately measure noble gas concentrations can be found in [3]. The velocity at periapsis, where sampling is to occur, is expected to be ~10.5 km/s, and the altitude is expected to be ~110 km.

One potential issue with this mission architecture relates to whether or not a sample that is collected by the spacecraft is representative (from a composition standpoint) of Venus' atmosphere. Due to the high velocity of the spacecraft and associated high enthalpy of the flow, complicated thermodynamic and fluid mechanical processes occur around the spacecraft and associated sampling system. Therefore, it should be demonstrated that elemental and/or isotopic fractionation processes do not significantly alter the relative concentrations of the gas to be measured by QITMS. In order to address this topic, both experimental and modeling work is being performed, though this work will focus solely on modeling efforts.

Numerical Simulations: The Direct Simulation Monte Carlo (DSMC) code SPARTA [5], an open source software package developed by SANDIA National Laboratories², is used in this work. SPARTA, based on Bird's DSMC method [6], is a molecular-level gas-kinetic technique. As SPARTA is able to model hypervelocity reacting flows in strong chemical and thermal non-equilibrium, this software package is well suited to determine relevant flow properties for the Cupid's Arrow mission concept, and to numerically investigate the possibility of elemental and/or isotopic fractionation in the sampled gases.



Figure 2: Cross-section view of a simplified geometry for the sampling system with one sampling tank shown.

Preliminary simulations have been run for simplified spacecraft and sampling system geometries (Figs. 2-3) in both 2D axisymmetric and full 3D configurations. The high-enthalpy rarefied flow around the probe cause the gas to be in a state of thermal and chemical non-equilibrium. This allows

²<http://sparta.sandia.gov>, accessed 10/31/2018

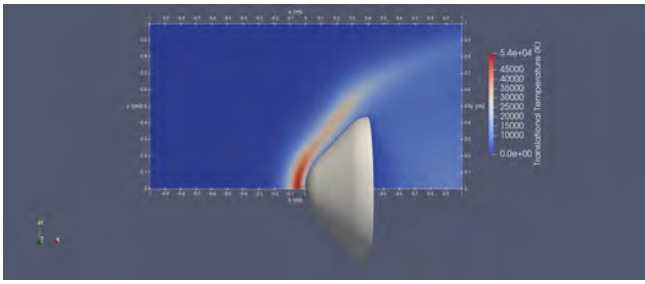


Figure 3: Preliminary translational temperature results for a 2D-axisymmetric simulation.

the Venus atmospheric gases to undergo chemical reactions as they travel through the thick bow shock in front of the vehicle, and form molecules that are not present in the original Venus atmosphere. Venus' atmosphere is dominated by CO_2 and N_2 . During sampling, other species, such as CO and O become dominant species, and additional species such as O_2 , N , and NO are formed. Having a list of predicted species in the sampling tanks is important for the interpretation of the eventual spectrograms produced by the mass spectrometer. The numerical simulations confirm that fractionation does happen during sampling. Fractionation can be quantified with the numerical simulations, and this effect can then be included in the performance model of the QITMS. Preliminary results show that while there is no significant isotopic fraction for Xe or Ar isotopes, the total ratio of Ar to Xe does change from the Venus atmosphere to the sampling tanks. The tank is enriched in Ar and Xe relative to the amount in Venus atmosphere. The enrichment is larger for Xe which is denser, than for Argon. As a result, the Xe/Ar ratio is 67% larger than in the Venus atmosphere, and this ratio remains constant as the tank is filled up. On the other hand, the isotope ratios are much less affected while the tank is filled (less than 5% for the $[40]\text{Ar}/[36]\text{Ar}$ and less than 1% for the $[128]\text{Xe}/[132]\text{Xe}$ - Fig. 4). As more results become available, the performance model will be improved. In particular, the Xe/Ar ratio will be varied to assess the fractionation effect at number densities closer to expected numbers in Venus' atmosphere. Preliminary results (Fig. 5) also predict that the spacecraft will have enough time during the sampling phase of the mission (~ 60 s) to acquire enough gas for QITMS. These preliminary results demonstrate that the mission should be able to handle the fractionation taking place during sampling and that enough sample can be acquired to perform the required measurements. Validation of the model will be performed by laboratory tests at the ArcJet facility at Ames Research Center.

Conclusions: Through a combination of numerical and experimental work, it is believed that a better understanding of the physical processes occurring during hypervelocity sampling in the upper atmosphere of Venus will be acquired. This knowledge will allow an optimized Cupid's Arrow spacecraft and sampling system to be designed, and also quantify the expected level of fractionation that is required to correct the observations. Numerical results will be compared against laboratory experiments in a forthcoming study.

Acknowledgments: Parts of this work have been performed at the Jet Propulsion Laboratory, California Institute of Technology, under contract to NASA. Sandia National Laboratories is a multi-mission laboratory managed and operated by National Technology and Engineering Solutions of Sandia, LLC, a wholly owned subsidiary of Honeywell International, Inc., for the U.S. Department of Energy's

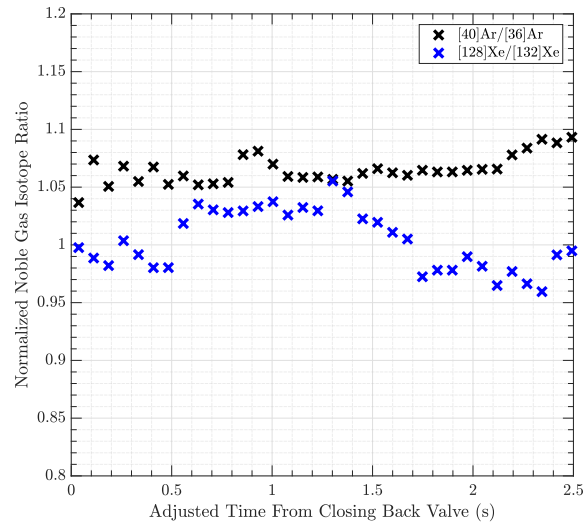


Figure 4: Preliminary fractionation predictions along the near-centerline of the sampling system.

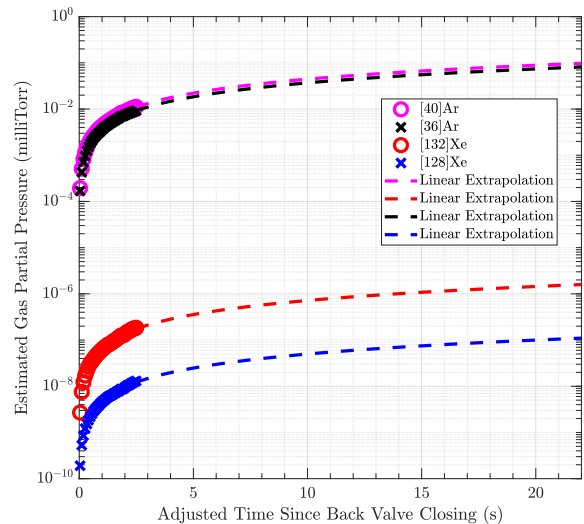


Figure 5: Preliminary predictions looking at tank fill times.

National Nuclear Security Administration under contract DE-NA0003525. The information in this abstract is pre-decisional and is presented for planning and discussion purposes only.

References:

- [1] E. Chassefière, R. Wieler, B. Marty, and F. Leblanc, "The evolution of venus: Present state of knowledge and future exploration," *Planetary and Space Science*, vol. 63-64, pp. 15 – 23, 2012, advances in Planetary Atmospheres and Exploration. [Online]. Available: <http://www.sciencedirect.com/science/article/pii/S0032063311001371>
- [2] C. Sotin, G. Avice, J. Baker, A. Freeman, S. Madzunkov, T. Stevenson, N. Arora, M. Darrach, G. Lightsey, and B. Marty, "Cupid's Arrow: A Small Satellite Concept to Measure Noble Gases in Venus' Atmosphere," in *49th*

Lunar and Planetary Science Conference, no. 1763, Mar. 2018. 1

- [3] G. Avice, A. Belousov, K. A. Farley, S. M. Madzunkov, J. Simcic, D. Nikolić, M. R. Darrach, and C. Sotin, “High-precision measurements of krypton and xenon isotopes with a new static-mode quadrupole ion trap mass spectrometer,” *Journal of Analytical Atomic Spectrometry*, 2018. [Online]. Available: <http://dx.doi.org/10.1039/C8JA00218E> 1
- [4] S. M. Madzunkov and D. Nikolić, “Accurate xe isotope measurement using jpl ion trap,” *Journal of The American Society for Mass Spectrometry*, vol. 25, no. 11, pp. 1841–1852, Nov 2014. 1
- [5] M. A. Gallis, J. R. Torczynski, S. J. Plimpton, D. J. Rader, and T. Koehler, “Direct simulation monte carlo: The quest for speed,” *AIP Conference Proceedings*, vol. 1628, no. 1, pp. 27–36, 2014. [Online]. Available: <https://aip.scitation.org/doi/abs/10.1063/1.4902571> 1
- [6] G. Bird, *Molecular Gas Dynamics and the Direct Simulation of Gas Flows*. Clarendon Press, 1994. 1

BALLOON-BORNE INFRASOUND AS A REMOTE SENSING TOOL FOR VENUS – PROGRESS IN 2018. S. Krishnamoorthy¹, A. Komjathy¹, J. A. Cutts¹, M. T. Pauken¹, D. C. Bowman², L. Martire³, R. F. Garcia³, D. Mimoun³, J. M. Jackson⁴

¹ Jet Propulsion Laboratory, California Institute of Technology, Pasadena, CA

² Sandia National Laboratories, Albuquerque, NM

³ Institut Supérieur de l'Aéronautique et de l'Espace (ISAE), Toulouse, France

⁴ Seismological Laboratory, California Institute of Technology, Pasadena, CA

Brief Presenter Biography: James A. Cutts is Program Manager in the Solar System Exploration Directorate at NASA's Jet Propulsion Laboratory (JPL), California Institute of Technology and is responsible for the development and demonstration of advanced concepts for solar system exploration. A major focus of this effort is planetary aerobots or robotic balloons. Prior to joining JPL, Cutts was Manager of the Planetary Science Institute of Science Applications International Corporation and a scientific investigator with the Mariner 9 and Viking Orbiter Imaging teams. He was also the Program Manager for Advanced Concepts and Deputy Director of the Center for Space Microelectronics Technology, from 1988 to 1991. He has served as Chair of NASA's Sensor Working Group from 1988 to 1990 and has served on other NASA and U.S. Air Force advisory committees. He has authored approximately 50 papers in planetary science, sensor technology and innovative space mission concepts. He holds a BA in Physics from Cambridge University, a MS degree (Geophysics) and Ph.D. (Planetary Science) from Caltech and a Certificate from UCLA's Executive Management Program.

Introduction: Over five decades have passed since the Mariner spacecraft visited Venus in 1962, but its interior structure remains unexplored. This is in large part due to the technological challenges in exploring Venus posed by its extremely high surface temperature and pressure conditions [1]. These adverse conditions have thus far rendered long-duration experiments on or near the surface impossible. Therefore, while Mars has hosted a fleet of rovers on the surface and the InSight lander has commenced seismology experiments, a similar experiment on Venus is decades away. In this presentation, we will explore the possibility of performing planetary science on Venus using infrasound (pressure waves with frequencies less than 20 Hz) as a remote sensing tool and discuss the progress our group has made in the last year.

Infrasound and Atmospheric Remote Sensing: Infrasound has been recorded from a variety of events on Earth. Of particular interest to planetary science are infrasound signals from quakes, volcanic eruptions, thunderstorms, and meteors [2,3,4,5]. While infrasound generation from quakes relies on the coupling between

the solid planet and the atmosphere, in the case of volcanic eruptions, thunderstorms, and meteors, energy is directly deposited into the atmosphere. Venus offers a unique opportunity for the use of infrasound as an investigative tool – due to its dense atmosphere, energy from seismic activity couples with the Venusian atmosphere up to 60 times more efficiently than Earth [6]. As a result, infrasound waves from Venusquakes are expected to be an almost exact replica of ground motion. Infrasound is also known to propagate long distances from generating events with relatively little attenuation, thereby making it an effective alternative to placing sensors on the surface of Venus. Lastly, acoustic sensors used to capture infrasound may also be used to investigate low-frequency, large-scale planetary atmospheric features such as planetary-scale gravity waves, which have recently been observed by JAXA's Akatsuki mission [7].

Balloon-based Infrasound Detections on Venus: The main advantage of performing balloon-based infrasound science on Venus is the extension of mission lifetimes by virtue of being in a more benign environment. Compared to 460 C temperature and 90 atmospheres pressure on the surface, atmospheric conditions are more Earth-like at 55-60 km altitude on Venus. Further, acoustic sensors greatly benefit from being on a platform that floats with the wind, leading to higher coverage and lower wind noise. Krishnamoorthy et al. [8, 9] recently showed that acoustic waves from artificially generated seismic signals can be detected from balloons, show the same spectral character as epicentral ground motion, and can be utilized to geolocate seismic activity by using an array of airborne barometers.

From a scientific perspective, there are also several challenges with performing such an experiment. Signals are often weak compared to the noisy background. Multi-channel correlation is difficult, since balloon platforms have payload restrictions and cannot feasibly support a large number of instruments. In the presence of a variety of infrasound-generating events, source discrimination and localization also represent challenges that need to be overcome.

Progress in 2018: Our team has been involved in a campaign to use the Earth's atmosphere as an analog

testbed for Venus to demonstrate the feasibility of balloon-based infrasound science on Venus and address the challenges associated with it.

In 2018, we focused our efforts on understanding the infrasound background on Earth for event discrimination, detecting stronger sub-surface seismic events, and sensor miniaturization. In July 2018, we conducted a stratospheric balloon flight as a secondary payload on a NASA Long-Duration balloon from Sweden to Canada. The recorded signal showed significant reduction in background noise in the Earth's stratosphere. Further, the recorded data are being examined for infrasound signals from events such as meteors, auroral activity, and ocean microbarom activity. In September 2018, we conducted the first successful demonstration of the "vector infrasound instrument" concept, which incorporates knowledge of the balloon's dynamic response to an arriving infrasound wave to determine its direction of arrival using a single station as opposed to an array of sensors. The development of a single-station instrument greatly reduces the mass, power and deployment requirements for an eventual Venus balloon-based seismic infrasound experiment. In December 2018, we conducted a balloon overflight of sub-surface chemical explosion at Nevada National Security Site (NNSS) in an attempt to record infrasound from seismic activity generated as a result of the explosion. Concurrently, we have been developing and refining coupled seismo-acoustic simulation techniques, which help simulate ground motion scenarios and generate expected signal profiles for the balloon [10]. Such simulation studies help us better understand the infrasound background at a lower cost than expensive balloon flight tests.

In this presentation, we will share a progress report using results from multiple flight tests and simulation studies in the past year. Further, we will present our plans for the future, which include balloon flights over naturally occurring quakes in the State of Oklahoma to demonstrate the detection of natural seismic activity from the stratosphere. The success of this remote sensing technique can greatly accelerate the study of Venus' interior by circumventing the need to use high-temperature electronics.

References:

[1] Wood, A. T., R. B. Wattson, and J. B. Pollack (1968), Venus: Estimates of the surface temperature and pressure from radio and radar measurements, *Science*, **162** (3849), doi:10.1126/science.162.3849.114.

[2] Arrowsmith, S. J., R. Burlacu, and K. Pankow et al. (2012), A seismoacoustic study of the 2011 January 3

Circleville earthquake, *Geophysical Journal International*, **189** (2), doi:10.1111/j.1365-246X.2012.05420.x.

[3] Matoza, R. S., A. Jolly, and D. Fee et al. (2017), Seismo-acoustic wavefield of strombolian explosions at yasur volcano, Vanuatu, using a broadband seismo-acoustic network, infrasound arrays, and infrasonic sensors on tethered balloons, *The Journal of the Acoustical Society of America*, **141** (5), doi:10.1121/1.4987573.

[4] Farges, T. and E. Blanc (2010), Characteristics of infrasound from lightning and sprites near thunderstorm areas, *Journal of Geophysical Research: Space Physics*, **115**(A6), doi:10.1029/2009JA014700.

[5] Donn, W. L. and N. K. Balachandran (1974), Meteors and meteorites detected by infrasound, *Science*, **185**(4152), doi:10.1126/science.185.4152.707.

[6] Garcia, R., P. Lognonné, and X. Bonnin (2005), Detecting atmospheric perturbations produced by Venus quakes, *Geophysical Research Letters*, **32** (16), doi:10.1029/2005GL023558.

[7] Fukuhara, T., M. Futaguchi, and G. L. Hashimoto et al. (2017), Large scale stationary gravity wave in the atmosphere of Venus, *Nature Geosciences*, **10**, doi:10.1038/ngeo2873.

[8] Krishnamoorthy, S., A. Komjathy, and M. T. Pauken et al. (2018), Detection of artificial earthquakes from balloon-borne infrasound sensors, *Geophysical Research Letters*, **45** (8), doi: 10.1002/2018GL077481.

[9] Krishnamoorthy, S., V. Lai, and A. Komjathy, et al. (2019), Aerial seismology using balloon-based barometers, *under review*, *IEEE Transactions on Geoscience and Remote Sensing*.

[10] L. Martire, Brissaud Q., and V. Lai et al. (2018), Numerical simulation of the atmospheric signature of artificial and natural seismic events, *Geophysical Research Letters*, **45**(21), doi: 10.1029/2018GL080485.

ALTITUDE-CONTROLLED BALLOON CONCEPTS FOR VENUS & TITAN - ENERGY, MASS, AND STABILITY TRADEOFFS

Jacob S. Izraelevitz, Jonathan M. Cameron, Michael T. Pauken, and Jeffery L. Hall. NASA Jet Propulsion Laboratory, California Institute of Technology (4800 Oak Grove Drive, Pasadena, CA 91109, jacob.izraelevitz@jpl.nasa.gov, michael.t.pauken@jpl.nasa.gov, jonathan.m.cameron@jpl.nasa.gov, jeffery.l.hall@jpl.nasa.gov)

Brief Presenter Biography: Dr. Jacob Izraelevitz is a robotics technologist at the NASA Jet Propulsion Laboratory in the Extreme Environments Robotics Group. Jacob holds a Ph.D. in experimental fluid mechanics and maintains research interests in controls, unsteady flows, and mechanical design.

Introduction: Long-duration aerobots are a promising mission platform for the hazy atmospheres of Venus and Titan, as they offer persistent in-situ access to the atmosphere and global-scale mobility. Furthermore, surface phenomena can still be investigated by probes deployed from the aerobot or indirectly from airborne sensors, such as Venus-quake induced pressure signals or low-altitude Titan imagery. Scientific ballooning has a long history on Earth, but the first non-terrestrial balloons flew in 1985 as part of the Soviet Union's two VEGA missions to Venus – each carried an identical superpressure balloon designed to passively maintain a single altitude of 54km with a 7kg payload [1]. Subsequent NASA mission proposals for Venus aerobots have often employed a similar single-altitude architecture, though with much larger payloads and more ambitious science goals [2-3].

However, the recent Venus Aerial Platforms [4] report has concluded that there is a science sweet-spot for Venus aerobot mission employing *variable* altitude balloons. This recommendation acknowledges recent terrestrial progress on long-duration variable altitude balloons that can be precisely controlled, which no longer require expendable ballast, venting, or hot air to adjust altitude. Beyond simply adjusting the altitude to sample different atmospheric layers, this precise control can also be used to direct the flight when winds vary in speed and direction with altitude. On Venus, the dominant winds “orbit” every 5-6 Earth-days, but some north/south control may be possible. On Titan, variable altitude aerobots may be able station-keep over an area of interest using circulating winds.

A number of these architectures have been demonstrated on Earth with considerable success, all of which could conceivably be adapted for Venus or Titan missions:

1. Helium Pump: A pump transfers helium between pressurized and unpressurized reservoirs, adjusting the total buoyancy [5].

2. Helium Compression: A single helium balloon is squeezed like an accordion to adjust the total buoyancy [6].
3. Air ballast: External atmospheric gas is pumped into a pressurized reservoir to add weight, while a separate unpressurized helium balloon provides buoyancy [7].
4. Air ballonet: A single balloon contains both helium and atmospheric gases, with internal membrane to separate them [8].

Objective: The objective of this study is to determine what variable-altitude balloon architectures, and at what altitude ranges, are suitable engineering implementations that can meet the science goals of the planetary science community on Venus and Titan.

Methodology: We evaluate all four of these concepts with first-order analytic models and compare their relative advantages. Scaling laws are derived for the power, mass, and loading using representative Venus and Titan atmospheric models and balloon material properties.

Results: We present detailed point designs for each concept on Venus and Titan, targeting a 100-200kg payload gondola below the balloon. Tradeoffs between altitude stability, delivery mass, and power are discussed.

Acknowledgements: The research described in this paper was funded by the Jet Propulsion Laboratory, California Institute of Technology, under a contract with the National Aeronautics and Space Administration.

References:

- [1] Huntress, Wesley T., and Mikhail Ya Marov. Soviet Robots in the Solar System: Mission Technologies and Discoveries. Springer Science & Business Media, 2011.
- [2] Klaasen, K. P., and R. Greeley. "VEVA Discovery mission to Venus: exploration of volcanoes and atmosphere." *Acta Astronautica* 52.2-6 (2003): 151-158.
- [3] Balint, T. S., and K. H. Baines. "Nuclear polar VALOR: an ASRG-enabled Venus balloon mission concept." AGU Fall Meeting Abstracts. 2008.
- [4] Venus Aerial Platforms Study Team, “Aerial Platforms for the Scientific Exploration of Venus”, JPL D-102569, October, 2018.

[5] Voss, Paul. "Advances in Controlled Meteorological (CMET) balloon systems." AIAA Balloon Systems Conference. 2009.

[6] de Jong, M. L. "Venus altitude cycling balloon." Venus Science Priorities for Laboratory Measurements. Vol. 1838. 2015.

[7] World View Enterprises. <https://worldview.space/> (Retrieved March 2019).

[8] Loon LLC. "Project Loon." <https://loon.co/> (Retrieved March 2019).

ADVANCES IN MECHANICAL COMPRESSION ALTITUDE CONTROL BALLOON TECHNOLOGY FOR VENUS AND TITAN.

M. de Jong¹, J. Thomas¹, and J. Cutts², ¹Thin Red Line Aerospace Ltd. (Chilliwack, Canada, maxim@thin-red-line.com), ²Jet Propulsion Laboratory, California Institute of Technology (Pasadena, CA, james.a.cutts@jpl.nasa.gov).

Brief Presenter Biography: Maxim de Jong is CEO and Chief Engineer at Thin Red Line Aerospace, (TRLA) a company specializing in softgoods development for manned and robotic space exploration.

Introduction: Significant science benefit is derived from persistent operation of a buoyant atmospheric vehicle in the atmospheres of Venus and Titan. This benefit is immensely augmented if the vehicle presents active mobility through precise control of its ascent and descent—especially if this control can be maintained over great altitude range, thereby additionally facilitating lateral navigation by taking advantage of favorable winds at different altitudes. Such an aerial platform represents a sweet spot in a trade of science merit, cost, and complexity [1].

TRLA has developed a robust, rapid altitude control, lighter-than-air vehicle. Ascent and descent is initiated and maintained by means of lifting gas density modulation through mechanical compression (*Figure 1, left*), while the balloon's accordion-like envelope simultaneously allows the lifting gas volume to adapt to atmospheric density throughout a very significant range of trajectory altitudes.

In December 2016 TRLA performed a successful proof of concept test flight of the proprietary mechanical compression ACB system (*Figure 1, right*).

An Advanced Altitude Control Balloon Testbed: This paper and associated presentation outline the most recent activities and objectives pertaining to development of TRLA's next generation, mechanical compression superpressure balloon. This terrestrial "analogue" aerial platform serves as advanced testbed to extend and adapt Altitude Control Balloon (ACB) technology for potential Venus and Titan mission insertion [2] [3]. The final build of this testbed ACB is progressing at time of writing.

Testbed Objectives: The advanced mechanical compression testbed is a high-fidelity, third generation ACB flight vehicle. As outlined in the associated poster session of the current IPPW [4], the ACB platform presents a broad range of hardware and software design advances that are specifically relevant to detailed consideration and evaluation in the context of Venus and/or Titan mission requirements. These design attributes are intended to foster sufficient insight to expedite design extrapolations to ultimate operational environments.

Beyond the aforementioned hardware advances, the scale and fidelity of the advanced ACB testbed will enable commensurately high-fidelity data acquisition to further insights and advance capabilities pertaining to:

1. Structural analysis of the multi-segment envelope for an operational range of envelope compression.
2. Test-anchored analytical correlation of mechanical compression force, super-pressure, and energy expenditure.
3. Flight dynamics and trajectory modeling.
4. Flight test anchored analytical correlation of super-pressure and ascent/descent velocity.
5. ACB platform compression, packaging, and deployment (COMPAD). Investigation of long duration "hard" packaging for planetary transit; post-entry in-flight system deployment and inflation.
6. Despite incorporating materials for terrestrial flight, the high-fidelity nature of the testbed envelope will provide invaluable insights w.r.t. material system response to cyclic compression.

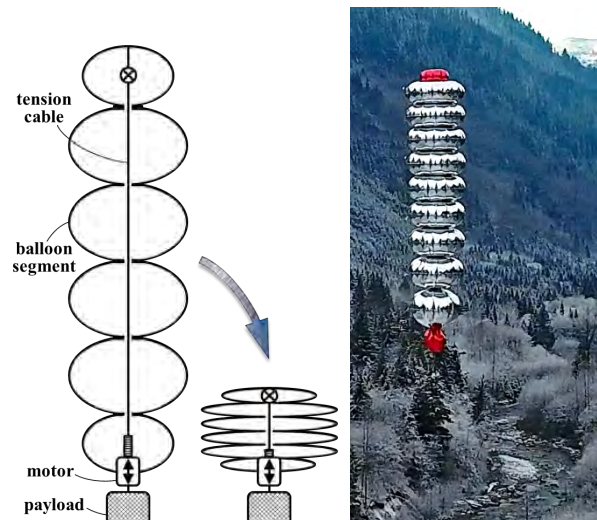


Figure 1. Thin Red Line mechanical compression Altitude Control Balloon (ACB) [5].

Flight Objectives: The ACB envelope comprises ten segments for a total distended volume of 14m³ (500ft³), 9.5m (31ft) height, and 1.6m (5.2ft) diameter. A primary end objective of the advanced ACB testbed is to demonstrate precise and continuous semi-autonomous control of flight altitude from ground level to 5500

meters (18,000 ft) above sea level, as well as throughout descent and return to ground level. Rapid appropriate response to pre-programmed altitude control directives will be sought, along with demonstration of the platform's inherent robustness, and simplicity of design, fabrication, and operation.

Acknowledgements: The advanced mechanical compression ACB flight system and associated research described in this paper is funded in whole by Thin Red Line Aerospace Ltd. as a technology demonstration and flight hardware development platform supporting future planetary missions.

References: [1] Cutts et al. "Aerial Platforms for the Scientific Exploration of Venus". Cutts et al, 2018. [2] De Jong, M., "Venus Altitude Cycling Balloon", Venus Lab and Technology Workshop, paper 4030. 2015. [3] De Jong, M. and Cutts, J., "Titan Altitude Cycling Balloon" IPPW-12, 2015. [4] Thomas, J., "Altitude Control Balloon Testbed for Planetary Atmospheres" IPPW-2019. [5] de Jong, M. "Systems and Methods including Elevation Control." U.S. Patent No. 10,196,123. 2019.

SAMPLING TITAN'S SURFACE WITH DRAGONFLY.

R. D. Lorenz¹, F. Rehnmark², T. Costa², J. Sparta², B. Yen², K. Zacny², ¹Johns Hopkins Applied Physics Laboratory, Laurel, MD (ralph.lorenz@jhuapl.edu), ²Honeybee Robotics (zacny@honeybeerobotics.com).

Brief Presenter Biography: Dr Ralph Lorenz worked in ESA on the Huygens probe to Titan, and is presently the project scientist for the Dragonfly Phase-A study at APL : he has participated in every IPPW. His interests center on planetary surface/atmosphere interactions, and on how spacecraft and instruments operate in planetary environments. He is author of eight books as well as over 300 publications in refereed and popular journals..

Introduction: Dragonfly [1,2,3] is a relocatable lander concept for Titan, using 8 rotors to effect atmospheric flight to permit exploration of a diverse range of sites on an organic-rich Ocean World. Dragonfly is presently under evaluation by NASA as one of two candidates for the New Frontiers 4 competition, with launch foreseen in 2025 and Titan arrival in 2034. A key science objective is to analyze surface material for prebiotic compounds using a sophisticated mass spectrometer (MS) [4]. A drill is mounted on each landing skid, and surface material is conveyed pneumatically [5] (using Titan ambient air driven by a centrifugal blower) to a sample delivery carousel derived from that used on MSL/Curiosity. Diverter valves (Fig.1) permit the selection of either drill as the source, delivery to a laser desorption (LD) or gas chromatography (GC) front end to the MS, and the use of either of two redundant blowers

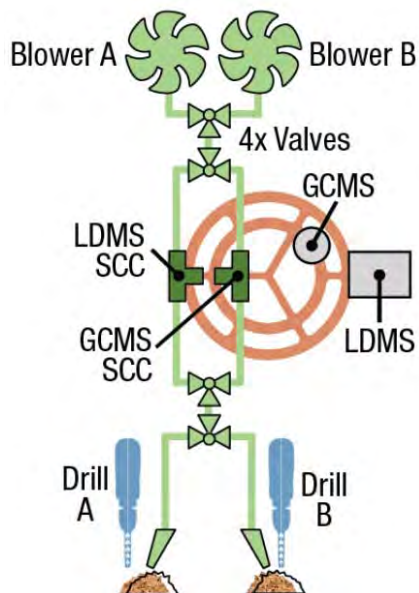


Figure 1. The Dragonfly sampling architecture provides flexibility and redundancy.

In addition to providing flexible operations (e.g. two different sample sites at one landing location without repositioning) the pneumatic transfer is very rapid and maintains the samples at ambient temperatures.

Recent Developments: Extensive testing of pneumatic transfer shows good results with a wide range of materials [5,6], including ice ‘bedrock’, organic and inorganic powders, and sticky oil/sand mixtures. A flight-like drill has been prototyped and tested on Titan materials including ice, frozen ammonia solution and organics [7] in a cold nitrogen bath at ~90K, and end-to-end sample delivery has been reliably demonstrated to a novel ‘deflector cup’ [5] which facilitates sample metering and presentation to the GCMS/LDMS instruments with minimal crosstalk between successive samples.

Operations Concept: Dragonfly’s other instrumentation [3] will provide elemental composition and surface physical properties (thermal, dielectric) soon after landing at each site, together with imaging at a variety of scales (including close-ups of the ground at the drill sites). The drill can be used to interrogate the surface via drill currents and the texture of cuttings. These data can inform the decision of which (if any) drill to sample. Multiple samples can be extracted from a single hole, to permit e.g. both LDMS and GCMS analyses, or to explore possible composition gradients. As with MSL, ‘throwaway’ samples can be acquired by drill/blower operation (without a cup in place in the sample collection chamber [SCC]) to ‘scrub’ the inner surfaces of the sampling system.

References: [1] dragonfly.jhuapl.edu [2] Turtle E.P. *et al.* (2018) Dragonfly: In Situ Exploration of Titan's Organic Chemistry and Habitability *LPSC 49*, #1641 [3] Lorenz R.D. *et al.* (2018) Dragonfly : A Rotorcraft Lander Concept for Scientific Exploration at Titan *APL Tech Digest*, 34(3), 374–387 [4] Trainer, M. *et al.*, *LPSC 49*, #2586 [5] Zacny, K. *et al.* (2019) Application of Pneumatics in Delivering Samples to Instruments on Planetary Missions, *IEEE Aerospace Conference*. [6] Sparta, J. *et al.* (2018) IPPW [7] Sparta, J. *et al.* (2018) Experimental Analysis of the Outer Solar System Workshop #3008

Additional Information: This work is supported in part by the NASA ColdTech Program.

Acknowledgments: The authors gratefully acknowledge the support of NASA as well as by the members of the Science Study Team, F. Ferri, A. Masters, O. Mousis and D. Turrini.

References: [1] *Ice Giants Pre-Decadal Study Final Report*, JPL D-100520, June 2017. [2] *CDF Study Report Ice Giants CDF-187(A) European Space Agency, December 2018*. [3] *CDF Study Report PEP (Planetary Entry Probe). CDF-106 European Space Agency, July 2010*.

THE DEEP COMPOSITION OF URANUS AND NEPTUNE FROM MASS SPECTROMETRY AND THERMOCHEMICAL MODELING.

T. Cavalié^{1,2}, O. Venot³, R. Bounaceur⁴, J. Leconte¹, M. Dobrijevic¹, V. Hue⁵, Y. Miguel⁶, P. Wurz⁷ and O. Mousis⁸,
¹Laboratoire d'Astrophysique de Bordeaux (Allée Geoffroy St Hilaire 33600 Pessac, France, thibaut.cavalié@u-bordeaux.fr), ²Laboratoire d'Études Spatiales et d'Instrumentation en Astrophysique (Meudon, France), ³Laboratoire Interuniversitaire des Systèmes Atmosphériques (Créteil, France), ⁴Laboratoire Réactions et Génie des Procédés (Nancy, France), ⁵Southwest Research Institute (San Antonio, TX, USA), ⁶Leiden Observatory (Leiden, The Netherlands), ⁷Berne University (Berne, Switzerland), ⁸Laboratoire d'Astrophysique de Marseille (Marseille, France).

Brief Presenter Biography: Dr. Thibault Cavalié is a CNRS research scientist at the Laboratoire d'Astrophysique de Bordeaux (LAB), and he is also affiliated with the Laboratoire d'Études Spatiales et d'Instrumentation en Astrophysique (LESIA) of the Paris Observatory. From 2015 to 2018, he was a CNRS research scientist at LESIA. He works on the formation and evolution of the Giant Planets by means of ground-based (ALMA) and space-based (Herschel) submillimeter observations, and photochemical and thermochemical modeling. He is a co-investigator of the Submillimetre Wave Instrument of the Jupiter Icy Moons Explorer. He is co-lead of the "Jupiter atmosphere" Working Group at the European Space Agency for the JUICE mission.

Dr. Cavalié has undergraduate degrees in Physics in 2003, a Master's degree in Physics in 2005, and a PhD in Astrophysics, Plasmas and Particles in 2008, all from the Bordeaux University. He has completed a Habilitation degree in 2018 at the Paris Observatory.

Introduction: The determination of the deep composition in the giant planets is an outstanding question as it bears implications on their formation processes. The situation is even worse for the Ice Giants as they have never been visited by an orbiting spacecraft and/or an atmospheric entry probe, though they seem to be a common type of planets in our Galaxy.

The abundances of heavy elements are key to understand the way these planets formed. For instance, oxygen was mainly carried by water beyond the snowline in the Solar System at the time of Giant Planet formation. As ices are responsible for the trapping of the other heavy elements, it is important not only to measure the heavy element abundances themselves, but also to understand under which form water condensed, either amorphous or crystalline, to constrain the deep oxygen abundance. The trapping of heavy elements in clathrates indeed requires a significantly larger initial water abundance than amorphous ice for similar heavy element enrichments.

In Uranus and Neptune, the deep tropospheric water will probably remain out of reach for remote sensing and in situ measurements as it condenses already at several hundred bars. In this paper, we will investigate how mass spectrometry performed by an in situ exploration probe could help shed light on the deep composition of

Uranus and Neptune, and on their deep oxygen abundance in particular, by combining the measurements with thermochemical modeling to link upper tropospheric measurements with deep tropospheric elemental abundances.

KEY ATMOSPHERIC SIGNATURES FOR DECIPHERING THE FORMATION CONDITIONS OF URANUS AND NEPTUNE IN THE PROTOSOLAR NEBULA.

O. Mousis. Aix Marseille Univ, CNRS, LAM, Marseille, France, Olivier.mousis@lam.fr.

Brief Presenter Biography: Prof. Olivier Mousis is a planetary scientist at Aix-Marseille Université/Laboratoire d'Astrophysique de Marseille, specializing in the field of solar system formation. He heads a team of 23 planetary and exoplanetary scientists at the Laboratoire d'Astrophysique de Marseille. His research is focused on the formation conditions of giant planets, satellites, and small bodies derived from measurements by spacecraft missions. Mousis has been PI of two Saturn probe proposals submitted to the ESA M4 and M5 calls, and is author or co-author of more than 180 refereed papers.

Introduction: The ice giant planets Uranus and Neptune represent a largely unexplored class of planetary objects, which fills the gap in size between the larger gas giants and the smaller terrestrial worlds. Uranus and Neptune's great distances have made exploration challenging, being limited to flybys by the Voyager 2 mission in 1986 and 1989, respectively. Uranus and Neptune are fundamentally different from the better-known gas giants Jupiter and Saturn. Interior models generally predict a small rocky core, a deep interior of 70% of heavy elements surrounded by a more diluted outer envelope with a transition at $\sim 70\%$ in radius for both planets. Uranus and Neptune's envelopes display substantial carbon enrichments, ranging from 20 to 120 times the protosolar value, suggesting global metallicities much higher than those of Jupiter and Saturn.

To derive some hints on their formation conditions, we investigate the possible reservoirs of volatiles that may have contributed to the compositions of Uranus and Neptune's atmospheres in both solid (amorphous ice, pure condensates, clathrates) and gas forms. We then discuss the atmospheric signatures that would be representative of each of these reservoirs, and that are potentially accessible to in situ measurements by an entry probe.

ICE GIANT AEROCAPTURE USING LOW-L/D AEROSHELLS: UNCERTAINTY QUANTIFICATION AND RISK ASSESSMENT. A. Pradeepkumar Girija^{1†}, S. J. Saikia^{2†}, and J. A. Cutts³, apradee@purdue.edu, ssaikia@purdue.edu, [†]School of Aeronautics and Astronautics, Purdue University, 701 W. Stadium Ave., West Lafayette, IN, 47907, ³NASA-Caltech Jet Propulsion Laboratory, 4800 Oak Grove Drive, Pasadena, CA, 91109, james.a.cutts@jpl.nasa.gov.

Brief Presenter Biography: Athul Pradeepkumar Girija is a Ph.D. candidate in School of Aeronautics and Astronautics at Purdue University. He obtained his Bachelors and Masters degrees in Aerospace Engineering from the Indian Institute of Technology, Madras. His Ph.D. dissertation work supervised by Dr. Saikia focuses on the development of a novel systems framework and software tool for aerocapture mission analysis. He is particularly interested in Venus and ice-giant mission concepts and science investigations.

The “Ice Giant” Planets: Uranus and Neptune are fundamentally different from gas giants and terrestrial planets and remains the only class of planets to not have a dedicated mission. Our knowledge is most lacking for ice giants, and most exoplanets discovered so far appear to be ice giant size. The Planetary Science Decadal Survey 2013 has identified an ice giant mission as the third highest priority for Flagship-class after Mars Sample Return and Europa orbiter [1]. It is anticipated that an ice giant mission will be flown in the next decade.

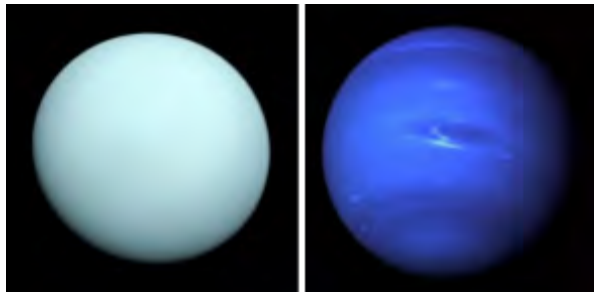


Figure 1: Uranus and Neptune, imaged by the Voyager 2 spacecraft in 1986 and 1989 respectively [2].

Preparing for the 2023 Decadal Survey: In 2016, JPL led the NASA Ice Giants Pre-Decadal Study to investigate candidate mission architectures [3]. The mid-term review of the 2013 Decadal Survey recommends that NASA performs a new mission study to determine if a more broad-based set of science objectives can be met within a \$2 billion cost cap. Aerocapture can greatly increase the science return and allow mission design flexibility for ice giant missions. Comprehensive analysis of the feasibility, benefit, and risk assessment of ice giant aerocapture is lacking in literature [4]. The present study will inform the upcoming decadal survey and allow the planetary science community to quantitatively assess the risk and readiness of aerocapture for an ice giant mission.

Mission Design Challenges: Due to the large heliocentric distance, reaching the ice giants with an acceptable transit time and sufficient delivered mass is a significant mission design challenge. Nominal flight times to Uranus and Neptune are 11 and 13 years respectively (with SEP stage for Neptune), which would allow 2–3 years for the science mission. The high orbit insertion ΔV and associated propellant mass severely limits the time-of-flight and delivered mass.

In contrast to propulsive orbit insertion, aerocapture allows for a much larger range of arrival velocities, which allows for a broader range of interplanetary trajectories. Thus a mission designer can potentially reduce the time-of-flight, increase delivered mass, or use a cheaper launch vehicle.

Ice Giant Aerocapture Assessment (2016): An assessment of aerocapture for ice giant missions was performed at Purdue University in support of the NASA Ice Giants Pre-Decadal Survey [3, 5]. The study concluded that ice giant aerocapture will require aeroshell with a mid lift-to-drag ratio (L/D) of 0.6–0.8.

Aeroshells with flight heritage such as Apollo and MSL, or those under development such as Orion Crew Module has a maximum L/D of 0.4. Currently there are no programs to develop a mid-L/D vehicle in the US, and it is unlikely that NASA will pursue the development of such a new vehicle in the near term due to budgetary constraints. The non-availability of a mid-L/D vehicle is a “long pole” that seriously hinders the use of aerocapture for ice giant missions.

Aerocapture using low-L/D aeroshells: A follow-on study to investigate techniques that may enable aerocapture at ice giants using heritage low-L/D aeroshells is underway at Purdue University in collaboration with JPL. Four possible solutions have been investigated: 1) refine approach navigation uncertainties, 2) quantify effect of atmospheric uncertainties, 3) a hybrid propulsive-aerocapture technique, and 4) a pathfinder probe concept. The investigations and preliminary results are as follows.

Refine Approach Navigation Uncertainties: Approach navigation errors from interplanetary trajectory were found to be the dominant uncertainty from the Neptune Aerocapture Systems Analysis study in 2004. Navigation analysis performed at JPL as part of the present study is used to better quantify the dispersions of the entry flight-path angle for a nominal

Neptune aerocapture approach trajectory. Table 1 shows key results from the navigation analysis.

Table 1: 3σ entry flight path angle dispersions in degrees (defined at 1000 km above 1 bar)

Data Cut Off (DCO), days	With OpNav (generic cam.)	With OpNav (LORRICam)
T - 09	± 3.18	± 0.78
T - 07	± 2.85	± 0.60
T - 04	± 2.22	± 0.33

The above navigation uncertainties were a crucial piece of information not available during the 2016 aerocapture assessment. Earlier estimate of the 3σ dispersion was ± 0.51 deg., and the refined estimate shows promise to lower the vehicle L/D requirement.

Effect of Density Dispersions: The aerocapture vehicle should have sufficient control authority to achieve desired exit conditions even with worst case density dispersions. Neptune-GRAM, an engineering model, incorporates all available data to predict the expected minimum and maximum density profiles. Table 2 shows the error in apoapsis altitude for combinations of navigation errors and mean density dispersions for a vehicle with L/D = 0.4, planet relative entry speed = 30 km/s (prograde near equator).

Table 2: Error (%) in apoapsis altitude for combinations of navigation and density dispersions*.

Entry Flight Path Angle (EFPA)	Min. atmos.	Nominal atmos.	Max. atmos.
Min. (shallow)	+ 1.9	- 0.03	+ 2.3
Nominal (mean)	+ 0.6	+ 0.05	+ 1.5
Max.(steep)	- 0.4	- 1.20	- 2.9

* Target apoapsis altitude = 400,000 km. A numerical predictor guidance with on-board density estimation from accelerometer measurement during the descending leg of the aerocapture maneuver is used.

Table 2 shows that even in worst case combinations of navigation and mean density uncertainties, the vehicle is able to achieve the desired apoapsis within a few percent error. The results do not incorporate high frequency density perturbations but are included in the Monte Carlo simulations discussed later. We note that the last study on effect of atmospheric dispersions at the ice giant planets were done in 2004 and since then advancements have been made. The present study incorporates the state-of-the-art knowledge in ice giant atmosphere for aerocapture analysis.

Hybrid Propulsive-Aerocapture Concept: Two variants of this technique have been investigated. In the first variant, the aerocapture vehicle initially targets a lower apoapsis than desired, and then propulsively boosts the apoapsis using a burn at the periapsis. The small capture orbit widens the corridor and lowers the

required L/D. In the second variant the desired science apoapsis is targeted, and a propulsive ΔV immediately after exit corrects for the excess/deficit in speed. Results indicate hybrid propulsive-aerocapture concept provides only marginal reduction in L/D (less than 10%) for propulsive ΔV allowable of 1000 m/s.

Biasing the target entry flight path angle towards the steep side corridor can significantly improve guidance performance. Entering steeper than the corridor results in a lower apoapsis than planned, and a small propulsive burn can raise the apoapsis.

Pathfinder Probe Concept: This concept investigates the possibility of sending a scout entry probe a few days/weeks ahead of the main aerocapture vehicle entering the atmosphere. Preliminary results indicate that if the concept were feasible, in-situ atmospheric density profile measured by the scout probe can be used to optimize the entry targeting of the aerocapture vehicle. Because the atmospheric uncertainty to be handled by the aerocapture vehicle is much lower, the required L/D is lower. Results will be presented on the feasibility, and benefit of the pathfinder probe concept for ice giant missions.

Monte Carlo Simulations and Risk Assessment:

To combine the effect of navigation uncertainties, density dispersions, and aerodynamic dispersions, Monte Carlo analysis is used to predict statistical performance estimate and quantitative risk assessment of aerocapture at the ice giants. The simulations use the refined navigation uncertainties, along with maximum range of mean density profiles along with high frequency perturbations from Neptune-GRAM. The simulations also include a small propulsive ΔV to raise the apoapsis if required from a steep entry, and if a pathfinder probe were available. The results will feed into the new mission concept studies involving aerocapture. This allows mission planners to quantitatively assess the readiness and risks of aerocapture for a future ice giant mission. The methodology and tools can also be applied to aerocapture at other planetary destinations.

Acknowledgement: The approach navigation uncertainty calculations were performed at JPL. The research described in this report was carried out at Purdue University and has been supported in part by the Jet Propulsion Laboratory, California Institute of Technology, under Contract Number 108436.

References: [1] SSB (2011), *Planetary Science Decadal Survey 2013-2022*. [2] JPL Photojournal, PIA18182, PIA01492. [3] Elliot J. *et al.* (2017), JPL-D 100520. [4] SSB (2018), *Planetary Science Decadal Survey 2013-2022: A Mid-Term Review*. [4] Spilker T. R. *et al.* (2016), JPL D-97058. [5] Saikia S. J. *et al.* (2016), PU-AAC-2016-MC-0002.

ATMOSPHERIC LINK SCIENCE AND COMMUNICATIONS WITH PLANETARY ENTRY PROBES VIA DIRECT-TO-EARTH AND RELAY RADIO LINK METHODS.

S. W. Asmar¹, D. H. Atkinson¹, I. G. Clark¹, F. Ferri², D. Firre³, R. E. Gladden¹, O. Karatekin⁴,
S. M. Krasner¹, J. Lazio¹, M. Mercolino³

¹NASA's Jet Propulsion Laboratory, California Institute of Technology, ²Università degli Studi di Padova,
³European Space Agency, ⁴Royal Observatory of Belgium

Biography: The presenter (S. W. Asmar) manages strategic partnerships at the Interplanetary Network Directorate and is an experienced radio scientist. He is an expert in the detection of weak and high dynamics signals during critical mission events and has led efforts to utilize radio telescopes for support of probes landing on Titan and Mars. He invented the carry-you-own-relay concept and developed the MarCO mission proposal. He is the receipt of several achievement medals from NASA and Space Ops, among other awards.

Introduction: One of the biggest technical challenges for planetary entry probes is communications of science and probe health to mission control centers during the risky descent phase. Traditional methods do not work reliably as a result of the high dynamics of the spacecraft motion and the corresponding Doppler profile and signal level as well as the release of heat shields and other layers along with switching antennas. In addition, compelling science about the planetary atmosphere that can be obtained during the descent and landing period.

This paper provides a review of techniques used at Jupiter via the Galileo Probe [1] and [2], Titan via the Huygens Probe [3], and several Mars missions [4, 5] and looks towards upcoming missions planning landing events. Experience from previous missions will be discussed along with a summary of the technologies used and lessons-learned.

Direct-to-Earth Radio Link: The link budget determines the feasibility of receiving the signal and extracting the telemetry at a ground station, such as the large stations of NASA's Deep Space Network, as long as the signal level is above the receiver threshold and the signal dynamics are within the acquisition limits. From the missions supported to date, very few supported a link budget that enable direct-to-Earth telemetry links.

Instead, for two reasons, an open-loop receiver is typically used: 1) the absence of tracking thresholds and 2) the increased sensitivity to lower received signal levels. However, this method has been successful in receiving the signal carrier only and not telemetry. From monitoring the carrier Doppler profile, important information about critical events, such parachute release, thruster firing, etc. are deduced in real-time.

Relay Radio Link: Many missions are fortunate to have assets in flight or orbit around the target planet

with geometries favorable for receiving the signal from the landing probe and relaying it to ground stations. When no assets are available in advance, the concept successfully utilized by the InSight mission can be applied; the MarCO CubeSats flew to Mars expressly to provide the relay during the critical landing phase [6]; this was one of three methods available and exercised by the InSight mission.

Science: Planetary atmospheric entry and descent probes provide an opportunity to examine the Doppler profile for studying the atmospheric dynamics, including winds, waves, tides, and turbulence, and measuring the integrated abundance profile of constituents that absorb at the microwave frequency of the probe telecommunication link.

References:

- [1] Atkinson, D. H., Pollack, J. B., and Seiff, A. (1998) *JGR*, 103(E10), 22911-22928. [2] Folkner, W. M., Preston, R. A., Border, J. S., Navarro, J., Wilson, W. E. and Oestreich, M. (1997) *Science*, 275(5300), pp.644-646. [3] Bird, M. K., Allison, M., Asmar, S. W., Atkinson, D. H., Avruch, I. M., Dutta-Roy, R., Dzierma, Y., Edenhofer, P., Folkner, W. M., Gurvits, L. I. and Johnston, D. V. (2005) *Nature*, 438(7069), p.800. [4] Esterhuizen, S. X., Asmar, S. W., De, K., Gupta, Y., Katore, S. N. and Ajithkumar, B., (2019) *Radio Science* 10.1029/2018RS006707 [5] Asmar, S. W., Oudrhiri, K., Kahan, D., Esterhuizen, S., Sarkissian, J., Jackson, S., Preisig, B., Karatekin, O., and Griebel, H. (2013) *IPPW-10* San Jose, CA. [6] Asmar, S. W. and Matousek, S., (2016) *14th International Conference on Space Operations* (p. 2483).

Thursday, July 11, 2019

Entry, Descent, and Landing Technologies - Conveners: Tom West, Rodrigo Haya Ramos, Milad Mahzari, Karl Edquist, and Eric Stern

12:00 PM (Wed July 10)	The Challenges of Landing on Uncertain Terrain	Alejandro San Martin	Jet Propulsion Laboratory, California Institute of Technology	Invited
8:45 AM	Study Of Neuromorphic Application Using Spiking Neural Network For Terrain Relative Navigation	Kazuki Kariya	The Graduate University for Advanced Studies	Student
8:57 AM	Crater-based Optical Navigation Technologies for Lunar Precision Landing in SLIM Project.	Takayuki Ishida	JAXA	
9:09 AM	Map matching during descent for terrain relative navigation on Titan	Larry Matthies	Jet Propulsion Laboratory, California Institute of Technology	
9:21 AM	Mars 2020 Hazard Map for Terrain Relative Navigation	Richard Otero	Jet Propulsion Laboratory, California Institute of Technology	
9:33 AM	Onboard Autonomous Trajectory Planner: A guidance routine to assist in enabling pinpoint landing and in-flight trajectory analysis	Justin Green	NASA Langley Research Center	
9:45 AM	Design Of The Pinpoint Landing GNC Of Space Rider.	Rodrigo Haya Ramos	SENER Aerospace	
10:18 PM	An Uncoupled Range Control Approach to Fully Numerical Predictor-Corrector Entry Guidance	Breanna Johnson	NASA Johnson Space Center	
10:30 PM	The SPLICE Project: Safe and Precise Landing Technology Development and Testing	Jay Estes	NASA Johnson Space Center	
10:42 PM	Stability Analysis and Control Design for a Deployable Entry Vehicle with Aerodynamic Control Surfaces	Wendy Okolo	NASA Ames Research Center	
10:54 PM	The Dragonfly Entry And Descent System	Michael Wright	NASA Ames Research Center	
11:06 PM	European Solutions for Heatshields of High Energy Entry Probes	Jean-Marc Bouilly	ArianeGroup SAS	
11:18 PM	Sustaining Phenolic Impregnated Carbon Ablator (PICA) For Future Nasa Missions Including Discovery And New Frontiers	Donald Ellerby	NASA Ames Research Center	
11:30 PM	ADEPT Sounding Rocket One Flight Test Overview	Alan Cassell	NASA Ames Research Center	
11:42 PM	Technology Readiness Assessment For HEEET TPS	Peter Gage	Neerim Corp at NASA Ames Research Center	
11:54 PM	The Challenges of Seam Design in Tiled Thermal Protection Systems	Cole Kazemba	NASA Ames Research Center	
1:34 PM	Damage Assessment During a Structural and Thermal Test Campaign of a 1-meter Diameter Heatshield with a 3-D Woven Thermal Protection System for Extreme Environments	Sarah Langston	NASA Langley Research Center	
1:46 PM	LOFTID Aeroshell System Overview	Stephen Hughes	NASA Langley Research Center	
1:58 PM	LOFTID Aeroshell Engineering Development Unit Structural Testing	Greg Swanson	NASA Ames Research Center	
2:10 PM	Retro Propulsion Assisted Landing Technologies (RETALT)	Ali Guelhan	DLR e.V.	
2:22 PM	Designing A Supersonic Retropropulsion Test For The NASA Langley Unitary Plan Wind Tunnel	Karl Edquist	NASA Langley Research Center	
2:34 PM	Experimental Investigation of Magnetohydrodynamic Energy Generation in Conditions and Configurations Relevant to Planetary Entry	Hisham Ali	Georgia Institute of Technology	Student
2:46 PM	Design And Qualification Testing Of Two European Parachute Mortars For The ESA Exomars 2020 Mission	Rudi Matthijssen	APP-ArianeGroup	

THE CHALLENGES OF LANDING ON UNCERTAIN TERRAIN.

A. M. San Martin, Jet Propulsion Laboratory, 4800 Oak Grove Dr., Pasadena, CA 91109

Biography: Inspired by Apollo and Viking missions, Miguel left his native Argentina to pursue his university studies and his dream of contributing to space exploration by working for NASA. After receiving his Bachelor's Degree in Electrical Engineering from Syracuse University and his Master's degree in Aeronautics and Astronautics Engineering from the Massachusetts Institute of Technology, he joined JPL. Early in his career, he participated in the Magellan mission to Venus and the Cassini mission to Saturn. He was then the Chief Engineer for the Guidance and Control systems for all four Mars rover missions: Pathfinder, Spirit, Opportunity, and Curiosity. He was a co-architect of Curiosity's innovative SkyCrane landing architecture and also served as its Deputy Chief for Entry, Descent, and Landing. Most recently, Miguel has served as the deputy Chief Engineer of the Europa Lander Study. For his Mars contributions he was named JPL Fellow in 2013 and received the NASA Exceptional Engineering Achievement Medal. He was elected to the National Academy of Engineering of the United States in 2019.

Abstract: Since the two Viking spacecraft landed successfully on Mars in 1976, we have not had to address the challenge of designing spacecraft to land successfully on a planetary surface we know very little about. Subsequent Mars landers like Mars Pathfinder, Spirit/Opportunity, Phoenix, and Curiosity, benefited from increasing information of the terrain from improved resolution images taken by orbiting spacecraft and previous landers. This broadened knowledge of the terrain was used to derive models of the Mars surface that were then used to design the next lander and, in conjunction with high-resolution orbital images, select its landing site. As we start planning to investigate and land on new worlds like Europa, the moon of Jupiter with a liquid ocean that may harbor life, we find ourselves, at best, in a similar situation as Viking: very little and low-resolution images of its surface, taken by the Galileo spacecraft, in this case. The options available to us at this point are either to send exploratory orbiters to gather high resolution surface images prior to designing and sending landers to those worlds, which would postpone those investigations for decades, or design and implement robust landing technologies that would reduce the risks of landing in those highly uncertain planetary surfaces to acceptable levels. This talk will first address the dangers to a lander that can be inflicted by terrain, followed by a quick historical retrospective on how the uncertain terrain challenges were addressed in the past, and ending with the description of a landing architecture

that is being considered for a future Europa Lander mission.

[The information to be presented on Europa Lander is pre-decisional and is provided for planning and discussion purposes only].

STUDY OF NEUROMORPHIC APPLICATION USING SPIKING NEURAL NETWORK FOR TERRAIN RELATIVE NAVIGATION.

K. Kariya¹ and S. Fukuda^{2,1}, ¹the Graduate University for Advanced Studies, 3-1-1 Yoshinodai Chuo-ku Sagamihara Kanagawa Japan, kariya.kazuki@ac.jaxa.jp, ²Institute of Space and Astronautical Science / Japan Aerospace Exploration Agency, 3-1-1 Yoshinodai Chuo-ku Sagamihara Kanagawa Japan.

Brief Presenter Biography: The presenter is a PhD student at the Graduate University for Advanced Studies, Japan. He is currently doing research in optical navigation, computer vision and neuromorphic computing.

Introduction: High precision landing capability is important technique to be acquired because it increases accessibility to scientifically interesting areas and makes safe landing. Terrain Relative Navigation (TRN), which extracts state estimates such as position and velocity of a spacecraft by comparing maps with landmarks in images of a planetary surface, is one of the GN&C functions to achieve that. Since time until landing is short in a case of landing on a gravitational celestial body, TRN requires on-board and real-time image processing algorithms performing image recognition, feature extraction, matching, tracking, etc. However, despite the demand for fast image processing task, space-grade computers have been slower than commercial ones, lagging behind them by 1-2 orders of magnitude in performance [1]. Future exploration missions will make more advanced landing to farther celestial bodies, and power consumption requirements for processors become severer and navigation algorithms become more complicated. Therefore, the gap between the complexity of algorithms and the performance of processors is an essential problem to be solved. To tackle the problem, we study applicability of a TRN algorithm for crater identification in architecture of neuromorphic processor chips which are expected to operate with low power consumption revolutionarily.

A neuromorphic processor chip operates asynchronously and in parallel mimicking neuro-biological architecture like our brain. Therefore, the processor operates as a Spiking Neural Network (SNN) based on biological spiking neuron models that communicate information by spike (pulse) current. Figure 1 (A) shows the spiking neuron model. The inputs of a spiking neuron are trains of sparse spike signals. When a spike arrives at a neuron, the spike is input to the neuron as an electric current having an amplitude called synaptic efficacy and decaying exponentially. The current pulses consequently drive its membrane potential to change over time, and trigger spikes as outcomes when the neuron's membrane potential reaches some threshold. As above, a SNN operates asynchronously by sparse spike current, so that the processors can be expected to have lower

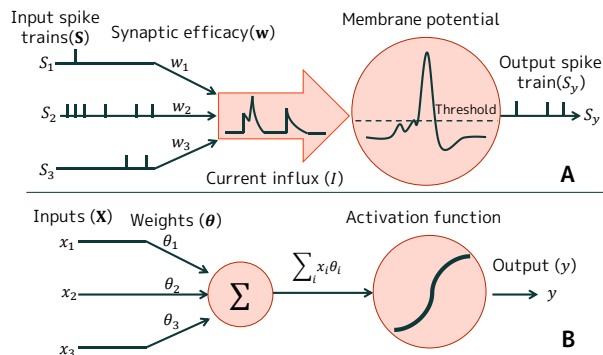


Figure 1: Neuron models, (A) A spiking neuron, (B) An artificial neuron.

power consumption than conventional clock-based circuits. The dynamics of spiking neurons are time dependent, while artificial neurons used for Artificial Neural Networks (ANNs) such as deep learning only cope with numerical values representing firing rate without timing information. The artificial neuron (Figure 1 (B)) takes numerical values as input and works as a weighted linear summation followed by an activation function (sigmoid, etc.). The difference in behavior between timing-based spiking neurons and rate-based artificial neurons has a problem that how to make SNNs with equivalent functions as ANNs.

To solve the problem, this study introduce a method to train a SNN by transferring weights of an ANN trained specially as synaptic efficacy of the SNN. The procedure of the training method is as follows:

1. Train a feed-forward ANN.
2. Re-train an artificial spiking neural network with layer architecture equivalent to Step 1 using transfer learning.
3. Transfer the weights trained in Step 2 directly to the SNN with layer architecture equivalent to Step 1.

In order to verify the effectiveness of this method, we train a network identifying craters [2]. The network uses 4-layer architecture of convolutional neural network (Figure 2). In this training, MATLAB was used for ANN training and pyNN [3] + NEST simulator were used for SNN simulation. As a result, the identification accuracy are 99.1% for the original network in Step 1, 97.8% for the network by the artificial spiking neuron in Step 2 and 95.6% for the inference in the SNN in Step 3. Moreover, the number of firing of all neurons in the

SNN was about 230 million times on average. The value indicates that it is possible to operate with about 50 mW of power consumption in IBM's neuromorphic processor [4]. Since it depends on specifications of processors, the power consumption is an approximate value, but we consider that the effectiveness of this method could be confirmed certainly from the viewpoint of low power consumption.

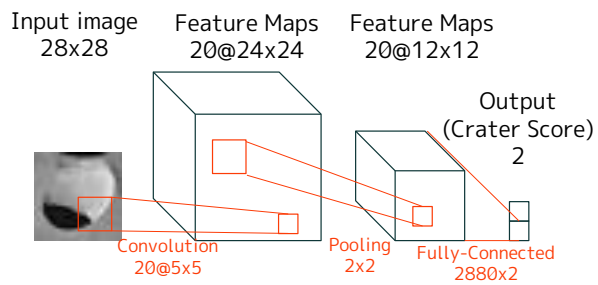


Figure 2: Architecture of crater identification network [2].

References: [1] Lentaris, G. et al. (2018) *J. Aerosp. Inf. Syst.*, 15(4), 178-192. [2] Ishida, T. et al. (2019) *ISTIS*, Abstract #d-073. [3] Davison, A. P. et al. (2008) *Front. Neuroinform.*, 2(11). [4] Merolla, P. A. et al. (2014) *Science*, 345(6197), 668-673.

Crater-based Optical Navigation Technologies for Lunar Precision Landing in SLIM Project.

T. Ishida¹, K. Kariya², H. Kamata³, K. Takadama⁴, H. Kojima⁵, S. Sawai¹, S. Sakai¹ and S. Fukuda¹, ¹Japan Aerospace Exploration Agency (3-1-1 Yoshinodai Chuo-ku Sagami-hara Kanagawa Japan, ishida.takayuki@jaxa.jp), ²SOKENDAI (3-1-1 Yoshinodai Chuo-ku Sagami-hara Kanagawa Japan), ³Meiji University (1-1 Kandasurugadai Chiyoda-ku Tokyo Japan), ⁴The University of Electro-Communications (1-5-1 Chofugaoka Chofu-shi Tokyo Japan), ⁵Tokyo Metropolitan University (1-1 Minamiosawa Hachioji Tokyo Japan).

Brief Presenter Biography: The presenter received the master's degree in engineering from Keio University, Yokohama, Japan, in 2015. His research interest includes terrain relative navigation for planetary precision landing.

Introduction: Japan Aerospace Exploration Agency (JAXA) is planning to launch a small lander to the Moon in 2022, which is called SLIM (Smart Lander for Investigating Moon) project. The aims of this project include two challenges, one is to build a small and light landing system, and the other is to demonstrate the precise landing technologies to land on the Moon within up to 100 m error. SLIM is to observe Olivine ejected from a fresh crater near Mare Nectaris. The predetermined landing site is the highly challenging since the area has steep slopes and is covered with boulders ejected from the crater. To achieve precision landing a crater-based terrain relative navigation technology is developed in SLIM project.



Figure 1: Conceptual image of SLIM landing.

After lunar orbit insertion, the main thruster is used to lower the orbit followed by powered descent phase. Figure 2 shows the concepts of this phase. To update the navigation errors, onboard cameras are used to obtain images of lunar surfaces in up to seven areas to collate them with onboard crater maps. Hazard detection and avoidance is performed just before landing to avoid obstacles harmful to the probe.

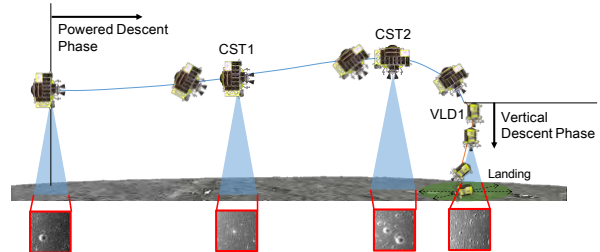


Figure 2: SLIM powered descent phase.

Approaches: The main technologies for crater-based optical navigation is described below.

Making crater maps. Onboard crater maps are generated before the launch using scientific data obtained by SELENE (Selenological and Engineering Explorer) and LRO (Lunar Reconnaissance Orbiter). Digital elevation maps (DEM) are made from obtained high-resolution image data, and craters are extracted in advance. Using craters as features makes it robust to illumination changes and possible to reduce map data size.

Crater detection [1]. In the landing phase, a navigation camera is used to obtain images of the surface of the moon, and craters are detected from the images. The first principal component of crater images obtained by the past probes is used as a template.

Crater Matching [2][3]. Detected craters are then collated with the onboard crater maps based on spatial relation. This approach searches for corresponding craters one by one using spatial relation between two or three craters at first, which leads robustness against detection errors.

Hazard detection [4]. In the end of vertical descent phase, a monocular camera is used to obtain images for the hazard detection. Since SLIM landing site is expected that boulders from the crater near the landing site are heavily distributed, obstacles are detected using variance in a local image patch. The deciding landing point is chosen as the safest area in the image from the detected obstacle map.

Simulation and Hardware verification Results: Montecarlo simulation results for one of the predetermined areas where the optical navigation is used are shown in Figure 3. Initial position error is up to about 2500 m, including orbit determination error and IMU error, but the results show the crater-based optical navigation is capable of reducing position error to less than 100 m (3σ).

These algorithms are implemented in RTG4 space grade FPGA. The algorithm design uses 61% of its logic resources, and processing time is 0.784 s in average for crater detection and matching, 0.396 s in average for hazard detection.

Acknowledgement: Hardware implementation of these algorithms is carried out by Mitsubishi Electric Corporation, and its verification is supported by Soliton Systems K.K..

[1] S. Okada et al. (2018) *AEROSPACE TECHNOLOGY JAPAN, JSASS*, 17, 61–67. [2] K. Kariya. et al. (2018) *AEROSPACE TECHNOLOGY JAPAN, JSASS*, 17, 79–87. [3] H. Ishii et al. (2018) *AEROSPACE TECHNOLOGY JAPAN, JSASS*, 17, 69–78. [4] T. Kuga et al. (2016) *JOURNAL OF THE JAPAN SOCIETY FOR AERONAUTICAL AND SPACE SCIENCES, JSASS*, 64 (6), 303–309.

Map Matching During Descent for Terrain Relative Navigation on Titan.

L. H. Matthies, B. Rothrock, S. Daftry, A. B. Davis, M. J. Malaska, Jet Propulsion Laboratory, 4800 Oak Grove Drive, Pasadena, CA, USA 91109, {lhm, brandon.rothrock, shreyansh.daftry, anthony.b.davis, michael.j.malaska}@jpl.nasa.gov.

Brief Presenter Biography: Larry Matthies has conducted research at JPL on vision systems for autonomous navigation in Earth and space applications since 1989. His work in this area has been used in all U.S. Mars surface missions since Pathfinder in 1997. He obtained his PhD in computer science from Carnegie Mellon University.

Introduction: Precision landing on planetary bodies uses terrain relative navigation (TRN) to estimate position during descent, by performing real-time, onboard registration of descent imagery to maps of the terrain created from prior orbital reconnaissance [1]. This is used to guide divert maneuvers to land close to desired targets or to avoid landing hazards that are known from prior reconnaissance. TRN is very mature for Mars, where descent images acquired at altitudes of approximately 3 to 4 km can be cross-correlated with map images to obtain position estimates with error on the order of 40 meters [2]. For Mars, orbital images have high resolution (30 cm/pixel) and the orbital and descent images have very similar spectral characteristics, which simplifies automatic image registration.

Titan's tall, dense, hazy atmosphere creates very different problems for precision landing. Here, we focus on the challenges of position estimation during descent. Position knowledge that is inertially propagated from entry will have large errors due to long descent times (up to 2.5 hours [3]). Position knowledge from TRN is limited by the low resolution of orbital images (currently 100s of meters to many km/pixel). TRN may be desired or required to start at altitudes of several 10s of km. However, atmospheric absorption and scattering limit the usable spectral bands for imaging and reduce image clarity with increasing altitude. We summarize progress in modeling descent imaging and in developing map matching algorithms for TRN on Titan.

Background: Descent cameras on the DISR instrument on the Huygens probe operated in a spectral band from 660 to 1000 nm (visible/near-infrared, or VNIR). Atmospheric scattering creates very diffuse scene illumination and adds significant scattered light to imagery. With post-processing, the surface was visible in DISR images beginning at an altitude around 40 km [3].

Without new orbital imaging, the only source of map imagery is the Cassini mission. Cassini's Imaging Science Subsystem (ISS) camera acquired images over much of Titan with a narrow band spectral filter cen-

tered at 938 nm. These have been processed into a mosaic with pixel sampling of 2.8 km [4]. The Visual and Infrared Mapping Spectrometer (VIMS) obtained images in the spectral region from 1 to 5 μm , which have been processed into mosaics with a best resolution of a few km/pixel [5]. This band is less affected by atmospheric scattering than VNIR, but atmospheric absorption makes only part of this spectral range useful. For TRN, the short-wave infrared (SWIR) window from 2 to 2.1 μm is of interest for descent imaging, because it is a good compromise between available light and reduced scattering. Cassini's radar obtained surface imagery with resolution of ~ 300 meters/pixel at closest approach [6], which is essentially unaffected by atmospheric scattering.

With these data sets, TRN can use maps from ISS, VIMS, or radar, and descent imaging spectral regions of interest are VNIR and the 2 to 2.1 μm SWIR band.

Modeling Descent Imaging: To evaluate expected imaging performance for VNIR and SWIR descent cameras, we modeled the entire process of solar illumination, surface reflection, and light propagation to the camera aperture using the DISORT radiative transfer code [7]. Atmospheric absorption and scattering data was drawn from the literature [8]. As notional camera spectral responses, for the VNIR case we used quantum efficiency curves for CMOS imagers from Mars 2020 rover engineering cameras, assuming filtering to restrict the range to 500 to 1000 nm. For the SWIR case, we used data for the HIRG infrared detector, assuming a filter for the 2 to 2.1 μm atmospheric window.

A standard paradigm for map matching with descent imagery is to use attitude and altitude data, assumed to be available from an IMU and altimeter, to project descent images onto the ground plane. These are then low-pass filtered and resampled at the resolution of the map image for use by image registration algorithms. For Titan, this effectively involves binning the descent image pixels to a degree that provides large SNR for reasonable exposure time and aperture values, regardless of the native imager well depth.

The main issue, therefore, is to model the relative amount of light reaching the camera directly from surface reflection vs. from multiple scattering in the atmosphere. Using DISORT, we evaluated this as a function of altitude. Figure 1 shows that SWIR is far superior to VNIR in this respect, so we focus on SWIR for map matching.

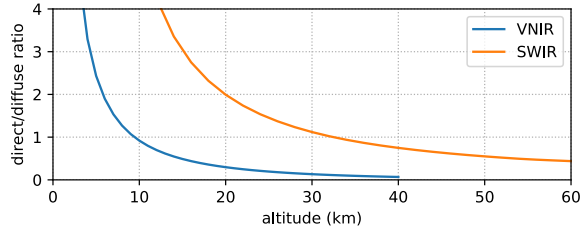


Figure 1. Modeled ratio of direct to scattered descent image irradiance vs altitude for VNIR and SWIR bands.

Estimating Position From Descent Imagery: The question now is how to register SWIR descent images to map images created from ISS, VIMS, or radar data. The best global mosaics are available from ISS; the best spatial resolution is available for selected locations from radar. Registering SWIR to either ISS or radar is a multi-modal registration problem. This problem has been explored for Titan data sets with some success using mutual information as registration criterion [10]. This approach has potential to apply to any landing site on Titan where the orbital imaging was adequate.

Regions of small lakes in northern latitudes are an interesting scenario, because they offer distinct science possibilities and the highest image contrast (between lake and ground regions) available on Titan, which may provide the best image registration performance. This scenario opens possibilities for a different approach to registration, because the contrast should enable reliable onboard segmentation of lake and non-lake regions in descent images, especially in the SWIR band. These binarized images could be registered to similarly binarized radar maps. This removes the differences in sensor phenomenology between radar and SWIR, and can benefit from the higher resolution of radar images.

We have experimented with both of these approaches by using Cassini VIMS mosaics to generate simulated descent images, with ISS and radar data as the map (Figure 2). We used the radiative transfer model to synthesize noisy descent images with a 90° field of view at a variety of altitudes. At several test altitudes, we created simulated descent images for many test locations to measure the mean and standard deviation of registration error (Figure 3). Results were better at higher altitudes because descent images project to shrinking patches on the ground as altitude decreases, which produces noisier matches. Non-zero mean errors are due to multiple factors, including imperfect registration of the Cassini mosaics used in the experiments; this could be improved with further work. Standard deviations of 1 to 1.5 km for altitudes of 30 to 40 km are quite promising.

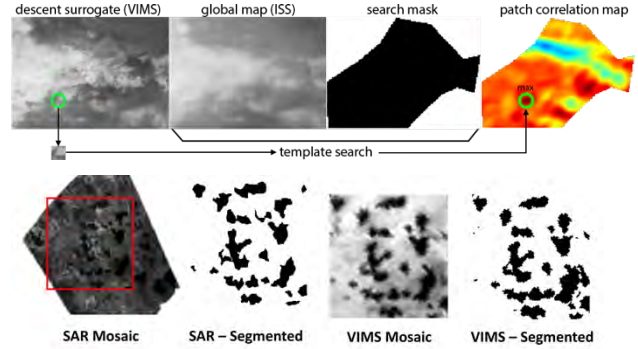


Figure 2. Top row: experiments with mutual information-based matching used data from the Huygens landing site region. The search mask limited tests to areas of the mosaics without distinct seams. The false color image shows match scores for one trial (deep red best, blue worst). Bottom row: Orbital mosaics of the Maracaibo Lacus region used for binary correlation experiments, which were constrained to the area in the red rectangle.

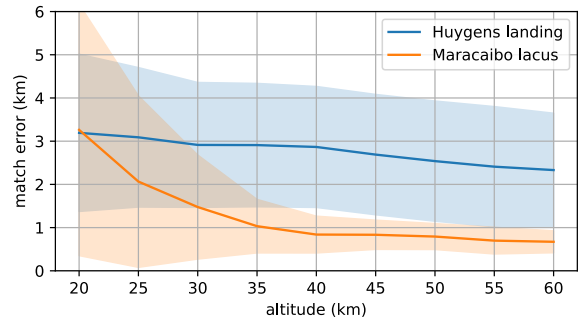


Figure 3. Match matching simulation results: mean position error and 1σ interval vs. altitude for ~ 1000 trials at each altitude. See text for interpretation.

Discussion: These results are encouraging and will be tested for other regions on Titan. Map matching will not work all the way to the ground, so other sensors and image processing algorithms are needed to bound position and velocity error growth at low altitude. Ongoing work will address this in simulations of navigation error from entry to landing.

References: [1] Johnson A. E. et al. (2007) *AIAA Infotech@Aerospace Conf.* [2] Johnson A. E. et al. (2015) *AIAA GNC Conf.* [3] Lebreton J.-P. et al. (2005) *Nature*, 438, 758-764. [4] Karkoschka E. et al. (2018) *AAS/DPS Meeting*, 50. [5] Le Moulic S. et al. (2018) *LPSC 49*, abstract 1889. [6] Stephan K. et al. (2009) ch. 19 in Brown R.H et al. *Titan from Cassini-Huygens*. [7] Stamnes K. et al. (1988) *Appl. Opt.*, 27, 415-419. [8] Doose L. R. et al. (2016) *Icarus*, 270, 355-375. [10] Ansar A. and Matthies L. H. (2009) *IROS Conf.*, 3349-3354.

Mars 2020 Hazard Map for Terrain Relative Navigation

R. E. Otero, Jet Propulsion Laboratory, California Institute of Technology, 4800 Oak Grove Drive, Pasadena, CA 91109.

Brief Presenter Biography: Richard has been a member of the EDL Systems and Advanced Technologies Group, at the Jet Propulsion Laboratory, since 2011. He is currently in charge of landed hazard map creation for Mars 2020 and co-manages the Mars 2020 Council of Terrains. Richard received a MS in Aerospace Engineering in 2009, a MS in Computer Science in 2010, and his PhD in Aerospace Engineering in 2012; all from Georgia Tech. He received his BS in Computer Science from SUNY New Paltz.

Introduction: Terrain relative navigation (TRN) has enabled many sites that would not have been considered viable for MSL; making use of the volume margin in the MSL propulsion tank design. If there is a sufficient distribution of safe zones, TRN can mitigate terrain-based landed hazards. These landed hazards are represented as an on-board map created before launch from satellite images, derived-terrain models, and assessments of the landing system capability.

This presentation will go into the elements of the Mars 2020 hazard map (Figure 1), the unique risk challenges of the selected landing site (Jezero), and the new characterization efforts to address those challenges.

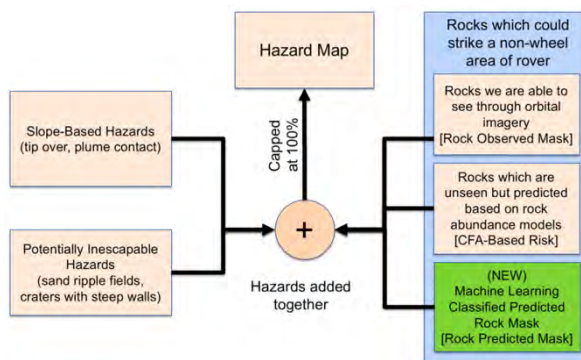


Figure 1: Components of the Mars 2020 Hazard Map

MSL used hazard characterization to select a landed ellipse location; this use case allowed them to coarsen the resolution of their hazard map to 150x150m. Mars 2020 is using their hazard map for both ellipse placement and for landing-day guidance. This required another order of accuracy for a 1x1m map (coarsened to 10x10m for flight use).

The Mars 2020 hazard map has a large amount of detail never before used for a flight mission hazard map. (Figure 2) Every rock identified from orbit is carried in the map with an additional new approach to identify rocks unseen by traditional techniques. MSL driving experience has also been incorporated into the hazard map by marking potentially inescapable sand ripple hazards.

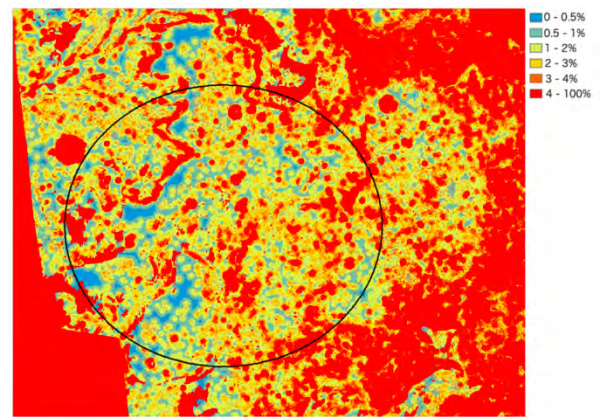


Figure 2: Example Hazard Map for Jezero

The use of a fine grained hazard map, paired with TRN, has made a site deemed unacceptably dangerous for MSL to one where we expect ~99% landed safety. A review of MSL analysis and better grounding our risk mappings to high fidelity simulation is expected to improve the accuracy of this hazard map relative to MSL.

Onboard Autonomous Trajectory Planner: A guidance routine to assist in enabling pinpoint landing and in-flight trajectory analysis

J. S. Green¹ and R. A. Williams¹, ¹NASA Langley Research Center, 1 NASA Dr., Hampton, VA 23666, justin.green@nasa.gov, robert.a.williams@nasa.gov.

Brief Presenter Biography: Justin Green graduated with his Bachelor of Science degree in Mechanical Engineering from the University of Nebraska – Lincoln in 2009, and his Master of Science degree in Mechanical and Aerospace Engineering degree in 2012 from the University of Virginia (UVA). In 2014, Green began his career at the NASA Langley Research Center. While at NASA, he has work on kinematic modeling of the Center of Gravity Offset Subsystem of Inflatable Reentry Vehicle Experiment (IRVE) – 3, early development of morphing hypersonic inflatable aerodynamic decelerator technology, and trajectory analysis of entry, decent, and landing vehicles. He is currently working on his doctorate on adaptable guidance and control strategies for powered descent vehicles.

Introduction: Given the complexity and requirements for current and future planetary missions, there is a strong need for enabling descent systems to obtain pinpoint landing. There are two major factors motivating this demand. The first is the ability to land at scientifically interesting sites that are located near hazardous terrain. The second motivator is the ability to land near already existing mission assets. One example is retrieving pre-cached specimens for a sample return, for which the Mars 2020 is beginning through the collection of Mars surface samples, [1]. Another example is landing crew and supplies near existing mission critical assets.

The ultimate goal of this work is the creation of an autonomous guidance and control strategy that allows for pinpoint landings in uncertain and dynamic environments with no human in the loop control or guidance. The guidance and control strategy needs to be autonomous because should conditions change during Entry, Descent, and Landing (EDL), whether vehicle or environmental, there is no time for the vehicle to communicate that information to engineers on Earth, then those engineers to re-evaluate or re-tune their guidance routine, and then communicate that back to the EDL vehicle. However, EDL vehicles can be enabled to perform trajectory path re-evaluation and re-tuning onboard by applying concepts first explored by Rogers and Slegers, [2,3,4]. To reach this goal, this work aims to lay the groundwork for enabling a guidance routine to take in information during flight to perform trajectory path re-evaluation and re-tuning onboard in real-time. The Onboard Autonomous Trajectory Planner (OATP) will be a large part of laying the ground work and achieving this ultimate goal.

Onboard Autonomous Trajectory Planner: The Onboard Autonomous Trajectory Planner (OATP) will generate candidate trajectories and evaluate the trajectory design space, see Fig 1 for example of the trajectory design space. The OATP guidance does this by reading in state information from onboard sensors, such as an inertial measurement unit (IMU), and planet parameters, such as gravity. Using this information, the OATP guidance samples the trajectory design space and executes a full six DoF simulation for each candidate trajectory. The simulated trajectories are then pruned and scored based on set metrics and cost functions, and a select trajectory is provided for the control system to follow. The pruning process includes evaluating whether the candidate trajectory passes through a keep-out-zone (an area it should be avoiding, such as terrain or already established assets), and whether or not the trajectory satisfies certain terminal conditions, such as the total vehicle attitude angle from nadir and the vehicle velocity. In order to complete the computations in a feasible amount of time, high performance computing (HPC) resources must be leveraged, such as multi-core central processing units (CPUs) and graphics processing units (GPUs). An additional goal is to enable in-situ Monte Carlo analysis techniques in the OATP guidance routine, which adds a layer of complexity. In this case, the OATP guidance will select a small number of candidate trajectories based on their score, and robustness and sensitivity analyses would be completed on each of these trajectories. By incorporating the Monte Carlo capability, more computations are being done onboard, and thus increases the need to utilize HPC resources. This capability being incorporated into the OATP guidance will be investigated in future work.

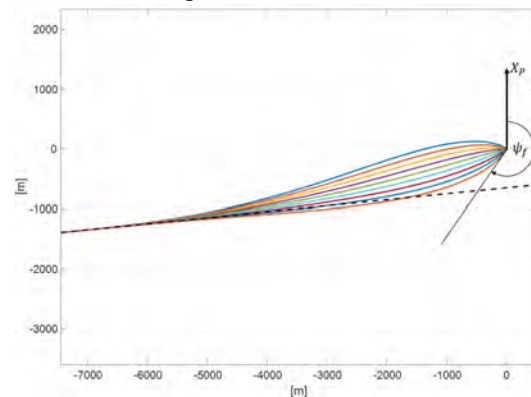


Figure 1: Trajectory design space.

Testing onboard the ISS: Starting in September 2017, Hewlett Packard Enterprise (HPE) began a year-long experiment onboard the ISS by running commercial off the shelf (COTS) multi-core CPU hardware. In December 2018, with the year-long experiment complete, HPE made the compute hardware available for testing software. Beginning December 20, 2018, the OATP guidance routine has begun testing on the multi-core CPUs on the ISS, and it has shown to produce identical results thus far when compared to the data gathered when run on local compute resources at NASA Langley Research Center.

References:

[1] L. E. Chu, K. M. Brown and K. Kriechbaum (2017) *IEEE Aerospace Conference*. [2] J. Rogers and N. Slegers (2013) Aerodynamic Decelerator Systems Technology Conferences. [3] J. Rogers and N. Slegers (2013) *Journal of Guidance, Control, and Dynamics*, 36, 5, 1336-1345. [4] N. Slegers, A. Brown and J. Rogers (2015) *Control Engineering Practice*, 36, 27-38.

DESIGN OF THE PINPOINT LANDING GNC OF SPACE RIDER.

R. Haya Ramos¹, A. Figueroa², J. Veenman³

¹ SENER Aerospace (Severo Ochoa 4, PTM, 28760 Tres Cantos, SPAIN rodrigo.haya@sener.es)

² SENER Aerospace (Severo Ochoa 4, PTM, 28760 Tres Cantos, SPAIN antonio.figueroa@sener.es)

³ SENER Aerospace (Severo Ochoa 4, PTM, 28760 Tres Cantos, SPAIN joost.veenman@sener.es)

Brief Presenter Biography: Mr. Haya is Aeronautical Engineer for the Polytechnics University of Madrid. He has more than 20 years of experience in atmospheric flight and space transportation, comprising re-entry systems, launchers and exploration probes. He is currently the project director for the Reentry Module GNC of Space Rider.

Introduction: Entry, Descent and Landing (EDL) faces several challenges in order to bring safely a vehicle from orbit flying at several km per seconds to rest onto the surface. The management of the energy drives the design and control of the EDL phases and if landing into a designated zone is required, the targeting of the landing area becomes the second EDL driver.

In case high precision at landing is required either by scientific interest or safety of the operation, more control authority is needed to reach the target within hundreds of meters. On the Earth, the use of wings allows runway landing (precise by definition) and re-usability, but the penalty on dry mass cannot be afforded in missions like beyond LEO exploration due to the snow ball effect in mass. Moreover, it has been widely demonstrated, either using capsules or lifting bodies, that wings are not necessary to perform a controlled hypersonic entry flight and hence alternatives are required for the descent and landing.

If the hypersonic guidance is able to leave the vehicle within a few kilometres before initiating the descent sequence the question is how to reduce the dispersion an additional order of magnitude. In case of the Earth, one alternative to the wings is the use of a guided parafoil, that on one side as decelerator continues the philosophy of “brake by free” of the entry and on the other it provides authority for trajectory control and hence targeting capability.

Based on the Intermediate eXperimental Vehicle (IXV) success and assets, an application programme called Space Rider, [1] has been proposed to develop an affordable and sustainable reusable European space transportation system to enable routine “access to” and “return from” space, operating in-orbit, de-orbiting, re-entering, landing on ground and being re-launched after limited refurbishment. Space Rider will perform in-orbit operation, experimentation and demonstration for applications like micro-gravity experimentation, orbit applications and In-Orbit Demonstration and validation

of technologies. These technologies suitable for demonstration inside Space Rider cover a wide spectrum: from Earth science to planetary Exploration. The re-entry module itself is a test bed for entry technologies as the IXV precursor was. The project is currently running Phase C heading towards CDR by the end of the year.

The vehicle used for re-entry is the IXV shape, which is a 5 m long lifting body weighting up to 2.7 Tons. The IXV flight demonstrated in can safely flight down to Mach 1.5 with a precision below 1 km at 25 kn altitude. The first challenge for Space Rider is to pass the transonic and once in subsonic how to achieve pinpoint landing. Resuming the heritage from the ESA/NASA X-38 program and the ESA Parachute Technology Demonstrator project, the landing under parafoil has been baselined in order to meet the 150 m accuracy requirement at landing on prepared terrain.

The landing under controlled parafoil has been mastered in military applications for precision cargo delivery since decades. However, significant differences arise in case of landing of a space vehicle. First, the need to compensate for the dispersion at the beginning of the descent accumulated during hypersonic and supersonic phases and second the need of a soft landing and safe ground roll with no lateral loads. Wind management is one of the main challenges due to the lack of a dedicated Air Data System. Thus, adaptiveness and prediction are key elements in the GNC design.

The Parafoil GNC (PGNC) design is based on a two loops approach (inner and outer), where the inner loop commands the required vehicle attitude to tack the reference descent profile and the outer loop sends the control surfaces deflection commands to the parafoil to achieve the required attitude and rates.

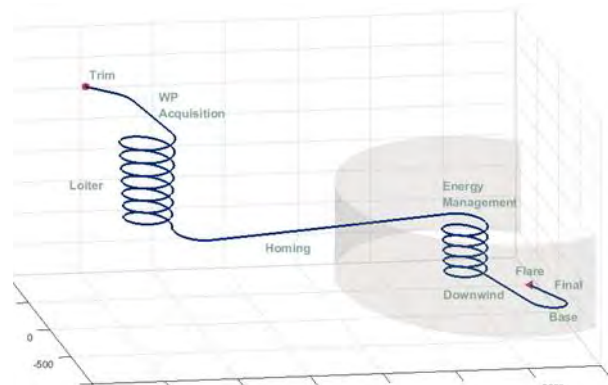


Figure 1 Parafoil Guidance concept for Space Rider

The compatibility with multiple landing sites, each of them with different constraints in terms of safety and environment characteristics, has led to a guidance design based on progressive energy management through waypoints with a final traffic pattern where precise targeting is achieved (Figure 1).

For what concerns the attitude control, the design process follows a systematic and incremental design cycle. The development and validation of the control algorithms relies on an uncertain linear parameter varying (LPV) plant and the control design presented is based on the H_∞ -control approach (Figure 2).

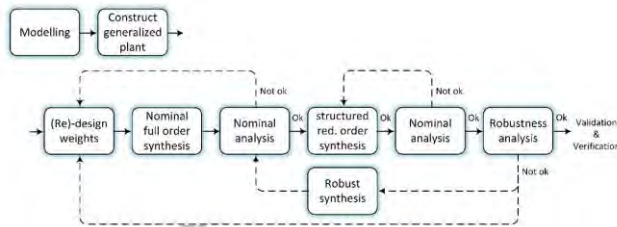


Figure 2 H_∞ design cycle for the parafoil controller

This paper presents an overview of Space Rider, the GNC of the Re-entry Module and in particular of the parafoil GNC. The requirements are presented and discussed as well as the current status of the parafoil GNC design and simulation results including dispersion analysis. Applicability of the precise landing GNC with parafoil to planetary probes is also discussed.

Acknowledgements: This work has been carried out in the frame of the Space Rider Programme of the European Space Agency with Thales Alenia Space Italia and Avio as co-primes. In this context, SENER is the main contractor for the Re-entry Module GNC.

References:

[1] Tumino G. (2018). The VEGA Space Transportation System Development: Status and Perspectives. 69th IAC, Bremen, Germany

An Uncoupled Range Control Approach to Fully Numerical Predictor-Corrector Entry Guidance

B. J. Johnson¹, B. E. Nikaido², Z. Hays², S. N. D'Souza², ¹NASA Johnson Space Center, (2101 E NASA Pkwy, Houston, TX, 77058, Breanna.J.Johnson@nasa.gov), ²NASA Ames Research Center.

Brief Presenter Biography: Breanna Johnson is a Flight Mechanics and Trajectory Design engineer at NASA Johnson Space Center (JSC) and serves as the trajectory design and G&C integration simulation lead for project Pterodactyl, G&C simulation lead for the Mars Mid-L/D Rigid Vehicle (MRV), and manual piloting backup flight software developer for Orion EM-2. Previous NASA projects supported at JSC and Jet Propulsion Laboratory include: MSL, SMAP, Mars 2020 sample return, ISS, and MARAIA capsule.

Introduction: NASA is investing in technologies that could revolutionize the way payloads are delivered to the surfaces of planetary bodies. One area of investment is in deployable entry vehicles (DEVs), a class of vehicles with the potential to increase effective drag, while using less mass than traditional blunt body rigid aeroshells. This increase in energy dissipation for less mass during hypersonic entry makes DEVs attractive options for a wide array of different applications. DEVs like Adaptive Deployable Entry and Placement Technology (ADEPT) and Hypersonic Inflatable Aerodynamic Decelerator (HIAD) have been demonstrated to be capable of transporting the equivalent science payload of a blunt body rigid aeroshell, while using a significantly smaller diameter when stowed in the launch vehicle [1, 2]. However, due to their unique ability to contract and expand, DEVs would also require advancements of current state-of-the-art guidance and control (G&C) architectures to deliver payloads safely and with precision. To close this technology gap, NASA's Space Technology Mission Directorate (STMD) has funded project Pterodactyl, which aims to determine the feasibility of different control system architectures for DEVs that could enable precision targeting. Pterodactyl is the first NASA project to delve into such a study with detailed packaging and structural analysis.

To test these integrated G&C architectures, a challenging lunar return demonstration mission is chosen to stress the developed technology capability. The Lifting Nano-ADEPT (LNA) vehicle is chosen as the DEV to demonstrate the integrated solution [3]. This submission details the trajectory design for the lunar return mission, using a new guidance approach that leverages the strengths of the Fully Numerical Predictor-Corrector Entry Guidance (FNPEG) algorithm [4]. The new guidance approach, FNPEG Uncoupled Range Control (URC), diverges from traditional bank angle guidances by producing angle of attack (α) and sideslip angle (β) commands to thereby decouple downrange and

crossrange control. FNPEG URC is exhibiting similar to better targeting performance to the bank angle commanded FNPEG trajectories, simulated for identical entry interface (EI) conditions for this blunt body vehicle.

Technical Approach: Structural and aerodynamic analyses for different control system architectures suggest an additional need for a non-bank angle guidance. The first control system explored in the feasibility study is a set of 8 aerosurfaces attached at the rib tips of the LNA aeroshell, all designed to increase the aerodynamic effectiveness of the resultant aerodynamic moments. A fully deployed view is shown in Figure 1.

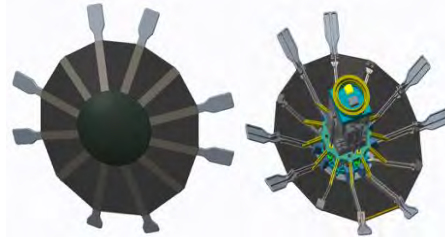


Figure 1. Lifting Nano-ADEPT vehicle model with aerodynamic control surfaces. Front view (left) and aft view (right).

Because of the locations of the control effectors, there was a need to have a guidance algorithm that could command the vehicle's lift vector by using pitching and yawing moments. Traditional bank angle entry guidance algorithms for low L/D blunt body vehicles (e.g. Apollo, MSL, Orion, etc.) and higher L/D vehicles like Space Shuttle, have all relied on the ability to roll the vehicle about its lift vector, in order to steer the vehicle towards the intended target. However, these guidances rely on table lookups to find the sensitivity coefficient gains from linearized reference trajectories to predict the real-time downrange errors and generate bank angle commands [5]. These tables can cause significant delays in the trajectory design process with a rapidly developing mission, as each new change to the vehicle or concept of operations changes the values within these tables. Large uncertainties in the upper atmosphere can also pose challenges in many of these guidances when transitioning between direct and skip entry phases of flight [4]. Because of these concerns, FNPEG became an attractive option to serve as the foundational algorithm for adaptation due to its reliance on fundamental equations of motion [6] during flight. Assumptions for FNPEG were revisited, resulting in the derivation of a more general set of equations to be used in the predictor-corrector, where side force from sideslip angle is desired and utilized as a command, in addition to lift and drag.

FNPEG URC, like FNPEG, may be used for a wide range of vehicles from low to high L/D, and may handle skip and direct entry for both orbital and sub-orbital entry problems. Due to its predictor-corrector nature, dispersions are more readily handled in real time and with minimal to no gain tuning for different trajectories. This flexibility, coupled with the strong convergence rates of guided solutions, makes FNPEG URC a strong candidate for such DEV control architectures. In order to ensure similar convergence rates as FNPEG, the new alpha-beta guidance was developed using the same Newton-Gauss method to iterate upon new angle of attack commands in exchange for bank.

The crossrange error that results from banking the vehicle to minimize downrange can result in different approaches to determine when to perform bank reversals, which can degrade overall targeting performance. Alpha-beta guidances like FNPEG URC and Direct Force Control (DFC) can, by their nature, handle this error in a way that does not affect downrange control using sideslip angle [7]. Crossrange error is nulled by using a proportional-derivative control to track azimuth and produce sideslip angle commands in FNPEG URC.

The adaptation of FNPEG to an alpha-beta guidance algorithm was successful, resulting in guidance profiles that stayed within heating rate and g-load constraints. Example energy profiles of the resultant FNPEG URC trajectories for different EI locations relative to the target (from 2000 to 2300 km) are shown in Figure 2. Through Monte Carlo analysis, this new guidance method was also shown to withstand the applied aerodynamic, atmospheric, and entry interface dispersions typical of a lunar return mission.

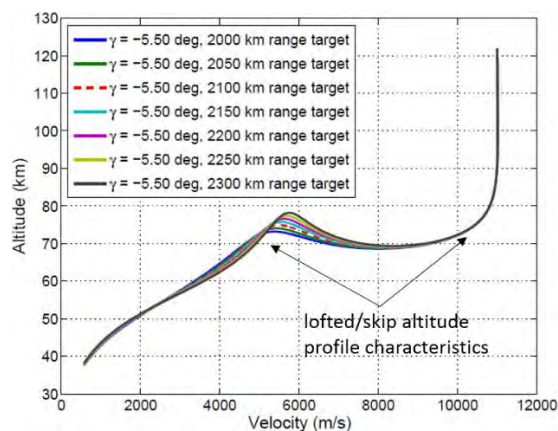


Figure 2. Example FNPEG URC Energy Profile demonstrates the FNPEG trajectory shaping feature, and flexibility is maintained for the alpha-beta guided trajectories.

References: [1] Cassell, A., et al. *ADEPT, A Mechanically Deployable Re-Entry Vehicle System, Enabling Interplanetary CubeSat and Small Satellite Missions*. (2018). [2] Cianciolo, A. D., Polsgrove, T. T. *Human Mars Entry, Descent, and Landing Architecture Study Overview*. SPACE 2016, AIAA 2016-5494. [3] D'Souza, S., et al. *Developing an Entry Guidance and Control Design Capability using Flaps for the Lifting Nano-ADEPT*. 2019 AIAA Aviation and Aeronautics Forum and Exposition. [4] Lu, P. *Entry Guidance: A Unified Method*. Journal of Guidance, Control, and Dynamics, Vol. 37, No. 3, 2014, pp. 713- 728. [5] Graves, C., Harpold, J. *Apollo Experience Report – Mission Planning for Apollo Entry*. (1972). [6] Vinh, N., Busemann, A., Culp, R. *Hypersonic and Planetary Entry Flight Mechanics*. Ann Arbor, Michigan, University of Michigan Press, 1980. [7] Cianciolo, A., Powell, R. *Entry, Descent, and Landing Guidance and Control Approaches to Satisfy Mars Human Landing Criteria*. AAS 2017.

The SPLICE Project: Safe and Precise Landing Technology Development and Testing

J. M. Carson¹, R. R. Sostaric¹, J. N. Estes¹, C. I. Restrepo², M. M. Munk³, A. D. Cianciolo³, ¹NASA Johnson Space Center, Houston, TX, 77058, ²NASA Goddard Space Flight Center, 8800 Greenbelt Rd, Greenbelt, MD, 20771, ³NASA Langley Research Center, 1 Nasa Dr., Hampton, VA, 23666

Brief Presenter Biography: Presenter will be Jay Estes (SPLICE Chief Engineer), Carolina Restrepo (SPLICE Hazard Detection Lead, COBALT Deputy Project Manager), or Alicia Dwyer Cianciolo (SPLICE ConOps Team Lead, Mars EDL Architecture Study Lead).

Introduction: Guidance, Navigation and Control (GN&C) technologies for precise and safe landing are essential for future robotic science and human exploration missions to solar system destinations with targeted surface locations that pose a significant risk to successful landing and subsequent mission operations. These Entry, Descent and Landing (EDL) technologies are a part of the NASA domain called PL&HA (Precision Landing and Hazard Avoidance) and are considered high-priority capabilities within NASA space technology development roadmaps to promote and enable new mission concepts. The SPLICE (Safe & Precise Landing - Integrated Capabilities Evolution) project is a multi-center, multi-directorate NASA project focused on continuing the decade-plus of NASA investments and projects focused on PL&HA technology development and infusion. Multiple GN&C technologies are under development within SPLICE, along with the simulation and field test plans for validation of the capabilities and Technology Readiness Level (TRL) maturation toward infusion into potential near-term robotic lunar landing missions.

NASA Technology Roadmaps [1, 2] and the NASA Space Technology Mission Directorate (STMD) EDL investment strategy deem precision landing and hazard avoidance (PL&HA) technologies as critical capabilities for future robotic science and human exploration missions to the Moon, Mars, icy bodies and other solid surface destinations. The PL&HA suite of technologies includes multiple sensors, algorithms, and avionics components that when integrated together enable a spacecraft to safely land in close proximity to specified surface locations. Such locations include landing within topographically diverse terrain consisting of lander-sized hazards (e.g., high slopes and/or large rocks), as well as in regions in close proximity of pre-positioned surface assets (e.g., cached science samples or human mission infrastructure). These technologies support the NASA Strategic Plan to enable exploration of new solar system destinations and allow access to new surface regions of scientific interest that are currently unreachable with current landing capabilities.

The SPLICE Project has been initiated with the STMD Game Changing Development (GCD) Program as a three-year project from government fiscal year (FY) 2018 through FY 2020. The project objective is to develop, mature, demonstrate and infuse PL&HA technologies into NASA and potential US commercial spaceflight missions. The SPLICE project is the focal PL&HA project within the agency and is the direct successor of the prior NASA ALHAT [3] (Autonomous precision Landing and Hazard Avoidance Technology) and COBALT (CoOperative Blending of Autonomous Landing Technologies) [4] Projects that ended in FY 2015 and FY 2017, respectively. The project also continues the multi-center partnerships within the agency PL&HA community at JSC, LaRC, GSFC, and JPL, and includes contributions from Armstrong Flight Research Center (AFRC) and Marshal Spaceflight Center (MSFC). Additionally, the SPLICE project is closely aligned to other agency focal projects in High Performance Spaceflight Computing (HPSC) and Entry Systems Modeling (ESM) for synergy in both infusion timelines and mission architectures.

SPLICE is developing multiple focal technologies in PL&HA sensing, computing, and algorithms. The SPLICE sensor developments include a NDL (Navigation Doppler Lidar) Engineering Test Unit (ETU) for ultra-precise velocity and range measurements and a HD (Hazard Detection) Lidar Engineering Development Unit (EDU) for high-resolution terrain imaging and safe landing site identification. Additionally, the project is developing a PL&HA DLC (Descent & Landing Computer) EDU that is incorporating a surrogate processor for the in-development NASA HPSC processor. The DLC and surrogate work are focused on preparation of PL&HA algorithms and computational architectures for accelerated migration to the flight HPSC processor once it is completed in the 2022-2023 timeframe. The NDL ETU will achieve TRL 6 in 2019, and the HD Lidar and DLC EDUs will achieve TRL 5 by late FY 2020.

The SPLICE project is also conducting robotic and human mission Concept of Operations (ConOps) studies to understand the relevance of the focal technologies (and to identify the capability gaps) for NASA near-term and long-term missions to the Moon, Mars, and elsewhere. Performance characterization and TRL maturation of the technologies are being accomplished through ground, airborne, and suborbital testing of the component and integrated technologies, as well as in Hardware-in-the-Loop (HWIL) simulation-based testing. Fundamental GN&C and PL&HA algorithms research is also being performed in SPLICE between the

supporting NASA centers and through partnerships with multiple US universities.

References: [1] Steering Committee for NASA Technology Roadmaps; NASA Space Technology Roadmaps and Priorities: Restoring NASA's Technological Edge and Paving the Way for a New Era in Space, *The National Academies Press* (2012). [2] Office of the Chief Technologist, 2015 NASA Technology Roadmaps. [3] Carson III, J. M., Robertson, E. A., Trawny, N., and Amzajerjian, F., "Flight Testing ALHAT Precision Landing Technologies Integrated Onboard the Morpheus Rocket Vehicle," AIAA 2015-4417, (2015). [4] Carson III, J. M., Restrepo, C. I., et al., "Open-Loop Flight Testing of COBALT Navigation and Sensor Technologies for Precise Soft Landing," AIAA 2017-5287, (2017). [5] Carson, J. M. et al., "The SPLICE Project: Continuing NASA Development of GN&C Technologies for Safe and Precise Landing", AIAA 2019-0660 (2019).

Stability Analysis and Control Design for a Deployable Entry Vehicle with Aerodynamic Control Surfaces

W. A. Okolo¹, B. W. L. Margolis¹, J. D. Barton², B. E. Nikaido¹, Z. Hays¹, B. J. Johnson³, B. Yount¹, S. N. D'Souza¹,
¹NASA Ames Research Center, (Mailstop 269-3, Moffett Field, CA, 94035, wendy.a.okolo@nasa.gov), ²Johns Hopkins University Applied Physics Laboratory, ³NASA Johnson Space Center.

Brief Presenter Biography: Dr. Wendy A. Okolo is an Aerospace Research Engineer at NASA Ames Research Center. She (i) leads a controls team to develop the G&C technologies to enable precision landing for entry vehicles, and (ii) serves as a sub-project manager for the System Wide Safety project to monitor, predict, and mitigate risks for unmanned aerial vehicles in the U.S. national airspace.

Introduction: The need to land high mass payloads and return samples from other planets is driving the development of innovative entry vehicle systems called Deployable Entry Vehicles (DEVs). A DEV has the potential to deliver an equivalent science payload with a stowed diameter 3 to 4 times smaller than a traditional entry system with a rigid aeroshell [1]. Traditional vehicles rely on reaction control systems mounted on the backshell to achieve guidance commands. In contrast, DEVs have no backshell, thus one of the primary design challenges for DEVs is the placement and integration of control systems.

NASA's Space Technology Mission Directorate (STMD) has successfully developed two types of DEVs, one that deploys mechanically (Adaptive Deployable Entry and Placement Technology - ADEPT) and another that deploys pneumatically (Hypersonic Inflatable Aerodynamic Decelerator - HIAD) [1]. In addition, STMD is funding a Pterodactyl project, which is a design, test, and build capability to (i) advance the current state of the art for entry vehicle guidance and control (G&C) and (ii) determine the feasibility of control system integration for various entry vehicle types, for example, those without aeroshells [2]. This capability is currently being used to develop novel and non-propulsive G&C solutions for the Lifting Nano-ADEPT (LNA) vehicle.

In this submission, we detail our efforts on the Pterodactyl project to (i) analyze and augment the stability of the LNA during entry and (ii) design a control system that will utilize aerodynamic surfaces to track reference angle-of-attack and side-slip angle commands from a guidance algorithm.

Technical Approach: First, the stability analysis of the asymmetric LNA will be presented, followed by the novel control design architecture for the vehicle to track guidance commands using eight control surfaces as seen in Fig. 1. Finally, simulation results of tracking the commanded angle-of-attack and sideslip angle will be shown.

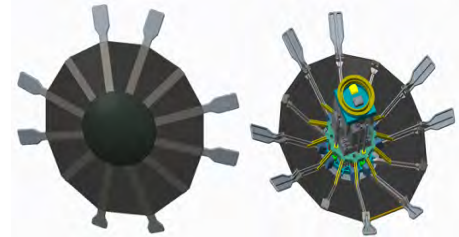


Figure 1. Lifting Nano-ADEPT vehicle model with aerodynamic control surfaces. Front view (left) and aft view (right).

Stability Analysis: Aerodynamic data for the vehicle was generated using CBAERO [3]. The database was post-processed to remove spurious solution errors and ensure symmetry, particularly with sideslip angle variation. Multivariate B-splines [4] were constructed to smoothly interpolate the clean aerodynamic database to obtain aerodynamic force and moment coefficient dependencies on Mach, dynamic pressure, angle-of-attack, and sideslip angle. The interpolating spline curves can then be differentiated to obtain the dimensionless stability derivatives. In Fig. 2 we show the pitch stiffness derivative, $C_{M\alpha}$ versus angle-of-attack at a Mach number of 25 and dynamic pressure of 0.015bars. This parameter is negative, indicating longitudinal static stability for the LNA. For brevity, only this stability derivative is depicted.

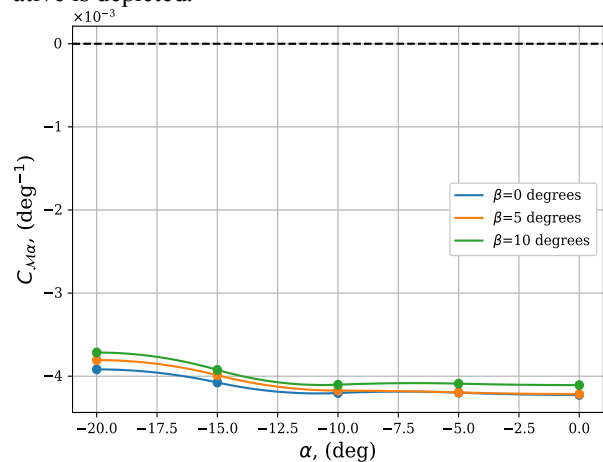


Figure 2. Pitch stiffness vs angle of attack

Control Design: A MIMO (multi-input multi-output) state-feedback integral controller is designed based on LQR (Linear Quadratic Regulator) optimal control techniques [5]. The LQR method is selected because it has attractive performance and stability characteristics.

These are important control requirements for the asymmetric LNA vehicle. In addition, the LQR control design technique allows for the relative allocation of the control variables through the choice of weighting matrices in the cost index. Thus, we can specify which and how much of the eight control surfaces to use.

Since the control system will be tracking angle of attack and sideslip angle commands from guidance, we will model the vehicle state

$$x(t) = [V \beta \alpha p q r \sigma \gamma z e_\beta e_\alpha e_\sigma]^T$$

where V is the velocity magnitude, β is the sideslip angle, α is the angle of attack, p , q , and r are the angular velocities about the body-fixed x , y , and z axes, σ is the bank angle, γ is the the flight-path angle, z is the radial distance from the planet center, and e_β , e_α , and e_σ are the augmented states of the integral error of sideslip angle, angle-of-attack, and bank angle, respectively.

The system control inputs

$$u(t) = [\delta_1 \delta_2 \dots \delta_8]^T$$

are the hinge deflection angles of the eight aerodynamic control surfaces into or out of the flow.

To develop the linear controller, we linearize the equations of motion, for the states defined above, at different points in the flight envelope to obtain state-space linear equations of the form

$$\Delta \dot{x} = A \Delta x + B \Delta u$$

where Δx and Δu are deviations from the linearization point x^* , u^* . The matrices A and B defined by

$$A = \left. \frac{\partial f}{\partial x} \right|_{x^*, u^*}$$

$$B = \left. \frac{\partial f}{\partial u} \right|_{x^*, u^*}$$

are called the state and input matrices respectively, where f is the vector-valued function of the non-linear dynamics for each state concatenated together.

Using these linearized dynamics, the LQR control law is given by

$$\Delta u = -K \Delta x$$

and the gain matrix K is computed to minimize the quadratic cost function

$$\int_0^\infty \Delta x^T Q \Delta x + \Delta u^T R \Delta u dt$$

where Q and R are tunable weighting matrices for the states and control surfaces respectively. The gain matrix K that minimizes the cost function for a particular linear system can be found using a number of numerically stable algorithms by constructing the appropriate Algebraic Riccati Equation or Linear Matrix Inequality [6].

Preliminary Simulation Results: To evaluate the control system, two simulation environments have been developed, in Python [7] and MATLAB. The simulations will be used to validate stability analyses and evaluate performance trends for different regimes in the

flight envelope. In Fig. [3] we show that for a fixed flight condition, the errors between the true signals (β , α , and σ) and the commanded signals (β_c , α_c , and σ_c) are driven to zero. The control system is able to regulate, stabilize, and control the LNA vehicle.

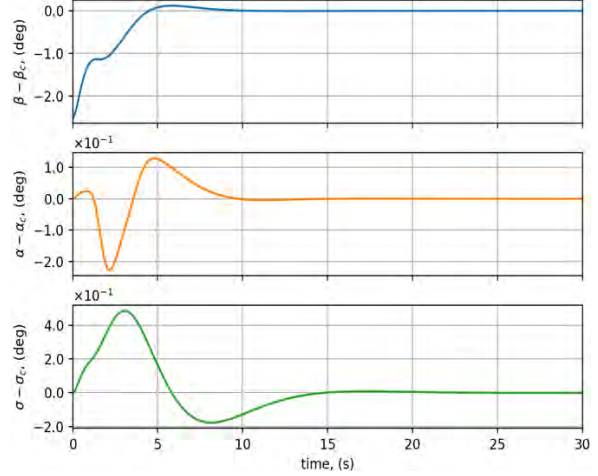


Figure 3. Simulation results depicting errors between commanded and actual signals.

References: [1] Cassell, A., et al. "ADEPT, A Mechanically Deployable Re-Entry Vehicle System, Enabling Interplanetary CubeSat and Small Satellite Missions." (2018). [2] D'Souza, S., et al. "Developing an Entry Guidance and Control Design Capability using Flaps for the Lifting Nano-ADEPT." 2019 AIAA Aviation and Aeronautics Forum and Exposition. [3] Kinney, D., et al. "Predicted convective and radiative aerothermodynamic environments for various reentry vehicles using CBAERO." 44th AIAA Aerospace Sciences Meeting and Exhibit. 2006. [4] de Boor, C. "A Practical Guide to Splines." Spring, 1978. [5] Kirk, D. E. Optimal control theory: an introduction. Springer, 1970. [6] Boyd, Stephen, et al. Linear matrix inequalities in system and control theory. Vol. 15. Siam, 1994. [7] Margolis, BWL "SimuPy: A Python Framework for Modeling and Simulating Dynamical Systems." Journal of Open Source Software, September 2017.

THE DRAGONFLY ENTRY AND DESCENT SYSTEM

M. J. Wright,¹ J. Herath,² H. H. Hwang,³ A. M. Brandis,⁴ D. Buecher,⁵ D. Adams,⁶ and R. Lorenz⁷

¹NASA Ames Research Center, Moffett Field, CA 94035. Michael.J.Wright@nasa.gov

²NASA Langley Research Center, Hampton, VA, CA 23681. jeffrey.a.herath@nasa.gov

³NASA Ames Research Center, Moffett Field, CA 94035. Helen.Hwang@nasa.gov

⁴AMA, Moffett Field, CA 94035. Aaron.M.Brandis@nasa.gov

⁵Lockheed Martin Space System, Littleton, CO 80120. David.Buecher@lmco.com

⁶Applied Physics Lab, Laurel, MD 20723. douglas.adams@jhuapl.edu

⁷Applied Physics Lab, Laurel, MD 20723. Ralph.Lorenz@jhuapl.edu

Brief Presenter Biography: Michael Wright has worked at NASA Ames Research Center for twenty years, specializing in Entry, Descent and Landing technologies, aerothermodynamics, and thermal protection systems. He is the primary developer of the aerothermodynamics code “DPLR,” 2007 NASA software of the year, and has supported EDL for many flight missions, including Orion, MSL, Stardust, Phoenix, and Huygens. Michael is currently the EDL Assembly lead for the proposed *Dragonfly* New Frontiers mission to Titan.

Introduction: *Dragonfly* is a proposed New Frontiers class mission that will send a nuclear powered octocopter to the surface of Titan for an extended science mission. This presentation will provide an overview of the Entry and Descent system that is under development to ensure the safe delivery of this unique “relocatable lander” to Titan.

Titan’s dense atmosphere, large atmospheric scale height, and low gravity allows for a slow-paced entry and descent sequence that lasts more than 100 minutes, as opposed to the “7 minutes of terror” that is characteristic of landed Mars missions. This slow pace allows for sufficient temporal separation between critical events of the EDL sequence to minimize overall risk.

The *Dragonfly* entry and descent system is composed of high-heritage components, minimizing overall risk. The aeroshell will be a scaled Genesis Sample Return capsule with a diameter of 3.75 meters, built by Lockheed Martin. The thermal protection system (TPS) is made up of Phenolic Impregnated Carbon Ablator-Domestic (PICA-D) on the heatshield, SLA-561V on the backshell, and SLA-220M on the aft cover and low gain antenna. Each material has extensive heritage for the chosen application. The spacecraft will enter Titan at a velocity of 7.3 km/s, resulting in a predicted fully margined stagnation point heating environment of 254 W/cm² heat rate and 13 kJ/cm² heat load, well within the tested limits of the chosen materials. The aeroheating environments, including the significant contribution of shock layer radiation from CN on both the heatshield

and backshell, are evaluated using state of the art models and codes that have been validated with appropriate ground testing.

Once the deceleration pulse is complete, a disk-gap-band (DGB) drogue parachute will be deployed at approximately Mach 1.5 to stabilize and further decelerate the spacecraft. Due to the dense atmosphere, the spacecraft will spend more than 80 minutes on this parachute, until reaching an appropriate altitude to deploy the subsonic main parachute. The lander is released after approximately 17 minutes on the main chute before releasing and transitioning to powered flight in order to navigate to its first landing site. The release of the lander from the backshell effectively ends the entry and descent portion of the mission.

The full presentation will provide additional details about the design of the EDL system hardware, engineering design, and overall con-ops. Preliminary aerothermal and TPS sizing analyses will be presented, and the parachute system will be described in greater detail. In addition, the *Dragonfly* spacecraft will carry an Engineering Science Investigation (ESI) package designed to obtain engineering data during EDL that will be used to validate the design methodology for future missions. An overview of the proposed ESI package will also be presented.

European Solutions for Heatshields of High Energy Entry Probes

Jean-Marc Bouilly – jean-marc.bouilly@ariane.group– Ariane Group SAS,
Site Issac, Rue du Général Niox, BP 30056, 33166 Saint Médard en Jalles Cedex, France
Marc Lacoste – marc.lacoste@ariane.group

Brief Presenter Biography: Jean-Marc Bouilly graduated from Ecole Centrale Paris in 1984. He joined Aerospatiale in 1985 (Issac site, now part of ArianeGroup), where he has been in charge of TPS development first for military applications, and then for the Atmospheric Reentry Demonstrator ARD and Huygens. Later, he managed the Thermal and Thermomechanical Engineering section for 11 years. Since 2008, he has served as the Deputy Head of ArianeGroup 'Reentry Systems & Technologies Department' and was appointed as a senior expert in thermal analysis and TPS. He is supporting advanced projects and preliminary projects phases for atmospheric entry vehicles (ExoMars, Marco Polo, Phootprint, MSR...). He also contributes to Space Debris Mitigation studies, and is leading ArianeGroup R&T activities on Reentry Technologies.

Abstract: It is unquestionable that the Thermal Protection System (TPS) is a key technology for planetary entry.

This is even more critical for the most demanding atmospheric entry missions, such as: Venus, Sample Return from Mars or far Solar System bodies to Earth, Ice Giants, Gas Giants. In each case, high robustness and good thermal performance are required, and the best suitable compromise has to be selected.

A significant heritage is available in the US, relying on successful entries of several missions: Pioneer-Venus, Galileo, Stardust, Genesis.

Even though appearing at less emblematic at a first glance, ArianeGroup also owns a robust background and can provide in Europe a wide range of solutions for heatshields and entry vehicles..

This talk will present the corresponding heritage in the domain with two main parts:

- An overview of ArianeGroup capabilities for entry probes (trajectory and aerothermodynamics analyses, probe design, material qualification in a relevant environment, elaboration of a reliable thermal and ablation model...) gained in several programmes: Huygens, ARD, Beagle2, ExoMars, IXV & SpaceRider, and defense projects as well.
- A particular focus on material and technologies which are mastered at industrial level for ArianeGroup rocket propulsion core business. Available materials such as carbon-phenolic or carbon-carbon can provide suitable solutions for heatshields, with adequate shape and dimensions.

- This part will be completed with an outline of the company experience about hybrid solutions (SPA, Sepcore, Hydra) associating a material layer resistant to ablation, and a second one providing insulation. Such concepts may be very useful in view of an optimal performance with a minimum mass.

This talk will highlight ArianeGroup readiness to provide adequate solutions for currently envisaged mission: Ice Giants, MSR, and other Sample Return missions as well.

SUSTAINING PHENOLIC IMPREGNATED CARBON ABLATOR (PICA) FOR FUTURE NASA MISSIONS INCLUDING DISCOVERY AND NEW FRONTIERS

D. Ellerby¹(Donald.T.Ellerby@nasa.gov), E. Venkatapathy¹, M. Stackpoole¹, M. Gasch¹, F. Milos¹, K. Peterson¹, Dinesh Prabhu² and Kristina Skokova², S. Violette³

¹NASA Ames Research Center, Moffett Field, CA 94035

²AMA, Inc. at NASA Ames Research Center, Moffett Field, CA 94035

³Fiber Materials Inc, Biddeford, ME 04005

Brief Presenter Biography: Don Ellerby is a materials scientist in the Entry Systems and Vehicle Development Branch at NASA Ames Research Center. Don's work primarily focuses on technology development for thermal protection systems. He has a B.S. in Ceramic Engineering and PhD in Materials Science and Engineering from the University of Washington.

Introduction: Phenolic Impregnated Carbon Ablator (PICA) was invented in the mid 1990's and due to its relatively low density and efficient performance has been the heat shield TPS of choice for a range of missions including, Stardust, OSIRIS-Rex, Mars Science Laboratory (MSL) and Mars 2020. PICA has also been the TPS solution on numerous Discovery and New Frontiers proposals, as both the heat shield and back shell TPS and is under consideration as both for the Mars Sample Return Earth Entry Vehicle (EEV) and the heat shield on the Sample Retrieval Lander (SRL).

Recently NASA's Science Mission Directorate (SMD) has funded an activity to develop a more sustainable version of PICA and to expand the demonstrated capabilities of PICA both in manufacturing and aerothermal performance.

Sustainability: PICA is formed by the infusion of a low density phenolic resin into a carbon bonded carbon fiber preform known by the trade name FiberForm®. A Rayon staple is utilized as the precursor of the carbon fibers used in the preforms. In the last 25 years the rayon precursor has had to be requalified at least twice, for use in the manufacturing of PICA and a third substitution is now required.

The challenges with sustaining the rayon precursor stem from the environmental concerns associated with the manufacturing processes, for instance there is no longer a domestic United States supplier of rayon fibers. In order to avoid the continued challenges with Rayon a cellulosic based fiber, known as Lyocell, that are produced in a more environmentally responsible process, and are produced domestically within the US, has been identified as a viable replacement for rayon as the precursor for the carbon fibers used in the preforms for PICA. This work will review the status of testing domestically produced PICA (PICA-D) utilizing the Lyocell precursor. Testing to date shows the PICA-D material to have

comparable performance to that of previous PICA materials utilizing different rayon sources.

Capability Extension: The second part of this work has been to look at extending the capability of PICA to larger size single piece heat shields and to demonstrate performance at more demanding aerothermal environments in the past.

To date the demonstrated limit for the size of a single piece PICA heatshield is ~0.8m in diameter, however there are many mission studies that would have benefited from the ability to utilize a larger single piece heatshield. NASA ARC has been working with Fiber Materials Inc. to demonstrate the near net shape casting of the FiberForm preform needed for a single piece heat shield up to ~1.4m in diameter, see figure 1, and the subsequent resin infusion of the part converting it to PICA.



Figure 1. Near net shape cast 1.4m diameter FiberForm Preform.

In addition the PICA extensibility work has focused on demonstration of material performance in more aggressive aerothermal environments through a series of ground based arcjet tests, coordinating conditions with potential near term missions.

The status of the manufacturing and aerothermal extensibility work will be reviewed in this work.

ADEPT Sounding Rocket-One Flight Test Overview.

A. M. Cassell¹, P. F. Wercinski¹, B. C Yount¹, O. Nishioka¹, J. Williams¹, S. Dutta², A. Korzun² and J. Tynis², ¹Entry Systems and Vehicle Development Branch, NASA Ames Research Center (Mailstop 229-1, Moffett Field, CA 94035, USA, Alan.M.Cassell@nasa.gov), ²NASA Langley Research Center (Hampton, VA 23681, USA).

Brief Presenter Biography: Alan is a Systems Engineer in the Entry Systems and Vehicle Development Branch at NASA Ames Research Center. He has contributed to various EDL systems development including aeroshell testing for the Mars Science Laboratory, Large-Scale HIAD ground testing, and ADEPT test and concept development. He is currently the Lead Systems Engineer for the ADEPT project.

Introduction: On September 12th 2018, a sounding rocket flight test was conducted on a mechanically-deployed atmospheric entry system known as the Adaptable Deployable Entry and Placement Technology (ADEPT). The purpose of the Sounding Rocket One (SR-1) test was to gather critical flight data for evaluating the vehicle's in-space deployment performance and supersonic stability. This flight test was a major milestone in a technology development campaign for ADEPT: the application of ADEPT for small secondary payloads. The test was conducted above White Sands Missile Range (WSMR), New Mexico on a SpaceLoft XL rocket manufactured by UP Aerospace. This paper describes the system components, test execution, and test conclusions [1].

Flight Test Objectives: the SR-1 flight test matured ADEPT in the areas of deployment and structural integrity (for missions employing <1 m deployed diameter), and improved aerodynamic knowledge [2] of the ADEPT open-back configuration. In addition, SR-1 was an integrated system demonstration in a partially relevant environment (SR-1 did not experience significant heating but reached supersonic speeds). The Key Performance Parameters (KPPs) for the ADEPT SR-1 flight experiment were:

- 1) Exo-atmospheric deployment to the desired entry configuration.
- 2) Aerodynamic stability without active control of the 1m-class ADEPT deployed flight configuration.

ADEPT Design: The SR-1 vehicle forms an octagonal pyramid with a spherical nose cap aeroshell when deployed. For this mission, the rectangular prism-shaped payload volume (~3U CubeSat form factor) is mostly filled with instrumentation, and the "payload" volume is integrated to the aft side of the aeroshell. The nominal dimensions of the stowed configuration are 0.24 m diameter, while the deployed configuration is 0.7

m diameter (rib-tip to rib-tip) with a 70° "half-cone" angle at the ribs. Figure 1 shows the ADEPT SR-1 entry configuration. The total mass was 11.0 kg (24.2 lb).

The ADEPT entry vehicle is comprised of a mechanical and electrical subsystems. The primary functional requirements of the mechanical system are to deploy and tension the 3D woven carbon fabric aeroshell, lock the structure in a fully-deployed and tensioned configuration, and maintain the required aerodynamic shape. The electrical subsystem is comprised of the battery, power distribution board, separation sensors, inertial measurement units, GPS receiver, C-band transponder and GoPro camera.

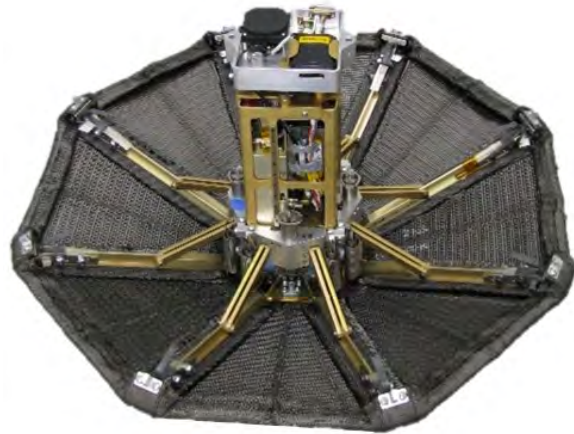


Figure 1- ADEPT SR-1 entry configuration.

Flight Test Overview and Results: The launch occurred from the vertical launch area at Spaceport America in New Mexico into the White Sands Missile Range (WSMR) on September 12, 2018 at 13:33 UTC (7:33 AM local). The ADEPT SR-1 flight unit was powered-on at approximately 5:30 AM local time, 2 hours prior to the launch window opening. After launch, booster burn-out occurred ~12 s into flight followed by high spin (>7 Hz) coast to the de-spin mechanism deploy point (launch + 55 s). Next, the nose was separated (launch + 60 s), followed by booster separation (launch + 90 s) and ADEPT separation (launch + 95 s). Sensing separation from the launch vehicle (LV) at + 95 s, ADEPT deployed 40 seconds later at + 135 s. Figure 2 shows a still image extracted from the onboard GoPro video camera just after deployment with the LED status indicator panel in view displaying that all systems were functioning as expected. The fully locked deployment indicator status LED is lit (leftmost LED), indicating the

project goal for fully locked deployment into the desired aerodynamic shape prior to entry was met (KPP #1). Apogee (~110 km) was reached at +156 s. As ADEPT descended it encountered atmospheric interface (defined as 85 km), which occurred at +229 s. ADEPT decelerated through the transonic flight regime at +290 s. Impact occurred at +857 s within WSMR. The ADEPT test article was radar tracked by WSMR as it returned to Earth. A Sikorsky UH-60 Black Hawk helicopter was dispatched around 1:30 PM in the afternoon of September 12 approximately 6 hours after SR-1 impacted the ground. The final radar location latitude and longitude were provided to the recovery team which quickly spotted the test article once the helicopter arrived at the impact location approximately 48 km (30 miles) E-NE from the launch site.

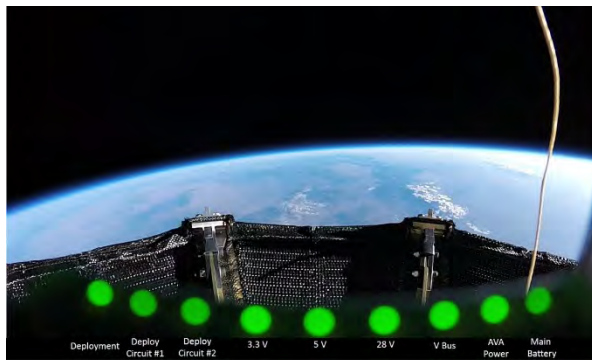


Figure 2- still frame taken from onboard GoPro video camera just after exoatmospheric deployment showing all 9 health status LEDs illuminated.

ADEPT SR-1 had several sensors on-board and also leveraged third-party data sources for post-flight analysis and trajectory reconstruction. Based upon data review, the LV met exo-atmospheric delivery performance requirements of spin rate, no re-contact, separation velocity, and delivery altitude. Radar tracking of SR-1 was achieved after apogee but before SR-1 re-entered the atmosphere. The three SR-1 on-board data sources: 1) primary IMU, 2) back-up IMU, and 3) Go-Pro camera were all operational and successfully stored in-flight data, which were recovered post flight. The primary data products were used to perform flight mechanics analysis [3] and reconstruct the as-flown trajectory [4]. Post-flight analysis showed that the vehicle met the threshold of achieving stable flight below Mach = 0.8 (KPP #2).

The ADEPT SR-1 flight test provided a low-cost means of achieving significant system level maturity for the 1 m class ADEPT configuration. Continued improvements in thermostructural design and predictive modeling tools are anticipated to prepare for a low earth

orbit re-entry demonstration test that will achieve mission readiness for secondary class payloads such as CubeSat and Small Satellite missions.

References:

- [1] Cassell, A. M., et al, "ADEOT Sounding Rocket One Flight Test Overview," *AIAA Aerodynamic Decelerator Systems Technology Conference*, Dallas, TX, 17-21 June 2019.
- [2] Korzun, A. M., Dutta, S., McDaniel, R. D., Karlgaard, C., Tynis, J. A., "Aerodynamics for the ADEPT SR-1 Flight Experiment," *AIAA Aerodynamic Decelerator Systems Technology Conference*, Dallas, TX, 17-21 June 2019.
- [3] Dutta, S., Green, J. S., "Flight Mechanics Modeling and Post Flight Analysis of ADEPT SR-1," *AIAA Aerodynamic Decelerator Systems Technology Conference*, Dallas, TX, 17-21 June 2019.
- [4] Tynis, J. A., Karlgaard, C., "Reconstruction of the Adaptable Deployable Entry and Placement Technology Sounding Rocket One Flight Test," *AIAA Aerodynamic Decelerator Systems Technology Conference*, Dallas, TX, 17-21 June 2019.

TECHNOLOGY READINESS ASSESSMENT FOR HEEET TPS.

P.J. Gage¹, D. Ellerby², E. Venkatapathy².

¹Neerim Corp. at NASA Ames Research Park (Mail Stop 229-3, NASA Ames Research Center, Moffett Field, CA 94035. E-mail: peter.j.gage@nasa.gov), ²Space Technologies Division, NASA Ames Research Center

Brief Presenter Biography: *Peter Gage runs Neerim Corp, a systems engineering organization that supports entry vehicle development at NASA Ames Research Center.*

The HEEET project was conceived to develop a heatshield with a high performance ablative thermal protection material that can withstand the extreme entry environment produced as a result of rapid deceleration during high speed entry into Venus, Saturn, Uranus or higher speed entry into Earth's atmosphere. Successful maturation of HEEET supports future New Frontiers and Discovery AO's, as well as Flagship and directed missions in the longer term. In addition, HEEET has the potential to evolve and to support re-entry to Earth, for missions such as Mars Sample Return.

The primary goal of the HEEET Project was to develop an ablative TPS heat-shield based on woven TPS technology to Technology Readiness Level (TRL) 6. Key evidence to support the TRL evaluation includes:

- Demonstration of reproducible manufacturing of a dual layer material over a range of thicknesses and integrated on to a heatshield engineering test unit at a scale that is applicable to near term Discovery as the highest priority and future NF missions as secondary priority set of missions.
- Demonstration of predictable and stable performance of the dual layer TPS over a range of entry environments that are applicable to near term Discovery and NF missions of interest to SMD.

- Includes completion of coupon arc jet and laser testing and development of a mid-fidelity thermal response model that correlates with test results.
- Demonstration of flight heatshield system design for a range of sizes and loads that are relevant to near term Discovery and NF missions of interest to SMD.
 - Includes completion of structural testing to validate analytic thermal/structural models and development of a material property database.
 - Includes structural testing of a ~1m Engineering Test Unit under relevant entry loads.

The NASA Systems Engineering Handbook [1] includes generic guidance for technology readiness assessment. A Government Accounting Office review of assessment approaches across multiple agencies identified a lack of consistency in methodologies that are applied [2]. The HEEET team chose to apply detailed guidance developed at JPL for TRL assessment [3].

The final presentation will summarize the self-assessment by the development team, and evaluation by an independent review team.

References: [1] NASA Systems Engineering Handbook. [2] Best Practices for Evaluating the Readiness of Technology for Use in Acquisition Programs and Projects GAO-16-410G, August 2016. [3] JPL Institutional Technology Readiness Levels and Technology Readiness Assessment DocID 78797, Rev. 0

THE CHALLENGES OF SEAM DESIGN IN TILED THERMAL PROTECTION SYSTEMS

C. D. Kazemba (cole.d.kazemba@nasa.gov),¹ K. H. Peterson¹, D. T. Ellerby, and P. J. Gage²

¹NASA Ames Research Center, Moffett Field, CA 94035

²Neerim Corp, Moffett Field, CA 94035.

Brief Presenter Biography: Cole Kazemba is an aerospace systems engineer in Entry Systems and Vehicle Development Branch at NASA Ames Research Center. Cole's work focuses on technology development of advanced thermal protection systems for planetary exploration. He has a B.S. in Aerospace Engineering and Mechanics from the University of Minnesota and an M.S. in Aerospace Engineering from the Georgia Institute of Technology.

Introduction: Heatshield systems face severe coupled structural and aerothermal environments during their entry into planetary atmospheres. Innovative solutions are often required to satisfy all requirements imposed by these environments, particularly when adding margin against one requirement increases the challenge associated with another requirement. For tiled thermal protection systems (TPS), the seam between tiles is the element in the heatshield system that typically requires the most design attention to meet mission-specific constraints.

Requirements: The seam elements in a tiled heatshield serve a vital function in a heatshield system by providing compliance to an otherwise rigid assembly, thereby maintaining acceptable stress levels as the aeroshell deforms under load. This functionality must be accomplished with a design that is feasible from a manufacturing perspective and compatible with the aerothermal requirements levied on the TPS materials.

Previous Designs: Several of NASA's most notable entry systems in recent years have employed tiled heatshields. In the trade study conducted to down-select the TPS system for the Orion vehicle, several tiled systems were explored. One seam solution demonstrated in that effort, RTV adhesive between tiles of PICA TPS, was later employed successfully by the Mars Science Laboratory (MSL) entry vehicle and is currently being implemented on Mars 2020. Another design known as "PICA on Edge" was developed for the tiled PICA TPS system, was patented, but ultimately was not implemented. Additionally, the recent design change to tiled Avcoat blocks for the Orion vehicle required significant development and verification effort for the seam solution.

HEEET: Heatshield for Extreme Entry Environments Technology (HEEET) is a new NASA-developed TPS that uses a 3D-woven preform for the tiles to provide a highly efficient and robust construction. For mission applications relevant to HEEET, the severe entry

pressures, shear levels, and heat fluxes drive the need for more robust seam solutions than those used for tiled PICA or Avcoat. A pure adhesive solution was demonstrated to be infeasible either from poor aerothermal performance or insufficient compliance to allow adequate deflections in the system.



Figure 1: HEEET Engineering Demonstration Unit

Given the limitations of adhesive-filled seams, the team ultimately developed a solution that builds on the PICA-on-Edge concept. The seam is comprised of a thin phenolic film adhesive on either side of a compliant gap filler material. The adhesive bonds the gap filler to the neighboring tiles and is thin enough to survive the aerothermal environment. The gap filler is a modified version of the base HEEET material that is subject to additional processing to improve its compliance, which minimizes compliance requirements on the adjacent. A novel integration approach is employed to achieve the required adhesive bondline thickness. The seam design has been validated through aerothermal and structural testing as well as a full scale manufacturing demonstration.

This presentation will discuss the overall challenges facing seam design in tiled TPS systems, provide examples of solutions implemented by past missions, and highlight the recent innovations developed by the HEEET team to develop a seam capable of meeting the most demanding environments ever levied on a tiled heatshield.

References:

Blosser, et al., 2015, "Space vehicle heat shield having edgewise strips of ablative material," US Patent No. 9,051,063

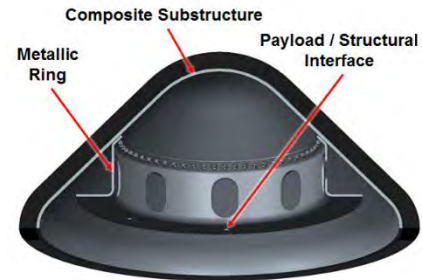
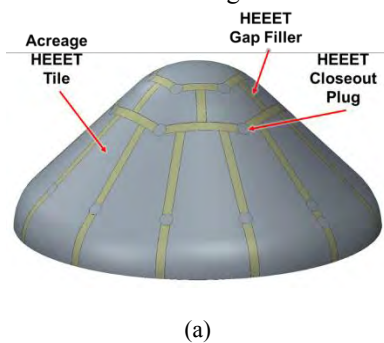
Damage Assessment During a Structural and Thermal Test Campaign of a 1-meter Diameter Heatshield with a 3-D Woven Thermal Protection System for Extreme Environments

S. L. Langston¹, S. C. Splinter¹, C. C. Poteet¹ and K. H. Peterson², ¹NASA Langley Research Center Hampton, VA 23681, ²NASA Ames Research Center Moffett Field, CA 94035

Brief Presenter Biography: Ms. Sarah Langston has been a research aerospace engineer at NASA Langley Research Center since 2015. Her primary research interests include thermal and structural analysis of space vehicles and flight dynamics.

Introduction: The Heatshield for Extreme Entry Environment Technology (HEEET) Project designed and manufactured a 3-D woven dual-layer thermal protection system (TPS) [1]. The TPS consisted of an outer recession layer comprised of densely woven carbon fiber and an inner less densely woven insulating layer comprised of blended carbon and phenolic yarns. The two layers were woven as one piece, and were mechanically interlocked using a 3-D layer to layer weave. The final material was infused with phenolic resin as a low density porous matrix. The material was designed to be used in extreme heating rate and pressure environments, such as missions to Venus, Saturn and the Ice Giants. To demonstrate a technology readiness level of six for the HEEET TPS, a 1-meter diameter prototype heatshield was built and structurally tested in relevant environments via ground testing at NASA Langley Research Center.

The prototype, or Engineering Test Unit (ETU), geometry was representative of a vehicle for a Saturn mission and was comprised of the HEEET material bonded to a composite substructure with an internal metallic ring for attaching ground support equipment. The rendering of the exterior and interior of the ETU, with key features labeled is shown in Figure 1.



(b)

Figure 1. Rendering of the exterior (a) and interior (b) of the ETU with key components labeled.

Test Campaign: The ETU test campaign took place from June 2018 through August 2018 at NASA Langley Research Center [2-4]. A static pressure test was performed at both room and elevated temperature. Two rounds of static point load testing were performed to obtain relevant deflections at critical joints and features. The second round of point load testing consisted of fewer test points, taken to higher loads than round one and occurred after thermal-vacuum testing. The thermal-vacuum test was performed to simulate the temperature changes experienced by the heatshield during on-orbit transit. Nondestructive evaluation (NDE) consisted of: a computed tomography (CT) scan taken of the entire ETU prior to the beginning and at the conclusion of the test campaign, and microscopic inspection of the heatshield seams performed between each test. The test campaign is outlined in Figure 2.

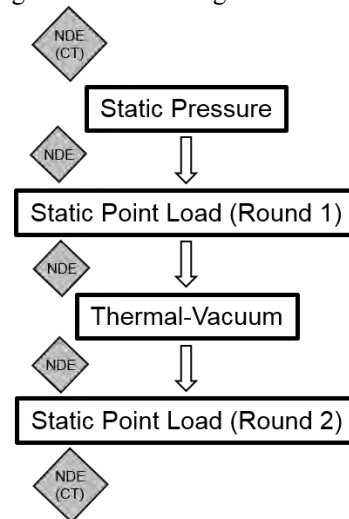


Figure 2. ETU test campaign outline.

The ETU had 79 strain gage instrumentation channels and 14 thermocouples to record data during the tests. The exterior of the ETU was instrumented with 17 biaxial strain gages, 12 uniaxial strain gages and 4 thermocouples. The interior of the ETU was instrumented with 7 biaxial strain gages, 19 uniaxial strain gages, and 10 thermocouples. The strain gages and thermocouples were primarily arranged in rays along the radial direction of the ETU, with additional gages placed elsewhere for defect tracking. The main purpose of the strain gage data was for comparison with expected strain results derived from pre-test analysis.

Test Campaign Results: An example of the comparison of collected strain gage data from the room temperature static pressure test and the expected strain from the analysis at the full pressure loading is displayed in Figure 3. The analysis and measured strain results were in good agreement for the majority of the tests. The collected strain data was used to confirm modeling techniques and material properties. Select strain gages were also monitored during testing to track any large changes in strain that may indicate damage.

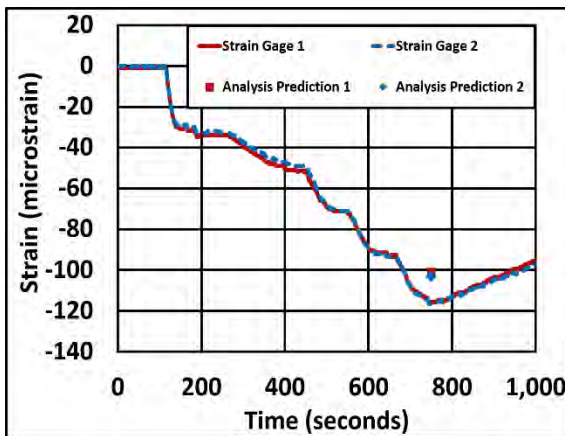


Figure 3. Comparison of the as collected strain data to the predicted strain from pre-test analysis during the room temperature pressure test.

In Situ NDE: While a CT scan of the entire ETU [5] was desired for inspecting the HEEET material and seams for internal defects, performing CT scans between each test series was not feasible. The seams were deemed one of the most critical areas to inspect between tests. Therefore, new methods were derived for inspecting the ETU seams in the test configuration and tracking differences found in the seam bondlines between tests. Two primary methods were implemented: inspection using a portable inspection microscope to take pictures of the bondline and with a jeweler's loupe. Prior to instrumentation, after the thermal-vacuum test, and after all tests were completed, microscope pictures (as shown in Figure 4) were taken

and mapped to all of the bondlines of the ETU. The pictures were then compared between tests to determine if any changes to the bondlines had occurred. In addition to the microscope pictures, inspection using a magnified jeweler's loupe was also performed between each test. The two bondline inspection methods were used in combination due to the amount of time that the full microscope survey took and because the jeweler's loupe was at a higher magnification than the microscope. Because the macroscope surveys were mapped to the ETU bondlines, any previously undocumented anomalies could be cross-referenced with previous pictures to determine if any change had occurred. Throughout testing, no changes to bondlines were detected.

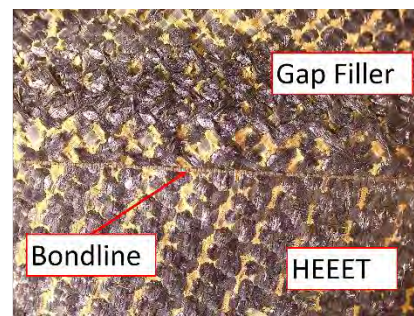


Figure 4 Microscope image for facilitating the inspection of the ETU bondlines before and after testing.

Concluding Remarks: Overall, the ETU test campaign was a success, with all planned testing being completed on schedule. The ETU performed as expected and had no indications of structural failure. The data collected is being used for model correlation and validation. The use of collecting pictures taken using a microscope and mapping the entirety of the ETU bondlines proved invaluable in assessing if any damage or change to the bondline had occurred during testing.

References:

- [1] Driver, D. M., et al. "Overview of Heatshield for Extreme Entry Environment Technology (HEEET)", 15th International Probe Workshop, 2018.
- [2] Splinter, S.C., et al. "HEEET ETU Static Pressure Tests", 10th Ablation Workshop, 2018.
- [3] Splinter, S.C., et al. "HEEET ETU Thermal-Vacuum Tests", 10th Ablation Workshop, 2018.
- [4] Splinter, S.C., et al. "HEEET ETU Static Point Load Tests", 10th Ablation Workshop, 2018.
- [5] Kazemba, C.D and Mahzari, M. "Computed Tomography Scanning of a 1-meter Demonstration Heatshield for Extreme Entry Environments", 15th International Probe Workshop, 2018.

LOFTID AEROSHELL SYSTEM OVERVIEW.

S. J. Hughes¹, F. M. Cheatwood¹, G. T. Swanson², C. D. Kazemba², M. C. Lindell¹, S. A. Tobin¹, R. J. Bodkin¹, R. A. Dillman¹, J. M. DiNonno¹, and R. K. Johnson¹. ¹NASA Langley Research Center, ²NASA Ames Research Center.

Brief Presenter Biography: Steve has worked at the NASA Langley Research Center for over 30 years on a wide array of projects and technologies, but for the last 16 years he has been pursuing HIAD technology development. Steve started his HIAD quest writing proposals in response to the In-Space Propulsion project NRA calls in 2003. He served as Lead Engineer for the IRVE and IRVE II sounding rocket flight tests, and was previously the Chief Engineer of the HIAD technology development project for GCD. Currently he is the Aeroshell Lead on the LOFTID flight project for TDM.

Introduction:

Hypersonic Inflatable Aerodynamic Decelerator (HIAD) is an atmospheric entry technology that has been determined to be enabling for human scale exploration of Mars, and enhancing for atmospheric entry at most celestial destinations with an atmosphere. NASA has been developing HIAD technology for the past 16 years and up until recently was a part of the Game Changing Development (GCD) Program, a part of NASA Space Technology Mission Directorate (STMD). In FY18 the Technology Demonstration Mission (TDM) Program in STMD initiated the Low-Earth Orbit Flight Test of an Inflatable Decelerator (LOFTID) project. LOFTID is the next step in HIAD technology development, an atmospheric entry from Low Earth Orbit. The LOFTID aeroshell must manage an order of magnitude more energy than the previous GCD sub-orbital flight test aeroshell, IRVE-3. The LOFTID aeroshell incorporates all of the HIAD system improvements matured over the last 16 years of development. Manufacturing process control improvements distribute the load more uniformly in the Inflatable Structure (IS) allowing the structure to carry more load. Material improvements have increased the maximum allowable temperature in the IS from 250C to in excess of 400C, at a reduced total system mass and reduced system leak rate.

Improvements in the Flexible Thermal Protection System (FTPS) have increased the allowable peak heat rate and can be tailored to the total integrated heat load. Previously demonstrated insulator ply tailoring was also used around the LOFTID aeroshell shoulder to improve the ability to fold and pack the aeroshell to stow for launch.

Finally, instrumentation was incorporated in the aeroshell using methods developed and demonstrated in the HIAD tech development. The LOFTID aeroshell has more embedded instrumentation than any aeroshell previously demonstrated. The instrumentation will not only provide data for correlation of the LOFTID aeroshell thermal and structural performance, but also capture data to help anchor tools used for the prediction of atmospheric entry environments on both the fore body and aft body of the aeroshell.

Construction of the LOFTID Engineering Development Unit (EDU) aeroshell has been completed and EDU system testing is underway. At the time of the Probe Workshop the flight unit build will be initiated with the goal of completion in late FY20. A successful LOFTID mission in FY22 will improve Technology Readiness Level (TRL) of a HIAD to a point that entry probes utilizing HIAD for EDL can be proposed without having to accept significant risk for the HIAD system. This presentation will discuss the improvements included in the LOFTID aeroshell from previous HIAD aeroshell experiments, the methods used verifying the aeroshell capabilities, and the predicted response to the environment the LOFTID aeroshell will be subjected to during atmospheric entry.



LOFTID Engineering Design Unit Inflatable Structure



LOFTID Engineering Design Unit Deployable FTSP



LOFTID Engineering Design Unit Nose FTSP

LOFTID AEROSHELL ENGINEERING DEVELOPMENT UNIT STRUCTURAL TESTING.

G. T. Swanson¹, C. D. Kazemba¹, S. J. Hughes², R. K. Johnson², M. C. Lindell², R. J. Bodkin², J. M. DiNonno², and F. M. Cheatwood². ¹NASA Ames Research Center, ²NASA Langley Research Center.

Brief Presenter Biography: Greg works on a variety of projects as part of the Entry Systems and Vehicle Development Branch at NASA Ames Research Center and is currently the Instrumentation Lead for the LOFTID flight demonstration project. He also spends a large part of his time supporting fabrication and testing of the HIAD aeroshell system. Greg received his Bachelors and Masters in Electrical Engineering from the University of Idaho.

Introduction: NASA's Hypersonic Inflatable Aerodynamic Decelerator (HIAD) technology was selected for a Technology Demonstration Mission under the Space Technology Mission Directorate in 2017. HIAD is an enabling technology that can facilitate atmospheric entry of heavy payloads to planets such as Earth and Mars using a deployable aeroshell. The deployable nature of the HIAD technology allows it to avoid the size constraints imposed on current rigid aeroshell entry systems. This enables use of larger aeroshells resulting in increased entry system performance (e.g. higher payload mass and/or volume, higher landing altitude at Mars).

The Low Earth Orbit Flight Test of an Inflatable Decelerator (LOFTID) is tentatively scheduled for FY22. LOFTID will be launched out of Vandenberg Air Force Base as a secondary payload on an Atlas V rocket. The flight test features a 6m diameter, 70-degree sphere-cone aeroshell and will provide invaluable high-energy orbital re-entry flight data. This data will be essential in supporting the HIAD team to mature the technology to diameters of 10m and greater. Aeroshells of this scale are applicable to potential near-term commercial applications and future NASA missions.

Currently the LOFTID project has completed fabrication of the engineering design unit (EDU) inflatable structure (IS) and the flexible thermal protection system (F-TPS). These two components along with the rigid nose and centerbody comprise the HIAD aeroshell system. This EDU aeroshell is the precursor to the LOFTID aeroshell that will be used for flight. The EDU was built to verify the design given the differences between the LOFTID aeroshell and past aeroshell designs that have been fabricated under the NASA HIAD project. To characterize the structural performance of the LOFTID aeroshell design, three structural tests will be performed.

The first test to be conducted is static load testing, which will induce a uniform load across the forward surface of the aeroshell to simulate the expected

pressure forces during atmospheric entry. The IS integrated with the rigid centerbody will first be tested alone to provide data for analytical model correlation, and then the F-TPS will be integrated for a second series of static load testing of the full aeroshell system. Instrumentation will be employed during the test series to measure component loads during testing, and a laser scanner will be used to generate a 3D map of the aeroshell surface to verify that the shape of the structure is acceptable at the simulated flight loads.

After static load testing, pack and deployment testing will be conducted multiple times on the integrated system to demonstrate the aeroshell's ability to fit within the required packed volume for the LOFTID mission without experiencing significant damage. Finally, the aeroshell will undergo modal testing to characterize its structural response.

This presentation will discuss the setup and execution of each of the three tests that the EDU aeroshell will undergo. In addition, initial results of the testing will be presented outlining key findings as LOFTID moves forward with fabrication of the flight aeroshell.



LOFTID Engineering Design Unit Inflatable Structure

RETRO PROPULSION ASSISTED LANDING TECHNOLOGIES (RETALT)

Ali Gülhan, Ansgar Marwege, Josef Klevanski, Daniel Kirchheck, and Johannes Rieher
German Aerospace Center (DLR e.V.), Supersonic and Hypersonic Technologies Department,
Linder Höhe, 51147 Köln, Germany, ali.guelhan@dlr.de

Brief Presenter Biography: Ali Gülhan is the head of the DLR's Department 'Supersonic and Hypersonic Technologies'. He was the PI of the EXOMARS 2016 Instrumentation Package COMARS+ and coordinator of the EU funded project RETALT.

Abstract: The development of reusable launch vehicle (RLV) is currently changing the global market of space transportation. The main game changer in this field are the technologies of retro propulsion assisted landing, which is a concept of decelerating the first stage of a Two Stage To Orbit (TSTO) RLV at its return to ground by firing its engines against the velocity vector.

To achieve a cost efficient and safe access to space there is not only an urgent need of building up the necessary know-how on state-of-the-art Vertical Take-Off Vertical Landing (VTVL) Two Stage To Orbit (TSTO) concepts, but also to go beyond this approach. Historically, many concepts of Reusable Launch Vehicle (RLV) are based on Single Stage To Orbit (SSTO) designs. Therefore, in the EU Horizon 2020 project RETALT (RETro propulsion Assisted Landing Technologies) the VTVL approach is investigated in a two-fold manner:

- A configuration similar to the SpaceX rocket "Falcon 9" serves as a reference for the state-of-the-art TSTO RLV.
- A configuration similar to the DC-X serves as a reference for a VTVL SSTO.

In this way, the concept of vertical landing with retro propulsion is investigated in a more general way and has the potential to be applied to more concepts of future RLV. The investigation for both reference configurations will be performed in the areas of aerodynamics, aerothermodynamics and flight dynamics and GNC as well as advanced structural parts and materials, health monitoring systems and advanced propulsion assisted landing systems.

The first configuration RETALT1 is a two stage to orbit (TSTO) vertical take-off vertical landing (VTVL) RLV. It is shown in Figure 1 as a conceptual sketch. It is similar to the Falcon 9 by SpaceX. The mission requirements for RETALT1 are to transport a payload of 30 tons to a low earth orbit (LEO) of approximately 340km, after separation of the second stage at Mach 7.1 at an altitude of 110 kilometers.



Figure 1: Conceptual sketch of the RETALT1 spacecraft. Configurations from left to right: launch, stage separation, first stage descent, first stage landing.

The configuration RETALT2 is a single stage to orbit (SSTO) vertical take-off vertical landing (VTVL) RLV with a comparable engine concept. It is similar to the DC-X. The mission of RETALT2 is to place smaller payloads in low earth orbits (LEO) or suborbital missions. It combines the use of retro propulsion and the novel aerodynamic control surfaces together with aerodynamic braking due to its capsule-like shape (e.g. like Soyuz, ExoMars, Hayabusa). The shaping results in a reduction of additional propellant for the descent. Atmospheric entry technologies are used for the study of the hot plume ground interaction and design of the base TPS.



Figure 2: Conceptual sketch of the RETALT2 spacecraft. Configurations from left to right: launch, descent and landing.

DESIGNING A SUPERSONIC RETROPROPULSION TEST FOR THE NASA LANGLEY UNITARY PLAN WIND TUNNEL. K. T. Edquist¹ and A. M. Korzun², ¹NASA Langley Research Center, Hampton, VA, USA, karl.t.edquist@nasa.gov.

Brief Presenter Biography: Karl Edquist has worked at NASA Langley Research Center since 2000. He received his Bachelor's and Master's degrees in Aerospace Engineering from the University of Colorado and the University of Maryland, respectively. He specializes in aerodynamic and aerothermodynamic analysis of planetary entry vehicles for NASA science missions and technology development projects. Currently, he is Aerothermal Lead for NASA's Mars 2020 project and the lead for Propulsive Descent testing in the Langley Unitary Plan Wind Tunnel.

Introduction: Future NASA human missions to the surface of Mars will require using retro-rockets beginning at supersonic freestream conditions (supersonic retropropulsion, SRP) in order to decelerate vehicles that are at least one order of magnitude heavier than all previous Mars landers [1]. All NASA robotic Mars missions to date, starting with the Viking missions in 1976, used a single supersonic disk-gap-band parachute prior to initiating powered descent at subsonic conditions. The renewed interest in SRP, which was first investigated prior to the Viking missions, will require testing and analysis to address the primary aerosciences risk associated with SRP: interactions between the retro-rocket exhaust plumes and the freestream flow that alter the aerodynamic behavior of the powered descent vehicle. Trajectory simulations that include a powered descent phase currently have simple aerodynamic interference models that are based on unvalidated computational fluid dynamics (CFD) flowfield predictions. Ground and flight test data are needed at relevant conditions in order to quantify uncertainties associated with the aerodynamic interference models. This paper will cover the status of planning for a sub-scale SRP wind tunnel test in the Langley Unitary Plan Wind Tunnel (UPWT) to occur in 2019, in which high-pressure air will be used to simulate the rocket engine exhaust.

Test Overview: NASA previously conducted SRP tests in 2010 (NASA Langley 4x4 UPWT) and 2011 (NASA Ames 9x7 Tunnel) as interest in SRP ramped back up after having been dormant for decades [2, 3]. The previous tests were designed to collect high-quality data against which CFD analysts could calibrate multiple codes [4, 5]. The same wind tunnel model was used in both tests, but the model was not designed to geometrically simulate any particular Mars reference vehicle. Another limitation of the previous tests is that

aerodynamic (non-thrusting) forces and moments were not measured.

For the upcoming test, geometric scaling and interference force and moment measurements will be added. The two available Mars reference powered descent vehicles are the low lift-to-drag (L/D) inflatable-based vehicle and the mid-L/D vehicle, shown in Figure 1. Each vehicle has eight LO₂/LCH₄ engines. Subscale versions of one or both vehicles will be tested in the UPWT.

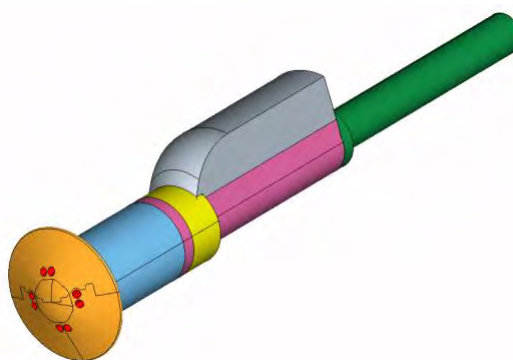


Figure 1. Sample Model Configuration.

The objectives of the current test are to: 1) Design and build a wind tunnel model that is geometrically-scaled from a current Mars reference powered descent vehicle. 2) Design nozzles that generate a range of aerodynamic interference forces and moments. 3) Collect data across a range of Mach numbers, angles of attack, and thrust: discrete surface pressure, global surface pressure, high-speed schlieren video, and non-thrusting forces and moments. 4) Compare CFD codes at wind tunnel conditions to measured data.

Testing will start in late 2019. The presentation will discuss the model designs, planned measurements, the test matrix (Mach numbers, angles of attack, and thrust coefficients), and sample CFD results.

References:

- [1] Dwyer Cianciolo A. et al. (2010) NASA TM-216720. [2].
- [2] Berry, S. et al. (2014) Journal of Spacecraft and Rockets, Vol. 51, No. 3, pp. 664-679.
- [3] Berry, S. et al. (2014) Journal of Spacecraft and Rockets, Vol. 51, No. 3, pp. 724-734.
- [4] Schauerhamer, D. et al. (2014) Journal of Spacecraft and Rockets, Vol. 51, No. 3, pp. 693-714.
- [5] Schauerhamer, D. et al. (2014) Journal of Spacecraft and Rockets, Vol. 51, No. 3, pp. 735-749.

EXPERIMENTAL INVESTIGATION OF MAGNETOHYDRODYNAMIC ENERGY GENERATION IN CONDITIONS AND CONFIGURATIONS RELEVANT TO PLANETARY ENTRY. H. K. Ali^{1*}, J. E. Polk², M. L. R. Walker^{3*}, and R. D. Braun, ¹Graduate Research Assistant, hisham.ali@gatech.edu, ²Principal Engineer, NASA Jet Propulsion Laboratory, California Institute of Technology, james.e.polk@jpl.nasa.gov, ³Professor of Aerospace Engineering, mitchell.walker@ae.gatech.edu, ⁴Dean, College of Engineering and Applied Sciences, University of Colorado Boulder, bobby.braun@colorado.edu, *High Power Electric Propulsion Lab, Daniel Guggenheim School of Aerospace Engineering, Georgia Institute of Technology, 270 Ferst Drive, Atlanta, GA 30331.

Brief Presenter Biography: Hisham is a Ph.D candidate in Aerospace Engineering at the Georgia Institute of Technology, where he is a dual member of the Space Systems Design and the High Power Electric Propulsion Laboratories. Hisham earned a Bachelor of Science in Aerospace Engineering with minors in Mathematics and Computer Based Honors from the University of Alabama in 2013 and a Master of Science in Aerospace Engineering from the Georgia Institute of Technology in 2015. Hisham's current research interests are in magnetohydrodynamics, hypersonics, plasma physics, and planetary entry systems.

Introduction: Many concepts for future missions to Mars, such as potential Mars Sample Return and eventual human exploration, could require much higher masses than have ever been landed on Mars. Previous Mars missions have relied primarily on Viking era technology for entry descent and landing [1]. The limit of this technology is being reached, with the Mars Science Laboratory (MSL) landing system in 2012 illustrating the difficulty in high mass Martian landings.

To achieve humanity's goals for Mars exploration, significant technology development is required. Mass reducing technologies are particularly critical in this effort. Not only does a larger mass require more fuel to launch, but it also carries significantly more kinetic energy that must be reduced to near zero if the vehicle is to land safely. For all previous Mars missions, this kinetic energy has been primarily dissipated through aerodynamic drag during the hypersonic phase, which is limited by the size of the entry vehicle. In addition, Previous Mars missions have shown that the majority of the vehicle's kinetic energy is dissipated during the hypersonic entry phase, about 92% in the case of Mars Pathfinder [2].

During this hypersonic entry phase, there exists a highly heated, ionized flow around the entry vehicle. This entry plasma is inherently conductive, and may thus be influenced by electromagnetic fields, facilitating magnetohydrodynamic flow interaction. This flow interaction can be used to provide a Lorentz force in addition

to aerodynamic drag, thereby enhancing deceleration capability without necessarily increasing the size and mass of the entry vehicle forebody.

Magnetohydrodynamic flow interaction for high speed aerospace applications has been studied since the dawn of the space race, with early theoretical studies dating back to the late fifties and early sixties [3][4]. At that time, practical implementation was limited due to the difficulties in generating high strength magnetic fields and electrical energy storage. Since that time, however, dramatic advances in superconductivity and electrical energy storage have been made, warranting additional study.

The number of experimental investigations of MHD interaction for conditions relevant to planetary entry is limited. There are a few experimental investigations dating back to the late 1950s and 1960s, mainly concerned with the effects MHD interaction has on shock standoff distance.[5][6][7][8] More recent studies describe various experimental campaigns aimed at investigating drag enhancement, heat-flux mitigation, artificial ionization, and energy generation through MHD interaction.[9][10][11][12] From all of these experiments, it is apparent that creating and testing MHD interaction in conditions relevant to planetary entry is a challenging task requiring specialized equipment, resulting in an overall limited data set that limits validation of numerical and analytical models. Experimental data related to MHD energy generation for planetary entry vehicles is particularly limited.

Traditional MHD energy generator concepts consist of an open channel design through which plasma flows. For a planetary reentry vehicle, it is undesirable to have plasma flowing through the vehicle's heatshield, due to the likelihood of damage or complete destruction from the high-temperature entry plasma. Previously, a non-channel type MHD energy generator concept was tested in an artificially ionized flow, and an extracted current was recorded, indicating an initial positive result. [11] However, this dataset was limited, and did not fully characterize the plasma, vary the test conditions, or vary the model design.

Thus there is a need for an experimental design that is capable of simulating MHD energy generation in both conditions and configurations relevant to planetary entry systems over a variety of test conditions and model geometries for which the plasma and models are well-characterized. This experimental design and initial dataset will allow for verification of the parametric dependence of the energy generated on various design parameters as well as extension to flight conditions relevant to planetary entry.

Methodology: The principal contribution made in this area is the design and execution of an experimental campaign to demonstrate MHD energy generation for a non-channel type MHD energy generation on a simulated blunt-body reentry vehicle. A gas source is accelerated to supersonic speed using a converging-diverging nozzle and mechanical vacuum pumping system, artificially ionized with a radio-frequency (RF) antenna and computer controlled impedance matching network to create a supersonic plasma, and allowed to pass over a permanently magnetized ceramic model representative of an atmospheric reentry vehicle. The key distinction here is that no plasma flows through the representative MHD energy generator, in contrast to a traditional channel-type Faraday MHD energy generator. This experimental design has been demonstrated over approximately 80 different combinations of experimental models and test conditions, and appears to show a positive effect for current through the MHD generator model when the supersonic plasma discharge is present. Figures 1, 2, and 3 present example discharges, results, and model designs from this experiment.

Expected Results: Expected results included characterization of the supersonic plasma discharge with regards to electron number density and temperature, as well as traces of MHD current collected for several variations of magnet orientation with respect to the electrodes and test conditions. Test conditions are specified by the gas mass flow rate, type of quartz converging-diverging nozzle and test-section used, and RF input power levels varying from 100W to 1000W. These results will provide an initial dataset with enough variation to provide a basis for experiment repeatability, parametric dependence of results, validation of computational models, and correlation or extrapolation to flight conditions experienced planetary entry.

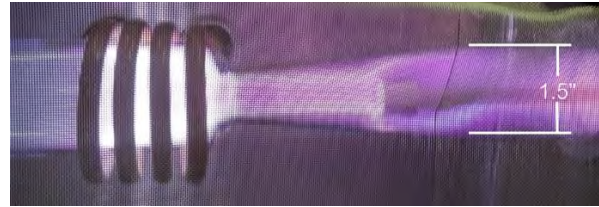


Figure 1. Supersonic plasma flowing over representative non-channel type MHD energy generator model. RF antenna and quartz converging-diverging nozzle pictured. Input RF power level is 1kW.

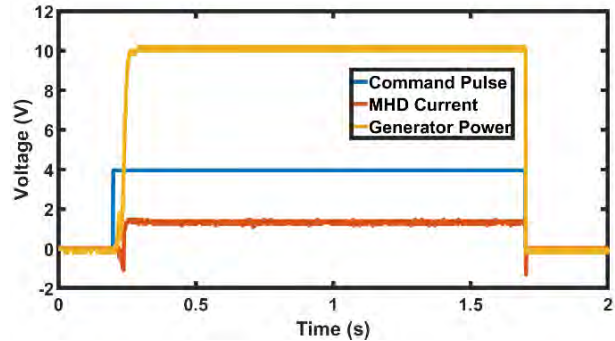


Figure 2. Sample data for voltage drop across 121Ω resistor due to MHD current collected across 1.5s 1kW RF powered pulse.

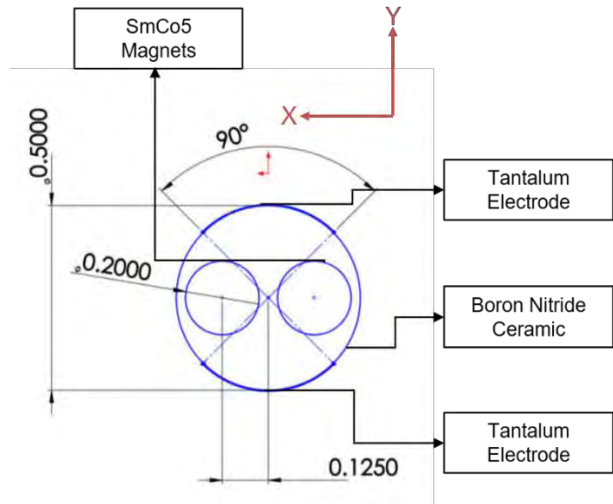


Figure 3. Front view of MHD energy generator model. The model is designed such that plasma does not flow through, only around model.

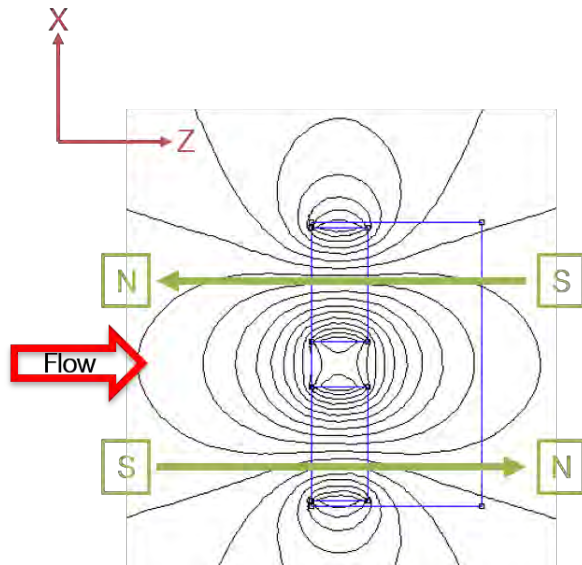


Figure 4. Top view of model with magnetic field due to two anti-parallel dipole cylindrical samarium-cobalt magnets. Maximum field strength is 0.2T.

Acknowledgments: This work was funded through a NASA Space Technology Research Fellowship, grant number NNX13AL82H. Also, support is provided from a NASA unsolicited research proposal award, grant number 80NSSC18K1429. This work was also funded by an Alfred P. Sloan foundation. Finally, the authors would like to thank Dr. Robert Moses of NASA Langley Research center for his assistance in the completion of this work.

References:

- [1] R. D. Braun and R. M. Manning, "Mars Exploration Entry, Descent and Landing Challenges," in *IEEE Aerospace Conference*, 2006.
- [2] D. A. Spencer, R. C. Blanchard, R. D. Braun, P. H. Kallemeyn, and S. W. Thurman, "Mars Pathfinder Entry, Descent, and Landing Reconstruction," *J. Spacecr. Rockets*, vol. 36, no. 3, pp. 357–366, 1999.
- [3] W. B. Bush, "A Note on Magnetohydrodynamic-Hypersonic Flow Past a Blunt Body," *Journal of the Aerospace Sciences*, vol. 26, no. 8, pp. 536–537, 1959.
- [4] P. O. Jarvinen, "On The Use of Magnetohydrodynamics During High Speed Re-Entry," Everett, Massachusetts, 1964.
- [5] R. W. Ziemer and W. B. Bush, "Magnetic Field Effects on Bow Shock Stand-Off Distance," *Phys. Rev. Lett.*, vol. 1, no. 2, pp. 58–59, 1958.
- [6] E. Locke, H. E. Petschek, and P. H. Rose, "Experiments with Magneto-hydrodynamically Supported Shock Layers," Everett Massachusetts, 1964.
- [7] G. R. Seemann and A. B. Cambel, "Observations Concerning Magnetoaerodynamic Drag and Shock Standoff Distance," *Proc. Natl. Acad. Sci. U. S. A.*, vol. 55, no. 3, pp. 457–465, 1966.
- [8] S. Kranc, M. C. Yuen, and A. B. Cambel, "Experimental Investigation of Magnetoaerodynamic Flow Around Blunt Bodies," Evanston, IL, 1969.
- [9] M. Kawamura, A. Matsuda, H. Katsurayama, H. Otsu, D. Konigorski, S. Sato, and T. Abe, "Experiment on Drag Enhancement for a Blunt Body with Electrodynamical Heat Shield," *J. Spacecr. Rockets*, vol. 46, no. 6, pp. 1171–1177, 2009.
- [10] A. Gülhan, B. Esser, U. Koch, F. Siebe, J. Riehmer, D. Giordano, and D. Konigorski, "Experimental Verification of Heat-Flux Mitigation by Electromagnetic Fields in Partially-Ionized-Argon Flows," *J. Spacecr. Rockets*, vol. 46, no. 2, pp. 274–283, 2009.
- [11] D. J. Drake, S. Popović, L. Vušković, D. J. Drake, S. Popović, and L. Vušković, "Characterization of a supersonic microwave discharge in Ar / H₂ / Air mixtures Characterization of a supersonic microwave discharge in Ar / H₂ / Air," *J. Appl. Phys.*, vol. 63305, no. 2008, 2008.
- [12] S. Popović, R. W. Moses, and L. Vuskovic, "System Development for Mars Entry in Situ Resource Utilization," in *Proceedings of the 8th International Planetary Probe Workshop*, 2011, no. 1, pp. 1–10.

DESIGN AND QUALIFICATION TESTING OF TWO EUROPEAN PARACHUTE MORTARS FOR THE ESA EXOMARS 2020 MISSION.

A. M. C. Matthijssen¹, ¹Aerospace Propulsion Products –ArianeGroup, Westelijke Randweg 25, 4791 RT Klundert – The Netherlands (r.matthijssen@appbv.nl)

Brief Presenter Biography: Rudi Matthijssen studied mechanical engineering and has worked in space industry since 2001. At APP he is systems engineer on various rocket motor igniter developments. From 2014 to 2016 he was involved in an ESA development program of a European parachute mortar and since end 2016 in the Exomars 2020 Parachute Deployment Devices (PDD).

Introduction: The PARachute System (PAS) for the ExoMars 2020 mission comprises two main parachutes deployed at different stages in the descent sequence, each extracted by pilot parachutes deployed by separate and different PDDs. The first-stage PDD is fired and the pilot parachute deployed while the Descent Module Composite (DMC) is supersonic, in order to stabilise the DMC, remove the canister lid and extract the first-stage main parachute. Once the DMC is subsonic, the first-stage main parachute is released; the second-stage PDD deploys the second-stage pilot parachute, which then extracts the second-stage main parachute.

APP has developed the PDD's for Exomars 2020, based upon a pre-development performed within ESA Technology Research Program (TRP). This makes this the first ESA mission using European sourced PDD's. Both mortars had to be fitted within the given constraints of the PAS (see Figure 1). Mortar 1 is attached by a top flange to the PAS lid structure, while mortar 2 is attached by a bottom flange to the base structure of the PAS canister. This required a flexible and scaleable mortar design with possibility of top or bottom flange mounting. Both mortars include a Gas Generator (GG), which uses heritage from the ESA PDD development and industrial GG designs within APP.

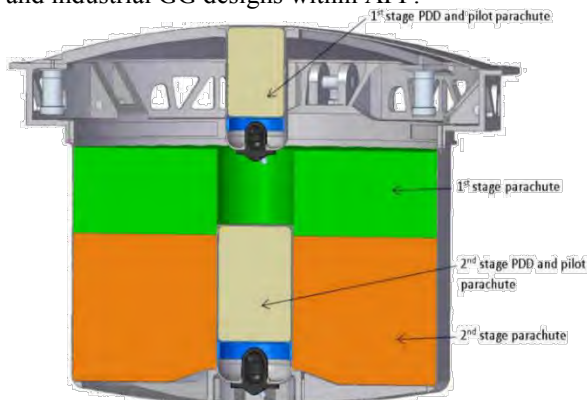


Figure 1: Mortar 1 and 2 location in the PAS canister

PDD design features: During the design phase it was required to make both GG and mortar designs generic and scaleable to the specific pilot parachute package size and ejected mass. Secondly, the use of European content in the PDD's has been maximized in order to avoid US export control requirements where possible. As a result none of the parts are subject to US-ITAR restrictions.

The mortar and GG designs were analysed and sized by Vorticity-UK against following requirements:

1st stage PDD:

- Parachute pack size: Ø126 mm x 154 mm
- Packed parachute + BoP mass: 1.5 to 1.85 kg
- Operational temperature range: +50 to -50 °C
- Ejection velocity range: 35 to 40 m/s
- Max reaction load: 12 kN

2nd stage PDD:

- Parachute pack size: Ø150 mm x 187.5 mm
- Bridle cut-outs: 3pce, 8mm height, 19 mm width
- Packed parachute mass range: 1.5 to 1.8 kg
- Operational temperature range: +50 to -50 °C
- Ejection velocity range: 35 to 40 m/s
- Max reaction load: 15 kN

The flight version mortar 1 and 2 including dummy GG are shown in Figure 2.



Figure 2: Mortar 1 and 2 flight designs

PDD1 uses a common Break-Out-Patch (BOP) with shear pins to retain the parachute package. However, for mass reduction purposes PDD2 is equipped with a so-called “soft-BOP” which is held in place by breaking

ords. Both PDDs include a Piston Capture Element (PCE) which catches the pistons after ejection.

The GG or cartridge contains the propellant in a propellant chamber, which provides hermetic sealing in order not to expose the propellant to space vacuum. The propellant is surrounded by foam and a mesh to withstand launch loads.

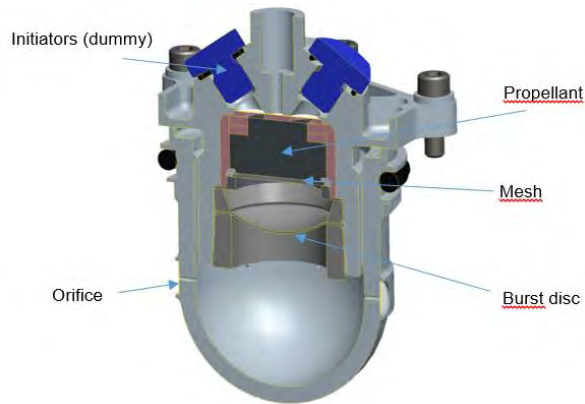


Figure 3: Gas Generator cross-section

The chamber is closed by a burst disc which has a defined opening pressure and creates a high-pressure environment to support complete combustion. When the propellant is ignited, the higher pressure gases are bled out through exhaust orifices at reduced pressure to the much larger low pressure mortar chamber to push the parachute pack forward. This enables a light-weight design with reduced recoil. Ignition source are two redundant pyrotechnic initiators. Performance of the GG against varying requirements is tuneable by the amount of loaded propellant.

PDD test program: For the Exomars 2020 PDD program, a major step had to be made enhancing the TRL of the PDD designs from TRL4, achieved during ESA TRP, to the current TRL8. For this purpose, a dedicated development, qualification and acceptance test campaign was applied, verifying all critical features of the design against the Exomars 2020 requirements.

The selected propellant was tested under accelerated ageing program and environmental loads to verify end-of-life performance.

The mortar and GG components were qualified against environmental loads, consisting of thermal cycling, vibration and shock. As the PDD is a fully integrated element of the PAS design, interfacing not only with PAS structure but also with the parachute approach was to verify environmentals in fully integrated configuration.

Performance of the PDD was verified during multiple ejection and deployment test campaigns. The first campaign demonstrated ejection velocity, reaction loads and PDD induced shocks over the full operational temperature range of $-50/+50^{\circ}\text{C}$. Subsequently deployment tests were performed with the mortars integrated into the lid or base structural elements of the PAS, also verifying capability of the PAS structure to withstand mortar firing loads. As a third campaign parachute deployment firings were performed in the final FM mortar and parachute configurations.

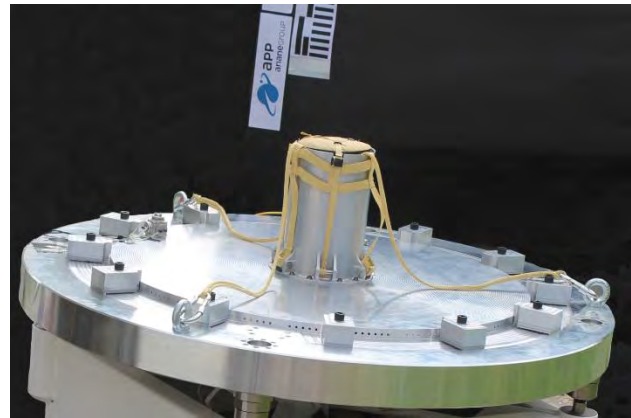


Figure 4: PDD2 integrated deployment testing

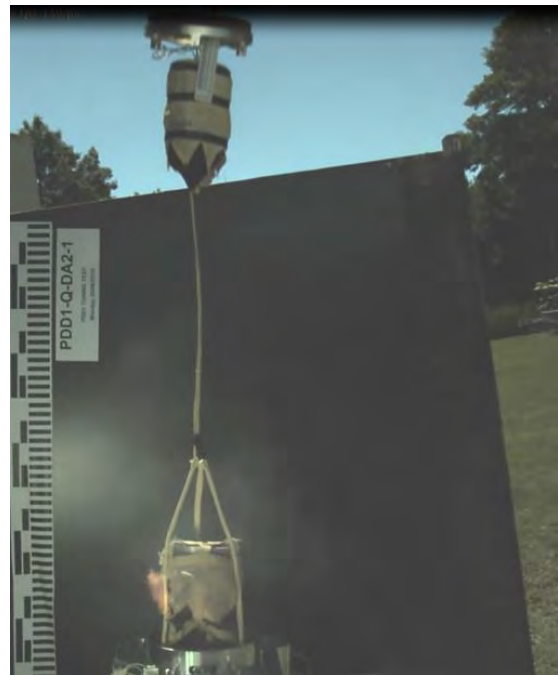


Figure 5: PDD1 QM parachute deployment test

Acceptance testing on the Flight Models was rather limited because of the pyrotechnic nature of the PDD components. However for planetary protection purposes a dedicated cleaning process was developed to achieve

required cleanliness levels before delivery. This was achieved by IPA wiping and microbial assays. Subsequent sterilisation (e.g. DHMR) will be performed by the prime (TASinI) at S/C level.

Conclusion: In the EXOMARS 2020 program, APP has developed the capability of a European sourced PDD that fills the severe requirements for planetary missions. Although the design is scaleable and flexible, the EXOMARS PDD designs are two dedicated PDD designs fully-integrated into the PAS. Qualification and acceptance tests were successfully performed and Flight Models delivered.

Thursday, July 11, 2019

Solar System Exploration II – Airless Planetary Satellites, Asteroids, and Comets - Conveners: Aline Zimmer, Christian Grimm, Michelle Rodio, and Benoit Pigneur

3:34 PM	Europa Lander Mission Concept Overview and Update	Steve Sell	Jet Propulsion Laboratory, California Institute of Technology	
3:46 PM	A New Mission Concept for Further Exploration of Enceladus	Stephanie Mottershead	University College London	Student
3:58 PM	Surface Accessibility with Vertical Controlled Landing on 67P / Churyumov-Gerasimenko	Alena Probst	Bundeswehr University Munich	Student
4:10 PM	Juventas - Attempting to Land a CubeSat on Didymoon for the Hera Mission	Hannah Goldberg	GomSpace	
4:22 PM	Moon Diver: A Discovery Mission Concept For The Exploration Of A Lunar Pit In Mare Tranquillitatis	Richard Kornfeld	Jet Propulsion Laboratory, California Institute of Technology	
4:34 PM	HERACLES - Human-Enhanced Robotic Architecture and Capability for Lunar Exploration and Science	Robert Buchwald	Airbus	
4:46 PM	Overview of NASA's Human Landing System for Lunar Exploration	Tara Polsgrove	NASA Marshall Space Flight Center	
4:58 PM	Technology Investments At The Moon To Enable Entry, Descent, And Landing For Humans At Mars	Alicia Dwyer Cianciolo	NASA Langley Research Center	

Europa Lander Mission Concept Overview and Update.

S. W. Sell¹, B. T. Cook¹, and A. K. Zimmer, ¹Jet Propulsion Laboratory, California Institute of Technology, 4800 Oak Grove Drive, Pasadena, CA 91109.

Brief Presenter Biography: Steve Sell is the Flight System Engineer for the Europa Lander pre-project at the Jet Propulsion Laboratory. Prior to joining the Europa Lander project, Steve served as the Powered Flight Systems Engineer for the Mars Science Laboratory Entry, Descent, and Landing team and was the Flight Systems Engineer for the Low Density Supersonic Decelerators test flights. Steve has a BS in Aerospace Engineering from the Florida Institute of Technology and an MS in Aerospace Engineering from the University of Maryland.

Introduction: The Europa Lander concept represents the next chapter in landed missions to explore the solar system. This mission would enable a nearly month-long, in-situ, investigation of the European surface including the excavation, processing and analysis of surface samples. The Europa Lander concept could be launch as early as 2026 with Europa landing occurring in the early 2030's. This paper outlines and updates the Europa Lander Mission concept as well as the new approaches to the many challenges of landing on Europa.

Many challenges exist for landed missions to Europa. The first is that very little is known about Europa's cryogenic surface. While some images exist from earlier missions such as Voyager and Galileo, they are of extremely low resolution (10's to 100's of meters per pixel) and are far insufficient to provide information with which to design a small (1-2m) lander. NASA's Europa Clipper mission will be able to provide meter-scale images of select locations on the surface, and while significantly richer in information content, will still be insufficient to identify sub-lander-scale hazards. The Europa Lander Mission concept addresses the lack of knowledge of the surface by employing a Sky Crane style landing similar to NASA's Mars Science Laboratory and Mars 2020 missions. This style of landing serves two purposes: 1) The landing engines remain far away from the cryogenic surface, and 2) it enables a controlled soft landing (on the order of 0.5 m/s). By leveraging this style of landing it minimizes the impact and interaction with the surface. Additionally, the Europa Lander concept has unique adaptive legs which provide a level and stable lander with up to 1 m of terrain relieve within the lander's footprint.

A second challenge is the harsh radiation environment around Europa. The month-long mission would encounter Total Ionizing Doses of radiation up to 3 Mrad, which is 20 times what typical radiation tolerant

electronics are designed to withstand. This presents obvious challenges for avionics design, forcing the design to have a high degree of redundancy and possibly triple voting schemes for critical events such as Deorbit, Descent, and Landing.

Finally, the trajectory for a landed mission to Europa involves a large allocation of delta-V – on the order of 3,000 to 4,000 m/s depending on Jupiter orbit insertion style, the availability of Mars flyby. This large delta-V requirement results in a total spacecraft wet mass at launch of over 15,000 kg for the concept presented. Although there are trajectory designs that use Venus and Earth flybys to reduce the delta-V, they present additional challenges from the thermal stress of a Venus flyby (approximately 0.7 AU) and significantly lengthen the transit time from Earth to Jupiter.

In November of 2018, the Europa Lander concept completed a Delta Mission Concept Review to reduce the estimated cost of the mission from the June 2017 Concept Review. This effort resulted in the mission concept undergoing significant changes aimed at reducing cost and complexity. Rather than using the carrier vehicle as a communications relay, the mission will instead use its updated telecommunications system to communicate directly to Earth. This change reduced both cost and mass, but also brought unique challenges such as communications during the critical event of Deorbit, Descent, and Landing. Additionally, a new landing trajectory to allow for a planetary protection compliant disposal of the carrier vehicle had to be implemented. This paper outlines and updates the Europa Lander Mission concept as well as the new approaches to the many challenges of landing on Europa.

The information presented about the Europa Lander mission concept is pre-decisional and is provided for planning and discussion purposes only.

A NEW MISSION CONCEPT FOR FURTHER EXPLORATION OF ENCELADUS.

S. J. Mottershead¹, Prof. A. Coates², Prof. G. Jones³, ¹University College London (UCL), Gower Street, London; ^{2,3}UCL Mullard Space Science Laboratory (MSSL), Holmbury St. Mary, Dorking, UK.

Brief Presenter Biography: Stephanie is a Masters student studying Space Science and Engineering at UCL, London. She has two undergraduate degrees in Geology and Environmental Science, and in Physics and Astronomy. After ten years following a very different career, she is now undertaking her Masters degree with a particular interest in planetary exploration and Earth observation. Her Master's thesis is supervised by Prof. Andrew Coates and Prof. Geraint Jones.

Introduction: There have been many missions and proposals to explore Saturn and its moons, starting with Pioneer in 1979, and the Voyager flybys in the 1980s [1]. Most recently, the 13-year Cassini mission delved deeper into the Saturnian system than ever before. As well as answering some questions, it also uncovered previously unknown activity and characteristics, and posed many new questions regarding its findings. Many of these new questions regard Enceladus, a small icy satellite of Saturn with a surprisingly active personality.

The observational evidence of the icy plumes coming from Enceladus' southern polar region is now far more comprehensive thanks to Cassini [2] and tells not only of the presence of an internal heat source [3], but also of liquid water subsurface oceans and even the possibility for life [4].

This master's thesis reviews the current knowledge of Enceladus and pinpoints the scientific questions that so far remain unanswered. The aim of the project is to develop and propose a new concept mission to revisit Enceladus and to answer as many of these questions as possible under a small or medium class ESA mission budget within their Cosmic Vision program. A shortlist of possible concepts is drawn up, after which a final concept is chosen and developed in more detail. This selected mission will ultimately be a new concept for Enceladus, and differ from any other proposals previously presented within the scientific community.

The scientific fields relating to Enceladus can be roughly grouped under eight topics: the composition, formation, and interior of Enceladus; surface geology and geochemistry; icy plume and ocean geochemistry; plume origin and mechanics; search for life and astrobiology; E-ring dynamics; Magnetic field interaction and radiation environment; and orbital and rotational dynamics. These topics are all inextricably linked but all have gaps in the scientific understanding. Central to almost all the topics however, are the plumes.

Acquiring a more comprehensive understanding of the plume, surface, and ocean geochemistry by means of remote sensing and planetary probes, will help to address questions such as the possible presence of hydrothermal vents on the subsurface ocean floor [5], the presence and concentrations of organic and minor species in the subsurface ocean and surface ice, and the temperatures of the deep oceans [3]. Therefore focusing a new mission on gathering extensive plume ejecta and surface geochemical data is likely to have significant impact upon almost all scientific fields with respect to Enceladus.

To achieve the scientific goal of acquiring comprehensive geochemical data from Enceladus, a Science Traceability Matrix (STM) is followed to assist in the selection of scientific instruments and subsequent design of the spacecraft and mission architecture. The project considers (to varying extents) a broad range of mission design topics including: spacecraft bus and payload design; thermal and mechanical engineering; scientific instrumentation; orbital mechanics; launchers; propulsion; mission lifetime; economics; justification for funding; and anticipated benefits. Trade-offs and optimisation of the mission as a whole are explained, and details of previous missions and proposals are drawn on for their successes and failures.

The short list of possible concepts includes, but is not limited to: a polar orbiting spacecraft with deployment of probes/surface landers at both the northern and southern polar regions; a penetrator deployed at the tiger stripes region to access the subsurface ocean geochemistry, multiple plume fly-throughs to obtain longer time-series data; deployment of seismic stations on the surface of Enceladus; and a single slingshot mission for plume sample return to Earth. The final mission concept to have been chosen and researched in more detail will be revealed at the IPPW conference as an early stage concept, with potential for further development.

References: [1] Coates, A. (2017) *A&G*, 58, 4.20–4.25. [2] Dougherty, M. K., et al. (2018) *Enceladus and the Icy Moons of Saturn*, 3–16. [3] Hemingway D. et al. (2018) *Enceladus and the Icy Moons of Saturn*, 57-77. [4] McKay C. P., et al. (2018) *Enceladus and the Icy Moons of Saturn*, 437-452. [5] Lunine J. I., et al. (2018) *Enceladus and the Icy Moons of Saturn*, 453-468.

JUVENTAS – ATTEMPTING TO LAND A CUBESAT ON DIDYMOON FOR THE HERA MISSION

H. R. Goldberg¹, Ö. Karatekin², B. Ritter², and C. Prioroc³, ¹GomSpace, (Langagervej 6, 9220 Aalborg Øst, Denmark, hrg@gomspace.com), ²Royal Observatory of Belgium, ³GMV-Romania.

Brief Presenter Biography: Hannah Goldberg is a systems engineer at GomSpace where she is the technical lead of the Juventas cubesat for the Hera mission. Previously, she worked at the NASA Jet Propulsion Laboratory on missions including the Mars Science Laboratory rover and the Orbiting Carbon Observatories.

Introduction: Juventas is a 6U CubeSat, as part of ESA’s planetary defense mission, HERA to the Didymos binary asteroid system. Juventas contains a low frequency radar as its primary observation instrument, to investigate details of the interior structure of Didymoon. The radar draws heritage from the CONSERT radar used for the ROSETTA mission [1]. The spacecraft will also conduct radio science experiments via inter-satellite link between Juventas and the HERA spacecraft as a means of gravity field measurements. After Juventas observations of radar and radio science are complete, the spacecraft will attempt to land on the surface on Didymoon. Through the monitoring of dynamics for landing or bouncing impacts as well as measurements from a gravimeter payload while on the surface, Juventas will use the data to determine the surface properties and dynamical properties of Didymoon.

Technical Design Approach: ESA’s HERA spacecraft is designed to accommodate two 6U form-factor CubeSats as deployable payloads to provide secondary means of contributing to asteroid research and mitigation assessment objectives of the mission. The 6U form-factor is chosen to take advantage of the standardization of CubeSat interfaces, allowing the stowage of the CubeSat inside the HERA spacecraft for the duration of the cruise phase from launch to arrival at Didymos. Juventas is one of two 6U CubeSats that HERA will deploy during the Detailed Characterization Phase of the mission.

Proximity operations for the Didymos system will be performed at a solar distance of approximately 1.8 AU, which requires the Juventas spacecraft to have large deployable solar arrays in order to generate sufficient power necessary for payload operations. The low-frequency radar payload, operating around 50 MHz also requires a large deployable antenna. These spacecraft requirements for the observation phase of the mission are in conflict with the landing and surface phases of the mission, where large deployed appendages create hazards and constraints for navigation during the landing process.

As landing on the Didymoon surface is a secondary objective for Juventas, the spacecraft design is not being

driven by landing requirements. Soft touch-down on an asteroid surface with a spacecraft not designed for landing has precedent from the NASA NEAR Shoemaker landing on the surface of Eros in 2001 [2]. Since that time, lander spacecraft including Philae [3] and MASCOT [4] have achieved asteroid landings for the Rosetta and Hayabusa2 missions, respectively.

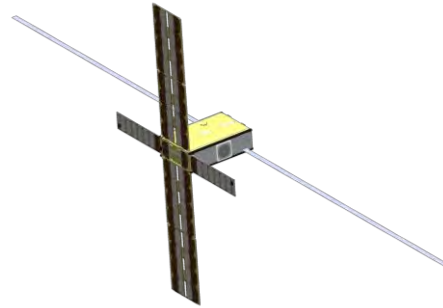


Figure 1: Juventas CubeSat in its deployed configuration

The Juventas CubeSat will be designed to achieve the mission requirements of the payloads both during the observation phase as well as the landing and surface operations phases. The small size and mass of Didymoon means that the escape velocity is very low, <10 cm/s, which provides a significant challenge to the landing trajectory design. During the landing event, the spacecraft IMU (accelerometers and gyros) will be sampled at a high rate to record the dynamics of the impact or bouncing events. Once settled on the surface, Juventas contains a three axis gravimeter payload used in surface operations. The goal of the spacecraft is to survive 1-2 days of surface operations and communicate the data back to the HERA spacecraft.

References: [1] Herique A., Kofman W. (2002). CEOS-SAR01-006. [2] Antreasian P.G., S. R. Chesley, J. K. Miller, and J. J. Bordi, and B. Williams (2001) *Advances in the Astronautical Sciences*, 109. [3] Boehnhardt H., et. al (2017) *Philosophical Transactions of the Royal Societ A: Mathematical Physical and Engineering Sciences*, 375. [4] Grundmann, J. et. al (2015) *Planetary Defense Conference*.

Acknowledgements: This work was performed in support of the European Space Agency’s Hera project. The authors wish to acknowledge contribution from the Juventas team including collaborators at ESA, GomSpace, the Royal Observatory of Belgium, GMV, the University of Grenoble-Alpes, the University of Bologna, Brno University of Technology, Astronika, as well as the entire Hera mission team.

MOON DIVER: A DISCOVERY MISSION CONCEPT FOR THE EXPLORATION OF A LUNAR PIT IN MARE TRANQUILLITATIS

R. P. Kornfeld, L. A. Kerber, I. A. Nesnas, A. Parness, R. G. Sellar, M. W. Smith, A. E. Johnson, and M. Vaquero, NASA/Caltech Jet Propulsion Laboratory, 4800 Oak Grove Dr., Pasadena, CA 91109

J. B. Hopkins, Lockheed Martin Space, 12257 S. Wadsworth Blvd., Littleton, CO 80128

Brief Presenter Biography: Richard Kornfeld, Ph.D., is a principal systems engineer, and currently the Deputy Chief Engineer of the Systems Engineering Division, at the Jet Propulsion Laboratory. He served as the Lead Systems Engineer during the Moon Diver proposal concept development.

Introduction: In 2009, the Japanese lunar orbiter Kaguya (aka Selene) discovered several pits on the surface of the Moon [1]. One pit, located in Mare Tranquillitatis, is over 100 m wide and deep and exposes a deep cross-section through both lunar regolith as well as tens of meters of bedrock lava layers, providing unprecedented access to the Moon's secondary crust (see Fig 1.) [2]. The Moon Diver mission concept, developed in response to NASA's 2019 Discovery Announcement of Opportunity, proposes to pin-point land a spacecraft near the pit and use the *Axel* rover, an extreme-terrain robotic explorer, to investigate the intact lava bedrock layers. Equipped with an instrument suite collecting information on chemistry, mineralogy, and morphology of the layers, Moon Diver will contribute to our understanding of the formation and evolution of the Moon's secondary crust, as a proxy for understanding the same processes across the solar system.

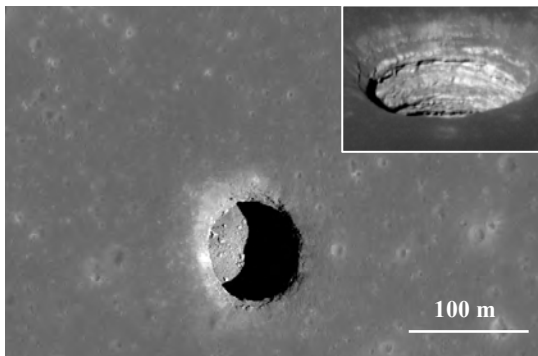


Fig. 1: The Mare Tranquillitatis Pit at (8.335° N, 33.222° E). Credit: NASA LROC M126710873R and M144395745L

Access to exposed lava layers in the selected pit is provided by two key technologies: 1) pin-point landing to deliver the *Axel* rover next to the pit funnel, and 2) extreme terrain mobility in the form of *Axel*, a rappelling rover, to deliver the instrument suite across the surface, and down the funnel and pit walls. Using a heritage lander design, derived from the successful Phoenix and Insight landers, pin-point landing is

achieved by leveraging Terrain Relative Navigation (TRN), also baselined for the Mars 2020 rover, to navigate during descent and landing [3]. The lander hereby compares images taken during the landing sequence with maps of the landing site stored onboard to establish its current position, and chart a course to the landing site. Once landed, expected to be within a 100 m diameter landing ellipse, the *Axel* rover egresses from the lander, traverses the lunar surface, enters the funnel of the pit, and rappels down the pit walls (see Fig. 2 & 3). The rover is anchored to the lander via a 300 m tether, which is released as the rover progresses away from the lander. In addition to providing mechanical support of *Axel*, the tether also provides power from the lander and communications between the lander and *Axel*.

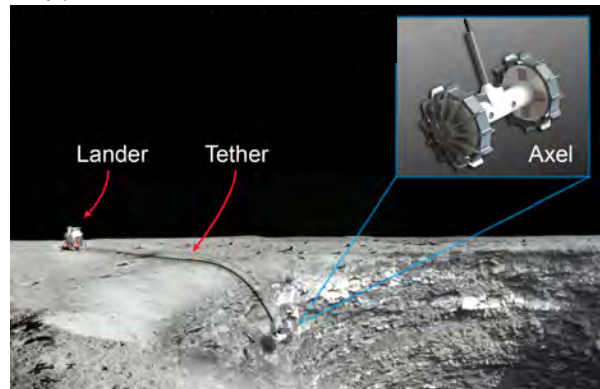


Fig. 2: Concept for the Moon Diver mission



Fig. 3: Artist's rendering of Axel rover rappelling into a lunar pit (left) and exploring the cavity below (right) as part of the Moon Diver mission

Axel's instrument suite consists of an Alpha-particle X-ray Spectrometer (APXS), a multi-spectral microscopic imager (MMI), a trio of context cameras, two of which are in stereo configuration, and a surface preparation tool. All instruments except the cameras are housed in separate bays that are enveloped and protected by Axel's wheels, and can be oriented and deployed independent of the wheel position, allowing the surface preparation tool, APXS, and MMI to be placed on the same target with high accuracy.

Landing shortly after lunar sunrise, the mission timeline is conceived to fit comfortably within the daylight hours of a lunar day (14 Earth days). The lunar surface operations are aided by using well established and validated operations processes in combination with the opportunity for near real-time commanding and telemetry. To test the surface operations concept, a prototype Axel rover was outfitted with a suite of representative instruments, and deployed to a terrestrial analog site, called "Devolites Pit" in Arizona.

This presentation provides a brief overview of the scientific goals, mission concept, mission and flight system elements, operations strategies, and payload capabilities for the proposed Moon Diver mission concept.

References: [1] Haruyama, J., et al., (2009) GRL 36, L21206. [2] Nesnas, I. A., et. al. "Moon Diver: A Discovery Mission Concept for Understanding the History of Secondary Crusts through the Exploration of a Lunar Mare Pit", IEEE Aerospace Conference, Big Sky Montana, March 2019. [3] Johnson, A.J., et al., "The Lander Vision System for Mars 2020 Entry, Descent and Landing", AAS 17-036.

Acknowledgments: This work was carried out at the Jet Propulsion Laboratory California Institute of Technology under a contract with NASA. The contributions of the entire proposal team at JPL, Lockheed Martin, and numerous additional institutions are hereby acknowledged. The information in this document is pre-decisional and is provided for planning and discussion only.

HERACLES - Human-Enhanced Robotic Architecture and Capability for Lunar Exploration and Science

R. Buchwald¹, F. Ebert¹, J. Hölzer¹, U. Soppa¹, M. Grallher¹, M. Landgraf², R. Schonenborg², A. Cropp², S. Vanden Bussche³, I. Gabiola⁴, D. Welberg⁵, T. Birck⁵, A. Götz⁵, T. Krone⁵, Airbus Defence and Space (mailto: robert.buchwald@airbus.com), ²European Space Agency, ³QinetiQ Space, ⁴SENER, ⁵ArianeGroup

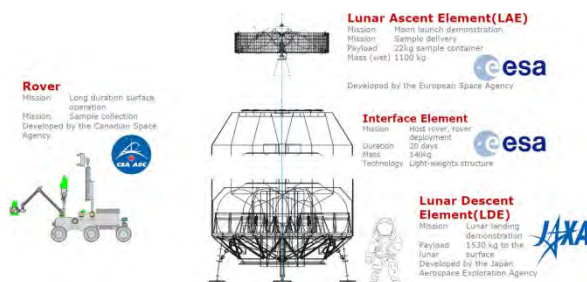
Presenter Biography: Robert started his career at Airbus in 2003 as development engineer for structural- and multi-body dynamics for various space missions. After working as system engineer and project manager for exploration and landing systems in the following years, he is now lunar logistics program manager in Airbus' advanced projects and products department.

Introduction: HERACLES is planned as an ESA-led international collaboration with Canada and Japan. HERACLES lands on the far side of the Moon in 2026, deploys a long range rover, and delivers 15 kg of surface samples to a crewed station orbiting the Moon called “the gateway”. The samples will be delivered to Earth by astronauts using Orion infrastructure.

By doing so, HERACLES serves as testbed for later crewed missions, enabling astronauts return to the Moon in the near future. The industrial team of Airbus, SENER, QinetiQ Space, and ArianeGroup analyzes and defines the mission and system specific aspects of the lunar ascent element (LAE) on behalf of ESA.

The HERACLES Demonstration Mission

The HERACLES stack consists of four main elements. A robotic lunar lander (LDE), a robotic lunar ascender (LAE), a long range rover, and an interface element which connects LDE and LAE, houses and deploys the rover, and supports sample transfer from rover to LAE.



The LAE Mission

The LAE provides power, communication, data storage, and attitude navigation support to the stack during outbound leg and landing. After landing, the LDE is decommissioned, the rover is deployed, and the LAE prepares for lunar night hibernation. After several weeks of sampling in the Southpole Aitken Basin, the rover returns to the LAE and a 22kg sample container with 15kg of surface samples from various locations of high scientific interest is handed over to the LAE.

After launch preparation, the LAE lifts off from the surface into an elliptical low lunar orbit. Following a

short loitering phase in LLO, the main engine is re-ignited for NRHO intersector orbit insertion burn before being isolated for crew safety reasons when approaching the gateway.



After several days of cruise and a small NRHO insertion burn at a distance of below 200km to the gateway, relative navigation and proximity operations start, ending with rendezvous and berthing by the gateway's robotic manipulator arm.

HERACLES architecture

The major objectives of the HERACLES mission are the in-flight demonstration of a to-be-developed human-rated main engine assembly (for later use in crewed ascender), in-orbit refueling demonstration, flight test of avionics and sensors for rendezvousing with a crewed station in near rectilinear halo orbit (NRHO), and technologies for surviving several lunar nights at minimum resources.

Following the HERACLES demonstration mission, various elements of HERACLES would eventually evolve into crewed elements.



Whilst the LDE could be re-used with minor modifications as small cargo lander and the LAEs rendezvous avionics and software could be identical for crewed versions to a wide extent, LDE and LAE would also be scaled to heavy lift versions by clustering the qualified and demonstrated engines, making the LAE a viable testbed for supporting the European leap to the Moon and beyond.

OVERVIEW OF NASA'S HUMAN LANDING SYSTEM FOR LUNAR EXPLORATION

D. G. Chavers¹, N. H. Suzuki¹, T. P. Polsgrove¹, S.L. Jackson¹, ¹NASA Marshall Space Flight Center, Huntsville, AL, USA, ²NASA Headquarters, Washington, D.C., USA, ³Stellar Solutions, Inc./NASA HQ, Washington, D.C., USA

Brief Presenter Biography: Dr. Greg Chavers is the formulation manager for NASA's efforts to return humans to the surface of the Moon. Prior to this role he managed NASA's Lander Technologies project. Dr. Chavers earned a bachelor's degree in Aerospace Engineering from Auburn University in 1990. He earned a Master's degree in physics in 1998 and a Doctorate in Physics in 2003, both from the University of Alabama in Huntsville.

Introduction: NASA is responding to the guidance of the U.S. Space Policy Directive-1 [1], "Beginning with missions beyond low-Earth orbit, the United States will lead the return of humans to the Moon for long-term exploration and utilization, followed by human missions to Mars and other destinations." NASA has identified a variety of exploration, science, and technology demonstration objectives via strategic knowledge gap analyses, decadal surveys, and exploration architecture studies that could be addressed by sending instruments, experiments, and humans to the lunar surface.

To address these objectives, NASA will build on its successful public-private partnership model to create a Human Landing System (HLS) to deliver human crews to the surface of the Moon. In addition to contributing to the establishment of the HLS, commercial and international partners can leverage new capabilities developed through this initiative for the execution of multiple other missions over the coming decades, including the potential to participate in regularly-recurring hardware and services procurements by NASA.

HLS is a key part of NASA's integrated lunar exploration campaign that includes the Orion crew module, Space Launch System rocket and Gateway outpost in lunar orbit. The agency is employing an approach to its human spaceflight strategy that is driven by the development of a suite of evolving capabilities that provide specific functions to solve exploration challenges. These investments in initial capabilities can be leveraged and reused continuously, enabling more complex operations over time and exploration of more distant solar system destinations.

While NASA expects to utilize commercial delivery services during the near term for early robotic missions, NASA also recognizes the need to foster the development of expertise and technologies required for reusable human landers. In addition, the agency understands that investments from the private sector are expected to

grow as market opportunities are identified and activities transition from science and exploration to resource utilization for both industry and government.

The reference architecture for the HLS employs a phased development approach starting with multiple flight demonstration missions [2].

NASA is planning for the launch of the first demonstration mission in 2024. The minimum objective of this mission is to demonstrate a lunar surface landing from the Gateway with a descent element capable of supporting a future human lander that includes both descent and ascent elements.

NASA plans to launch the second demonstration mission in 2026. The objectives of this mission are to demonstrate:

- Docking or berthing of the ascent element to the Gateway to support transfer of crew from Orion in a future mission.
- Aggregation of descent, ascent, and transfer vehicle elements at Gateway
- Transfer of the aggregated elements to low lunar orbit
- Lunar surface landing of the aggregated descent and ascent elements
- Return of the ascent element to Gateway, including docking or berthing
- Return of the transfer vehicle to Gateway

The first crewed human lunar landing is targeted for the third mission, which NASA plans to launch in 2028. The objectives of this mission include those of the 2026 mission, as well as demonstrating:

- Refueling and reusability of the 2026 Transfer vehicle and ascent elements
- Transfer of crew to and from the ascent element at Gateway
- Lunar surface extra-vehicular activity

References:

- [1] *Presidential memorandum on reinvigorating America's human space exploration program.* (2017). Washington: Federal Information & News Dispatch, Inc. Retrieved from ProQuest Central
- [2] *Human Landing System - Studies, Risk Reduction, Development and Demonstration - Federal Business Opportunities: Opportunities*, 07-Feb-2019. [Online]. Available: <https://www.fbo.gov/index?s=opportunity&mode=form&tab=core&id=13ca9566b575d496988122e66efc8230>.

TECHNOLOGY INVESTMENTS AT THE MOON TO ENABLE ENTRY, DESCENT, AND LANDING FOR HUMANS AT MARS. A. D. Cianciolo, NASA Langley Research Center, MS 489 Hampton, VA, 23681 USA (Al-
icia.m.dwyercianciolo@nasa.gov). T. P. Polsgrove, NASA Marshall Space Flight Center, Huntsville, Alabama,
35812, USA (tara.polsgrove@nasa.gov).

Introduction: 2019 marks the 50th anniversary of landing humans on the Moon. In the decades since, NASA has been working to define architectures and entry, descent, and landing (EDL) concepts to deliver humans to the surface of Mars [1,2,3]. As NASA, with commercial and international partners, considers returning to the Moon, the question remains: what technologies required to deliver humans to Mars are common with the lunar lander architecture and can be demonstrated at or around the Moon?

The return to the moon employs a *Mars Forward* philosophy that will leverage hardware elements, capabilities, technologies, and operations that exist for human use on the lunar surface with those that are either common, extensible, or are otherwise practical for crewed Mars surface exploration. The commonality extends beyond surface activities to all phases of a Mars mission including arrival, EDL, ascent and return to Earth.

Several major element commonalities may be possible. First, common propulsion technologies for landing and ascent stage for lunar and Mars surface missions would be *Mars Forward* because key technologies such as cryogenic fluid management (CFM) could be demonstrated in a lunar mission before using a more challenging Mars mission. Lunar missions may last days or weeks, but a mission to Mars would require long-term CFM to maintain propellant levels over months or years during in-space transit and to transport crew to the surface of Mars. Second, commonality in propellant and engine type are still being explored. A common lander development can leverage design, development, test, and evaluation considerations and minimize cost. Third, Solar Electric Propulsion(SEP)/Chemical Hybrid Propulsion System (HPS) type tug for Near Rectilinear Halo Orbit/Low Lunar Orbit transfers in cislunar space can test systems necessary for crew and cargo transfers to Mars. Fourth, surface kilowatt elements deployed on the Moon can demonstrate the types of contained and long-term use energy sources necessary to power Mars surface elements. Finally, common landing site requirements and surface mobility on the Moon demonstrate crucial operational aspects of the Mars Surface Field Station concept.

While in-space transportation, descent vehicles, and propellant types are visible aspects of Moon/Mars architecture commonalities, work continues on other aspects of the architecture that directly relate to EDL and are more subtle. For example, guidance, navigation, and

control algorithms and sensors, as well as design philosophies for approach and landing can be tested at the Moon [4,5]. Common on-board high-performance computing capabilities employed in various aspects of the Lunar architecture may offer equally significant impacts and opportunities for Mars missions. Some examples include performing guidance trajectory Monte Carlo calculations onboard during EDL and enabling the use of high-performance sensors, like terrain relative navigation, that can process measurements in a fraction of the time. These less obvious aspects critical to Mars EDL can be demonstrated at the Moon. Several such guidance algorithms and navigation sensors designs are under development.

In addition to the hardware and software, and technology and operation commonalities for Moon and Mars missions, the EDL community strives to maintain the human capital commonality, namely individuals who have worked both Mars EDL architecture studies and Lunar mission design and implementation. Other efforts to maintain common simulation frameworks, which are constantly updated to incorporate latest model data and perform analysis, are ongoing. Maintaining corporate knowledge of the goals of multiple destination architectures is also critical to the *Mars Forward* philosophy.

This presentation will review NASA's basis of comparison architecture for Mars exploration including the latest concepts for human scale EDL. Likewise, it will summarize NASA's the current architecture for returning to the Moon. Common hardware and software elements, specifically those relevant to EDL, being developed to support human missions to the Moon and Mars are presented. Finally, a brief summary of key Mars human scale EDL elements that remain unverifiable at the Moon will be discussed.

References: [1] Drake, B. G., editor., (2009) NASASP-2009-566. [2] Dwyer Cianciolo A. M. et al. (2010) NASA TM-216720. [3] Dwyer Cianciolo A. M. et al. (2018) AIAA 2018-5190. [4] Carson, J. et al. AIAA 2019-0660 [5] Dwyer Cianciolo A. M. et al. (2018) AIAA 2019-0661.

Friday, July 12 2019

Modeling, Simulation, Testing, and Validation - Conveners: Clara O'Farrell, Michael Wright, Julia Kowalski, Al Witkowski, and Aaron

8:30 AM	Further Aerodynamic Characterization Of The Esa Huygens Probe And Its Appendages : A Combined Testing And Modeling Approach	Simon Couche	Polytech Orleans - University of Orleans	Student
8:42 AM	Dragonfly: Modeling, Testing, and Validation for Atmospheric Flight on Titan	Douglas Adams	Johns Hopkins Applied Physics Laboratory	
8:54 AM	Integrated Modeling And Simulation Of Autonomous Parafoil Descent On Titan	Larry Matthies	Jet Propulsion Laboratory, California Institute of Technology	
9:06 AM	Static And Dynamic Testing Of Blunt Bodies In A Subsonic Magnetic Suspension Wind Tunnel	Mark Schoenenberger	NASA Langley Research Center	
9:18 AM	Recent Developments in Free-Flight CFD	Joseph Brock	AMA Inc. at NASA Ames Research Center	
9:30 AM	Plume-Surface Interaction (PSI): A New (Old) Challenge for Descent and Landing	Michelle Munk	NASA STMD	
9:42 AM	Application of Petascale Computing to Simulation of Powered Descent in Atmospheric Environments	Ashley Korzun	NASA Langley Research Center	
10:18 AM	Reconstructed Disk-Gap-Band Parachute Performance During the Third ASPIRE Supersonic Flight Test	Christopher Tanner	Jet Propulsion Laboratory, California Institute of Technology	
10:30 AM	ADEPT SR-1 Flight Test Performance Summary	Soumyo Dutta	NASA Langley Research Center	
10:42 AM	Aeroheating Tests Of Hayabusa Sample Return Capsule In Shock Tunnel And Expansion Tube	Hide Tanno	JAXA Kakuda	
10:54 AM	Challenges In Qualification Of Thermal Protection Systems In Extreme Entry Environments	Milad Mahzari	NASA Ames Research Center	
11:06 AM	Progress Towards Modeling The Mars Science Laboratory Pica-Nusil Heatshield	Brody Bessire	NASA Ames Research Center	
11:18 AM	Preliminary Results from Shock-layer Radiation Experiments in the T6 Aluminium Shock Tube	Peter Collen	University of Oxford	Student
11:30 AM	Current Status of Shock Layer Radiation Studies for Planetary Probes	Brett Cruden	AMA Inc. at NASA Ames Research Center	
11:42 AM	Mars 2020 EDL System Test Design and Progress	Mallory Lefland	Jet Propulsion Laboratory, California Institute of Technology	
11:54 AM	Validation Of The Mars 2020 Dsends Simulation Of Entry, Descent, And Landing Using Msl Reconstruction Data	Clara O'Farrell	Jet Propulsion Laboratory, California Institute of Technology	

FURTHER AERODYNAMIC CHARACTERIZATION OF THE ESA HUYGENS PROBE AND ITS APPENDAGES : A COMBINED TESTING and MODELING APPROACH. S. Couche¹, A. Beraud¹, C. De Tienda¹, R. Jochmans¹, L. Kovacs¹, A. Leroy², S. Loyer², P. Devinant^{1,2}, J-P. Lebreton³, ¹Polytech Orleans, Engineering school of University of Orleans, France (simon.couche@etu.univ-orleans.fr) ; ²PRISME Laboratory, UPRES 4229, University of Orleans, France ; ³LPC2E, CNRS-University of Orleans-CNES, Orleans, France.

Brief Presenter Biography: Simon Couche is a final year student at the Polytech Orleans Engineering School, in the TEAM department (Energy, Aerospace and Power Technologies).

Introduction and context : Huygens, part of the NASA/ESA/ASI Cassini-Huygens mission, is an atmospheric probe that landed under parachute on the surface of Titan, one of the several natural satellites of Saturn, on January 14th 2005. The goal of the mission was to study the physical properties and chemical composition of the atmosphere and the surface of Titan. The bottom of the probe was equipped with a set of spin vanes to control the spin during the descent (see Figure 1). External devices accommodated on the rim of the probe also contributed to the spin torque. Although the probe was released from its carrier Cassini with the correct spin, the spin started to slow down and eventually reverse during the descent under parachute [1,2]. Following previous studies aiming at explaining this issue, a study is currently carried out jointly by LPC2E (CNRS/Université d'Orléans/CNES), and the PRISME laboratory of University of Orléans in the framework of 2-year project (ESA Contract:4000121841/17/ES/JD started in November 2017). The results presented in this communication were achieved within a 2-month engineer student project which was conducted to investigate the contribution of the external appendages to the spin control, via experimental and modeling approaches.

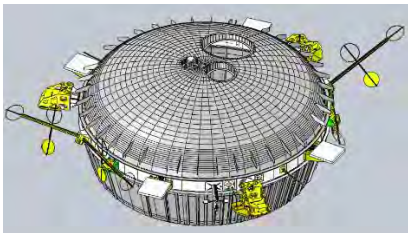


Figure 1: View of the Huygens probe from CAD modelisation and its appendages.

Methodology: The experimental approach consisted in testing a 1/3 size mock-up of the probe equipped with its appendages (Figure 1) in the Lucien Malavard subsonic wind-tunnel located at the University of Orleans. The mock-up was designed during the first year of the project and carefully chosen taking into

consideration the descent parameters of Huygens in Titan's atmosphere and the performances of the subsonic wind tunnel [2,3]. Appendages and vanes were 3D-printed in the laboratory. The objective was focused on the aerodynamic characterization of the mock-up achieved by aerodynamic load (forces and moments) measurements in static configuration using a 6 component aerodynamic balance located under the test section of the wind tunnel and a high sensitivity torque meter for the roll moment measurement (0.01 N.m) defined in Figure 2. The latter allows to measure smaller torques than possible with the balance.

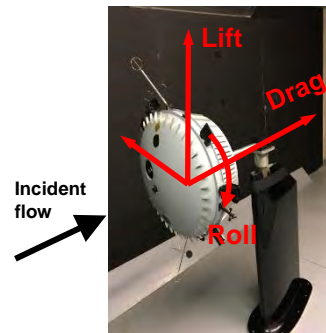


Figure 2: Picture of the mock-up mounted in the wind tunnel test section and linked to the balance via a shaped mast. Roll moment definition.

A test protocol was established that included a large number of combinations of appendages in order to characterize individually the effect of each of them and their combination on the aerodynamic behavior of the mock-up. Variable flow velocities (up to 40 m/s which corresponds to a Reynolds number of $1.2 \cdot 10^6$ based on the mock-up diameter) and angles of attack were also considered (up to $\pm 15^\circ$). Three inclination angles of vanes have been designed (2.2° , 2.8° , 6.8°). Different HASI (Huygens Atmospheric Structure Instrument) boom configurations have been investigated (closed, fully deployed and partly deployed) as well as different orientations of the DISR sensor head according to the considered definition of the angle of attack. About 200 tests were carried out.

In order to deepen this experimental approach, an analytic simulation tool was developed based on the original approach developed during the Huygens probe design phase [4] and adapted by Vorticity [5]. It consists

in solving the fundamental principle of dynamics of rotation about the probe axis of symmetry : $I_{xx}\omega = \sum_k C_k$ where ω is the rotational velocity and C_k represents the contribution of the indexed appendage k. At the time of writing, the tool is being validated with data obtained by the experimental tests. The validation will be pursued in April-May 2019 and hopefully terminated by the time of IPPW 2019.

Results: The roll moment was more particularly analysed during the tests according to different configurations of the mock-up. It is defined by $M_{roll} = \frac{1}{2}\rho SV^2 LC_{Mroll}$ where ρ is the air density, S is the reference area without appendages ($S = 0.147 \text{ m}^2$), V is the wind speed and L is reference length to calculate the moment induced by the corresponding force. Indeed, different appendages were mounted on the mock-up separately or in combination to observe their influence on the roll moment. Firstly it was highlighted that the vanes induce a roll moment in the predicted rotation direction but the different appendages all around the mock-up induced a reverse roll moment (Figure 3). It was also shown that each of the two booms provides an opposite torque of the same amplitude as the one provided by the vanes [3]. In Figure 3, the fixed appendages which have the highest influence on the negative reverse roll moment are the SEPS (Heat Shield Separation Subsystems) and the RAA (Radar Altimeter Antennae). Moreover, there might be some aerodynamic interactions between them which could increase the amplitude of the reverse roll moment. A study was also conducted to study the effects of the partial deployment (see Figure 4) of the booms as any asymmetry in their configuration (partial deployment of one boom) may affect the spin. The measurements provide inputs for the study of the change of boom configuration during the descent under parachute. The roll moments induced by the three tested inclination angles of vanes are plotted in Figure 5. It can be observed the quasi linear behavior of the roll moment against the inclination angle. In addition to Figure 3, it also shows that spin vanes with 2.8° inclination did not have enough authority to robustly control the spin rate as previously concluded in [5], and so the spin could have been affected by the appendages. The results finally demonstrate that each individual appendage contributes differently to the aerodynamic characteristics of the mock-up. A data base of all the test data is set-up in order to archive properly the test results. It will facilitate their further analysis taking account some data provided by specific instruments during the descent under parachute in order to find out some possible causes to explain this spin anomaly.

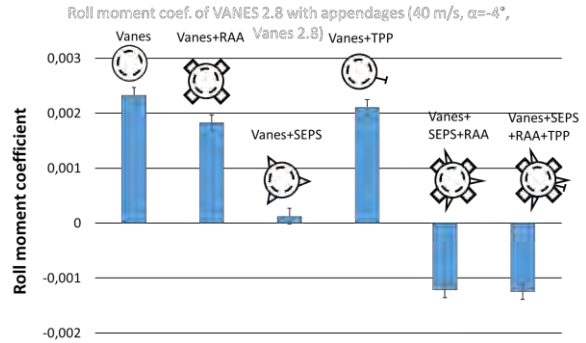


Figure 3: Roll moment coefficient for different mock-up configurations, 2.8° inclination angle vanes.

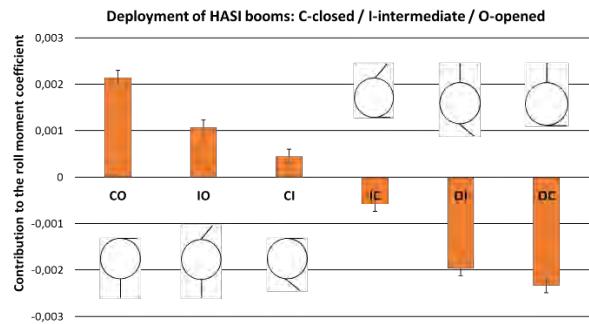


Figure 4: Contribution of different HASI boom configurations to the roll moment coefficient measured for a fully equipped mock-up (2.8° vanes, SEPS, RAA, TPP).

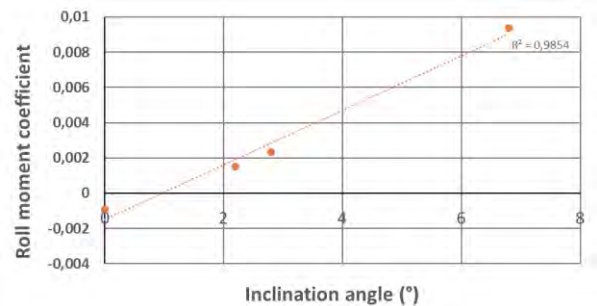


Figure 5: Roll moment coefficient for different vane inclination angles.

References:

[1] Lebreton J.-P . et al.. (2005) *Nature*, **438**,8. [2] Leroy et al., (2018), IPPW2018 oral paper. [3] Thébault et al (2018), IPPW2018 poster. [4] Aerospatiale Espace and Defense (1993). HUY-AS/m-120-PL-0009. [5] Vorticity Ltd Report (2015) Huygens in flight performance validation, ESA Contract Report : VOR-RE-1508, Iss 2.

***Dragonfly*: Modeling, Testing, and Validation for Atmospheric Flight on Titan**

D. S. Adams,¹ K. E. Hibbard,¹ B. F. Villac,¹ J. W. Langelaan,² J. R. Cruz,³ and J. A. Stipes¹

¹Johns Hopkins Applied Physics Laboratory, 11100 Johns Hopkins Road, Laurel, MD 20723.

²Pennsylvania State University, Old Main, State College, PA 16801.

³NASA Langley Research Center, 1 Nasa Dr, Hampton, VA 23666.

Presenter email: douglas.adams@jhuapl.edu

Brief Presenter Biography: Douglas Adams is a senior member of the Space Systems Engineering Group at the Johns Hopkins Applied Physics Laboratory (APL) where he has been for 6 years. During that time he has worked on Europa Clipper, Europa Lander, advanced concept development of future space missions, and is currently the *Dragonfly* Flight System Engineer. Prior to joining APL he spent 12 years at the California Institute of Technology's Jet Propulsion Laboratory (JPL) working on numerous programs including the *Mars Exploration Rovers (MER)*, and was the Entry, Descent, and Landing Mechanical Systems Engineer for the *Phoenix* Mars Scout mission. He served as the Parachute Cognizant Engineer for the *Mars Science Laboratory (MSL)* project, the Parachute Deployment Cognizant Engineer for the Low Density Supersonic Decelerator program (LDS), and was the Dynamics System Engineer for the *Soil Moisture Active Passive (SMAP)* rotating radar platform mission.

Introduction: *Dragonfly* is a proposed New Frontiers class mission that will send an MMRTG-powered rotorcraft lander to the surface of Titan to study the composition of a wide variety of surface sites and complete the first comprehensive *in situ* study of Titan's chemical diversity and complexity [1]. This presentation will provide an overview of the modeling, testing, and validation plans for the autonomous flight of this "relocatable lander."

Several key capabilities are required in order to enable *Dragonfly*'s mobility on the surface of Titan including: terrain-relative navigation (TRN), safe landing-site assessment, rotorcraft flight dynamics and aerodynamics, and software and control algorithms. The low gravity (1/7 Earth's) and high atmospheric density (4.4× Earth's) make Titan an ideal place to fly and enable an extensive, and economical, pre-flight testing and validation campaign that makes use of common-off-the-shelf (COTS) hardware and existing test facilities and infrastructure.

TRN is simulated using detailed environmental models based on terrestrial terrain analogs and Titan surface lighting models, permitting extensive development and testing of algorithms. These simulations include a 14-DOF dynamic model and an aerodynamic database that allows development of the event-driven flight mode

manager (FMM) and guidance, navigation, and control (GNC) algorithms for autonomous flight.



The aerodynamic database is developed for both terrestrial subscale and Titan full-scale flight through wind-tunnel testing. In particular, the National Transonic Facility (NTF) at NASA/Langley permits testing of full-scale hardware matching all of the relevant aerodynamic parameters 1:1 with Titan surface conditions. Other traditional facilities are used to develop an aerodynamic database for a subscale model that can be flown under standard temperature and pressure (STP) conditions on Earth using COTS hardware. This low-cost platform will allow extensive testing of flight algorithms on flight-representative computer boards using development versions of the flight sensors.

In particular, the subscale platform will be capable of lofting a flash lidar which can be used in combination with flight-representative COTS avionics to develop and validate the landing-site identification algorithms. In this way the landing sequence can be comprehensively tested prior to launch, which will develop field experience for the team and validate the algorithms. The same platform is used to test the transition to powered flight during EDL. The ability to perform these tests is a unique feature of the *Dragonfly* mission that is facilitated by the Titan environment.

The presentation will provide additional details about the planned testing, test facilities, test platforms, and the validation of *Dragonfly*'s planned surface concept of operations (ConOps).

References: [1] Lorenz, R. D., et al., "Dragonfly: A Rotorcraft Lander Concept for Scientific Exploration at Titan," Johns Hopkins APL Technical Digest, Vol. 34, No. 3, Oct. 2018, pp. 374-387.

INTEGRATED MODELING AND SIMULATION OF AUTONOMOUS PARAFOIL DESCENT ON TITAN[†]. Marco B. Quadrelli[‡], Aaron Schutte[†], Giacomo Bonaccorsi[‡], [†] Jet Propulsion Laboratory, California Institute of Technology, Pasadena, CA, 91109, U.S.A., [‡]Politecnico di Milano (Italy).

Introduction: The objective of this work is to address the problems of and investigate appropriate solutions to Guidance & Control aspects of autonomous Precision Aerial Delivery Systems for payload delivery using parafoils on Titan. Saturn’s moon Titan is the richest laboratory in the solar system for studying prebiotic chemistry, which makes studying its chemistry from the atmosphere to the surface one of the most important objectives in planetary science. Landing dispersions with existing technology are hundreds of kilometers wide, precluding landing in any liquid body except the large seas at high northern latitudes. Access to shorelines or other smaller features on Titan, which may present liquid-solid interfaces or more dynamic environments conducive to more chemical evolution, is only conceivable by relying on wind drift after landing on large seas. Therefore, there is a critical need for more precise landing capability to explore the unique potential for prebiotic chemistry on Titan’s surface. Our ultimate goal is to substantially reduce Titan lander delivery error at the end of the terminal descent. Lowest delivery error would be achieved with a multi-stage parachute system, with an unguided drogue parachute that descends rapidly through altitudes with high winds, followed by a guided parafoil with a high glide ratio that flies out position error at lower altitudes. One of the main risk areas in this concept is the uncertainty involved in parafoil guidance and control (G&C) performance. Parafoil aerodynamic performance has not been characterized yet for the dense Titan atmosphere and parafoil G&C algorithms must be adapted to unique characteristics of Titan missions, including the uncertainty in the density and the wind. Parafoil deployment at altitudes up to 40 km, where proven descent camera technology could see the surface to enable position estimation, could reduce delivery error by 100 km or more. The main risk areas in this concept are uncertainty in the precision of descent navigation and in parafoil guidance and control (G&C) performance. For autonomous descent, the only possible source of adequate position knowledge is onboard terrain-relative navigation (TRN), using a camera to recognize and track features of Titan’s surface during descent.

Guidance and Control Approach: We investigated the dynamics and control of the autonomous descent under parafoil. A six degrees of freedom model has been implemented to efficiently simulate the desired conditions for the whole descent and landing phase. This model was also used to perform some preliminary studies on the feasible glide range, expected wind drifts and average descent speed, as well as to investigate details of the final flare maneuver. A complete 40 km descent was simulated for glide ratios 2 and 3 in different conditions: no wind, upwind, and downwind descent. Both longitudinal and lateral wind speed were then varied to obtain a map of expected divert ranges, as shown in Table 1 and Figure 1. The Guidance & Control aspects [2] are divided into three parts: a heuristic approach (T-approach) for which no previous motion planning is required, optimal trajectory planning, and optimal trajectory tracking. The T-approach is particularly relevant in situations where no offline motion planning is desired and/or computational resources are limited. An expected wind drift is constantly taken into account to generate virtual waypoints in real-time: these waypoints guide the parafoil to an area close to the Intended Point of Impact, perform eight-patterns for energy management, and then to perform a final landing maneuver against wind. The results of Monte Carlo simulation (with different starting position/wind speed) indicate a maximum obtained error is 239 m and 332 m along Easting and Northing direction, respectively (Figure 2 and 3).

Motion Planning: Motion planning considers two distinct phases. An initial homing phase is considered, during which a minimum-time path is followed to reach an area above the target as quickly as possible as to maximize the residual altitude. The optimal trajectory for the final portion of the descent is obtained during this first phase by solving the Euler-Lagrange problem typical of the optimal control theory. If the complete state and control action history is needed, a 6-DOF model must be integrated in its entirety. If, instead, only trajectory waypoints are of interest, a 3-DOF model can be used to greatly improve integration speed. In cases where the complete state and control actions history is available, it is possible to perform trajectory tracking by means of a Linear-Quadratic Regulator (LQR) which, through the use of

[†] © 2019 California Institute of Technology. Government sponsorship acknowledged. This research was carried out at the Jet Propulsion Laboratory, California Institute of Technology, under a contract with the National Aeronautics and Space Administration. Thanks for Dr. Larry Matthies, Evgeniy Sklyanskiy, Emily Lylek, and Erik Bailey for useful technical discussions.

weight matrices, gives the appropriate feed-back control action in the neighborhood of the optimal nominal trajectory, provided small perturbations are present. If the whole state and input vectors are not available for each time instant (i.e. only waypoints to be followed are given), it is not possible to use a LQR. A Waypoint-Tracking Model Predictive Control (WT-MPC) was implemented for this eventuality. Given a sequence of spatial waypoints, the WT-MPC allows to accurately track them by linearizing the system (whose state matrices have been previously computed offline in symbolic form) at every time step and computing the optimal control action, given a desired time horizon which depends on the available computational power. Finally, a reduced-order Dynamic Programming (DP) implementation which makes use of successive grid-refinement has been investigated for the final approach. This would allow, through offline calculations, to obtain the optimal feed-back action to apply in every point close to the landing site.

Integrated Simulation: In parallel, we have extended our in-house Dynamics Simulator for Entry, Descent and Landing (DSENDS) [3] with libraries of vehicle dynamics models to handle the parafoil concept proposed here and the specific state estimation, tracking, and control capability in conditions relevant to Titan’s environment. TRN estimation is based on a SLAM-MCKF algorithm and is a key component in this study for determining lander delivery error. For simulation purposes, the TRN estimation is carried out independently from the DSENDS simulation on a Robot Operating System (ROS) node. This tool will be available for future Titan precision landing studies with different design points. Figure 4 shows a snapshot of the of the six-DOF DSENDS simulation.

References: [1] Folkner, W. M., et al. "Winds on Titan from ground based tracking of the Huygens probe." *Journal of Geophysical Research: Planets* 111.E7 (2006). [2] Yakimenko, Oleg A. "Precision Aerial Delivery Systems: Modeling, Dynamics, and Control" AIAA, Volume 248 Progress in Astronautics and Aeronautics, 2015. [3] <https://dartslab.jpl.nasa.gov>

Table 1. Divert range [m] for the case of low and high glide ratio (nominal wind conditions, $h_0 = 40$ km).

Glide ratio (L/D)	Upwind divert range	No wind divert range	Downwind divert range
2	74406	77146	78102
3	113647	119734	122015

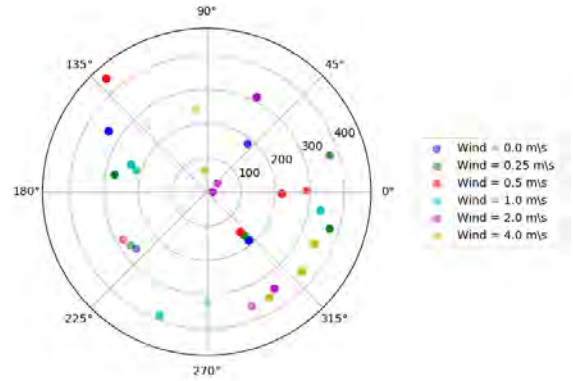


Figure 1. Final landing error [m] given the starting x,y position and wind speed.

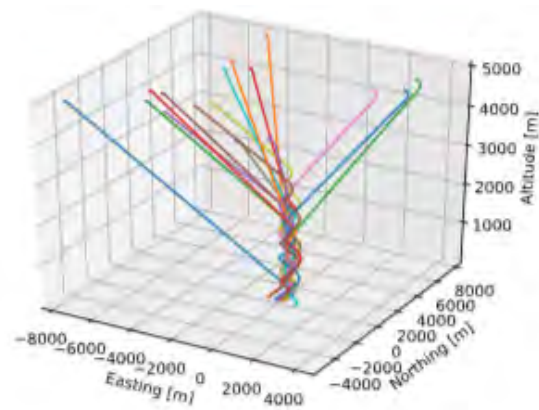


Figure 2. T-approach simulation with different initial conditions.

		Wind [m/s]											
		0.00		0.25		0.50		1.00		2.00		4.00	
Initial x, y	Position [m]	x	y	x	y	x	y	x	y	x	y	x	y
4755	1545	-286	179	-267	52	-293	332	-220	80	144	279	312	-151
0	5000	123	-141	109	-126	96	-116	328	-52	196	-282	277	-231
-4755	1545	121	-140	356	-106	218	-5	-137	-360	15	-0.5	181	-306
-2939	-4045	118	140	357	107	290	6	-207	64	29	27	-7	63
2939	-4045	-205	-164	-222	-155	-222	-139	-2	-320	131	-334	-34	241

Figure 3. T-approach simulation: landing coordinates with multiple winds and initial conditions.

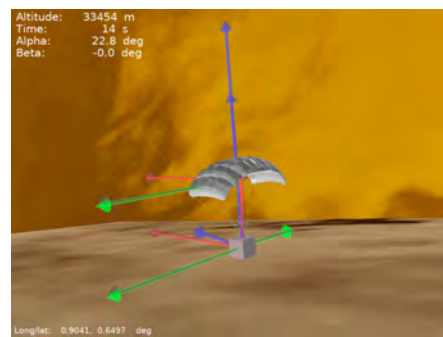


Figure 4. Snapshot from DSENDS simulation.

STATIC AND DYNAMIC TESTING OF BLUNT BODIES IN A SUBSONIC MAGNETIC SUSPENSION WIND TUNNEL

M. Schoenenberger¹, C. Finke², C. Britcher³, D. E. Cox¹ and T. Schott¹

¹NASA Langley Research Center, NASA Drive, Hampton, VA, 23666, United States, ²Texas A & M University College Station, Texas, 77843, ³Old Dominion University Hampton Blvd, Norfolk, VA, 23529

Brief Presenter Biography: Mark Schoenenberger NASA Langley Research Center's Atmospheric Flight and entry Systems Branch. He was the lead aerodynamicist for the Mars Exploration Rover and Mars Science Laboratory entry vehicles and has recently been working on bringing magnetic suspension test capabilities back to NASA Langley. The MSBS is being used to develop dynamic stability test methods which will help validate unsteady CFD calculations of blunt entry vehicles which will fly to Mars, Titan, Venus and other destinations in the solar system.

Introduction: The MIT 6-inch magnetic suspension wind tunnel [1] has been refurbished through a partnership between NASA and Old Dominion University. The tunnel is being used to develop test methods to measure pitch damping characteristics of blunt entry vehicles. Wind-on levitation was achieved in the fall of 2017. This was followed by calibration of the MSBS and characterization of different core materials as well as the first static drag measurements [2]. Test procedures are being developed to measure lift forces with models suspended at angles of attack and dynamic testing where the model is free to pitch, while constrained in the other degrees of freedom. Work has focused on demonstrating the feasibility of static and dynamic testing without moment control of the test articles.

MSBS Operation: Levitated models are controlled using a state estimator and Linear Quadratic Regulator (LQR) feedback design, with integral feedback to reject steady disturbances. Rotational states of the model are not sensed or commanded, and so were not part of the regulator design. The control system was implemented in Simulink, and autcoded to create software compatible with a real-time computer operating at 1000 Hz. Position feedback comes from an Electromagnetic Position Sensor (EPS) system. The intended use for this tunnel is to measure the dynamic stability of blunt bodies by measuring free oscillation histories. Separating dynamic aerodynamic moments from static aerodynamic moments and magnetic moments with a full 6-DoF controller was deemed impractical.

Model Test Configurations: To achieve free oscillation a number of model materials (permanent magnets and iron alloys) were assessed to see if a spherical core would rotate freely when levitated. The coercive forces of all materials tested were too high to achieve free oscillations. However, each levitated core would freely rotate about the magnetizing field. In normal operation

this results in models rolling freely in the flow. Neodymium-iron-boron (NdFeBo) permanent magnet cores were shown to stiffly align with the magnetizing field, while remaining free to rotate about the N-S axis. This feature was employed to create a set of models held at fixed angles of attack to measure lift. The MSBS was then rotated 90 degrees to demonstrate that models can pitch freely about the magnetizing axis. Figure 1 shows the two test configurations. A new smaller test section (2.375-in. H x 2.664-in. W) was fabricated that could pass through the side viewing ports of the MSBS. The rotation meant that the duties of the side and drag force coils are swapped.

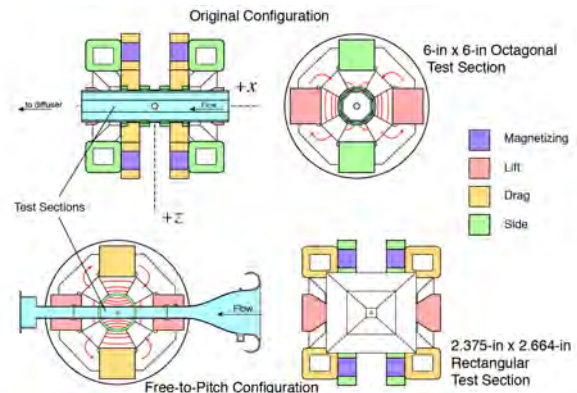


Figure 1 MSBS orientations for force and oscillation testing

Wind Tunnel Models for Lift and Pitching: Models of the Stardust capsule [3] and an approximation of the Orion entry vehicle were 3D printed with PLA plastic. 0.75-inch diameter x 0.75-inch length cylindrical NdFeBo magnets were located inside the models, canted at 8 and 16-degree angles relative to the model axes of symmetry. When levitated in the baseline MSBS configuration, the magnets would align with the magnetizing field, parallel to the tunnel freestream, holding the models at 8 and 16 degrees angle of attack. Dynamic pressure sweeps were run to measure the lift coefficient at these angles.

Another Stardust model was 3D printed to accommodate a 0.75-inch diameter NdFeBo sphere, which allowed for a smaller model to fit around the magnetic core so as to reduce blockage in the smaller free-to-pitch test section. The poles of the magnet were oriented to be orthogonal to the spin axis of the model, though a small sideslip was observed when levitated. In the transverse tunnel, the model was free to pitch and oscillated in tunnel flow due to its static pitch stability.

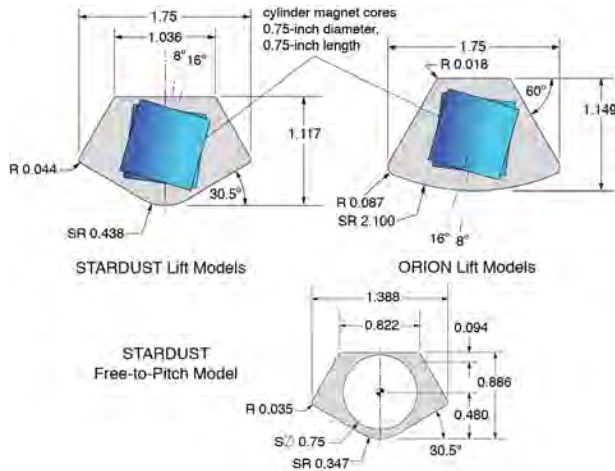


Figure 2 Lift and Free-to-Oscillate Wind Tunnel Models (dimensions in inches)

Lift Tests: Lift coefficient data from the Stardust and Orion canted-core models are plotted against reference wind tunnel data in Fig 3. Agreement is good for this preliminary assessment. The wind-off levitation current was subtracted from the lift current history and root-sum-squared with the side force current to determine the total lift force. The variation due to dynamic pressure needs to be investigated further. Signal-to-noise improved as dynamic pressure was increased. During testing the models rolled about the tunnel centerline. The 16-degree models showed more roll and lateral translation due to their increased lift, limiting the maximum dynamic pressure.

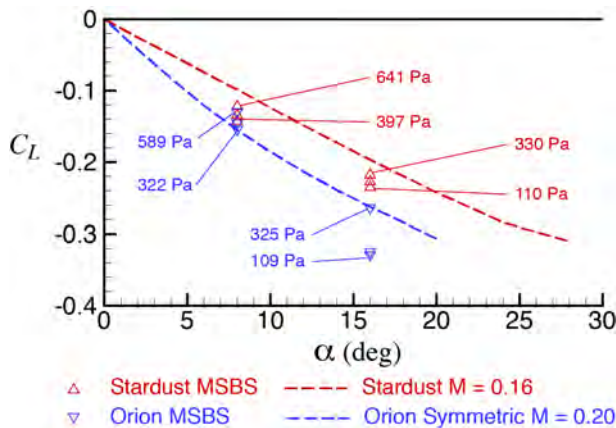


Figure 3 MSBS lift compared to historical wind tunnel data

Free to Oscillate Tests: The small Stardust free-to-pitch model is shown levitating in the transverse tunnel in Fig. 4. Video data at a small dynamic pressure (estimated to be approximately 50 Pa) was recorded and digitized to determine the attitude history. The planar attitude history can be approximated by the equation shown in Fig. 5 [4]. This model was fit to the measured attitude

history to identify the oscillation frequency and nose-down trim angle (the model cg was slightly forward of the magnet centroid). Future work will use this model to extract static and dynamic moment coefficients.

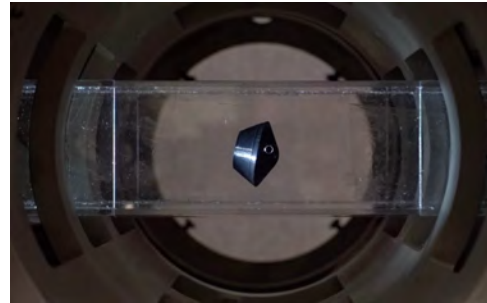


Figure 4 Free-to-pitch Stardust capsule in transverse tunnel

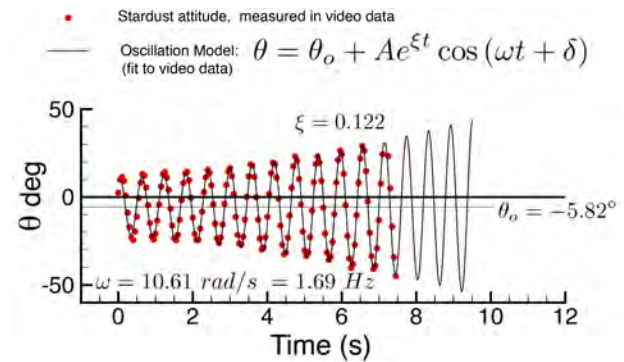


Figure 5 Planar oscillation model fit to Stardust video data

This free-to-oscillate configuration was intended as a proof of concept test to demonstrate that models would oscillate freely and capsule oscillations would grow or decay due to dynamic damping properties of the capsule. This demonstration was successful, although several sources of error must be addressed before the accuracy of aerodynamic coefficients can be determined. Model blockage affected dynamic pressure measurements during this test. The active control of the MSBS acting at a (small) distance from the model cg can introduce non-aerodynamic oscillation growth or decay. The MSBS control inputs can produce plunging motions that affect the angle of attack history, complicating pitch damping measurements as well.

Conclusion: Static lift forces were measured and free pitch oscillations recorded to extract damping information of blunt bodies. Future work will assess error sources and measure capsule pitch damping with uncertainties. Lessons learned from the transverse configuration can be applied to future MSBS designs for dynamic testing.

References:

[1] Stephens T., "Design, construction, and evaluation of a magnetic suspension and balance system for wind tunnels," NASA CR-66903; 1969.

- [2] Schoenenberger et al, "Preliminary Aerodynamic Measurements from a Magnetic Suspension and Balance System in a Low-Speed Wind Tunnel," AIAA 2018-3323, 2018.
- [3] Mitcheltree et al, "Aerodynamics of Stardust Sample Return Capsule," AIAA-97-2304, 1997.
- [4] Schoenenberger and Queen, "Limit Cycle Analysis Applied to the Oscillations of Decelerating Blunt-Body Entry Vehicles," NATO RTO-MP-AVT-152-006, 2008.

Recent Developments in Free-Flight CFD Joseph M. Brock¹ and Eric C. Stern², ¹Analytical Mechanics Associates, Inc., ²NASA Ames Research Center, Moffett Field, CA, USA (joseph.m.brock@nasa.gov)

Abstract: A Free-Flight Computational Fluid Dynamics (FF-CFD) capability has been developed within US3D under the Entry Systems Modeling (ESM) project [1]. Prior to this effort, aerodynamic stability coefficients have been exclusively derived from ballistic range experimentation and flight reconstruction. The FF-CFD project seeks to leverage advancements in high-fidelity CFD to characterize dynamic stability of entry probes. Previous presentations[2, 3, 4] have shown validation of the FF-CFD solver in the supersonic regime through comparison with ballistic range data. The current status report will present the extension of previous validation work from the supersonic down into the transonic flow regime. Additional discussion of the multi-body capability for modeling proximal bodies in supersonic flight.

To begin, a brief overview of previous regimes of the FF-CFD capability and comparisons with experiments will be presented. Qualitative and quantitative comparisons of the solver with ballistic range data for the Supersonic Inflatable Aerodynamic Decelerator (SIAD) and Adaptable Deployable Entry Placement Technology (ADEPT) geometries have been performed. The SIAD set of experiments provide coverage of Mach 3.5 down to Mach 2, while the ADEPT cases provide coverage from Mach 2.3 down to 1.2. The level of agreement with experimental data is discussed and an assessment on solver capability is proposed.

Next, new results from the low supersonic to transonic regime will be presented via comparisons with experimental data from the Orion MPCV ballistic range experiment[5]. The Mach numbers for these cases span 1.35 down to 1.03 providing subsonic flight for later portions of experiments.

Finally, the ability to simulate aerodynamic interactions of multiple bodies has been implemented in the FF-CFD solver. Preliminary validation of this capability has been performed using free-flight experimental data from the H2K wind tunnel facility at DLR, Cologne. If time allows, additional capabilities of the solver under development, as well as on-going applications to technology development and flight projects, will be discussed.

References

- [1] Eric C. Stern, Vladimir M. Gidzak, and Graham V Candler. Estimation of Dynamic Stability Coefficients for Aerodynamic Decelerators Using CFD. In *30th AIAA Applied Aerodynamics Conference*, pages 1–14, New Orleans, June 2012.
- [2] Joseph M Brock and Eric C. Stern. Dynamic CFD Simulations of the Supersonic Inflatable Aerodynamic Decel-

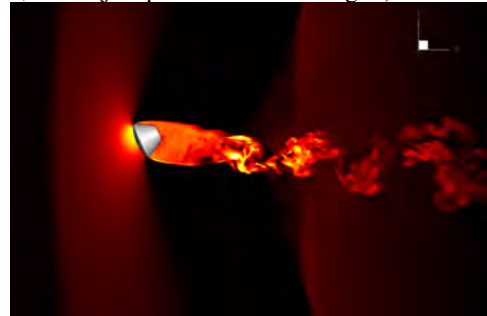


Figure 1: Temperature contours on the pitch-plane showing the extended unsteady wake of transonic CEV ballistic range model.

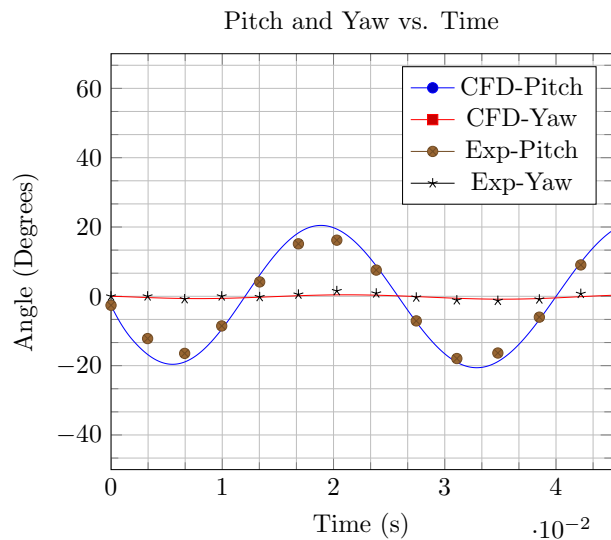


Figure 2: Pitch and yaw predictions from FF-CFD for the CEV geometry compared to ballistic range data.

erator (SIAD-R) Ballistic Range Tests. In *International Planetary Probe Workshop*, Laurel, Maryland, June 2016.

- [3] Eric C. Stern, Joseph M Brock, Alan M Schwing, Mark Schoenenberger, Michael C Wilder, Brandon P Smith, and Jakob Hergert. Progress on Free-Flight CFD Simulation for Entry Capsules in the Supersonic Regime. In *International Planetary Probe Workshop*, The Hague, June 2017.
- [4] Joseph M Brock and Eric C. Stern. Progress on free-flight cfd simulation for blunt bodies in the supersonic regime. In *International Planetary Probe Workshop*, 2018.
- [5] Jeffrey D Brown, David W Bogdanoff, Leslie A. Yates, and Gary T Chapman. Transonic Aerodynamics of a Lifting Orion Crew Capsule from Ballistic Range Data. *Journal of Spacecraft and Rockets*, 47(1):36–47, January 2010.

PLUME-SURFACE INTERACTION (PSI): A NEW (OLD) CHALLENGE FOR DESCENT AND LANDING.

M. M. Munk¹ and M. Mehta², ¹NASA-Langley Research Center (1 N. Dryden Street, Mail Stop 489, Hampton, VA 23681, Michelle.M.Munk@nasa.gov), ²NASA-Marshall Space Flight Center (MS 3421/EV33, Building 4600 Rideout Road, MSFC, AL 35812, Manish.Mehta@nasa.gov).

Brief Presenter Biography: Ms. Munk has served as NASA's Entry, Descent and Landing System Capability Lead since 2017. In that role, she is responsible for assessing technology, workforce, tool and facility needs for upcoming NASA missions and advising Agency leadership about investments. Ms. Munk's background is in flight mechanics, and she has spent over 20 years coordinating and leading entry system technology efforts.

Introduction: NASA is preparing to send larger payloads, some up to human-class, to the moon and Mars, in the next decade. Heavier landers mean more powerful descent engines, and those engines will disturb their environment more than ever before. The challenges of predicting the effects on the landing vehicle, and the surrounding area, are significant.

Current Efforts: Current modeling capabilities are being used in systems studies to give some indication of the potential damage to neighboring vehicles when a high-powered landing occurs. For example, human-scale Mars landers may spread ejecta up to 700 m from the lander [1]. Large site alteration and aerodynamic and aerothermal plume-induced effects on the lander during descent can lead to vehicle instability and violate landing constraints. These results drive requirements on landing precision, landing site spacing, and surface operations. Apollo landings showed that Lunar dust can achieve orbital velocities, which could damage overhead assets. Understanding these potential results is critical to designing vehicles and missions. However, state-of-the-art tools lack validation data and uncertainty quantification. Analysis results can be compared against analyses for other landing vehicles, and trends can be observed, but there is little confidence in an established "truth." In addition, the physics that govern the movement of ejecta at the Moon and Mars are quite different, due to the differences in the gravity field, atmosphere, and soil properties. Although computational methods can be applied across destinations, validation data is needed for both applications. Critical data need to be gathered both in ground test and in flight, regarding the engine plume, the crater shape and evolution, and the ejecta size/mass and velocity, to fully characterize this problem. Recent and upcoming robotic Mars missions like InSight and Mars 2020 are key opportunities for gathering flight data sets. At the Moon, commercial landers can deliver instruments for obtaining relevant data, in the next 1-3 years.

Conclusions: This presentation will discuss the state-of-the-art, and gaps, in the current NASA capability for modeling Plume-Surface Interaction. Modeling needs, ground test data needs, and flight test data needs are all important to recognize, as these components form the "three-legged stool" for validation. This talk will explain the structure of a proposed NASA technology project, establishing a coordinated effort to advance predictive models. The project involves multiple NASA centers and includes validation through ground test and flight test, as well as the possibility for international, university and commercial partnerships.

References:

[1] Liever, P. et al. (2018) "Gas-Granular Flow Solver for Lunar and Mars Plume-Surface Interaction Simulations," presented at the PSI TIM, November 14-15, 2018, Huntsville, AL.

Application of Petascale Computing to Simulation of Powered Descent in Atmospheric Environments

A.M. Korzun¹, E.J. Nielsen¹, A.C. Walden¹, ¹NASA Langley Research Center, Hampton, VA 23681 (ashley.m.korzun@nasa.gov)

Brief Presenter Biography: Ashley Korzun is a research aerospace engineer at NASA Langley Research Center. Her work focuses on the development of technologies to significantly increase payload mass to the surface of Mars, namely propulsive descent and landing and aerodynamic decelerators. She was the Aerodynamics Lead for the 2018 InSight Mars Lander and currently supports a variety of lander developments for the Moon and Mars. She holds a B.S. in Aerospace Engineering from the University of Maryland and an M.S. and Ph.D. in Aerospace Engineering from Georgia Tech.

Abstract: The entry, descent, and landing (EDL) systems for NASA's eight successful landings on Mars have all relied on technology developed for the Viking missions of the mid-1970s. The most ambitious of these missions, the Mars Science Laboratory, delivered a rover the size of a small automobile to the surface of Mars in 2012. While incremental improvements to these technologies, namely rigid aeroshells, supersonic parachutes, and subsonic propulsive terminal descent, have increased payload mass capability, new approaches to EDL are necessary to support the goal of human exploration at Mars. Recent work at NASA has identified and begun developing technologies that enable delivery of significantly larger payloads to the surface of Mars [1-3]. The goal of this effort is to assist in advancing the understanding of the underlying flow physics associated with novel approaches to aerodynamic and propulsive deceleration for atmospheric entry at Mars. Specifically, this work supports NASA efforts to characterize environments and requisite computational approaches to enable implementation of this technology into a flight vehicle.

Investigations of retropropulsion aerodynamics in ground testing require substantial compromises on physical scale, instrumentation and data products, configuration, and environments. The problem is challenged further by the very low pressure, density, and predominantly carbon dioxide composition of the Martian atmosphere. The inability to fully simulate relevant physics through ground testing requires a strong reliance on high-fidelity computational analyses to identify and evolve the knowledge basis for retropropulsion aerodynamics [3]. Simulating the interactions between the atmosphere and the retropropulsion exhaust plumes at sufficient spatial resolution to resolve governing phenomena with a high level of confidence is not feasible

with current, more conventional, computational capabilities. Present capabilities yield a single solution (one point along a trajectory at one attitude and one thrust level) requiring hundreds of thousands of CPU hours with additional limitations on spatial resolution. This work demonstrates the application of state-of-the-art, petascale computing capabilities to enable high-fidelity simulation of retropropulsion aerodynamics at flight-relevant scale. This is one of the first known efforts to efficiently apply a GPU-accelerated computational environment to high-fidelity computational fluid dynamics [4-7].

The investigation has yielded data that are unachievable with conventional high-performance computing (HPC) resources, targeting identification of the limits of dependence on spatial resolution and applicability of detached eddy simulation (DES) methods for retropropulsion in atmospheric environments. Retropropulsion is necessary for in-situ human space exploration, and the uniquely large size and complexity of the flow interactions for flight-relevant environments can only be examined through computational analysis. The effort is constructed around examination of bounding environments and conditions for nominal operation of a low-L/D, human-scale Mars lander concept. Design of the test matrix and scaling approach to explore differential throttling to produce pure pitch maneuvers and varied nozzle expansion conditions are also discussed.

This presentation will provide an overview of the ongoing computational campaign, the relationship between computational analysis of powered descent and ground and flight testing, preliminary results focused on nominal operating conditions for a low-L/D, human-scale vehicle concept, and the challenges facing the development of powered descent into a viable flight implementation.

This work is supported by resources received through 2019 Innovative and Novel Computational Impact on Theory and Experiment (INCITE) and Summit Early Science Program awards at the Oak Ridge National Laboratory Leadership Computing Facility, which is a U.S. Department of Energy Office of Science User Facility supported under Contract DE-AC05-00OR22725. The scientific objectives of the effort are in collaboration with the NASA Langley High Performance Computing Incubator and the NASA Space Technology Mission Directorate's Descent Systems

Studies Project and aligned with the NASA Aeronautics Research Mission Directorate's Aerosciences Evaluation and Test Capability Challenge.

References:

- [1] A.D. Dwyer Cianciolo and T.T. Polsgrove (2016) "Human Mars Entry, Descent, and Landing Architecture Study Overview" *AIAA Space Conference*. [2] K.T. Edquist, A.M. Korzun, et al. (2014) "Development of Supersonic Retropropulsion for Future Mars Entry, Descent, and Landing Systems" *Journal of Spacecraft and Rockets*, Vol. 51, No. 3, pp. 650-663. [3] Korzun, A.M. et al. (2019) "Design Considerations and Development Status for Atmospheric Powered Descent of High-Mass Payloads at Mars" *Submitted to the 2019 International Astronautical Congress*. [4] A. Walden et al. (2018) "Unstructured-Grid Algorithms for a Many-Core Landscape" *International Conference on Parallel Computational Fluid Dynamics*. [5] M. Zubair et al. (2018) "An Optimized GPU Implementation for CFD on Unstructured Grids" *The NVIDIA GPU Technical Conference*. [6] E.J. Nielsen et al. (2017) "Unstructured-Grid CFD Algorithms on the NVIDIA Pascal and Volta Architectures" *International Conference for High Performance Computing, Networking, Storage and Analysis (SC)*. [7] R.T. Biedron et al. (2018) "FUN3D Manual 13.3" *NASA/TM-2018-219808*.

RECONSTRUCTED DISK-GAP-BAND PARACHUTE PERFORMANCE DURING THE THIRD ASPIRE SUPERSONIC FLIGHT TEST.

C. O'Farrell¹, B. S. Sonneveldt¹, and I. G. Clark¹

¹Jet Propulsion Laboratory, California Institute of Technology, 4800 Oak Grove Drive, Mail Stop 321-220, Pasadena, CA 91109, ofarrell@jpl.nasa.gov

Introduction: The Advanced Supersonic Parachute Inflation Research Experiments (ASPIRE) project was aimed at developing and exercising a capability for testing supersonic parachutes at Mars-relevant conditions [1]. The initial series of ASPIRE flights were targeted as a risk-reduction activity for NASA's upcoming Mars 2020 project [2]. For this effort, two candidate Disk-Gap-Band (DGB) parachute designs were tested at conditions relevant to Mars 2020: a build-to-print version of the DGB used by the Mars Science Laboratory (MSL) in 2012 and a full-scale strengthened version of this parachute that has the same geometry but differs in materials and construction.

Over a three-flight campaign, the parachutes were delivered to targeted deployment Mach number and dynamic pressure conditions representative of flight at Mars by sounding rockets launched out of NASA's Wallops Flight Facility (WFF). The 21.5-m parachutes were mortar-deployed, and the deployment, inflation, and aerodynamics of the parachute were analyzed by a suite of instruments including: a three-camera high-speed/high-resolution stereographic video system trained on the parachute, situational awareness video cameras, a set of load pins at the interface of the parachute triple-bridle and the payload, and a GPS and inertial measurement unit (IMU) onboard the payload.

The first flight test (SR01) of the build-to-print parachute took place on October 4, 2017, followed by the first test of the strengthened parachute during flight SR02 on March 31, 2018 [3]. This presentation will describe the performance of the strengthened DGB parachute during the third ASPIRE test (SR03), which took place on September 7, 2018. During this test, the parachute was deployed successfully at a Mach number of 1.85 and a dynamic pressure of 932 Pa. The high speed camera footage captured the deployment and inflation of the parachute. The peak load at full inflation was found to be 67.4 klpf, the highest load survived by a supersonic parachute to date. Following completion of the mission, the parachute and payload were recovered from the ocean and inspected for damage.

The presentation will discuss the performance of the mortar system, the deployment and inflation of the parachute, its aerodynamic performance in subsonic and supersonic flight, and the results of the post-flight inspection. The observed performance will be compared against pre-flight models [4, 5] as well as the results from SR01 and SR02 and historical flight tests. Lessons

learned from the three flights, avenues for further investigation using the data collected during the tests, and the impact of the results on Mars 2020's risk-reduction campaign will be discussed.

Brief Presenter Biography: Clara O'Farrell is an engineer in the Entry, Descent, and Landing Guidance and Control Systems Group at JPL. She received a PhD in Control and Dynamical Systems from Caltech in 2013, and a BSE in Mechanical and Aerospace Engineering from Princeton University in 2008. Since joining JPL in 2013, she has worked on the Low-Density Supersonic Decelerators, ASPIRE, and Mars 2020 projects.

References:

- [1] O'Farrell, C., Clark, I.G., and Adler, M. "Overview of the ASPIRE Project," presented at the 14th International Planetary Probes Workshop, The Hague, NL, June 2017.
- [2] Tanner, C.L., Clark, I.G., and Chen, A. "Overview of the Mars 2020 Parachute Risk Reduction Plan" presented at IEEE Aerospace Conference, Big Sky, MT, March 2018.
- [3] O'Farrell, C., Sonneveldt, B.S., and Clark, I., G.. "Reconstructed disk-gap-band parachute performance during the first two ASPIRE supersonic flight tests" presented at the 15th International Planetary Probes Workshop, Boulder, CO, June 2018.
- [4] Muppidi, S., O'Farrell, C., Tanner, C.L., Van Norman, J.W., and Clark, I. G. "Modeling and Flight Performance of Supersonic Disk-Gap-Band Parachutes In Slender Body Wakes", to be presented at the AIAA Atmospheric Flight Mechanics Conference, Atlanta, GA, June 2018.
- [5] Way, D. W., "A Momentum-Based Method for Predicting the Peak Opening Load for Supersonic Parachutes", IEEE Aerospace Conference Paper No. 2817, Big Sky, MT, March 2018.

ADEPT SR-1 Flight Test Performance Summary

S. Dutta¹, A.M. Korzun¹, J.A. Tynis², J.S. Green¹, C.D. Karlgaard², J.M. Williams², A.M. Cassell³, P.F. Wercinski³, and B.C. Yount³, ¹NASA Langley Research Center, Hampton, VA 23681 (soumyo.dutta@nasa.gov), ²Analytical Mechanics Associates, Hampton, VA 23681, ³NASA Ames Research Center, Moffett Field, CA 94035

Brief Presenter Biography: Soumyo Dutta is an Aerospace Engineer in the Atmospheric Flight and Entry Systems Branch at NASA Langley Research Center. His current research focus is flight mechanics simulation and modeling of planetary entry systems. Soumyo has a Ph.D. and M.S. in Aerospace Engineering from the Georgia Institute of Technology and a B.S. in Mechanical Engineering from the University of Tennessee, Knoxville.

Abstract: Adaptable Deployable Entry and Placement Technology (ADEPT) is a deployable aeroshell that is stowed during the launch and then deployed after launch to increase the drag area of the spacecraft. The deployable aeroshell yields lower ballistic coefficients for planetary entry missions than heritage rigid aeroshells constrained to the volume requirements for existing or proposed launch vehicles.

The ADEPT Sounding Rocket One (SR-1) test was performed successfully on Sept. 12, 2018 within the grounds of White Sands Missile Range (WSMR) in New Mexico. ADEPT SR-1 was the first flight test of the ADEPT concept, and the flight vehicle was a 0.7 m-diameter, 70 deg. half-angle spherecone aeroshell with a 11 kg cubesat as the payload (Fig. 1).

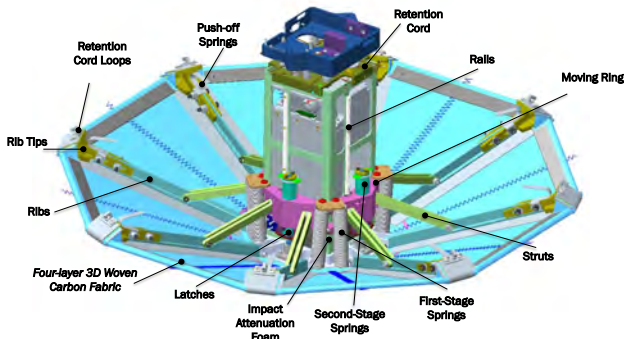


Fig. 1. ADEPT SR-1 flight vehicle description [1].

ADEPT SR-1 successfully separated from the spent booster in its stowed configuration, deployed above 100 km altitude (one of the key performance parameters of the mission), and then landed and was successfully retrieved from the grounds of WSMR. ADEPT SR-1 reached a peak Mach number of 3.1 and peak dynamic pressure of 818 Pa [2], both of which were well within 2 standard deviations of the pre-flight performance predictions. In addition, ADEPT SR-1 showed pitch and yaw stability through supersonic and high subsonic

flight, with total angles of attack below 20 deg. down to Mach 0.4 (see Fig. 2), satisfying the flight key performance parameter to maintain stability during supersonic and transonic flight.

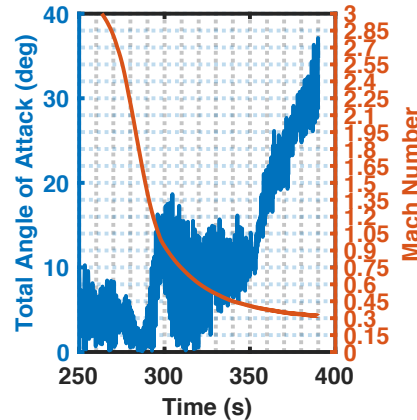


Fig. 2. Total angle of attack and Mach number of ADEPT SR-1 in supersonic and subsonic flight [3].

ADEPT SR-1 experienced unexpected rolling motion during the supersonic flight after the peak Mach number was achieved. The spacecraft had a planned rolling rate of 40 deg/s for gyroscopic stability during the exoatmospheric phase of flight. Gyroscopic stability was maintained through peak Mach number, but shortly after that, the rolling rate rapidly increased to 375 deg/s by the time ADEPT slowed down to Mach 0.5. This unexpected roll rate occurred while dynamic pressure increased (see Fig. 3) and is a focus of post-flight analysis. It is believed to be captured in aerodynamic simulations where an axisymmetric assumption is not enforced [4].

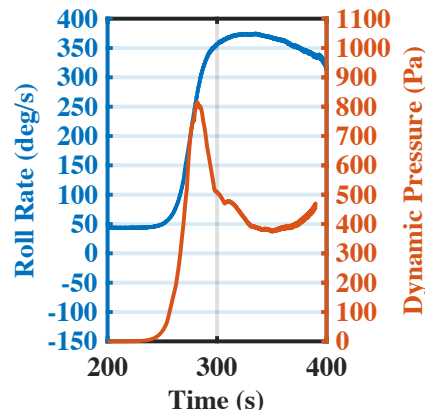


Fig. 3. Roll rate and dynamic pressure of ADEPT SR-1 in supersonic and subsonic flight [3].

This work will summarize the flight performance of the ADEPT SR-1 flight. Pre-flight flight dynamics predictions will be compared with post-flight reconstruction of the on-board data.

References:

- [1] Cassell, A.M. et. al. (2019) "ADEPT Sounding Rocket One Flight Test Overview," *AIAA Aviation 2019*.
- [2] Tynis, J.A. et al. (2019) "Reconstruction of the Adaptable Deployable Entry and Placement Technology Sounding Rocket One Flight Test" *AIAA Aviation 2019*.
- [3] Dutta, S. et. al. (2019) "Flight Mechanics Modeling and Post-Flight Analysis of ADEPT SR-1" *AIAA Aviation 2019*.
- [4] Korzun, A.M. et. al. (2019) "Aerodynamics for the ADEPT SR-1 Flight Experiment" *AIAA Aviation 2019*.

AEROHEATING TESTS OF HAYABUSA SAMPLE RETURN CAPSULE IN SHOCK TUNNEL AND EXPANSION TUBE

H. Tanno¹, K. Yamada³, B. K. Shimamura³, ¹JAXA KSPC Kakuda Miyagi 981-1525 Japan tanno.hideyuki@jaxa.jp, ²JAXA-ISAS Sagamihara Kanagawa Japan, ³University of Tsukuba, 1-1-1 Tennodai, Tsukuba-shi, Japan

Brief Presenter Biography: Hideyuki TANNO received his BSc., MSc. and Ph.D. degrees in Mechanical Engineering from Tohoku University in 1989, 1991 and 2005, respectively. He started to work as a researcher at National Aerospace Laboratory (Predecessor: Japan Aerospace Exploration Agency (JAXA)) Kakuda Research Centre since 1992. He is a senior researcher in high-enthalpy shock tunnel HIEST in the Research and Development directorate and a visiting professor in Tohoku University department of aerospace engineering. He belongs to HAYABUSA and HAYABUSA-II asteroid sample return missions (JAXA-ISAS). His current research interest is hypersonic aerothermodynamics including measurement technique and test facilities.

In JAXA, aiming at the development of the next generation reentry capsules for sample return missions¹, several aerodynamic and aerothermodynamic researches are undergoing. For the design of the sample return capsules, highly accurate numerical codes to predict aerodynamic heating become extremely important to reduce the mass of TPS (thermal protection systems), which suppresses payload budget. However, the accuracy of present numerical prediction codes are not enough due to lack of reliable experimental data for the codes validation. In order to obtain experimental data as benchmark for the code validation, JAXA is focusing on ground tests under the following two condition. (1) Turbulent boundary layer condition and (2) Super-orbital condition. In the present paper, the current status of aeroheating tests conducting in JAXA Kakuda Space Center was reported. A aero heating characteristics of HAYABUSA Sample return capsule configuration were investigated in the free-piston shock tunnel JAXA-HIEST² and the super-orbital expansion tube JAXA HEK-X³.

For the aero heating test under turbulent boundary layer, a Hayabusa SRC (sample return capsule) 70% scale model was tested in JAXA-HIEST, which model was 282mm diameter and has forty-eight fast-response coaxial thermocouples on the windward and back-shell to measure the heat flux distribution. Eight piezo-resistive pressure transducers were also mounted on the aft of the model and were used to determine flow establishment around the model. In the test campaign, stagnation enthalpy and pressure were $H_0=13\text{MJ/kg}$ and $P_0=83\text{MPa}$, respectively. Under the condition, the Reynolds number based on the model diameter under was $Re=0.8$ million, which Re number is expected for

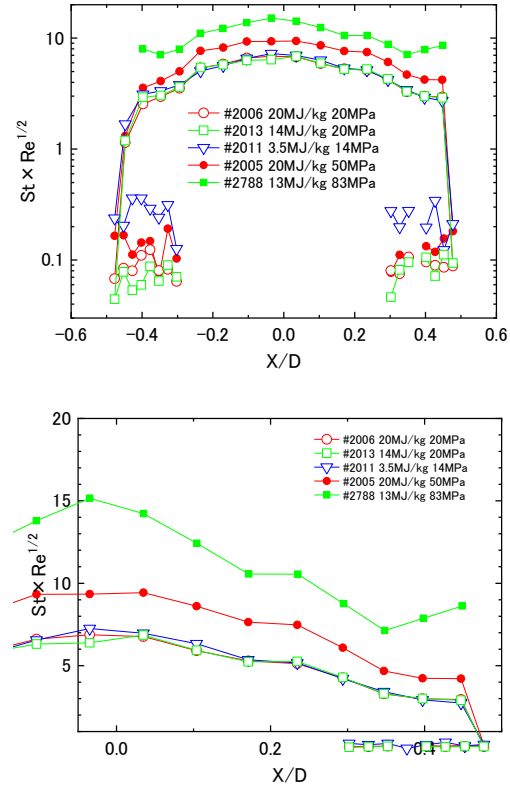


Fig.1 (Top) Measured heat flux distribution of the windward (heat shield side) of the model. Heat flux was normalized as a product of Stanton number and square root Reynolds number. (Bottom) Magnified heat flux distribution in the vicinity of the capsule shoulder.

boundary layer transition. Surface heat-flux distribution was observed around the model at the angle of attack 0 degree (Fig.1), which distribution showed heat-flux augmentation in the vicinity of the model heat shield edge. The cause of the augmentation was suspected the onset of the boundary layer transition. The Nomarski differential interferometry was applied to observe the flow around the model⁴ (Fig.2), which indicated high-density region around the edge.

For the aero heating test under superorbital flow, a Hayabusa SRC (sample return capsule) 10% scale model was tested⁵, which model was 40mm diameter and has four fast-response coaxial thermocouples on the windward to measure heat flux. In the test campaign, stagnation enthalpy and pressure were $H_0=40\text{MJ/kg}$

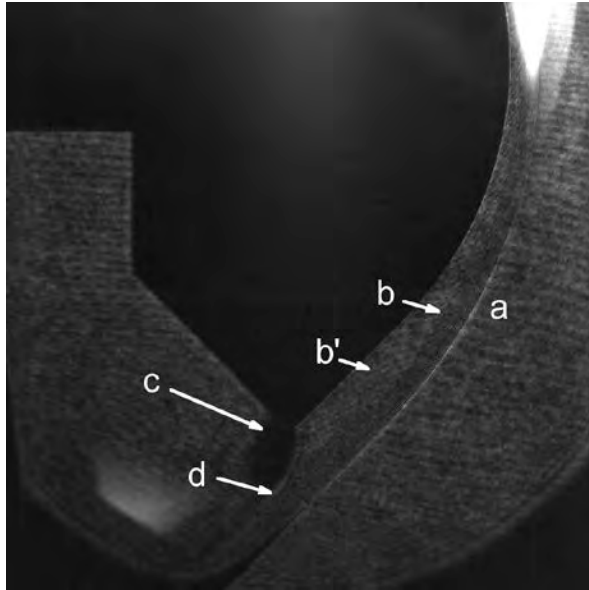


Fig.2 An interferometry image around the Hayabusa SRC shoulder, which image was taken with the Normarski differential interferometer. In the figure, a:bow shock, b:shock layer, c:separation bubble like structure and d:shock wave.

(Flow velocity =9km/s). Surface heat-flux was observed (Fig.3) around the model at the angle of attack 0 degree .

References:

[1]MMX: <http://mmx.isas.jaxa.jp/index.html>
 [2] Itoh, K., Ueda, S., Tanno, H., Komuro, T., and Sato, K."Hypersonic aerothermodynamic and scramjet research using high enthalpy shock tunnel", Shock Waves, 12, pp.93-98, (2002).
 [3]Tanno, H., Komuro, T., Sato, K., Itoh, K., Arai, K. and Yamada, K, "Basic characteristics of the free-piston driven expansion tube JAXA HEK-X", 32nd AIAA Aerodynamic Measurement Technology and Ground Testing Conference, AIAA AVIATION Forum, (AIAA 2016-3817)
 [4]Uchibe, G., et.al.: Flow visualization around Hayabusa ample return capsule using high-enthalpy shock tunnel (HIEST), to be published in the Proceedings of the 32nd International Symposium on Shock Waves (2019)
 [5]Fujiwara, Y., et.al.: Measurement of Stagnation Heat Flux in HEK-X Expansion Tube, to be published in the Proceedings of the 32nd International Symposium on Shock Waves (2019)

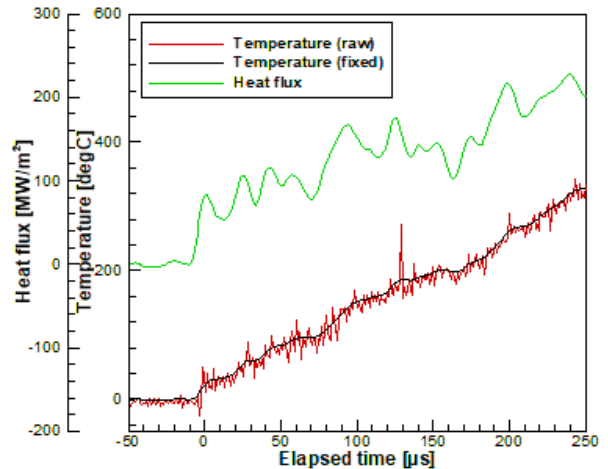


Fig.3 Temperature and surface heat flux histories measured with hemisphere probe (diameter 20mm) in HEK-X superorbital expansion tube. The flow velocity was 9km/s ($H_0=40\text{MJ/kg}$).

CHALLENGES IN QUALIFICATION OF THERMAL PROTECTION SYSTEMS IN EXTREME ENTRY ENVIRONMENTS

Milad Mahzari¹, Donald T. Ellerby², Peter J. Gage³

¹NASA Ames Research Center, milad.mahzari@nasa.gov, ²NASA Ames Research Center, donald.t.ellerby@nasa.gov, ³Neerim Corp, peter.j.gage@nasa.gov.

Brief Presenter Biography: Milad Mahzari is an Aerospace Engineer in the Entry Systems and Vehicle Development Branch at NASA Ames Research Center. He has been involved in the design and analysis of entry vehicles and Thermal Protection Systems (TPS) for multiple NASA projects including Orion, Mars2020, HEEET and MEDLI2. He is currently serving as the TPS lead for Dragonfly, a proposed mission to Titan.

Introduction: Planetary entry vehicles employ ablative TPS materials to shield the aeroshell from entry aeroheating environments. To ensure mission success, it must be demonstrated that the heatshield system, including local features such as seams, does not fail at conditions that are suitably margined beyond those expected in flight. Furthermore, its thermal response must be predictable, with acceptable fidelity, by computational tools used in heatshield design. Mission assurance is accomplished through a combination of ground testing and material response modelling. A material's robustness to failure is verified through arcjet testing while its thermal response is predicted by analytical tools that are verified against experimental data. Due to limitations in flight-like ground testing capability and lack of validated high-fidelity computational models, qualification of heatshield materials is often achieved by piecing together evidence from multiple ground tests and analytical simulations, none of which fully bound the flight conditions and vehicle configuration. Extreme heating environments (>2000 W/cm² heat flux and >2 atm pressure), experienced during entries at Venus, Saturn and Ice Giants, further stretch the current testing and modelling capabilities for applicable TPS materials. Fully-dense Carbon Phenolic was the material of choice for these applications; however, since heritage raw materials are no longer available, future uses of re-created Carbon Phenolic will require re-qualification. To address this sustainability challenge, NASA is developing a new dual-layer material based on 3D weaving technology called Heatshield for Extreme Entry Environments (HEEET) [1]. Regardless of TPS material, extreme environments pose additional certification challenges beyond what has been typical in recent NASA missions.

Scope of this presentation: This presentation will give an overview of challenges faced in verifying TPS performance at extreme heating conditions. Examples include:

- Bounding aeroheating parameters (heat flux, pressure, shear and enthalpy) in ground facilities. How to certify TPS if environments

can't be bounded or aeroheating parameters can't be simultaneously achieved.

- Higher uncertainties in ground test environments (facility calibration and analytical predictions) at extreme conditions
- Testing in flows similar to planetary atmosphere composition (H₂/He for Gas and Ice Giants)
- Test sample size limitations for qualifying seam designs
- Lack of computational tools capable of simulating all significant aspects of TPS performance (including initiation and propagation of failures)

This presentation will provide recommendations on how the EDL community can address these challenges and mitigate some of the risks involved in flying TPS materials at extreme conditions. Examples include:

- Dedicated activity to understanding TPS failure modes. Develop computational tools capable of modelling fluid interaction with material's thermostructural response. Validate these tools through failure testing. A better understanding of failure mechanisms may eliminate the need to fully bound all aeroheating parameters in ground testing
- Enhancements to current testing facilities to simulate flight-like ablation mechanism (ex. testing in Nitrogen at Ames Interaction Heating Facility to limit oxidation in favor of more sublimation)
- Improved characterization of test conditions with new diagnostic methods and determination of environment uncertainty through rigorous statistical analysis of available data
- Design margin policies that are directly tied to uncertainties in ground test environments and modelling fidelity

References:

[1] D. Ellerby, et al., "Overview of Heatshield for Extreme Entry Environment Technology (HEEET)", 15th International Planetary Probe Workshop, Boulder, CO, June 2018.

PROGRESS TOWARDS MODELING THE MARS SCIENCE LABORATORY PICA-NUSIL HEATSHIELD

A. Borner¹, B. Bessire², J. B.E. Meurisse¹, F. Panerai³, J. Monk², N. N. Mansour⁴ and T. White⁴, ¹Science and Technology Corporation at NASA Ames Research Center (arnaud.p.borner@nasa.gov & jeremie.b.meurisse@nasa.gov), ²AMA Inc. at NASA Ames Research Center (brody.k.bessire@nasa.gov & joshua.d.monk@nasa.gov), ³University of Illinois at Urbana-Champaign (fpanerai@illinois.edu), ⁴NASA Ames Research Center (nagi.n.mansour@nasa.gov).

Brief Presenter Biography:

Dr. Arnaud Borner is a Senior Research Scientist with Science and Technology Corporation, and an on-site contractor at NASA Ames Research Center working in the Advanced Supercomputing Division.

Abstract:

The data collected by the Mars Science Laboratory (MSL) Entry, Descent and Landing Instrumentation, MEDLI, have become an established reference to assess the performance of engineering models of the Phenolic Impregnated Carbon Ablator, PICA and to validate hypersonic computational fluid dynamics (CFD) tools for entry systems [1-4]. MEDLI measurements are also extensively used as validation reference for current developments of high-fidelity material response models for PICA [5], such as those implemented in the Porous Materials Analysis Toolbox based on OpenFOAM (PATO) [6]. So large has been the scientific output and impact of MEDLI that a follow-up instrumentation suite MEDLI2 is underway for the upcoming Mars 2020 mission [7].

A feature neglected thus far in the modeling of the MSL heatshield, is the presence of a silicone-based room temperature vulcanizing coating designated NuSil CV-1144-0. NuSil was used to coat the entire MSL heatshield, including the MEDLI plugs, to mitigate the spread of phenolic dust from PICA, and limit contamination during clean room operations. NuSil CV-1144-0 is a space grade siloxane copolymer, designed as an oxygen protection barrier for extreme low temperature environment. Notable applications of the material were coating solar arrays of the Space Hubble Telescope and the Long Duration Space Environment Candidate Material Exposure (LDCE-3) experiment on board of the STS-46 Orbiter mission [8,9]. As a coating of the MSL heatshield the material was applied using a light spray overcoat, after being diluted with Naphtha to a specific target viscosity

level. The application of NuSil to the MSL heatshield and MSL ground test articles is not immediately observable from photographs, as the coating is optically transparent.

Assessments conducted during MSL development demonstrated that the presence of NuSil had no adverse effect on the performance of PICA. However, evidence from ground testing of PICA-NuSil (PICA-N) models in arcjets suggests that the silicone fundamentally changes the high temperature response of PICA. It is therefore critical to assess the importance of modeling the coating in ongoing code validation efforts.

The overarching goals of studying the aerothermal response of PICA-N are: 1) to revisit MEDLI data analysis in the light of NuSil, 2) to support the development and exploitation of MEDLI2 instrumentation plugs, also determined to be coated with NuSil, and 3) to prepare NASA's design and analysis tools for future flight applications using PICA or analogous carbon/phenolic systems such as HEEET to include contamination controls, water proofing, and/or thermal control in the form of coatings or paints. The near-term objective of this research is to build a high-fidelity material response capability for PICA-N and assess how critical it is to consider the effect of NuSil on TPS numerical analyses and inverse environment reconstructions from TPS data.

This presentation will report on the status of ongoing efforts aimed at studying PICA-N. First, we will describe the phenomena involved in the response of PICA-N as observed from the analysis of old arcjet data from MSL era. We will then perform a preliminary revisited assessment of MEDLI data. Additionally, we will describe ongoing efforts dedicated to develop a rigorous spraying process for NuSil application on PICA and characterization of PICA-N. Finally, we will give an outlook on planned

experimental and model efforts in support of developing computational tools for the PICA-N system.

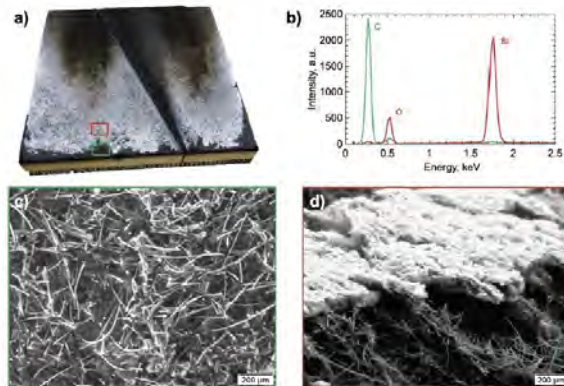


Figure 1: SEM and EDX of the PICA-N panel model tested in the PTF arcjet. a) Post-test photograph of the panel (flow from bottom to top) showing the formation of a whitish silica surface layer. b) EDX measurements of at two locations featuring the silica layer (red) and the underneath charred PICA (green). c,d) Micrographs of bare charred PICA at the location where the silica layer has peeled off (c) and of the silica layer formed on top of PICA (d).

References:

- [1] Bose, D. *et al.* (2013), *51st AIAA Aerospace Sciences Meeting*, AIAA 2013-908.
- [2] Mahzari, M. *et al.* (2013), *51st AIAA Aerospace Sciences Meeting*, AIAA 2013-185.
- [3] Bose, D. *et al.* (2014), *J. Spacecraft Rockets*, Vol. 51, pp. 1174–1184.
- [4] Mahzari, M. *et al.* (2015), *J. Spacecraft Rockets*, Vol. 52, pp. 1203–1216.
- [5] Meurisse, J. *et al.* (2018), *Aerosp. Sci. Technol.*, Vol. 76, pp. 497–511.
- [6] Lachaud, J., and Mansour, N. N. (2014), *JTHT*, Vol. 28, pp. 191–202.
- [7] Hwang, H. *et al.* (2016), *46th AIAA Thermophysics Conference*, AIAA 2013-3536.
- [8] Silverman, E. (1995), *NASA CR-4661, Part 1*.
- [9] Burns, H. *et al.* (1989), *16th International Conference on Metallurgical Coatings*, Vol. 39–40, pp. 627–636.

Preliminary Results from Shock-Layer Radiation Experiments in the T6 Aluminium Shock Tube.

P.L. Collen¹, L. J. Doherty¹, T. A. Hermann¹ and M. McGilvray¹, ¹ University of Oxford (Osney Thermofluids Institute, Southwell Building, Osney Mead, Oxford, OX2 0ES, United Kingdom).

Brief Presenter Biography: Peter is currently a DPhil student at the University of Oxford Hypersonics Group. To date, the majority of his work has involved the commissioning of T6, the United Kingdom's first high enthalpy hypersonic facility. His thesis focuses on the experimental investigation of shock layer radiation for re-entry vehicles.

Introduction: Super-orbital atmospheric entry typically occurs at very high velocities, from around 10 km s⁻¹ for lunar return to in excess of 40 km s⁻¹, as experienced during Galileo's Jupiter entry [1]. At these velocities, the sudden deceleration of the gas through the bow shock ahead of the entry vehicle causes significant heating with temperatures commonly in excess of 10,000K. These conditions are sufficient to cause thermochemical changes in the flow, including dissociation and ionization [2]. Radiative emission also becomes significant, and for sufficiently high velocities, large vehicles or certain atmospheric compositions the heating from this source can exceed that from convective sources [3]. Radiative heating is thus a significant consideration for thermal protection system (TPS) design, but high uncertainties present a challenge to accurate predictions of heat load [4].

The problem of radiative heat transfer to an entry vehicle is complex, potentially involving thermochemical non-equilibrium, radiation/flow-field coupling and optically thick radiative effects [5]. Validation of computational models thus requires high quality experimental data to build confidence in their ability to inform TPS design. Ground test facilities present a means to gather this validation data without the high costs associated with flight testing.

High enthalpy shock and expansion tubes have been used to simulate many flight conditions at which radiative heating is a potential issue (for example, [6-8]). However, these facilities have also encountered problems at certain trajectory points, for example due to limited test time or low signal-to-noise. In addition, discrepancies have been observed between models and experiments in several facilities [9,10]. The T6 Aluminium Shock Tube has been developed with the intention to address some of these issues, as well as to provide an additional source of cross-facility validation data.

Abstract: The T6 free-piston driver has recently been commissioned at the University of Oxford [11]. The driver can be coupled to a range of downstream ar-

chitectures to permit operation as a reflected shock tunnel, expansion tube or shock tube [12]. Two shock tube configurations are currently available: a 96.3mm diameter steel tube and a 225mm diameter aluminium shock tube. The predicted performance envelope of both modes is shown in Fig. 1.

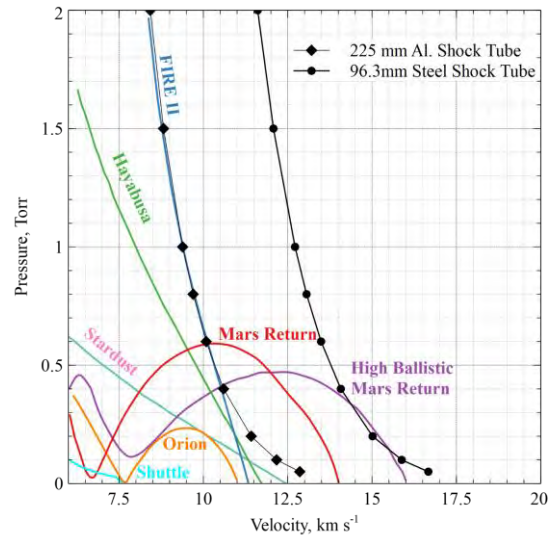


Figure 1: Predicted T6 Shock Tube Mode Performance (adapted from McGilvray et al. [12]).

The T6 Aluminium Shock Tube has been designed specifically for shock-layer radiation studies. The tube features a large, 225mm bore which increases test time [13] and provides a longer integration path for optical diagnostics. Diaphragms at either end of the tube isolate the test gas volume, which can be evacuated to approximately 1 mPa before filling. These measures ensure that the fill composition during the test is known to within 0.1% accuracy. Thirteen flush-mounted pressure sensors in the tube wall allow calculation of shock speed at the measurement location via time-of-flight methods. Finally, two 200mm long, diametrically opposed axial windows provide access for a range of optical techniques.

For shock layer radiation experiments a shock wave is passed through the stationary test gas. The shock speed and test gas fill pressure are matched to a flight trajectory point and an analogy made between the stagnation line of an entry vehicle and the normal shock passing through the tube. The radiative emission is collected using a series of UV-enhanced aluminium mirrors and focused onto the slit of a Princeton Instruments

IsoPlane-320 spectrometer, coupled to an Andor Intensified sCMOS camera. This arrangement allows a single image of the shock to be captured as it passes through the field of view, yielding a 2D map of the variation in radiance with wavelength and distance behind the shock. This data can then be used to gain insight into the sources and mechanisms of radiative heat transfer to entry vehicles.

This work will present initial measurements of radiative emission behind hypervelocity shocks in air, at conditions relevant for super-orbital earth entries. A comparison will also be made to existing results from other facilities and to computational tools.

References:

- [1] Gnoffo, P. A. (1999) *Annu. Rev. Fluid Mech.* 31, 459-94.
- [2] Anderson, J. D. (2006) *Hypersonic and High Temperature Gas Dynamics*.
- [3] Brandis, A. M. and Johnston, C. O. (2014) *AIAA Aviation*, Paper AIAA-2014-2374.
- [4] Johnston, C.O. et al. (2012) *43rd AIAA Thermophysics Conference*, Paper AIAA-2012-2866.
- [5] Boyd, I.D. and Jenniskens, P. M. (2010) *J Spacecraft Rockets* 47 (6), 901-909.
- [6] Brandis, A. M. et al. (2017) *J. Thermophys. Heat Tr.* 31(1), 178-192.
- [7] Brandis A. M. et al. (2010) *J. Thermophys. Heat Tr.* 24(2), 291-300.
- [8] Takayanagi, H. and Fujita, K. (2012) *43rd AIAA Thermophysics Conference*, Paper AIAA-2012-2744.
- [9] Brandis, A. et al. (2010) *10th AIAA/ASME JTHTC*, Paper AIAA-2010-4510.
- [10] Cruden et al. (2014) *11th AIAA/ASME JTHTC*, Paper AIAA-2014-2962.
- [11] Collen, P. L. et al. (2019) *AIAA SciTech*, Paper AIAA-2019-1941.
- [12] McGilvray, M. et al. (2015) *20th AIAA ISPHSC*, Paper AIAA-2015-3545.
- [13] Mirels, H. (1963) *Phys. Fluids* 6(9), 1201-1214.

Current Status of Shock Layer Radiation Studies for Planetary Probes

B. A. Cruden¹ and A. M. Brandis¹, ¹AMA Inc. at NASA Ames Research Center, Moffett Field, CA 94035, brett.a.cruden@nasa.gov.

Brief Presenter Biography: Brett Cruden is the Branch Technical Lead for the Aerothermodynamics branch at NASA Ames Research Center. He has served as the principal investigator of the Ames Electric Arc Shock Tube facility for the past ten years and is a co-developer of the NEQAIR radiation code.

Introduction: Radiative heating by the shock layer gases surrounding an entry probe is an important heating mechanism for many planetary entries. The magnitude of radiative heating for planetary atmospheres may be characterized with flight similarity in a shock tube capable of obtaining flight relevant velocities and atmospheric density/composition. Over the last decade, studies performed in the Electric Arc Shock Tube (EAST) at NASA Ames have characterized the radiative heating magnitudes for most relevant planetary destinations: Mars, Venus, Titan, Saturn, Uranus. Predictions of heating for a given entry trajectory are simulated by a combination of hypersonic flowfield modeling and the radiation code, NEQAIR, and then compared to the EAST test data. This paper will discuss the measurements, summarize the current simulation capability and provide indications for destination specific radiative heating uncertainties.

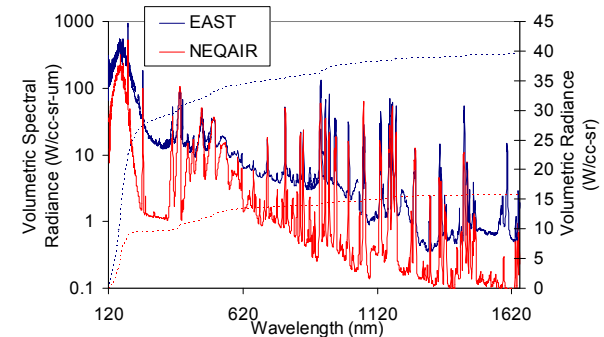
Approach: EAST is a 10.16 cm aluminum tube, separated from a 1.3L driver section by aluminum or stainless steel diaphragms. A 1.3 mF capacitor bank with up to 1.2 MJ energy storage is discharged into the driver section via an electric arc, creating a high temperature/pressure gas slug that drives strong shock waves (up to Mach 50) down the tube. The test section, 7.9 m beyond the driver diaphragm, is equipped with 4 spectrometers all imaging the same axial section of the shock tube in different wavelength ranges spanning from the vacuum ultraviolet to mid-infrared (120-5500 nm). The driven section is filled with planetary mixtures at densities that are representative of altitudes surrounding the radiative heat pulse.

Over the past 10 years, numerous tests in EAST have been performed in support of the Orion program¹, Mars Science Laboratory/MEDLI and future planetary probe missions. Of particular interest for this talk are Tests 49 (Venus: 97% CO₂, 3.5% N₂ by mole) [1], 54 (Mars: 95.8% CO₂, 2.7% N₂, 1.5% Ar) [2], 56 (Saturn/Uranus: 89% H₂, 11% He) [3] and 61 (Titan: 98% N₂, 1.5% CH₄, 0.5% Ar) [4]. The use of spectral and

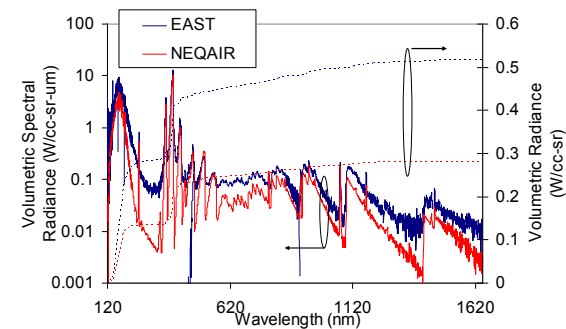
spatially resolved data from the spectrometers allow for the measurements to be understood in terms of particular radiative features, reactive intermediates and non-equilibrium phenomena.

Results are compared to simulations using the DPLR flow field code and NEQAIR radiation code. A pseudo-1D flow is extracted from the stagnation line solution over a blunt sphere to obtain temperature and species profiles behind the shock. These serve as inputs to NEQAIR which predicts the radiation magnitude with spectral resolution.

Results: The following general observations are made regarding each entry scenario and will be discussed in more detail for the final talk:



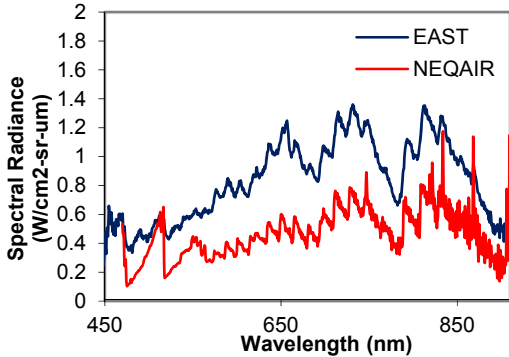
Venus: Radiation for Venus entries are dominated by atomic line emission in the vacuum ultraviolet and molecular band radiation from CO and CN in the VUV through UV. The largest unknown is bound-free radiation from the Carbon electron-ion recombination in the VUV.



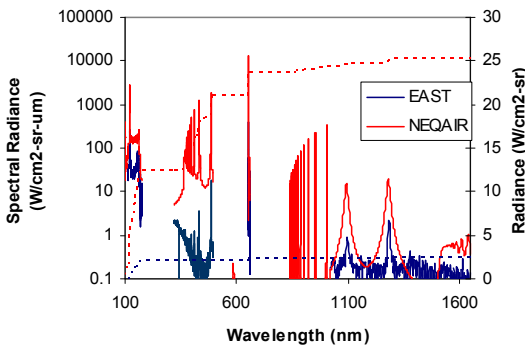
Mars: Martian entry radiation depends on the entry regime. At low velocities, mid-infrared radiation from CO₂ is the dominant mechanism. Predictions of fundamental CO₂ radiation are relatively accurate, while the

¹ <https://www.nasa.gov/exploration/systems/orion/index.html>

overtone bands are less well predicted. At higher velocity, CN and CO 4th Positive radiation become larger contributors. There is significant variations in what models may predict for CO 4th Positive radiation.



Titan: Significant overpredictions of radiation were noted for Titan entries in studies made around the time of the Huygens probe. More recent data suggest the earlier studies to have been biased by impurities and newer data sets indicate a higher level of radiation that is more consistent with current models.



Uranus/Saturn: For entries into Hydrogen atmospheres below 25 km/s (typical of Uranus), no radiation could be measured, consistent with models. At higher velocity (i.e. Saturn), relatively slow ionization rates prevents the attainment of equilibrium or Boltzmann levels of radiation and the radiative intensity is correspondingly small. However, the presence of small amounts of CH₄ in the upper Saturn atmosphere may increase the ionization rate and the impact of this has not yet been studied in EAST.

References:

[1] Cruden B. A. et al. (2012) *Journal of Spacecraft and Rockets*, 49, 1069-1079. [2] Cruden B. A. et al. (2013) *44th AIAA Thermophysics Conference*, 2013-2502. [3] Cruden B. A. and Bogdanoff D. W. (2017) *Journal of Spacecraft and Rockets*, 54, 1246-1257. [4] Brandis A. M. and Cruden B. A. (2017) *AIAA Aviation*, 2017-4534.

Mars 2020 EDL System Test Design and Progress. Mallory Lefland¹, ¹Jet Propulsion Laboratory, California Institute of Technology, 4800 Oak Grove Drive, Pasadena, CA 91109

Abstract: The Mars 2020 Mission test program in the Assembly, Test and Launch Operations (ATLO) Phase integrates the software and hardware for the first time to do large scale scenario testing. This testing facilitates the verification of requirements and overall validation of the system.

This paper will review the verification and validation aspects of the Mars 2020 EDL System Test Program and the progress since completing the first System Test in January of 2019. It will focus on the EDL scenario test runs, the outcome of the tests, and lessons learned that we can apply to future system tests and vehicle operation in flight. As well as how this test data is used as a comparison to validate tests performed in other venues.

The current plan is to do up to three more system tests on the EDL system prior to launching in July of 2020. This paper will cover the scenarios planned in future system tests including test objectives which were descoped from the first one. The first system test planned to do four EDL Runs – one nominal, one off-nominal Second Chance [2] landing, and two targeted testbed validation runs. Due to timing issues and simulation equipment, we descoped the off-nominal landing Second Chance and one of the testbed validation runs. A goal of the future tests will be to incorporate the Second Chance landing objective to ensure that that build of software has at least one ATLO landing prior to launch.

This first System Test uncovered issues that will change not just our future test campaigns but some aspects of how we intend to fly the vehicle. This test highlighted differences between the ATLO and testbed venues, providing the team with an understanding of the differences that they must account for to make the testbed as flight-like as possible. Additionally, as this was the first time a test had stitched together a scenario that takes the vehicle through Launch, Cruise, Landing, and early Surface, we were able to track various parameters and their use through the mission phases. Based on the performance, the EDL team has changed some system parameters to optimize their use across all of these phases, including Landing.

All in all, the first System Test was a huge success considering that the scope was just as comprehensive as the final Mars Science Laboratory System Test. The team is currently working on incorporating the lessons learned and planning the next System Test.

References:

[1] Allen Chen. Et al (2014) *Mars 2020 Entry, Descent, and Landing System Overview*, IPPW11 Presentation #8015.

[2] Chris Roumeliotis et al. (2013) *The Unparalleled systems engineering of MSL's backup entry, descent, and landing system: second chance*, 8th Annual System of Systems Engineering Conference, 2013, 13-1045.

VALIDATION OF THE MARS 2020 DSENDS SIMULATION OF ENTRY, DESCENT, AND LANDING USING MSL RECONSTRUCTION DATA. P. D. Burkhart¹, S. Aaron¹ and C. O'Farrell¹, ¹NASA Jet Propulsion Laboratory, California Institute of Technology (4800 Oak Grove Drive, Pasadena CA 91109).

Brief Presenter Biography: Dan Burkhart earned a PhD from The University of Texas at Austin in 1995 and has since worked at the Jet Propulsion Laboratory in Pasadena, California. He started as a navigation analyst supporting multiple Mars flight projects and studies including MGS, Mars 98 lander, Mars Odyssey and MSL. He started doing EDL flight dynamics analysis in 2005 and since has supported MSL, Mars 2020, and various proposals to planets, moons, and asteroids. He is currently a senior mission design engineer and is the DSENDS simulation group lead in the guidance and control section along with team lead for the Mars 2020 JPL EDL Flight Dynamics team.

Abstract: The Mars 2020 project will land a large rover on Mars in February of 2021 with an entry, descent, and landing (EDL) architecture that is mostly inherited from Curiosity [1][2]. With the reliance on simulation analysis to show the EDL system works, an independent verification and validation (IV&V) using the Dynamics Simulator for Entry, Descent and Surface landing (DSENDS) will be performed. DSENDS inherent capability is augmented for Mars 2020 with project-specific models of atmosphere, aerodynamics, sensors and thrusters, along with GN&C flight software, to enable high-fidelity trajectory simulation. While much of the required capability is inherited from Mars Science Laboratory [2], significant updates in DSENDS capability and new functionality needs for Mars 2020 meant significant updates for Mars 2020 were made, which was presented to this forum previously [3].

The final step in the capability checkout is a comparison with the MSL EDL reconstruction results.

The comparison process is as follows. A set of simulation parameters were identified by the MSL project as parameters of interest both as inputs that are varied in a defined fashion and as outputs that are tracked to measure performance. An uncertainty quantification (UQ) analysis was performed, in this case a standard Monte Carlo, by varying the parameters of interest and tabulating the results of interest with simulation runs for each set of dispersed parameters. A subset of these results was also determined from MSL flight data as part

of the reconstruction effort, along with information on how the flight performance compared with the expected values, specifically whether the values were higher or lower than predicted/expected. These results and expectations are used to compare how well the DSENDS analysis matches the expected values, treated as truth values, for MSL's EDL performance. Reconstruction values used for this comparison were gathered from [4].

A summary of the results is shown in Table 1. The values chosen here reflect metrics that span EDL from atmospheric entry to touchdown. Of particular note are the places where values don't agree with the reconstruction, for example the altitude when the radar-based onboard nav solution is available (TDS Nav Init), and related time in GN&C Mode 21. This difference is as expected, since the actual radar provided measurements at a much larger slant range than the model in simulation predicted (based on requirements), so the filter converges much earlier than predicted and also means a much larger time spend after the nav filter converges but before backshell separation and the start of powered flight. Additional details on the comparison will be provided.

References:

- [1] Allen Chen et al. (2015) *2015 Update: Mars 2020 Entry, Descent, and Landing System Overview*, IPPW-2015 Presentation #2104
- [2] P. Daniel Burkhart et al. (2013) *Mars Science Laboratory Entry Descent and Landing Simulation Using DSENDS*, AAS 13-421
- [3] P. Daniel Burkhart et al. (2018) *DSENDS Simulation of Mars 2020 Entry, Descent, and Landing*, IPPW-2018 presentation #558
- [4] D. Way et al. (2013) *Assessment of the Mars Science Laboratory Entry, Descent, and Landing Simulation*, AAS 13-420

CL#19-1211

Table 1: Summary Comparison of DSEDS Monte Carlo and MSL Reconstruction values

Score Card Item		DSEDS EDL Simulation Monte Carlo Results			MSL Flight Reconstruction	
Description	Units	1%	Mean	99%	Value	Quantile
Peak Entry Deceleration	Earth g's	12.262	12.707	13.228	12.609	-0.469σ
Peak Entry Lateral Loads	Earth g's	0.361	0.455	0.553	0.492	0.885σ
Downrange at HDA	km	76.311	81.452	86.17	83.242	0.780σ
Downrange at SUFR	km	8.249	14.233	20.388	12.819	-0.533σ
Downrange at PD	km	1.534	7.466	13.658	4.966	-0.947σ
Peak Parachute Deceleration	Earth g's	5.098	6.717	8.583	6.068	-0.823σ
Altitude AGL at TDS Nav Init	km	5.695	6.729	7.454	8.346	4.164σ
Time in GN&C Mode 21 (Timeline Margin)	s	31.375	43.91	56.192	62.5	3.491σ
Fuel Use, Powered Flight (no flyaway)	kg	244.962	252.004	259.388	247.5	-1.465σ
Downrange at TD	km	-6.564	-0.038	6.597	-2.329	-0.783σ
Landing Accuracy	km	0.274	2.666	7.348	2.385	1.139σ*

*Note: One-sided distributions are compared to standard Rayleigh quantiles

Friday, July 12 2019

Closing Session - Conveners: Pat Beauchamp and Jean-Pierre Lebraton

1:57 PM	White Papers For The Next Decadal Survey: Thermal Protection Systems And Instrumentation	Helen Hwang	NASA Ames Research Center	
---------	--	-------------	---------------------------	--

WHITE PAPERS FOR THE NEXT DECADAL SURVEY: THERMAL PROTECTION SYSTEMS AND INSTRUMENTATION.

H. H. Hwang¹, R. A. Beck², D. T. Ellerby², M. J. Gasch², J. A. Santos³, and T. R. White², ¹NASA Ames Research Center, Moffett Field, CA, USA (helen.hwang@nasa.gov), ²NASA Ames Research Center, Moffett Field, CA, USA, ³Sierra Lobo, Inc., Moffett Field, CA, USA.

Brief Presenter Biography: Dr. Helen Hwang has been at NASA Ames Research Center for over 20 years. She has been the Thermal Protection Systems Project Manager for MSL, Mars 2020, and previously was the MEDLI2 Principal Investigator. She is currently the Science Missions Development Manager for the Entry Systems Technology Division.

Introduction: NASA is anticipated to commission the next Planetary Science Decadal Survey (PSDS) with preparation expected in early calendar year 2020. The new PSDS will outline the priorities of science missions for the decade spanning 2023-2032. For the previous PSDS [1], the science and technology communities have been invited to submit white papers to the PSDS sub-panels as background information to guide the PSDS recommendations. The National Research Council has previously stated that white papers that represent the opinion of many authors from different institutions carried more significance and weight, and the recommendations from the previous PSDS attempted to reflect more of a consensus opinion.

In 2009, a total of 4 white papers were submitted to the PSDS panels regarding thermal protection system (TPS) readiness for missions [2] – [5], as well as one on TPS instrumentation [6]. The TPS readiness papers were co-authored by 90 individuals from many institutions. These white papers surveyed the TPS materials for both forebody and afterbody of a probe and analyzed the suitability of materials for missions to each destination. In addition, each paper outlined the ground testing required and ongoing technology development. Recommendations were provided for further technology development and ground test capability in order to fulfill future missions.

Planning for the next PSDS: Many improvements and changes have occurred in the past 10 years with regard to TPS materials and instrumentation. New materials have been developed and tested, such as the high density material Heatshield for Extreme Entry Environment Technology (HEEET), and new capabilities for ground testing for high heating and high pressures have been added such as the 3” nozzle at the Ames arc jet. NASA has also flown several TPS instrumentation suites, such as MEDLI and EFT-1.

In order to provide the PSDS sub-panels with the most current information about the state-of-the-art suit-

ability for TPS materials for entry missions, we are beginning to update and draft new white papers. We will present the outline for material to be covered in the white papers, and we invite all IPPW attendees to participate in co-authoring these papers.

References: [1] S. Squyres et al., “Vision and Voyages for Planetary Science in the Decade 2013-2022,” National Academies Press (2011). [2] E. Venkatapathy et al., “Thermal Protection System Technologies for Enabling Future Venus Exploration,” *White Paper to the NRC Decadal Survey Inner Planets Sub-Panel* (2009). [3] E. Venkatapathy et al., “Thermal Protection System Technologies for Enabling Future Sample Return Missions,” *White Paper to the NRC Decadal Survey Primitive Bodies Sub-Panel* (2009). [4] E. Venkatapathy et al., “Thermal Protection System Technologies for Enabling Future Mars/Titan Science Missions,” *White Paper to the NRC Decadal Survey Sub-Panels Mars & Outer Planet Satellites/Primitive Bodies* (2009). [5] E. Venkatapathy et al., “Thermal Protection System Technologies for Enabling Future Outer Planet Missions,” *White Paper to the NRC Decadal Survey Outer Planets Sub-Panel* (2009). [6] E. R. Martinez and R. V. Frampton, “Thermal Protection System Sensors,” *White Paper to the NRD Decadal Survey Mars and Outer Planets Sub-Panels* (2009).

Poster Session Abstracts

Tuesday, July 9 2019

Session	Title	Name	Affiliation	Status
Science Instrumentation, Experiments, and In-Situ Measurements	INES-a flexible and innovative payload for measuring radiation in the presence of ablation	Gilles Bailet	CentralesSupélec	
Science Instrumentation, Experiments, and In-Situ Measurements	Laboratory-Based Thermal Shock Investigation of Heat Flux Sensors for the Mars 2020 Backshell	Ruth Miller	AMA Inc. at NASA Ames Research Center	
Science Instrumentation, Experiments, and In-Situ Measurements	The LONSCAPE (Light Optical Nephelometer Sizer and Counter for Aero-sols in Planetary Environments) instrument: concept and application for the in situ detection of liquid and solid particles	Jean-Baptiste Renard	LPC2E-CNRS	
Science Instrumentation, Experiments, and In-Situ Measurements	GeMini Plus: Preparing the Way for Future Planetary Elemental Composition Measurements Throughout the Solar System Using Gamma-Ray Spectroscopy	John Goldsten	Johns Hopkins Applied Physics Laboratory	
Science Instrumentation, Experiments, and In-Situ Measurements	High Temperature Operation of Gallium Nitride Hall-Effect Sensors	Hannah Alpert	Stanford University	Student
Science Instrumentation, Experiments, and In-Situ Measurements	An Energetic Particle Monitor for Ice Giant Atmospheric Probes	Nicolas Andre	IRAP, CNRS, UPS, CNES	
Science Instrumentation, Experiments, and In-Situ Measurements	Radio Science from Venus Probe/Lander Mission	Robert Frampton	Boeing	
Mars Exploration	InSight's Reconstructed Aerothermal Environments	Jarvis Songer	Lockheed Martin Space	
Mars Exploration	Reconstruction of the Performance of Mars InSight Lander's Supersonic Parachute	Ian Clark	Jet Propulsion Laboratory, California Institute of Technology	
Mars Exploration	Landing Radar Performance Reconstruction for Entry, Descent, and Landing of the InSight Mars Lander	Dave Eckart	Lockheed Martin Space	
Mars Exploration	InSight Entry, Descent and Landing Operations Overview	Julie Wertz Chen	Jet Propulsion Laboratory, California Institute of Technology	
Mars Exploration	InSight Entry, Descent, And Landing Post-Flight Simulation Assessment	Carlie Zumwalt	NASA Langley Research Center	
Mars Exploration	InSight Landing Safety Assessment During Approach	Evgeniy Sklyanskiy	Jet Propulsion Laboratory, California Institute of Technology	
Mars Exploration	Trajectory Analysis of the ExoMars Schiaparelli Descent Probe	Emma Johnstone	Fluid Gravity engineering	
Mars Exploration	Challenges For Mars 2020 EDL At The Jezero Crater Landing Site	Erisa Stille	Jet Propulsion Laboratory, California Institute of Technology	
Mars Exploration	AMELIA: The EDL Science Experiment For The Entry And Descent Module Of The EXOMARS 2020 Mission	Francesca Ferri	CISAS - Univ. Padova	
Mars Exploration	Modelling Sensitivities and Knowledge Gaps Associated with Mars-atmosphere Destructive Entry Applied to Planetary Protection	James Merrifield	Fluid Gravity engineering	
Mars Exploration	Aerothermal Analysis and Thermal Protection System [TPS] Design of the Mars Sample Retrieval Lander [SRL] Concept	Suman Muppidi	AMA Inc. at NASA Ames Research Center	
Mars Exploration	ExoMars Rover and Surface Platform Mission: Technical Status	Andrew Ball	European Space Agency ESTEC	
Sample Return to Earth	A Dynamic Topology Optimization Method for Sizing Internal Components of the Potential Mars Sample Return Earth Entry Vehicle	Cameron Grace	University at Buffalo	Student
Sample Return to Earth	Implementing CubeSat Avionics Components to Full-Scale Capsule Return Missions	Zachary Hughes	San Jose State University	Student
Sample Return to Earth	Mars Sample Return - Earth Return Orbiter: Design and Validation of a Guidance, Navigation and Control System for Martian Rendezvous	Marc Chapuy	Airbus Defence and Space	
Sample Return to Earth	Structural Analysis of Impact-Tolerant Latched Containment Mechanisms for Mars Sample Return	Emma Shupper	Jet Propulsion Laboratory, California Institute of Technology	
Sample Return to Earth	High Velocity Impact Performance of a Dual Layer Thermal Protection System for the Mars Sample Re-turn Earth Entry Vehicle.	Benjamin Libben	NASA Ames Research Center	
Innovative Concepts for Exploration	TOUTATIS-Ex: A CubeSat testbed for entry experiments on Mars	Chloe Gentgen	CentralesSupélec	Student
Innovative Concepts for Exploration	Lunar Gateway LASC Module for Innovative Concepts for Exploration: A Laser-powered Apparatus for Satellite Charging	Brandon Biggs	San Jose State University	Student
Innovative Concepts for Exploration	Virtual Validation and Verification of the VaMEx Initiative	Philipp Dittmann	University of Bremen	Student
Modeling, Simulation, Testing, and Validation	Aerodynamic heating estimation of deployable inflatable aeroshell for Martian penetrator entry system	Tomoya Kazama	Tokyo University of Science	Student
Modeling, Simulation, Testing, and Validation	Modal Analysis of the Orion Capsule Two Parachute System	Jing Pei	NASA Langley Research Center	
Modeling, Simulation, Testing, and Validation	Multi-Fidelity Modeling for Efficient Aerothermal Prediction of HIAD Configurations with Surface Scalloping	Mario Santos	Missouri University of Science and Technology	Student
Modeling, Simulation, Testing, and Validation	Deployable Mars Aero-Decelerators: Rib Deformation Modelling and Testing	Lisa Peacocke	Imperial College London / Airbus	Student
Modeling, Simulation, Testing, and Validation	Modeling Thermal and Fluid Response of MMOD Impacted Thermal Protection Systems	Olivia Schroeder	University of Minnesota	Student
Solar System Exploration II - Airless Planetary Satellites, Asteroids, and Comets	Enceladus Lander Mission Concept	Leora Peltz	Boeing	

INES: AN INNOVATIVE AND FLEXIBLE SYSTEM FOR IN-FLIGHT RADIATION MEASUREMENTS IN THE PRESENCE OF AN ABLATIVE TPS. G. Bailet¹, A. Bourgoing², T. Magin³ And C. O. Laux⁴, ¹Technical Lead CS³, Laboratoire EM2C, CentraleSupélec, 91190 Gif-sur-Yvette, France . gilles.bailet@centralesupelec.fr, ²ArianeGroup, Route de Verneuil, 78133 Les Mureaux CEDEX, France, ³Associate Professor, Von Karman Institute for fluid dynamics, Aeronautics & Aerospace Dept, Chaussée De Waterloo 72, 1640 Rhode-St-Genèse, Belgium, ⁴Professor, Laboratoire EM2C, CentraleSupélec, 91190 Gif-sur-Yvette, France.

Brief Presenter Biography: Gilles is the technical lead of CentraleSupélec Space Center. With 9 years of experience the CubeSat and EDL field, he is leading teams in the design and development of 4 different CubeSat missions ranging from solar system exploration to debris mitigation. Fond of space exploration and multicultural work environment, Gilles is hoping to host IPPW-2021 in Paris.

Introduction: Reentry radiation is one of the key phenomena to take in account while designing a EDL phase of a mission for gas/ice giants and sample return. In the case of an ablative Thermal Protective System (TPS), the physico-chemical processes involved are producing a large amount of dust and phenolic gas.

The QARMAN mission [1] (Flight 2019 Q2) gave us the opportunity to develop a dedicated payload named INES (Imbedded Nano-platform-size Emission Spectrometer) to study the radiation of the reentry plasma in the presence of an ablative heatshield (Cork P50 [2]). This payload is also able to measure recession/swelling of the TPS at the same location.

The poster presents the different aspects of the payload design and the new design to push the envelope of the payload to a highly compact/low-cost instrument.

INES for QARMAN: The QARMAN vehicle (34 cm long for 5 kg) will reenter the Earth's atmosphere from an initial altitude of 400 km by the end of 2019. Located inside the payload bay, INES (left on Fig. 1) will take measurements of the radiation along the stagnation line (336-822nm spectral range with 1nm resolution for 350g).

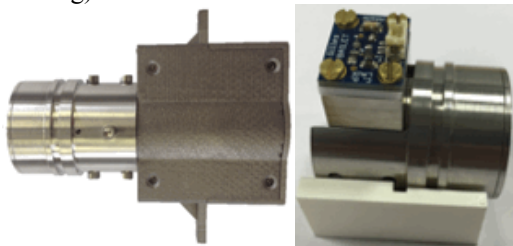


Figure 1: Full INES (left) and mini-INES (right)

Pushing the INES envelop: The INES payload effectively measure radiation without being impacted by the pollution of an ablative TPS, even after several minutes of plasma exposure. Efforts at EM2C and von Karman Institute ground test facilities (ICP torches)

allowed for successful testing of INES on a wide range of missions, from low heat flux (300 kW/m²) with PTFE TPS material to high heat flux (> 8 MW/m²) and for a Mars entry (2.6 MW/m²). Tests will start in the coming months to demonstrate the interest of INES payload for its integration within reentry/entry vehicles for sample mission return and Giant atmospheric probing.

Mini-INES: Following the success of the INES payload in different configuration, two patents were published [3] and [4]. In the idea of using the technology of INES for every type of entry/reentry vehicle, the payload was miniaturized, still fully passive, in order to provide for a fully qualified and highly compact payload able to measure the total radiative flux and the recession at the same location. Called Mini-INES (right on Fig. 1), the payload is only weighing 150g.

Conclusion: The INES payload will be rated TRL9 during QARMAN reentry by the end of 2019. In the meantime, the qualification tests are planned to expand the use of INES and mini INES and offer it to the EDL community.

References:

- [1] G. Bailet, A. Bourgoing, T. Magin and C. O. Laux (2014), *Qarman: an Atmospheric Entry Experiment on CubeSat Platform*, 11th International Planetary Probe Workshop.
- [2] NASA-CR-170881 (1979), *SRB TPS Materials Test Results in an Arched Nitrogen Environment*, Lockheed Missiles and Space Co.
- [3] G. Bailet, (2018), *Apparatus reduction liability of pollution of an optical access of an optical instrument*. Patent WO2018100255A1.
- [4] G. Bailet, (2018), *Method and device for detecting and assessing a thickness variation of a workpiece*. Patent WO2018100256A1.

LABORATORY-BASED THERMAL SHOCK INVESTIGATION OF HEAT FLUX SENSORS FOR THE MARS 2020 BACKSHELL.

R. A. Miller¹, G. T. Swanson², J. A. Santos³, and T. R. White², ¹AMA Incorporated at NASA Ames Research Center, ²NASA Ames Research Center, ³Sierra Lobo, Inc. at NASA Ames Research Center.

Brief Presenter Biography: Ruth Miller earned a PhD in Aeronautics and Astronautics from Stanford University. She is currently working as a Systems Engineer for AMA Inc. at NASA Ames Research Center in the Entry Systems and Vehicle Development Branch.

Abstract: In 2012 during the entry, descent, and landing of the Mars Science Laboratory (MSL), the MSL Entry, Descent, and Landing Instrumentation (MEDLI) sensor suite was collecting in-flight heatshield pressure and temperature data. The data collected by the MEDLI instruments has since been used for reconstruction of vehicle aerodynamics, atmospheric conditions, aerothermal heating, and Thermal Protection System (TPS) performance as well as material response model validation and refinement. The Mars Entry, Descent, and Landing Instrumentation 2 (MEDLI2) sensor suite for the Mars 2020 heatshield and backshell is being designed to expand on the measurements and knowledge gained from MEDLI. Similar to MEDLI, MEDLI2 will measure the pressure and temperature of the heatshield. MEDLI2 will additionally measure the temperature, pressure, total heat flux, and radiative heat flux on the backshell.

Since the backshell instrumentation is new to MEDLI2, Do No Harm (DNH) testing was conducted on instrumented backshell TPS (SLA-561V) panels [1]. The panels consisted of four pressure port holes, one Mars Entry Atmospheric Data System (MEADS) pressure port plug, one MEDLI2 Integrated Sensor Plug (MISP) thermal plug, and one heat flux sensor. DNH testing was conducted to ensure the performance of the TPS was not degraded due to sensor integration and to characterize any TPS performance changes. The testing consisted of environmental testing— vibration, shock, thermal vacuum (TVAC) cycling— and bounding aerothermal (arc jet) testing.

During arc jet testing, the heat flux sensors embedded in the SLA-561V panels exhibited an unexpected temporary reduction in the heat flux sensor temperature and response. After review of the test results, it was determined that this unexpected response was confined to the two heat flux sensors that experienced the greatest thermal shock condition. This condition consisted of a liquid nitrogen (LN₂) bath that induced temperatures of approximately -190°C, and then a transition (thermal shock) to an arc jet test at a heat rate of approximately 21 W/cm². Both heat flux sensors that were exposed to

this thermal shock experienced a blister in the thermal coating (see Figure 1) during the arc jet test.

Two heat flux sensor thermal shock test series were performed to investigate the cause of the blistering and subsequent energy release. In these tests, the heat flux sensor was first cold soaked in either a dry ice or LN₂ bath to induce temperatures of approximately -78°C or -190°C, respectively. Then the sensors were thermally shocked using two propane torches with a heat rate of either approximately 8 W/cm² or 21 W/cm². The key findings indicated that there is a correlation between thermal shock and the blistering observed in the DNH test series, and that the cause appeared to be rooted in the heat flux sensor epoxy that encapsulates the sensor thermopile. Blistering was experienced after cold soaks of -78°C and -190°C and a heat rate of approximately 21 W/cm². However, blistering was not observed after cold soaks of -78°C and -190°C and exposure to heating at approximately 8 W/cm².

Since the heat flux sensors are required to measure heat fluxes up to 15 W/cm² during the Mars 2020 entry, a third test series was designed to determine if blistering is an issue at this maximum expected flight heat flux. The third test series used a linear actuator table to simulate a flight-like time-varying heat pulse as opposed to the square heat pulse used in the two previous test series. A schematic of the test setup is shown in Figure 2.

Results from all three thermal shock test series and a discussion about whether or not blistering of the heat flux sensor thermal coating could be an issue for the Mars 2020 mission will be presented.

References: [1] Swanson, G. T. et al., (2017) 14th IPPW, The Hague, Netherlands, June 12-16.

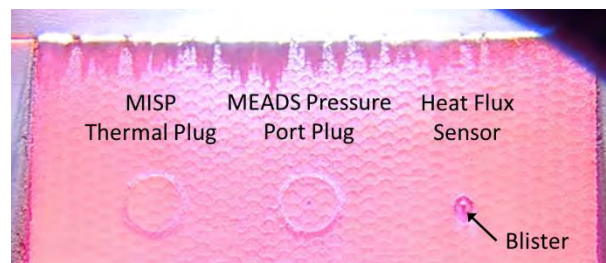


Figure 1. DNH backshell panel during arc jet testing.

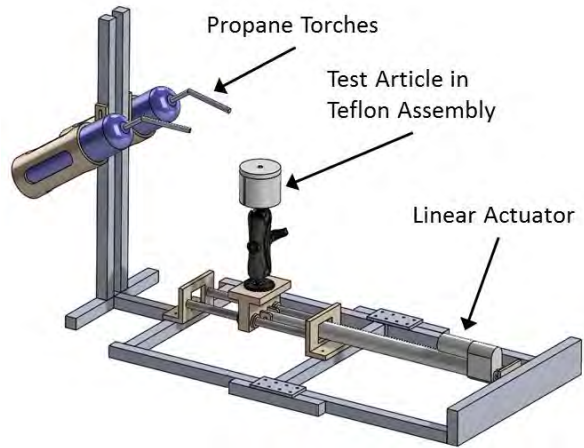


Figure 2. Test setup to expose a heat flux sensor to a time-varying thermal shock.

The LONSCAPE (Light Optical Nephelometer Sizer and Counter for Aerosols in Planetary Environments) instrument: concept and application for the in situ detection of liquid and solid particles

J.-B. Renard¹, O. Mousis², G. Berthet¹, D. Daugeron¹, J.-M. Geffrin³, A.C. Levasseur-Regourd⁴, P. Rannou⁵ and N. Verdier⁶

¹LPC2E, 3A avenue de la recherche scientifique, F-45071 Orléans, France, jean-baptiste.renard@cnsr-orleans.fr, ²LAM, 38 rue Frédéric Joliot Curie, F-13013 Marseille, France, ³Aix Marseille University, Centrale Marseille, Institut Fresnel, F-13013 Marseille, France, ⁴LATMOS – Sorbonne University, 4 place Jussieu, F-75005 Paris, France, ⁵GSMA, Campus SEN, Université de Reims, BP 1039, F-51687 Reims, France, ⁶CNES, 18 avenue Edouard Belin, F-31400 Toulouse, France.

Brief Presenter Biography: Dr. J.-B. Renard has been involved in the detection of liquid and solid particles since 25 years. He has developed several instruments for the study of the optical properties of the particles in atmosphere under balloons, and in laboratory at ground and during parabolic flights. He is author and co-authors of more than 120 peer review papers.

Introduction: Liquid and solid particles are present in the environment of many solar system objects: terrestrial planets, ice giants, cometary coma, interplanetary medium. Measuring aerosols properties can provide major constraints about both atmospheric composition and dynamic, and the surface of the objects. While some bulk aerosols properties can be estimated using remote measurements, their size distributions, which are related to their formation process, their origin and their evolution, are often poorly known. In particular, large uncertainties remain in remote derivation of the size distribution of aerosols.

Optical counter: We have been using since 2013 a light aerosols counter, LOAC (Light Optical Aerosol Counter) to perform measurements of liquid and solid particles at ground and under all kinds of balloons in the Earth atmosphere [1,2]. In particular, LOAC is regularly launched under weather balloons and more than 150 flights have been conducted to date. The total weight of the gondola, including the instrument, the battery, meteorological sensors and the telemetry system is of 1 kg, for an electric consumption below 3 W. Also, LOAC is involved in the Strateole 2 project which consist of long duration flights (at least 3 months) of poly-instrumented gondolas in the equatorial lower stratosphere (first technical flight at the end of 2020).

The particles cross a laser beam and their scattered light is recorded by photodiodes. In its current version, measurements are performed at two scattering angles. The first one is around 12° and is almost insensitive to the refractive index of the particles; the second one is

around 60° and is strongly sensitive to the refractive index of the particles. By combining measurements at the two angles, it is possible to retrieve the concentrations for 19 sizes between 0.2 and 50 μm and to estimate the light absorbing properties of the particles related to their typology (droplets, carbonaceous particles, minerals particles, salts, ices) by comparison with calibration charts obtained in the laboratory with real particles.

Space instrument: The French Space Agency CNES has funded studies for space applications of the LOAC instrument. The aim is to first improve the existing version of LOAC in terms of performance for the detection of sub-micronic aerosols and secondly to be able to use the instrument in space conditions (low temperatures, low and high pressures, electro-magnetic radiations). Also, the possibility of adding several angles of measurements (up to ten) is proposed to be able to retrieve the whole scattering function for better identification of the typology of the aerosols, for radiative transfer calculations and for comparison with remote-sensing measurements. The number of additional angles can be defined following the science objectives of the mission. Thus, we propose a new instrument that combines the counting for an accurate determination of the size distribution and nephelometric measurements to accurately retrieve the refractive index, the nature and the shape of the particles for different size classes. This instrument is called LONSCAPE (Light Optical Nephelometer Sizer and Counter for Aerosols in Planetary Environments).

Projects: LONSCAPE will be involved in future space projects. A collaboration starts to be established with the JPL/NASA for technological developments to study the Venus atmosphere. Also, LOSNCAPE could participate to a future mission to the ice giants inside an atmospheric probe [3].

References: [1] Renard et al., *Atmos. Meas. Tech.* 9, 1721-1742, 2016. [2] Renard et al., *Atmos. Meas. Tech.* 9, 3673-3686, 2016. [3] Mousis et al., *Planet. Space Sci.* 155, 12-40, 2018.

GeMini Plus: Preparing the Way for Future Planetary Elemental Composition Measurements Throughout the Solar System Using Gamma-Ray Spectroscopy.

David J. Lawrence¹, Morgan T. Burks², Samuel Fix¹, John O. Goldsten¹, Lena E. Heffern^{2*}, Patrick N. Peplowski¹; Zachary W. Yokley¹; ¹Johns Hopkins University Applied Physics Laboratory, Laurel, MD (David.J.Lawrence@jhuapl.edu), ²Lawrence Livermore National Laboratory, Livermore, CA. *now at Arizona State University.

Brief Presenter Biography: Dr. David Lawrence is a staff scientist at Johns Hopkins University Applied Physics Laboratory, and has over 20 years of experience in the development and use of spaceflight instrumentation for planetary, magnetospheric, and solar physics measurements. Dr. Lawrence is currently leading the development of the Gamma-Ray and Neutron Spectrometer (GRNS) on NASA's Psyche mission, and is the Principal Investigator of the MEGANE gamma-ray/neutron spectrometer that will fly on the Japanese Martian Moons eXploration (MMX) mission to Mars' moons Phobos and Deimos.

Introduction: Knowing the elemental composition of a planetary surface is key to understanding its formation and evolution. Planetary gamma-ray spectroscopy is a well-established technique for remotely measuring planetary elemental concentrations for a variety of major and trace elements. Orbital gamma-ray measurements have resulted in significant discoveries from the Moon, Mars, Mercury, and a number of asteroids [1–4].

Here we present work to develop a new instrument called GeMini Plus, which is a high-purity Ge (HPGe) Gamma-Ray Spectrometer (GRS) that can accomplish laboratory quality, high-precision gamma-ray measurements at various planetary bodies throughout the solar system. This abstract provides an overview of a GRS known as GeMini Plus, including improvements made from prior instruments, as well as future science applications for the use of GeMini-Plus technology.

GeMini Plus Gamma-Ray Spectrometer: GeMini Plus is based on the MESSENGER GRS [5] and a miniature HPGe instrument known as GeMini. GeMini was developed by Lawrence Livermore National Laboratory for national security applications [6]. GeMini Plus uses the same size and type of Ge sensor as the MESSENGER GRS, and so achieves the same sensitivity.

GeMini Plus includes a newly-developed Data Processing Unit (DPU), which uses a digital pulse processing and a new cryocooler controller board. The fully digital pulse processor (in contrast to the hybrid analog/digital solution used for MESSENGER) allows increased flexibility for on-board pulse processing. GeMini Plus works with various types of pulsed-tube cryocoolers while retaining the capability to operate the lower cost but shorter life rotary cryocoolers, such as the MESSENGER-heritage Ricor cryocooler.

A particular area of interest for this development program was to understand how to better mitigate for radiation damage effects due to energetic cosmic rays and solar particles. These radiation damage effects degrade the energy resolution of Ge detectors by creating crystal defects that result in incomplete detector charge collection, thus worsening the resolution. Typically, this radiation damage can be partially reversed by heating the crystal to high temperatures (85°C) for number of hours to days [7], but, at this temperature full recovery is not typically observed. Various evidence [8] has suggested that higher temperatures (105–115°C) are needed to achieve a full recovery. We tested the idea of using higher annealing temperatures with a comprehensive test program where we irradiated three separate Ge crystals with energetic protons (100 MeV to 1 GeV) to induce radiation damage. We then annealed the crystals at both 105°C and 115°C, and achieved full recovery. Figure 1 shows the results of one irradiation/annealing cycle (105°C) that achieved full recovery [9].

GeMini Plus Applications: GeMini Plus can be tailored for a wide variety of planetary science applications. Such applications include missions to asteroids, Mars, the Moon, and outer planetary bodies. Here, we highlight three such applications.

16 Psyche: The NASA Psyche mission will orbit and characterize the large (211 km diameter) M-class asteroid 16 Psyche [10], and includes a GRNS that will quantify and characterize the elemental composition of the asteroid [11]. Of particular interest is 16 Psyche's Ni concentration. Measurements of Ni concentration will directly test the hypothesis that Psyche is an exposed core, and if so, how it may have formed and solidified. The Psyche GRNS uses GeMini-Plus technology along with a borated plastic anticoincidence shield for background rejection and fast-neutron measurements. Thermal and epithermal neutron measurements are accomplished using ³He sensors. The GRS cryocooler is a miniature (500 g) pulsed-tube cryocooler built by Lockheed Martin [12]. The primary Ni measurements will be accomplished by measuring the 1.454 MeV inelastic Ni line. With the expected energy resolution of 3.6 keV @ 1.454 MeV (equivalent to 3.4 keV @ 1.332 MeV), the Ni line will be clearly distinguished from a nearby K line.

Mars' moon Phobos: The Mars moons Phobos and Deimos are important targets for future exploration

[13]. Besides the Earth's moon, they are the only other moons of terrestrial planets, and therefore they provide important insights into the evolution of the inner solar system. Measurements of the elemental compositions of Phobos and Deimos are required to test the competing hypotheses for the origins of these moons, and to understand surface processes that are operating on these Moons. The Japanese Martian Moons eXploration (MMX) mission will carry out comprehensive measurements at Phobos and Deimos, and will bring a Phobos regolith sample back to Earth [14]. To accomplish its orbital measurements, MMX is carrying the Mars moon Exploration with GAMMA rays and NEutrons (MEGANE) instrument that will use lessons learned from the GeMini Plus development for its GRS [15].

Titan Exploration: Saturn's moon Titan presents a unique opportunity to explore and investigate solar-system prebiotic chemistry. A key part of such exploration includes making the first in-situ composition measurements of its surface [16]. Elemental composition can be determined via gamma-ray spectroscopy. Because Titan's atmosphere is sufficiently thick that cosmic-rays cannot reach the surface, gamma-ray measurements at Titan require the use of a pulsed neutron generator (PNG) to generate elemental gamma rays. Titan's surface is 90 K, therefore a cryocooler is not needed. High-precision concentration and possibly layering measurements of key elements (H, C, O, N) can be achieved using a HPGe sensor. A few-hour measurement at Titan's surface can strongly discriminate between different types of materials thought to be at Titan's surface.

References: [1] Lawrence, D. J. et al. (1998), *Science*, 281, 1484; [2] Boynton, W. V. et al. (2007), *JGR*, 112, E12S99, 10.1029/2007JE002887; [3] Peplowski, P. N. et al. (2011), *Science*, 333, 1859, 10.1126/science.1211576; [4] Prettyman, T. H. et al. (2012), *Science*, 10.1126/science.1225354; [5] Goldsten, J. O. et al. (2007) *Space Sci. Rev.* 131, 339–391.; [6] Burks, M. (2008), *IEEE Nucl. Sci. Symp.*, 1375; [7] Evans, L. G., et al., *Icarus*, 288, 186, 2017; [8] Roques, J. P. et al., *Astron. & Astrophys.*, 411(1), L91, 2003; [9] Peplowski, P. N. et al., *Nuc. Inst. & Meth.*, in preparation, 2019; [10] Elkins-Tanton, L. T. et al., *48th LPSC*, Abstract #1718, 2017; [11] Lawrence, D. J. et al., *50th LPSC*, Abstract #1544, 2019; [12] Nast et al. (2014) *Cryocoolers 18*, 45 – 50; [13] Murchie, S.L. et al. (2015), in *Asteroids IV*, UofA Press, pp. 451-467. [14] Kuramoto, K. et al., *49th LPSC*, Abstract #2143, 2018; [15] Lawrence, D. J. et al., *49th LPSC*, Abstract #2121, 2018; [16] Turtle, E. P et al., *50th LPSC*, Abstract #2888, 2019.

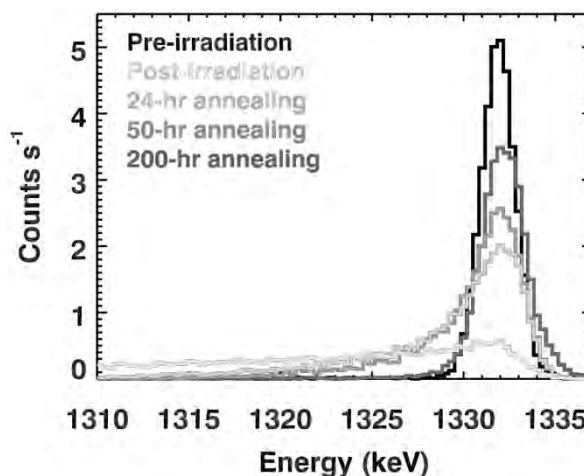


Fig. 1. A representative sample of 1332-keV photopeak measurements in a HPGe sensor, acquired at different annealing times after being irradiated with high-energy protons. The data illustrate the Gaussian shape of a gamma-ray photopeak, the tailing induced by radiation damage, and the recovery following annealing operations.

HIGH TEMPERATURE OPERATION OF GALLIUM NITRIDE HALL-EFFECT SENSORS.

H. S. Alpert¹, C. A. Chapin¹, K. M. Dowling², S. Benbrook², H. Köck³, U. Ausserlechner³, and D. G. Senesky¹, ¹Stanford University Department of Aeronautics and Astronautics (halpert@stanford.edu, cchapin3@stanford.edu, dsenesky@stanford.edu), ²Stanford University Department of Electrical Engineering (kdow13@stanford.edu, sbenbroo@stanford.edu) ³Infineon Technologies Austria AG (helmut.koeck@infineon.com, udo.ausserlechner@infineon.com).

Brief Presenter Biography: Hannah Alpert received her B.S. in Physics and Astronomy from Yale University and her M.S. in Aeronautics and Astronautics from Stanford University, where she is currently pursuing her Ph.D in the EXtreme Environments Microsystems Lab. Her research interests include designing and building sensors for space applications.

Introduction: Magnetic field sensors are used for position and velocity sensing in land and space vehicles, current sensing in power electronics, and position and torque control in motors. Most commercial Hall-effect sensors are made of silicon because it is inexpensive, easy to manufacture, and compatible with integrated circuit technologies. However, the narrow bandgap of silicon (1.1 eV) limits its functionality to temperatures below 200°C [1]. Meanwhile, wide bandgap semiconductors like gallium nitride (GaN) have shown operation up to 1000°C [2] as well as radiation hardness beyond that of silicon [3]. GaN heterostructures, created by depositing an unintentionally doped layer of aluminum gallium nitride or indium aluminum nitride (AlGaN or InAlN) on top of GaN, are of particular interest; the differences in the polarization fields of the two layers leads to the formation of a 2-dimensional electron gas (2DEG). This 2DEG demonstrate high electron mobility not prone to the diffusion and scattering effects that doped junction devices experience at elevated temperatures, thus enabling high sensitivity devices. Here, we evaluate the performance of InAlN/GaN Hall-effect sensors at high temperatures (up to 400°C), to investigate their potential for applications related to space exploration (e.g., the Venus environment).

Device Operation: The Hall voltage (V_H) is measured perpendicular to both the applied current (I) and the external magnetic field (B). It is defined as:

$$V_H = \frac{IBr_n G_H}{qn_s}. \quad (1)$$

where r_n is the scattering factor of the material (~ 1.1 for GaN) [4], G_H is the shape factor (dependent on the relative lengths of the sides with and without contacts), q is the electronic charge, and n_s is the sheet electron density. The principle of the Hall effect is illustrated in Fig. 1.

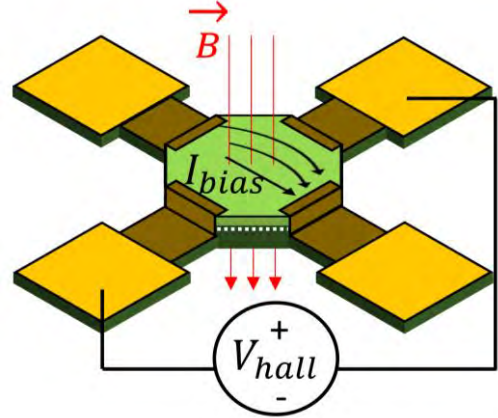


Fig. 1. Illustration of the Hall effect, where Hall voltage (V_{hall}) is measured perpendicular to the supply current (I_{bias}) and the magnetic field (B).

The sensitivity of a Hall-effect device with respect to supply current (S_i) is inversely proportional to n_s ;

$$S_i = \frac{V_H}{IB} = \frac{r_n}{qn_s} G_H. \quad (2)$$

Meanwhile, the sensitivity with respect to supply voltage (S_v) is proportional to the Hall mobility of the electrons, μ_H ;

$$S_v = \frac{V_H}{V_s B} = \mu_H r_n \frac{G_H}{\left(\frac{L}{W}\right)_{eff}}. \quad (3)$$

where $(L/W)_{eff}$ is defined as the ratio of the internal resistance over the sheet resistance, and like G_H it solely depends on the geometry of the device [5].

Device Fabrication: The device under test was fabricated on a commercial InAlN/GaN-on-Si wafer with a room temperature sheet resistance of 248 Ω/\square and room temperature electron mobility of 1143 $\text{cm}^2/\text{V}\cdot\text{s}$. The InAlN stack consisted of a 300 nm buffer structure, 1 μm GaN layer, a 0.8 nm AlN spacer, and 10 nm $\text{In}_{0.17}\text{Al}_{0.83}\text{N}$ barrier layer. The fabrication process is described by us elsewhere [6], with the only difference being the thickness of the Al_2O_3 passivation layer (20 nm). The tested Hall-effect plate was a regular octagonal (the lengths of the sides with and without contacts were equal), and the sensing region was 100 μm across (Fig. 2).

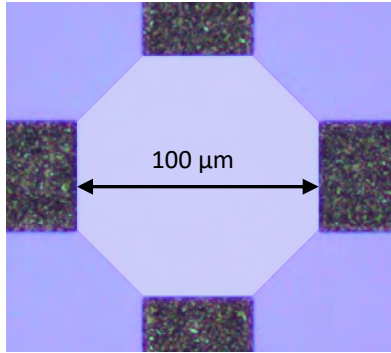


Fig. 2. Optical image of 100- μm -diameter Hall-effect plate.

Experimental Methods: The sensitivity with respect to current and voltage of the InAlN/GaN Hall-effect plate was tested using a constant supply voltage of 1 V and a magnetic field of 2 mT. Ten measurements were performed at multiple temperatures between room temperature and 400°C, in increments of 55°C. The devices were then returned to room temperature to investigate recovery characteristics. A current-spinning technique, described by us elsewhere [6], was implemented to eliminate high offset voltages.

Results and Discussion: Between room temperature and 400°C, the current-related sensitivity of the Hall-effect plate decreased in a linear fashion by 9% total. The slope of the best fit line shows a decreasing sensitivity of 268 ppm/°C, corresponding to a slight increase in sheet density with increasing temperature. It is important to note that the device followed the same trend as the temperature was decreased from 400°C back to room temperature (Fig. 3).

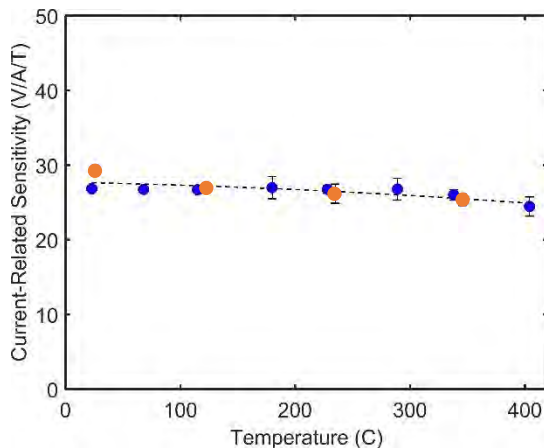


Fig. 3. Sensitivity with respect to supply current, measured from room temperature to 400°C. The blue points represent increasing temperature, the orange points show the return characteristics, and the dashed line is the best fit line to the data.

The sensitivity with respect to supply voltage decreased by a factor of 5.2 from 0.058 V/V/T to 0.011 V/V/T. The decrease in voltage-related sensitivity is due to a significant reduction in mobility as temperature increases [1]. Again, the return characteristics followed the same trend, allowing the sensitivity to recover back to its original value (Fig. 4). This full recovery suggests a lack of degradation of the device and its component materials at temperatures up to 400°C.

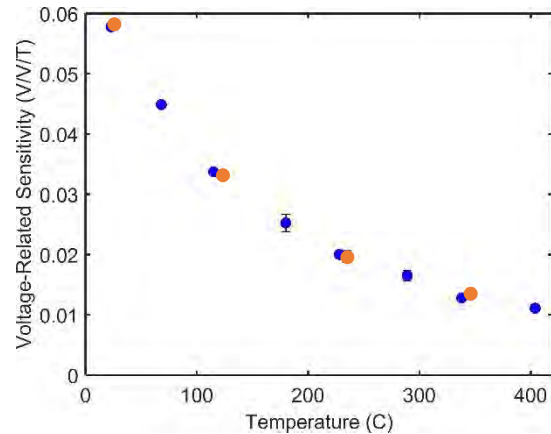


Fig. 4. Sensitivity with respect to supply voltage, measured from room temperature to 400°C. The blue points represent increasing temperature and the orange points show the return characteristics.

The noise in the ten measurements was not highly dependent on temperature. This, combined with the recovery behavior, suggests that this sensor can be calibrated for sensitivity over a wide temperature range; it can be used in conjunction with a temperature sensor to reliably measure currents or magnetic fields up to temperatures of 400°C.

Future Work: Future work will push the temperatures even higher, to investigate the limit of operability of these sensors. We also plan to conduct reliability and lifetime studies to understand the long-term behavior of the sensors, which is important for a real space mission. Additionally, operation in cold environments and radiation-rich environments will be studied to more fully encompass the variety of extreme environments encountered in space.

References: [1] H. Lu, et al., (2006) *JAP*, 99. [2] D. Maier, et al. (2012) *IEEE Electron Dev. Lett.*, 60, 985-987. [3] A. Abderrahmane, et al., (2014) *IEEE Electron Dev. Lett.*, 35, 1130-1132. [4] B. K. Ridley, et al., (2000) *Phys. Rev. B*, 61, 16862-16869. [5] U. Ausserlechner (2016), *Solid-State Electronics*, 116, 46-55. [6] H. S. Alpert, et al., (2019) *IEEE Sensors J.*, in press.

An Energetic Particle Monitor for Ice Giant Atmospheric Probes.

N. André¹, P. Devoto¹, Q. Nenon¹, and L. Griton¹, ¹Institut de Recherche en Astrophysique et Planétologie, IRAP, UPS, CNRS, CNES, Toulouse, France (IRAP, 9 avenue du colonel Roche, BP44346, 31028 Toulouse Cedex 4, France nicolas.andre@irap.omp.eu)

Brief Presenter Biography: Nicolas André is CNRS Research Staff Scientist at IRAP. His main research interests deal with planetary magnetospheres. He is actively involved in the development of space instrumentation for future missions like BepiColombo and JUICE.

Introduction: The Voyager 2 flybys of Uranus and Neptune provided limited measurements of energetic particles in the magnetospheres of the planets. The energetic particle instrument onboard the spacecraft detected significant fluxes of energetic electrons and protons in the regions of their magnetosphere where these particles could be stably trapped. We will review these observations and discuss the need for a more detailed modeling of the energetic particle environment of these two planets in the context of their future exploration.

An Ice Giant Atmospheric Probe will provide a unique platform in order to measure energetic particles in the innermost regions of the magnetospheres of Uranus and Neptune – within a few radii of the cloud tops – and into the upper atmosphere, as was done with the Galileo Probe EPI instrument at Jupiter or during the Cassini Grand Finale at Saturn.

We will propose an instrument onboard an Ice Giant Atmospheric Probe in order to provide omnidirectional as well as sectorized measurements of electrons (30 keV – 1 MeV) and ions (30 keV – 6 MeV) in the magnetospheres of Uranus and Neptune. The foreseen instrument will operate during the pre-entry phase of the Ice Giant Atmospheric Probe and provide unique measurements in order to understand the innermost magnetospheric structure, dynamics, and electrodynamical coupling between the dust, rings, moons, and atmosphere of Uranus and Neptune that can not be achieved with an orbiter.

ABSTRACT

IPPW-2019 -- Oxford, United Kingdom

Radio Science from Venus Probe/Lander Mission

Robert Frampton and Leora Peltz, The Boeing Company

Introduction: Boeing Research and Technology (BR&T) in Huntington Beach, CA was recently awarded a Contract under NASA's Hot Temperature Technology Program (HOTTech) to develop electronics for Venus lander missions. Boeing is teaming with the Nanofabrication Group at The California Institute of Technology (Caltech) to develop a nano-vacuum tube electronics technology for the Venus surface environment of 500 degrees C to: (1) demonstrate Nano-triode devices based on Field Emission Vacuum (FEV) Electronics Technology; (2) design and fabricate small FEV integrated circuit (oscillator for frequencies corresponding to S-band, 2 to 4 GHz); (3) verify the operation of devices and oscillator circuit at 500 Celsius, for over 1,500 hours (60 days).

Technical Background: Most semiconductor devices can operate only up to 250 C. Recent advances in SiC and gallium nitride semiconductors hold promise for higher temperatures, yet are associated with high R&D costs. The well-established technology of microwave vacuum tubes is demonstrated for 500 C, yet its dimensions limit severely the complexity of circuits. There is need for a technology with the simplicity of vacuum tubes that can be reduced to micron sizes. The Boeing/Caltech project is following this path, to demonstrate feasibility for the FEV nano-triode technology in silicon with tungsten metallization. Goals include: Implementation with Zirconiated Tungsten (Zr-W), to reduce work-function, increase the emitted current, and to enable sustained operation, over 60 days; and Demonstrate an innovative gate structure that alters the electric field at the surface of the anode to reduce (modulate) the Fowler-Nordheim current [1].

We are currently fabricating prototype devices, using a simple lithography process and leveraging nano-scale patterning, etching, and oxide growth. This will yield stable, reproducible sub-50nm gaps between emitter, collector and gate. Heating the device to 500 C in vacuum is compatible with the device operation, since they are not susceptible to traditional semiconductor limitations of carrier leakage, temperature dependence, and crystal imperfections.

We will use this technology to develop and fabricate an oscillator circuit for 2 GHz (S-band). This implementation will be complemented by theoretical/simulation analysis for a path to X-band circuits. Tests for operation at high temperatures are performed with local heating (with temperature control), on a simplified packaging/substrate. Our effort includes: (1) development of device model for HSpice circuit simulations; and (2) simulation using first-principles (atomic-level) modeling tools, of metal migration for tungsten with alloy of thorium or zirconium at high temperature.

Application to Radio Science Experiment at Venus. This technology can provide circuitry for front-end stages for spacecraft transmitters, for L-Band, S-Band or X-Band, that can operate on a Venus probe or lander mission, and provide direct-to-Earth communications during descent and landing and for communications from the surface. During descent the transmission sequence could provide a radio-science experiment to determine the microwave opacity of the Venusian atmosphere, as a function of altitude.

Observational data for Venus atmospheric absorption of sulfuric acid (H_2SO_4), SO_2 , and CO_2 has been obtained from both radio occultation measurements of Venus spacecraft and from radio astronomy measurements from ground observatories. The spacecraft radio occultation data are from Pioneer Venus Orbiter as well as Mariner 5 and Mariner 10, in S-Band (13 cm, 2.24 GHz) and X-Band (3.6 cm, 8.42 GHz). This is obtained from the attenuation of the radio signal from the orbiter to Earth passing through the Venus atmosphere during Earth occultation. These observational data are compared to quantum modelling and to laboratory measurements. The laboratory measurements by Paul Steffes are reported in References [2.], [3.], [4.] and [5.]. The largest part of absorption and signal attenuation is due to sulfuric acid, and very little attenuation is due to either SO_2 or CO_2 . The region of sulfuric acid concentration is above 30 km altitude. Below 30 km the temperature is great enough to dissociate sulfuric acid into SO_2 and water. Thus not much microwave absorption is expected below 30 km. The Venus cloud layers are around 46 to 48 km altitude, due to condensation of supersaturated sulfuric acid. However, the large part of the microwave absorption (and attenuation) is below the clouds, between 45 km and 30 km altitude, Ref. [3.].

Neither the Russian Venera nor the Pioneer Venus Probes yielded attenuation measurements, nor did the Vega balloons, because the ground stations had not been configured to measure signal attenuation with depth Ref. [6.]. So there is need for further *in situ* measurements of atmospheric absorption by a future Venus descent probe, either a lander, or deployment of a balloon. A radio science experiment on such a descent probe would need to have an ultra-stable oscillator (USO), and an S-Band and/or X-Band transmitter (preferably both) of around 10 to 15 watts. During descent it would operate in an environment of 6 to 10 bars and temperature of 560 to 575 Kelvin (286 to 300 Celsius).

For a lander, the electronics would need to be operational at 500 Celsius to accommodate operation for 30 to 60 days of operation on the surface. Simultaneous S and X Band uplink from a lander is preferred for a comprehensive radio science experiment. The simultaneous S and X rf signals, which are related in a fixed frequency multiple (e.g. 11/3) is used to separate the Doppler shift due to relative motion of the lander and Earth tracking stations from the dispersive media effects, due to propagation of the rf waves through various levels of the Venus atmosphere and interplanetary medium.

Session: Solar System Exploration: Venus

Biographical:

Robert V. Frampton (Presenter) is a Senior Systems Engineer at Boeing in Huntington Beach, CA. He holds a MS degree in Astrophysics from Louisiana State University in Baton Rouge. Mr. Frampton has been Principal Investigator on two NASA technology development projects: (1) development of precision landing and hazard avoidance (PL&HA) for planetary landers, and (2) characterization of mechanical and thermal properties of icy lunar regolith simulant, at 40 Kelvin in vacuum, conditions of the permanently dark polar lunar craters.

Dr. Leora Peltz (Co-Author) is a Technical Fellow in the Boeing Research and Technology division, in the Solid State Electronics Design (SSED) group in Huntington Beach, California. She

has a PhD in electrical engineering from Case Western Reserve University in Cleveland. Dr. Peltz was the Boeing lead on the NASA project to develop silicon germanium (SiGe) radiation hardened cryo-electronics that can function at 40 Kelvin, She is currently principal investigator for a NASA HOTTech project to develop micro-vacuum-tube electronics for Venus Landers that can operate at 500 Celsius for 30 days.

References:

- [1.] R.H. Fowler and L. Nordheim – Proceedings of the Royal Society of London, May 1928.
- [2.] Paul Steffes and Von R. Eshleman, “Sulfuric Acid Vapor and Other Cloud-Related Gases in the Venus Atmosphere: Abundances Inferred from Observed Radio Opacity”, *Icarus* **51**, 322-333 (1982).
- [3.] Paul Steffes, “Laboratory Measurements of the Microwave Opacity and Vapor Pressure of Sulfuric Acid Vapor under Simulated Conditions for the Middle Atmosphere of Venus”, *Icarus* **64**, 576-585 (1985).
- [4.] Paul Steffes, Michael Klein, and Jon Jenkins “Observations of the Microwave Emission of Venus from 1.3 to 3.6 cm”, *Icarus* **84**, 83-93 (1990).
- [5.] Paul Steffes et al, “Laboratory measurements of the 3.7 to 20 cm wavelength opacity of sulfur dioxide and carbon dioxide under simulated conditions for the deep atmosphere of Venus”, *Icarus* **245**, pg 153-161 (2015).
- [6.] R.Z. Sagdeev et al, “The VEGA Balloon global ground network”. *Pis'ma Astron Zh*, **12**, pg 16-18, (1986)

InSight's Reconstructed Aerothermal Environments

R. A. Beck¹, J. T. Songer², C. E. Szalai³, D. A. Saunders¹, K.T. Edquist⁴, S.A. Sepka¹, M. A. Lobbia³, C. Karlgaard⁴,
¹NASA Ames Research Center, ²Lockheed Martin Space Systems, ³Jet Propulsion Laboratory, ⁴NASA Langley Research Center

Brief Presenter Biography: Poster presenter TBD, bio will follow

Introduction: The InSight Mars Lander successfully landed on the surface on November 26, 2018. This poster will describe the methodologies and margins used in developing the aerothermal environments for design of the thermal protection systems (TPS), as well as a prediction of as-flown environments based on the best estimated trajectory. The InSight mission spacecraft design approach included the effects of radiant heat flux to the aft body from the wake for the first time on a US Mars Mission, due to overwhelming evidence in ground testing for the European ExoMars mission (2009/2010) [1] and 2010 tests in the Electric Arc Shock Tube (EAST) facility [2]. The radiant energy on an aftbody was also recently confirmed via measurement on the Schiaparelli mission [3]. In addition, the InSight mission expected to enter the Mars atmosphere during the dust storm season, so the heatshield TPS was designed to accommodate the extra recession due to the potential dust impact. This poster will compare the predicted aerothermal environments using the reconstructed best estimated trajectory to the design environments.

Design Approach: The InSight spacecraft was planned to be a near-design-to-print copy of the Phoenix spacecraft. The determination of the heatshield TPS requirements was approached as if it was a new design due to the new requirement of flying through a dust storm. The baseline for aftbody was build-to-print, and all analyses focused on ensuring adequate margin. This proved to be a challenge because the Phoenix aftbody was designed to withstand only convective heating and the InSight aftbody was evaluated for both convective and radiative heating. Aerothermal environments were predicted using the Langley Aerothermodynamic Upwind Relaxation Algorithm (LAURA) and the Data Parallel Line Relaxation (DPLR) CFD codes, and the Nonequilibrium Radiative Transport and Spectra Program (NEQAIR) utilizing bounding design trajectories derived from Monte Carlo analyses from the Program to Optimize Simulated Trajectories II (POST2). In all cases, super-catalytic flowfields were assigned to ensure the most conservative heating results. Two trajectories were evaluated: 1) the trajectory with the maximum heat flux was utilized to determine the flowfield characteristics and the viability of the selection of TPS materials; and

2) the trajectory with the maximum heat load was used to determine the required thicknesses of the TPS materials. Evaluation of the MEDLI data [4], along with ground test data [5] led to the determination of whether or not the flow would transition from laminar to turbulent on the heatshield, which also determined the TPS sizing location for the heatshield. Aerothermal margins were added for the convective heating and developed for the radiative heating. TPS material sizing was determined with the Reaction Kinetic Ablation Program (REKAP) and the Fully Implicit Ablation and Thermal Analysis program (FIAT) using a three-branched approach to account for aerothermal, material response, and material properties uncertainties. In addition, the heatshield recession was augmented by an analysis of the effect of entry through a potential dusty atmosphere using a methodology developed in References [6] and [7]. These analyses resulted in an increase to the Phoenix heatshield TPS thickness.

Reconstruction Efforts: Once the best estimated trajectory is reconstructed by the team, the LAURA/HARA (High-Temperature Aerothermodynamic Radiation model) and DPLR/NEQAIR code pairs will be used to predict the as-flown aerothermal conditions. In these runs, fully-catalytic flowfields will be assigned because it is a more physically accurate description of the chemistry in the flow. Once again, determination of the onset of turbulence on the heatshield will be evaluated. The as-flown aerothermal environments will then be compared to the design environments.

References:

- [1] LeBrun, et al. "Investigation of Radiative Heat Fluxes for EXOMARS Entry in the Mars Atmosphere" Proceedings of the 4th International Workshop on Radiation of High Temperature Gases in Atmospheric Entry, 2010.
- [2] Brandis, et al. "Investigation of Nonequilibrium Radiation for Mars Entry", 51st AIAA Aerospace Sciences Meeting, Jan 2013, Grapevine, TX.
- [3] Gulhan, et al. "Aerothermal Measurements from the ExoMars Schiaparelli Capsule Entry", JSR, Vol. 56, NO. 1, January-February 2019.
- [4] Edquist, et al. "Mars Science Laboratory Heat Shield Aerothermodynamics: Design and Reconstruction", JSR, Vol 51, No. 4, July-August 2014.

[5] Reda, et al. "Transition Experiments on Blunt Cones with Distributed Roughness in Hypersonic Flight", JSR, Vol 50, No. 3, May-June 2013.

[6] Keller, et. al., "Dust Particle Erosion During Mars Entry," AIAA 2010-6283, July 2010.

[7] Papadopoulos, et al. "Heatshield Erosion in a Dusty Martian Atmosphere," JSR, Vol. 30, No. 2, March-April 1993.

Reconstruction of the Performance of Mars InSight Lander's Supersonic Parachute.

I. G. Clark¹ and C. O'Farrell¹

¹ Jet Propulsion Laboratory, California Institute of Technology, 4800 Oak Grove Drive, Mail Stop 321-400, Pasadena, CA 91109, ian.g.clark@jpl.nasa.gov

Brief Presenter Biography: Ian Clark is a Systems Engineer at JPL, and a specialist in the area of Planetary Entry, Descent, and Landing (EDL). Dr. Clark is the recipient of a number of awards including the Presidential Early Career Award for Scientists and Engineers, the JPL Lew Allen Award, and the JPL Explorer Award. He was Principal Investigator of the Low-Density Supersonic Decelerators and ASPIRE projects. He holds B.S., M.S., and Ph.D. degrees in Aerospace Engineering from the Georgia Institute of Technology, where he also previously served as a Visiting Assistant Professor.

Abstract: The Mars InSight lander launched on May 5th, 2018 on a mission to investigate the fundamental processes of terrestrial planet formation and evolution [1]. Six months later, on November 26th, InSight entered the Martian atmosphere and successfully landed at Elysium Planitia to begin its 26 month prime mission.

The Entry, Descent, and Landing sequence utilized by InSight included a supersonically deployed Disk-Gap-Band parachute. The 11.8 m nominal diameter parachute was a largely build-to-print version of the parachute that was used to successfully land the Phoenix mission on Mars in 2008 [2] [3]. Both parachutes were scaled versions of the Viking lander parachute that has been used in a number of successful Mars missions.

This presentation covers the reconstruction of the performance of the supersonic parachute used by InSight. Data provided by the onboard inertial measurement unit, along with assumptions about the vehicle's aerodynamics and atmosphere models, has been used to reconstruct the trajectory flown by InSight. This trajectory provides details of the conditions leading up to, and after, the point of parachute deployment, including Mach number, dynamic pressure, total angle of attack, and flight path angle. Furthermore, the measured rates and accelerations are used in conjunction with the vehicle's mass properties to calculate the forces and moments applied by the parachute during inflation, supersonic flight, and subsonic descent. This data is used to provide estimates of the peak load and aerodynamics provided by the parachute. Time histories of the parachute pull angles are also derived to gain an understanding of the dynamics of the parachute during flight. Measured rates are used to intuit the dynamics of the vehicle and how it responded to the parachute's behaviors. Lastly, the performance of the deployment system is analyzed based on known and derived event times, providing estimates of the mortar velocity, reaction loads, snatch loads, and parachute inflation times.

The similarity of the InSight mission to the earlier Phoenix mission allows for comparisons between the two parachutes. Using an updated reconstruction for Phoenix, comparisons of inflation time, inflation distance, peak loads, parachute pull angle and aerodynamics, and vehicle response are also provided.

References:

- [1] Hoffman, T., "InSight: Mission to Mars," IEEE Explore, June 2018., DOI: 10.1109/AERO.2018.8396723
- [2] Witkowski, A., Kandis, M., and Adams, D. "Mars Scout Phoenix Parachute System Performance," AIAA 2009-2907.
- [3] Adams, D., Witkowski, A., Kandis, M. "Phoenix Mars Scout Parachute Flight Behavior and Observations" IEEE Aerospace, Big Sky, MT, March 2011. DOI: 10.1109/AERO.2011.5747499

Landing Radar Performance Reconstruction for Entry, Descent, and Landing of the InSight Mars Lander

A. Zimmer¹, E. D. Skulsky¹, E. Bonfiglio¹, T. Kennedy², C. Chen¹, J. Hoffman¹, and D. Howell², ¹Jet Propulsion Laboratory, California Institute of Technology, 4800 Oak Grove Drive, Pasadena, CA 91109. ²Lockheed Martin Space, 12257 S. Wadsworth Blvd, Littleton CO 80125.

Biography: Aline Zimmer is a systems engineer for Mars Entry, Descent, and Landing for InSight as well as Europa Deorbit, Descent, and Landing for the Europa Lander Concept. After InSight's successful landing in November 2018, Aline joined the Europa Clipper team as phase lead for the science tour phase. Aline received her M.Sc. in Aerospace Engineering from the Georgia Institute of Technology and her Ph.D. in Aerospace Engineering from the University of Stuttgart in Germany.

Abstract: The Interior Exploration Using Seismic Investigations, Geodesy, and Heat Transport (InSight) Mission successfully executed its Entry, Descent, and Landing (EDL) phase on November 26, 2018. InSight's landing radar played a critical role during the parachute and terminal descent stages of EDL, providing Mars surface-relative range and velocity.

The radar was not originally designed for planetary landings; it was adapted from a commercial altimeter used in fighter aircraft to include the measurement of the Doppler spectra of the return echoes. After undergoing comprehensive testing, the landing radar performed as expected during the successful EDL phase of the Phoenix mission. The InSight flight system incorporated a flight spare of the Phoenix landing radar.

The radar utilizes eight broad-beam patch antennas mounted to the bottom of the lander to form four separate beams. Each beam consists of a separate transmit and receive antenna and is activated sequentially during radar operation. Altitude is measured exclusively from the nadir-pointed beam. Doppler spectra are measured from the nadir beam as well as from each of three beams that are canted approximately 40° off nadir and equally spaced in azimuth. This additional Doppler data allows the spacecraft to solve for the three-axis Mars surface-relative velocity state of the lander.

After atmospheric entry, peak heating and deceleration, parachute deployment, heat shield jettison, and landing leg deployment, the radar is activated and begins searching for the ground. From cruise stage separation until radar acquisition, the vehicle relies exclusively on inertially propagated state information for position and velocity knowledge. However, the ground-relative accuracy of the inertially propagated state is inadequate for terminal descent, so radar acquisition is essential for a successful landing. Radar acquisition is expected at an altitude of about 2,400 m and is a prerequisite for backshell separation. Although the radar is in Altitude-only mode at this time and does not produce

ground-relative velocity measurements, the 10 Hz altitude measurements yield a reasonably accurate altitude and altitude rate estimate when processed by the onboard navigation filter, which is sufficient for computing the optimal backshell separation altitude. The radar is commanded to Altitude/Velocity mode at a navigated altitude of 1,700 m. In this mode, the radar generates 10 Hz altitude and Doppler spectra. However, the Doppler spectra measurements are cycled through each of four antennas, completing a full four-beam cycle every 0.4 sec. After backshell separation and thus the start of terminal descent, radar data allow the lander to meet its touchdown requirements: a vertical velocity between 1.4 m/s and 3.4 m/s and a horizontal velocity less than 1.4 m/s. Although the radar is designed to operate down to zero altitude, the flight system stops incorporating radar measurements into the navigated state at 30 m altitude due to concerns about radar performance at very low altitudes.

This poster will provide an overview of the reconstructed InSight landing radar performance and behavior.

InSight Entry, Descent, and Landing Operations Overview

J. Wertz Chen¹, E. Bonfiglio¹, M. Grover¹, E. Skulsky¹, C. Szalai¹, and M. Johnson², ¹Jet Propulsion Laboratory, California Institute of Technology, 4800 Oak Grove Drive, Pasadena, CA 91109, ²Lockheed Martin Space Systems, 12257 S. Wadsworth Blvd, Littleton, CO 80127.

Brief Presenter Biography: Julie Wertz Chen is a systems engineer at JPL. She is currently the Group Supervisor for the Autonomy and Fault Protection group and was recently an Entry, Descent, and Landing (EDL) systems engineer on the InSight project. Previously, she was the EDL and then the Project Verification and Validation lead on InSight. She graduated from MIT with her SB in 2000, SM in 2002, and PhD in 2006 - all in Aeronautics and Astronautics.

Abstract: The Interior Exploration Using Seismic Investigations, Geodesy, and Heat Transport (InSight) mission to Mars made a successful entry, descent, and landing (EDL) onto the Martian surface on November 26, 2018. InSight was joined in its journey to Mars by two CubeSats called Mars Cube One, or MarCO, that were launched at the same time as InSight and flew independently to the red planet. The MarCO mission was a technology demonstration to show that deep space communications was possible using a CubeSat, and both spacecraft were able to provide near real-time communications from the InSight spacecraft back to Earth during the EDL event. [1]

While the EDL phase of the mission is only approximately 6 minutes long, the EDL team is performing operations functions to prepare the spacecraft for EDL during all of the cruise and approach phases. Additionally, while the actual EDL events on the spacecraft occur autonomously, the public interest in the event itself makes the telemetry and ability to interpret what is actually happening during this event extremely important. This poster will explore the aspects of the InSight mission that made operations, both during approach and during the EDL event itself, unique and challenging.

One challenge that faces all missions is flexibility. During design and preparations for operations, the InSight team spent a significant amount of effort creating tools to facilitate the operations process. These tools were developed with the planned operations concept in mind. As is the case with most complex systems and problems, in several cases we found that the specific analysis that was planned in the original operations concept had to be adjusted somewhat to account for unexpected circumstances. It became clear throughout operations that it was imperative that both the tools, and the team itself, were flexible enough to handle these adjustments and be able to customize analyses as the situation dictated.

Several of the analyses that the team completes during operations are to inform decisions on whether or not to execute a Trajectory Correction Manuever (TCM). TCM-6, which was the final planned TCM, was scheduled for approximately 22 hours prior to entry into the martian atmosphere. The team ran through all of the analyses to determine whether or not to execute TCM-6, and assessment tools indicated a maneuver was not required, based on criteria that had been agreed to prior to end-game operations. While the navigation estimate put the predicted landing ellipse inside the pre-determined safe landing area, it was pushed up against one edge. Using a combination of analysis results and previous experience, it was decided to execute TCM-6 even though a maneuver was not required to meet the EDL and landing safety criteria. [2] [3] After the landing, a small calibration error was discovered in the navigation data that showed that InSight was actually on a trajectory that would have put it closer to the center of the safe landing area than thought during operations. We will re-examine the decision to execute TCM-6 given the new information that has become available since operations.

An additional challenge that InSight faced during operations for InSight EDL was how to determine what we would reliably know and when we would know it during the EDL event. The InSight team was relying on several different sources of information. The MarCO spacecraft were a technology demonstration mission, and it was unclear if we would be able to reliably achieve a communications link from InSight to the MarCO spacecraft and then back to Earth. Additionally, there was not enough bandwidth to send all the InSight telemetry plus the MarCO engineering telemetry at the same time. This meant that a latency would build up in the InSight telemetry. The size of the latency was uncertain, but estimated at one point to be up to several minutes by touchdown. In addition to the detailed engineering telemetry that InSight was sending through the MarCO spacecraft, there were also direct to Earth (DTE) tones being sent throughout the EDL event. These tones were only for major events, such as parachute deployment or touchdown, and it was uncertain how reliably the ground stations would be able to lock on to the tones (and whether engineers would be able to interpret the tones) given the dynamic nature of the EDL event itself. A third source of data during the EDL event was the Doppler signature of the telemetry that InSight was sending, captured by ground stations on Earth. These three sets of data (detailed telemetry through

MarCO, DTE tones, and Doppler) all provided unique views into what was occurring on Mars, but all had different reliability and latency challenges associated with them. [1] Pulling the different sources of information together to form one understanding of what was happening, and when, during the EDL event proved to be more difficult than originally thought.

Given the small number of EDL events that occur across our community, it is important that we relook at each EDL and gather all relevant lessons to be passed on to future missions. This poster will provide a look into several of the more interesting and unique challenges that InSight faced during EDL operations, including those discussed above.

References:

[1] Wallace, et al. "Orbiters, Cubesats, and Radio Telescopes, Oh MY; Entry, Descent, and Landing Communications for the 2018 InSight Mars Lander Mission" AAS 19-291, 29th AAS/AIAA Space Flight Mechanics Meeting

[2] Abilleira, et al. "2018 Mars InSight Trajectory Reconstruction and Performance from Launch through Landing," AAS 19-204, 29th AAS/AIAA Space Flight Mechanics Meeting

[3] Halsell, et al. "Navigation Performance of the 2018 InSight Mars Lander Mission" AAS 19-228, 29th AAS/AIAA Space Flight Mechanics Meeting

INSIGHT ENTRY, DESCENT, AND LANDING POST-FLIGHT SIMULATION ASSESSMENT

R. W. Maddock¹, C. H. Zumwalt¹, A. M. Dwyer-Cianciolo¹, and D. K. Litton¹, ¹NASA Langley Research Center

Brief Presenter Biography: Carlie Zumwalt is an aerospace engineer in the Atmospheric Flight and Entry Systems Branch at the Langley Research Center. She received her bachelors in aerospace engineering from The University of Texas at Austin and has been involved with projects such as InSight, Mars2020, and the Commercial Crew Program during her time at Langley.

Introduction: On November 26, 2018, the Interior Exploration using Seismic Investigations, Geodesy and Heat Transport (InSIGHT) mission touched down on the surface of Mars. Landing in a large flat plain, the entry, descent and landing (EDL) of the ballistic trajectory performed as expected. This poster will provide comparisons of preflight trajectory simulation predictions and postflight reconstruction analysis to date.

NASA LaRC's Program to Optimize Simulated Trajectories II (POST2) was used for InSight from early on in the project implementation phase to assess EDL performance against related requirements across the full range of possible environmental and spacecraft conditions. Much of the simulation code heritage was derived from the Phoenix mission, for which this vehicle is very similar. The InSight six degree-of-freedom (6DOF) simulation included models for Mars atmosphere, gravity and landing digital elevation maps of the landing location. Additionally, vehicle specific aerodynamic, parachute, engines, navigation sensors, flight software and landing radar models were also included.

This poster will present results of the pre- and post-flight performance assessment, as well provide a comparison of key EDL metrics to the nominal and three sigma bound predictions. Focus will also be given to comparing the final trajectory prediction prior to EDL to the reconstructed flight trajectory, with emphasis on entry interface to parachute deploy. This post flight assessment provides important verification of the POST2 models and analysis techniques used for InSight, providing critical feed-forward information to future Mars lander missions.

INSIGHT LANDING SAFETY ASSESSMENT IN APPROACH NAVIGATION.

E. Sklyanskiy¹, E. D.Gustafson¹, M.R.Grover¹, M.A.Johnson², R. W.Maddock³, E. P. Bonfiglio¹, M. P. Golombek¹, D. M. Kipp¹, ¹Jet Propulsion Laboratory, California Institute of Technology, ²Lockheed Martin Space, ³NASA Langley Research Center

Brief Presenter Biography: Evgeniy Sklyanskiy is the trajectory analyst as part of the InSight Entry, Descent & Landing (EDL) and Navigation teams at the Jet Propulsion Laboratory. Previously the author has supported the Hayabusa I (MUSES-C) sample return mission, Space X Red Dragon project and various Discovery/New Frontier proposal activities. He has Applied Mathematics and Aerospace degrees from University of Illinois at Urbana-Champaign.

Introduction: The Interior Exploration using Seismic Investigations, Geodesy, and Heat Transport (InSight) spacecraft was launched on May 5, 2018 and arrived at Mars on November 26, 2018. Six nominal trajectory correction maneuvers (TCMs) were designed to ensure that InSight would enter the atmosphere of Mars ballistically and land in a preselected characterized safe zone known as Elysium Planitia. The nominal EDL trajectory targeting and landing ellipse assessment, in conjunction with the hazard maps, are the key elements for approach navigation strategy to ensure a safe landing on Mars. This paper will focus on the InSight nominal EDL trajectory design for the unguided lander in the presence of various atmospheric conditions, as well as statistical methods of analyzing the landing dispersions and the probability of successful landing coupled with the terrain hazard map. The paper will address the effectiveness of the Landing Site Assessment Tool (LSAT) in the maneuver design.

NAV/EDL Ground Targeting:

The InSight is a three-axis-stabilized spacecraft during the cruise phase. Six trajectory correction maneuvers were scheduled to target an atmospheric reference point of Mars with Entry Flight Path Angle (EFPA) of -12 deg. The TCMs 5 and 6 are the most critical as they were designed to adjust the entry condition of the nominal EDL trajectory to minimize errors to the desired landing target on the ground. Landing in dust storm season created additional targeting challenges where the NAV/EDL team had to consider a range of possible arrival atmospheric conditions in the final approach phase. One of the most robust strategies was to let the nominal EFPA be a floating parameter bounded by -12.15deg to -11.85deg in addition to the ground target optimized location based on the daily

atmospheric updates from the Council of the Atmospheres (CoA)[1].

Final Landing Target Assessment:

Two days prior to EDL the InSight Navigation Team and Spacecraft Team met the flight path angle (EFPA) requirement at -11.936° , well within the required corridor of $-12.0 \pm 0.21^\circ$ [2]. Based on this nominal trajectory, the ground ellipse of 92kmX25km would have marginally met the probability of landing within the landing site area imaged by the Mars Reconnaissance Orbiter (MRO) HiRISE instrument. The center of this ellipse was 11.6 km down-track from the InSight official target (4.51° N, 135.99° E). To mitigate the landing safety concerns in the poorly characterized region outside of the HiRISE map, the TCM-6 was executed at E-22 hours which resulted in a final EFPA of -12.046° . The predicted footprint based on EDL errors and NAV plus TCM execution errors was 101kmX25km[2]. The final NAV Orbit Determination (OD) solution, od133, at E-45min showed that the nominal landing point was 6.73km up-track from the TCM-6 target location. The landing footprint of 86kmX24km for this trajectory was mostly driven by the EDL error sources. Two hours after landing, the spacecraft team reported that the lander location was 20km up-track from TCM-6 target in the predominant cross-track direction. This result was based on the IMU onboard state propagation. On Dec 10, 2018 HiRISE imaging revealed that the lander was 13.87 km up-track from the latest reconstructed NAV solution and 19.36 km up-track from the TCM-6 ground target location [2].

Figure 1. Final Landing Site Assessment for od133.

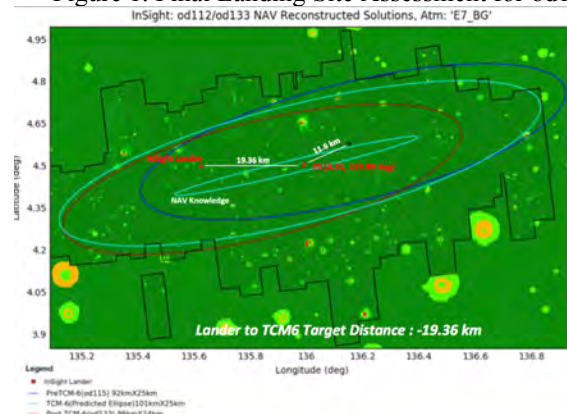


Figure 1 illustrates the EDL/NAV ground target strategy in combination with the landing assessment analysis used routinely during the TCM design process. The footprint location for a given set of NAV states allowed the team to quickly evaluate the landing hazards and compute the overall probability for a successful landing.

References:

[1] Bonfiglio, et al. “Atmospheric Impact on Maneuver Targeting for the InSight Mission and Unguided Mars Landers,” AAS 19-264, 29th AAS/AIAA Space Flight Mechanics Meeting.

[2] Abilleira, et al. “2018 Mars InSight Trajectory Reconstruction and Performance from Launch through Landing,” AAS 19-204, 29th AAS/AIAA Space Flight Mechanics Meeting.

¹ © 2018 Jet Propulsion Laboratory, California Institute of Technology. Government sponsorship acknowledged.

Trajectory Analysis of the ExoMars Schiaparelli Descent Probe.

E. M. Johnstone¹, F. R. Willcocks² and L. Ferracina³, ¹Fluid Gravity Engineering Ltd, Emsworth, PO10 7DX, UK, ²University of Cambridge, Magdalene College, Magdalene Street, Cambridge CB3 0AG, UK, ³ESA ESTEC, Keplerlaan 1, Postbus 299, 2200 AG Noordwijk, NL. Corresponding author: emma.johnstone@fluidgravity.co.uk

Brief Presenter Biography: Emma Johnstone has worked in the field of high speed aerodynamics, aerothermodynamics and high temperature material response for over ten years. During this time, she has been responsible for trajectory rebuilds associated with several flights including Earth Return Capsule balloon drop testing and the ExoMars Schiaparelli Descent Module.

Introduction: The ability to send telemetry during the descent of the ExoMars Schiaparelli probe has given the community a unique set of validation data for the approach followed in the design phases of the ExoMars 2016 descent module (Schiaparelli). Flight data is a very valuable resource in this context. It covers many environments and does not suffer some of the complications that commonly affect the interpretation and utility of ground experiments, especially at high enthalpy. These include stings and mounting systems as well as the specification of the flow conditions produced by high enthalpy facilities.

Fluid Gravity Engineering led an international consortium tasked with performing the aerodynamic and aerothermodynamic activities to support the design justification of the Schiaparelli descent module. FGE's in-house Thermal and Chemical Non-Equilibrium Navier Stokes Algorithm (TINA) contributed to the generation of the hypersonic portion of the aerodynamic and aerothermodynamic database. The same techniques were successfully used to support the Beagle2 flight.

General Findings: In this work, the open literature flight data has been utilised and analysed from the perspective of those familiar with the work performed to construct design-level databases. The key objectives were to assess how successful the approach taken was and to highlight what lessons can be learnt for application to future missions. In this paper, the work concerning the trajectory data is presented and the aerodynamic database (AEDB) is assessed.

The work has focused on assessing the quality of the aerodynamic database and the associated uncertainties pre-parachute deployment (entry phase). The analysis has primarily been carried out in the hypersonic portion of the descent trajectory of the Schiaparelli probe. The axial and normal force coefficients, pitch and roll moment coefficients and pitch damping coefficients are all considered.

The FGE six degrees of freedom trajectory code, TRAJ6D was used to perform the analysis and predict a best estimate of the trajectory based on all the collated

literature data. The corrections required to match the trajectory have been compared with the uncertainties specified in the AEDB.

Through the analysis it was found that the AEDB performed very well and most of discrepancies found were well within the margins specified by the database application rules. This provides validation and justification for the techniques developed and used within the ExoMars 2016 design phase.

References:

- [1] D. Bonetti, G. De Zaiacomo and G. B. Arnao, "EXOMARS 2016: Post Flight Mission Analysis of Schiaparelli Coasting, Entry, Descent and Landing," in 14th IPPW, The Hague, The Netherlands, June. heat shield," in IPPW14, The Hague, June 2017 [2] ThalesAlenia Space, "ExoMars 2016 Schiaparelli Mission: Real Time Telemetry and Post-Flight Results," in IPPW-14, The Hague, June 2017 [3] B. Van Hove, O. Karatekin, T. Schleutker and A. Guelhan, "Surface pressure data from ExoMars Schiaparelli instrumented heat shield," in IPPW14, The Hague, June 2017

CHALLENGES FOR MARS 2020 EDL AT THE JEZERO CRATER LANDING SITE.

E. K. Stilley¹, R.E. Otero¹, ¹Jet Propulsion Laboratory, California Institute of Technology, Pasadena, CA, 91109

Brief Presenter Biography: Erisa Stilley is a member of the EDL systems team for Mars 2020. Previously, she enjoyed planning drives for the Curiosity rover currently operating on Mars. Erisa has an MS in Aerospace Engineering from MIT and a BS in Mechanical Engineering from the University of Miami, Florida.

Abstract: On February 18, 2021, the public will witness the landing of the next US-led rover mission to the red planet. Much about this mission, currently titled “Mars 2020”, is considered a heritage design, both in terms of software and hardware, as well as from a cruise and EDL phase perspective[1].

A handful of notable improvements to the EDL system capability including Range Trigger, improved cruise attitude initialization, and Terrain Relative Navigation (TRN), have greatly affected the type of landing sites considered for the Mars 2020 mission: the former two have reduced the size of the landed ellipse by approximately 40%[2]; the latter has provided capability to pre-designate safe landing zones[3]. In addition, the confidence with which the hazards in the landing ellipse are being evaluated has improved through changes like new methods of rock detection.

The combined effect of these changes allowed the science community to consider landing sites for the Mars 2020 mission that would have been deemed far too risky for previous missions. NASA commonly places a requirement on the statistical probability of landing safely for the Mars robotic missions. Though flat locations are sometimes driven by science, more often the combination of this requirement and limited system capability has led NASA Mars missions to target locations believed to be relatively flat and free of rocks.

In November 2019, NASA announced the selection of the Mars 2020 landing site: Jezero Crater[4]. A site believed to once have harbored a lake, rich with details to explore, it is not thought of as a flat, terrain-less place. Jezero Crater’s topography inherently provides some notable terrain-related challenges for the EDL system. This talk will discuss the different hazards within the Jezero Crater site, how they differ from past missions, and how they have constrained and led to refinements of the Mars 2020 ellipse placement.

Typically, the choice of ellipse placement at a given site is affected by 1) system-level margins such as timeline, fuel, and accuracy, and 2) the probability of landing on a hazard. For Mars 2020, the system margins are sufficiently good across the final landing sites and within Jezero Crater. In addressing the probability of

landing on a hazard, there are the traditional hazard categories of slopes, rocks, and inescapable hazards all present at Jezero. There is also a new addition of large relief within the ellipse. With TRN, most “known” hazards are now manageable given sufficient distribution of “safe” places to land among the hazards. Until recently, large relief hadn’t been included as a landing hazard. Previous missions (and Mars 2020) had to consider large relief as part of the overall EDL trajectory, but not necessarily internal to the targeted ellipse. The system-level challenges related to the high relief features, such as communications around the time of EDL and sensor interactions, and how they are currently being addressed, will be presented.

As part of the recent work to support the Mars 2020 Landing Site Safety Assessment, the team assessed the relative safety of different target placements within the crater. While a more western ellipse target showed an improvement in landed safety probability using TRN, this movement also placed the delta and other high-relief features more centrally in the ellipse. This resulted in a handful of landed points showing up very close to the delta wall. While a detailed review of the landed points and maps is planned as part of the V&V efforts, this provided an opportunity for the team to refresh the assumptions about how the heritage EDL system works and the implications of landing so close to these unique high relief features.

References:

- [1] A. Stehura et. Al. (2013) *10th IPPW, Mars 2020 Entry, Descent, and Landing Overview*. [2] Al Chen (2017) *14th IPPW, Mars 2020 EDL Update*. [3] P. B. Brugarolas et al. (2017) *14th IPPW, Mars 2020 On-Board Terrain Relative Navigation*. [4] D. Brown et al. (2018) <https://www.nasa.gov/press-release/nasa-announces-landing-site-for-mars-2020-rover>.

EXOMARS 2020 – AMELIA: THE EDL SCIENCE EXPERIMENT FOR THE ENTRY AND DESCENT MODULE OF THE EXOMARS 2020 MISSION

F. Ferri¹, A. Aboudan¹, G. Colombatti¹, C. Bettanini¹, S. Debei¹, O. Karatekin², S. Lewis³, F. Forget⁴, S. Asmar⁵, A. Lipatov⁶, I. Polyanskiy⁶, A. M. Harri⁷, G. G. Ori⁸, A. Pacifici⁸, K. Machenkov⁶, D. Rodionov⁶, N. Modzhina⁹

¹Università degli Studi di Padova, Centro di Ateneo di Studi e Attività Spaziali “Giuseppe Colombo” (CISAS) (francesca.ferri@unipd.it);

²Royal Observatory of Belgium (ROB), Brussels, Belgium;

³School of Physical Sciences, The Open University, Walton Hall, Milton Keynes MK7 6AA, UK;

⁴Laboratoire de Météorologie Dynamique, UPMC BP 99, 4 place Jussieu, 75005, Paris, France;

⁵Jet Propulsion Laboratory, California Institute of Technology - NASA, Pasadena, CA, USA;

⁶IKI, Moscow, Russia;

⁷Finnish Meteorological Institute (FMI), Helsinki, Finlandia;

⁸IRSPS, Pescara, Italy;

⁹TsNIIMASH, Russia

Brief Presenter Biography: PI of AMELIA: EDL science experiment of the ESA ExoMars project.

She was deputy PI for the HASI instrument on the ESA Huygens probe of the NASA/ASI/ESA Cassini mission; Co-proposer/CoI of several *in situ* instruments (e.g. for Mars NetLander, ExoMars PASTEUR, M2020 MEDA, Titan, Venus). She was acting as Project Scientist of the NetLander project within the French Mars Sample Return programme at CNES (2000-2002). She has been studying planetary atmospheres and martian dust devils by *in situ* measurements

Abstract: The AMELIA – EDL science experiment on Schiaparelli, was officially selected by the *Joint ESA and NASA ExoMars2016 AO* (Nov 2010). AMELIA aimed at exploiting the EDLS engineering measurements for scientific investigations of Mars’ atmosphere and surface [1].

Following the Schiaparelli’s crash landing, the AMELIA team was part and valuably contributed to the ESA Schiaparelli Anomaly Investigation Group (SAIG) for identifying the reasons of the failure (e.g. [2], [3]). From the limited returned EDL flight data, AMELIA managed to reconstruct the correct trajectory and attitude of Schiaparelli EDM and to retrieve the atmospheric profiles and low altitude wind profiles [4]. Therefore ESA has finally decided for extending the AMELIA –EDL science proposal for application to the interpretation of the ExoMars2020 Entry, Descent and Landing (EDL) engineering data.

As per the previous mission, the experiment AMELIA 2020 will rely on the *in situ* measurements by the GNC (Guidance, Navigation and Control) sensors of the descent module: 2 Inertial Platforms (IMU) and the Radar Altimeter (RDA) and also by the ExoMars 2020 Surface Platform (SP) payload (e.g. the meteorological package MTK-L and the television camera system TSPP) and from the tracking of the radio signal during EDL.

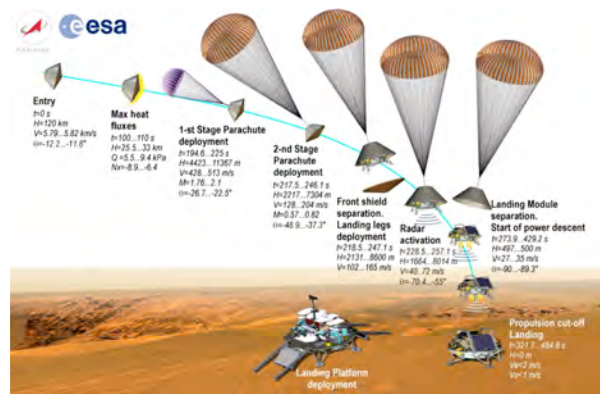


Figure 1: ExoMars 2020 EDL scenario

From the measurements recorded during entry and descent, we will retrieve an atmospheric vertical profile along the entry and descent trajectory.

Different algorithms, methods, data sets and their assimilation will be used for simulation and reconstruction of the EDM trajectory and attitude during the entry and descent phases in order to retrieve the most accurate atmospheric profile.

A near real time reconstruction of the trajectory will be done using the radio communication link between the EDM and the radio receiver on board the orbiter and by the carrier signal detection by ground telescopes. Atmospheric vertical profiles in terms of density, pressure and temperature, will be derived directly from deceleration measurements, by matching atmospheric standard model with Extended Kalman filtering (EKF) of a 6 DoF EDM dynamic model and from hypersonic dynamic pressure data recorded during entry.

The dynamical behaviour of the EDM during the descent under parachute will be modeled, simulated and reconstructed using different data, methods and data assimilation (e.g. IMU, radio link, radar, imaging and auxiliary data). Wind profile along the entry probe path will be retrieved by using the Doppler shift in the

radio link between the Descent Module and a radio receiver and by modeling the dynamic response of the pendulum system composed by the EDM and the parachute line.

Scientific analysis of the landing measurements will be aimed at the determination of the landing site context (e.g. surface mechanical characteristics, geomorphology, etc.), its characterization and assessment also in combination with remote sensing imaging.

ExoMars 2020 will provide the opportunity for new direct *in situ* measurements exploring an altitude range not covered by remote sensing observations from an orbiter. AMELIA results together with the measurements of the meteorological package MTK-L at the surface of Mars will provide a surface and atmosphere “ground truth” for remote sensing observations and important constraints for validation of Mars atmosphere models.

The experience and lessons learned in the framework of the Schiaparelli EDM and expertise in Mars observations and modelling are being put in perspective for the AMELIA ExoMars 2020 Entry, Descent and Landing (EDL) science experiment.

References:

- [1] Ferri, F. et al. (2019) *Space Science Review* **215**: 8. <https://doi.org/10.1007/s11214-019-0578-x>
- [2] Portigliotti S., et al. (2017) *14th International Planetary Probe Workshop IPPW#14*, The Hague, The Netherlands, June 2017
- [3] Bonetti, D., et al (2018) *Acta Astronautica* **149**, 93-105
- [4] Aboudan, A., et al. (2018) *Space Science Reviews*, **214**, doi: 10.1007/s11214-018-0532-3

Acknowledgements: AMELIA is an experiment for scientific investigations of Mars’ atmosphere and surface by means of the ExoMars measurements during its entry, descent and landing on Mars. The International AMELIA team led by Francesca Ferri (CISAS-Univ. Padova) as *Principal Investigator*, includes scientists and experts from Italy, Belgium, France, UK, Finland, USA and Russia. The support of the national funding agencies of Italy (ASI, grant no. 2017-03-17 and I/018/12/3), Belgium (BELSPO and PRODEX), UK (UKSA, grant no. ST/M00306X/1) and France (CNES) is gratefully acknowledged.

Modelling Sensitivities and Knowledge Gaps Associated with Mars-atmosphere Destructive Entry Applied to Planetary Protection

J. A. Merrifield¹ and J. C. Beck², ¹Fluid Gravity Engineering Ltd, Emsworth, PO10 7DX, UK, ²Belstead Research Ltd, 387 Sandyhurst Lane, Ashford, Kent, UK. Corresponding Author: jim.merrifield@fluidgravity.co.uk

Brief Presenter Biography: Jim Merrifield has worked in the field of high speed aerodynamics, aerothermodynamics and high temperature material response for over ten years. He has been involved in a number of assessments for flight vehicles and wind tunnel test campaigns and has been actively involved in destructive entry analysis since 2013. He is a main developer of the Spacecraft Aerothermal Model (SAM) which is jointly maintained and developed by Fluid Gravity Engineering and Belstead Research Limited.

Introduction: Within the context of space exploration, there is an obligation on space agencies and mission planners to sensibly limit the potential for biological contamination of celestial bodies. These limits are most stringent for celestial bodies that are of significant interest for chemical evolution or the origin of life, and where there is a significant chance that contamination could compromise future or present investigations. Mars[1] and Icy Moons are prime examples of celestial bodies for which careful planetary protection is mandated and mission planners are required to justify and document their approach to demonstrate compliance with the relevant COSPAR recommendations.

These do not only apply to probes, but also to any carrier vehicle that might impact on the surface of the celestial body. For celestial bodies with an atmosphere, there is an opportunity to auto-sterilize material during planned destructive entry due to aeroheating. The justification of this approach requires a modelling capability for destructive entry which includes high speed aerodynamics, aerothermodynamics and high temperature material response.

This analysis is currently undergoing a resurgence of interest in Europe and elsewhere, mainly to support ground casualty risk assessments associated with end-of-life disposal of satellites in LEO. The cost-benefit of a destructive entry when compared with a controlled re-entry motivates this interest. This has resulted in the creation of several investigative activities within the last five years aimed at increasing the understanding of destructive entry and ultimately improving predictive methodologies. Lessons learnt from these investigations can be applied to planetary protection scenarios. This presentation aims at highlighting the possible impact of this new knowledge with respect to Mars planetary protection.

Numerical Method: This study uses the Spacecraft Aerothermal Model (SAM) to demonstrate known sensitivities to modelling approach for aerothermal sterilization in the context of planetary protection. This involves disciplines associated with: trajectory propagation, aerothermal heating, fragmentation and high temperature material response. In common with studies associated with terrestrial destructive entry, the empirical evidence required to support this modelling is still being accumulated, and is being rapidly incorporated into numerical tools, so some judgement is required to establish realistic best practice. A key decision here is the level of modelling fidelity required as well as the level of modelling granularity.

SAM is well suited to this study, since a range of modelling fidelities and granularities are possible spanning: 6DoF and 3Dof trajectory propagation, various fragmentation criteria including joint based fragmentation, various heating approaches, including the ability to calculate pre-heating to components prior to catastrophic fragmentation, various material models including specialist models for glasses, metals, insulators and ablaters, the application of thermal network models to assess the heating of sub-components, and nested fragmentation models for component/sub-component level analysis. The code also allows a Monte-Carlo assessment of the likelihood of sterilization given modelling inputs and submodel uncertainties. This provides additional insight into the likelihood of sterilization and enables additional efforts to be expended on marginal cases.

General Findings: The number of objects that can be considered auto-sterilised is strongly driven by fragmentation altitude. For a given fragmentation altitude, debris items that can be considered to almost always sterilize, and those that will most likely not sterilize can be quickly determined. Models which provide gently conservative sterilization assessments should be used for this initial screening. Those debris items which contribute strongly to bio-burden, or which lie close to a sterilisation threshold can then be analysed in more detail to assess the accuracy of the initial screening. This can result in a relatively small list of high impact components. Further detailed investigation of these components could then include: more sophisticated internal heat transfer approaches (thermal networks), nested fragmentation models and more sophisticated aerothermal heating methodologies, including the application of CFD. In particular, nested fragmentation of components

can lead to debris items that are far from sterilization when considered monolithically becoming auto-sterilised. In these circumstances, the modelling approach for the nested fragmentation needs to be carefully justified.

References:

[1] D.L.DeVincenzi, P.Stabekis and J.Barengoltz, "Refinement of planetary protection policy for Mars missions", *Advances in Space Research*, Volume 18, Issues 1-2, 1996, Pages 311-316

Aerothermal Analysis and Thermal Protection System [TPS] Design of the Mars Sample Retrieval Lander [SRL] Concept.

S. Muppidi¹, M. K. McGuire², D. Kinney², D. Saunders¹, K. Bensassi¹, H. Hwang², J. Olejniczak², K. Edquist³, and M. Ivanov⁴. ¹AMA, Inc., NASA Ames Research Center, Moffett Field, CA 94035, ²NASA Ames Research Center, Moffett Field, CA 94035, ³NASA Langley Research Center, Hampton, VA 23666, ⁴Jet Propulsion Laboratory, California Institute of Technology, Pasadena, CA 91109.

Brief Presenter Biography: Suman Muppidi is an Aerothermal Engineer based at NASA Ames Research Center, and leads the Mars SRL aerothermal design team. Dr. Muppidi has previously worked on the Low Density Supersonic Decelerators (LDS) project.

Introduction: Mars Sample Return (MSR) is a proposed mission to return samples from the surface of Mars to Earth. The current concept uses robotic systems and a Mars ascent rocket to collect and send samples of Martian rocks, soil and atmosphere for detailed chemical and physical analysis at Earth [1][2]. The mission architecture includes a Sample Retrieval Lander (SRL) which carries a rover and the ascent rocket to the surface of Mars, an Earth Return Orbiter (ERO) which collects the Martian sample from the ascent vehicle, and the Earth Entry Vehicle (EEV) which transports the sample to Earth. This presentation discusses the design options and constraints relevant to the SRL portion of the overall mission.

The estimated landed payload mass for the SRL is larger than that of MSL or Mars2020 [3], and enhancements to EDL capability are necessary. To that end, the proposed SRL vehicle has a 4.7 m diameter, spherical heatshield, similar to Orion. This is a first for a Martian entry, as all previous capsules that have entered Mars have featured a 70-deg sphere-cone geometry. This new geometry requires detailed analyses of the aerodynamic and aerothermal environments of this capsule in a Martian atmosphere, along with the development of databases. As with the InSight and Mars 2020 missions [4], aerothermal analysis and design includes calculating the radiative heating environment; efforts are particularly geared towards developing scaling rules for radiative heating on the fore- and aft- surfaces of this new geometry at various angles of attack and velocity. The convective heating environment on the spherical heatshield differs from the 70-deg sphere-cone, in terms of magnitude and location of peak heating.

While the various Entry options are still being evaluated, the current baseline involves a faster entry speed and a higher angle of attack (compared to MSL and Mars2020) resulting in a differences to the trajectory and the heat pulse. While the starting point in terms of the design of the Thermal Protection System (TPS) is very similar to that of MSL and Mars2020, these differences (geometry, trajectory, heat pulse) require investigation of alternate, mass-efficient TPS[5,6].

Scope: The presentation will describe (i) the expected entry environments including Martian atmospheric characteristics, (ii) aerothermal environment including CO₂ and CO radiation, and turbulent convective heating on the large spherical heatshield, (iii) aerothermal and Thermal Protection System (TPS) design methodology (with comparisons to MSL and Mars 2020 mission designs) and (iv) the envisioned path forward with respect to aerothermal analysis, design and testing.

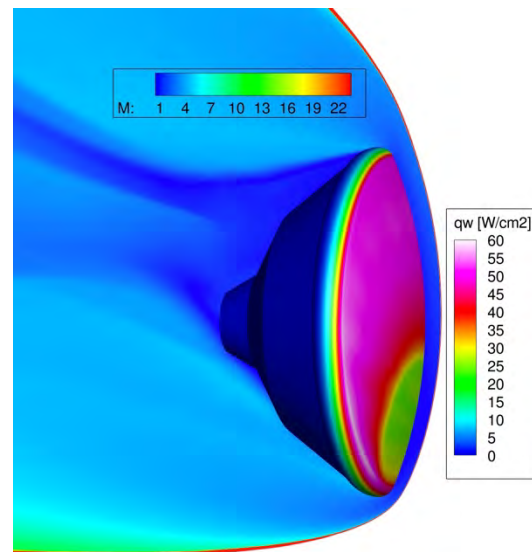


Figure 1 Flowfield Visualization: Contours of convective heat flux (on the surface) and fluid Mach number (on the symmetry plane) from hypersonic flow simulations used to characterize the aerothermal environment

References:

- [1] <https://www.jpl.nasa.gov/missions/mars-sample-return-msr/>
- [2] E. Venkatapathy, "Mars Sample Return: Grand Challenge for EDL", 10th Ablation Workshop, 2018, Burlington, VT, United States.
- [3] A. Wise, D. K. Prabhu, D. A. Saunders, C. Johnston, and K. Edquist, "Computational Aerothermodynamic Environments for Mars2020 Entry Capsule", AIAA Aviation Forum 2018, Atlanta, GA, United States.
- [4] A. Brandis, C. Johnston and K. Edquist, "Radiative Heating Indicators and Uncertainty Analysis for Mars2020", AIAA Aviation Forum 2018, Atlanta, GA, United States.

[5] I. Cozumta and M. K. McGuire, “Thermal Protection System Margins Management Standardized Policy for Safer and Reliable NASA and Commercial Missions”, CRASTE, Moffett Field CA, Oct 2010

[6] A. D. Cianciolo, T.A. Zang, R. R. Sostaric and M. K. McGuire, “Overview of the NASA Entry, Descent and Landing Systems Analysis Exploration Feed-Forward Study”, IPPW-8 Portsmouth VA, June 6-10, 2011

ExoMars Rover and Surface Platform Mission: Technical Status

A. J. Ball, O. Bayle, L. Lorenzoni, T. Blancquaert, S. Langlois, A.F.C. Haldemann and the ExoMars Project team, ESA ESTEC, Noordwijk, The Netherlands. andrew.ball@esa.int

Brief Presenter Biography: Andrew Ball is an Instrument Systems and Operations Engineer for ExoMars at ESA ESTEC, where he has been since 2008. Having worked previously on Rosetta and Huygens, this is Andrew's 14th IPPW.

Abstract: We present the latest status on the ExoMars Rover and Surface Platform Mission, with particular emphasis on the European contributions. ExoMars is a joint mission of ESA and Roscosmos. ESA's 300 kg ExoMars Rover, now named Rosalind Franklin, carries nine payload instruments, with hardware contributions from Europe, Russia and the US. The Rover will use survey instruments (panoramic, high-resolution and close-up cameras, IR spectrometer, ground-penetrating radar, neutron spectrometer) to prospect for promising drilling sites, and samples of astrobiological interest extracted by the 2 m drill (which also incorporates an IR spectrometer) will be passed via a crushing and dosing system to a carousel for analysis by four analytical instruments (imaging Vis/NIR microscope, Raman spectrometer, LDMS and GCMS).

The Russian-led Surface Platform carries Russian and European instruments. Furthermore an Entry, Descent and Landing science investigation (AMELIA) is foreseen, using telemetry from the descent module.

Launch of the Spacecraft Composite (Carrier Module + Descent Module enclosing the Surface Platform and Rover) is due in July 2020 on a Proton-M from Baikonur. The DM will be attached (at 8 points around the back shell) to the CM via a separation assembly. Following its separation (with nominal 2.75 rpm rotation) on approach to Mars, the DM will follow a ballistic entry, two-stage parachute descent and propulsive braking, targeting a landing site in Oxia Planum (120 km × 19 km landing ellipse to be located in proximity of an area centred at 335.70°E, 18.15°N, and having an elevation w.r.t. MOLA of -2 km). Nominal relative speed and IFPA at 120 km entry interface point are 5.6 km s⁻¹ (5.8 km s⁻¹ inertial) and -12.4°, respectively.

The DM is a 2000 kg, 3840 mm diameter, 70° sphere-cone with truncated conical (37°) back shell ('Rear Jacket'). During entry, real-time telemetry will be transmitted via UHF at 8 kbps via an antenna array on the RJ.

A two-stage parachute sequence will be initiated below Mach 2.1, based on GNC output informed by IMU data (*g* thresholds for EIP detection and falling deceleration).

The first stage comprises a 2.4 m diameter DGB pilot parachute followed by a 15 m DGB main supersonic parachute, and the second stage a 4.8 m DGB pilot followed by a 35 m RingSlot main subsonic parachute.

After the second stage parachute deployment the Front Shield will be released and the four landing legs deployed. The surface platform propulsion system then performs rate damping. The Radar Doppler Altimeter (identical to that flown on Schiaparelli, 4-beam, Ka band at 35.76 GHz) is then activated and brought into the GNC control loop. Braking engines are then activated and the landing platform separates from the Rear Jacket to continue to the surface on propulsion. A back-shield avoidance manoeuvre is performed. Touchdown is detected by means of contact sensors protruding from the landing legs, and the braking engines are shut down.

Following touchdown, the surface platform deploys its solar arrays, helix UHF antenna (identical to that on the Schiaparelli Surface Platform) and Rover egress ramps.

Transmission of the full set of data from the EDL phase will then be performed.

Introduction: An overall mechanical structure capable of transporting Martian samples from space to the Earth's surface must be specifically designed to ensure the alleviation of excessive dynamic loading and heating conditions. The proposed Mars Sample Return (MSR) mission architecture utilizes a passively and aerodynamically stable Earth Entry Vehicle (EEV) containing an Orbital Sampler (OS) designed to protect samples upon impact at terminal velocity onto the national landing site of the Utah Test and Training Range (UTTR). In the potential architecture, the EEV must be designed to absorb and redirect kinetic energy in a way that avoids damage to the Orbiting Sample (OS) and the sample tubes held within [1, 2, 7]. To successfully deliver high-quality Martian rock and regolith samples the MSR relies on a robust EEV design for mitigating the impact energy away from primary seals to meet the planetary protection (PP) protocols.

The EEV must be designed to guarantee sample integrity and containment assurance during impact landing. Thus, a dynamic Topology Optimization (TO) methodology for the crashworthiness and energy absorption of potential internal EEV support structures has been explored using Fusion 360 and LS-TaSC.

Traditional Topology Optimization Geometry: A geometry which has undergone Topology Optimization (TO) may be considered the best potential arrangement of materials for a given loading condition within a fixed domain. This optimization, will result in a reduction of the total amount of material required to complete the components' functionality and will directly contribute to an overall reduction of structural mass.

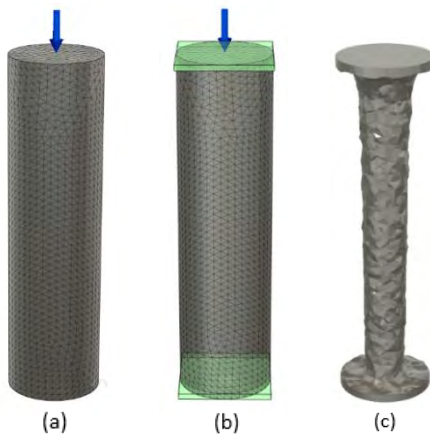


Fig. 1. Simple static topology optimization using a tetrahedral mesh: (a) cylindrical component under static load (b) initial boundary conditions applied (c) resulting geometry from uniform force distribution

Designs which have undergone TO are classified as either discrete or continuous. The discrete TO is conducted after the discretization of the solid geometries into finite elements, and the continuous TO is conducted via the modeling of the densities within continuous variables [3, 4, 5, 6].

Dynamic Topology Optimization: The implications of reducing the mass of a potential EEV can have significant mission benefits. One of which could be the reduction of the ballistics coefficient during the Entry Decent and Landing (EDL) phase of the mission; thus, lowering the overall kinetic energy upon landing. However, the traditional TO is to be used for static loading conditions, as discussed earlier. These static techniques would not be capable of optimizing a structures which experiences a transient impact. The research presented will show progress in the feasibility and implementation of TO when investigating simple geometries that experience dynamic loading (Fig. 2 below), and will build up on the progress made within this emerging field of research found in existing literature. This methodology would enable the implementation of more efficient advanced topologies within the internal components of complex systems, such as of EEV.

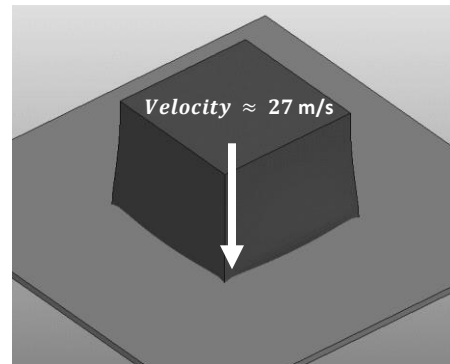


Fig. 2. Simple FEA geometry used to showcase the dynamic topology optimization methodology developed

Conclusion: A successful MSR mission would expand our knowledge and accelerate our understanding of our solar system. The samples which are to be gathered and transported back to Earth must remain intact and contained not to violate PP. The dynamic TO efforts presented in this presentation will further the goals of effective energy dissipation using only mechanical structures upon the EEV landing in UTTR. The EEV is a critical structure to the success of the MSR mission and thus in order to secure the payload successfully, the entire design space must be explored. This presentation will expand upon the topics discussed and the potential for future work.

References:

[1] Perino, S. V., et al, "The Evolution of an Orbiting Sample Container for Potential Mars Sample Return," IEEE Aerospace Conference, Big Sky, MT, 2017, pp. 1-16. doi: 10.1109/AERO.2017.7943979.

[2] Mitcheltree, R. A., Kellas, S., Dorsey, J. T., Desai, P. N., and Martin, C. J., "A Passive Earth-Entry Capsule for Mars Sample Return," 7th AIAA/ASME Joint Thermophysics and Heat Transfer Conference, Albuquerque, NM: AIAA, 1998.

[3] Gladman, B., "The LS-TaSC Tool Theory Manual," Livermore Software Technology Corporation (LSTC), Livermore, CA, 2015, pp.1-31.

[4] Beekers, M. "Topology Optimization Using a Dual Method with Discrete Variable," LTAS – Aerospace Structures, Liege, Belgium, 1999.

[5] Grace, C. M., Perino, S. V., "Exploring Impact Attenuating Interfaces for a Potential Mars Sample Return Earth Entry Vehicle," Jet Propulsion Laboratory, California Institute of Technology, Pasadena, CA, 2018

[6] Siddens, A. J., Perino, S. V., Komarek, T. A., "Recent Developments for an Orbiting Sample Container for Potential Mars Sample Return," Jet Propulsion Laboratory, California Institute of Technology, Pasadena, CA, 2018

[7] Perino, S. V., Bayandor, J., "A structural dynamics analysis methodology for development of Earth entry vehicles," AIAA, SciTech, 2014

Acknowledgments: Portions of the research described in this paper were carried out at the following institutions:

[1] The University at Buffalo, Buffalo, NY 14260

Implementing CubeSat Avionics Components to Full-Scale Capsule Return Missions .

Z. M. Hughes¹, M.S. Murbach², and R. D. Ntone¹, ¹San José State University, ²NASA Ames Research Center

Brief Presenter Biography: Zachary Hughes graduated from San José State University with a bachelor of science in aerospace engineering and is currently pursuing his masters degree. While at San José State University Zachary was an intern at NASA Ames Research Center where he worked along side the TechEdSat team who has a proven flight history of successful CubeSat missions. During his internship Zachary was exposed to CubeSat avionics components and realized their wide variety of applications.

Introduction: Returning samples from Low Earth Orbit (LEO) is no simple task. Whether the samples are scientific experiments or surveillance footage, engineers must overcome many challenges to achieve mission success. In August of 1960, the first payload recovered from LEO, the Corona capsule, carrying “more photographic coverage of the Soviet Union than all previous U-2 missions” [2]. The Corona program proved that returning samples from LEO is possible, the program is still referenced today when designing new sample return missions. Although there are many crucial subsystems that make up a sample return capsule such as the structural, thermal, and parachute subsystem the avionics subsystem demands the most attention.

This paper will discuss how current CubeSat avionics components can be applied to large sample return missions. The advantage of CubeSat avionics components is they are small and compact and can fit into a 1.5 U (10x10x15 cm) compartment leaving more room for the payload. This paper is broken down as follows. First, the reader is introduced to the history of sample return projects, the major outcomes and design strengths are analyzed and applied to the current design. Next, the typical trajectory of a capsule is presented along with mission requirements and operations. During the re-entry phase the avionics subsystem is responsible for commanding the deployment of the parachute, back shell ejection, and the heatshield ejection. Next, the power subsystem is discussed in detail including the trade studies of battery selection and voltage regulators. Next, the interface between the Ground Support Equipment (GSE) and the avionics components is discussed. It is important that the capsule is able to provide avionics system state of health to ensure proper functionality before the capsule is launched into LEO. Next, an in depth analysis of current TechEdSat avionics components, with proven flight history, are presented [2]. The various components such as radios, GPS, IMU, temperature sensors, altitude sensors, and ejectors are discussed and their applications to a sample return project

are analyzed. After, the wiring diagram is presented along with a discussion of the design. Next, a summary of how the avionics components are tested and validated are provided. Finally this article will present current sample return missions the proposed avionics components are being applied to.

CubeSat Avionics can be applied to almost all sample return missions due to the compact configuration and their proven space flight heritage. The TechEdSat team is currently making great progress in returning samples from the International Space Station (ISS) and is eager to present how their avionics components can be applied to full-scale sample return missions.

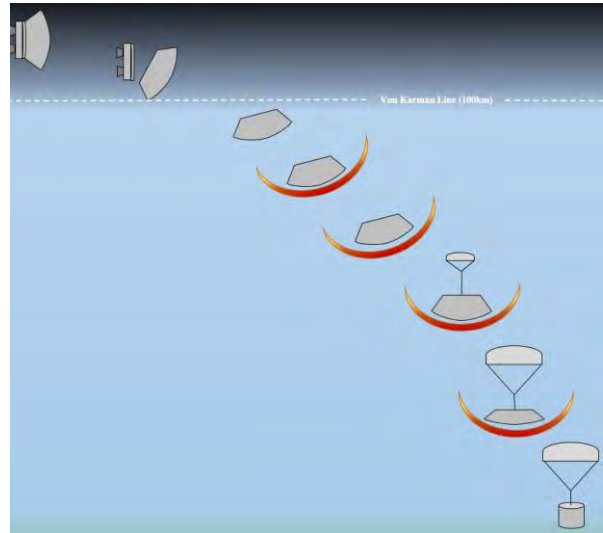


Figure 1: Mission Operation Sequence

References:

- [1] NASA Ames Research Center, "TechEdSat-N Procedures".
- [2] J. K. McDonald, "Corona: Americas First Satellite Program".

MARS SAMPLE RETURN – EARTH RETURN ORBITER: DESIGN AND VALIDATION OF A GUIDANCE, NAVIGATION AND CONTROL SYSTEM FOR MARTIAN RENDEZVOUS

M. Chapuy¹, F. Capolupo¹, B. Le Bihan¹, L. Whittle¹, A. Falcoz¹, A. Masson¹, R. Brochard¹, M. Baudry¹, K. Kani¹, ¹Airbus Defence and Space, 31 Rue des Cosmonautes, 31400 Toulouse, France, marc.chapuy@airbus.com

Brief Presenter Biography: Marc Chapuy is Guidance, Navigation and Control (GNC) architect for the Mars Sample Return – Earth Return Orbiter phase A/B1 at Airbus Defence and Space, Toulouse. He has worked as GNC system designer and analyst for the past 8 years at Airbus, contributing to the preparation of the future ESA exploration missions such as Jupiter Icy Moon Explorer (JUICE), Phobos Sample Return, and other concepts related to small body and Mars landing, as well as hazardous asteroid deflection.

Introduction and Mission Context: The NASA-led Mars Sample Return (MSR) program is an ambitious concept: it consists of four missions aiming at bringing samples of Martian soil to Earth, for analysis in state-of-the-art facilities, before 2032. The first mission, in charge of collecting and caching the samples, is the Mars2020 rover and is well known to the IPPW community. The other missions include the Sample Fetch Rover (SFR), the Mars Ascent Vehicle (MAV) and the Earth Return Orbiter (ERO), currently under preparation by NASA in collaboration with ESA.

The European contribution to the MSR program includes in particular the design, development and operation of the ERO vehicle. The mission of this spacecraft is to autonomously detect and rendezvous with the Orbiting Sample (OS) container in low Mars orbit, capture it, seal it, and safely bring it back to Earth. As such, it will be the first spacecraft to carry out rendezvous around a planet other than the Earth, which is all the more challenging considering that the OS is a small, non-cooperative target, injected by the MAV on an orbit with significant dispersions [1].

Airbus Defence and Space is currently leading the Phase A/B1 study for the ERO design, under ESA contract. In particular, Airbus is designing the vision-based GNC system for the rendezvous and capture of the OS, leveraging on the Automated Transfer Vehicle (ATV) heritage and decades of experience in vision-based navigation.

GNC System Design and Validation: This paper first presents context information on the MSR mission and the MSR-ERO design, a large spacecraft which will use a hybrid propulsion system (both electrical and chemical) to reach the Low Mars Orbit (LMO) and then return to Earth. Subsequently, an overview of the whole rendezvous scenario is provided, from injection of the OS in LMO by the MAV to capture. The rendezvous phases are then detailed individually, with a

focus on the most critical ones: the OS detection and orbit determination, and the terminal rendezvous. For each phase, the concept of operations is described, together with the GNC technical solution developed to satisfy mission performance and reliability requirements. The design is justified by end-to-end performance evaluation. The image processing chain used during the whole rendezvous mission is also detailed, as it constitutes an essential component of the relative navigation solution, which relies on passive optical sensors.

From an OS detection and orbit determination phase heavily supported by ground, the GNC system gradually and safely transitions to a system which is, although still monitored by operators, able to perform rendezvous autonomously.

Technology Readiness Acceleration: Even if the MSR-ERO rendezvous GNC design is inherited from the strong experience of Airbus, in particular from the ATV, the MSR-ERO rendezvous target and operational environment are very different from an International Space Station cargo mission, which implies that dedicated validation of the involved GNC technologies is required, beyond performance analysis in a simulated environment. The activities implemented in order to reach a technology readiness level (TRL) of 5-6 in 2019 and guarantee feasibility of a launch in 2026 are thus also described in this paper.

References: [1] Didion A. M., Nicholas A. K., Riedel J. E., Haw R. J. and Woolley R. C. (2018) *Methods for Passive Optical Detection and Relative Navigation for Rendezvous with a Non-Cooperative Object at Mars*, AAS 2018.

Structural Analysis of Impact-Tolerant Latched Containment Mechanisms for Mars Sample Return .

E.R. Shupper¹, M. L. Hendry¹. ¹Jet Propulsion Laboratory, California Institute of Technology, 4800 Oak Grove Drive, Pasadena, CA 91109, Emma.Shupper@jpl.nasa.gov, Morgan.Hendry@jpl.nasa.gov

Introduction: NASA is currently studying a potential Mars Sample Return (MSR) campaign that would return samples from the surface of Mars to Earth. A key component in the baseline MSR design is breaking the chain of contact (Break the Chain, or BTC) with Mars via high-reliability, backward planetary protection techniques. Sample containment and sterilization mechanisms would be used to ensure the protection of Martian samples from terrestrial contamination, while reducing the remote but non-zero risk associated with uncontained Martian samples causing adverse changes to the Earth's environment. Redundancy in these features is a primary driver in assuring a robust BTC containment methodology [1].

The first phase of containment will be achieved during the acquisition and caching of Martian surface samples in hermetically-sealed tubes during the Mars 2020 mission. The next phase of sample collection, including containment and sterilization for Earth return, would be conducted during the potential MSR campaign. Current concepts involve the insertion of sample tubes into a non-spherical container, the Orbiting Sample (OS), and sequential packaging into two additional sealed containers, the Primary Containment Vessel (PCV) and the Secondary Containment Vessel (SCV). Each vessel would be separated by layers of crushable foam. This Contained Orbiting Sample (C-OS) assembly would then be placed into the Earth Entry Vehicle (EEV) for Earth return and would be required to withstand the dynamic load environment associated with entry, descent, and impact landing (Figure 1).

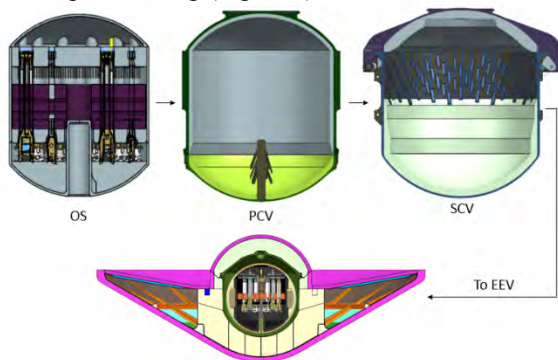


Figure 1. Schematic of the OS, PCV, SCV, and EEV design concepts.

Recent design efforts have focused on maturation of the EEV energy absorption mechanisms, which currently consists of a composite web and crushable foam

structure responsible for attenuating the impact response of the C-OS and thus reducing the risk of containment failure during nominal and off-nominal landing events [2].

While a variety of studies have been performed on the structural design of the OS and OS-internals to ensure sample survival during peak loading [3], the viability of specific containment mechanisms on the PCV and SCV under these dynamic conditions has not yet been investigated. Impact-tolerant lid latch and seal designs are critical to maintaining a redundant containment architecture and to achieving the containment assurance reliability requirements of the mission. This poster will discuss the current advanced structural simulations and methodology that is being utilized to assess the performance of lid latch mechanisms under nominal and off-nominal impact loading events in order to further mature the design of C-OS and increase confidence in containment assurance reliability.

Pawl-Latch Design and Analysis: The current lid latch design concept for the SCV consists of a logarithmic-derived, zero-backlash pawl mechanism (Figure 2). Initial pawl geometry was sized assuming a static 1000 g landing load.



Figure 2. Secondary Containment Vessel lid latch conceptual design.

A key focus in the early design stages is ensuring viability of the pawl-latch lid mechanism under both quasi-static and dynamic impact events. In order to (1) assess initial reliability of the pawl-latch lid design at the C-OS sub-assembly level, including material yielding and gapping, and to (2) size various design features for assumed worst-case loading conditions, explicit, nonlinear finite element analysis in the advanced solver LS-DYNA was employed (Figure 3). As the maturity of the design increases, additional modeling of internal mechanisms will be included to reach the goal of full system-level modeling

Displacement-controlled lid closure was first simulated in order to verify proper pawl engagement and

mechanism performance. Quasi-static loading was applied to the fully-assembled C-OS to mimic attempts to pry the containment lid from the bottom vessel and to assess the presence of contact gapping at the interface. Dynamic impact loads of varying magnitude and orientation were then applied in order to assess mechanism performance, as measured by maintaining of lid closure and sealing, and sub-system structural performance during nominal and off-nominal landing conditions. This poster will further provide an overview of the analysis, including assumptions and idealizations that were imposed and detailed results summaries as related to both structural reliability and overall BTC containment assurance goals.

Administration. The information presented about potential MSR is pre-decisional and is provided for planning and discussion purposes only.

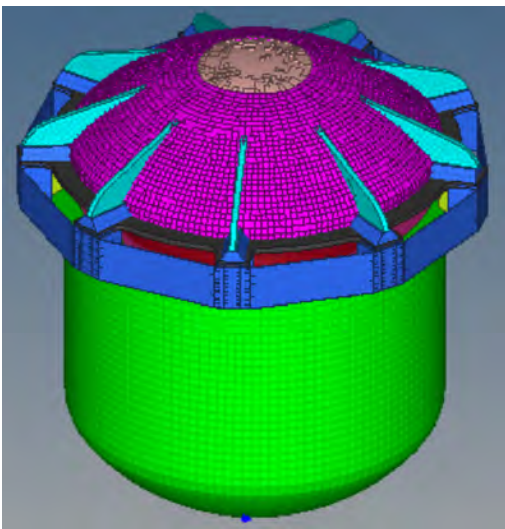


Figure 3. Finite element model representation of the C-OS assembly.

References:

- [1] Mitcheltree, R. A. et. al., “Earth Entry Vehicle for Mars Sample Return,” 51st International Astronautics Federation Congress, Rio de Janeiro Brazil, AIAA, 2000.
- [2] Kellas, S., “Energy Absorption Design, Fabrication, and Testing for a Passive Earth Entry Vehicle,” 43rd Annual AIAA/ASME/ASCE/AHS/ASC Structural Dynamics, and Materials Con, Denver Colorado. AIAA 2002.
- [3] Perino, S. et al, “The Evolution of an Orbiting Sample Container for Potential Mars Sample Return,” 2017 IEEE Aerospace Conference, Big Sky MT, 2017.

Acknowledgements: A portion of this research described in this paper was carried out at the Jet Propulsion Laboratory, California Institute of Technology, under contract with the National Aeronautics and Space

High Velocity Impact Performance of a Dual Layer Thermal Protection System for the Mars Sample Return Earth Entry Vehicle.

B.J.Libben¹, J.T. Needels², D.T. Ellerby³, J.C. Vander Kam³, T.R. White³, ¹AMA Incorporated at NASA Ames Research Center, ²Neerim Corporation at NASA Ames Research Center, ³NASA Ames Research Center.

Brief Presenter Biography: Ben Libben earned a Masters in Aeronautics and Astronautics from Purdue University. He is currently working as a Systems Engineer for AMA Inc. at NASA Ames Research Center in the Entry Systems and Vehicle Development Branch.

Abstract: The Mars Sample Return (MSR) Earth Entry Vehicle (EEV) is currently planned on being released from its Micro-Meteorite/Orbital Debris (MM/OD) shielding housing about two days before the Earth entry phase. This leaves the EEV exposed to incoming MM/OD impacts, potentially damaging the heat shield and compromising its Entry, Decent, and Landing (EDL) integrity.

Currently, two materials are proposed to comprise the MSR-EEV heat shield, a dual layer material called Heatshield for Extreme Entry Environment Technology (HEEET) or a single layer Phenolic Impregnated Carbon Ablator (PICA). PICA has been well characterized for OD class impacts, ~7 km/s high mass impacts, from previous testing done in the Orion program, but hasn't undergone extensive MM impact testing. HEEET is a relatively new material with minimal prior testing in regards to High Velocity Impacts (HVI). In order to inform the selectability of a material, it is crucial to understand the material performance when faced with an HVI, directly affecting mission success probability.

The current measure of a Thermal Protection System's (TPS) performance against an HVI is evaluating a thermally sized material against its derived Ballistic Limit Equation (BLE). A BLE is generated empirically from multiple shots of HVI testing and is used as a first order method in evaluating TPS's performance against the expected MM/OD environment. This method has proved useful for previous uniform density TPS materials, but has never been validated against a dual layer recession material such as HEEET.

Testing in the MSR program for FY19 has a requirement to assess the effects of a dual layer TPS by testing various thicknesses of HEEET's Recession Layer, seen in Figure 1. While flying solely Insulation Layer can theoretically close the system from an aerothermal standpoint, adding a thin stack of Recession Layer has potential to provide a "whipple shield" like effect, increasing the HS robustness. From FY19 test data, BLE's will be derived for the individual thickness ratio samples, as well as the material as a whole to evaluate if a heritage form of the BLE can capture the complex phys-

ics associated with a dual layer system. Crater morphology will also be assessed with post-test Non-Destructive Evaluation (NDE) methods such as CT scanning to visualize if a BLE can predict the associated penetration depths, since a BLE assumes full disintegration of the impacting particle and is generally only used to size a spherical crater – disregarding any shrapnel effects from a high density impactor.

To inform this analysis, expected MM environments from the Meteoroid Engineering Model (MEM) and analytical equations for mass flux of incoming MM were evaluated against the notional MSR-EEV trajectory [1]. Using those dispersions, a Monte Carlo simulation was run to determine the most probable particle parameters, as well as the riskiest in terms of full bondline penetration. From these probabilities, a test matrix was designed to test against bounding cases for the various parameters of the BLE: projectile density, projectile mass, projectile velocity, and the impact angle.

This presentation will discuss the performance of the dual layer TPS material HEEET against a wide range of impact kinetic energies and densities, as well as the comparison of HEEET to PICA in terms of MM/OD performance and selectability criteria.

References: [1] Moorhead, A. V., Koehler, H. M., & Cooke, W. J. (2015). NASA Meteoroid Engineering Model Release 2.0.

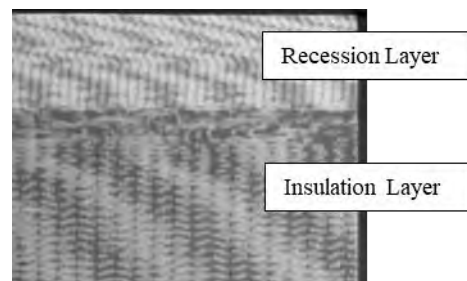


Figure 1. Cross section CT scan of the dual layer HEEET material anatomy. Recession Layer comprises the Outer Mold Line (OML) of the TPS.

TOUTATIS-Ex: A CUBESAT TESTBED FOR ENTRY EXPERIMENTS ON MARS C. Gentgen¹, T. Krzymuski¹, G. Villaret¹, A. Michaud¹, H. Brodeau¹, C. Duval¹, V. de Broesses¹, A. Duhamel¹, G. Bailet², L. Bourgois², C. O. Laux². ¹CentraleSupélec, Université Paris-Saclay, 3 rue Joliot Curie, 91192 Gif-sur-Yvette cedex, France, ²Laboratoire EM2C, CNRS, CentraleSupélec, Université Paris-Saclay, 3 rue Joliot Curie, 91192 Gif-sur-Yvette cedex, France (gilles.bailet@centralesupelec.fr).

Brief Presenter Biography: Chloé Gentgen is an Engineering Student in CentraleSupélec in France. Highly involved in her School's Space Center, the "Centre Spatial de CentraleSupélec pour les CubeSats", she has the position of System Engineer on the TOUTATIS-Ex mission, and is thus one of the leaders of the project. TOUTATIS-Ex is a testbed for entry experiments on Mars.

Introduction: Designing a planetary probe for Mars or other planetary bodies with an atmosphere relies on the use of a Thermal Protection System (TPS) material composing the heat shield. Considering the delivery of a payload, such as a rover or a Human crew, every reduction on the design margin of the TPS will save valuable mass for the payload and/or reduce thermal/structural loads. The study of the entry phenomenon is a critical point when it comes to the design of the future missions to Mars after M2020. In this study, TOUTATIS-Ex is presented. Based on the CubeSat 12U standard, TOUTATIS-Ex follows the missions pushing the design envelop (MarCO [1] and QARMAN [2]). The proposed design will be composed of two main parts, a carrier/radio relay and an atmospheric probe capsule called SERENADE-Ex. Brought to the Martian vicinity as a piggyback mission by a larger spacecraft, the CubeSat will autonomously conduct entry experiments within the atmosphere and downlink the data to Earth without the use of another orbital relay. This poster will expose the platform and mission design as well as the way to solve the key issue of data return.

Platform(s) design: The 12U CubeSat (34x22x22 cm³ for <20kg) will consist of two main elements.

The first half will be dedicated to SERENADE-Ex, an entry capsule (22 cm in diameter, <10kg) which will be ejected from TOUTATIS-Ex. Equipped with a full set of sensors, the capsule will transmit its data in real time to the carrier/relay spacecraft with a S-band patch antenna. SERENADE-Ex will have a heat shield composed of cork based TPS material to resist the harsh environment of entry.

The second half of the spacecraft, the carrier, equipped with an electric propulsion system and small cold gas thrusters for attitude control, will remain in space (martian orbit or hyperbolic fly-by). Equipped with a S-band receiving antenna and a X-band transmitting antenna,

TOUTATIS-Ex will be a dedicated orbital relay in order to send the collected data directly back to Earth through the Deep Space Network.

Possible orbits for TOUTATIS-Ex: For the carrier, both hyperbolic (fly-by style, no insertion within the martian orbit) and elliptic orbits are possible. The financing agency will decide which is chosen depending on the planetary protection assessment. If the elliptical orbit is selected, the carrier/relay spacecraft will use its electric thruster to deorbit to an altitude where the upper layer of the atmosphere will induce a natural orbital decay.

SERENADE-Ex instrumentation: The capsule is equipped with a full set of sensors in order to conduct experiments during its entry of the Martian atmosphere. Those compact instruments will measure material response (using thermocouple plugs and recession/swelling sensors) and the flow environment around the vehicle (pressure spools, FAD system [3] and mini-INES, a total radiative sensors [4]). Mini-INES is an innovative payload able to measure radiative flux in a presence of an ablatif TPS without any contamination. It is also able to measure recession, sublimation and swelling at the same location.

Conclusion: TOUTATIS-Ex represents an innovative testbed for entry experiments on Mars due to its entry capsule embarking a full suite of instrumentation, and its orbital relay which will send back a high volume of data back to Earth. This high risk/high reward approach is enabled by the low-cost of the CubeSat platform and a few platforms could be embarked on a larger missions for redundancy and testing of different entry path parameters.

References:

- [1] A. Klesh (2018), *MarCO*, 15th International Planetary Probe Workshop.
- [2] G. Bailet, A. Bourgoing, T. Maginand C. O. Laux (2014), *Qarman: an Atmospheric Entry Experiment on CubeSat Platform*, 11th International Planetary Probe Workshop.
- [3] S. A. Whitmore, et al. (1995), *In-flight Demonstration of a Real-Time Flush Airdata Sensing (RT-FADS) System*. NASA Technical Memorandum 104314.
- [4] G. Bailet, (2018), *Apparatus reduction liability of pollution of an optical access of an optical instrument*. Patent WO2018100255A1.

Lunar Gateway LASC Module for Innovative Concepts for Exploration: A Laser-powered Apparatus for Satellite Charging.

B. C. Biggs¹, A. B. Biggs², P. Papadopoulos³, ^{1,2,3}San Jose State University, 1 Washington Sq, San Jose, CA 95192

Introduction: With the inevitable retirement of the International Space Station (ISS) approaching in the year 2024, there exists a significant movement toward lunar-based missions. NASA is leading this expedition with the creation of a lunar outpost known as the Gateway. The Gateway will serve as an all-in-one solar-powered communications hub, science laboratory, short-term habitation module, and holding area for rovers and other robots. The design architecture can be seen in figure 1 [1].

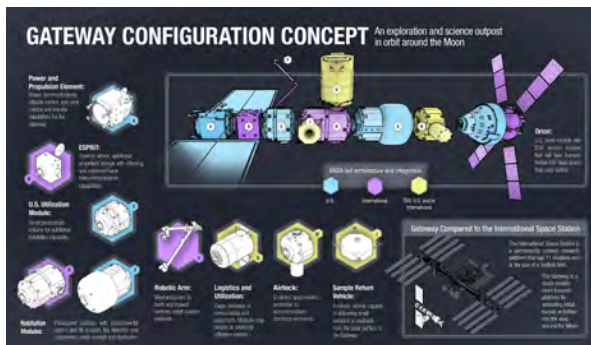


Figure 1: View of Gateway configuration concept [1]

The Gateway will promote human exploration of the solar system starting at the moon with the help of state-of-the-art technology and innovative research. LASC is a researched-based proposed lunar CubeSat charging and transmitting spacecraft platform that will be stationed on and operated from the Gateway. Details of the LASC design, including technical requirements, will be presented as follows.

Mission: LASC is a power station that can directly support multiple CubeSat lunar missions. LASC provides direct power transmission to CubeSats co-orbiting the Gateway all the way to near the lunar surface an example of which can be seen in figure 2.

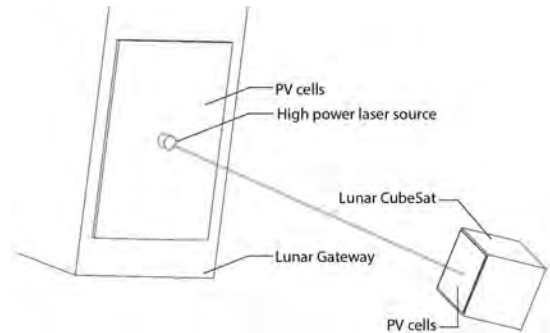


Figure 2: System overview: CubeSat in lunar orbit receiving power transmission via high power laser source mounted on the Lunar Gateway

With the abilities of LASC, the time of flight of lunar CubeSats will be significantly extended, enabling longer periods to conduct in-situ measurements, observations, and increase the bandwidth for data transmission. The addition of a charging station on The Gateway is a compact, modular subsystem that can be used on demand as needed to support Gateway to lunar surface missions. The solar collector and solar array subsystems are positioned and oriented to collect the abundant amount of sunlight available in space. Solar energy is transformed into electric energy and is stored until energy transmission to a nearby CubeSat is required. The current project has designed mission ops and autonomous maneuvering procedures for recharging CubeSats. When a lunar CubeSat requires a re-charge, the CubeSat's on-board GNC system orients the CubeSat such that it is within operating range of the laser aboard LASC. The functionality of the system is shown below in figure 3.

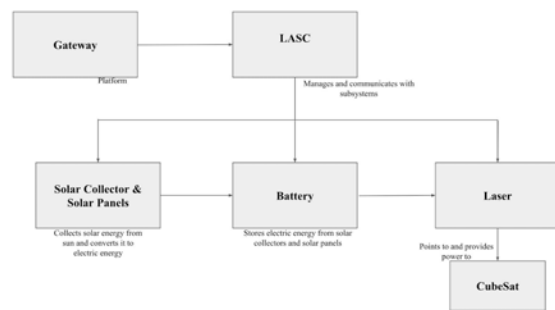


Figure 3: Functional flow block diagram of LASC

The specific operating range, accuracy, and precision of the laser will be presented at the conference. The design set forth by the authors utilizes a MHGoPower LSM-010 laser in conjunction with a modified aperture diameter greater than 3mm that meets the requirement as presented in reference [4]. An N2 diagram of the interface between systems can be viewed below in figure 4.

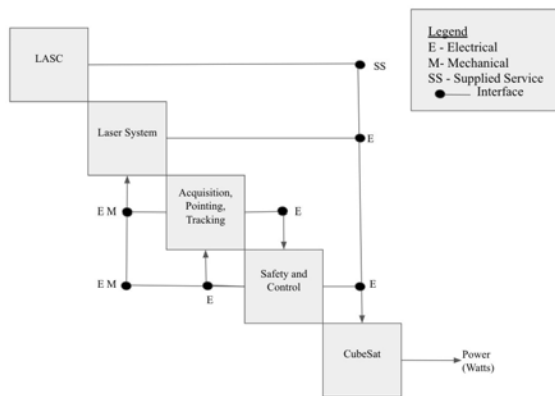


Figure 4: N2 Diagram displaying functionality of the laser system.

The innovation of LASC is that it miniaturizes a solar collecting system architecture to a CubeSat form factor. The innovation highlights the implementation of a low-cost, reusable, rechargeable lunar CubeSat architecture for extended operation life.

From a power point of view, a major limiting factor for CubeSats is the amount of onboard power that can be supplied to the spacecraft. On average, a 3U CubeSat draws around 11 watts of power. This power requirement is based on varying spacecraft mass, instrumentation needs, GNC requirements amongst others. LASC is a game-changing design of an external power module aboard the Gateway that provides on-demand recharging of lunar CubeSats in situ, in-orbit. The utilization of a centralized power hub significantly enhances the capabilities of orbiting CubeSats. LASC removes the current power constraints for small satellites thus enables high-power demanding experiments to take place in space.

According to NASA's list of current state-of-the-art solar cell technology, MMA's eHAWK solar panel configuration possesses 29.5%-30.7% efficiency while providing anywhere between 36-112 watts of peak power performance, depending on the solar panel configuration [3],[4]. The solar panel configurations range in size and are easily scalable. MMA's solar panel is currently one of the most efficient and reliable designs for space-based missions. Using the various configurations and the technical specifications listed on the MMA website, the LASC design stays within

the area requirement of 20cm by 30cm (the surface area of one face of a 6 unit CubeSat) in order to sufficiently provide at least 15 watts of power. This design allows for the demonstration of successful solar power collection, laser transmission, and charging of one 3 unit CubeSat in space. LASC is specially designed such that, once proven to successfully supply power on a small scale transmission, the system can be scaled up in size, depending on the need and available space on the Gateway.

The final presentation will address the limitations of the current solar panel interface and suggest viable solutions. The initial, primary focus of the platform is on the low cost, reusable and rechargeable power capabilities of LASC. Forthcoming innovations for the module includes the coupling and integration of both photonic propulsion and laser-based telecommunication subsystems for small satellites. Research on the propulsion and telecommunication subsystems will be presented at the conference.

LASC is a valuable and multifunctional technology that can reduce life-cycle costs while mission longevity for small satellites conducting solar system exploration.

References:

- [1] Dunbar, Brian. (2018). Competition Seeks University Concepts for Gateway and Deep Space Exploration Capabilities. <https://www.nasa.gov/feature/competition-seeks-university-concepts-for-gateway-and-deep-space-exploration-capabilities>
- [2] Iyer Vikram. (2017). Charging a Smartphone Across a Room Using Lasers <https://dl.acm.org/citation.cfm?id=3161163>
- [3] MMA Design. (2019). Existing Hawk Configurations. <https://mmdesignllc.com/>
- [4] Yost, Bruce. (2019). State of the Art Small Spacecraft Technology. <https://sst-soa.arc.nasa.gov/03-power>

Biography



Brandon Biggs is currently in his senior year of the Bachelor of Science in Aerospace Engineering (BSAE) at San Jose State University. His concentration is in

spacecraft design. Current projects, beyond LASC, include the construction of a low-cost hyperspectral imaging CubeSat and a supersonic rocket.



Ashleigh Biggs is currently in her senior year of the Bachelor of Science in Aerospace Engineering (BSAE) at San Jose State University. Her

concentration is in spacecraft design. Current projects, beyond LASC, include the construction of a low-cost hyperspectral imaging CubeSat and a supersonic rocket.

Virtual Validation and Verification of the VaMEx Initiative

Jörn Teuber¹, Rene Weller¹, Luisa Buinhas², Daniel Kühn³, Philipp Dittmann¹, Abhishek Srinivas¹,
Frank Kirchner^{1,3}, Roger Förstner², Oliver Funke⁴, Gabriel Zachmann¹

¹ University of Bremen, Germany

² Bundeswehr University Munich, Germany

³ German Research Center for Artificial Intelligence, Germany

⁴ German Aerospace Center (DLR), Space Administration, Germany

Abstract— We present an overview of the *Valles Marineris Explorer (VaMEx)* initiative, a DLR-funded project line for the development of required key technologies to enable a future swarm exploration of the Valles Marineris on Mars. The Valles Marineris is a wide canyon range, near the Martian equator. The so far still fictive VaMEx mission scenario comprises a swarm of different robots, including rovers, flying drones and a hominid robot. Here, we present VaMEx-VTB, a virtual testbed (VTB) with a digitalized map of the large and fragmented terrain of the Valles Marineris. The VaMEx-VTB allows an adjustable validation as well as verification of the complex mission design in virtual reality, due to its modular design. It shall also be used in preparation of field tests in the near future for validation of each swarm element’s ability for interactive swarm cooperation and collaboration.

1. INTRODUCTION

The goal of the VaMEx initiative, funded by the German Aerospace Center (DLR) as part of the Explorer Initiatives, is the investigation of new technologies for the exploration of the Valles Marineris on Mars. This Martian region is the largest connected canyon landscape in the solar system with a length of more than 4000 km. In the deep and protected areas of these canyons, it is possible to find valuable resources like water or even signs of extraterrestrial life. However, due to the ragged nature of the canyons, the development of new technologies is required in order to pursue exploration tasks in a robust, reliable and autonomous manner.

The VaMEx initiative proposes to use a swarm of different autonomous robots that complement each other, including UAVs, wheeled ground vehicles and walking robots, supported by a satellite in Mars orbit. In a first phase, we focus on the development of concepts, the hardware but also algorithms, e.g. to allow a flawless cooperation of the individual elements. A key feature for a mission consisting of an heterogeneous and autonomous swarm is a stable real-time communication system.

The validation and verification of such a complex mission, consisting of several interdisciplinary teams with many communication interfaces to exchange different kinds of data, is nontrivial. Real-world field tests for the individual parts are already expensive, time-consuming and not very realistic, because the environments on Earth differ significantly from the environmental conditions on Mars. The logistical effort in performing real-world field tests to evaluate swarm performance is considerable and out of reach in terms of the financial resources.

In order to identify design gaps and inconsistencies at an early stage of mission planning we have developed a *virtual* testbed

(VaMEx-VTB) that simulates the communication interfaces, sensor input and important physical properties of the local topography in a virtual environment. This allows the project partners to test the software components of their systems before a real-world field test, diagnose flaws and correct them already at initial research stages. Moreover, our VTB allows to rebuild the Martian environmental conditions and it supports a user-adjustable modification of the terrain.

A main challenge for VaMEx-VTB are the large amounts of data that have to be handled. Actually, we have recreated a 3D model of $40km^2$ of the Martian surface based on digital terrain models (DTMs) provided by HiRise [1]. Moreover, we will present the integration of the different communication systems where we guarantee a real-time simulation of the data exchange between the individual VaMEx components. Finally, the VaMEx-VTB is not only a desktop application, but the integration of virtual reality technologies allows the engineers a more natural and immersive interaction with the systems.

In the presented manuscript, we will give a brief overview on the individual parts of the VaMEx initiative and then focus on our novel verification and validation platform, VaMEx-VTB.

2. VAMEX OVERVIEW

The VaMEx initiative consists mainly of four parts to explore the unknown terrain of the Valles Marineris: a swarm of unmanned aerial vehicles (UAVs) and wheeled rover that can cover large distances (VaMEx-CoSMiC), a hominid robot platform to explore also hardly reachable places like caves (VaMEx-UIPE), a ground-based localization and navigation network (VaMEx-LAOLa) and orbital support for global localization and communication (VaMEx-NavComNet).

VaMEx-CoSMiC

The VaMEx Cooperative Swarm Navigation, Mission and Control (VaMEx-CoSMiC) project focuses on the swarm exploration using autonomous rovers and UAVs (see Fig. 1). The main goals are the development of efficient algorithms for surveying large areas without human supervision. The different vehicles are equipped with different sensor types, such as inertial sensors and monoscopic and stereoscopic cameras. Swarm communication is used for the distributed simultaneous localization and mapping (SLAM). Beyond the goal of using the sensor output for the navigation of the VaMEx-CoSMiC vehicles, it is used to create a map of the explored terrain and made available to other members of the VaMEx swarm.

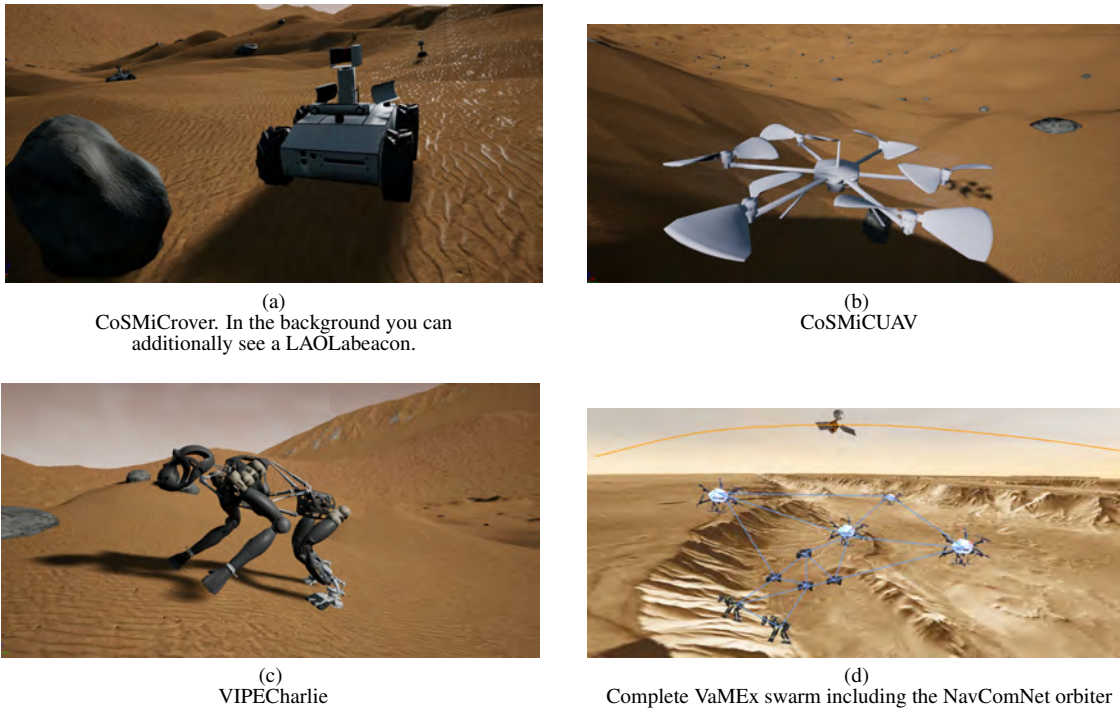


Figure 1: Models of the VaMEx swarm members in VaMEx-VTB.

VaMEx-VIPE

For an extensive exploration of the Valles Marineris, a robotic platform that can move within the fissured rock formations and navigate in caves and crevices that are unreachable by the rovers of VaMEx-CoSMiC is desired as part of the heterogeneous team. The hominid robot Charlie [2], developed by DFKI, closes the remaining gap in the swarm (see Fig. 1).

To put the project into practice efficiently and cost-effectively, expertise and hardware built in previous projects from different areas, such as deep-sea robotics [3], [4], [5], was used. Charlie, a four-legged walking robot, is well suited to overcome difficult terrain due to its light and highly integrated construction and agility. In addition, the tactile sensors are powerful tools in many applications [6]. In order to keep the weight of the robot platform low (important for the agility and transport costs of the system), only light sensors were used.

Visual navigation is a very suitable technology based on light, passive sensors, which allows a reliable position determination due to the high redundancy but usually requires a robust semantic representation of environmental objects and features like described in [7]. In contrast to radio-based positioning, no (visual) connection to other swarm participants is necessary. The position determination based on continuous visual odometry using a stereo camera, as it is used for the rovers and flight systems, can only be applied to a limited extent to Charlie. Especially in areas with low brightness, the exposure times would be too long or would require a continuous, and thus resource-intensive, illumination.

Particularly when overcoming a rugged terrain, it is crucial to place the legs of the walking robot precisely on stable surfaces [8]. In order to make this possible, a proprioceptive approach was researched that uses tactile sensors to record body position and movement in space and converts them into position information. This is a prerequisite for motion

planning and reactive motion control, which makes it possible to overcome obstacles. By merging tactile data with visually-perceived surface structures such as edges and gaps, these two technologies complement each other to form a very promising approach for reliably pursuing exploration tasks in topographically-challenging areas.

The reactive motion control in Charlie was extended by further behavior modules, so that a safe locomotion over leveled and uneven ground as well as the overcoming of obstacles with the robot could be shown. In addition, an algorithm for optimal foot placement was developed. This adaptive foot-placement algorithm makes it possible to find an optimal foot contact point for each leg either between or including various obstacles with the help of a local map. It has to be mentioned that this is not a purely planning-based control of the robot. The reactive walk control is maintained, the planning level is only allowed to write offsets on the respective walking pattern of the different legs. This procedure takes place in real time and extends the robot's mobility in that it is not necessary to stop on uneven ground or in front of obstacles in order to plan the next steps. Even if the ground does not behave as expected (e.g. due to the flexibility of an obstacle, where a contact between foot and obstacle has been planned into the step cycle), the robot is able to continue its locomotion stably due to the permanently active reactive control level.

VaMEx-LAOLA

The goal of the VaMEx-LAOLA (*Lokales Ad-hoc Ortungs- und Landesystem*²) project is to provide systems for the communication between the individual members of the swarm, as well as enabling a localization to determine their positions relative to other swarm members. The local position is important for the coordination of the swarm members and to find the way back to the lander. The accuracy of

²German for: local ad-hoc localization and landing system

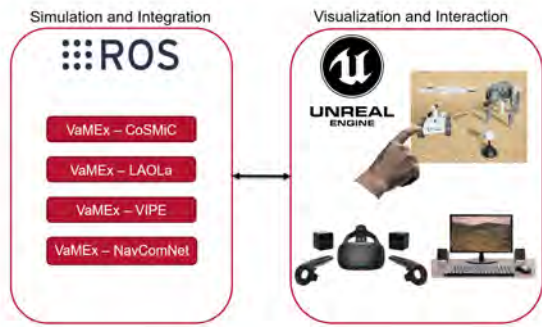


Figure 2: High-level overview of VaMEx-VTB structure.

the local reference frame is higher than that of the global reference frame. The system is based on a set of beacons that are equipped with Frequency Modulated Continuous Wave (FMCW) secondary radar. For the communication, the beacons contain additionally a 2.4 GHz module.

VaMEx-NavComNet

The VaMEx-NavComNet (*Navigation and Communication Network*) has the concrete aim of serving as a science data, telemetry and telecommand relay between Earth and the in-situ users, as well as a cross-communication relay between users, but also providing a near real-time positioning system for surface, aerial and (potential future) space-based users. An ideal solution would consist of four satellites dispersed at different altitudes [9], ranging between 800 and 1200 km, and orbital inclinations up to 35 degrees, allowing for data exchange volumes of up to 300 Mbits per Sol (or Martian day). We are currently investigating more cost-efficient solutions consisting of a single satellite or nano satellites.

3. VAMEX-VTB

Virtual testbeds are already successfully used in fields like autonomous automotive development [10], physically-based automotive control [11], supply chain planning [12] but also planetary exploration [13], [14]. In general, virtual testbeds are software solutions that enable the validation and verification of arbitrary simulation models in user-definable virtual environments. They mainly help to reduce the need to build expensive physical prototypes by moving, especially early testing, into a pure virtual simulation environment. Consequently, VTBs reduce development time and cost significantly. Moreover, VTBs can be used as a common development and evaluation platform [15].

The main goals of VaMEx-VTB are:

- to serve as a common validation and verification platform for the VaMEx initiative,
- to simulate all relevant environmental aspects, including sensor synthesis, distribution of resources, collision detection,
- to deliver immersive natural interaction with the system and to provide a highly detailed graphical feedback,
- and to allow extensions and exchangeability of the individual parts of the system.

In the following we will briefly sketch some design details and discuss the features of VaMEx-VTB with respect to the requirements defined above.

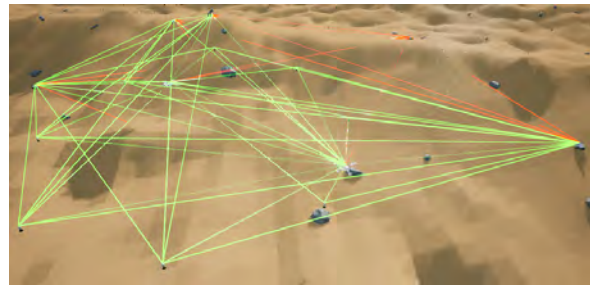


Figure 3: The line-of-sights connecting the VaMEx-LAOLA beacons.

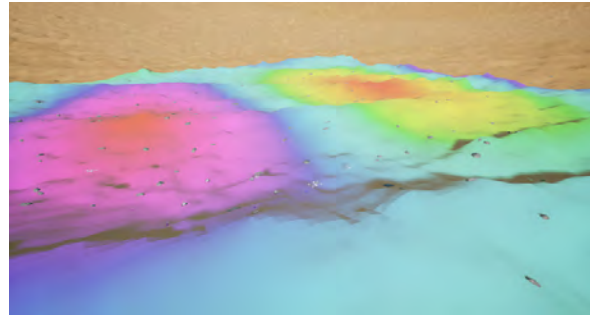


Figure 4: Visualization of the process to be measured by the swarm in VaMEx-VTB.

General Design

Figure. 2 provides a broad overview on the design of our virtual testbed. One core element of our VaMEx-VTB is a high-end visualization in combination with the possibility of virtual reality (VR) interaction. We decided to use a state-of-the-art game engine, the Unreal 4 Engine, that supports the most modern visualization effects and has an integration for a large amount of VR hardware devices.

Moreover, we have manually created a $40km^2$ terrain of the Valles Marineris based on data available from the NASA. However, the accuracy of the data is limited, hence we included the possibility to easily add surface details. For instance, our systems supports simply painting the specific terrain type (e.g. sandy, rocky, etc) directly on the surface. This includes also different texturing and even different physical properties for the simulation depending on the terrain type.

In order to connect the individual VaMEx components, which are predominantly implemented in the widely used robot operating system (ROS) [16], to the VTB we integrated and extended an interface to ROS. More specifically, the VTB establishes a connection to a ROSbridge server [17] via a websocket to which the components can register to receive and send data. This fast ROS interface allows a simple modular design of practical relevance while maintaining real-time capability of our VTB.

VaMEx-VTB Features

A main feature of our VaMEx-VTB is the synthesization of sensor input that can be delivered to the specific modules via the ROS connections. This includes images of RGB(D) cameras, the odometry and the generation of LIDAR data via ray tracing. The same technique is used to compute the line-

of-sights between the LAOLA beacons and the swarm units (see Fig. 3). All this data is generated in real time.

The simulation in our VTB is based on detailed models of the individual swarm members, including working vehicle wheel physics for the VaMEx-CoSMiC rovers, working rotors of the VaMEx-CoSMiC UAVs and a skeletal model with physically-based movement of the VaMEx-UIPE robot. Obviously, the number of vehicles, beacons and humanoid robots is user-definable. The VaMEx-NavComNet satellites fly in a realistic orbit as calculated by SPICE kernels, providing position updates in a Mars-centered absolute reference frame.

Our interactive data visualization includes ellipsoidal uncertainty visualizations based on covariance matrices, ghost models to display the differences between real and expected positions of the vehicles, the planned paths of the swarm units and a visualization of the process that is being measured by the swarm, both ground-truth and currently measured (see Fig. 4).

4. CONCLUSIONS AND FUTURE WORKS

We have presented a brief overview on the VaMEx initiative for the swarm-based exploration of the Valles Marineris on Mars. Moreover, we have introduced VaMEx-VTB, a virtual testbed for the verification and validation of complex planetary surveying missions.

We are confident that the modular and future-proof design of our VaMEx-VTB qualifies it to serve as a testing platform for other space projects, especially for planetary surface exploration scenarios. Additionally, the navigation and communication technologies researched within the VaMEx initiative are of interest for future missions.

ACKNOWLEDGMENTS

The authors thank the DLR Space Administration for funding this project line.

REFERENCES

- [1] A. S. McEwen, E. M. Eliason, J. W. Bergstrom, N. T. Bridges, C. J. Hansen, W. A. Delamere, J. A. Grant, V. C. Gulick, K. E. Herkenhoff, L. Keszthelyi *et al.*, “Mars reconnaissance orbiter’s high resolution imaging science experiment (hirise),” *Journal of Geophysical Research: Planets*, vol. 112, no. E5, 2007.
- [2] D. Kuehn, M. Schilling, T. Stark, M. Zenzes, and F. Kirchner, “System design and field testing of the humanoid robot charlie,” *Journal of Field Robotics*, vol. 34, no. Issue 4, pp. 666–703, 4 2016.
- [3] J. Albiez, S. Joyeux, C. Gaudig, J. Hilljegerdes, S. Krofke, C. Schoo, S. Arnold, G. Mimoso, P. Alcantara, R. Meireles Saback, J. Britto Neto, D. Cesar, G. Neves, T. Watanabe, P. Merz Paranhos, M. Reis, and F. Kirchner, “Flatfish- a compact subsea-resident inspection auv,” *Proceedings of the MTS/IEEE OCEANS 2015*, pp. 1–8, 01 2015.
- [4] J. Lemberg, J. de Gea Fernandez, M. Eich, D. Mronga, P. Kampmann, A. Vogt, A. Aggarwal, Y. Shi, and F. Kirchner, “Aila - design of an autonomous mobile dual-arm robot.” in *ICRA*. IEEE, 2011, pp. 5147–5153. [Online]. Available: <http://dblp.uni-trier.de/db/conf/icra/icra2011.html#LembergFEMKVASK11>
- [5] M. Hildebrandt, J. Albiez, and F. Kirchner, “Computer-based control of deep-sea manipulators,” in *OCEANS 2008 - MTS/IEEE Kobe Techno-Ocean*. IEEE, 2008, pp. 1–6.
- [6] A. Aggarwal and F. Kirchner, “Object recognition and localization: The role of tactile sensors,” *Sensors*, vol. 14, no. 2, pp. 3227–3266, 2014.
- [7] M. Eich and M. Goldhoorn, “Semantic labeling: Classification of 3d entities based on spatial feature descriptors,” in *Best Practice Algorithms in 3D Perception and Modeling for Mobile Manipulation*, 2010.
- [8] D. Spenneberg, M. Albrecht, T. Backhaus, J. Hilljegerdes, F. Kirchner, A. Strack, and H. Zschenker, “Aramies: A four-legged climbing and walking robot,” in *Proceedings of 8th International Symposium iSAIRAS. International Symposium on Artificial Intelligence, Robotics and Automation in Space (iSAIRAS)*, Munich, Munich, 2005.
- [9] L. Buinhas, G. Peytaví, and R. Förstner, “Navigation and Communication Network for the Valles Marineris Explorer (VaMEx),” in *Proceedings of the 69th International Astronautical Congress (IAC)*, 2018.
- [10] F. Dion, J. Oh, and R. Robinson, “Virtual testbed for assessing probe vehicle data in intellidrive systems,” *IEEE Transactions on Intelligent Transportation Systems*, vol. 12, no. 3, pp. 635–644, Sep. 2011.
- [11] D. Davis and D. Brutzman, “The autonomous unmanned vehicle workbench: Mission planning, mission rehearsal, and mission replay tool for physics-based x3d visualization,” *14th International Symposium on Unmanned Untethered Submersible Technology (UUST)*, 2005.
- [12] S. Chick, P. Sanchez, D. Ferrin, and D. Morrice, “A simulation test bed for production and supply chain modeling,” in *Proceedings of the 2003 Winter Simulation Conference, 2003.*, vol. 2, Dec 2003, pp. 1174–1182 vol.2.
- [13] J. Rossmann and B. Sommer, “The virtual testbed: Latest virtual reality technologies for space robotic operations,” *9th International Symposium on Artificial Intelligence, Robotics and Automation in Space (iSAIRAS)*, 2005.
- [14] J. Rossmann, B. Sondermann, and M. Emde, “Virtual testbeds for planetary exploration: The self-localization aspect,” *11th Symposium on Advanced Space Technologies in Robotics and Automation (ASTRA)*, 03 2019.
- [15] P. Lange, R. Weller, and G. Zachmann, “Multi agent system optimization in virtual vehicle testbeds,” in *EAI SIMUtools*. Athens, Greece: EAI, Aug. 2015.
- [16] M. Quigley, B. Gerkey, K. Conley, J. Faust, T. Foote, J. Leibs, E. Berger, R. Wheeler, and A. Ng, “Ros: an open-source robot operating system,” in *Proc. of the IEEE Intl. Conf. on Robotics and Automation (ICRA) Workshop on Open Source Robotics*, Kobe, Japan, May 2009.
- [17] C. Crick, G. Jay, S. Osentoski, B. Pitzer, and O. C. Jenkins, “Rosbridge: Ros for non-ros users,” in *ISRR*, 2011.

AERODYNAMIC HEATING ESTIMATION OF DEPLOYABLE INFLATABLE AEROSHELL FOR MARTIAN PENETRATOR ENTRY SYSTEM.

T. Kazama¹, K. Yamada², Y. Takahashi³ and J. Koyanagi⁴, ¹Tokyo University of Science (125-8585 Nijuku, Katshika Ward, Tokyo Japan, 8214028@ed.tus.ac.jp), ²ISAS/JAXA (252-5210 Yoshinodai, Chuo-ku, Sagamihara City, Kanagawa Prefecture, Japan), ³Hokkaido University (060-8628 Kita 13 Nishi 8, Kita-ku, Sapporo, Hokkaido, Japan).

Brief Presenter Biography: Mr. Tomoya Kazama is a master course student in Tokyo university of science. I have been studying on the aerodynamics and material science. My research topic is EDL system of Martian penetrator. This work is collaborating with JAXA/ISAS, Hokkaido university and MAAC group.

Introduction: The penetrator is one of the unique concept in planetary probes. This is the stake-shape hard lander which impacts on the planetary surface in order to penetrate into the ground and make meteorological and geological observation under the ground. The penetrator can be embedded under the ground simultaneously with landing and doesn't require a soft-landing system. This probe which is lighter and more simple than soft-landing probe has the significant advantage for the Martian distributed network exploration if a spacecraft carries many small probes to a planet in limited resources such as weight and capacity. Some penetrator probe missions have planned or launched in the world, but now they have not succeeded to explore yet.

In Japan, the LUNAR-A penetrator mission, which is a lunar exploration probe, was planned by ISAS, but was canceled. However, the development of penetrator technology continues, and this LUNAR-A penetrator technology has matured [1]. We have been expected to discuss about the new mission using the heritage of LUNAR-A penetrator.

Martian exploration mission: Our group has proposed the Martian distributed network exploration Nano probe mission SPUR using the next generation entry system of deployable inflatable aeroshell [2]. The goal of SPUR is to demonstrate the technology of distributed exploration to build a network between some nano-class landers and small orbiters. The Martian penetrator probe with deployable inflatable aeroshell that further improved LUNAR-A is one of candidate for the Nano landers in SPUR concept (Fig. 1). To realize the Martian penetrator is important to design the EDL system. Last year, we planned the EDL sequence of Martian penetrator concept (Fig. 2) [3]. We discussed that Martian penetrator has the deployable inflatable aeroshell and the cross parachute as entry and descent systems. This sequence has designed under the constraints on landing and entry system. Especially, it is essential for this inflatable aeroshell as entry system to keep the aerodynamic heating experienced when entering the Martian atmosphere below the heat resistant performance of

inflatable ring, because the aeroshell has a single inflatable torus ring to sustain the aeroshell structure. We have estimated the aerodynamic heating at entry by the simple Tauber equation previously [4]. We need to estimate the heat distribution from the stagnation point to the inflatable torus ring to optimize the aeroshell design and to update the EDL sequence. So, we calculated the heat flux by CFD using RG-FaSTAR which can perform highly efficient calculation with unstructured grid jointly developed by JAXA and Hokkaido university. The result of CFD calculation indicates that Tauber equation may overestimate heat flux for the inflatable aeroshell. Therefore, heat flux on inflatable torus is about 80% of it at stagnation point (Fig. 3). So, the Martian penetrator can use the smaller and lighter aeroshell at entry and descent phase than preliminary concept.

EDL sequence design: CFD analysis has made it possible to be smaller the deployable inflatable aeroshell in the Martian penetrator mission. If we can use that small aeroshell than the preliminary concept, we can expect a solution that is to use only the aeroshell from entry to descent phase without using the cross parachute. And we have begun to discuss about the new EDL sequence of Martian penetrator according to this estimation. In the near future, we will estimate the more accurate entry environment of Martian penetrator by CFD and also obtain the detailed constraints at landing by penetrating test using vertical ballistic range in JAXA to update the EDL sequence of its concept.



Fig. 1. Half model of Martian penetrator and strage case of this probe (left side)
2.5 m deployable inflatable aeroshell (right side)

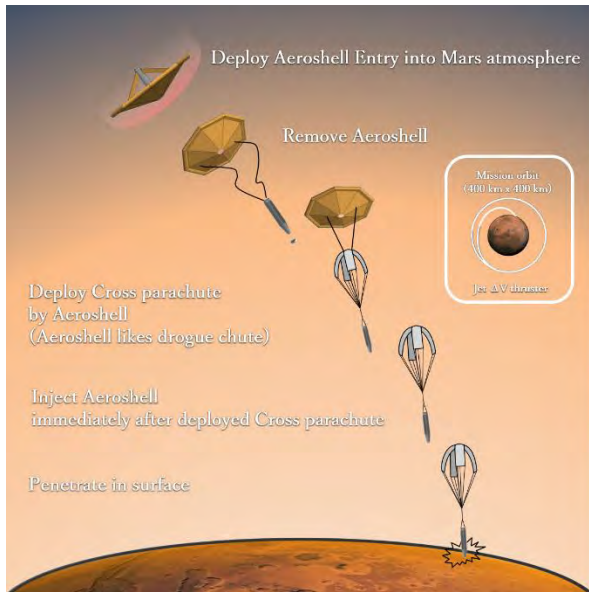


Fig. 2. EDL sequence concept of Martian penetrator. (entry: deployable inflatable aeroshell, descent: cross parachute)

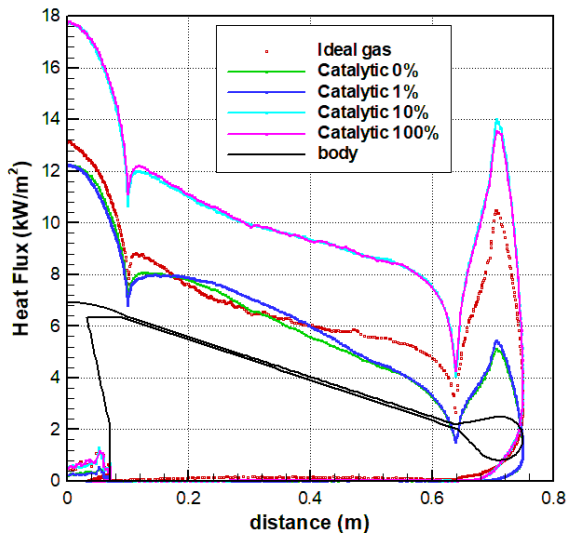


Fig. 3. Aerodynamic heating distribution of Martian penetrator applied ideal gas, real gas (Catalytic 0%, 1%, 10%, 100%) and penetrator probe body are showed.

References: [1] T. Nakajima, M. Hinada, H. Mizutani, H. Saitoh, J. Kawaguchi and A. Fujimura (1996) LUNAR PENETRATOR PROGRAM:LUNAR-A, Acta Astronautica Vol. 39.

[2] K. Yamada (2018) SmallSat Efforts in JAPAN for future planetary exploration, IPPW-2018 Short Course : Small Satellite

[3] T. Kazama, K. Yamada and J. Koyanagi (2018) Study on EDL sequence of Martian penetrator, IPPW-2018

[4] M. E. Tauber, J. V. Bowlest, LiLy Yang, Use of Atmospheric Braking During Mars Missions, AIAA 1990

Modal Analysis of the Orion Capsule Two Parachute System

J. Pei¹, C. Roithmayr¹, R. Barton², D. Matz³, J. Beaty⁴, ¹NASA Langley Research Center, Hampton VA 23681. ²Retired. NASA Johnson Space Flight Center, Houston TX 77058. ³NASA Johnson Space Flight Center, Houston TX 77058. ⁴Retired. NASA Langley Research Center, Hampton VA 23681.

Brief Presenter Biography: Jing Pei works in the Vehicle Analysis Branch at NASA Langley Research Center and is a member of NASA's Engineering and Safety Center (NESC) flight mechanics technical discipline team. His interests include: atmospheric flight mechanics, orbital dynamics, Guidance Navigation & Control, modeling and simulation for launch vehicles, aircraft, UAVs, spacecraft, and re-entry systems.

Introduction: As discussed in ref [1], it is apparent from flight tests that the system made up of two main parachutes and a capsule can undergo several distinct dynamical behaviors. The most significant and problematic of these is the pendulum mode in which the system develops a pronounced swinging motion with an amplitude of up to 24 deg. Large excursions away from vertical by the capsule could cause it to strike the ground at a large horizontal or vertical speed and jeopardize the safety of the astronauts during a crewed mission. In reference [1], Ali et al. summarized a series of efforts taken by the Capsule Parachute Assembly System (CPAS) Program to understand and mitigate the pendulum issue. The period of oscillation and location of the system's pivot point are determined from post-flight analysis [2].

Other noticeable but benign modes include: 1) flyout (scissors) mode, where the parachutes move back and forth symmetrically with respect to the vertical axis similar to the motion of a pair of scissors; 2) maypole mode, where the two parachutes circle around the vertical axis at a nearly constant radius and period; and 3) breathing mode, in which deformation of the non-rigid canopies affects the axial acceleration of the system in an oscillatory manner. Because these modes are relatively harmless, little effort has been devoted to analyzing them in comparison with the pendulum motion.

Motions of the actual system made up of two parachutes and a capsule are extremely complicated due to nonlinearities and flexibility effects. Often it is difficult to obtain insight into the fundamental dynamics of the system by examining results from a multi-body simulation based on nonlinear equations of motion (EOMs). As a part of this study, the dynamics of each mode observed during flight is derived from first principles on an individual basis by making numerous simplifications along the way. The intent is to gain a better understanding into the behavior of the complex multi-body system by studying the reduced set of differential equations associated with each mode. This approach is analogous to the traditional modal analysis technique used to study airplane

flight dynamics [3], in which the full nonlinear behavior of the airframe is decomposed into the phugoid and short period modes for the longitudinal dynamics and the spiral, roll-subsidence, and dutch-roll modes for the lateral dynamics. It is important to note that the study does not address the mechanisms that cause the system to transition from one mode to another, nor does it discuss motions during which two or more modes occur simultaneously.

Pendulum Mode: Over the past 50 years, a number of analytical, numerical, and experimental investigations have been performed with the goal of understanding parachute pitch-plane dynamics (e.g., refs. [4]–[6]). Reference [7] used computational fluid dynamics (CFD) to study the stability of various main parachute configurations from the Apollo and Multi-Purpose Crew Vehicle (MPCV) Programs. It was demonstrated that an increase in the porosity of the parachute improved its stability characteristics, and hence reduce the severity of the pendulum motion. Figure 1 shows representative plots of C_N and C_A comparing a stable versus an unstable main parachute configuration. It is apparent from the C_N versus α plot that the unstable configuration has a negative slope at $\alpha = 0$ and two stable equilibrium points at $\pm\alpha_o$. As described in ref. [7], by adding a "gap" in the parachute (increased porosity), the C_N slope becomes close to zero at $\alpha = 0$ and is considered the stable configuration. In addition, the two stable α_o shift closer to $\alpha = 0$. However, this modification comes at a cost in the reduction of the C_A , which results in a higher descent velocity. References [6] and [8] provide similar insights regarding the flow physics associated with non-porous and porous configurations and how these affect the parachute stability characteristics. The current study focuses on the unstable MPCV main parachute design (modeled by the red curves in Figure 1), which is highly susceptible to the pendulum motion under the two-main cluster configuration.

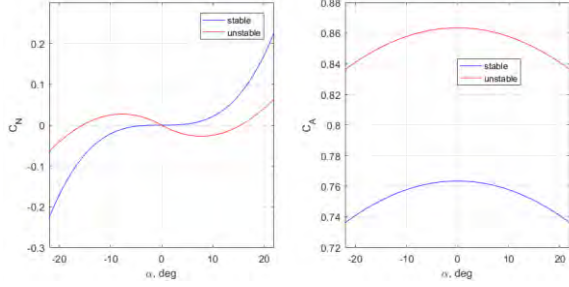


Figure 1. C_N and C_A Coefficients Representative of Unstable versus Stable Parachute Configurations

The planar dumbbell model used to study the underlying dynamics of the pendulum motion is illustrated in Figure 2. The capsule is modeled as a particle rather than an extended rigid body, and aerodynamic forces acting on the capsule are ignored [4]. The two parachutes are treated as a single particle. The rigid body B contains two particles. Particle P_C has a mass of m_C , the total mass of two parachutes, which includes dry mass as well as the mass of air trapped in each of the canopies. Particle P_L has a mass of m_L and represents the capsule. Body B moves such that P_C and P_L remain at all times in a plane fixed in a Newtonian reference frame N . A right-handed set of mutually perpendicular unit vectors n_1, n_2 , and n_3 is fixed in N . Unit vectors n_1 and n_3 lie in the plane in which motion takes place, and are directed as shown in Figure 2; n_1 is horizontal, n_2 is directed into the page, and n_3 is vertical, directed downward. A right-handed set of mutually perpendicular unit vectors b_1, b_2 , and b_3 is fixed in B . Unit vectors b_1 and b_3 are directed as shown in Figure 2; b_1 has the same direction as the position vector $\mathbf{r}^{P_C P_L}$ from P_C to P_L . Unit vector b_2 is directed into the page; note that it is fixed in N as well as in B .

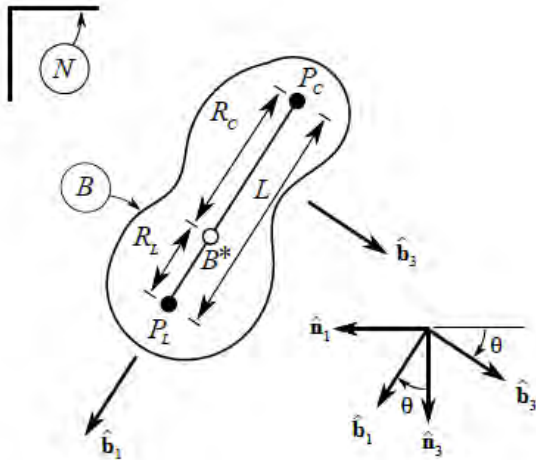


Figure 2. Dumbbell Model for Pendulum Motion

The following two relationships governing translation and rotation of the dumbbell are derived in reference [8]:

$${}^N \mathbf{a}^{B*} = \frac{1}{m_C + m_L} \{-[A_x \sin \theta + A_z \cos \theta] \mathbf{n}_1 + [W_C + W_L - A_x \cos \theta + A_z \sin \theta] \mathbf{n}_3\} \quad (1)$$

$$\ddot{\theta} + \frac{1}{m_C L} [(m_C g - W_C) \sin \theta - A_z] = 0 \quad (2)$$

where $W_L = m_L g$ and g is the magnitude of the local gravitational force per unit of mass. W_C is the sum of the dry weights of the two parachutes; the weight of the air trapped in their canopies is ignored because the gravitational force exerted on that air is assumed to be counteracted by buoyancy effects from the ambient atmosphere. A_x , the magnitude of the resultant of the aerodynamic axial forces applied to the two parachutes, can be expressed as:

$$A_x = 2q_\infty S_{\text{ref}} C_A \quad (3)$$

where q_∞ is the dynamic pressure, S_{ref} is the reference area of a single parachute, and C_A is the drag coefficient for a single parachute. The absolute value of A_z is the magnitude of the resultant of the aerodynamic normal forces applied to the two parachutes; A_z can be expressed as:

$$A_z = -2q_\infty S_{\text{ref}} C_N \quad (4)$$

where C_N is the aerodynamic normal force coefficient for a single parachute. As discussed in references [4] and [5], C_A and C_N are nonlinear functions of α , the instantaneous angle of attack of the parachute:

$$C_A(\alpha) = C_{A_0} + \frac{1}{2} C_{A_\alpha} \alpha_0 \left(\frac{\alpha^2}{\alpha_0^2} - 1 \right) \quad (5)$$

$$C_N(\alpha) = \frac{C_{N_\alpha}}{2\alpha_0^2} (\alpha^3 - \alpha_0^2 \alpha) \quad (6)$$

Here, α_0 is the stable trim angle of attack and C_{N_α} is the slope of the C_N curve at α_0 . An additional damping term $C_{N_{\dot{\alpha}}}$ was added to Eq. (6) to account for unsteady time lag effects in the rotational DOF ref. [3] and [10].

Much insight into the stability of the parachutes can be obtained by assuming that C_N is a linear function of α in the neighborhood of a stable equilibrium point, α_0 . For small-amplitude oscillations, the rotational equation of motion is found to have the form of the second-order linear differential equation governing damped, free vibrations, and a general solution of the differential equation is given. A point on the dumbbell whose trajectory is nearly a straight line for undamped, small-amplitude oscillations is identified. The distance from this pivot

point to the capsule is of interest because the capsule moves as though that distance is the length of a simple pendulum. In the case of a simple pendulum, the length of the string between the pivot point and pendulum bob determines the distance traveled by the bob on a circular arc as the pendulum swings. The length of the string also determines the period of oscillations. Analogously, the distance from the pivot point to the capsule is an important parameter in capsule-parachute pendulum motion. When this distance is minimized, undesirable swinging motion of the capsule is also minimized.

When θ remains small, Eq. (2) can be approximated as

$$\ddot{\theta} + \frac{W_{\text{tot}}}{m_C L C_A} (C_{N\dot{\alpha}})_{\text{tot}} \dot{\theta} + \frac{1}{m_C L} \left[(m_C g - W_C) + \frac{W_{\text{tot}}}{C_A} C_{N\alpha} \right] \theta = 0 \quad (7)$$

This second-order linear differential equation has the form

$$\ddot{x} + 2b\dot{x} + \omega_n^2 x = 0 \quad (8)$$

which governs damped free vibrations. ω_n is referred to as the circular natural frequency, and b/ω_n is the fraction of critical damping, or damping ratio. We define b and ω_n^2 as:

$$b = \frac{W_{\text{tot}}}{2m_C L C_A} (C_{N\dot{\alpha}})_{\text{tot}} \quad (9)$$

and

$$\omega_n^2 = \frac{1}{m_C L} \left[(m_C g - W_C) + \frac{W_{\text{tot}}}{C_A} C_{N\alpha} \right] \quad (10)$$

The general solution of Eq. (7) is then given by

$$\theta = e^{-bt} [C_1 \sin(\omega_d t) + C_2 \cos(\omega_d t)] \quad (11)$$

where the damped natural frequency, ω_d , is given by

$$\omega_d = \sqrt{\omega_n^2 - b^2} \quad (12)$$

and the constants C_1 and C_2 can be expressed in terms of the initial values $\theta_0 = \theta(t=0)$ and $\dot{\theta}_0 = \dot{\theta}(t=0)$,

$$C_1 = \frac{1}{\omega_d} (\dot{\theta}_0 + b\theta_0) \quad (13)$$

$$C_2 = \theta_0 \quad (14)$$

The constants appearing in the fraction on the right-hand side of Eq. (9) are all positive; therefore, the sign

of b is determined by the sign of $(C_{N\dot{\alpha}})_{\text{tot}}$. Exponential decay in θ occurs for $(C_{N\dot{\alpha}})_{\text{tot}} > 0$, whereas there is exponential growth in θ for $(C_{N\dot{\alpha}})_{\text{tot}} < 0$. In either case, the damped frequency ω_d of oscillations in θ is smaller than ω_n ; consequently, the period of damped oscillations is larger than that of undamped oscillations.

Solutions of dynamical equations governing planar motions of the dumbbell reveal the existence of a point Q , on the line joining P_L and P_C , whose trajectory in N is very nearly a straight line; from this observation, it can be inferred that the magnitude of the acceleration ${}^N a^Q$ of Q in N is nearly zero. In what follows, we find the distance L_L from P_L to Q such that ${}^N a^Q \cdot b_3 = 0$ for undamped oscillations having small amplitude. It is also shown that, under the same conditions, ${}^N a^Q \cdot b_1$ is small when the initial values θ_0 and $\dot{\theta}_0$ are zero and small, respectively. Q is referred to as the pivot point; the smaller the value of L_L is, the better the landing conditions will be for the capsule.

The acceleration ${}^N a^Q$ of Q in N is, with the aid of Eq. (1), given by

$${}^N a^Q = \left[\frac{(W_C + W_L) \cos \theta - A_x}{m_C + m_L} + (L_L - R_L) \dot{\theta}^2 \right] b_1 + \left[\frac{(W_C + W_L) \sin \theta + A_z}{m_C + m_L} + (L_L - R_L) \ddot{\theta} \right] b_3 \quad (15)$$

One can determine the value of L_L such that ${}^N a^Q \cdot b_3 = 0$ when θ remains small and oscillations are undamped [8]:

$${}^N a^Q \cdot b_3 = \frac{(W_C + W_L) \sin \theta + A_z - m_C L \ddot{\theta}}{m_C + m_L} + L_L \ddot{\theta} = 0 \quad (16)$$

In view of Eq. (2) and the fact that $W_L = m_L g$, we have

$$\frac{(W_C + W_L) \sin \theta + (m_C g - W_C) \sin \theta}{m_C + m_L} + L_L \ddot{\theta} = g \sin \theta + L_L \ddot{\theta} = 0 \quad (17)$$

Thus, after substitution from Eq. (28) of [8] with $(C_{N\dot{\alpha}})_{\text{tot}} = 0$,

$$-L_L \ddot{\theta} = \frac{L_L}{m_C L} \left[(m_C g - W_C) \sin \theta + \frac{W_{\text{tot}}}{C_A} C_{N\alpha} \theta \right] = g \sin \theta \quad (18)$$

When θ remains small, L_L can be expressed as

$$L_L = \frac{m_C g C_A}{(m_C g - W_C) C_A + W_{\text{tot}} C_{N\alpha}} L \quad (19)$$

It is easily shown that $L_L = R_L$ when $C_A = C_{N\alpha}$, in which case Q is coincident with B^* . When $C_{N\alpha} = 0$, it is evident that L_L slightly exceeds L because the numerator in Eq. (19) becomes the sum of the masses of the dry parachutes and entrapped air, whereas the denominator consists only of the masses of entrapped air.

As the distance L_L decreases the pivot point moves closer to the capsule, which decreases the distance the payload travels over a circular path during pendulum motion. Equation (19) is a key relationship for a two-parachute system that substantiates observations made in previous studies of pendulum motion; 1) increasing the parachute $C_{N\alpha}$ moves the pivot point towards the payload and reduces the distance traveled by the capsule as it swings; 2) decreasing the parachute drag coefficient (by increasing its porosity) moves the pivot point towards the payload and reduces the distance traveled by the capsule as it swings; however, this benefit comes at the expense of increasing the steady-state descent rate, which may not be desirable; 3) decreasing the payload mass (the largest contributor to W_{tot}) shifts the pivot point towards the parachutes and increases the distance traveled by the capsule as it swings, and 4) an increase in the atmospheric density increases the mass of the air entrapped in the canopy (the larger part of m_C) and moves the pivot point towards the parachutes. These observations are consistent with conclusions drawn in Refs. [4], [6], and [7].

Flyout Mode: Reference [2] describes the flyout, or scissors, motion as two parachutes moving sinusoidally away from or toward the vertical axis in a symmetrical manner, while the capsule descends at nearly constant speed. A simple planar model involving three particles is used to study the underlying dynamics of the scissors motion, as shown in Figure 3. Particle P_L has a mass of m_L and represents the capsule. The two parachutes are treated as identical particles, P_B and P_C ; each has a mass of m_C , which includes dry mass as well as the mass of air trapped inside the canopy. The system moves such that the three particles remain at all times in a plane fixed in a Newtonian reference frame N . A right-handed set of mutually perpendicular unit vectors n_1 , n_2 , and n_3 is fixed in N . Unit vectors n_1 and n_3 lie in the plane in which motion takes place and are directed as shown in Figure 3; n_1 is horizontal, n_2 is directed out of the page, and n_3 is vertical, directed downward. P_B and P_C each are connected to P_L by a massless, rigid link; the two links are connected by a revolute joint whose axis is parallel to n_2 . P_B and one link are fixed in a reference frame B , whereas P_C and the other link are fixed in a reference frame C . The orientations of B and C in N are described by angles θ_1 and θ_2 , respectively. A dextral

set of mutually perpendicular unit vectors b_1 , b_2 , and b_3 is fixed in B and directed as shown in Figure 3; b_2 is directed out of the page. A similar set of unit vectors c_1 , c_2 , and c_3 is fixed in C ; c_2 is directed into the page. Note that b_2 and c_2 are each fixed in the three reference frames N , B , and C . The resultant external forces acting on P_L , P_B , and P_C are denoted by F_L , F_B , and F_C , respectively.

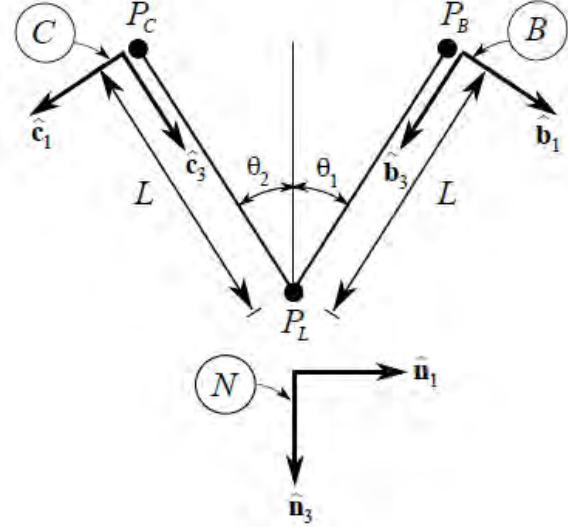


Figure 3. Scissors Mode Planar Model

Maypole Mode: Maypole motion described in reference [1] consists of two parachutes orbiting about the vertical axis. A simplified model used to study maypole motion is illustrated in Figure 4. The three particles P_L , P_B , and P_C are the same as those described in Fig 3; in the present model, however, all three are assumed to be fixed in a rigid body B . A right-handed set of mutually perpendicular unit vectors b_1 , b_2 , and b_3 is fixed in B and directed as shown in Figure 4; b_2 is normal to the plane containing P_L , P_B , and P_C ; and b_3 is parallel to an axis of symmetry of B , which is therefore a central principal axis of inertia of B . A dextral set of mutually perpendicular unit vectors n_1 , n_2 , and n_3 is fixed in a Newtonian reference frame N . n_1 is horizontal, n_2 is directed out of the page, and n_3 is vertical, directed downward. B moves in N such that $b_3 = n_3$ at all times. Moreover, the velocity in N of every point on the axis of symmetry of B has the same constant magnitude and the same direction as n_3 . Two additional sets of dextral, mutually perpendicular unit vectors are introduced for convenience in conducting kinematic analysis and expressing the forces applied to B . Both sets of unit vectors are fixed in B . The first set contains e_1 , e_2 , and e_3 , whereas the second set contains f_1 , f_2 , and f_3 .

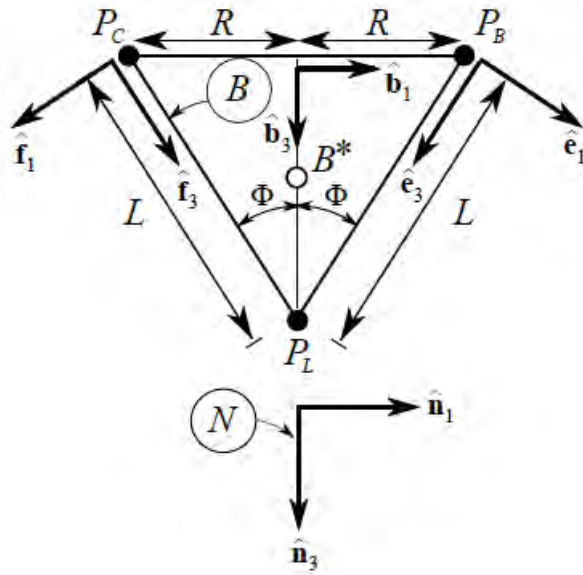


Figure 4. Maypole Mode Model

Breathing Mode: Reference [1] describes the breathing mode

Conclusions:

References:

[1] Ali, Y., Sommer, B., Troung, T., Anderson, B., and Madsen, C., "Orion Multi-Purpose Crew Vehicle Solving and Mitigating the Two Main Cluster Pendulum Problem," No. 2017-4056, *24rd Aerodynamic Decelerator Conference*, AIAA, 2017.

[2] Ray, E. S., and Machin, R. A., "Pendulum Motion in Main Parachute Clusters," No. 2015-2138, AIAA, 2015.

[3] Etkins, B., *Dynamics of Atmospheric Flight*, Dover Publications, Mineola, NY. 2000.

[4] White, F. M., and Wolf, D. F., "A Theory of Three-Dimensional Parachute Dynamic Stability," *Journal of Aircraft*, Vol. 5, No. 1, 1968, pp. 86–92.

[5] Ginn, J. M., Clark, I. G., and Braun, R. D., "Parachute Dynamic Stability and the Effects of Apparent Inertia," No. 2014-2390, AIAA, 2014.

[6] Knacke, T. W., *Parachute Recovery Systems Design Manual*, Para Publications, Santa Barbara, 1991.

[7] Greathouse, J., and Schwing, A., "Study of Geometric Porosity and Drag using Computational Fluid Dynamics for Rigid Parachute Shapes," No. 2015-2131, *23rd Aerodynamic Decelerator Conference*, AIAA, 2015.

[8] Wolf, D., and Heindel, K., "A Steady Rotation Motion for a Cluster of Parachutes," No. 2005-1629, AIAA, 2005.

[8] Roithmayr, C. M., Beaty, J., Pei, J., Barton, R. L., and Matz, D. A., "Linear Analysis of Two-Parachute System Undergoing Pendulum Motion," submitted, 25th Aerodynamic Decelerator Conference, AIAA, 2019.

[9] Pei, J., "Nonlinear Analysis of a Two-Parachute Cluster System Undergoing Pendulum Motion," submitted, 25th Aerodynamic Decelerator Conference, AIAA, 2019.

[10] Pamadi, B. N., *Performance, Stability, Dynamics, and Control of Airplanes*, 3rd Ed, AIAA, 2015, pp. 427-428.

[11] Morelli, E. A., and Klein, V., *Aircraft System Identification, Theory and Practice*, Sunflyte Enterprises, Williamsburg, VA. 2016.

[12] Morelli, E. A., "System IDentification Programs for AirCRAFT (SIDPAC)," <http://software.nasa.gov>.

Multi-Fidelity Modeling for Efficient Aerothermal Prediction of HIAD Configurations with Surface Scalloping. M. Santos¹, S. Hosder², and T. K. West³, ¹Missouri University of Science and Technology, Department of Mechanical and Aerospace Engineering, Toomey Hall, Rolla MO, 65409, ms474@mst.edu, ² Missouri University of Science and Technology, Department of Mechanical and Aerospace Engineering, , Toomey Hall, Rolla MO, 65409 hosders@mst.edu, ³ NASA Langley Research Center, Vehicle Analysis Branch, Bldg. 1201, Hampton, VA 23666, thomas.k.west@nasa.gov.

Introduction and Motivation: Currently NASA is developing deployable re-entry technologies that will allow for an increase in mission possibilities and flexibility over that of rigid aero-shells by allowing for an increase in possible landing sites and maximum deliverable payload mass to planetary surfaces. These technologies include NASA’s Hypersonic Inflatable Aerodynamic Decelerator (HIAD) and the Adaptable Deployable Entry and Placement Technology (ADEPT) concepts (Fig 1.) For the HIAD, the aeroheating on the vehicle during the EDL phase can increase significantly due to surface scalloping of the thermal protection system (TPS) surface. Thus accurate prediction of the surface heat flux, including the increase due to scalloping effects, is needed in the design process to ensure that a robust and reliable TPS is in place.

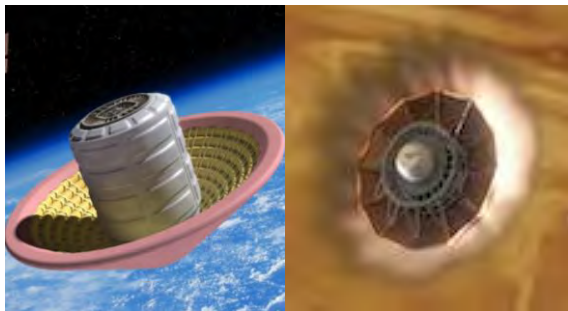


Figure 1. HIAD^[1] (left) and ADEPT^[2] (right) conceptual designs.

This design process can include total heat load calculations, fluid-structure interaction calculations, and Uncertainty Quantification (UQ) of the aerothermal loads, all which may require hundreds or thousands of high accuracy predictions. Unfortunately, high-fidelity computational fluid dynamics (CFD) can be extremely computationally expensive due to the complex physics in these flow regimes (turbulence modeling, non-equilibrium thermo-chemistry, radiation heat transfer, etc.). Therefore using purely high-fidelity CFD simulations for these analyses is not practical and a more computationally efficient modelling process is needed that retains the accuracy of the high-fidelity CFD simulations. By incorporating information from different models of varying fidelity, multi-fidelity modeling has the potential to produce highly efficient, high accuracy models of aerothermal loads on HIAD vehicles with a scalloped TPS surface.

The objective of the project to be presented in this poster is to implement and demonstrate co-Kriging based multi-fidelity modeling approach for efficient turbulent aerothermal prediction of HIAD configurations with surface scalloping in Mars entry. With this study, the multi-fidelity model will incorporate multiple prediction model fidelity levels as well as multiple surface geometry representation fidelity levels. Previous work by the research group, presented at the 2018 IPPW conference, has shown that a co-Kriging based multi-fidelity modeling approach can accurately predict aerothermal loads on a smooth large diameter HIAD under fully laminar flow. This project improves upon the previous work by extending the analysis to turbulent boundary layer flow and by incorporating multiple surface geometry fidelities into the analysis. The co-Kriging based multi-fidelity methodologies developed during this research can also be applied to a wide range of other entry technologies such as rigid aeroshells, ADEPT configurations, and mid L/D configurations.

Approach: To predict the aerothermal response of HIAD geometries, a refined co-Kriging based multi-fidelity method will be used [3]. This method includes determining the sample space, creating a sampling plan, evaluating the different model fidelities at the sample locations, and finally building the co-Kriging multi-fidelity model.

Trajectory and Sample Space. An 18.8 m diameter HIAD in Mars entry will be used in this study. Assuming ballistic entry and using NASA’s exploration feed forward [4] (EFF) study as a guide, it was determined that the vehicle would have a velocity range of 2 to 7 km/s over an altitude range corresponding to atmospheric densities of $6.675e-5$ to $1.00e-3$ kg/m³. The possible nose radius of the vehicle are assumed to range from 4 to 20 m. These velocity, density, and nose radius ranges made up the three-dimensional model sample space.

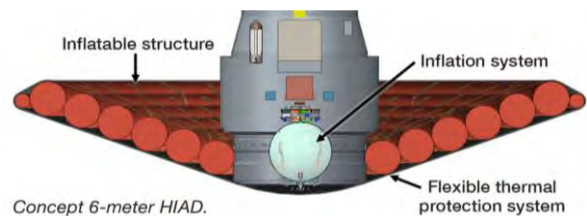


Figure 2. Cross section of a HIAD vehicle^[5].

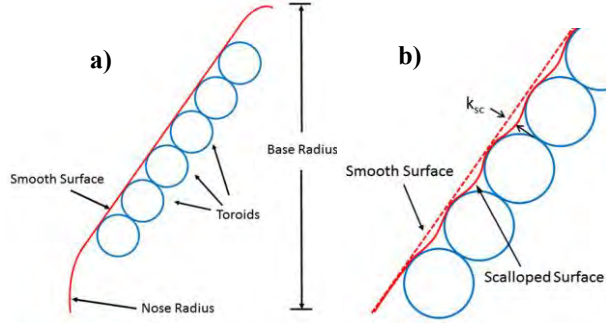


Figure 3 Vehicle geometry with a.) smooth surface and b.) scalloped surface.

Geometry Surface Models. As can be seen in Fig. 2, the HIAD vehicle consists of several concentric inflated toroids with a flexible TPS material stretched over the outside. During planetary entry, surface forces will cause the TPS to deform and be pushed inward in the regions between toroids, known as “scalloping”, as illustrated in Fig. 3. The maximum distance a scalloped surface region deforms from the smooth surface is known as the scallop depth, k_{sc} . Two surface geometry models will be considered in this study, a smooth surface and surface with constant scallop depth.

Prediction Models. Three different prediction model fidelities will be used in the project: engineering correlations [6][7][8], high-fidelity laminar CFD solutions, and high-fidelity turbulent CFD solutions [9]. The high-fidelity models will be based on the LAURA CFD solutions with thermochemical non-equilibrium and 10-species gas. The turbulent CFD solution will use the algebraic Cebeci-Smith turbulence model.

The augmented heating due to scalloping will be modeled by the correlation developed by Hollis [6]. The heating augmentation is dependent on scallop depth and is given by the sum between the laminar and turbulent CFD solutions for a smooth surface geometry.

$$h_{k,turb} = (A_k)(h_{lam}) + (B_k/B_0)(\Delta h_{turb}) \quad (1)$$

Here $h_{k,turb}$ is the augmented turbulent heat transfer coefficient for scallop depth k_{sc} , h_{lam} is the laminar heat transfer coefficient from the LAURA CFD solution, Δh_{turb} is the difference in heat transfer coefficients between turbulent and laminar LAURA solutions, B_0 is a constant, A_k is a constant dependent on scallop depth, and B_k is a constant dependent on scallop depth.

Multi-Fidelity Model. A refined co-Kriging based approach will be used as the multi-fidelity modeling methodology in this study. The approach uses an adaptive sampling scheme based on the root-mean-square error (RMSE) of the multi-fidelity model stagnation point heat flux prediction to determine training point

locations. Also in this approach, the distribution predictions of the aerothermal loads over the vehicle are parameterized using Hicks-Henne bump functions. An autoregressive co-Kriging process [10] is then applied, using the distribution parameters as the model response values. In our multi-fidelity approach, separate multi-fidelity models will be built for the laminar and turbulent heat flux on a smooth surface geometry. The correlation by Hollis will be applied to the laminar and turbulent multi-fidelity models to obtain a multi-fidelity model of heat flux on a scalloped surface geometry.

Preliminary Results. The refined co-Kriging based multi-fidelity modeling process has been applied to fully laminar flows for smooth HIAD geometries. To obtain a multi-fidelity model within 10% mean heating rate accuracy when compared to LAURA over 36 test points, required 24 and 48 high-fidelity training points for convective and radiative heating, respectively. Figures 4 and 5 show the convective and radiative heat flux predictions for a randomly selected test case with smooth TPS surface and fully laminar flow at a velocity of 6.86 km/s, density of 8.42×10^{-5} kg/m³, and nose radius of 12.69 m. From these figures it can be seen that multi-fidelity model prediction is very close to that of the high-fidelity model, outperforming both a single fidelity surrogate model using the same training points and the low-fidelity engineering correlations. Once built, the computational cost of a single evaluation of the multi-fidelity model is on the same order as that of low-fidelity engineering correlations, and five orders of magnitude less than that of the high-fidelity LAURA model.

Work To Be Done. The convective heat flux for fully turbulent flow will be modeled using the co-Kriging based multi-fidelity approach developed for laminar flow. Alongside this a scalloped geometry surface will be used as a third fi-

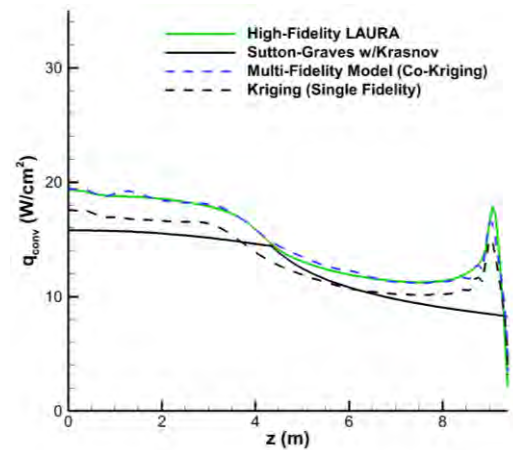


Figure 4. Convective heating prediction for selected test case.

delity level, demonstrating the ability of the developed approach to incorporate different levels of physics and geometric fidelities into the same model. The co-Kriging based multi-fidelity modeling computational framework is fully developed and will not require any further work to model turbulent boundary layer heating or surface scalloping effects.

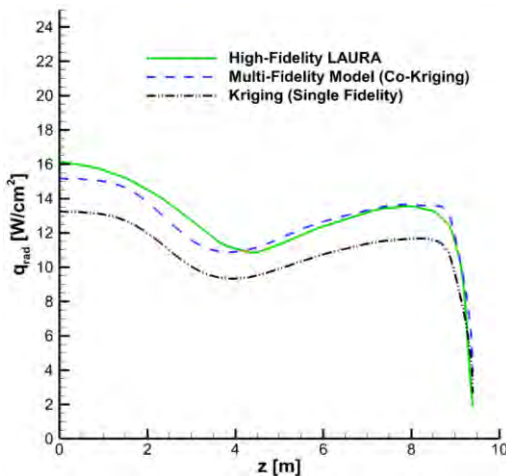


Figure 5. Radiative heating prediction for selected test case.

Acknowledgements. This work was funded by a NASA Space Technology Research Fellowship, Grant No. 80NSSC17K0170.

References:

[1] http://www.nasa.gov/directorates/spacetech/game_changing_development/HIAD, Accessed: 2017-06-12.
 [2] <https://flightopportunities.nasa.gov/technologies/> 139, Accessed: 2017-06-12. [3] Santos M. et al. (2018) *AIAA ISPHSTC* [4] Dwyer-Ciancolo A. et al. (2011) *Tech. Rep. TM-217055*, NASA. [5] https://gameon.nasa.gov/gcd/files/2017/11/HIAD2_FS_170331-5.pdf, Accessed: 3/4/2019 [6] Hollis B. *JSR*, 55, 4, 856-876. [7] Sutton K. and Graves R.A. (1971) *Tech. Rep. TR-R-376*, NASA [8] Krasnov N. (1970) *Aerody. of Bodies of Rev.* [9] Mazaheri A. et al. (2013) *Tech. Rep. TM-2013-217800*, NASA [10] Forrester A. et al. (2008) *Eng. design via surr. modelling: a practical guide*.

Presenter Biography. Mario Santos is a doctoral student in aerospace engineering at Missouri University of Science and Technology where he also obtained a bachelor's degree in aerospace engineering. In 2017 he was awarded a NASA Space Technology Research Fellowship for Multi-Fidelity Modeling and Simulation for the Analysis of Deployable Re-Entry Technologies Under Uncertainty.

DEPLOYABLE MARS AERO-DECELERATORS: RIB DEFORMATION MODELLING AND TESTING.

L. Peacocke¹, P.J.K. Bruce¹, and M. Santer¹, ¹Department of Aeronautics, Imperial College London, London, SW7 2AZ, United Kingdom, l.peacocke16@imperial.ac.uk.

Brief Presenter Biography: Lisa Peacocke is researching deployable Mars entry vehicles as part of her PhD at Imperial College London. Prior to this she worked as a systems engineer for 10 years in the Future Missions department of Airbus UK.

Abstract: Large diameter entry vehicles (> 5 m) for landing high mass payloads at Mars are not currently feasible due to launch vehicle fairing size limitations. One solution is a mechanically deployable aero-decelerator, that increases the diameter of the entry vehicle significantly. This class of entry vehicle uses mechanical ribs and struts to deploy outwards once in space, with flexible thermal protection system (TPS) material tensioned over the deployable structure.

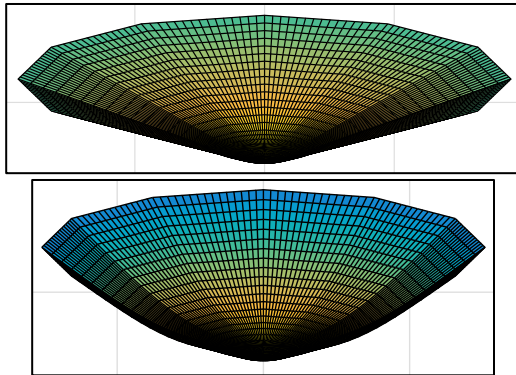


Fig. 1: Undeformed and deformed shape of a 16 m diameter deployable aero-decelerator.

Deployable elements inherently have some flexibility associated with them as they deform due to the aerodynamic pressures experienced during atmospheric entry, as shown in Fig. 1. We have developed a 6 degree of freedom entry trajectory simulator coupled to an aero-structural model that simulates the deformation the ribs experience, and the effect on the trajectory. In previous work [1], we have shown that some deformation can be beneficial for the entry trajectory if the associated mass savings from allowing some deformation can be used to increase the diameter of the entry vehicle. This is shown in Fig. 2, where the total entry vehicle mass has been maintained between test cases, but where mass savings taken from greater rib taper ratios have been used to increase the overall diameter. The larger diameter entry vehicles, even with greater deformation, decelerate higher in the atmosphere.

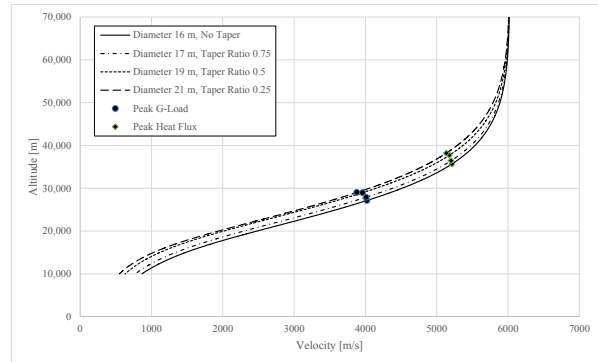


Fig. 2: Velocity-Altitude plots of varying taper ratio and diameter, with peak-load and heat flux loci [1].

Our analysis so far has assumed that the TPS material gores remain flat during aerodynamic loading, while the ribs bend – a simplification that enables speedy coupled analysis for a variety of early phase designs. As a next step, we have developed a test capability to investigate the behavior of an entry vehicle panel under representative loading conditions, to determine the accuracy of our flat TPS assumption, and any required modifications to our code.

A 2.5 m diameter deployable test rig has been developed, along with a single panel rig consisting of two ribs and the flexible TPS gore. These two test rigs allow us to study a section of a deployable aero-decelerator under differential loading, and different TPS attachment and tensioning architectures. Photogrammetry and direct measurement will be used to measure the rib and TPS deformation for the different test cases, with a focus on the flexure and shape of the TPS for different load cases and attachments. It is noted that a flexible TPS architecture with a high pre-tension and strong attachment may well remain largely flat between ribs.

This poster will outline the motivation for the testing, describe the test rigs, provide the latest results from the test campaign to validate rib bending and determine TPS flexure, and interpret the results in terms of potential impact on aerodynamics and entry trajectory. This will contribute to our knowledge of the potential benefits of flexible TPS and mechanically deployable architecture strategies.

[1] Peacocke, L., Bruce, P.J.K. and Santer, M. (2019) *JSR*, 56(2).

Modeling Thermal and Fluid Response of MMOD Impacted Thermal Protection Systems

Olivia Schroeder¹, Eric Stern², and Graham Candler¹, ¹Department of Aerospace Engineering and Mechanics, University of Minnesota, Minneapolis, MN, 55455 (schr1581@umn.edu), ²NASA Ames Research Center, Moffett Field, CA 94035

Introduction: Predictive models for spacecraft planetary entry are challenging to develop due to the multi-physical and multi-scale nature of the problem. Computational modeling has increasingly proven to be an effective way in which we can study high-enthalpy flows, ablation, and their interaction given that it offers high flexibility (can isolate physical phenomena we wish to study), repeatability (useful for obtaining statistical information and risk quantification), and (relatively) low cost. These aspects are more challenging in experimental settings because of the ground-to-flight traceability problem and the high cost associated with ground facilities.

For NASA's missions, thermal protection system (TPS) margins for design are applied successfully by adding thickness (mass) to the heat shield to meet system requirements such as bondline temperature and total recession. Here, the uncertainties associated with these parameters are quantified from extensive aerothermal and thermal response analysis (computational and experimental). However, as NASA's planetary probe and sample return missions become increasingly extreme (higher entry speeds and heating) and more mass restrictive, uncertainty quantification becomes highly important. Additionally, risk quantification associated with failure modes of TPS becomes a critical aspect of the analysis.

This project aims to provide a better understanding of the physical mechanisms by which thermal protection systems fail in the event of an impact with a micrometeoroid or orbital debris (MMOD). These bodies can travel at speeds between 1-70km/s and, upon impact with a spacecraft, may generate cavities or even holes through the heatshield. This is a particular concern for the Mars Sample Return and the Orion missions due to the large amount of time spent in low earth orbit, where the density of orbital debris has been increasing rapidly over the past sixty years, see Fig. 1.

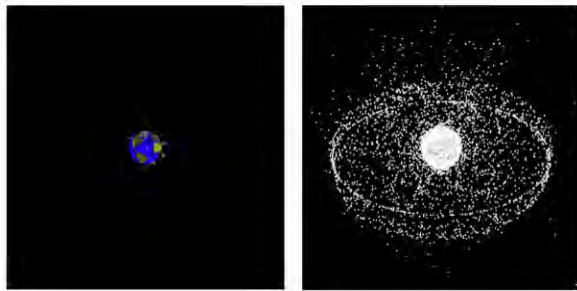


Figure 1: Catalogued orbital debris in 1960 (left) and 2009 (right), from Ref. [3].

Therefore, it is highly important for designers to understand how the heatshield reacts to the flow environment if it contains a cavity, and whether or not the spacecraft can survive reentry in these conditions.

The objective of this work is to assist in the development of models that can help predict TPS failure under known reentry conditions, impact velocity, angle, and location on the body as well as projectile size.

To approach this problem, we first need to consider the aerothermal environment that surrounds the cavity's space. It has been shown that the presence of a cavity increases local heating due to greater shearing [1]. It was also shown that the relative increase in heating, termed "bump factor", was largely dependent on, not only flow parameters, but also the geometric configuration of the cavity (length to width ratio) and depth to boundary layer height ratio. An extensive experimental campaign to investigate these effects was conducted for the Shuttle program. Some noteworthy modeling efforts were also conducted on simulating these experiments [5]. However, these experiments were conducted in a cold-gas facility which implies that the non-equilibrium processes that occur during flight and significantly affect heating rates are not accounted for. Furthermore, there is a need to determine the importance of simulating realistic cavity shapes, see Fig. [2], as opposed to rectangular cuts.

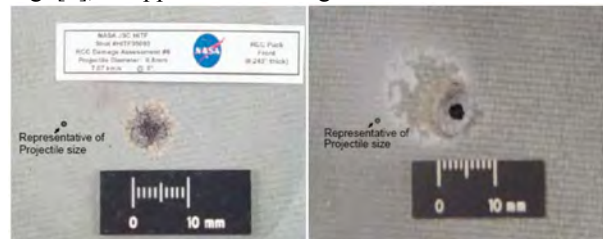


Figure 2: Carbon-Carbon sample after MMOD impact test pre- (left) and post- (right) arc-jet test, from Ref. [4].

In this work, we begin by using the aforementioned experimental campaign as a baseline, and then expanding upon its findings with a computational parametric study. We will first verify the computational methods using these experiments. Once this task is completed, we can begin to change flow configurations to understand how these affect the fluid dynamics and heating augmentation. Finally, we will incorporate real gas effects characteristic of high enthalpy flows and non-equilibrium chemistry. These affects will lastly be studied on realistic cavity shapes predicted empirically for various commonly used TPS materials.

At this stage, the US3D unstructured, finite-volume, hypersonic flow solver [2] is used for simulating the

aerothermal environment of one test case from the experimental setup in Ref. [1]. Simulations are tested for grid convergence and shock alignment. A perfect gas air mixture in thermal equilibrium is used, and thus only one energy equation is solved. Noteworthy is that the fluid dynamic processes are highly coupled to the solid. However, in this preliminary stage, the solid response will be neglected and there will be no effect of the dynamics of the wall boundary on the fluid.

Future plans include the study of heat conduction in anisotropic materials, as well as capturing the ablative processes that the cavity region undergoes. Of particular interest is to characterize the dominant ablation process i.e. whether the mass removal is dominated by shearing processes or by oxidation. Finally, the dynamic interaction between the solid and the gas will be studied.

In summary, this work aims to better understand the physical mechanisms that dominate the reentry flow and material response of an MMOD impacted thermal protection system.

Acknowledgements: This work is supported by a NASA Technology Research Fellowship, under grant number 80NSSC18K1150.

References: [1] Everhart, J., Berger, K., Merski, R., Wood, W., Hollingsworth, K., Hyatt, A., and Prabhu, R., (2010) *NASA/TM-2010-216846*. [2] Nompelis, I., Drayna, T., and Candler, G., (2005) *AIAA Paper 2005-4867*. [3] Christiansen, E., and Rollis, M., (2012) *NASA JSC In space NDI workshop* [4] Christiansen, E., (2009) *NASA/TM-2009-214785*. [5] Palmer, G., Alter, S., Everhart, J., Wood, W., Driver, D., Brown, J., Prabhu, R., (2007) *AIAA Paper 2007-4254*

ABSTRACT

IPPW-2019 -- Oxford, United Kingdom

Enceladus Lander Mission Concept

Leora Peltz and Robert Frampton, The Boeing Company

The plumes of Europa are the source of material in Saturn's E-Ring, an extremely wide and diffuse ring composed of microscopic ice and dust particles. Enceladus' orbit is within the E-Ring; so the E-ring materials are constantly bombarding the surface of Enceladus. Cassini has shown a global variation of surface albedo related to re-accumulation of E-Ring material and plume deposits. The temperature of Enceladus' sunlit surface is around 75 Kelvin. The active south polar surface of Enceladus is exposed to strong chemical processing by direct interaction with charged plasma and energetic particles from the local magnetospheric environment. Chemical oxidation activity is suggested by detection of H_2O_2 at the surface and by substantial presence of CO_2 , CO , and N_2 in the plume gases. Molecular composition of the uppermost surface, that includes ejecta from plume activity, is radiolytically transformed, mostly by penetrating energetic electrons with lesser effects from energetic protons. These molecular ions and the dust grains are chemically processed by magnetospheric interactions that further impact surface chemistry on return to Enceladus' surface. For example, H_2O neutrals dominating the emitted plume gas return to the surface mostly as H_3O^+ ions after magnetospheric processing. Surface oxidant loading is further increased by return of radiolytically processed ice grains from the E-ring. The bombardment of the surface by charged particles leads to changes in the structure of the ice, as well as chemical changes in its composition [1.]. Action by high energy electron bombardment could cause chemical changes, including the formation of peroxides. The charged particles (electrons, protons and heavy ions) and UV radiation induces chemical changes by breaking bonds in the surface ice and regolith, resulting in chemical alteration. Laboratory work with ice in a simulated Enceladus environment suggests that these chemical alterations could produce hydroxyl ions, hydrogen peroxide, and eventually combine with carbonaceous compounds on the surface that may have been deposited there by micrometeorite bombardment.

Investigations are needed to characterize surface alteration by these different mechanisms, under the thermal conditions of the surface and subsurface. These surface observations from a lander could address the questions of how these processes change the physical state of exposed surface materials over time. What differences can be found between the native comminuted regolith, accreted ring material, the plume jet fallout, and thermally segregated materials.

A lander mission would be able to characterize the range of regolith physical properties that characterize the different terrains. Lander *in situ* investigations could yield an understanding of how the surface has evolved over time through impact cratering, tidal tectonics, icy volcanism, thermal relaxation of the topography, and thermal segregation of the materials. This lander would need complex navigation and landing autonomy software. And the option of allowing the lander to hop to a second surface location would add even more cost and complexity, but would allow investigation of surface diversity. Lander instruments could characterize surface ice and mineral composition and study the surface effects of bombardment by grains from the E-ring and charged particles from Saturn's magnetosphere.

Typical lander instruments, such as GCMS, magnetometer, heat flow instruments, accelerometers for seismic activity, and camera, have been considered in a 2010 JPL study conducted for input to the Decadal Survey [2.]. It would also be useful to have a Dual Versatile Langmuir Probe (VLP). The VLP would be designed with cryo-electronics that can function on

the surface of Enceladus in the range 50 to 75 Kelvin, without heaters. This Versatile Langmuir Probe instrument can function as both a classic Langmuir Probe, for measuring electron plasma characteristics, and also, in the dual mode, as an electric field sensor. The VLP can study near-surface plasma environments to provide context for modeling the surface environment and, in particular, the interactions between the surface and dust and charged particle bombardment of the surface. Dust charging in near-surface plasmas encompasses a number of complex processes, including the collection of electrons and ions, photoemission of electrons, secondary electron impact and emission, thermionic emission, and field emission of electrons. The Langmuir Probe has proven to be a valuable instrument for capturing scientific data on charged particles in tenuous space plasmas. Understanding particles and fields at the surface of Enceladus is critical to developing a comprehensive picture of its surface environment. In addition to obtaining the electron temperature and plasma density of the surface plasma environment, a VLP probe also will be capable of measuring DC and low-frequency electric fields and the propagation velocities of plasma waves. The VLP would also be used in the dual mode to measure the horizontal electric field at the surface. This requires two voltage probes near the surface, with a sufficient horizontal separation (several meters). The electric field is determined by subtracting the two potentials from these probes.

In the single Langmuir Probe mode, the VLP would be an extremely valuable instrument to study the vapor plume emitted from Enceladus' south pole. This plume exhibits a complex interaction with surrounding magnetospheric plasma, and in this region, VLP's determination of electron density and temperature holds the potential to enable critical measurements of the Enceladus plume. Also there may be a free-electron plasma near the surface, induced by cosmic UV radiation and by bombardment of heavy ions from the Saturn magnetic field. In the Dual VLP mode, electromagnetic sounding measures the horizontal electric field, and the electrical conductivity of the subsurface from its response to a time-varying source. Conductivity is sensitive to the temperature and composition, and thus is complementary to seismology and heat flow measurements in understanding the subsurface and, perhaps, the nature of the subsurface oceans. [3.]

Some technology development is needed to enhance the functional design of an Enceladus lander. Two of the technology developments needed are.

.1) Battery technology. The lander will require primary batteries that can operate at a low temperature (e.g. minus 60 Celsius or below). The new Lithium-Oxygen battery technology (sometimes called "Lithium-Air) is promising, but low TRL, a technology that could have ten times the energy density of Lithium Ion batteries.

.2) Cryo-electronics. Electronics in a lander at Enceladus need to operate at cryo-temperature, at 70 Kelvin or below. Extensive work has been done with the silicon germanium (SiGe) and gallium nitride (GaN) technologies to develop integrated circuits that operate at these cryo-temperatures. But cryo-electronic circuits are not available commercially as commercial off-the-shelf (COTS); so all electronics for the secondary elements must be custom designed and fabricated as ASICs. Boeing has participated in NASA-funded research to develop SiGe cryo electronics, for analog and digital circuits that can operate below 70 K and can be radiation tolerant.

.3) Regolith electrical properties. The dielectric permittivity ϵ is required for interpreting the electric sounding data. The value can be a function of temperature, composition and compactness of the regolith, as well as frequency of the sounding wave. Laboratory measurements of regolith simulant, at Enceladus temperatures and compactness (from sintering) should be carried out.

Session: Solar System Exploration: Airless Planetary Satellites

Biographical:

Dr Leora Peltz (Presenter) is a Technical Fellow in the Boeing Research and Technology division, in the Solid State Electronics Design (SSED) group in Huntington Beach, California. She has a PhD in electrical engineering from Case Western Reserve University in Cleveland. Dr. Peltz was the Boeing lead on the NASA project to develop silicon germanium (SiGe) radiation hardened cryo-electronics that can function at 40 Kelvin, She is currently principal investigator for a NASA HOTTech project to develop micro-vacuum-tube electronics for Venus Landers that can operate at 500 Celsius for 30 days.

Robert V. Frampton (Co-Author) is a Senior Systems Engineer at Boeing in Huntington Beach, CA. He holds a MS degree in Astrophysics from Louisiana State University in Baton Rouge. Mr. Frampton has been Principal Investigator on two NASA technology development projects: (1) development of precision landing and hazard avoidance (PL&HA) for planetary landers, and (2) characterization of mechanical and thermal properties of icy lunar regolith simulant, at 40 Kelvin in vacuum, conditions of the permanently dark polar lunar craters.

References:

[1.] P.D. Cooper, J.F. Cooper and E.C. Sittler, "Saturn Magnetospheric Impact on Surface Molecular Chemistry and Astrobiological Potential of Enceladus", AGU Fall Meeting 2008, Abstract P23B-1369.

[2.] Mark Adler, et al, "Rapid Mission Architecture Trade Study of Enceladus Mission Concepts" 2010 IEEE Conference, Big Sky, Montana, March 2011, DOI: 10.1109/AERO.2011.5747289

[3.] R.E. Grimm and G.T. Delory, "Next Generation Electromagnetic Sounding of the Moon". Advances in Space Research, 50 (2012) 1687-1701.

Tuesday, July 9 2019

Session	Title	Name	Affiliation	Status
Solar System Exploration I - Mercury, Venus, Giant Planets, and Titan	Altitude Control Balloon Testbed For Planetary Atmospheres	Jasper Thomas	Camosun College	Student
Solar System Exploration I - Mercury, Venus, Giant Planets, and Titan	Investigation Of Suggested Atmospheric Microbes On Venus And Similarities With Earth's Atmosphere.	Denise Lainez	San Jose State University	Student
Solar System Exploration I - Mercury, Venus, Giant Planets, and Titan	Venus Cloud Village: An EDL Sequence For Bringing Humans To The Venusian Atmosphere	Stephen Hunt	University of Southern California	Student
Solar System Exploration I - Mercury, Venus, Giant Planets, and Titan	A Compact, Versatile Net Flux Radiometer For Ice Giant Probes.	Shahid Aslam	NASA Goddard Space Flight Center	
Solar System Exploration I - Mercury, Venus, Giant Planets, and Titan	Science Drivers And Measurement Targets For The In-Situ Study Of Venus' Unidentified Cloud Absorber	Kandi Jessup	Southwest Research Institute	
Solar System Exploration I - Mercury, Venus, Giant Planets, and Titan	Latitudinal variation in abundance of hydrogen sulphide and methane in the atmospheres of Uranus and Neptune: Implication for future entry probes	Patrick Irwin	University of Oxford	
Solar System Exploration I - Mercury, Venus, Giant Planets, and Titan	Investigation of Aerocapture G&C for Ice Giants Missions	Benjamin Tackett	AMA Inc. at NASA Langley Research Center	
Solar System Exploration I - Mercury, Venus, Giant Planets, and Titan	The Annwn Probe: A Scalable Titan Mission Concept for Tracking the Hydrocarbon Cycle	David Davies	UCL/MSSL	Student
Entry, Descent, and Landing Technologies	SERENADE-Ex: an entry capsule designed to characterize the Martian atmosphere and to provide flight data	Tanguy Krzymuski	CentraleSupélec	Student
Entry, Descent, and Landing Technologies	AeroDrop: Dual Aerocapture-Entry Architecture for Multiple Spacecraft Missions	Samuel Albert	University of Colorado, Boulder	Student
Entry, Descent, and Landing Technologies	Obstacle Avoidance With Sequential Convex Optimal Powered Descent Guidance	Padraig Lysandrou	University of Colorado, Boulder	Student
Entry, Descent, and Landing Technologies	Optimal Lift and Drag Modulation Hypersonic Control Options for High Ballistic Coefficient Entry Vehicles at Mars	Nicklaus Richardson	University of Illinois at Urbana-Champaign	Student
Entry, Descent, and Landing Technologies	Atmospheric Neural Net Application To Martian Entry, Descent, And Landing	Shayna Hume	University of Colorado, Boulder	Student
Entry, Descent, and Landing Technologies	Deployable Martian Aero-Decelerators: Design Of A Novel TPS Folding Concept	Danielle O'Driscoll	Imperial College London	Student
Entry, Descent, and Landing Technologies	Analytical Assessment Of Hypersonic Separation Dynamics For Drag Modulation Systems.	Michelle McClary	University of Illinois at Urbana-Champaign	Student
Entry, Descent, and Landing Technologies	Supersonic Retro-Propulsion For Launch Vehicle Stage Recovery And Entry, Descent And Landing Applications.	Kieran Montgomery	Imperial College London	Student
Entry, Descent, and Landing Technologies	An Accessory Minimization Problem for Robust Numerical Predictor-Corrector Aerocapture Guidance	Casey Heidrich	University of Colorado, Boulder	Student
Entry, Descent, and Landing Technologies	Operations Plans for the LOFTID 6-meter HIAD Flight Demonstration	Robert Dillman	NASA Langley Research Center	
Entry, Descent, and Landing Technologies	Scalable Non-Propulsive Dynamic Mass-Shifting Control System For Entry, Descent, And Landing Systems.	Kayla Parcerero	San Jose State University	Student
Entry, Descent, and Landing Technologies	Analysis of Tip-Off Rates During Discrete-Event Drag Modulation for Venus Aerocapture	Annika Rollock	University of Colorado, Boulder	
Entry, Descent, and Landing Technologies	Flight Control Techniques for Optimal Aerocapture Guidance	Rohan Deshmukh	Purdue University	Student
Solar System Exploration II - Airless Planetary Satellites, Asteroids, and Comets	Science investigations of small solar system bodies with a landed CubeSat platform	Ozgur Karatekin	Royal Observatory of Belgium	
Solar System Exploration II - Airless Planetary Satellites, Asteroids, and Comets	Icy Moon Sub-Surface Probe Radioisotope Heat Source Considerations	Daniel Kramer	University of Dayton	
Solar System Exploration II - Airless Planetary Satellites, Asteroids, and Comets	Sample Return from a Relic Ocean World: the Calathus Mission to Occator Crater, Ceres	Lucy Kissick	University of Oxford	Student
Modeling, Simulation, Testing, and Validation	Maturation of Heatshield for Extreme Entry Environment Technology (HEEET) through Extreme Aero-thermal Ground Testing at Arnold Engineering Development Complex (AEDC).	Joseph Williams	AMA Inc. at NASA Ames Research Center	
Modeling, Simulation, Testing, and Validation	Heatshield Entry Modeling Using A Design, Analysis, And Optimization Toolbox	Jeremie Meurisse	STC at NASA Ames Research Center	
Modeling, Simulation, Testing, and Validation	Hypersonic Flows in Thermochemical Nonequilibrium with Immersed Boundary Method and Adaptive Mesh Refinement	Monal Patel	Imperial College London	Student
Modeling, Simulation, Testing, and Validation	Comparison of Chemical Kinetic Models for Aerothermal Simulations of Entry into Gas Giants	Alex Carroll	University of Michigan - Ann Arbor	Student
Modeling, Simulation, Testing, and Validation	Commissioning of the Oxford T6 Stalker Tunnel in Reflected Shock Tunnel Mode	Suria Subiah	University of Oxford	Student
Modeling, Simulation, Testing, and Validation	Status Of Global Reference Atmospheric Model (GRAM) Upgrades	Hilary Justh	NASA Marshall Space Flight Center	
Modeling, Simulation, Testing, and Validation	Development of Patch Integral Method for Hypersonic Thermal Imaging Analysis	Jon Cheatwood	Virginia Tech	Student
Modeling, Simulation, Testing, and Validation	DSMC Simulation Of Hypersonic Flow Over TPS Microstructures	Sahadeo Ramjatan	University of Minnesota	Student

ALTITUDE CONTROL BALLOON TESTBED FOR PLANETARY ATMOSPHERES.

J. Thomas and M. de Jong, Thin Red Line Aerospace (208-6333 Unsworth Rd., Chilliwack, BC, Canada V2R 5M3, jasper.thomas@thin-red-line.com).

Presenter Biography: Jasper Thomas is a student aerospace engineering research assistant at Thin Red Line Aerospace (TRLA). He is tasked with supporting advancement of Thin Red Line's mechanical compression Altitude Control Balloon (ACB) flight hardware as testbed for planetary science aerial platform application.

Introduction: In December 2016 TRLA performed a successful proof of concept flight test of their proprietary mechanical compression ACB system [1]. This paper and associated poster describe development of hardware and software components for TRLA's next generation, high fidelity mechanical compression super-pressure balloon. This latest terrestrial flight vehicle serves as advanced testbed to support ACB system extensibility to Venus and Titan mission insertion [2] [3].

Hardware and Software components: The terrestrial ACB flight system testbed comprises the following primary elements:

1. Multi-segment ACB balloon envelope
2. Mechanical compression winch and tension cable system
3. Power supply system
4. Winch housing
5. Onboard computer systems and software
6. Onboard communication systems
7. Onboard flight control and diagnostic systems sensor suite
8. Redundant payload cutdown systems
9. Emergency flight termination system
10. Experimental payload and test interfaces

1. Multi-segment ACB envelope.

The envelope comprises ten segments for a total distended volume of 14m^3 (500ft^3), 9.5m (31ft) height, and 1.6m (5.2ft) diameter. A primary end objective of the advanced ACB testbed is to demonstrate precise and continuous semi-autonomous control of flight altitude from ground level to 5500 meters ($18,000$ ft) above sea level, with similarly controlled return to ground level. Despite incorporating materials for terrestrial flight, the high-fidelity nature of the testbed envelope will provide invaluable mechanical and materials behavior insights relevant to Venus and Titan environments.

2. Mechanical compression winch and tension cable system. A custom-designed and fabricated servo motor-driven winch system weighing less than 1 kg (2.2 lbs) is capable of applying operational loads of 4.4 kN (990 lbf) to the mechanical compression tension cable. The winch system is mounted in a robust housing which, in

turn, is attached to the exterior bottom of the multi-segment balloon stack. An onboard computer semi-autonomously controls the winch, adjusting the balloon's density and facilitating rapid altitude mobility (*Figure 1*).

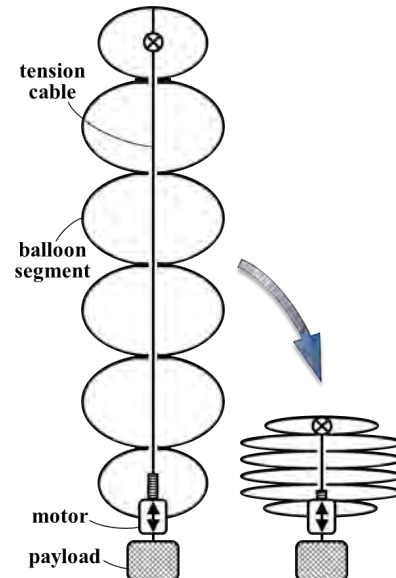


Figure 1. Thin Red Line mechanical compression Altitude Control Balloon (ACB) [4].

3. Power supply system. Redundant high-amperage 14.7V batteries power the mechanical compression system, with 3.7V power supply to the onboard computer. The batteries are positioned in the winch motor housing for investigation of power supply heating during the planned $18,000\text{ft}$ flight. Future flight testing of the high-fidelity ACB platform can support preliminary correlation of flight energy expenditure with potential solar energy contributions.

4. Winch housing. The winch housing consists of a modular and interchangeable, three-part 3D-printed assembly to support design adaptation to mission requirements. It contains the battery bank, gas ports, and the mechanical compression winch system. The winch housing is sealingly attached to exterior of the balloon's bottom apex.

5. Onboard computer systems and software. A modular integrated computer system provides semi-autonomous flight control and remote radio control of the ACB test platform. A single-chip computer communicates via long range radio modem, sending flight and diagnostic data and telemetry, and receiving command inputs.

Onboard telemetry is compared against pre-programmed target setpoints, with offsets triggering autonomous response from the compression system.

6. *Onboard communication systems.* A long-range 433MHz radio modem has been tested to 130km (81mi) line of sight in whiteout snow conditions. While the ACB altitude control is designed to operate autonomously, the ground station can override and modify flight commands. A third layer of control redundancy is provided by a control terminal that can be flown on a chase plane.

7. *Onboard flight control and diagnostic systems sensor suite.* A large array of tracking, flight data, diagnostic, and mechanical compression control loop sensors are positioned throughout the balloon stack.

8. *Redundant payload cutdown systems.* A custom designed, redundant hot-wire cutdown assembly is mounted between winch housing and payload. For payload release the wire is heated with power from the primary ACB batteries, severing the payload train support cable. Cutdown system development supports extrapolation to mission requirements for a variety of deployment options. Dropsonde sensor packages may be similarly deployed by sequential cutdown.

9. *Emergency flight termination system.* A likewise developed heating wire system is mounted near the upper apex of the balloon stack. When triggered, it melts an aperture to release lifting gas.

10. *Experimental payload and test interfaces.* The exterior of the winch housing is outfitted with integration hardpoints for tethered flight and for a variety of camera equipment, sensors, and other instrumentation. The plug-and-play payload train connects to the base of the winch housing. By segregating flight and payload systems, the ACB testbed facilitates testing of numerous payload configurations.

Acknowledgements: The advanced mechanical compression ACB flight system and associated research described in this paper is funded in whole by Thin Red Line Aerospace Ltd. as a technology demonstration and flight hardware development platform supporting future planetary missions.

References: [1] Cutts et al. "Aerial Platforms for the Scientific Exploration of Venus". Cutts et al, 2018. [2] De Jong, M., "Venus Altitude Cycling Balloon", Venus Lab and Technology Workshop, paper 4030. 2015. [3] De Jong, M. and Cutts, J., "Titan Altitude Cycling Balloon" IPPW-12, 2015. [4] de Jong, M. "Systems and Methods including Elevation Control." U.S. Patent No. 10,196,123. 2019.

INVESTIGATION OF SUGGESTED ATMOSPHERIC MICROBES ON VENUS AND SIMILARITIES WITH EARTH'S ATMOSPHERE.

D. Lainez¹, C. Sarmiento¹, L. Rivera¹, M. Boursier¹, U. T. Sou¹ and P. Papadopoulos¹,

¹ San Jose State University, 1 Washington Sq, San Jose, CA 95192

Biography: Denise Lainez is a graduate of San José State University, with a B.S. in Aerospace Engineering focused in Astronautics. Through her education in the Aerospace Engineering department and internship at NASA Ames Research Center in Mountain View, California, Denise has had the opportunity to participate and assist in the development of scientific projects in hopes of making her own contribution to the aerospace industry and our society. .

Introduction: Venus has often been compared to Earth due to the similar size, mass and makeup of the two planets. At approximately 50 kilometers above the surface of Venus, the atmosphere has a similar chemical composition to that of Earth's atmosphere. Gases found in Venus' atmosphere include Hydrogen Sulfide (H₂S), Sulfur Dioxide (SO₂) and Carbonyl Sulfide (COS). High concentrations of H₂S and SO₂ found in Venus' atmosphere suggest that these two gasses are constantly being produced by a catalyst. This is due to the reaction that occurs when H₂S and SO₂ come in contact with one another, in which water and solid Sulfur are produced by this reaction.

For both Carbonyl Sulfide and Sulfur Dioxide to exist, as previously mentioned, a catalyst is needed. On Earth, microbes are the catalysts for these kinds of reactions. The existence of these microbes would also explain the lack of Carbon Monoxide (CO) in Venus' atmosphere. Due to the large amounts of radiation and lightning found on the planet, one would expect high concentrations of Carbon Monoxide. The lack of this byproduct then supports the idea that microbial life could be present on the planet serving as the catalyst for H₂S and SO₂, and metabolising the CO being produced by solar radiation and lightning. Studies also suggest that both H₂S and SO₂ could be produced by volcanic activity on Venus and whose reactions could be catalyzed by metals or chemicals. However the lack of CO cannot be explained by volcanic activity which supports the

idea of microbial life acting as both the catalyst for H₂S and SO₂, and digesting the CO.

Sample Collection: To further confirm the suggestion of these microbes present in Venus' atmosphere, the Venus Atmospheric Research Satellite (VARS) provides a means from which to test for the possible existence of microbial life in Venus' clouds.

The VARS payload is a small satellite system fully instrumented to collect microbial samples from Earth's atmosphere. This research experiment will initially launch on a NASA mission in collaboration with a high-altitude balloon. The payload will be tested at stratospheric altitudes to demonstrate performance at similar Venusian atmospheric conditions. Our initial flight will be confirmation of the payloads capabilities, where samples collected on Earth's atmosphere will serve as a control experiment and will be examined for any signs of microbial life. On Venus the aerobiology in the sample would be analyzed for any signs of H₂S, SO₂, and/or COS. The mission objective of VARS is to successfully collect, retrieve, and preserve atmospheric samples for further analysis through studying the types of organisms or matter collected on the payload.

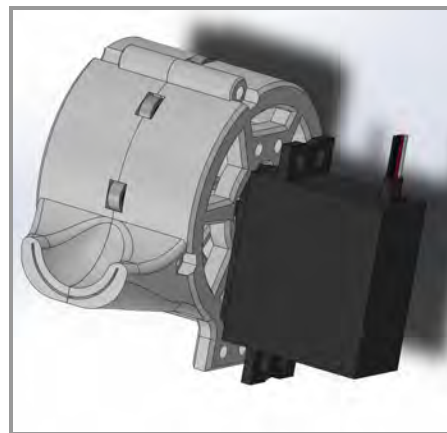


Figure 1: Courtesy of NASA TechEdSat Team

The system includes a probing mechanism known as the automated retractable mechanism (ARM), shown in Figure 1, that utilizes an onboard timer to command and control the probe. A GPS unit is also installed to track the location of the VARS system during all phases of its airborne mission, including ascent, altitude sampling and descent. The ARM is kept in a sterile filter-lined enclosure which conforms to a 1U cubesat form factor.

Summary: The samples collected from potential future missions with the use of VARS could further suggest the existence of bioaerosols or microbial life in a particular part of Venus' atmosphere. This idea could be implemented on future missions to Venus, with a similar objective. The samples obtained on Venus would allow scientists to determine whether Venus' atmospheric composition is similar to that of Earth's. Similarities in composition may suggest the possibility of sustaining life on Venus or the possible effects of climate change on Earth.

References:

^[1] Chisabas, R. S. S., Loureiro, G., de Oliveira Lino, C., "Method for Cubesat Thermal-Vacuum Cycling Test Specifications," *Internatonal Conference on Environmental Systems*, 47th, ICES, Charleston, SC, 2017.

^[2] Blumenthal, Kay, Palen, Smith, "Atmosphere", *Understanding Our Universe*, New York: W.W. Norton and Company, 2012, ISBN 9780393912104.

^[3] "Surviving Extreme Conditions in Space", *European Space Agency*, ESA, 2004.

^[4] Chisabas, R. S. S., Burger, E. E., Loureiro, G., "Space Simulation Chambers State-of-the-Art", *Internatonal Conference on Environmental Systems*, 67th, ICES, Guadalajara, MX, 2016.

^[5] "Thermal Vacuum BakeOut Specification For Contamination Sensitive Hardware", *National Aeronautics and Space Administration*, MSFC-SPEC-1238, NASA, Marshall Space Flight Center, AL, 2007.

^[6] "Chapter 06: Flight Certification Documentation", *Cubesat 101 National Aeronautics and Space Administration Cubesat Launch Initiative*, NASA, 2017.

^[7] Sarafin, T., Doukas, P., Demchak, L., Browning, M., "Vibration Testing of Small Satellites," *Instar Engineering and Consulting*, Revision B, Instar Inc., 2017.

^[8] Williams, D., "Venera: Soviet Missions to Venus," *National Aeronautics and Space Administration*, NASA Goddard Space Flight Center, Greenbelt, MD, 2005.

VENUS CLOUD VILLAGE: An EDL Sequence for Bringing Humans to the Venusian Atmosphere

S. J. Hunt¹ and B. J. Landis², ¹University of Southern California, Los Angeles, CA, huntstep@usc.edu, ²University of Southern California, Los Angeles, CA, blandis@usc.edu

Presenter Biographies: Stephen Hunt and Brian Landis are both graduate students at the University of Southern California in Los Angeles, California. Stephen is pursuing his Master of Science degree in Astronautical Engineering while working in industry as a software engineer at Northrop Grumman. Brian is pursuing his Master of Science degree in Aerospace Engineering while working at Collins Aerospace (UTC) as a Mechanical Design Engineer.

Introduction: It is well known within the space community that the surface of Venus is inhospitable to human life, with surface pressures approximately ninety times that of Earth's, surface temperatures north of four hundred and fifty degrees Celsius, and sulfuric acid clouds dominating the atmosphere [1]. However, at around fifty kilometers altitude, the environment is more welcoming. Pressures drop to about one atmosphere, temperatures to around seventy-five degrees Celsius, and the sulfuric acid clouds are much thinner [1]. This understanding along with Venus' proximity to Earth has brought up the question of whether it is viable to deliver humans to Venus' atmosphere and if so, how it would be done.

Landing a space vehicle within any planet's atmosphere provides unique, interesting challenges, like how to end the landing sequence in buoyant equilibrium with the planet's gravitational forces. Add humans to the mission and issues become exacerbated with needs for larger masses delivered, lower entry decelerations, and a reliable way to leave the planet. Despite these challenges, NASA Langley Research Center has already done research into the problem under project HAVOC [2], and there are surely other mission concepts and vehicle architectures within the solution space.

The Study: The primary focus of this exercise was to explore Entry Descent and Landing (EDL) sequences which enable a human presence in Venus' atmosphere. The motive was pure curiosity and the belief that humans would provide a level of exploration to Venus not attainable by robots. In addition, if systems could be designed to deliver humans, they would also be capable of delivering large amounts of cargo or probes.

Mission Requirements. The mission was to deliver approximately 35 MT of payload, with a minimum crew of 4, to an altitude of 71 km while not exceeding 5 g's of acceleration during entry. Mass requirements were based off what would be necessary to allow initial manned missions of approximately 30 days. It was also

assumed that multiple cargo ships would be delivered alongside the astronauts.

EDL Design. Various EDL architectures were explored as potential solutions, including those that incorporated parachutes and trailing spheres. Ultimately, a multi-staged Hypersonic Inflatable Aerodynamic Decelerator (HIAD) was chosen. A HIAD's ability to decelerate higher in the atmosphere is attractive as well as the potential for it to contribute as a flotation device. A CG offset and corresponding angle of attack provided a positive lift to drag ratio during the HIAD decent, and allowed for a sequence that reduced deceleration loads, while deploying additional inflatable stages lower in the atmosphere enabled the vehicle to further decelerate and float after final "splash down" in the upper atmosphere. System level mass, volume, power, and data link budgeting were created to illustrate the effects of various design decisions on mission parameters.

Analysis Methods. Level two systems design was performed using first-order mathematical models. Equations for acceleration, velocity, down range distance, heat flux, and heat load as a function of altitude were derived from first principles and used to analyze the viability of various architectures. Computational results were then synthesized with engineering data from previous research and mission architectures to identify and select technologies for the mission.

Final Remarks: The entirety of a manned mission to Venus was not considered during this analysis. The findings presented will serve as the foundation for future research. The attempt to have one subsystem serve multiple functions (HIAD would be used for deceleration, flotation, and habitable volume) would particularly be of interest.

References: [1] Arney D. and Jones C. (2015) *High Altitude Venus Operational Concept (HAVOC): An Exploration Strategy for Venus*, Figure 3. [2] Arney D. and Jones C.

A COMPACT, VERSATILE NET FLUX RADIOMETER FOR ICE GIANT PROBES.

S. Aslam¹, R. K. Achterberg², S. B. Calcutt³, V. Cottini², N. Gorius⁴, T. Hewagama², P. G. J. Irwin³, C. A. Nixon¹, A. A. Simon¹, G. Quilligan¹ and G. Villanueva¹. ¹Planetary Systems Laboratory, NASA Goddard Space Flight Center, Greenbelt Rd., MD 20771, USA, ²University of Maryland College Park, College Park, MD 20742, USA, ³Atmospheric, Oceanic and Planetary Physics, Department of Physics, Parks Rd, Oxford OX1 3PU, UK, ⁴The Catholic University of America, Washington DC 20064, USA.

Brief Presenter Biography: Dr. Shahid Aslam is an Instrument Scientist in the Planetary Systems Laboratory, at NASA Goddard Space Flight Center, USA. Apart from working on maturing the net flux radiometer technology readiness level for probe payloads, he is also developing non-dispersive infrared, and Raman and fluorescence spectroscopy instrumentation for planetary landers.

Introduction: The recent Ice Giants Pre-Decadal Survey Mission Report, 2017 (IGPDS) [1] recommended the scientific importance and high priority of sending a mission with an orbiter and a probe to one of the ice giants with preferential launch dates in the 2029-2034 timeframe. Such a mission will advance our understanding of the Solar System, exoplanetary systems, planetary formation and evolution.

Ice giant meteorology regimes depend on internal heat flux levels. Both incident solar insolation and thermal energy from the planetary interior, can have altitude and location dependent variations. Such radiative energy differences cause atmospheric heating and cooling, and result in buoyancy differences that are the primary driving force for Uranus and Neptune's atmospheric motions [2]. The three-dimensional, planetary-scale circulation pattern, as well as smaller-scale storms and convection, are the primary mechanisms for energy and mass transport in the ice giant atmospheres, and are important for understanding planetary structure, circulation, and evolution [3]. These processes couple different vertical regions of the atmosphere, and must be understood to infer properties of the deeper atmosphere and cloud decks. While on Jupiter and Saturn ammonia, ammonium hydrosulfide (NH₄SH) and water are predicted to be key cloud-forming species in the troposphere, the colder atmospheres of Uranus and Neptune are expected to form clouds from methane ice and hydrogen sulfide at observable pressure levels (Fig. 2). It is not known in detail how the energy inputs to the atmosphere—solar insolation from above and the remnant heat-of-formation from below interact to create the planetary-scale patterns seen on these ice giants [1]. An understanding of circulation in these planetary systems requires knowledge of the vertical profile of radiative heating and cooling and also its horizontal distribution. *In situ* measurements with a Net Flux Radiometer (NFR), Fig.

1, using judiciously chosen filter channels, will contribute to our understanding of the balance between the upward and downward radiation streams to evaluate effects due to primary opacity sources, and to establish the extent of solar heating *e.g.*, below 1 bar pressure for Neptune (Fig. 2).

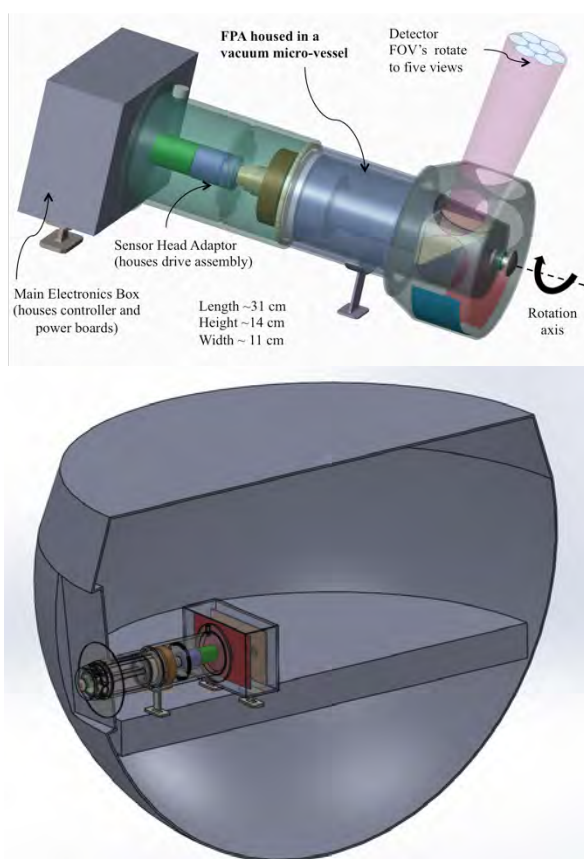


Figure 1. *Top:* Goddard's NFR concept responds to the IGPDS science objectives of a future probe mission to either Uranus or Neptune, but is also applicable to missions to other planets with atmospheres. The NFR will be capable of measuring energy flux in seven spectral bands covering the 0.2-300 μm spectral range, each with a 5° FOV projected into the sky. *Bottom:* Graphic showing accommodation of the NFR on a 1-m diameter probe deck.

***In situ* Net Flux Measurement:** The net energy flux, the difference between upward and downward radiative energy crossing a horizontal surface per unit area

SCIENCE DRIVERS AND MEASUREMENT TARGETS FOR THE IN-SITU STUDY OF VENUS' UNIDENTIFIED CLOUD ABSORBER

K-L. Jessup¹, L. Zasova², S. Limaye³, N. Ignatiev², Y-J. Lee⁴, S. Perez-Hoyos⁵, D. Crisp⁶, R. W. Carlson⁶, D. Grinnspon⁷, M. Bullock⁸, F. P., Mills⁹

1. 1050 Walnut Street, Suite 300 Southwest Research Institute, Boulder CO, USA (jessup@boulder.swri.edu); 2. Space Research Institute for Russian Academy of Sciences, Moscow, Russia; 3. University of Wisconsin, Madison, Wisconsin, USA; 4. University of Tokyo, Japan 5. Universidad del Pais Vasco, UPV/EHUS, Spain; 6. Jet Propulsion Laboratory, California Institute of Technology, Pasadena, California USA 7 Planetary Science Institute 8. Science and Technology Corporation, Boulder, CO, USA; 9 Australian National University, Australia;

Brief Presenter Biography: Dr. Jessup is a solar system scientist who specializes in the observation and modeling of planetary atmospheres. Her current research involves spectroscopic observation, radiative transfer modeling, photochemical modeling and microphysical modeling of the atmosphere of Venus; as well as the development of UV and IR instrumentation for space based solar system atmospheric observing. She is actively involved in international Venus missions including working as a Participating Scientist for JAXA's *Akatsuki* mission to Venus, and serving as member of the joint NASA-Roscosmos Venera-D Mission Science Definition Team. In addition to studying Venus' atmosphere she has published work on the atmospheres of Titan, Pluto and Io.

Introduction: Photos of Venus' distinctive near-

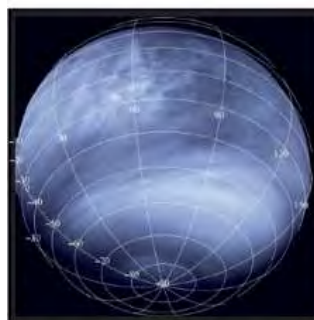


Fig. 1 Venus Monitoring Camera image of Venus at 0.365 μm [9].

UV contrasting cloud features provided the first evidence of Venus' infamous UV absorber [1]. Barker et al. [2] was the first to show the spectral signature of the absorber and assert that broad its absorption at 0.33-0.39 μm occurs ubiquitously at the cloud tops in UV bright and dark regions. Detailed studies of radiative properties of the atmosphere indicate that absorption occurring at the cloud tops at these wavelengths is responsible for 50% of the solar energy deposited in Venus' atmosphere [3]. Consequently, it is understood that the UV absorber must play a key role in planetary energy budget and is expected to be a key factor in the dynamics of the atmosphere including the superrotation of the clouds. For this reason, studying the nature of the UV absorber has been assigned a high priority science target for both in-situ and remote sensing Venus observing programs proposed and executed throughout the decades. However, in spite of on-going research efforts a unique chemical identification of the absorption species—from which extrapolations of the

absorber's chemical reactivity, temperature, UV sensitivity and broad wavelength (UV-visible-IR) spectral response might be made have remained elusive.

Science Drivers for In-Situ Studies: In the absence of a unique chemical identification, modeling of Venus' radiative balance (and energy budget) on cloud characteristics derived from a handful of in-situ probe observations obtained by Pioneer Venus [3, see references therein], cloud top spectroscopy via remote sensing techniques [2,4-7] and two single trajectory in-situ profiles of Venus' atmospheric absorption in the 0.2-0.4 μm region obtained on Venus' night side during the VEGA missions [8]. While these data provide a reasonable standard for climate and general circulation modeling, remote sensing observations continue to reveal the complexity of the absorber—even confirming the potential for multiple absorbing species as first inferred from the VEGA data [8]. For example, long-term image monitoring of the cloud tops at NUV (~0.34-0.39 μm) wavelengths completed by multiple missions to Venus indicates that the morphology of the NUV markings is highly variable. Analysis of Venus Express imaging data [9] indicates that the NUV contrast boundaries are linked to important changes/boundaries in the cloud top altitude and temperature [10]—and may be linked to/or dependent on dynamic, chemical and/or microphysical processes [11]. Thus, the intrinsic characteristics of the absorber such as its state (gas/solid/aerosol), poly-molecular bonding, and/or compositional identity may be highly spatially and/or temporally variant.

Spatially resolved spectra obtained with VIRTIS [4], HST [5,6] and MESSENGER [7] during the Venus Express era all confirm inferences made by [2] that Venus' NUV bright, dark and minimal contrast regions all have significant absorption between 0.33 and 0.39 μm . However, the VIRTIS data also show that the shape of the 0.3 to 0.6 μm cloud top absorption spectra is variant, and that the onset of the absorption from the unidentified species commonly occurs at wavelengths longward of 0.5 μm . In fact, only the relatively NUV bright regions have an 0.3-0.7 μm absorption structure that can be well replicated by the species fit to the disk-integrated Barker et al. data [2,12]. Preliminary analysis of the remotely sensed spectral data also implies that the

variations in the NUV brightness at the cloud tops may correspond to changes in the particle size, age and/or composition of the primary absorber. The observed range of NUV brightness levels may additionally be an indication that a variety of absorbers [7,12-14] with different lifetimes (or responses to UV exposure) contribute to the observed spectral signatures—some of which may even be organic [15,16]. The possibility that an organic species contributes to the unidentified absorption has been repeatedly speculated over the decades [15, 16 and references therein]. This hypothesis has yet to be excluded, especially as on-going research supports (rather than refutes) the compatibility of microbial species within Venus' cloud layer environment and also shows that microbial species may produce spectral signatures compatible with the spectral signature of Venus' unidentified cloud dwelling species as observed via both in-situ and remote sensing techniques [15-17].

Unfortunately, detailed mapping of the vertical distribution of the unidentified absorber relative to LST remains unquantified. As a result, lacking chemical identity, the sensitivity of the absorber's abundance and absorption properties to LST dependent changes in T, pressure, available solar radiation and vertical profiles of other co-located trace Venus atmosphere species is undefined.

In-situ Observation Measurement Targets:

To identify how the changes in the cloud contrasts observable at the cloud tops at UV and NIR wavelengths relates to changes in the nature of the UV absorber and the cloud microphysics **multiple in-situ measurements of Venus' atmospheric properties must be obtained contemporaneously over a broad range of altitudes, LSTs and wavelengths**. These properties include: the 0.2-1.1 μm atmospheric spectral signature, measurements of the atmospheric aerosol particle composition, size and density distribution, temperature profiles measurements, and measurements of the horizontal and vertical wind shears. The high spatial variability of the day-side spectral signature of the absorber at the cloud tops and the impact of its vertical distribution on the planetary energy budget and radiative balance strongly also motivates the need to map the spectrum of the absorber over multiple altitudes at all possible local times **consistently through the full duration of a cloud rotation cycle if not a full Venus day (i.e., 117, 24hr periods of time)**. Access to these data would be monumental in advancing our understanding of Venus' planetary energy budget and superrotation mechanism.

Recent NASA funded aerial platform study shows the capabilities of different aerial options, focusing on payload capacity per platform. Access to the 50 to 60 km range seems within reach for the next generation large capacity aerial platform, and such vehicles would be highly valuable for large flagship style missions. An in-situ aerial platform payload consisting of

UV-visible spectrograph, raman-lidar sensor (with capabilities for organic material detection), anemometer and temperature sensors would make significant strides in understanding the nature and possibly the identity of Venus' unidentified absorbing species. Though technically challenging, the 60-70 km altitude range is also an extremely critical in-situ target for spectroscopic observation because it covers the gap between the cloud top altitude sensed remotely at UV and NIR wavelengths and the altitudes over which in-situ probe spectra have been obtained.

References: [1] Ross, F. E.. (1928), *Astrophys. J.*, **68**, 57-92.; [2] Barker, E. S., et al. (1975). *J.Atmos. Sci.*, **32**, 1205-1211.; [3] Crisp, D. (1986). *Icarus*, **67**, 484-514.; [4] Carlson, et al. (2016) *International Venus Conference*, Oxford, UK; [5] Jessup et al., 2019 *Icarus*, submitted; [6] Jessup. et al. (2017) *15th VEXAG*, 8040; [7] Perez-Hoyos et al., (2018) *JGR-Planets*, **123**, 145-162. [8] Lee et al. (2012), *Icarus*, **217**, 599-609; [9] Titov et al. (2008). *Nature*, **456**, 620-623; [10] Ignatiev, et al. (2009). *J. Geophys. Res.* **114**. E00B43.; [11] Bertuax et al. (1996) *Geophys Res* **101**, 2709–12746; [12] Zasova et. al (1981) *Adv. Science Research*, **1**, 13-16; [13] Pollack et al. (1980) *J Geophys Res* **85**(A13):8141–8150 [14] Krasnopolsky et al. (2018), *Icarus* **299**, 294-299. [15] Grinspoon and Bullock (2007) In: *Exploring Venus as a Terrestrial Planet*, eds L.W. Esposito, E.R. Stafan, and T.E. Cravens, American Geophysical Union, 191–206.; [16] Limaye, S. S. et al. (2018). *Astrobiology*, **18**, 1-17.[17] Limaye et al. (2018), *16th VEXAG*, 8051.

LATITUDINAL VARIATION IN ABUNDANCE OF HYDROGEN SULPHIDE AND METHANE IN THE ATMOSPHERES OF URANUS AND NEPTUNE: IMPLICATION FOR FUTURE ENTRY PROBES

P.G.J. Irwin¹, S.B. Calcutt¹, L.N. Fletcher², N.A. Teanby³, G.S. Orton⁴, D. Toledo¹, A. Braude¹, B. Bézard⁵, S. Aslam⁶, D. Atkinson⁴. ¹Atmospheric, Oceanic and Planetary Physics, Department of Physics, Parks Rd, Oxford OX1 3PU, UK, ²Department of Physics & Astronomy, University of Leicester, University Road, Leicester, LE1 7RH, UK, ³School of Earth Sciences, University of Bristol, Wills Memorial Building, Queens Road, Bristol, BS8 1RJ, UK, ⁴Jet Propulsion Laboratory, California Institute of Technology, Pasadena, CA 91109, USA, ⁵LESIA, Observatoire de Paris, PSL Research University, CNRS, 92195 Meudon, France, ⁶NASA, GSFC, Planetary Systems Laboratory, Greenbelt, MD, 20771, USA.

Brief Presenter Biography: Patrick Irwin is a Professor of Planetary Physics in the University of Oxford. He was a Co-investigator of the Composite Infrared Spectrometer (CIRS) on the NASA Cassini spacecraft and a co-I on the Visible and Infrared Thermal Imaging Spectrometer (VIRTIS) on ESA's Venus Express and Rosetta spacecraft. More recently he has been involved in ground-based spectroscopic observations of the Giant Planets and specializes in retrieving atmospheric composition and temperature from these data.

Introduction: The bulk composition of the atmospheres of Uranus and Neptune is very difficult to constrain since the planets are so cold that many gases condense into clouds well below observable pressure levels. Until recently, the only gases that had been detected were hydrogen, helium, methane, and photochemical products of methane. The composition of the main cloud deck, with tops at pressures of 2 – 3 bar has also been a mystery, but it was generally concluded by researchers to be composed primarily of either ammonia (NH₃) or hydrogen sulphide (H₂S). Observations at the VLA in the 1980s and 1990s[1] found a missing absorption that was attributed to H₂S. This observation implied that the deep abundance of H₂S must exceed that of NH₃ in which case all NH₃ would combine with H₂S to form a cloud of NH₄SH at a pressure of ~40 bar, leaving H₂S alone at the pressure levels sounded by VLA. Such a scenario would then imply that the observable cloud seen at 2 – 3 bar is primarily H₂S ice. However, while this model seemed plausible, there was no direct detection of H₂S in the atmospheres of either Uranus or Neptune (or indeed any of the Giant Planets) to confirm this.

Observations and Analysis: Observations of the visible and near-infrared spectra of Uranus and Neptune have been made recently with three integral-field spectrometers: the MUSE and SINFONI instruments at ESO's Very Large Telescope, and the NIFS instrument at the Gemini/North telescope. These observations image the entire observable disc at sub-arcsecond resolution with each 'pixel' containing a complete spectrum from 1.45 – 1.80 μm for NIFS and SINFONI

(Uranus and Neptune), and 480 – 930 nm for MUSE (Neptune only).

The Gemini/NIFS and VLT/SINFONI spectral ranges include a weak absorption band of hydrogen sulphide (H₂S) and from these observations we have directly detected, for the first time, the presence of this gas in the atmospheres of both Uranus[2] and Neptune[3]. For Uranus we find that the cloud-top abundance (at 2 – 3 bar) of H₂S is 0.4 – 0.8 ppm, at all observable locations, while for Neptune we find a weaker detection of H₂S, but with a clearer signal near Neptune's south pole. The observed cloud-top presence of H₂S constrains the deep bulk sulphur/nitrogen abundance to exceed unity and adds to the weight of evidence that H₂S ice likely forms a significant component of the main observable cloud deck.

At shorter wavelengths, the VLT/MUSE spectral range includes a collision-induced absorption band of hydrogen near 825 nm and the observed spectra can be used to disentangle latitudinal variations in methane (CH₄) abundance from variations in cloud-top pressure of the H₂S cloud. We find that deep abundance of methane in Neptune's atmosphere decreases from a mole fractions of ~ 4-5% at equatorial and mid latitudes to values closer to 3-4% at polar latitudes[4], in broad agreement with an earlier analysis of HST/STIS observations [5].

We have also analysed our MUSE/SINFONI/NIFS data using a Principal Component Analyses (PCA) and find that this technique allows us to map very efficiently the vertical and latitudinal distribution of cloud, hydrogen sulphide and methane in the atmospheres of Uranus and Neptune.

Relevance to planetary probe community: These observations are relevant to the planetary probe community in two ways. First, they can be used to more accurately simulate the likely spectra observed by a Net Flux Radiometer being considered for future missions to Uranus and Neptune [6,7] and thus inform the optimal set of filters needed to maximise scientific return. Secondly, the direct detection of H₂S at the cloud tops confirms that the abundance of NH₃ must be depleted at pressures less than ~ 40 bars. This has an important implication on the telecommunications link

between an entry probe and its orbiter in that there will be much lower absorption if the atmosphere contains more H₂S and less NH₃. This means that a probe could potentially sound to much greater pressure levels than previously anticipated.

References: [1] de Pater, I. et al. (1991) *Icarus*, 91, 220 – 233. [2] Irwin, P.G.J. et al. (2018) *Nature Astronomy*, 2, 420 – 427. [3] Irwin, P.G.J. et al. (2019) *Icarus*, 321, 550 – 563. [4] Irwin, P.G.J. et al. (2019) *Icarus* (under review). [5] Karkoschka, E. and Tomasko, M.G. (2011) *Icarus*, 211, 780 – 797. [6] Aslam, S., et al. (2017) *ESPC Abstracts*, 11, EPSC2017-772-3. [7] Olivier, M., et al. (2018) *Plan. Space Sci.*, 155, 12 – 40.

INVESTIGATION OF AEROCAPTURE G&C FOR ICE GIANTS MISSIONS.

B. M. Tackett¹, S. Dutta², R. W. Powell³, R. A. Lugo⁴. ¹Analytical Mechanics Associates, 21 Enterprise Pkwy., Suite 300, Hampton, VA 23666, benjamin.m.tackett@nasa.gov, ²NASA Langley Research Center, Hampton, VA 23681, soumyo.dutta@nasa.gov, ³Analytical Mechanics Associates, 21 Enterprise Pkwy., Suite 300, Hampton, VA 23666, richard.w.powell@nasa.gov, ⁴NASA Langley Research Center, Hampton, VA 23681, rafael.a.lugo@nasa.gov

Brief Presenter Biography: Ben Tackett is an AMA flight mechanics engineer at NASA Langley working in the Atmospheric Flight and Entry Systems Branch; graduate of Purdue University in Aeronautics and Astronautics.

Introduction: Aerocapture is defined as an intra-atmospheric orbital transfer maneuver where the aerodynamic forces of the vehicle are used to provide the required ΔV needed to transition from a hyperbolic approach trajectory to a desired captured orbit around a target planet. Since aerodynamic forces rather than propulsive systems provide the change in velocity, aeroassist capture techniques generally provide a large savings in propulsion needed to reduce the velocity of the vehicle to orbital speeds. Aerocapture as a technology requires an integrated system level design, including thermal protection systems, actuator systems for aerodynamic modulation, and guidance and control systems that can autonomously command changes in the aerodynamic forces.

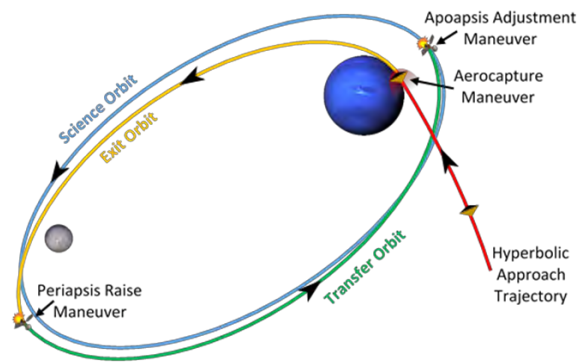


Figure 1: Neptune Aerocapture with a Triton Flyby Science Orbit (not to scale)

Prior Studies: Aerocapture has been assessed and proposed for many targets within our solar system, namely Mars, Venus, Titan, Saturn, Uranus, and Neptune orbiters as well as for Earth demonstration missions, but it has not been attempted on any missions. Many studies performed over the past few decades that have considered aerocapture as a design option have concluded that there are large mass savings that come from using aerodynamic forces rather than propulsive forces to reduce the velocity of a spacecraft and insert into a captured orbit. The benefits of aerocapture are

destination dependent, but some of the largest mass savings occur for the Ice Giants planets. The large velocities of hyperbolic trajectories approaching Uranus and Neptune require a large amount of propulsion to be used to slow down and insert a spacecraft into a science orbit around one of these planets. Aerocapture has been proposed as a maneuver to reduce the propulsion needs by dissipating energy in the atmospheres of the Ice Giants. NASA commissioned a detailed study [3] to quantify the benefits, if any, for use at Neptune which found that aerocapture could deliver 40% more payload than an all-propulsive vehicle, even while having to provide a heat shield. Aerocapture was also found to enable a 3-4 year reduction in trip time compared to all-propulsive options because aerocapture allows for higher approach velocities. Mass savings are also expected at Uranus when using aerocapture for the orbital insertion phase of a mission. The entry environment at Neptune is characterized by large aeroheating and g-loads due to high entry velocities and based on previous studies[1,2,3,7], it was expected that a vehicle with higher lift to drag ratio, L/D, capabilities would be necessary for aerocapture at Neptune. However, recent advances in thermal protection systems, TPS, [3,7,8] and guidance and control, G&C, systems [4,5,] show a path enabling heritage vehicle shapes with more traditional aerodynamic capabilities.

Discussion: The discussion will provide an overview of the capabilities of multiple G&C techniques for the potential Neptune mission described in [Lockwood et al.]. The capabilities of each G&C technique will be determined using a Monte Carlo with the same uncertainties as described in [Lockwood et al.] and the POST2 atmospheric flight simulation tool. The goal is to compare their capabilities for the guidance algorithms and control techniques and the impact on vehicle design. Potential ΔV savings compared to a propulsive orbital insertion will also be provided for each technique as a performance metric.

References:

- [1] Wercinski P. et al. (2002) *Neptune Aerocapture Entry Vehicle Parameters*, AIAA Paper, Vol. 4812.
- [2] Lockwood M. K. et al. (2006) *Aerocapture Systems Analysis for a Neptune Mission*. NASA/TM-2006-214300.
- [3] Spilker T. R. et al. (2018) *Qualitative Assessment of Aerocapture and Applications to Future Missions*, Journal of Spacecraft and Rockets.
- [4] Hiedrich C. R. et al. (2018) *Modern Aerocapture Guidance*

to Enable Reduced-Lift Vehicles at Neptune, AAS 19-221. [5] Deshmukh R. G. et al. (2018) *Investigation of Direct Force Control for Planetary Aerocapture at Neptune*, AAS 19-212. [6] Lu P. et al. (2015) *Optimal Aerocapture Guidance*, AIAA Guidance, Navigation, and Control Conference. [7] Munk M. M. (2008) *Aerocapture Technology Developments by the In-Space Propulsion Program*, Planetary Science Subcommittee Meeting. [8] M. Hofstadter et al. (2017) *Ice Giants Pre-decadal Survey Mission Study Report*, JPL D-100520.

The Annwn Probe: A Scalable Titan Mission Concept for Tracking the Hydrocarbon Cycle

David Aled Davies
University College London
Mullard Space Science Laboratory
Holmbury St. Mary
Dorking, RH5 6NT
07415 455865
david.davies.18@ucl.ac.uk
United Kingdom

Co-Authors: Prof Andrew Coates, Prof Geraint H. Jones

INTRODUCTION

The Cassini mission has enlightened us about many of the conditions of the Saturnian system. One of these discoveries, is of a large population of hydrocarbons in Titan's environment (Waite et al., 2007; Coates et al., 2007). These hydrocarbons are initially formed in the upper atmosphere, however it has been observed that the mass and density of these hydrocarbons increases as the altitude decreases (Coates et al., 2007; Wellbrock et al., 2013). The purpose of this proposed mission would be to explore the hydrocarbon cycle down through the atmosphere, to explore the dunes and surface ice. Due to the Cassini mission coming to an end very recently, now would be an opportune time for another mission to the Saturn system for a long time. As such, this mission concept has been designed to be scalable to different mission sizes, depending on demand for a new mission to Titan as part of a larger Saturnian mission. This masters project concept is being developed so that it could hypothetically be launched in tandem with another mission. As it is part of the thesis, the concept is still in its infancy; however, it will be developed much further by the time of the conference.

MISSION OUTLINE

The basic concept is to use an aerobot (balloon) to glide through Titan's atmosphere, and make measurements at different altitudes. A balloon system is the preferred option, as it would allow to gather data at higher altitude than drones, and does not require as much energy to stay airborne. The air inside the balloon would be heated using the waste heat from an RTG, allowing the balloon to be lifted for minimal power, and also allowing the heat to be radiated away from sensitive electronics. The nature of a balloon would allow the payload to intermittently land on the surface dunes and ice, allowing for further exploration of the hydrocarbon cycle. The hydrocarbon chains are understood to be created high up in the atmosphere, and fall down into the more dense atmosphere (Coates et al., 2009). In order to make these measurements, the balloon would be equipped with a negative ion, positive ion, and neutral particle detector, with design considerations for the negligible ram velocity. The underneath of the craft would contain a drill, and a spectrometer that would be used after landing on dunes or ice sheets in order to conduct the necessary measurements

of what happens to these hydrocarbons after falling to the surface (Hörst, 2017). The underneath would also include a 360° camera that would not only allow the aerobot to view the ground below for possible landing sites, but also provided ample public engagement content.

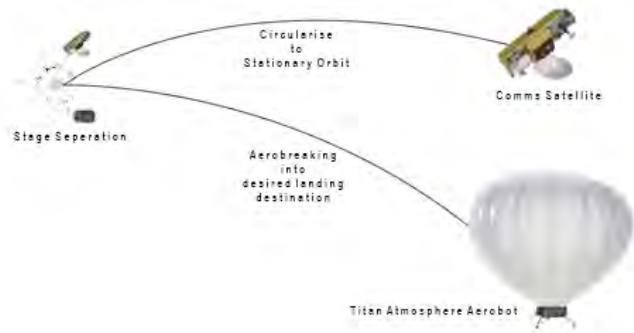


Figure 1. A basic diagram of the separation of the aerobot and Comms Satellite

SCALABILITY

A large part of this proposal is the aforementioned scalability. This allows the mission concept to fit into a future mission in the same way Huygens was carried by Cassini, or allow it to launch as its own larger mission. Lower end of the scale accommodates a single aerobot and a communications satellite. Therefore, the mission outline is the total extent of the mission, with only a small orbital craft to allow for communication with Earth. Scaling up the mission budget can add more aerobots (As they take up a relatively smaller fraction of the mission budget), with each one either being identical, or varying in instrumentation as the mission objectives might evolve. Further increases to the budget can add remote sensing orbital craft (polar orbit) to observe how the climate can change, and how this can effect the measurements from the aerobots. Finally, budget increases beyond this point add more craft to the constellations of aerobots and remote sensing satellites.

The scalable aspect of this mission proposal allows flexibility in fitting into a wide range of possible future missions. A large part of the initial work done for the thesis involved

researching previously proposed Titan exploration missions. Many of these proposals were written as full missions in their own right, and though that allows to explore deeper scientific objectives, it reduces the likelihood of selection by a significant margin. With the Cassini mission still within recent memory, a new Saturn mission with space for smaller attachments is more probable. Therefore, should a mission to the Saturn system be proposed in the future, a scalable mission concept allows for the development of a mission that could accompany the larger mission, whilst still exploring a range of possible mission techniques.

REFERENCES

- Coates, A., Cray, F., Lewis, G., Young, D., Waite, J. and Sittler, E. (2007), 'Discovery of heavy negative ions in titan's ionosphere', *Geophysical Research Letters* **34**(22).
- Coates, A. J., Wellbrock, A., Lewis, G. R., Jones, G. H., Young, D., Cray, F. and Waite Jr, J. (2009), 'Heavy negative ions in titan's ionosphere: Altitude and latitude dependence', *Planetary and Space Science* **57**(14-15), 1866–1871.
- Hörst, S. M. (2017), 'Titan's atmosphere and climate', *Journal of Geophysical Research: Planets* **122**(3), 432–482.
- Waite, J., Young, D., Cravens, T., Coates, A., Cray, F., Magee, B. and Westlake, J. (2007), 'The process of tholin formation in titan's upper atmosphere', *Science* **316**(5826), 870–875.
- Wellbrock, A., Coates, A. J., Jones, G. H., Lewis, G. R. and Waite, J. (2013), 'Cassini caps-els observations of negative ions in titan's ionosphere: Trends of density with altitude', *Geophysical Research Letters* **40**(17), 4481–4485.

BIOGRAPHY



Aled Davies received his B.S. in Space Science and Robotics from Aberystwyth University last year, and is currently working towards the completion of his MSc in Space Science and Engineering from UCL. His academic pursuits includes Systems Engineering, Planetary Physics, Solar Physics, Instrumentation, and Mission Design.

SERENADE-Ex: AN ENTRY CAPSULE DESIGNED TO CHARACTERIZE THE MARTIAN ATMOSPHERE AND TO PROVIDE FLIGHT DATA

T. Krzymuski¹, C. Gentgen¹, A. Michaud¹, G. Villaret¹, H. Brodeau¹, P. Chambon¹, V. de Brosse¹, A. Duhamel¹, C. Duval¹, G. Bailet², L. Bourgois², C. O. Laux². ¹CentraleSupélec, Université Paris-Saclay, 3 rue Joliot Curie, 91192 Gif-sur-Yvette cedex, France, ²Laboratoire EM2C, CNRS, CentraleSupélec, Université Paris-Saclay, 3 rue Joliot Curie, 91192 Gif-sur-Yvette CEDEX, France (gilles.bailet@centralesupelec.fr).

Brief Presenter Biography: Tanguy Krzymuski is a student at CentraleSupélec and a member of the Space Center of CentraleSupélec for CubeSats (CS³).

Introduction : Thermal Protection System (TPS) design of Martian missions has suffered from high margins due to the lack of flight-proven data and unknown processes of ablation and radiation. We propose to fly an entry experiment mission with a compact and low cost platform based on the CubeSat standard (12 U, 34x22x22 cm³ and a mass inferior to 20 kg). This mission consists of the entry capsule for the flight experiment and a data relay staying in orbit. A full suite of instrumentation embedded in the capsule will characterize the entry environment and the response of the thermal shield to these harsh conditions. This paper will present the design of the entry capsule and its instrumentation.

CN : a crucial constraint for the leeward-side TPS: The atmosphere of Mars is composed of 95.97% of CO₂ (against 0.04% on the Earth). During the entry, the CO₂ molecules are dissociated to high energy levels in front of the capsule, mixed with ablation products from the heatshield and recombined downstream. Energy will then be radiated in the direction of the capsule, mainly by CN molecular systems. High uncertainties on the non-equilibrium radiation processes of CN cause increased margins on the total heatflux estimation at the wall. Even if the back side of the capsule is subjected to lower heatfluxes compared to the front, it represents at least 2/3 of the vehicle's surface. With only few centimeters of TPS, a slight margin on the heatflux assessment can conduct to a non-negligible increase of the TPS thickness and therefore of the TPS mass.

Capsule design: Fitting within the CubeSat platform, the 22 cm diameter capsule called SERENADE-Ex will be composed of an outer protective layer of cork P50 [1]. This thermal shield will be able to resist to the harsh environment of entry and will integrate measuring instruments. Within the platform, all the essential subsystems (CPU, data acquisition board, mass memory, COMS) to run the mission will be present in addition of the instrumentation. For the downlink capabilities, the S-Band will be selected with a UHF back-up to ensure the downlink capabilities needed.

Role of TOUTATIS-Ex: The orbital relay TOUTATIS-Ex will inject SERENADE-Ex on the entry

trajectory, and stay in orbit to receive the experimental data through S-band and then relay it back to Earth through to a deployable X-band antenna.

Entry condition representativity : To ensure that the flight data could be used to reduce the margins of TPS design, the entry loads should be representative of recent and future EDL (Entry-Descent-Landing) phases of Martian missions.

The capsule will match the ballistic coefficient of missions like MSL and M2020 (146 kg/m²) and their heat flux (peak at 2.6 MW/m²).

The efficiency of CORK P50 in those conditions has been assessed with ICP (Inductively Coupled Plasma) torch and CO₂ gas mixture (Fig. 1)

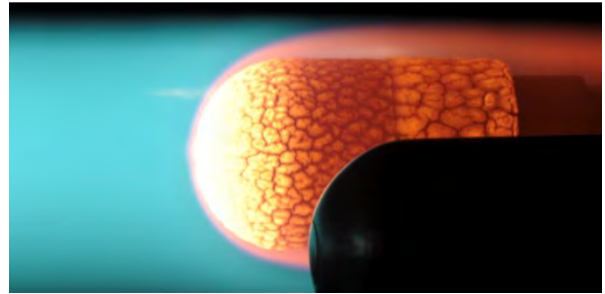


Figure 1 : CORK P50 tested for Mars entry conditions.

Instrumentation : The instrumentation will be composed of conventional means (thermocouple plugs and pressure spools) and innovative ones for plasma radiation measurements [2]. This set of instrumentation will allow to characterize the aerothermal environment around the capsule and the material response of the CORK P50.

Conclusion : SERENADE-Ex is an efficient, cost-effective and compact solution solving the issue of unknown phenomena during the entry to Mars. It will allow a more efficient and safer sizing of TPS for future Mars entry vehicles.

References:

- [1] NASA-CR-170881 (1979), *SRB TPS Materials Test Results in an Arched Nitrogen Environment*, Lockheed Missiles and Space Co.
- [2] G. Bailet, (2018), *Apparatus reduction liability of pollution of an optical access of an optical instrument*. Patent WO2018100255A1.

AERODROP: DUAL AEROCAPTURE-ENTRY ARCHITECTURE FOR MULTIPLE SPACECRAFT MISSIONS

S. W. Albert¹ and R. D. Braun², ¹University of Colorado Boulder (samuel.albert@colorado.edu), ²University of Colorado Boulder (bobby.braun@colorado.edu)

Brief Presenter Biography: Sam Albert is a first-year graduate student in the Entry Systems Design Laboratory at the University of Colorado Boulder. He received a Bachelor of Science in Aeronautical and Astronautical Engineering from Purdue University in 2018.

Introduction: One of the key technologies for entry, descent, and landing (EDL) of deep space missions that needs to mature to enable the next generation of interplanetary missions is aerocapture [1]. Aerocapture is the process of flying through a planet's upper atmosphere upon arrival in order to slow down enough to enter into an elliptical orbit, followed by a maneuver to raise the periapsis out of the planet's atmosphere. This process has significant mass and cost savings for a variety of mission architectures [2].

Separately, smallsats - primarily CubeSats - are revolutionizing the satellite industry [3]. With the recent success of MarCo, the two CubeSats communications relays accompanying the InSight Mars lander, smallsats have proven their merit in deep space applications as well [4]. The low mass, cost, and complexity of smallsats have the potential to yield significant new benefits to interplanetary missions.

In this presentation, I introduce AeroDrop, an innovative EDL concept which addresses both trends above. AeroDrop consists of two spacecraft, a primary and a secondary. The spacecraft travel together during the cruise phase, and have the same approach trajectory. Upon entry, one spacecraft (either the primary or secondary) performs aerocapture, and the other lands via direct atmospheric entry. This method has potential benefits for mass, risk, and engineering and operational complexity for missions delivering orbiters and/or landers to other planets or back to Earth from deep space.

Trade Study: AeroDrop is currently at the trade study stage of development, where the range of its feasibility is being explored. Using an atmospheric flight simulator, I set up a nominal case for the primary spacecraft (be it orbiter or lander), then iterate over one or more parameters to find the viable range for the secondary spacecraft. In every case, the two spacecraft have the same entry conditions (flight path angle, velocity, point of entry, etc.), so the only differences between primary and secondary are geometric properties. The primary spacecraft performs ballistic entry, whereas the secondary is either ballistic or uses simple lift modulation. For example, in a scenario where the primary is an

orbiter performing aerocapture, the secondary could fly fully lift-down with some realistic L/D in order to land.

This trade study will answer a series of questions regarding the range of valid AeroDrop scenarios, including:

- Which destinations are suitable for AeroDrop? Prime candidates so far include Earth return, Mars, or Titan.
- Given a primary spacecraft, what L/D is required for the secondary? Initial results show some valid scenarios with both spacecraft being ballistic.
- Given a primary spacecraft, what range of ballistic coefficients for the secondary result in valid AeroDrop?
- What is the range of flight path angles for a primary orbiter for which a secondary spacecraft can land - and vice-versa for primary lander, secondary orbiter?

In performing this trade study, all parameters will be bounded by current or high-TRL state of the art.

Applications of AeroDrop: By combining the cruise phase and using a single approach trajectory, AeroDrop reduces the overall mass and complexity required for the two spacecraft by avoiding duplicate systems and maneuvers on two independent spacecraft. Operationally, AeroDrop is an efficient way to deliver multiple spacecraft because it is not necessary to divert the primary spacecraft after separation.

A wide variety of mission scenarios would benefit from these advantages of AeroDrop. For example, a small telecom orbiter could be placed in Mars orbit secondary to delivery of a science lander. Alternatively, sample return canisters could perform entry at Earth upon return from the Moon while the primary "cargo" spacecraft enters orbit for refueling. AeroDrop could also have been used on several missions that were proposed but never flew, such as the THOR mission, which would have entered Mars orbit while delivering two high-velocity impactors to the surface [5].

Results: Early simulations have shown multiple valid scenarios for AeroDrop. The results presented at IPPW 2019 will establish and bound the feasibility of AeroDrop, paving the way for further conceptual development and investigation.

References: [1] - NASA Technology Roadmaps TA 9: Entry, Descent, and Landing Systems, 2015. [2] - Hall, J.L., Noca, A.N., Bailey, R.W., "Cost-Benefit Analysis of the Aerocapture Mission Set," *Journal of Spacecraft and Rockets*,

Vol. 42, No. 2, 2005, pp. 309-320. [3] - Bok, C. B., Comeau, A., Dolgoplov, A., Halt, T., Juang, C., and Smith, P., "Small-sats by the Numbers 2018," 2018, pp. 0–21. [4] - Asmar, S. W., and Matousek, S., "Mars Cube One (MarCO): Shifting the Paradigm in Relay Deep Space Operation," SpaceOps 2016 Conference, 2016, pp. 1–7. [5] – "THOR – Tracing Habitability, Organics, and Resources," web, <http://thor.asu.edu/overview/index.html>

OBSTACLE AVOIDANCE WITH SEQUENTIAL CONVEX OPTIMAL POWERED DESCENT GUIDANCE

P. S. Lysandrou¹ and R. D. Braun², ¹University of Colorado Boulder (padraig.lysandrou@colorado.edu), ² University of Colorado Boulder (bobby.braun@colorado.edu).

Presented Biography: Padraig is a first-year graduate student in the Entry Systems Design Lab at the University of Colorado Boulder. He graduated from Cornell University with a Bachelors of Science in Electrical and Computer Engineering.

Introduction: Current and proposed space missions show consistent interest in the exploration of the surface of Mars and other planets. Having sophisticated guidance which allows for pin-point landing in regions of interest, for scientific or colonization reasons, is becoming increasingly important in missions to come. Pin-point powered descent guidance employing online optimization gives us the ability to maximize divert capability, minimize fuel consumption, provide obstacle avoidance, and increase landing zone repeatability for the development of permanent bases. This addresses the key challenge of being robust to uncertainty in initial conditions.

It has recently been shown that online convex optimization is promising for active guidance due to deterministic convergence criteria and low computational cycle times [1]; it is amenable to online implementation. However, the nonlinear dynamics and inherent system constraints are nonconvex, so the problem statement must be manipulated to follow the disciplined convex programming ruleset. The problem is posed as a second-order cone program (SOCP) solved with interior-point methods. This manipulation is done utilizing "lossless" convexification, "successive" linearization, dynamic relaxations, and trust regions.

Atmospheric stochasticity contributes much of the down-range error accumulated in entry and landing phases. Therefore, it is important to implement guidance laws that maximize the divert capability, under large entry atmospheric entry variance, of the rocket-powered platform and simultaneously generate trajectories which are robust to potential adversarial surface features.

The convex optimization framework is widely adaptable to many fields and has recently found successful application in the vertical-takeoff vertical-landing reusable launch vehicle (RLV) industry [2]. With suitable real-time properties, these methods are amenable to implementation on RLVs for their final landing-pad divert maneuvers.

I present a modified version of the Szmuk Açıkmeşe [3] 6DoF successive, or sequential, convexification guidance algorithm, and demonstrate encoding of convex geometrical constraints which denote obstacles or

target wells. The base algorithm iteratively solves the 6DoF free-final-time problem by iteratively solving the linear time variant dynamics with a time dilation coefficient. It can be initialized with a trivial, dynamically inconsistent, point-to-point trajectory. Each iteration makes sure to stay within trust-regions and minimize dynamic and feasibility relaxations. For each sequential iteration, the nominal trajectory approaches a dynamically consistent optimal solution. Each iteration is an informed SOCP sub-problem that can be solved quickly.

I modify this algorithm by modifying the dynamics to include drag and other useful parameters. I also show how to encode geometric convex constraints demonstrating how information from terrain relative navigation can be used on a planetary lander to avoid dangerous regions and to land in precarious positions. Additionally, I show deterministic convergence times results from code generation tools.

References:

- [1] I Ploen, S., Açıkmeşe, B., and Wolf, A., AIAA GNC Conference and Exhibit, Keystone, CO, 2006.
- [2] Blackmore, L., "Autonomous Precision Landing of Space Rockets," NAE Winter Bridge, Vol. 4, No. 46, 2016.
- [3] Szmuk, M., Açıkmeşe, B., "Successive Convexification for 6-DoF Mars Rocket Powered Landing with Free-Final-Time", 2018 AIAA Guidance, Navigation, and Control Conference, AIAA SciTech Forum, (AIAA 2018-0617)

Optimal Lift and Drag Modulation Hypersonic Control Options for High Ballistic Coefficient Entry Vehicles at Mars

N. O. Richardson¹ and Z. R. Putnam², ¹University of Illinois at Urbana-Champaign (noricha2@illinois.edu), ²University of Illinois at Urbana-Champaign (zputnam@illinois.edu).

Brief Presenter Biography: Nicklaus Richardson is a graduate student at the University of Illinois at Urbana-Champaign graduating in May 2019 with his Masters of Science in Aerospace Engineering. He received his Bachelors of Science in Aerospace Engineering also from the University of Illinois at Urbana-Champaign in 2017.

Introduction: Future Mars entry, descent, and landing (EDL) missions will require larger mass vehicles and payloads, especially if humans are to land on the planet. Due to the reliance of supersonic parachutes on Viking-era technology and poor sizing scalability [1], these missions will likely need some form of propulsive terminal descent phase after completing the hypersonic portion of flight. It therefore becomes beneficial to target a terminal descent initiation state that minimizes required propellant. Both the maximization of terminal descent initiation (TDI) altitude and minimization of required propellant are examined in this study.

In order to target an optimal TDI state, one must use some form of hypersonic flight control. There are several options available to do this. The state-of-the-art method for this at Mars is lift modulation through bank angle control as demonstrated by Mars Science Laboratory. By changing the orientation of the entry vehicle, through reaction control system thrusters, the direction of the lift vector can be modulated through a full 360° to provide control.

Another form of hypersonic flight control is drag modulation. Vehicles using a drag skirt to increase the vehicle's drag area can use a deployment or jettison event to change the ballistic coefficient and energy dissipation rate during hypersonic flight, enabling trajectory control. While drag modulation has been previously studied [2] [3], it has yet to be demonstrated by a spacecraft.

A third option may be available by combining both lift and drag modulation techniques. A lift-controlled vehicle may be able to deploy or jettison a decelerator to provide more overall controllability to the system. It may also be advantageous for a vehicle to have this combination of capabilities to mitigate initial risks of flying an unproven technology such as drag modulation.

The benefits and trades to these three hypersonic flight control options to target optimal TDI states are assessed in this study and build upon previous work by Lorenz [4]. The two objective functions examined in

this study are the maximization of TDI altitude and the minimization of propellant mass fraction (PMF) of the propulsive descent system.

The TDI maximum altitudes for each control method were compared along with associated control profiles for various entry conditions. This was done using the 2-degree of freedom equations of motion and an optimal control solver to find a control history to maximize the final altitude during hypersonic flight for a notional vehicle configuration. Direct control of the lift-to-drag ratio and ballistic coefficient were used with no constraint on control rates to represent lift and drag modulation, respectively. Inverse-square gravity and an exponential atmosphere was assumed. Different control modes for each method were characterized, and the combined lift and drag control system was found to be beneficial at near skip-out initial conditions.

The minimization of the PMF was examined by finding the TDI states that were reachable for a given method and calculating which reachable state corresponds to the minimum PMF state. The lift-to-drag ratio of a lift modulation system or the ballistic coefficient ratio of a drag modulation system were varied to characterize how these vehicle parameters effect the reachable TDI states and minimum PMF. Generally, it was found that the increased controllability of a lift and drag control system provided a smaller required PMF and larger reachable set of TDI states with the inclusion of the other control method providing greater benefits to systems of lower controllability i.e. drag modulation systems of low ballistic coefficient ratios or lift modulation systems of low lift-to-drag ratios.

References: [1] Braun R. D. and Manning R. M. (2007) JSR 44, 310-323 [2] Putnam Z. R. and Braun R. D. (2014) JSR, 51, 128-138 [3] Putnam, Z. R., and Braun, R. D., (2014) JSR, 51, 139-150. [4] Lorenz, C. G. Putnam Z. R. (2019) JSR, 0, 1-12

ATMOSPHERIC NEURAL NET APPLICATION TO MARTIAN ENTRY, DESCENT, AND LANDING

S. Hume¹ (shayna.hume@colorado.edu), J. McMahon¹ (jay.mcmahon@colorado.edu), R. Braun¹ (bobby.braun@colorado.edu), ¹University of Colorado, Boulder

Presenter Biography: Shayna is a Ph.D. student at the University of Colorado, Boulder, in Astrodynamics and is conducting research in the area of Entry, Descent, and Landing (EDL). She is currently working to implement predictor-corrector algorithms to improve re-entry systems' reactions to stochastic atmospheric conditions and is working to improve accuracy and capabilities of landing systems. In addition, she is also part of the inaugural class of Isakowitz Fellows, and aims to integrate space technologies into the new space industry.

Introduction: EDL serves as one of the 16 NASA official technology roadmaps – however, many of the NASA developments in atmospheric flight from as distant as the 1960's remain the basis of our capabilities. At this time, the state of the art for planetary re-entry is generally the models used for the Mars Curiosity Laboratory, based on Viking-era EDL technology and augmented by the Sky Crane touchdown delivery system. One of the goals of both public and private industry is to update these heritage methods and implement new knowledge in the areas of aeroassists, descent and targeting, and landing systems in order to use them for upcoming missions to both planets and atmosphere-retaining moons. The development such systems only has the benefit of not only implementing recent advances in machine learning, but also of obtaining concrete space-flight systems outcomes such as increased mass delivery, delivery accuracy, and stochastic robustness, and expanded entry speed envelopes which will help in critical upcoming missions. [3,7]

Abstract: This research is based around the development and use of a robust Martian landing algorithm that will ensure a vehicle's completed mission in the presence of performance and perturbation uncertainties. Predictor-corrector methods are commonly used for on-board guidance in dynamic environments, however, has shortcomings that comes from its assumption of mean state evolution and model parameters. [5] During re-entry, the stochastic nature of the atmosphere and aerodynamic performance often leads to these predictions being inaccurate. [4] By understanding the uncertainty in the propagated mean, it is possible to maximize guidance robustness for future missions. One way this is currently being pursued is in the application of machine learning algorithms to the atmospheric perturbations experienced during the re-entry process.

Method. First, in order to apply the benefits of machine learning onto re-entry problems, it was necessary to create a re-entry framework to train the method on.

To this end, a bank-modulated landing baseline code was created to test simple ballistic and guided results. At this time, such an entry simulation has been created and is being verified against alternate models. The results of this model are being measured against a goal entry corridor and landing zone to ensure high probability success before implementation of a neural net.

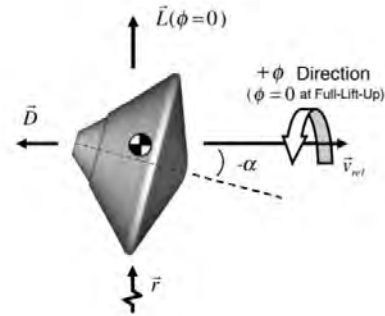


Figure 1: Bank-modulated flight yields higher ranges.

As stated, one of the biggest problems in high-fidelity EDL simulations is the propagation of data which has to keep chasing errors as new stochastic conditions arise. A neural network is comprised of a system of nodes and connections, the basic building blocks of which, neurons, represent information-processing sites. The weighting of the synapses allow the net to learn as it goes, transforming the framework of the net itself (input layer, hidden layer(s), and output layer) into a solution that specifically handles the problem it was trained on. In this work, a neural net will be trained on a series of monte carlo landing simulations for years of data of Martian atmospheric conditions through GRAM 2010, a NASA software being used for this research. The resulting net can then handle a new implementation of a trajectory with significantly less error than previous predictor-corrector models even for non-linear aerodynamic models, because of its training on atmospheric perturbations. A multi-layer, feedforward backpropagation neural network, as shown in Fig. 2, has been chosen for use due to its proven ability to handle unsteady dynamical systems. [12]

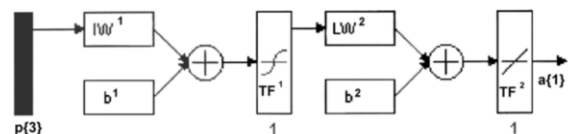


Figure 2: Multilayer feed-forward diagram. [12]

In several studies that applied this type of neural network to aerodynamics, specifically, the output of the net was concluded to be well-equipped to handle roll angle approximations. [12] The result of the application of such successes to Martian landings would be a bank-modulated algorithm that updates based not only on specific range destinations but stochastic changes in the environment it has woven into the output of a trained neural net. By applying the uses of neural nets to these stochastic atmosphere changes, any amount of guidance correction required as conditions change in the trained model will be reduced and the stability, efficiency, and precision of Martian landing systems will be greatly enhanced.

Extensions. Continuing in this work, there are other applications of neural nets to planetary entry in other bodies, “skipping” energy-deflation methods, and aerocapture and other aeroassist maneuvers. In future, the algorithm for Martian entry will be made more robust, and this work will be applied to other opportunities for improving entry during unpredictable conditions.

References: [1] Terejanu, Gabriel, et al. (2008) *JGCD* 31.6. [2] Behcet and Ploen. (2007) *JOG*. [3] Adler, Wright, et al. (2012) *NASA TA09*. [4] Braun and Manning (2007) *JSR*. [5] Brunner and Lu (2014) *JAS*. [6] Christian, Braun et al. (2008) *JSR*. [7] Cianciolo. (2010) *NASA*. [8] DiCarlo. (2003) *MIT Thesis*. [9] Julier and Uhlmann. (2004) *IEEE*. [10] Meginnis et al. (2013) *JSR*. [11] Hunt et al. (1992) *Automatica*. [12] Henderson (2002) *UTK*.

DEPLOYABLE MARTIAN AERO-DECELERATORS: DESIGN OF A NOVEL TPS FOLDING CONCEPT

D.S. O’Driscoll¹, M. Santer² and P. Bruce³, Imperial College London ([1dso13@ic.ac.uk](mailto:dso13@ic.ac.uk), [2m.santer@imperial.ac.uk](mailto:m.santer@imperial.ac.uk), [3p.bruce@imperial.ac.uk](mailto:p.bruce@imperial.ac.uk))

Brief Presenter Biography: Danielle O’Driscoll obtained her Master’s in Aeronautical Engineering from Imperial College London. After completing a year at the European Space Agency (ESTEC) as a graduate trainee she returned to Imperial College in 2018 to research for a PhD.

Introduction: To land successfully on the Martian surface a spacecraft must decelerate to an appropriate speed to avoid destructive impact. Past Mars EDL missions have achieved this deceleration during the entry phase by utilising a rigid heat shield. The sizing of a rigid heat shield is constrained by the diameter of the launcher fairing, currently at a maximum of 4.5m [1], and so to maintain a sufficiently low ballistic coefficient the payload mass is limited. However, if the diameter of the heat shield is increased a higher payload would be possible, for example, human missions and larger robotic systems. A potential means of achieving this is a deployable heat shield that is stowed during launch.

At Imperial College, work is ongoing to develop a deployable lander architecture. To ensure a stable and symmetrical deployment, an umbrella-like configuration has been selected (see figure 1), drawing inspiration from NASA’s ADEPT spacecraft [2]. The ribs retract to a vertical position around the lander body, maximising deployment range. The deployment and retraction of the ribs are controlled by the vertical motion of an actuated ring around the lander body. Both flexible and rigid options for the TPS material between the ribs are being considered.

Aero-structural model: A coupled aero-structural model was developed [3] to investigate the effects of the flexibility of the ribs during entry, and whether this is aerodynamically and structurally beneficial. The ribs were modelled as Euler-Bernoulli beams bending under aerodynamic forces and the TPS panels were assumed to stay in tension during the simulation.

It was found that allowing some rib flexibility offered significant mass savings and, to a certain degree, enables higher stability by damping attitude oscillations during entry.

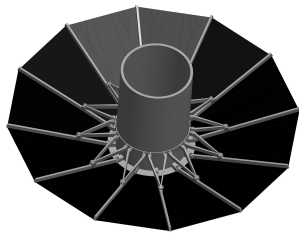


Figure 1: Deployable design concept.

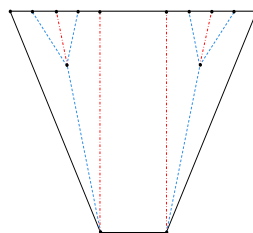


Figure 2: Panel fold pattern.

Objectives: Since rib flexibility has been shown to offer certain advantages, further investigation is being made into this design. In particular, the behaviour of the integrated panels and whether they can meet specific criteria:

- Robust, repeatable deployment and stowage, to ensure mission success,
- Optimal aero-structural performance, to maximise drag and avoid heat transfer hot spots,
- Predictable surface deflection, to mitigate undesired deformations during entry.

This poster will explore the viability of a rigid-panel TPS concept in meeting these objectives.

Selected TPS concept: To maximise deployment range and available payload volume the panels must be stowed flat against the lander central body. Both fold constraints and the dynamics of stowage influence this.

Folding geometry. Whether the panels are made from a flexible or rigid material, a fold pattern will need to be imposed on them to ensure flat stowage. Once the ribs are fully deployed each TPS panel will assume a rigid trapezium shape, and when stowed it must fold into the assigned area between the two vertical ribs, seen in figure 3. The number and length of folds must be minimised, to reduce stacking thickness, and the angle between each fold must be maximised, to reduce the number of sharp intersections which are not aligned with the flow. A symmetrical fold pattern is required for a uniform deployment and to minimise stacking thickness, so subpanels must not fold over the panel centre-line.

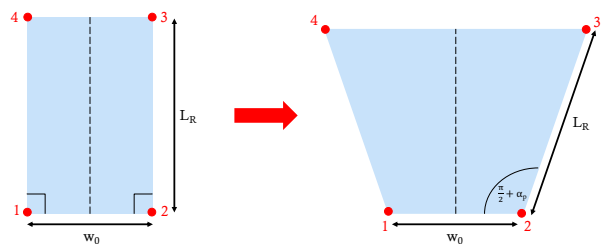


Figure 3: Initial (stowed) and final (deployed) panel geometry.

The final optimised design can be seen in figure 2. Following fundamental origami principals the creases must alternate between valley and mountain folds to ensure stowage and deployment are viable.

Stowage simulation. Since the aero-decelerator has rotational symmetry of order N_R (number of ribs) only one ‘segment’ is needed to simulate stowage (figure 4). The segment is modelled with rigid, zero-thickness subpanels which rotate about spherical joints. An optimum

torsional stiffness between the subpanels and ring displacement rate directs the subpanels into their current stowed state.

This poster will explore the above design process, and how an optimum deployment and stowage configuration is found through analysis and verified through an experimental model.

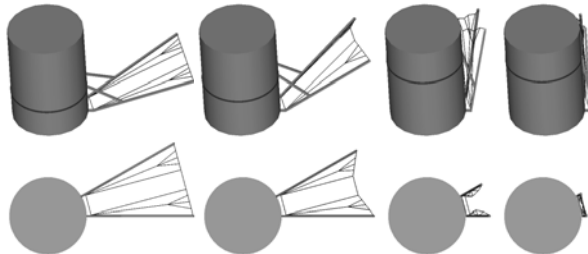


Figure 4: Panel segment stowage sequence.

Continuing work: A scale model will be manufactured to demonstrate the repeatability of the stowage and deployment sequence. The model will also undergo wind-tunnel testing to replicate the aerodynamic forces that will act on the aero-decelerator during entry to the Martian atmosphere. The aero-structural model will be updated to include the panel fold geometry and material properties, and the impact of architecture on trajectory will be examined. This will give greater insight into panel deflection and aero-structural performance.

References:

[1] Braun, R., and Manning, R. (2007) "Mars Exploration Entry, Descent and Landing Challenges", *Journal of Spacecraft and Rockets*, Vol. 44, No. 2, pp. 310-323.

[2] Venkatapathy, E., Hamm, K., Fernandez, I., Arnold, J., Kinney, D., Laub, B., Makino, A., McGuire, M., Peterson, K., Prabhu, D., Empey, D., Dupzyk, I., Huynh, L., Hajela, P., Gage, P., Howard, A., and Andrews, D.. "Adaptive Deployable Entry and Placement Technology (ADEPT): A Feasibility Study for Human Missions to Mars", *21st AIAA Aerodynamic Decelerator Systems Technology Conference and Seminar, Aerodynamic Decelerator Systems Technology Conferences*.

[3] Peacocke, L., Bruce, P.J.K., Santer, M., (2018) "Coupled Aero-Structural Modelling of Deployable Aero- Decelerators for Mars Entry."

ANALYTICAL ASSESSMENT OF HYPERSONIC SEPARATION DYNAMICS FOR DRAG MODULATION SYSTEMS.

M. N. McClary¹ and Z. R. Putnam², ¹Graduate Research Assistant, Aerospace Engineering, University of Illinois at Urbana-Champaign, MC-236, 104 S. Wright Street, ²Assistant Professor, Aerospace Engineering, University of Illinois at Urbana-Champaign, MC-236, 104 S. Wright Street.

Brief Presenter Biography: Michelle McClary is a first year Master's student in Aerospace Engineering at the University of Illinois at Urbana-Champaign.

Introduction: Large, potentially deployable, drag areas have been shown to be a viable option for landing large mass payloads on planetary surfaces. Deployable drag areas may be deployed and inflated prior to atmospheric entry and have the advantage of not being limited by fairing vehicle size constraints. With an increase in drag area, the vehicle's ballistic coefficient is lowered which corresponds to lower heat rates and integrated head loads during hypersonic flight in addition to deceleration at higher altitudes. The drag area may be jettisoned during descent to allow for further configuration changes and entry, descent, and landing (EDL) events. The jettison event can also be used to control the range of the vehicle by jettisoning the drag area at a specified appropriate time during EDL [1].

NASA's Mars Design Reference Architecture 5.0 – Addendum #2 investigates and ranks different EDL architectures for robotic and human missions to the surface of Mars. In the architectures produced in this study, the drag area jettison event was chosen to be a forward or rear exit method to leverage the difference in ballistic coefficients between the vehicle and drag area. The forward exit was determined to be the best alternative because of mechanical simplicity and rapid execution. It was also identified that there is the possibility of recontact of the drag area with the vehicle during the jettison event. Of the architectures investigated, some of these vehicle configurations were determined to have higher risks of recontact. In the case of forward exit vs rear exit, rear exits have a higher probability of recontact [2]. Other work done on this topic has assumed the jettison event to take place at an angle of attack of zero and to be instantaneous with a period of free fall following to ensure no recontact. In this work separation time scales are provided as estimates based on the assumptions made [3]. With the possibility of recontact, work must be done to model the dynamics of the jettison event to reliably predict if the drag area will recontact the vehicle and to provide accurate separation time scales.

This study analyzes the jettison event where the vehicle performs a forward exit through the drag area. Closed-form analytical relationships are developed that relate separation dynamics to vehicle properties. Accurate modeling of this event is imperative to ensuring that

separation time scales are accurate and the risk of recontact after jettison is minimized. Flight trajectories are modeled using the two degree-of-freedom equations of motion. The vehicle is modeled as a blunted spherecone and the drag area is modeled as a rigid conical frustum. The aerodynamic coefficients are determined using Modified Newtonian Aerodynamics. Atmospheric density is modeled using exponential atmosphere. Separation time scales and recontact scenarios are identified over a range of vehicle properties and freestream conditions. Analysis of vehicle and drag area parameters will demonstrate which vehicle and drag area properties are most influential in separation time scales and recontact scenarios.

References:

- [1] Putnam, Z. R., Braun, R. D., (2014) *JSR*, 51, 128-138.
- [2] Drake, B. G., (ed), (2014) "Mars Design Reference Architecture 5.0 – Addendum #2".
- [3] Cianciolo, A. D., Davis, J. L., Shidner, J. D., Powell, R. W., (August 2010) "Entry, Descent and Landing Systems Analysis: Exploration Class Simulation Overview and Results".

SUPERSONIC RETRO-PROPULSION FOR LAUNCH VEHICLE STAGE RECOVERY AND ENTRY, DESCENT AND LANDING APPLICATIONS.

K. Montgomery¹, S. Navarro-Martinez² and P. Bruce³. Department of Mechanical Engineering, Imperial College London, Kensington, London, SW7 2AZ. k.montgomery17@imperial.ac.uk

Brief Presenter Biography: Kieran Montgomery is a first year PhD student at Imperial College London working in the thermofluids research group within the Department of Mechanical Engineering.

Motivation: As we attempt to land larger and heavier craft on Mars, current entry, descent and landing (EDL) systems are reaching their limits[1]. Supersonic parachutes become larger and heavier with increased payload mass, therefore for manned missions to Mars, these EDL techniques are not sufficient. Supersonic retro-propulsion (SRP) is a novel technology that aims to rectify this. Not only SRP will reduce the payload's velocity, it could also provide a more controlled and accurate re-entry. However, SRP is an immature concept, and much research is needed before we can realise the full potential of this promising EDL technology.

State-of-the-art: The basic flow physics of a lander using SRP are yet not well-understood [2]. Very few studies exist in the open literature detailing how force coefficients vary with parameters such as jet thrust coefficient C_T , jet number and position, Mach number M , and craft orientation. Experiments on SRP are particularly challenging, due to the mismatch in physical scales between wind-tunnel test models and the real application and practicalities of simulating a jet exhaust in a laboratory environment. Numerical studies can overcome some of these issues but high fidelity methods are required to accurately capture the complex flow physics and its interactions in a typical SRP environment.

Objectives: This poster presents preliminary results from a computational study using state-of-the-art tools to systematically explore the flow physics of SRP on a realistic candidate geometry. The variation of basic parameters such as pressure drag and shock stand-off distance with flow conditions are studied and reported. The ultimate goal of the work is to develop a set of design guidelines that can be used as a tool to assess the potential impact of SRP on an EDL mission.

CompReal: Simulations have been performed using CompReal: a compressible Navier-Stokes solver, with capability to capture real-gas effects and thermochemical non-equilibrium. Shock-capturing is performed using an hybrid second/fourth order accurate HLLC-Riemann/finite difference solver. Simulations have been carried out with non-uniform grids, using adaptive mesh refinement. Validation of the code is ongoing.

Test case definition: Tests have been performed using the Phoebus lander geometry (Figure 1), provided by the European Space Agency [3] (ESA) in a supersonic free-stream. Simulations have been performed with and without SRP over a range of different jet thrusts (determined by the ratio of tank stagnation pressure to nozzle exit pressure), angles of attack and Mach number. The model for the Martian atmosphere is The Mars atmosphere model by NASA[4].

Preliminary results: Study of the work done on the Phoebus geometry concluded that there exists a reduction in pressure drag once the SRP is activated. Furthermore, this reduction increases as we increase the strength of the SRP. Simulations for a range of conditions are ongoing.

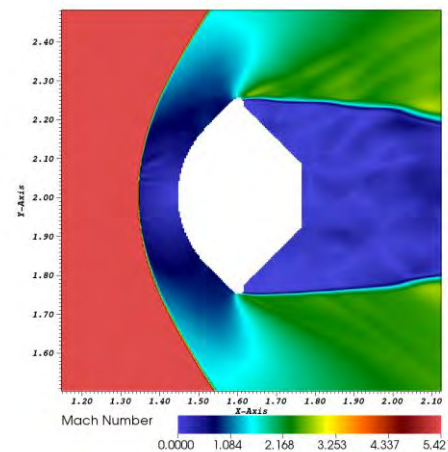


Figure 1: Mach number contours around the Phoebus craft in a Mach 5.4 flow, at 20 km above the Martian surface.

References:

- [1] Bakhtian, N.M., (2012) *Drag Augmentation via Supersonic Retropropulsion for Atmospheric Deceleration* (Doctoral dissertation, Stanford University).
- [2] Bakhtian, N.M. and Aftosmis, M.J., (2011) *Maximum Attainable Drag Limits for Atmospheric Entry via Supersonic Retropropulsion*. In 8th International Planetary Probe Workshop, 1-28.
- [3] Ferracina, L., Marraffa, L. and Longo, J., (2012) December. *Phoebus: A Hypervelocity Entry Demonstrator*. In ESA Special Publication (Vol. 714).
- [4] Grc.nasa.gov. (2019). *Mars Atmosphere Model - Metric Units*. [online] Available at: <https://www.grc.nasa.gov/WWW/k-12/airplane/atmosmrm.html>

An Accessory Minimization Problem for Robust Numerical Predictor-Corrector Aerocapture Guidance

C. R. Heidrich¹ and R. D. Braun², ^{1,2}University of Colorado Boulder, CCAR 431 UCB, Boulder, CO 80309, USA.

Brief Presenter Biography: Casey Heidrich is a PhD student at University of Colorado Boulder in the Entry Systems Design Lab. His research concerns flight mechanics and guidance of reentry vehicles.

Introduction: Aerocapture has received considerable attention in the research community for decades as a means of orbit insertion with significant improvements in delivered mass to orbit. The maneuver consists of a single pass through a planet's upper atmosphere to generate aerodynamic lift and drag forces. Upon exiting the atmosphere, the vehicle has sufficiently reduced its kinetic energy and captured into a bounded orbit. The precision of this final orbit is of high concern, as it dictates the necessary mass margins to ensure final trajectory correction capability. Mission concept studies have identified atmospheric flight performance as a limiting factor for aerocapture applications. [1] There also exists uncertainty regarding aerocapture in general due to the lack of any true flight demonstration to date.

For years, studies assessing aerocapture performance employed approximate methods for simulated guidance. Such methods relied on piecewise analytical solutions to the entry guidance problem, utilizing rather severe assumptions on dynamics and atmosphere models. Examples include the Apollo skip entry guidance, HYPAS semi-analytical aerocapture scheme, and reference trajectory tracking methods.

In response to apparent shortcomings in approximate entry guidance, a new generation of numerical predictor-corrector (NPC) shooting methods have gained popularity in the literature. These strategies reduce the entry control problem to a line search optimization problem, where the full nonlinear equations of motion are numerically integrated each iteration to calculate exit conditions. NPC methods have shown promise to provide higher accuracy over heritage guidance schemes. However, the reliability of these methods in highly uncertain entry environments is still unclear and a subject of ongoing research.

In this work, we study a class of aerocapture control problems that fall into a broader category of degenerate singular control, with the bang-bang solution representing the extremal optimal control. We investigate the possibility of a minimum-variance solution robust to stochastic state uncertainties.

Background: The work by Lu [2] identified a class of aerocapture problems with an optimal solution of bang-bang form. In this strategy, the vehicle must use the full magnitude of its control authority, with instantaneous changes in magnitude defined by a switching

function. The results apply to many aerocapture problems, but do not fully account for degenerate cases where the control solution is ambiguous, requiring further constraints or assumptions.

A general strategy in optimal control is to minimize a cost functional of the form

$$J = \phi[\mathbf{x}(t_f), \mathbf{u}(t_f), t_f] + \int_{t_0}^{t_f} \mathcal{L}[\mathbf{x}(t), \mathbf{u}(t), t] dt$$

The problem is subject to the dynamic constraint

$$\dot{\mathbf{x}}(t) - \mathbf{f}[\mathbf{x}(t), \mathbf{u}(t), t] = 0$$

as well as constraints on the final state and control magnitude

$$\psi[\mathbf{x}(t_f), t_f] = 0, \quad |\mathbf{u}(t)| \leq 1$$

Objectives in aerocapture typically concern problems of the *Mayer* type, where the cost is a function of the final state only (i.e. no integral terms). The aerocapture cost may include apoapsis radius error, Delta-V correction, or other objectives. The end time is free, subject to a stop condition specified by the final state constraint.

We now consider the endpoint targeting problem, where we seek to minimize the quadratic error of a desired cost with open end time. The cost function takes the form

$$\phi[\mathbf{x}(t_f), t_f] = \frac{1}{2} \tilde{\phi}^2[\mathbf{x}(t_f)]$$

where it is assumed on the optimal trajectory

$$\tilde{\phi}[\mathbf{x}^*(t_f)] = 0.$$

For this class of problems, it can be shown that a degenerate singular control exists over a finite time interval. [3] The proof is omitted for brevity, but it results from the free end-time and stop conditions allowing for non-convex stationary points in the Hamiltonian. It turns out that the optimal control is potentially time-varying but bounded by the control magnitude constraint. The extremal control is the bang-bang solution.

Singular control is a continuing topic of current research. Determining the singular control is rarely straight-forward, especially for nonlinear systems. Even in the easiest cases, the solution is still highly problem-specific. In this research, we consider methods to disambiguate the control while improving the reliability of NPC methods.

Approach: Problems involving singular control can be reduced by imposing additional constraints or minimization objectives that bring out the optimal control in the Hamiltonian. The problem can also be simplified using parametric control, where a form of the

control is assumed (e.g. a step function or transcendental function) and a set of parameters defining its shape are left to solve for.

First, we employ a strategy concerning the second moment (or variance) of the cost function. In practice, we often have not only a state estimate, but an estimation error covariance provided by coalescing sensor measurements via a navigation filter. Since the exact vehicle state is never known outside of this precision, errors will accumulate in the integration of the system dynamics. This in turn diminishes the prediction accuracy. To compensate, a so-called *accessory minimization problem* is solved, where we seek a trajectory that simultaneously minimizes the cost function along with its variance. For example, consider the continuous time matrix Lyapunov equation and endpoint constraint

$$\dot{P} = -\frac{\partial^2 H}{\partial \mathbf{x}^2} + AP + PA^T$$

$$P(t_f) = \frac{\partial^2 \phi[\mathbf{x}(t_f), t_f]}{\partial \mathbf{x}^2}$$

In theory, solving the accessory problem will minimize the variance of the cost function along an optimal singular arc. Unfortunately, these problems are difficult to solve in practice, especially for nonlinear systems.

Another method of simplification is to utilize a parametric control. For this study, it was reasonable to choose a parametric control of the form

$$u^*(\mathbf{k}, t) = \begin{cases} u_{max} & t < t_s \\ u_{min} & t \geq t_s \end{cases} \quad \mathbf{k} = [u_{min}, u_{max}, t_s]^T$$

$$-1 < u_{min} < u_{max} \leq 1$$

The control is not strictly bang-bang, as we have freedom to vary the control bounds and switching time independently. Note the control input is bank angle which is related to $u(t)$ as

$$u(t) = \cos \sigma(t), \quad \sigma(t) \in [0, \pi]$$

Results: A Neptune aerocapture concept was chosen for the problem statement above. The target orbit was a high-energy science orbit with apoapsis and periapsis altitudes of 430,000 km and 3,986 km, respectively. The vehicle had a ballistic coefficient of 896 kg/m² and moderately high L/D of 0.8. The endpoint cost function was chosen as the apoapsis correction Delta-V squared. An initial state covariance matrix P_0 was adopted from an MPF statistical reconstruction study, [4] with distance and time units scaled to Neptune using canonical units. The initial state and covariance were propagated to atmospheric exit using (1) a linear time-varying system about the optimal trajectory and (2) Monte Carlo methods with the initial state perturbed by P_0 . The process was repeated across a range of admissible controls $u^*(t)$ for various switching times, with $u_{max} = 1$ and u_{min} solved iteratively using a first-order numerical optimizer. The final covariance

matrix was then used to estimate the Delta-V cost variance using statistical simulation.

The existence of singular optimal arcs in the aerocapture problem is supported by Figure 1. For the chosen switching times, an optimal control was found without utilizing maximal effort. Figure 2 illustrates the apoapsis error Delta-V cost 2- σ bounds. The expected cost is zero across all switching times. There is an apparent bottlenecking of the 2- σ bounds near 190 seconds providing about a 64% decrease. This point indicates an admissible control solution of the accessory minimization problem. The method shows promise to minimize NPC targeting errors subject to state uncertainty. This will in turn reduce propellant mass margins required to perform exo-atmospheric Delta-V maneuvers. Further research is necessary to determine if this problem can be solved in real time, as required by an on-board NPC algorithm.

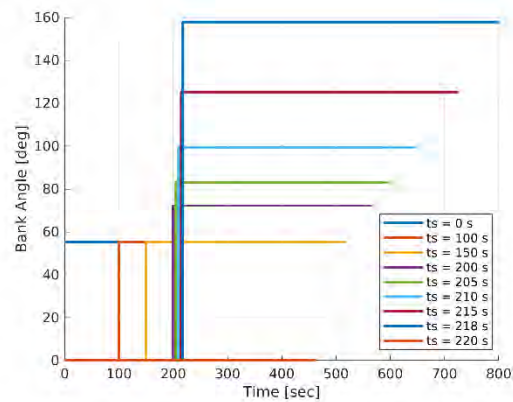


Figure 1. Admissible controls found to minimize the apoapsis correction quadratic Delta-V cost.

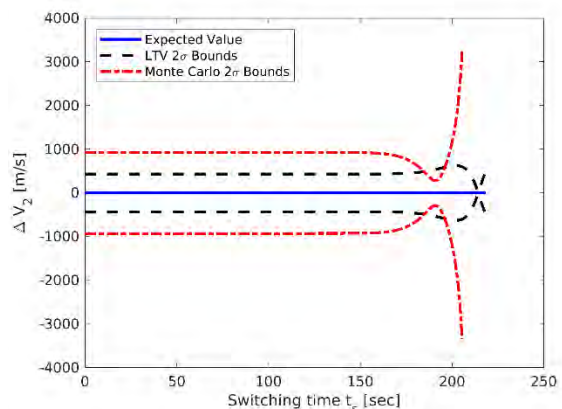


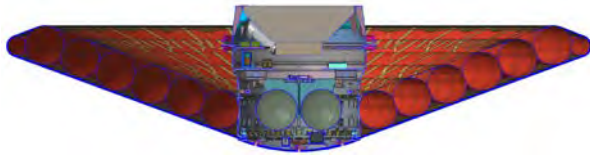
Figure 2. Final Delta-V cost uncertainty across switching times.

References: [1] Lockwood M. K. (2003) *AIAA/ASME*, 4799. [2] Lu P. et al. (2015) *AIAA*, 1771. [3] Jacobson, D. (1971). *IEEE* 16(6), 651-658. [4] Christian, J. et al. *AIAA*, 6192.

OPERATIONS PLANS FOR THE LOFTID 6-METER HIAD FLIGHT DEMONSTRATION.

R. A. Dillman^{1,2}, J. M. DiNonno¹, R. J. Bodkin¹, S. J. Hughes¹, H. Blakeley¹, F. M. Cheatwood¹, R. L. Akamine¹, and A. Bowes¹; ¹NASA Langley Research Center, ²Robert.A.Dillman@nasa.gov.

Brief Presenter Biography: Robert Dillman has been a flight hardware engineer at NASA Langley Research Center since 1989. He has a Bachelor of Science in Aerospace Engineering, and a Masters of Materials Science, both from the University of Virginia. He was project chief engineer for IRVE-II and IRVE-3, the successful suborbital flight tests of 3-meter diameter HIAD's, and is currently the Operations Lead for the LOFTID 6m diameter HIAD flight demonstration.



Abstract: NASA has funded LOFTID, the Low Earth Orbital Flight Test of an Inflatable Decelerator, to perform a flight demonstration of a 6m diameter HIAD reentry vehicle. LOFTID is planning to launch in 2022 as a secondary payload on an Atlas V mission. After release of the primary payload, LOFTID will deploy from its launch configuration and be de-orbited by the launch vehicle's Centaur upper stage.

One major requirement on the LOFTID mission is that, as a secondary payload, it does no harm to the primary payload with which it flies. As with previous HIAD's that were flown on sounding rockets, the LOFTID reentry vehicle contains significant quantities of material that do not meet the typical low-outgassing requirements for space flight. LOFTID also will not be assembled in a clean room, and some facilities that will be used for flight qualification testing are not clean either. Current plans for integration to the Atlas V call for the LOFTID reentry vehicle to be sealed inside the payload adapter structure, the outside of which will then be thoroughly cleaned before integration of the primary payload on top. LOFTID will remain sealed in the payload adapter through launch. While on the launch pad, dry nitrogen purge gas flowing from the primary payload past LOFTID and other auxiliary payloads before reaching vents placed low in the launch fairing will keep contaminants from reaching the primary payload even if the protective covers leak. After launch, the dry nitrogen in the launch fairing will expand as the pressure drops during ascent to orbit, keeping the gas flow moving away from the primary payload toward the vents in the fairing. After the launch fairing is jettisoned, the free stream atmospheric flow will provide the same protection. On orbit, contamination

protection will be provided by a radial shield that will block line-of-sight travel of any contaminants from the secondary payloads to the primary.

Another major facet of the mission is the planned recovery of the 6-meter HIAD after splashdown. The recovery ship will be pre-positioned near the predicted splashdown location. GPS data will be used to guide the ship to the reentry vehicle after splashdown, and to the second data recording stored in a floating buoy that will be ejected before deployment of the reentry vehicle's terminal descent parachute.

This presentation will discuss the details of the LOFTID operations plans, including launch site integration and contamination control, in-flight monitoring, and post-flight recovery.

SCALABLE NON-PROPULSIVE DYNAMIC MASS-SHIFTING CONTROL SYSTEM FOR ENTRY, DESCENT, AND LANDING SYSTEMS.

S. Krzesniak¹, B. Baeza¹, K. Parcero¹, I. Besemer¹, K. Luongo¹, P. Papadopoulos², and S. Swei². ¹Undergraduate Student, Aerospace Engineering, 1 Washington Square, San Jose, CA 95192, brandon.baeza@sjsu.edu, ¹Undergraduate Student, ian.pradodebesemer@sjsu.edu, ¹Undergraduate Student, kayla.parcero@sjsu.edu, ¹Undergraduate Student, kiana.luongo@sjsu.edu, ¹Undergraduate Student, stanley.krzesniak@sjsu.edu. ²Faculty Advisor.

Brief Presenter Biography: Stanley Krzesniak is an undergraduate student at San Jose State University studying astronautics with an emphasis on systems design and embedded systems for hypersonic vehicles. He has played a role in many aeronautics- and astronautics-related projects at San Jose State involving electronics, programming, and conceptual design. He will continue to focus on hypersonic systems during his graduate studies at San Jose State.

Introduction: NASA's Moon to Mars campaign calls for human exploration on the Martian surface by the mid 2030's time frame. As a result, thermal protection systems (TPS) of the future must adhere to payload volume constraints and enable precision landing and thermal protection abilities to deliver large payloads during Martian aerocapture and subsequent entry, descent, and landing (EDL). The control system design supports NASA's Adaptable Deployable Entry and Placement Technology (ADEPT) [1] and Pterodactyl development efforts by proving scalability of a control system which utilizes commercial off the shelf (COTS) microcontrollers, MathWorks software, and a prototype semi-rigid TPS design. The unification of ADEPT and Pterodactyl would result in a low-ballistic maneuverable TPS fitting completely into 5-meter and larger fairings, which would be impossible for rigid low ballistic coefficient TPS of similar specifications to fit into [2]. The developed GN&C architecture and hardware for such a mission will be presented in this publication.

Overview: The current system comprises primarily of COTS components or parts manufactured from COTS tools: two high voltage servo motors, two inertial measurement unit sensors, a microcontroller, 3D-printed servo motor and PCB mounts, onboard power supply, timing belts for 2D

linear motion, and 100mm 3D printed diameter aeroshell. The small-scale design is intended to experimentally validate vehicle dynamics and to provide an experimental testbed to ensure high-level issues are worked out of the base controller design. Following completion of validation, a much larger, semi-rigid model will be designed, with an optional ability to completely fold into the size of a 1U CubeSat. This further design and testing will take occur at the NASA Ames SpaceShop and the Intelligent Robotics Laboratory facilities, potentially culminating in a test flight in a vertical wind tunnel facility or by high altitude balloon.

GN&C Subsystem: C.G. shifting is accomplished by two high voltage Hitec Multiplex servos, capable of rotating 60° in .13 seconds with 7.4V of power provided by onboard batteries. Bosch Inertial Measurement Unit sensors utilize gyroscopes, accelerometers, and magnetometers to provide real time position orientation. A microcontroller then executes velocity profile based commands, orientation positioning, and provides lift vector control.

Acknowledgments: This research was conducted in partnership with NASA Ames Research Center and the Space Engineering Laboratory at San Jose State University in fulfillments of university undergraduate requirements.

References:

- [1] Venkatapathy, R. (2011) *Adaptive Deployable Entry and Placement Technology (ADEPT): A Feasibility Study for Human Missions to Mars*. 21st AIAA Aerodynamic Decelerator Systems Technology Conference and Seminar. [2] D'Souza, S. (2018) *Pterodactyl: Integrated Control Design for Precision Targeting of Deployable Entry Vehicles*, 15th International Planetary Probe Workshop

ANALYSIS OF TIP-OFF RATES DURING DISCRETE-EVENT DRAG MODULATION FOR VENUS AEROCAPTURE.

A.E. Rollock¹, R. D. Braun¹, and M. S. Werner¹.

¹University of Colorado Boulder, Department of Aerospace Engineering, 429 UCB, Boulder, CO 80309

Brief Presenter Biography: Annika Rollock is a first-year graduate student in the Entry Systems Design Lab at the University of Colorado, Boulder. After graduating from MIT in 2018 with a degree in aerospace engineering, she now does work on the aerodynamics of spacecraft re-entry. In her free time, she enjoys running, biking, reading, and writing.

Introduction: Aerocapture is an aeroassist maneuver that uses a single braking pass through the planet's atmosphere in order to capture into a target orbit. This technique has the potential to greatly increase the payload mass delivered to orbit when compared to traditional propulsive maneuvers. [1] Drag modulation is one method of control that allows for a simple but elegant control approach, without a need for the center-of-gravity offset or propulsive reaction control used by traditional bank-to-steer vehicles. Discrete-event drag modulation is a subset of drag modulation that relies on discrete changes in the vehicle's ballistic coefficient in order to alter the vehicle's trajectory through the atmosphere. The simplest way of achieving discrete-event drag modulation is through the jettison of a high-drag device, such as a trailing ballute or a rigid drag skirt. This method of drag modulation has been proven to provide ample control authority for an aerocapture mission. [2]

While this method of aerocapture is promising, there has been little work done on the analysis of the hypersonic separation event in literature. Previous work has focused on assessing recontact risk during nominal separation [3] but did not investigate the addition of tip-off forces. This investigation is focused on analyzing the aerodynamics and dynamics of the separation event across a range of tip-off angles and rates between the front and trailing bodies, in order to better characterize the stability of both bodies after jettison and assess the risk of recontact. In order to ensure relevance to the results of this study, a Venus aerocapture mission concept is analyzed. This mission is an ongoing joint effort by the Jet Propulsion Laboratory, Ames Research Center, and the University of Colorado Boulder, and aims to study of the feasibility of aerocapture for use in the Venus environment. This mission concept utilizes a rigid drag skirt in order to change the vehicle's ballistic coefficient and provide control authority during the aerocapture event.

The analysis of the separation event will utilize the Cart3D computational fluid dynamics (CFD) software

developed by NASA Ames Research Center. Cart3D will be used to generate aerodynamic force and moment time histories following the jettison of the drag device with initial tip-off angles and angular rates. For the purpose of this mission, the study is limited to initial angles between -5 and 5 degrees, with a 0.5 degree resolution. The work will be extended to examine tip-off rates, beginning at a 0 degree initial offset with 1 degree/s angular rate, and then 0.5 degree initial offset with 1 degree/s angular rate in order to further examine the sensitivity around the 0 degree mark.

The work done in this study will provide valuable insight into the complex dynamics of hypersonic separation events as well as the intricacies of the aerocapture maneuver. The effects of tip-off rates will contribute to understanding the margin of stability for such vehicles. Ultimately, these results can be applied to other hypersonic separation events and extended to similar aerocapture missions around other bodies, and will further validate aerocapture as a flightworthy technology.

References:

- [1] Hall, J. L., Noca, M. A., and Bailey, R. W., "Cost-Benefit Analysis of the Aerocapture Mission Set," *Journal of Spacecraft and Rockets*, Vol. 42, No. 2, 2005, pp. 309-320.
- [2] Werner, M. S., and Braun, R. D., "Characterization of Guidance Algorithm Performance for Drag Modulation-Based Aerocapture," AAS 17-032, 2017 AAS Guidance, Navigation and Control Conference, Breckenridge, CO, February 2017.
- [3] Werner, M. S., Roelke, E., and Braun, R. D., "Dynamic Propagation of Discrete-Event Drag Modulation for Venus Aerocapture," *Interplanetary Probe Workshop*, Boulder, CO, July 2018

FLIGHT CONTROL TECHNIQUES FOR OPTIMAL AEROCAPTURE GUIDANCE

Rohan. G. Deshmukh¹ and David. A. Spencer², ¹Purdue University, 480 W Stadium Ave, West Lafayette, IN, 47906, deshmur@purdue.edu, ²Purdue University, 480 W Stadium Ave, West Lafayette, IN, 47906, dspencer@purdue.edu

Brief Presenter Biography: Rohan Deshmukh is currently a PhD candidate in the Space Flight Projects Laboratory at Purdue University School of Aeronautics and Astronautics. His dissertation involves the systems analysis of optimal guidance architectures for planetary aerocapture. He has previously interned at the National Aeronautics and Space Administration Langley Research Center in the Atmospheric Flight and Entry Systems Branch where he worked on planetary aerocapture mission studies. His research interests include guidance, navigation, and control of planetary aeroassist vehicles, mission design, and systems engineering. He received his BS in Aerospace Engineering from Georgia Institute of Technology and his MS in Aerospace Engineering from Purdue University.

Introduction:

Aerocapture is a promising propellant-saving orbital insertion technique for planetary destinations with an atmosphere. Although not flight-proven, previous aerocapture systems studies in the literature have demonstrated both the validity and robustness of the technique. At certain destinations, such as Neptune, aerocapture is mission enabling by significantly reducing propellant mass requirements as compared to an all-propulsive mission while at other destinations, such as Venus, aerocapture is mission enhancing by increasing the delivered mass to orbit for the same launch vehicle as compared to the best non-aerocapture alternative [1].

The technology that enables robust aerocapture performance is the guidance algorithm, which autonomously commands the vehicle's flight control during flight to achieve the desired orbit at atmospheric exit. Such flight control techniques envisioned for aerocapture vehicles include bank angle modulation (BAM), drag modulation (DM), and direct force control (DFC) as shown in Figure 1 [2].

Almost all of the existing literature has focused on bank angle guidance [3][4] while limited and a lack-thereof of literature exists for drag modulated [5] and direct force control guidance, respectively [6]. Despite the existence of these different techniques, there does not exist a unifying architecture that allows for critical guidance trade studies to be conducted in preparation for flight projects. To address this limitation, this work presents the formulation of a modular aerocapture guidance architecture that is suitable for application utilizing all three flight control techniques.

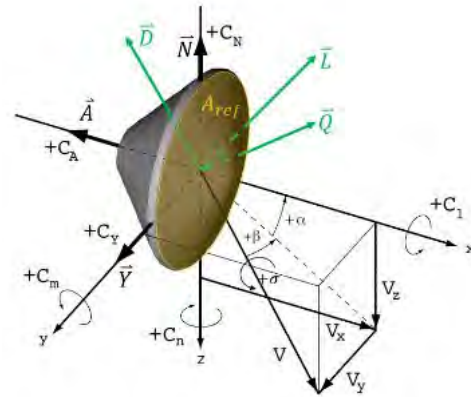


Figure 1. Visualization of aerocapture flight control techniques. Bank angle modulation rotates lift vector L about relative velocity vector V , by bank angle σ . Ballistic drag modulation changes aerodynamic reference area A_{ref} to control drag vector D . Direct force control changes angle of attack α and side-slip angle β to control all aerodynamic forces, including side force vector Q .

To achieve optimal guidance that minimizes orbit insertion ΔV , optimal control theory is applied to each flight control parameter. A first-order linear aerodynamics model is developed for a flight-heritage blunt-body aeroshell utilizing the Mars Science Laboratory aerodatabase [7]. The linear model facilitates the derivation of “bang-bang” optimal control laws for bank angle, drag area, and combination of angle of attack and side-slip angle. This unified control structure enables the modular application of a closed-loop numerical predictor-corrector (NPC) guidance architecture.

An assessment of the theoretical entry flight path angle corridor width for each flight control is conducted. Investigation of the effect of different vehicle trim angle of attack, angle of attack ranges, and reference area ranges, on the corridor width associated with BAM, DFC, and DM flight controls are conducted. The results demonstrate that the corridor width significantly increases increased vehicle L/D capability.

Using a Mars aerocapture mission set, nominal performance testing of the NPC guidance architecture is conducted. The simulated trajectories utilizing each flight control demonstrate similar orbit insertion performance but noticeable differences vehicle aero-heating and aero-loading profiles. Furthermore on the same mission set, robustness trade studies are performed for each flight control in a Monte Carlo setting. Robustness testing includes approach trajectory delivery errors, vehicle

mass and trim attitude uncertainties, atmospheric density variations, and aerodynamic characteristic uncertainties. The simulated trajectories are demonstrated to be robust to the applied dispersion but show noticeable differences in the orbit insertion statistics for each flight control technique.

The results presented in this paper demonstrate both the necessity and viability of utilizing the designed modular guidance architecture for facilitating further technological trade studies at other planetary destinations.

References:

[1] Hall J., Noca M., and Bailey, R. (2005) Cost-Benefit Analysis of the Aerocapture Mission Set, *Journal of Spacecraft and Rockets*, Vol.42, No.2, 309-320.

[2] Spilker T. R. et al. (2019) Qualitative Assessment of Aerocapture and Applications to Future Missions, *Journal of Spacecraft and Rockets*, Article in Advance, 1-10.

[3] Braun R. D. and Powell R. W. (1992) Predictor-corrector guidance algorithm for use in high-energy aerobraking system studies, *Journal of Spacecraft and Rockets*, Vol. 15, No. 3, 672-678.

[4] Lu P. et al. (2015) Optimal Aerocapture Guidance, *Journal of Guidance, Dynamics, and Control*, Vol. 38, No. 4, 553-565.

[5] Putnam Z. R. and Braun R. D. (2014) Drag-Modulation Flight-Control System Options for Planetary Aerocapture, *Journal of Spacecraft and Rockets*, Vol. 51, No. 1, 139-150.

[6] Deshmukh R. G., Dutta S., and Spencer D. A. (2019) Investigation of Direct Force Control for Planetary Aerocapture at Neptune, *29th AAS/AIAA Space Flight Mechanics Meeting*, Ka'anapali, HI, 13-17 Jan 2019.

[7] Dyakonov, A. A., Schoenenberger M., and Van Norman, J. W. (2012) Hypersonic and Supersonic Static Aerodynamics of Mars Science Laboratory Entry Vehicle *43rd AIAA Thermophysics Conference*, New Orleans, LA, June 2012.

Science investigations of small solar system bodies with a landed CubeSat platform . Ö. Karatekin¹, H. Goldberg², B. Ritter¹, B. Van Hove¹, M. Noeker¹. ¹Royal Observatory of Belgium, Ringlaan 3, Brussels/Uccle 1180, Belgium, (ozgur.karatekin@observatory.be), ²GomSpace, Langagervej 6, 9220 Aalborg Øst, Denmark

Brief Presenter Biography: Özgür Karatekin is a research scientist at the Royal Observatory of Belgium. He is the science lead of the Juventas CubeSat for the Hera mission. Previously, he was the PI of the Asteroid Geophysical Explorer AGEX CubeSat study. He has been involved with the Entry Descent Landing investigations of ExoMars 2016 & ExoMars 2020 as well as with the radio science investigations with planetary entry probes and landers.

Introduction: The Hera mission [1] is currently under study at ESA in the framework of the AIDA project associated to the NASA DART impactor mission to the binary asteroid Didymos. It foresees landing of the Juventas 6U CubeSat on the surface of the secondary of the Didymos system, called Didymoon [2]. This will be the first time a rendezvous mission with the binary asteroid Didymos and touchdown on the smallest asteroid ever visited. Juventas will have a dedicated mission phase for the surface geophysical investigation [3]. In parallel to Juventas, there are additionally similar mission studies considering landing of small platforms and CubeSats on asteroids for the ESA Fast Class mission opportunities. Here, we will present the science objectives, payloads and operations concept for the “surface science” mission phase of Juventas. In addition, we will extend the payloads and operation concepts to other potential asteroid targets.

Science Investigation: Our knowledge of asteroids is still limited, especially for the smallest ones. These small bodies are very diverse, have highly complex histories and their low-gravity environment challenges our intuition. They are irregularly-shaped in general and may possibly have complicated interior structure, being fragments of larger asteroids or gravitational aggregates thereof. In addition to the formation process (e.g., fragmentation and re-accumulation), the interior structure and mechanical properties are affected by the subsequent collisional history resulting in crater formation on the surface and shock-wave induced interior compaction vs. fracturing. Juventas’ main objective is to investigate details of the interior structure and dynamical properties of Didymoon.

Juventas focuses on the geophysical analysis of Didymoon, its subsurface structure, density and porosity distribution as well as its surface properties. Fur-

thermore, its dynamical state will be investigated which will give insights into the dynamics of the binary system and the formation of Didymoon. In order to do so, Juventas will perform a direct measurement of the local gravity vector on the surface of Didymoon, which has never been done on an asteroid. In addition, it will infer mechanical properties of near-surface material from CubeSat landing and bouncing. The surface gravity field will be analysed with remote radio and low frequency Radar sensing. The complementarity of the payload will allow a comprehensive geophysical investigation of Didymoon in support to the HERA investigation on the exploration and characterization of the Didymos asteroid binary system and the effects of the DART impact on Didymoon.

References: [1] Michel, et al (2018) *Advances in Space Research* 62, 2261-2272. [2] Goldberg et al (2019) *International Planetary Probe Workshop 2019*, Oxford UK. [3] Karatekin et al 2018 *Hera Community Workshop*, Berlin, Germany.

Acknowledgements: This work was performed in support of the European Space Agency’s Hera project. The authors wish to acknowledge contribution from the Juventas team including collaborators at ESA, GomSpace, the Royal Observatory of Belgium, GMV, the University of Grenoble-Alpes, the University of Bologna, Brno University of Technology, Astronika, as well as the entire Hera mission team.

ICY MOON SUB-SURFACE PROBE RADIOISOTOPE HEAT SOURCE CONSIDERATIONS

D.P. Kramer¹, C.E. Whiting¹, C.D. Barklay¹, R.M. Ambrosi², E.J. Watkinson², J. Weston², Z.A. Magre², and S.A. Botta²

¹University of Dayton Research Institute, 300 College Park, Dayton, Ohio 45459 USA

daniel.kramer@udri.udayton.edu

²University of Leicester, Space Research Centre, University Road, Leicester, UK, LE1 7RH

rma@leicester.ac.uk

Brief Presenter Biography: Dr. Kramer has been associated with the U.S. nuclear space power program since the 1990s when he was at Mound Laboratories, where he worked on the RTGs (Radioisotope Thermoelectric Generators) for the Cassini/Saturn mission. After joining the University of Dayton, he has remained very active in the nuclear space power program including contributing to Mars2020. He currently holds joint appointments at the university as a Professor in the Chemical and Materials Department and at the Research Institute where he is a Distinguished Research Engineer.

Introduction: Over the last several decades, RTG powered exploratory spacecraft have enabled the identification of several icy moons within the solar system which may contain sub-surface oceans of water below a thick ice cap. It is expected that some of these ice caps may be as many as tens of kilometers thick. Positioning a probe into one of the icy moon oceans may help to determine whether life forms have existed in other locations within the solar system besides Earth. Several sub-surface probe concepts discussed in the literature employ the radioisotope plutonium-238, as the heat source material within a probe, to melt through an icy moon's ice cap down to the liquid ocean [1-2]. This would allow for the first time the investigation of an icy moon sub-surface ocean environment.

Over the last several decades U.S. RTGs have employed the radioisotope plutonium-238 in the form of $^{238}\text{PuO}_2$ as the heat source material. Plutonium-238 has a half life of ~87 years and a thermal output of ~0.5W_{th/g}. While the relatively long half-life of plutonium-238 is advantageous for long space missions, shorter half-life radioisotopes may have benefits in terms of greater thermal output for an icy moon probe mission which could have an estimated duration of ~12 to 20⁺ years. A first-order analysis suggests that other radioisotopes exhibit a number of characteristics making them attractive for a future icy moon sub-surface probe. For example, Curium-244 similar to plutonium-238 is an alpha emitter but with a shorter half-life of ~18.1 years. Therefore, curium-244 generates an initial thermal output per gram several times greater compared to plutonium-238. The use of higher thermal output radioisotopes could enhance the overall performance of an

icy moon sub-surface probe. While the application of a greater thermal output radioisotope could be beneficial for such an icy moon mission, the authors are aware that the selection/application of any new radioisotope heat source material will require extensive; radiological considerations, realistic evaluation of obtainability, cost factors, and launch safety considerations.

References:

- [1] Zimmerman, W., et al., "A Radioisotope Powered Cryobot for Penetrating the European Ice Shell," STAIF-2001, CP552 American Institute of Physics, Albuquerque, NM (2001).
- [2] Hendricks, T., "Sub-Surface RTG Systems and New Heat Sources," Proceedings of the 2018 Conference on Advanced Power Systems for Deep Space Exploration, Jet Propulsion Laboratory, Pasadena, CA (2018).

SAMPLE RETURN FROM A RELIC OCEAN WORLD: THE *CALATHUS* MISSION TO OCCATOR CRATER, CERES.

G. Acciarini¹, H. Bates², N. Berge³, M. Caballero⁴, P. Cambianica⁵, M. Dziewiecki⁶, Z. Dionnet⁷, F. Enengl⁸, O. Gassot⁹, S. B. Gerig¹⁰, F. Hessinger¹¹, N. Huber⁸, R. Hynek¹², B. Kędziora¹³, L. Kissick², A. Kiss¹⁴, M. Martin¹⁵, J. Navarro Montilla¹⁶, M. Novak¹⁷, P. Panicucci¹⁷, C. Pellegrino¹⁹, A. Pontoni²⁰, T. Ribeiro²¹, C. Riegler²²

¹Delft University of Technology, ²University of Oxford, ³Université d'Orléans, CNES ⁴Universitat Politècnica de Catalunya, ⁵University of Padova, ⁶Wroclaw University of Science and Technology, ⁷DIST-Università Parthenope, ⁸KTH Royal Institute of Technology, ⁹Univerté Grenoble Alpes, IPAG, CNRS ¹⁰University of Bern, ¹¹Luleå University of Technology, ¹²University of West Bohemia, ¹³Warsaw University of Technology, ¹⁴Budapest University of Technology and Economics, ¹⁵University of Stuttgart, ¹⁶Institut national des sciences appliquées, ¹⁷University of Technology Vienna, ¹⁸ISAE-SUPAERO, CNES, ¹⁹Technical University of Munich, ²⁰Swedish Institute for Space Physics, Kiruna, ²¹University of Porto, ²²University of Würzburg

This work was initially developed during the 42nd edition of the Alpbach Summer School (SSA) and subsequently during the Post-Alpbach Summer School Event 2018 (PASSE), both co-organised by the Austrian Research Promotion Agency (FFG) and the European Space Agency (ESA). All authors, in alphabetical order, met and worked on a mission proposal under the theme “Sample return mission from small solar system bodies”.

Introduction: ESA's Cosmic Vision program 2015–2025 is the current cycle of ESA's long-term planning for space science missions [1]. It aims at furthering Europe's achievements in space science for the benefit of all mankind. One of the programs main objectives is the question about the conditions of life and habitability of the solar system, as well as the formation and composition of small bodies. Based on these ideas, the Cosmic Vision program targeted sample return missions as significant candidate projects for European space activities.

Here we present Calathus, a mission concept that aims to return a sample from Ceres' Occator Crater and search for the presence of the ingredients of life.

Dawn's Ceres. Occator Crater, as revealed on Ceres by NASA's *Dawn* orbiter, is 92 km in diameter and contains two distinct bright regions – called *faculae* – composed of salt-rich carbonates believed to be the solid residues of brines erupted from a cryomagma chamber [2]. These carbonates are younger than 2 Myr in age, and smaller, darker faculae across Ceres are likely older remnants of similar deposits [3]; the Occator Crater faculae therefore represent a geologically-widespread activity.

Planetary evolution models suggest an ocean may have once existed at shallow depths [3], which may persevere today as localised brine reservoirs, with one perhaps below Occator [4]. As such, to understand the composition and evolution of Occator is to understand the inner workings of a relic – potentially extant – ocean world [5] providing a snap-shot inside not only Ceres but a whole class of ice-rich small bodies including Europa, Ganymede, and perhaps Kuiper Belt Objects such as Pluto.

In discovering such an unprecedented feature and linking Ceres with the wider Solar System, *Dawn*

created as many questions as it answered. These may be broadly divided into two main categories of interest:

Q1) Ceres appears to contain the three vital prerequisites for life: sources of water, carbon, and energy. Do ice-rich bodies like Ceres represent a widespread, astrobiologically-favourable niche?

Q2) Ceres' spectral features do not match any known meteorite groups [6], nor can the location of its formation be pinpointed to a specific region. Where and how did Ceres form, and did asteroids of similar composition play any role in the delivery of water/organics to proto-Earth?

A return mission to Ceres to sample material from Occator Crater would provide invaluable insight into both of these categories, the former of which is in particular an ESA *Cosmic Visions* priority, as well as further the study of a world fascinating in its own right.

Sample return: Given the high priority of exploring as-yet technologically unreachable worlds such as Europa for their astrobiological interest, and given complimentary missions such as NASA's OSIRIS-REx to the C-type asteroid Bennu, a return mission to Ceres to sample material from Occator Crater would provide insight into both of these categories of interest.

From the Dawn mission, we know that the chemical composition of Occator's bright material is very complex and there is evidence for the presence of organics [7]. A precise assignment of the chemical groups and their respective abundances can only be achieved by performing analysis on Earth, where we have a wide range of advanced analytical techniques available. A meticulous sample analysis is needed to unravel the exact composition of the crater and its interior, to evaluate the role of the possible aqueous and thermal processes and to better understand the crater evolution.

Science Objectives: Besides sample return, the Calathus mission has some additional objectives which are intended to be completed while in orbit and on the surface of Ceres. These include mapping the surface of Ceres on a global scale and mapping

the sampling site on a local scale. The mission plans to do this both with an optical camera and a thermal infrared mapper to provide compositional information and to build context for the returned samples. Calathus also intends to probe the near subsurface of Ceres to a depth of 100m using a radar instrument, which should provide information on geological structures and inform on the presence of brines below bright spots. For sampling, a lander module will descend to the surface of Ceres. This lander module will be equipped with cameras which allow choices to be made on specific sampling sites once the module has landed. Finally, Calathus also aims to do some preliminary compositional analysis on the surface using a gas chromatography mass spectrometer.

Mission Payload: The spacecraft is composed of two main parts: the orbiter and the lander. The mission payload will consist of instruments, split between these modules, based on the Calathus scientific objectives and dedicated to answering the scientific questions:

	Instrument	Q1	Q2
Orbiter	Mapping Camera	✓	
	Subsurface radar	✓	
	Thermal infrared mapper	✓	
	Orbiter Sample	✓	✓
Lander	Mapping Camera	✓	
	Mass Spectrometer	✓	✓
	Sampling Module	✓	✓

Technical approach: In order to address the complexity of a sample return mission, a system engineering approach has been used by employing ESA OCDT software [8].

Operational modes have been defined according to the mission phases, shown in Figure 1, taking into account the interplanetary and Ceres orbital phase and operational constraints, viz. eclipses, communication and safe modes. The duration of all the mission is 9.6 years at the current design phase.

The orbiter: The main driver of the orbiter design, in Figure 2, has been the use of the low thrust ion engine whose employment is state-of-the-art for interplanetary missions to small bodies [9][10][11]. This drive clearly limits the propellant mass and avoids multiple flybys and a long duration mission,

but requires large surface area solar panels in order to provide the needed power. All engineering subsystems have been developed considering the TRL and interfaces with other subsystems, in order to obtain a feasible and competitive design with state-of-the-art technology.

The lander: The lander is used to fulfil the main goal of Calathus mission: sample collection. It will be released for the orbiter at a low altitude, as in the Rosetta and Hayabusa 2 missions, and will safely reduce its velocity using hydrazine propulsion. Once on the surface, a ground-in-the-loop process will decide which the relevant sampling sites are and the lander will perform sampling and sample storing.

The samples will then be sent to orbit using an ascending module, as in the Mars Sample return Mission [12] or in the current Airbus DS lunar sample return mission design [13].

Two critical subsystems have been identified:

1. The sampling subsystem is composed of a manipulator arm with cameras, a grinding device to minimize hydrazine contamination and a hammering Drill with 5 sample holding bits. In the nominal case, four samples will be collected.
2. The on-orbit catching subsystem aims at relative navigation between the spacecrafts. Optical navigation and 3-way radar ranging will be used to perform cooperative localization between the orbiter and the ascending module. At close range, the canister will be released and non-cooperative catching will be performed using laser ranging, visual navigation and beacon-radar data. As with the Hayabusa 2 artificial marker [14], the canister will be covered with LEDs and mirrors to increase visual and laser navigation respectively.

Planetary protection: Ceres is a class V restricted body, implying forward and backward protection actions need to be taken. The spacecraft will be sterilized prior to launch, and approval will be given from a planetary protection officer for launch from Earth, Ceres and Earth re-entry. Any returning hardware must also be contained or sterilized for re-entry. The sample will be curated in the EURO-CARES facility to remove chances of contamination.

Acknowledgements:

The authors acknowledge funding from ESA and FFG during PASSE 2018. The authors would also like to thank all SSA and PASSE tutors and lecturers for their valuable inputs into the subject of the present work. This study benefited from the work of 45 other students during the above mentioned summer school.

References : [1] B. Schutz C. Turon. (2002). ESA. [2]. De Sanctis, M. C., et al. (2016) *Nature* 536.761 [3] Castillo-Rogez, J. C., et al.. (2010). *Icarus*, 205 (2), 443-459. [4] Neveu, M., & Desch, S.

J. (2015) *Geophysical Research Letters*, 42(23), 10-197 [6] McSween et al. (2018). *Meteoritics & Planetary Science*, 53(9), 1793-1804. [7] De Sanctis M. C. et al. (2017) *Science*, 355, 719-722. [8] De Koning, Hans Peter, et al. (2014) “6th International Conference on Systems and Concurrent Engineering for Space Applications”

[9] Kuninaka, Hitoshi, et al. (2009) *31st Intern. Electric Propulsion Conference*. [10] Tsuda, Yuichi, et al. (2013) *Acta Astronautica* 91 : 356-362. [11] Polansky, C. A. et al. (2011) in *The Dawn Mission to Minor Planets 4 Vesta and 1 Ceres* [12] Price, H., et al. (2000) *IEEE Aerospace Conference* Vol. 7. [13] R. Buchwald, F. Ebert, O. Angerer. (2015). *IPPW 15*. [14] Hashimoto, Tatsuaki, et al. (2010) *IFAC Proceedings Volumes* 43.15 (2010): 259-264.

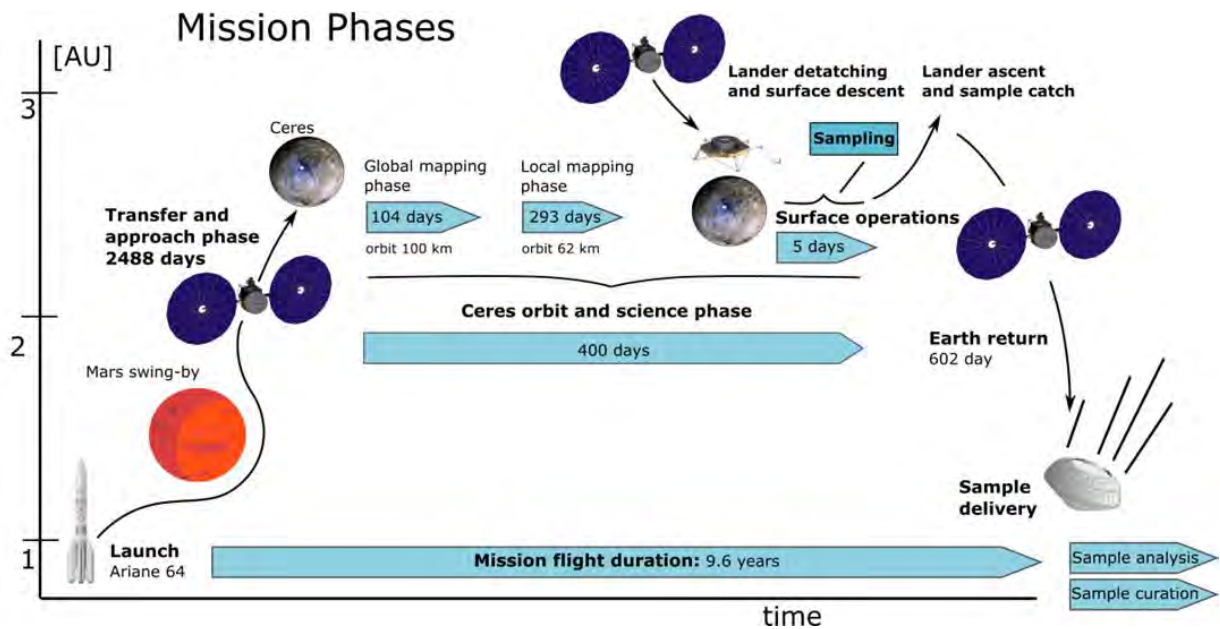


Fig. 1 Calathus Mission Phases

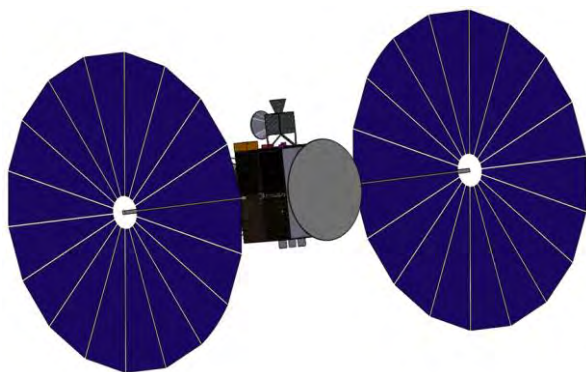


Fig. 3. Calathus Orbiter

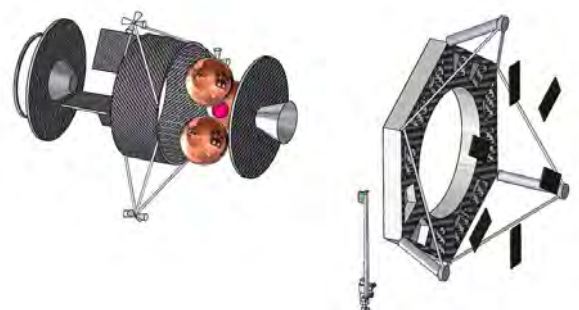


Fig. 2 Calathus lander. In details, the scientific module on the right and the ascending module on the left

Maturation of Heatshield for Extreme Entry Environment Technology (HEEET) through Extreme Aerothermal Ground Testing at Arnold Engineering Development Complex (AEDC).

J. Williams¹, D. Ellerby², C. Kazemba², M. Mahzari², ¹AMA Incorporated at NASA Ames Research Center, ²NASA Ames Research Center

Brief Presenter Biography: Joseph Williams earned a Masters in Aeronautics and Astronautics from Purdue University. He is currently working as a Systems Engineer for AMA Inc. at NASA Ames Research Center in the Entry Systems and Vehicle Development Branch.

Introduction: The Heatshield for Extreme Entry Environment Technology (HEEET) project is developing a thermal protection system (TPS) capable of flight in extreme entry environments such as Venus, Saturn, Ice Giants and very high speed Earth returns. The goal of the project is to develop an alternative heatshield material that is more mass efficient and more sustainable than fully dense carbon phenolic (CP).

HEEET's aerothermal capabilities are demonstrated through ground based arcjet testing. At the extreme conditions that HEEET is targeting, there are very few facilities capable of attaining relevant environments. The project identified the Arnold Engineering Development Complex (AEDC) as the preferred facility to provide mission-relevant levels of shear stress and has conducted multiple test series there. These tests are particularly useful for identifying any shear induced failure modes in the system, particularly at the seams.

One of the challenges when testing at these extreme entry environments is that the test article sizes can become small, on the order of the size of the features being tested. This is particularly true for the tiled HEEET solution, illustrated in Figure 1. The gap fillers are ~2.5cm wide and geometries can consist of intersecting gap fillers and other features of similar size. The wedge-shaped test coupons tested at AEDC are large enough to test all features of interest in the HEEET system. However, the nature of the flow generates environments that vary significantly over the surface of the coupon. Therefore, careful placement of the features of interest is required. This is shown in Figure 2.



Figure 1. HEEET Engineering Test Unit design features.

A passive leading edge is utilized on the wedge test articles. The environments along the leading edge are very aggressive and result in substantial recession of the leading edge, which slightly impacts the environment across the sample, but more importantly limits the total run duration. Given that the HEEET seam design shows some differential recession compared to the acreage material, the project is testing seam articles with simulated differential recession machined into the coupon at the start. This provides some ability to explore longer test durations to investigate the evolution of the differential recession behavior.



Figure 2. Pre-test image of a seamed HEEET test article.

The severity of the test conditions can make seemingly mundane activities, such as retaining the samples during testing, challenging. During early testing some articles were lost mid-test, not due to a failure in the TPS system, rather due to a test artifact. A thorough investigation of the root cause of the loss of the test articles was performed and resulted in a substantial re-design of the articles that eliminated the issues.

Finally, in the high shear environment of the AEDC arcjet, roughness augmentation plays a role in the experienced recession and needs to be accounted for to properly predict the recession and understand the material performance.

This work will review some of the nuances of testing at AEDC. The facility provides a unique capability to test relatively large test articles at the extreme environments of interest. HEEET has successfully completed multiple test series at AEDC and the results have provided the evidence supporting HEEET maturation and readiness to support future missions.

HEATSHIELD ENTRY MODELING USING A DESIGN, ANALYSIS, AND OPTIMIZATION TOOLBOX

J. B.E. Meurisse¹, A. Borner¹, M. Karimi¹, J. Fegghi² and N. N. Mansour³, ¹Science and Technology Corporation at NASA Ames Research Center (jeremie.b.meurisse@nasa.gov, arnaud.p.borner@nasa.gov, mona.karimi@nasa.gov), ²University of Michigan (joseph.fegghi@nasa.gov), ³NASA Ames Research Center (nagi.n.mansour@nasa.gov).

Brief Presenter Biography:

Mr. Meurisse is a Research Scientist with Science and Technology Corporation, and an on-site contractor at NASA Ames Research Center working in the Supercomputing Division.

Abstract:

The Mars Science Laboratory (MSL) was protected during its Mars atmospheric entry by an instrumented heatshield that used NASA's Phenolic Impregnated Carbon Ablator (PICA) [1]. PICA is a lightweight carbon fiber/polymeric resin material that offers excellent performances for protecting probes during planetary entry. The Mars Entry Descent and Landing Instrument (MEDLI) suite on MSL offers unique in-flight validation data for models of atmospheric entry and material response. MEDLI recorded, among others, time-resolved in-depth temperature data of PICA using thermocouple sensors assembled in the MEDLI Integrated Sensor Plugs (MISP).

The objective of this work is to showcase the capability of the Design, Analysis, and Optimization of Thermal Protection Materials (DAO-TPM) toolbox. DAO-TPM is a Python based framework that works as a link between mission design, aerothermal and radiative environment computation, Thermal Protection Systems (TPS) microstructure analysis, material response and optimization tools. The toolbox has a Graphical User Interface (GUI) (Fig. 1) that allows the user to build as well as run the various software and utilities used to design, analyze and optimize a heatshield.

The General Mission Analysis Tool (GMAT) [2] provides an open source software system for space mission design, optimization, and navigation. The Direct Simulation Monte Carlo SPARTA code [3] computes the environment around the MSL aeroshell in the rarefied regime, while the in the continuum regime, the aerothermal properties will be computed using the Data Parallel Line Relaxation (DPLR) CFD code [4]. The environment radiative heating at Mars entry conditions is provided by the Nonequilibrium air radiation (NEQAIR) program [5].



Fig. 1 - Graphical User Interface (GUI) of DAO-TPM.

The Porous Microstructure Analysis (PuMA) software [6] provides the effective material properties of PICA through a combination of predictive simulations and experiments. Mutation++ library [7] computes the thermodynamic and chemistry properties. The Porous material Analysis Toolbox based on OpenFOAM (PATO) software [8,9,10] is used to perform the heatshield material response. The DAKOTA library [8] is used to calibrate physical models in PATO and PuMA. In future work, DAKOTA will be used to do sensitivity analysis and quantification of margins and uncertainty of the thermal response at the MISP locations.

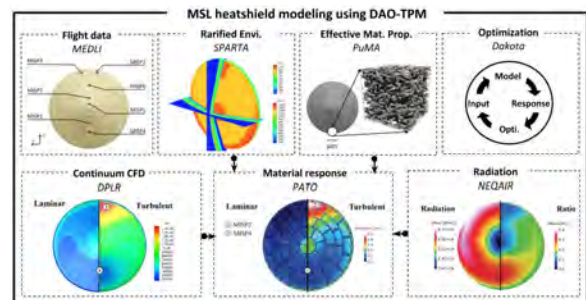


Fig. 2 - MSL heatshield modeling using DAO-TPM.

NASA's next mission to Mars, the Mars 2020, will use the spare heatshield of the Mars Science Laboratory (MSL) for thermal protection during entry, descent and

landing. In preparation to Mars 2020 post-flight analysis, the predictive material response capability is benchmarked against flight data from the MSL Entry, Descent, & Landing Instrument (MEDLI) (**Fig. 2**). This work represents an important milestone toward the development of validated predictive capabilities for designing thermal protection systems for planetary probes.

References:

- [1] M.J. Wright et al. (2009), *AIAA Paper*, 2009-423.
- [2] General Mission Analysis Tool (GMAT) Architectural Specification, *NASA NTRS* (2007).
- [3] M. A. Gallis et al. (2014), *AIP Conf Proc* 1628, 27.
- [4] M.J. Wright et al. (2009), *DPLR Code User Manual: Acadia-Version 4.01.1*.
- [5] Park C., "Nonequilibrium air radiation (NEQAIR) program: User's manual." (1985).
- [6] Ferguson J., et al. "PuMA: the Porous Microstructure Analysis software." *SoftwareX* 7 (2018): 81-87.
- [7] J. B. Scoggins and T. E. Magin (2014), *AIAA Paper*, 2014-2966.
- [8] J. Lachaud and N. N. Mansour (2014), *J Thermophys Heat Tran*, 28, 191–202.
- [9] J. Lachaud et al. (2017), *Int J Heat Mass Tran*, 108, 1406–1417.
- [10] J. B.E. Meurisse et al. (2018), *Aerosp Sci Technol*, 76, 497-511.

HYPERSONIC FLOWS IN THERMOCHEMICAL NONEQUILIBRIUM WITH IMMERSED BOUNDARY METHOD AND ADAPTIVE MESH REFINEMENT

M. Patel¹ and S. Navarro-Martinez¹

¹Department of Mechanical Engineering, Imperial College London, Kensington, London, SW7 2AZ

Corresponding Author: monal.patel12@imperial.ac.uk

Brief Presenter Biography: 2nd Year PhD Student at Imperial College London within the Department of Mechanical Engineering. Working title of PhD is Fully Coupled Ablation in Thermochemical Nonequilibrium.

Introduction: Hypersonic flows are very energetic flows with stagnation enthalpies in the order of MJ/kg, leading to high temperatures when the fluid is decelerated. High temperatures lead to various physical processes, vibrational and electronic energy mode excitation, chemical reactions, ionization and gas-surface interactions. All of which are rate controlled processes and have a timescale associated with them. Thermochemical nonequilibrium refers to situations where the flow time scales are of a similar order of magnitude to these high temperature rate processes. These can affect the aerothermodynamics of high speed vehicles. Therefore, planetary entry flow conditions demand an understanding of thermochemical nonequilibrium phenomena [1].

Problem: Modelling planetary reentry flows involves a large range of spatial and temporal scales within the flowfield. Especially in the presence of complex geometries, shapes with curved edges. Thermal nonequilibrium and chemical reaction timescales can be exponential functions of temperature. Reentry flowfields have temperature ranging from $O(10^2)$ K to $O(10^4)$ K which means timescales as small as 10^{-9} s can be present. Furthermore, high speed planetary reentry involves high Reynolds number flows ($> 10^5$), which induce large range of spatial and temporal scales. Therefore, high mesh densities and small computational time steps are required to capture the range of scales. Such simulations are computationally expensive. A method to reduce the expense is Adaptive Mesh Refinement (AMR). It allows local addition of spatial resolution within the domain as required, depending on the local flow. Although various validated thermochemical nonequilibrium (TCNE) codes exist: Structured, LAURA [2] and DPLR [8] ; Un-

structured, US3D [5] and LeMANS [6]. Only some have been coupled with AMR, in order to reduce computation time. The existing codes contain intricate meshing routines needed for unstructured methods. For conventional structured methods, stitching algorithms linking various parts of domain together are required, adding unnecessary computation time and algorithmic complexity. An alternative computational method of representing boundaries is Immersed boundary methods (IBM). This approach allows simple Cartesian grids to represent complex geometries, moving or stationary [4]. In the author's knowledge, no attempt of combining AMR with IBM for planetary reentry application exists. The combination of TCNE, AMR and IBM is well suited for high-fidelity ablative thermal protection systems and satellite/meteor burn up modelling.

Approach In-house explicit finite difference solver is used, *CompReal*. It solves mass, species mass fractions, momentum, total energy and vibrational energy conservation equations. Euler fluxes can be calculated using Riemann solver, Dispersion Relation Preserving Scheme (DRP) finite difference or conservative skew-symmetric formulation. Viscous fluxes can be calculated using central difference schemes. A two-temperature model is implemented with mixture vibrational energy. Vibrational-translational energy transfer source term is modelled with Landau-Teller and Millikan-White interspecies relaxation rates with Park's correction for high temperatures. Thermodynamic and transport properties of the flow are calculated using Mutation++ library and are valid up to 15,000K for partially ionized plasmas [7]. AMR is implemented using Boxlib libraries, developed at the Center for Computational Sciences and Engineering within Lawrence Berkeley National Laboratory. IBM is implemented via discrete forcing approach with direct boundary condition imposition using ghost-cells.

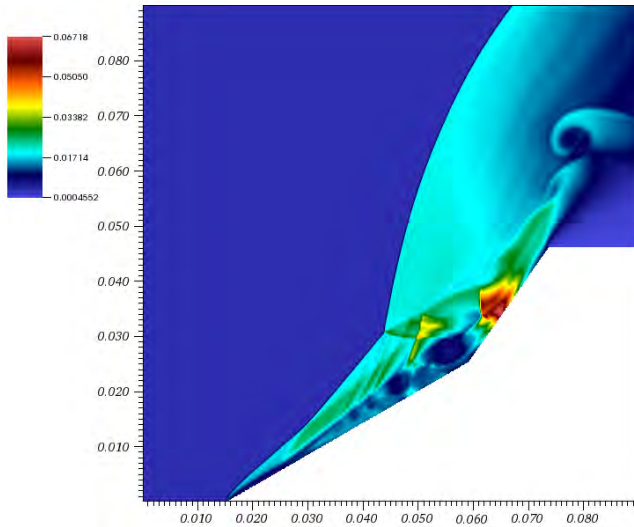


Figure 1: Density field around double ramp at Mach 7.14 and stagnation enthalpy 8 MJ/kg

Results: Implementaion of AMR and IBM with TCNE suitable for reentry applications is validated compared with experiments and other codes. Flows with Mach number less than 15 with simple geometries like spheres,wedges,etc., are simulated. Surface pressure coefficient, heat transfer distributions, shock shape and stand-off distances are examined. Figure 1 shows a double ramp based on [3] with modelled with *CompReal*.

References

- [1] G. V. Candler. Rate effects in hypersonic flows. *Annual Review of Fluid Mechanics*, 51(1), 2019.
- [2] P. A. Gnoffo and F. M. Cheatwood. User’s manual for the langley aerothermodynamic upwind relaxation algorithm (laura). 1996.
- [3] D. Knight, O. Chazot, J. Austin, M. A. Badr, G. Candler, B. Celik, D. de Rosa, R. Donelli, J. Komives, A. Lani, et al. Assessment of predictive capabilities for aerodynamic heating in hypersonic flow. *Progress in Aerospace Sciences*, 90:39–53, 2017.
- [4] R. Mittal and G. Iaccarino. Immersed boundary methods. *Annu. Rev. Fluid Mech.*, 37:239–261, 2005.
- [5] I. Nompelis, T. W. Drayna, and G. V. Candler. A parallel unstructured implicit solver for hypersonic reacting flow simulation. In *Parallel Computational Fluid Dynamics 2005*, pages 389–395. Elsevier, 2006.
- [6] L. Scalabrin and I. Boyd. Numerical simulation of weakly ionized hypersonic flow for reentry configurations. In *9th AIAA/ASME Joint Thermophysics and Heat Transfer Conference*, page 3773, 2006.
- [7] M. J. B. Scoggins. *Development of numerical methods and study of coupled flow, radiation, and ablation phenomena for atmospheric entry*. PhD thesis, PhD thesis, Centralesupélec. Le laboratoire énergétique moléculaire et , 2017.
- [8] M. J. Wright, G. V. Candler, and D. Bose. Data-parallel line relaxation method for the navier-stokes equations. *AIAA journal*, 36(9):1603–1609, 1998.

Comparison of Chemical Kinetic Models for Aerothermal Simulations of Entry into Gas Giants

Alex T. Carroll,¹ Savio J. Poovathingal,² and Iain D. Boyd³

Department of Aerospace Engineering, University of Michigan, Ann Arbor, MI 48109

¹ Undergraduate Researcher, atm carr@umich.edu, ² Research Fellow, spoovath@umich.edu, ³James E. Knott Professor, iainboyd@umich.edu

Brief Presenter Biography: Alex Carroll is an undergraduate researcher at the University of Michigan’s Nonequilibrium Gas and Plasma Dynamics Laboratory. He is double majoring in Aerospace Engineering and Computer Science, with research interests in hypersonic aerothermodynamics and CFD.

Abstract: Computational fluid dynamics (CFD) simulations are used to analyze bulk flow field properties and variations in flow composition for entry of planetary probes into ice and gas giants. Atmospheres of ice and gas giants are primarily composed of hydrogen and helium, and the high velocities associated with entry vehicles often results in the formation of strong shocks that dissociate hydrogen molecules into atoms. In this study, the rate constants of hydrogen dissociation reactions for entry flows in Saturn’s atmosphere at entry velocities of 10 km/s were varied systematically to determine their influence on flow properties and composition surrounding the entry vehicle, as well as shock stand-off distances. It was found that increasing the rate constant of the dissociation reaction between $H_2 + H$ affected flow properties the most of all studied reactions. It was also found that increased dissociation of H_2 resulted in larger shock stand-off distances, while increasing the rate constant of the $H_2 + H$ reaction by three magnitudes from the baseline rates of Leibowitz led to a 13% increase in shock stand-off distance. The results of systematically varying the rate constants of these dissociation reactions, and their key implications for the design requirements of entry vehicles into Saturn will be presented at the conference.

Introduction: The 2013-2022 decadal survey [1] for planetary exploration has identified probe missions to the gas giants Uranus and Saturn as priorities. The design of these probes, and especially their thermal protection systems (TPS) remains challenging, due to the high-temperature, hypersonic, non-equilibrium flows encountered by these vehicles on entry. One of the problems associated with characterizing such flow fields is the lack of understanding on how varying rates of dissociation reactions in such flows influences bulk flow field properties and fluid composition near the surface of such vehicles. While the flow fields surrounding entry probes in atmospheres composed mainly of inert gases such as CO_2 , O_2 , N_2 , and air (such

as Earth and Mars) have been fairly well characterized [2], the atmosphere of gas giants such as Jupiter, Saturn, Uranus, and Neptune are composed primarily of H_2 and He. Additionally, the lack of adequate experimental test facilities for reactive H_2 -He mixture flows since the closing of NASA’s Giant Planet Facility [3] presents an additional challenge in studying such flow phenomena. Therefore, computational analysis through hypersonic CFD simulations is necessary to investigate the feasibility of different entry vehicle and TPS designs for future probe missions to gas and ice giants.

Methods: Flow calculations are performed using the hypersonic CFD solver, LeMANS. LeMANS is a Navier-Stokes solver developed at the University of Michigan specifically for applications involving hypersonic flow with thermal and chemical nonequilibrium. It can handle unstructured three-dimensional meshes, and the governing equations are solved using the finite volume method. LeMANS has been extensively benchmarked (DPLR, LAURA), verified, and validated (Apollo, Fire II, RAM-C). The development of LeMANS and additional details are provided in Reference [4].

The reactions and rates used for the baseline simulation are taken from Leibowitz [5], and have been modified to only include neutral species (H_2 , H , and He). These reactions and rates are given below in Table 1. These baseline rate constants were then systematically increased and decreased by three orders of magnitude. The first six simulations involved independently increasing or decreasing rate constants from the baseline rates for each of the three dissociation reactions in Table 1, whereas the last two involved simultaneously increasing or decreasing the rate constant for all three reactions.

Table 1: Reactions and rates for baseline simulation

Reaction	Rate Constant [$\frac{cm^3}{mol-s}$]
$H_2+H_2 \rightarrow H+H+H_2$	$1.839 \times 10^{19} \exp(-52340/T)$
$H_2+H \rightarrow H+H+H$	$6.07 \times 10^{19} \exp(-52340/T)$
$H_2+He \rightarrow H+H+He$	$4.33584 \times 10^{18} \exp(-52340/T)$

Results: It was found that increasing the rate constant of the H_2+H reaction led to the greatest

dissociation of H_2 in front of the vehicle, as well as the greatest changes in bulk flow field properties when compared to the baseline simulation. Additionally, the influence of increasing the rate constant of the H_2+H was so large that the difference in results from increasing just the rate constant of the H_2+H reaction versus all three reactions simultaneously was nearly negligible. This trend can be seen in Figure 1, where for the simulation corresponding to an increase in the rate constant of the H_2+H reaction, the minimum mole fraction of H_2 decreased by approximately 79% versus 2% in the baseline simulation.

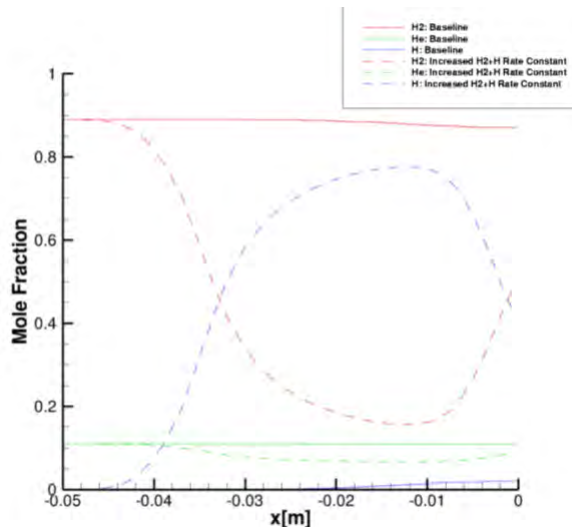


Figure 1: Increasing rate constant of H_2+H reaction leads to greatest dissociation of H_2

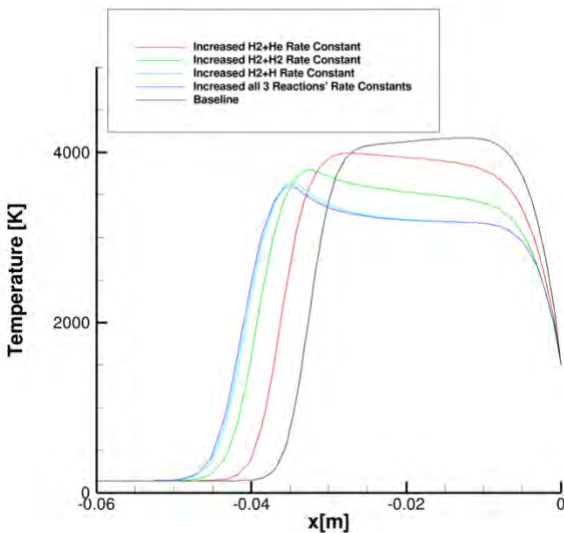


Figure 2: Increase in dissociation of H_2 associated with larger shock stand-off distances

The increase in dissociation of H_2 was also associated with the largest shock stand-off distances. From Figure 2, it can be seen that the simulations that were associated with larger amounts of dissociation of H_2 led to larger shock stand-off distances, with the simulation corresponding to an increase in the rate constant of the H_2+H reaction having a shock stand-off distance that was 13% larger than that of the baseline simulation.

Finally, it was observed that decreasing the rate constants of any of the three reactions had a negligible effect on the flow properties and composition surrounding the vehicle. This result was as expected, as there was close to no dissociation of H_2 in the baseline simulation, and so decreasing the rate constants of the reactions led to no further dissociation reactions in the flow.

References:

- [1] "Vision and Voyages for Planetary Science in the Decade 2013-2022," National Research Council Rept., National Academy Press; Washington, D.C., 2011.
- [2] Park, C. "Nonequilibrium hypersonic aerothermodynamics", Wiley Publications, 1990.
- [3] Laub, B., and Venkatapathy, E., "Thermal protection system technology and facility needs for demanding future planetary missions," Planetary Probe Atmospheric Entry and Descent Trajectory Analysis and Science, Vol. 544, 2004, pp. 239–247.
- [4] Scalabrin, L. C., Numerical Simulation of Weakly Ionized Hypersonic Flow Over Reentry Capsules, Ph.D. thesis, University of Michigan, Ann Arbor, MI, 2007) and Martin et al. Martin, A., Scalabrin, L. C., and Boyd, I. D., "High Performance Modeling of Atmospheric Re-entry Vehicles," Journal of Physics: Conference Series, Vol. 341, No. 1, 2012, pp. 1-12
- [5] Leibowitz, L. P., and Kuo, T.-J., "Ionizational nonequilibrium heating during outer planetary entries," AIAA Journal, Vol. 14, No. 9, 1976, pp. 1324–1329.

Commissioning of the Oxford T6 Stalker Tunnel in Reflected Shock Tunnel Mode

S. D. Subiah¹, P. L. Collen¹, L. J. Doherty¹, M. McGilvray¹, ¹Oxford Thermofluids Institute, University of Oxford, Osney Mead Industrial Estate, Oxford, OX2 OES, suria-devi.subiah@eng.ox.ac.uk

Brief Presenter Biography: Suria Subiah received her BSc. Aeronautical Engineering from the University of the Witwatersrand, South Africa and is a Fulbright Scholar with an MSc. Aerospace Engineering from the Georgia Institute of Technology, USA. She is a first year DPhil student at the Oxford Thermofluids Institute where she is researching the high temperature effects of transpiration cooling as a re-usable thermal protection system in hypersonic flows.

Introduction: In the development of future space vehicles, the understanding of hypersonic flow phenomena is of extreme importance. Whilst flight testing is optimal, it can be prohibitively expensive for a wide range of flight trajectories. Computational models can provide additional information, but they require validation against experimental data and this is where ground testing facilities, such as Oxford University's T6 Stalker Tunnel are critical.

The T6 Stalker Tunnel is the United Kingdom's first high total enthalpy hypersonic facility (Fig. 1). It is a free piston driven facility and is able to operate in three main modes: expansion tunnel, shock tube and reflected shock tunnel [1]. Extensive work has been done in commissioning of the tunnel in shock tube mode by Collen, et al. [2]. This paper will outline the work done to commission the facility in reflected shock tunnel (RST) mode and detail the process of developing the conditions. In particular, a condition has been developed for testing of the HIFiRE-1 model which is in air with a total enthalpy of 2.39 MJ/kg, Mach number of 7 and unit Reynolds number of 18.08×10^6 /m.

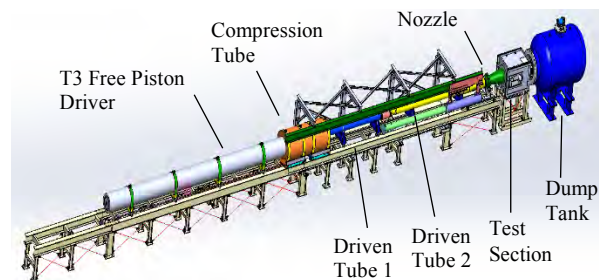


Figure 1: Oxford T6 Stalker Tunnel

To obtain the required fill conditions in the facility in RST mode, a calculation procedure is undertaken in four parts, shown in Fig. 2. Part I uses the aimed nozzle exit conditions and assumes isentropic and thermochemical equilibrium to calculate the stagnation pressure. Part II

calculates the required fill pressure in the shock tube and the shock speed required to achieve the stagnation conditions. Part III calculates the required driver conditions at primary diaphragm rupture to drive the desired shock whilst generating a tailored condition, using an additional expansion mechanism using the method outlined in Hong et al. [3] and Gildfind et al. [4]. Part IV investigates the free piston driver initial conditions, including a model of the piston dynamics to achieve a tuned condition with a piston soft landing. This used the method described by Hornung [5], and the effects of varying orifice sizes were compared to give the optimal test time and piston trajectory.

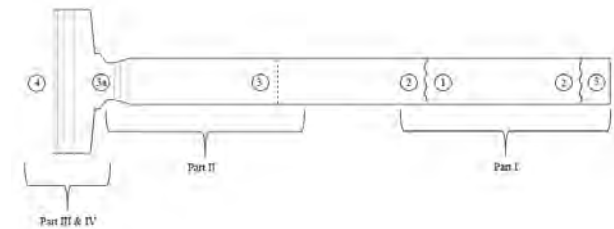


Figure 2: Flow features and numbering convention in reflected shock tube mode

The results were validated using the University of Queensland's quasi-one-dimensional gas dynamics simulation code, L1d3 [6] and the equilibrium gas facility simulation tool PITOT [7]. Blank off tests of the piston were undertaken to confirm losses in the free piston driver. The proposed condition was operated in T6 and the results for the first commissioning tests in reflected shock tunnel mode are presented here and compared with the predicted values.

References:

- [1] McGilvray M. et al. (2015) *20th Int. Space Planes and Hypersonic Syst. and Tech. Conf.*, 1-11.
- [2] Collen P. L. et al. (2019) *AIAA Scitech Forum*.
- [3] Hong Z. et al. (2009) *Shock Waves*, 19:331-336.
- [4] Gildfind D. E. et al. (2015) *Shock Waves*, 25:169-176.
- [5] Hornung H. G. (1988) *FM 88-1, California Institute of Technology*.
- [6] Jacobs P. A. (1988) *Research Report 13/98, University of Queensland*.
- [7] Gildfind, J. C. et al. (2017) *Shock Waves*, 28:349-377.

STATUS OF GLOBAL REFERENCE ATMOSPHERIC MODEL (GRAM) UPGRADES.

H. L. Justh¹, A. M. Dwyer Cianciolo², K. L. Burns³, J. Hoffman⁴, R. W. Powell⁵, and P. W. White⁶. ¹NASA, Marshall Space Flight Center, Mail Code EV44, Marshall Space Flight Center, AL, 35812, hilary.l.justh@nasa.gov, ²NASA, Langley Research Center, Mail Stop 489, Hampton, VA 23681, alicia.m.dwyercianciolo@nasa.gov, ³Jacobs Space Exploration Group, 1500 Perimeter Pkwy., Suite 400, Huntsville, AL 35806, kerry.l.burns@nasa.gov, ⁴Analytical Mechanics Associates, 21 Enterprise Pkwy., Suite 300, Hampton, VA 23666, james.hoffman-1@nasa.gov, ⁵Analytical Mechanics Associates, 21 Enterprise Pkwy., Suite 300, Hampton, VA 23666, richard.w.powell@nasa.gov and ⁶NASA, Marshall Space Flight Center, Mail Code EV44, Marshall Space Flight Center, AL, 35812, patrick.w.white@nasa.gov.

Brief Presenter Biography: Hilary L. Justh is a scientist with the Terrestrial and Planetary Environments team in the Natural Environments Branch of the Engineering Directorate at NASA's Marshall Space Flight Center (MSFC). As planetary Global Reference Atmospheric Model (GRAM) lead, she has utilized the MSFC developed planetary GRAMs for diverse mission applications including Mars Reconnaissance Orbiter (MRO), Mars Science Laboratory (MSL), Cassini, Mars Ascent Vehicle (MAV), and others. Hilary Justh is the atmosphere modeling lead for the GRAM Upgrade task.

Introduction: The Global Reference Atmospheric Model (GRAM) is one of the most widely used engineering models of the atmosphere. GRAM is developed and maintained by the NASA Marshall Space Flight Center (MSFC). The NASA Science Mission Directorate (SMD) has provided funding support to upgrade the GRAMs in Fiscal Year 2018 and 2019. This presentation will provide a summary of the upgrades that have been made to the GRAMs, the release status of the upgraded GRAMs, the new GRAMs that are under development, and future GRAM upgrade plans.

Global Reference Atmospheric Model (GRAM): The GRAMs are engineering-level atmospheric models applicable for engineering design analyses, mission planning, and operational decision making. They provide mean values and variability for any point in the atmosphere as well as seasonal, geographic, and altitude variations. GRAM outputs include winds, thermodynamics, chemical composition, and radiative fluxes. They have been widely used by the engineering community because of their ability to create realistic dispersions; GRAMs can be integrated into high fidelity flight dynamic simulations of launch, entry, descent and landing (EDL), aerobraking and aerocapture. MSFC has been developing and updating GRAMs since 1974 with GRAMs currently available for Earth, Mars, Venus, Neptune, and Titan.

GRAM Upgrade Status:

Code Upgrades. The GRAM atmosphere models have been redesigned around a common C++ framework. The source code for the GRAM suite has been

reorganized in a modular fashion. A common framework has been developed upon which all GRAM models are built which is then coupled with the models specific to that particular planetary body. This will make the user interface with all of the planetary GRAMs uniform. The first C++ releases of the existing planetary GRAMs will be a straight conversion from the latest Fortran version.

Model Upgrades. The focus of the model upgrade task has been to improve the atmosphere models in the existing GRAMs and to establish a foundation for developing GRAMs for additional destinations. The GRAM ephemeris has been upgraded to the NASA Navigation and Ancillary Information Facility (NAIF) SPICE toolkit (version N0066). Meetings with planetary modelers, mission data providers, and experts are ongoing to determine new data sets and models that are currently available to upgrade existing planetary GRAMs and to develop new planetary GRAMs (Saturn, Uranus, and Jupiter-GRAM).

Upcoming GRAM Releases. The first upgraded planetary GRAM that will be released is Neptune-GRAM. This release will include the new common C++ framework as well as SPICE. A user's and programmer's guide will be released with Neptune-GRAM.

Uranus-GRAM is currently being developed as a new planetary GRAM. Uranus-GRAM will be based on data generated by the Ames Research Center Uranus model. An overview of Uranus-GRAM, Neptune-GRAM, and a schedule of additional upcoming GRAM releases will be provided during the presentation.

Conclusions: Upgrades of the existing planetary GRAMs and development of new planetary GRAMs are continuing with release dates TBD. The funding provided by the NASA SMD has been essential to upgrading this critical tool set.

Acknowledgments: The authors gratefully acknowledge support from the NASA SMD.

Speaker Biography:

Jonathan Cheatwood is a Junior at Virginia Tech currently majoring in aerospace engineering. He interns at NASA Langley Research Center and is planning on attending graduate school for Aerospace Engineering.

Introduction:

Hypersonic thermal imaging methods have been used for many years to assist in modeling the surface temperature and heat flux of models while in hypersonic flow. The two most commonly used methods are infrared and phosphor, both of which use cameras to detect energy. Images of the model are only taken while the model is on the centerline of the tunnel; thus, during the model’s injection sequence there is no imaging data being taken. Since preliminary images of the model are taken, there exists a gap in the recorded imagery data. Because of this gap, approximations had to be made in order to be able to model the heat flux on the model. One of the main approximations that was made was assuming that the profile for heating coefficient during model injection was a step function. The computation power required for the step approximation was extremely low; however, the assumption did not model injection heating accurately and prevented variable thermal properties to be modeled. Due to the fact that model injection heating was not accurately modeled, the step approximation method took a significant amount of time to reach a near enough approximation for the heat flux. Because of these factors, and the advancement of computational capabilities in recent years, the

creation of an alternative method was preferable, one that modeled the heat flux of the model much more accurately, accounted for variable thermal properties, and, most importantly, collapsed to an accurate approximation of heating within a small amount of time. In 2006, Brian Hollis developed a parabolic bridge function that approximated the heat that the model saw during its injection phase. As a result of this approximated patch the heating data obtain from imagery could be treated as and direct methods to analyze the data, including the use of variable thermal properties. In the summer of 2018, the parabolic bridge function was revisited, leading to the development of the Patch Integral Method (PIM). The major difference between PIM and the parabolic bridge function is that PIM more accurately models the injection heating curve. The PIM approach to creating continuous data is to “patch” the gap in imagery data with an S-shaped curve which more accurately approximates the physical heating that the model sees during injection. PIM is also written in Python and the code can utilize a finite-difference method to model variable thermal properties and calculate heat flux values, a luxury that wasn’t available in the code written for the original step approximation method. This allows for much more accurate modeling of surface heat flux values. An illustration of the differences between the step approximation method and PIM can be seen in Figure 1. PIM (seen in orange) accurately matches the thin film data (seen in black) within half a second after the model reaches the centerline, while the Step-Approximation Method (seen in dashed blue) takes multiple seconds to produce comparable results.

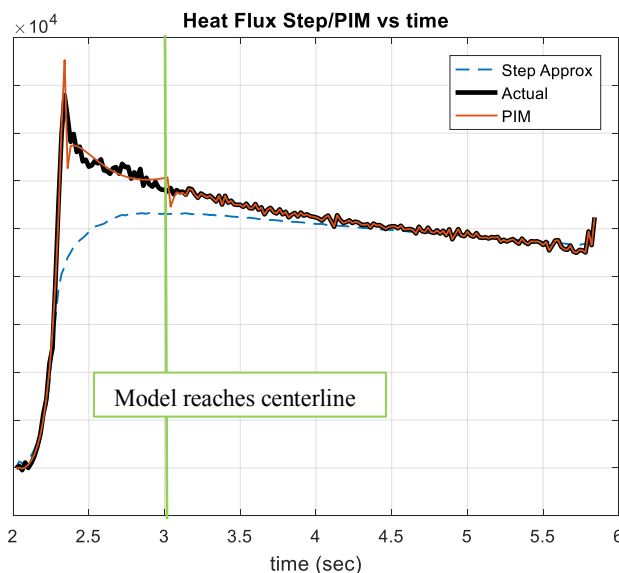


Figure 1: PIM vs Step-Approximation Method

DSMC SIMULATION OF HYPERSONIC FLOW OVER TPS MICROSTRUCTURES

S. Ramjatan¹ and Thomas E. Schwartzentruber¹,

¹Aerospace Engineering & Mechanics, University of Minnesota, Minnesota, USA,

Brief Presenter Biography: Sahadeo Ramjatan is currently a graduate student at the University of Minnesota working on his PhD under Prof. Schwartzentruber.

Introduction: Future robotic science missions to Venus, a Mars sample return, or asteroid mission involve high reentry velocities that are beyond PICA capability. Hence, higher reliability ablative TPS are needed to handle more challenging flight conditions. During the ablation process, thermal stresses and traction forces combined with oxidation could affect the structural integrity of the TPS resulting in failure. For example, spallation or the ejection of disconnected fibers or chunks of material into the flow field can occur and spalled particles can alter the aerodynamic heating rate by changing the chemical composition of the flow field thereby affecting the heat flux [1]. The objective of this work is to improve the predictive modeling of the chemical and structural failure of porous ablative materials. Hypersonic boundary layer flow is simulated over TPS microstructures using the Direct Simulation Monte Carlo (DSMC) method. This work examines the local surface properties including the heat flux and traction force on the microstructure at flight relevant conditions. Another aim of this work is to isolate fibers of interest from the microstructure, e.g. based on centroid or angle from the normal, and average them onto a representative fiber for use in thermo-structural analysis.

Novelty of Research: Using the DSMC method allows one to study the overall stress and heat flux at a microscopic level [2]. In addition, at high altitudes the characteristic length scale of the microstructure approaches that of the mean free path justifying the use of the DSMC particle-based approach. Simulations are performed using boundary layer profiles from real flight conditions including the Stardust and a Mars Sample Return reentry condition using state of the art gas-surface and gas-phase reactions.

Microstructure: Microstructures are modeled as a random array of carbon fibers where each fiber is modeled as a cylinder that is made up of several elements, each of which is in turn made up of triangles. The software FiberGen [3], developed at the University of Minnesota, has the capability of generating a set of fibers where the distributions of three-dimensional orientations, fiber diameters, and material characteristics such as bulk porosity can be controlled. Standard FiberForm microstructures are created using FiberGen and inputted into the DSMC simulation where hypersonic boundary layer flow is simulated as shown in Fig. 1 [4].

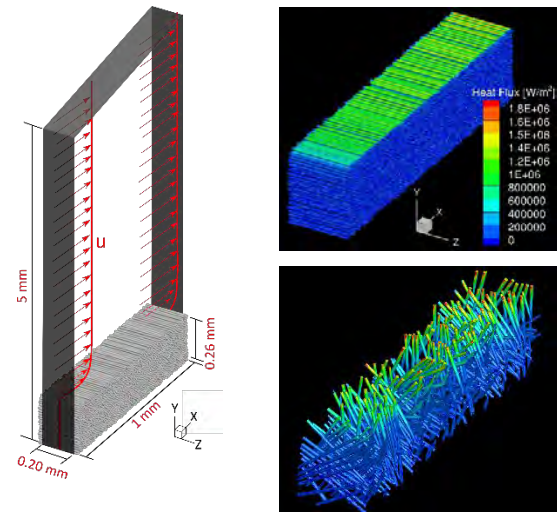


Figure 1: Boundary Layer flow over microstructure.

Results & Conclusions: This work applies the DSMC method in simulating boundary layer flow over TPS microstructures. Boundary layer profiles from the Stardust and a Mars Sample Return mission are both simulated and accurate estimates of the heat flux and traction force are obtained and discussed. The oxygen mass flux to the microstructure, which is responsible for the pitting and failure of TPS, is plotted at various trajectory points and discussed. Most importantly, individual fibers of interest are averaged onto a representative fiber for use in thermo-structural analysis. The results acquired in this work provides insight into designing more reliable TPS for upcoming missions and amounts to a greater understanding of the ablation process.

References:

- [1] R. Davuluri, H. Zhang and A. Martin, "Numerical study of spallation phenomenon in an arc-jet environment," *Journal of Thermophysics and Heat Transfer*, vol. 30, no. 1, pp. 32-41, 2015.
- [2] A. D. Achambath, S. Ramjatan and T. Schwartzentruber, "Surface Properties on Thermal Protection System Microstructure during Hypersonic Ablation," in *AIAA Scitech 2019 Forum*, 2019, San Diego, 2019.
- [3] E. Stern, S. Poovathingal, I. Nompelis, T. Schwartzentruber and G. Candler, "Nonequilibrium flow through porous thermal protection materials, Part I: Numerical Methods," to appear in *Journal of Computational Physics*, 2017.
- [4] S. Ramjatan and T. Schwartzentruber, "DSMC Simulation of Flow Over Various TPS Microstructures," in *2018 Ablation Workshop*, Burlington, VT, 2018.